Annals of Computer Science and Information Systems
Volume 32

Communication Papers of the 17th Conference on Computer Science and Intelligence Systems

September 4–7, 2022. Sofia, Bulgaria

Maria Ganzha, Leszek Maciaszek, Marcin Paprzycki,
Dominik Ślęzak (eds.)

PTI

Annals of Computer Science and Information Systems, Volume 32

Communication Papers of the 17th Conference on Computer Science and Intelligence Systems

Maria Ganzha, Leszek Maciaszek, Marcin Paprzycki, Dominik Ślęzak (eds.)

POLSKIE TOWARZYSTWO INFORMATYCZNE
POLISH INFORMATION PROCESSING SOCIETY

2022, Warszawa, Polskie Towarzystwo Informatyczne

Annals of Computer Science and Information Systems, Volume 32

Communication Papers of the 17th Conference on Computer Science and Intelligence Systems

USB: ISBN 978-83-965897-5-0
WEB: 978-83-965897-4-3

ISSN 2300-5963
DOI 10.15439/978-83-965897-4-3

Ul. Solec 38/103
00-394 Warsaw
Poland

Contact: secretariat@fedcsis.org
http://annals-csis.org/

Cover art:
Barbara Borysewicz,
Elbląg, Poland

Also in this series:

Volume 31: Position Papers of the 17th Conference on Computer Science and Intelligence Systems, **ISBN WEB: 978-83-965897-2-9, ISBN USB: 978-83-965897-3-6**
Volume 30: Proceedings of the 17th Conference on Computer Science and Intelligence Systems, **ISBN WEB: 978-83-962423-9-6, ISBN USB: 978-83-965897-0-5**
Volume 29: Recent Advances in Business Analytics. Selected papers of the 2021 KNOWCON-NSAIS workshop on Business Analytics**ISBN WEB: 978-83-962423-7-2, ISBN USB: 978-83-962423-6-5**
Volume 28: Proceedings of the 2021 International Conference on Research in Management & Technovation, **ISBN WEB: 978-83-962423-4-1, ISBN USB: 978-83-962423-5-8**
Volume 27: Proceedings of the Sixth International Conference on Research in Intelligent and Computing in Engineering, **ISBN WEB: 978-83-962423-2-7, ISBN USB: 978-83-962423-3-4**
Volume 26: Position and Communication Papers of the 16th Conference on Computer Science and Intelligence Systems, **ISBN WEB: 978-83-959183-9-1, ISBN USB: 978-83-962423-0-3**
Volume 25: Proceedings of the 16th Conference on Computer Science and Intelligence Systems, **ISBN WEB 978-83-959183-6-0, ISBN USB 978-83-959183-7-7, ISBN ART 978-83-959183-8-4**
Volume 24: Proceedings of the International Conference on Research in Management & Technovation 2020, **ISBN WEB: 978-83-959183-5-3, ISBN USB: 978-83-959183-4-6**
Volume 23: Communication Papers of the 2020 Federated Conference on Computer Science and Information Systems, **ISBN WEB: 978-83-959183-2-2, ISBN USB: 978-83-959183-3-9**
Volume 22: Position Papers of the 2020 Federated Conference on Computer Science and Information Systems, **ISBN WEB: 978-83-959183-0-8, ISBN USB: 978-83-959183-1-5**
Volume 21: Proceedings of the 2020 Federated Conference on Computer Science and Information Systems, **ISBN Web 978-83-955416-7-4, ISBN USB 978-83-955416-8-1, ISBN ART 978-83-955416-9-8**
Volume 20: Communication Papers of the 2019 Federated Conference on Computer Science and Information Systems, **ISBN WEB: 978-83-955416-3-6, ISBN USB: 978-83-955416-4-3**

DEAR Reader, it is our pleasure to present to you Communication Papers of the 17th Conference on Computer Science and Information Systems (FedCSIS 2022), in Sofia, Bulgaria, and in the hybrid mode.

In the context of the FedCSIS conference series, the *communication papers* were introduced in 2017, as a separate category of contributions. They report on research topics worthy of immediate communication. They may be used to mark a hot new research territory or to describe work in progress in order to quickly present it to scientific community. They may also contain additional information omitted from the earlier papers or may present software tools and products in a research state.

The main Conference Chair of FedCSIS 2022 was Stefka Fidanova, while Nina Dobrinkova acted as the Chair of the Organizing Committee. This year, FedCSIS was organized by the Polish Information Processing Society (Mazovia Chapter), IEEE Poland Section Computer Society Chapter, Systems Research Institute Polish Academy of Sciences, Warsaw University of Technology, Wrocław University of Economics and Institute of Information and Communication Technologies, Bulgarian Academy of Sciences.

FedCSIS 2022 was technically co-sponsored by: IEEE Bulgarian Section, IEEE Poland Section, IEEE Czechoslovakia Section Computer Society Chapter, IEEE Poland Section Systems, Man, and Cybernetics Society Chapter, IEEE Poland Section Computational Intelligence Society Chapter, IEEE Poland Section Control System Society Chapter, Committee of Computer Science of the Polish Academy of Sciences, Mazovia Cluster ICT, Poland and Bulgarian Section of SIAM.

Moreover, last year the FedCSIS conference series formed the strategic alliance with QED Software, a Polish software company developing AI-based technologies and acting as the technological co-founder in the AI-driven start-ups. This collaboration has been continued.

During FedCSIS 2022, the keynote lectures were delivered by:

- Krassimir Atanassov, Bulgarian Academy of Sciences, Sofia, Bulgaria: "*Remarks on Index Matrices",*
- Chris Cornelis, Ghent University, Department of Applied Mathematics, Computer Science and Statistics: "*Hybridization of Fuzzy Sets and Rough Sets: Achievements and Opportunities",*
- Ivan Lukovic, University of Belgrade, Faculty of Organizational Sciences, *"Organizational Capability for Information Management – Do We Feel a Big Data Crisis?",*
- Stefano Mariani on behalf of Franco Zambonelli (due to serious health issues encountered right before the conference), University of Modena e Reggio Emilia, Italy: "*Individual and Collective Self-development*".

Moreover, this year, two special guests delivered invited talks:

- Bogusław Cyganek, who was awarded the 2021 Wiley-IEEE Press Award, for his recent book *"Introduction to Programming with C++ for Engineers",*
- Andrzej Skowron, who delivered the talk: "*Rough Sets Turn 40: From Information Systems to Intelligent Systems*", which was devoted to the 40th anniversary of introduction, by late Professor Zdzisław Pawlak, of the theory of Rough Sets.

FedCSIS 2022 consisted of five Tracks and a special event for Doctoral School Students. Within each Track, topical Technical Sessions have been organized. Each Technical Session was split into fully on site and fully online sub-sessions. The on-site part of the conference took place in the facilities of the Crisis Management and Disaster Response Centre of Excellence in Sofia, Bulgaria.

Some of Technical Sessions have been associated with the FedCSIS conference series for many years, while some of them are relatively new. The role of the technical Sessions is to focus and enrich discussions on selected areas, pertinent to the general scope of each Track. The list of Tracks, and topical Technical Sessions organized within their scope, was as follows.

- **Track 1: Advanced Artificial Intelligence in Applications (17th Symposium AAIA'22)**
  - Artificial Intelligence for Next-Generation Diagnostic Imaging (1st Workshop AI4NextGenDI'22)
  - Artificial Intelligence in Machine Vision and Graphics (4th Workshop AIMaViG'22)
  - Personalization and Recommender Systems (1st Workshop PeRS'22)
  - Rough Sets: Theory and Applications (4th International Symposium RSTA'22)
  - Computational Optimization (15th International Workshop WCO'22)
- **Track 2: Computer Science & Systems (CSS'22)**
  - Computer Aspects of Numerical Algorithms (15th Workshop CANA'22)
  - Concurrency, Specification and Programming (30th International Symposium CS&P'22)
  - Multimedia Applications and Processing (15th International Symposium MMAP'22)
  - Scalable Computing (12th Workshop WSC'22)
- **Track 3: Network Systems and Applications (NSA'22)**
  - Complex Networks - Theory and Application (1st Workshop CN-TA'22)
  - Internet of Things – Enablers, Challenges and Applications (6th Workshop IoT-ECAW'22)
  - Cyber Security, Privacy, and Trust (3rd International Forum NEMESIS'22)
- **Track 4: Advances in Information Systems and Technology (AIST'22)**
  - Data Science in Health, Ecology and Commerce (4th Workshop DSH'22)
  - Information Systems Management (17th Conference ISM'22)
  - Knowledge Acquisition and Management (28th Conference KAM'22)
- **Track 5: Software and System Engineering (S3E'22)**
  - Cyber-Physical Systems (9th International Workshop IWCPS'22)
  - Model Driven Approaches in System Development (7th Workshop MDASD'22)

- Software Engineering (42nd IEEE Workshop SEW'22)

- **7th Doctoral Symposium on Recent Advances in Information Technology (DS-RAIT'22)**

Each contribution, found in this volume, was refereed by at least two referees.

The program of FedCSIS 2022 required a dedicated effort of many people. We would like to express our warmest gratitude to all Committee members, of each Track and each Technical Session, for their hard work in attracting and later refereeing 290 submissions.

We thank the authors of papers for their great contribution to the theory and practice of computing and intelligence systems. We are grateful to the invited speakers for sharing their knowledge and wisdom with the participants.

Last, but not least, we thank Stefka Fidanova and Nina Dobrinkova. It should be stressed that they made all the preparations to organize the conference in Bulgaria for three years in a row, while only in 2022 the conference actually happened there. They also worked with us diligently to adapt the conference formula to organize it in hybrid mode. We are very grateful for all your efforts!

We hope that you had an inspiring conference. We also hope to meet you again for the 18th Conference on Computer Science and Intelligence Systems (FedCSIS 2023) which will take place in Warsaw, Poland on September 17-20, 2023.

Co-Chairs of the FedCSIS Conference Series:

Maria Ganzha, *Warsaw University of Technology, Poland and Systems Research Institute Polish Academy of Sciences, Warsaw, Poland*

Leszek Maciaszek*, Macquarie University, Sydney, Australia*

Marcin Paprzycki, *Systems Research Institute Polish Academy of Sciences, Warsaw Poland and Management Academy, Warsaw, Poland*

Dominik Ślęzak, *Institute of Informatics, University of Warsaw, Poland*

Communication Papers of the 17th Conference on Computer Science and Intelligence Systems

September 4–7, 2022. Sofia, Bulgaria

TABLE OF CONTENTS

4TH INTERNATIONAL SYMPOSIUM ON ROUGH SETS: THEORY AND APPLICATIONS

15TH INTERNATIONAL WORKSHOP ON COMPUTATIONAL OPTIMIZATION

COMPUTER SCIENCE AND SYSTEMS

15TH WORKSHOP ON COMPUTER ASPECTS OF NUMERICAL ALGORITHMS

30TH INTERNATIONAL SYMPOSIUM ON CONCURRENCY, SPECIFICATION AND PROGRAMMING

15TH INTERNATIONAL SYMPOSIUM ON MULTIMEDIA APPLICATIONS AND PROCESSING

NETWORK SYSTEMS AND APPLICATIONS

1ST WORKSHOP ON COMPLEX NETWORKS: THEORY AND APPLICATION

6TH WORKSHOP ON INTERNET OF THINGS - ENABLERS, CHALLENGES AND APPLICATIONS

3RD INTERNATIONAL FORUM ON CYBER SECURITY, PRIVACY AND TRUST

ADVANCES IN INFORMATION SYSTEMS AND TECHNOLOGIES

7TH WORKSHOP ON MODEL DRIVEN APPROACHES IN SYSTEM DEVELOPMENT

17th International Symposium Advances in Artificial Intelligence and Applications

THIS track is a continuation of international AAIA symposiums, which have been held since 2006. It aims at establishing the synergy between technical sessions, which encompass wide range of aspects of AI. With its longest-tradition threads, such as WCO focusing on Computational Optimization, it is also open to new initiatives categorized with respect to both, the emerging AI-related methodologies and practical usage areas. Nowadays, AI is usually perceived as closely related to the data, therefore, this track's scope includes the elements of Machine Learning, Data Quality, Big Data, etc. However, the realm of AI is far richer and our ultimate goal is to show relationships between all of its subareas, emphasizing a cross-disciplinary nature of the research branches such as XAI, HCI, and many others.

AAIA'22 brings together scientists and practitioners to discuss their latest results and ideas in all areas of Artificial Intelligence. We hope that successful applications presented at AAIA'22 will be of interest to researchers who want to know about both theoretical advances and latest applied developments in AI.

TOPICS

Papers related to theories, methodologies, and applications in science and technology in the field of AI are especially solicited. Topics covering industrial applications and academic research are included, but not limited to:

- Decision Support
- Machine Learning
- Fuzzy Sets and Soft Computing
- Rough Sets and Approximate Reasoning
- Data Mining and Knowledge Discovery
- Data Modeling and Feature Engineering
- Data Integration and Information Fusion
- Hybrid and Hierarchical Intelligent Systems
- Neural Networks and Deep Learning
- Reinforcement Learning
- Bayesian Networks and Bayesian Reasoning
- Case-based Reasoning and Similarity
- Web Mining and Social Networks
- Business Intelligence and Online Analytics
- Robotics and Cyber-Physical Systems
- AI-centered Systems and Large-Scale Applications
- AI for Combinatorial Games, Video Games and Serious Games
- Evolutionary Algorithms and Evolutionary Computation
- Artificial Intelligence for Next-Generation Diagnostis Imaging (1st Workshop AI4NextGenDI'22)
- Artificial Intelligence for Patient Empowerment with Sensor Systems (1st Workshop AI4Empowerment'22)
- Artificial Intelligence in Machine Vision and Graphics (4th Workshop AIMaViG'22)
- Intelligent Ambient Assisted Living Systems (1st Workshop IntelligentAAL'22)
- Personalization and Recommender Systems (1st Workshop PeRS'22)
- Rough Sets: Theory and Applications (4th International Symposium RSTA'22)
- Computational Optimization (15th Workshop WCO'22)

TRACK CHAIRS

- **Zdravevski, Eftim,** Ss. Cyril and Methodius University, Macedonia
- **Szczuka, Marcin,** University of Warsaw, Poland
- **Matwin, Stan,** Dalhousie University, Canada

PROGRAM CHAIRS

- **Corizzo, Roberto,** American University, USA
- **Sosnowski, Łukasz,** Systems Research Institute, Polish Academy of Sciences, Poland
- **Świechowski, ,** Maciej, QED Software, Poland

PROGRAM COMMITTEE

- **Azad, Mohammad,** Jouf University, Saudi Arabia
- **Bellinger, Colin,** National Research Council of Canada – Ottawa, Canada
- **Bianchini, Monica,** Dipartimento di Ingegnegneria dell'Informazione, Università di Siena, Italy
- **Boukouvalas, Zois,** American University – Washington DC, USA
- **Calpe Maravilla, Javier,** University of Valencia, Spain
- **Chelly, Zaineb,** Université Paris-Saclay, UVSQ, DAVID, France
- **Colantonio, Sara,** ISTI-CNR, Italy
- **Corizzo, Roberto,** American University, USA
- **Cyganek, Bogusław,** AGH University of Science and Technology, Poland
- **Dey, Lipika,** TCS Innovation Lab Delhi, India
- **Durães, Dalila,** Universidade do Minho, Portugal
- **Filipe, Vitor,** UTAD, Portugal
- **Girardi, Rosario,** UFMA, Brasil
- **Goleva, Rossitza,** New Bulgarian University, Bulgaria
- **Hullam, Gabor,** Budapest University of Technology and Economics, Hungary

- **Hussain, Shahid,** Institute of Business Administration, Pakistan
- **Jakovljevic, Niksa,** University of Novi Sad, Faculty of Technical Sciences, Bulgaria
- **Jaromczyk, Jerzy W.,** University of Kentucky, USA
- **Kaczmarek, Katarzyna,** Instytut Badań Systemowych Polskiej Akademii Nauk, Poland
- **Kasprzak, Włodzimierz,** Warsaw University of Technology, Poland
- **Kwaśnicka, Halina,** Wroclaw University of Technology, Poland
- **Laskov, Lasko,** New Bulgarian University, Bulgaria
- **Lerga, Jonatan,** Rijeka Tehnical University, Croatia
- **Lingras, Pawan,** Saint Mary's University, Canada
- **Ljubić, Sandi,** University of Rijeka, Faculty of Engineering, Croatia
- **Matwin, Stan,** Dalhousie Unbiversity, Canada
- **Meneses, Claudio,** Universidad Católica del Norte, Chile
- **Mignone, Paolo,** Università degli studi di Bari, Italy
- **Mihajlov, Martin,** Jozef Stefan Institute, Slovenia
- **Moore, Neil,** University of Kentucky, Department of Computer Science, USA
- **Moshkov, Mikhail,** King Abdullah University of Science and Technology, Saudi Arabia
- **Mozgovoy, Maxim,** University of Aizu, Japan
- **Muñoz, Andrés,** Universidad de Cádiz, Spain
- **Myszkowski, Paweł,** Wroclaw University of Science and Technology, Poland
- **Noguera, Manuel,** University of Granada, Spain
- **Pataricza, András,** Budapest University of Technology and Economics, Hungary
- **Peters, Georg,** Munich University of Applied Sciences & Australian Catholic University, Germany
- **Petrovska, Biserka,** Goce Delcev University, North Macedonia
- **Pires, Ivan Miguel,** Instituto de Telecomunicações, Universidade da Beira Interior, and Universidade de Trás-os-Montes e Alto Douro, Portugal
- **Po, Laura,** Universitá di Modena e Reggio Emilia, Italy
- **Porta, Marco,** University of Pavia, Italy
- **Przybyła-Kasperek, Małgorzata,** Uniwersytet Śląski, Poland
- **Raghavan, Vijay,** University of Louisiana at Lafayette, USA
- **Ramanna, Sheela,** Department of Applied Computer Science, University of Winnipeg, Canada
- **Rauch, Jan,** University of Economics, Prague, Czech Republic
- **Schaefer, Gerald,** Loughborough University, United Kingdom
- **Sosnowski, Łukasz,** Systems Research Institute, Polish Academy of Sciences, Poland
- **Spinsante, Susanna,** Università Politecnica delle Marche, Italy
- **Stańczyk, Urszula,** Silesian University of Technology, Poland
- **Stoean, Catalin,** University of Craiova, Romania
- **Stojanov, Riste,** Faculty of Computer Science and Engineering, Skopje
- **Subbotin, Sergey,** Professor, Zaporozhye National Technical University, Ukraine
- **Szczuka, Marcin,** University of Warsaw, Poland
- **Szczęch, Izabela,** Poznan University of Technology, Poland
- **Trajkovik, Vladimir,** Ss. Cyril and Methodius University, Faculty of Computer Science and Engineering, North Macedonia
- **Turukalo, Tatjana Loncar,** FTN, University of Novi Sad, Bulgaria
- **Unland, Rainer,** University of Duisburg-Essen, ICB, Germany
- **Verstraete, Jörg,** Instytut Badań Systemowych Polskiej Akademii Nauk, Poland
- **Weber, Richard,** Universidad de Chile
- **Zakrzewska, Danuta,** Institute of Information Technology, Technical University of Lodz, Poland
- **Zdravevski, Eftim,** Ss. Cyril and Methodius University, North Macedonia
- **Zielosko, Beata,** Univeristy of Silesia, Institute of Computer Science, Poland
- **Świechowski, Maciej,** QED Software, Poland
- **Żurek, Dominik,** AGH, Poland

Communication Papers of the of the 17th Conference on Computer Science and Intelligence Systems pp. 3–9
DOI: 10.15439/2022F56
ISSN 2300-5963 ACSIS, Vol. 32

Treating Dataset Imbalance in Fetal Echocardiography Classification

Guilherme Ferreira Gusmão
Dept. of Informatics, PUC-Rio, Rio de Janeiro, Brazil
Email: gusmaof@tecgraf.puc-rio.br

Renato Cherullo de Oliveira
Tecgraf Institute, PUC-Rio, Rio de Janeiro, Brazil
Email: cherullo@tecgraf.puc-rio.br

Carlos Roberto Hall Barbosa
Postgraduate Programme in Metrology, PUC-Rio, Rio de Janeiro, Brazil
Email: hall@puc-rio.br

Alberto Barbosa Raposo
Dept. of Informatics, PUC-Rio, Rio de Janeiro, Brazil
Email: abraposo@inf.puc-rio.br

Abstract— **Deep learning has been a trending topic during the last few years, notably in medical imaging that employs neural networks for image manipulation, computer-aided detection of diseases, and many other tasks depending on the clinical practices. One possible application that would benefit from these methods is the fetal cardiac view classification, where these different views are useful to obtain valuable information about the patient's heart development. A trained network could help reduce variance in interpretation and speed up data annotation. Alas, in this context we can face two challenges: datasets may contain a lot of information not relevant to the outcome of the classifier's training, and the view classes may be unbalanced in the sense that certain classes may have much more samples than others. This paper presents a series of attempts to solve these issues and can be used as a practical guide for training viable classifiers in this context.**

Index Terms—fetal echocardiography, cardiovascular imaging, image processing, machine learning, data augmentation.

I. Introduction

DEEP learning has found a lot of traction in recent years, especially focusing on automating big data analysis. With the rise of new technologies, like more powerful GPU allowing faster parallel processing of data, many new applications can be explored [1]. One field that is taking advantage of these developments is Medical Imaging. It uses deep neural networks for image reconstruction, enhancement, segmentation, computer-aided detection of diseases, and many other tasks depending on the clinical practices, such as chest, neuro, cardiovascular, abdominal, and microscopy imaging. In this paper, we will be focusing on echocardiography tasks [2-4].

Echocardiography is the mainstay of cardiovascular imaging, as it is a fast method for image acquisition that avoids the use of radiation. The method produces grayscale videos containing sufficient information to diagnose alterations in the development of the patient's heart even in the gestational period [2]. The interpretation of the resulting images is typically made manually by a cardiologist, and it could take a lot of time and effort. To improve this method, many researchers are focusing on transforming this process into a partially automated pipeline for interpreting cardiovascular imaging using deep neural networks.

One difficult task that would benefit from deep learning methods is the fetal cardiac view classification. These views are standardized imaging planes defined in the medical literature, which cardiologists use to obtain valuable information about the development of the different valves and chambers of the heart. A trained network could help reduce variance in interpretation and speed up data annotation [5-8]. Another noteworthy use would be to find a specific heart view among the frames of a fetal echocardiography video. This is very important for the detection of congenital heart diseases that are still being missed during diagnostics [9-10]. This analysis may be made by the cardiologist through the appraisal of the four standard heart views:

- Four-chamber (4CH) view that contains aorta descendens, left atrium, left ventricle, right atrium, and right ventricle;
- Left Ventricular Outflow Tract (LVOT) view that contains aorta ascendens, left atrium, left ventricle, right atrium, and right ventricle;
- Right Ventricular Outflow Tract (RVOT) view that contains ductus arteriosus, superior vena cava, aorta ascendens, and main pulmonary artery; and
- Three Vessels View (3VV) that contains ductus arteriosus, superior vena cava, aorta ascendens. The 3VV can have a few variations, for example, in our dataset we also have the Three Vessels and Trachea (3VT) view.

Funding: This study was financed in part by the Coordenação de Aperfeiçoamento de Pessoal de Nível Superior—Brasil (CAPES)—Finance Code 001.

Acknowledgments: The authors thank for the financial support provided by the Brazilian funding agencies CNPq, CAPES, FINEP, and FAPERJ.

These five heart views are exemplified in Fig. 1.

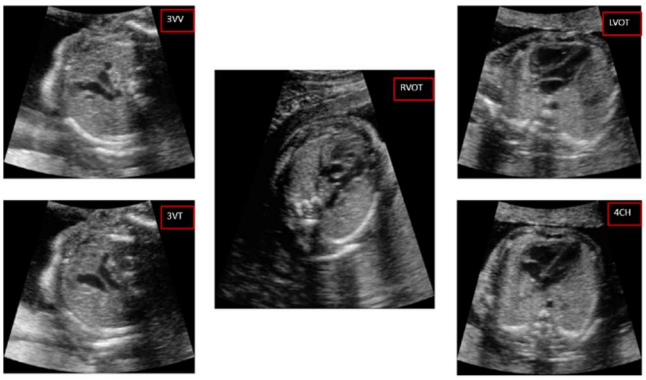

Fig. 1. The four standard fetal heart views: 3VV (+ 3VT), RVOT, LVOT and 4CH.

However, in this context we face two challenges: first, echocardiography datasets contain a lot of information that may or may not influence the outcome of the classifier's training, and there is not a default annotation format to follow. The second is that fetal echocardiography datasets typically have a large imbalance, in the sense that certain classes contain many more samples than others, as is the case of the 4CH view in relation to the other more complex views, as it is the starting point and most important view in fetal echocardiography [5-8]. Meanwhile, other views may be used only when investigating rare, specific conditions.

Unbalanced datasets are a very common issue in deep learning, not only in medical imaging, and many researchers tried to reduce its impact during training [11-14].

In [11], the authors developed a self-contained deep architecture with the synthetic minority oversampling technique (SMOTE) for artificial instance generation that doesn't need a discriminator during the synthetic image generation process, instead depending only upon a penalty function for improving the generator.

The authors of [12] proposed a generative adversarial network (GAN) with a three-player adversarial game: a generator that produces synthetic images of the minority classes to fool both the discriminator of real/fake images and a multi-class classifier. This min-max game, in time, will adjust all players for better outputs, reducing misclassifications of the underrepresented classes.

In [13], a training technique called ReMix leverages batch resampling, instance mixing and soft-labels to induct robust deep models from imbalanced and long-tailed datasets.

The RetinaNet [14] tries to solve the problem of extreme foreground-background class imbalance encountered during training of dense detectors by reshaping the standard cross entropy loss to downplay the more prevalent classes.

While most of the other works focus on the models' architectures and loss function, in this paper we tackle these imbalance challenges for training viable classifiers with a more data-centric approach, as our primary effort being on parsing, pruning, and organizing the fetal echocardiography dataset, while using readily available convolutional neural networks.

This manuscript is structured as follows: Section II presents the dataset characteristics and a brief mention of the model used in our experiments; the methods for balancing the dataset and their impact upon training are shown in Section III; conclusions of the manuscript, including recommendations for future works, are described in Section IV.

II. Dataset and Model

Deep learning applications have four fundamental cornerstones: the layers that build the network; the dataset, with the training and ground truth data; the loss function, which defines how well modeled the network is; and the optimizer, which reduces overall loss by helping better define the model weights [15].

The literature shows that we have reached a high level of maturity in the development of effective neural networks, optimizers, and loss functions, allowing for easy implementation and fine-tuning of the model hyperparameters. However, it is important to do more dataset-driven explorations [15].

Usually, the *modus operandi* for neural networks is to train them with the largest number of samples possible, but, sometimes, we have only a small collection of relevant data to work with [15]. This is especially true in medical imaging when analyzing rare occurrences or rarely performed exams. It is still possible to successfully train a network with relatively little data if all samples are representative and correctly annotated.

The dataset used for training our neural network model comes from private data supplied by another project in development at the Tecgraf Institute. It originally contained a set of Excel tables and DICOM files (Digital Imaging and Communications in Medicine) but it has been already pre-processed into a single, consolidated Excel file describing the results of each exam and referencing a set of gray-scale PNG (Portable Network Graphics) files, each containing a single frame of an exam. Although it is possible to figure out if two images belong to the same exam or even if they belong to the same patient, it is worth noting that all data is anonymized.

These exams were acquired using different machines and were annotated by different doctors. Each row contains a bit of information about either a point, a line, a region of a frame, a whole frame, a range of frames, or all the frames in an exam video. This means that there can be many rows related to a single exam frame, and some exam frames may not have any kind of annotation associated with them at all.

To evaluate the dataset's class balance, we selected all the frames annotated with view type information, and belonging to the classes 3VT, 3VV, 4CH, LVOT, and RVOT, producing the histogram presented in Fig. 2.

Right off the bat, we can see how unbalanced the dataset is: there are around forty-five times more frames in the most represented class than in the least represented class. We will tackle this imbalance in the following sections.

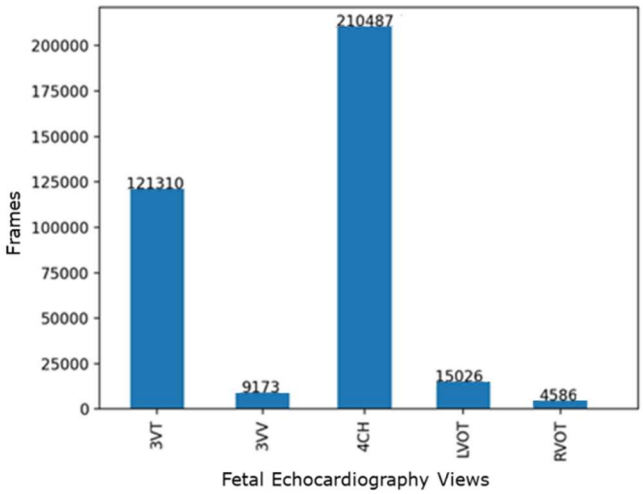

Fig. 2 Histogram with classes distribution throughout the dataset.

Inspecting the pixel value range in each image, that is, the value of the brightest pixel minus the value of the darkest pixel in each image, we produced the histogram in Fig. 3 that shows the images' pixel value range, considering that the value 1.0 corresponds to white and that the value 0.0 corresponds to black.

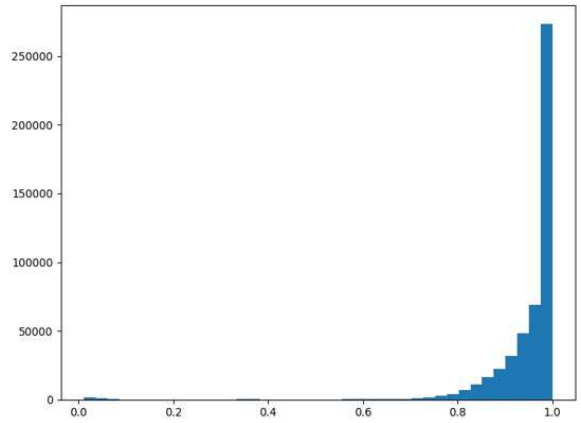

Fig. 3 Histogram of the pixel value range in each image.

Although it's not perfect, most of the images have a pixel value range above 0.8, so simply adjusting for range should not have much impact on the classifier's performance.

For our classifier model, we chose the EfficientNets [16] family of models. It is a convolutional neural network (CNN) and scaling method that uniformly scales all dimensions of depth/width/resolution using a compound coefficient, a user defined parameter that manages the resources availability, optimizing the network. We choose this architecture due to a few reasons: its baseline model has good performance and low resource requirements; it can be easily scaled up if needed; it's flexible since it can run on Tensorflow 1.15, and it was known to work to classify fetal echocardiograms since it was formerly used in a previous project at the Tecgraf Institute.

Finally, we can start rebalancing our dataset to better fit our training, as described in the next section.

III. Balancing the Data: Preprocessing and Augmentation

As seen in Fig.2, the dataset is very unbalanced. Therefore, to counteract this, many methods found throughout the literature were tested. Since the goal of this paper is to present guidelines, we decided to present our findings in a streamlined manner: instead of showing the results of each dataset preprocessing or augmentation technique individually and additively, we packed those techniques in thematic, coherent sets.

We created a baseline test using the first 8 % of the dataset for training and used the last 2 % for validation, preserving the class imbalances and without using any enhancement. We used a fraction of our data to reduce the time taken during training, so we could quickly iterate towards a working solution. It also prevents data leakage, when samples in the training set are equal or extremely similar to samples in the validation set, since the dataset was sorted by patient.

The class distributions in both sets are shown in Fig. 4.

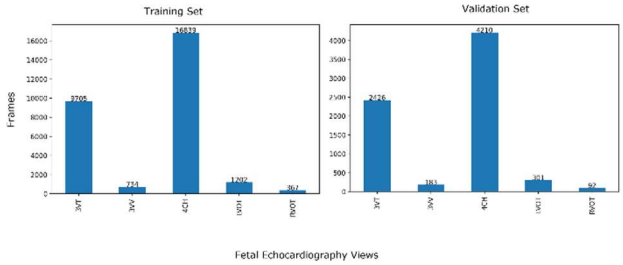

Fig. 4 Class distribution in the training and validation sets. Both keep the imbalance of classes in the dataset.

We used for training the EfficientNet B0 model with Adam as the optimizer with learning rate 0.001 (well known for its great performance in image classification problems). We reduced the learning rate on plateau monitoring the validation loss, with patience as 7, factor as 0.5 and minimum learning rate as 10^{-9}. All these values were found through empirical experiments that provided the best results for training the model. Categorical cross-entropy was chosen, as our output has five possible outcomes. EfficientNet allows you to start training with pre-trained weights from ImageNet, but we opted for training without it. Beyond that, the EfficientNet family employs a softmax activation function, so the dataset labels were codified by one-hot encoding [16].

Looking at the baseline learning history, in Fig. 5, we can see that the network quickly overfits the training set with no further improvements to the validation set loss. Whereas the confusion matrix over the validation set, in Fig. 6, shows that most of the achieved accuracy was due to the 3VT and 4CH classes (the most represented ones). The LVOT class got a F1-score of 0.11 and the network didn't predict a single image in the RVOT and 3VV classes. The weighted average F1-score was 0.54, as seen in Table I.

Things look dire for our dataset with these results, but the following subsections will bring techniques that will better improve the data quality.

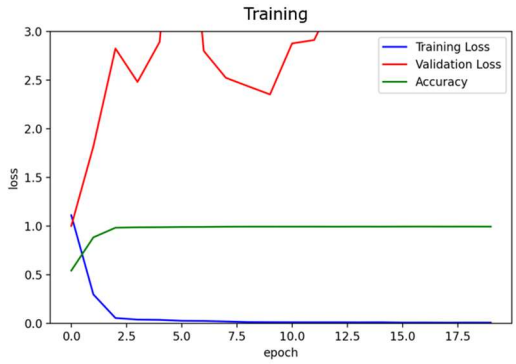

Fig. 5 Learning history with accuracy, training loss, and validation loss.

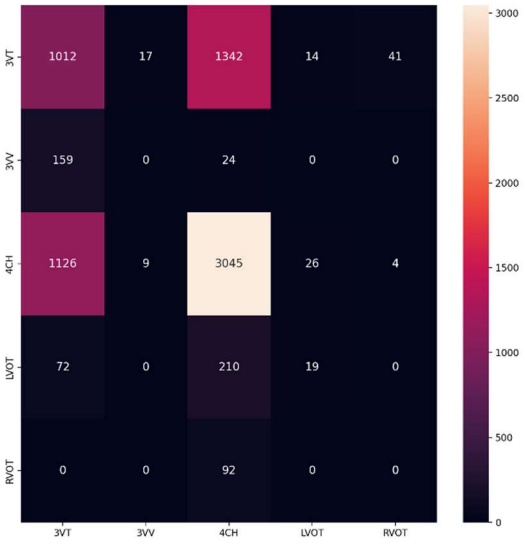

Fig. 6 Baseline Model's Confusion Matrix.

A. Preprocessing Selection

Stride

Echocardiogram exams are video data, but we opted, as suggested in other papers [5-6], to develop our classifier with still images sampled from the video. Consequently, in earlier experiments, we sampled all the images from each successive exam in a class, up to the desired frame count for that class. But, since consecutive video frames change very little from one another, the network was being fed with many similar frames, reducing the learning potential. So, instead of sampling frames contiguously in an exam, we tried sampling frames with a stride. In our case, one frame was selected every 5 frames. This brought an increase in data diversity, as a greater volume of exams from a variety of patients were sampled.

Shuffle

First and foremost, never forget: always shuffle your data after every epoch! This will help escape bad batches and minimize variance, increasing the generalization of the model for unseen data. Disregarding this truth can hinder the advances in your research [15].

So, after striding, we shuffled the entire dataset before selecting 8 % of samples for training and 2 % for validation, avoiding shared frames between the sets and once again preserving the class distributions.

This step greatly increased the diversity of the samples in each class again, by using frames from more exams and avoiding any bias that could be present at the beginning or the tail-end of the original dataset.

Stratified Batch

Another interesting technique used in unbalanced scenarios is to do what is called stratified batching [17]. It consists in, instead of feeding all images of the training set to the network every epoch, randomly choosing a fixed number of images of each class, so that at the end of each epoch, the network will have been trained with the same number of images from each class. This prevents bias toward predominant views, as it reduces the number of samples from the same patient to be used. These batches must have their size limited by the total amount of samples of the least prevalent class. In our case, we used batches of size 300.

New training was implemented with these three methods to better understand their impact on the model performance. In Fig. 7 and Fig. 8, the learning history and confusion matrix can be investigated.

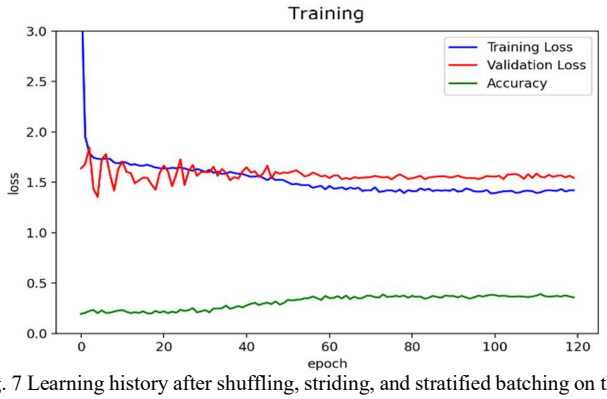

Fig. 7 Learning history after shuffling, striding, and stratified batching on the dataset.

TABLE I.
BASELINE TEST REPORT

Class	Precision	Recall	F1-score	Number of Samples
3VT	0.43	0.42	0.42	2426
3VV	0.00	0.00	0.00	183
4CH	0.65	0.72	0.68	4210
LVOT	0.32	0.06	0.11	301
RVOT	0.00	0.00	0.00	92
Weighted Acc	0.53	0.57	0.54	7212

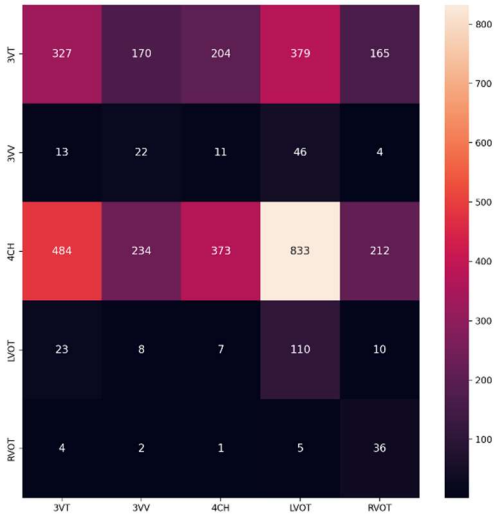

Fig. 8 Confusion Matrix after shuffling, striding, and stratified batching on the dataset.

Although the results are still bad, as the accuracy and loss don't even converge and the weighted average F1-score lowers to 0.27 in Table II, we can observe a reduction in bias towards most represented classes, as it can identify all the classes now and confounds itself more between them.

B. Augmentation

For the next improvement to the dataset, we can generate more instances of the less prevalent classes, so the model can see them more times during training. This is easily achieved with image augmentation techniques. Before going forth with our findings, we give a warning: any change to medical images should be evaluated by a professional in the area, as altering them too forcefully could result in unrealistic data being fed to the model and confounding the view classes features. We consulted a cardiologist that validated our proposed augmentation methods and other image manipulation techniques applied in our research. Not all of them will be presented here. For this paper, we chose only two: rotation and brightness.

Different from other works where augmentation is applied to all images of the training set, we use augmentation to increase the number of samples in the underrepresented classes 3VV, LVOT, and RVOT, as further explained below.

Rotation

As the name suggests, we transformed our images by rotating samples of the underrepresented classes. This was accomplished by using the scikit-image library [18], which is an open-source image processing library for the Python programming language that includes segmentation, geometric transformations, and many others.

We applied the rotate function, turning the images by a random angle in the range from -20° to +20°for each epoch. Rotating an exam image makes sense during training because the orientation of the heart is not standardized in the views, and what matters is the section plane.

Brightness

We decided to implement multiplicative brightness change in part due to its simplicity [18]. This process is defined by the following brightness and contrast adjustment equation:

$$T(i,j) = \alpha . I(i,j) + \beta \quad (1)$$

where i, j are pixels coordinates, I is the input image, T is the transformed image, α represents gain, and β represents bias. The change in brightness can easily be done by just multiplying each pixel by a set value close to 1 and then clipping it into the range [0, 1].

Small changes to the exam's brightness help the network identify features affected by shadows and generalize equipment differences and/or tissue density differences.

Another round of training was executed with all proposed methods. As mentioned before, the rotation and brightness augmentation were only applied to the less favored classes, effectively creating new samples. In Fig. 9, we can see the increase of those samples on the training set. This increase allows us to choose larger batch sizes for the stratified batching. Using all these techniques helped reduce the difference between the most prevalent class (4CH) and the less prevalent class (RVOT) from 45 to around 11 times more frames than the other.

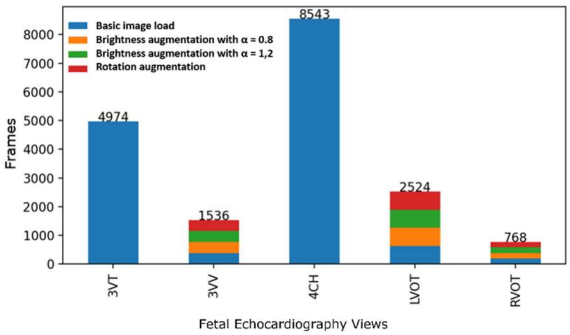

Fig. 9 Training set after preprocessing and augmentation methods. Blue are samples loaded normally, Orange are samples loaded with brightness augmentation with alpha = 0.8, Green are samples loaded with brightness augmentation with alpha = 1.2, and Red are samples loaded with rotation augmentation.

TABLE II.
SHUFFLE, STRIDE AND STRATIFIED BATCHING TEST REPORT

Class	Precision	Recall	F1-score	Number of Samples
3VT	0.38	0.26	0.31	1245
3VV	0.05	0.23	0.08	96
4CH	0.63	0.23	0.27	2136
LVOT	0.08	0.70	0.14	158
RVOT	0.08	0.75	0.15	48
Weighted Acc	0.50	0.24	0.27	3683

In Fig. 10 and Fig. 11, the learning history and confusion matrix can be further examined.

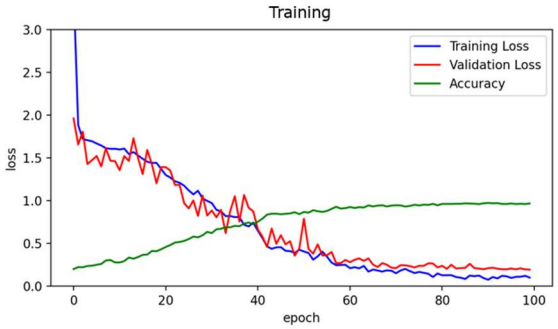

Fig. 10 Learning History after adding rotation and brightness augmentation

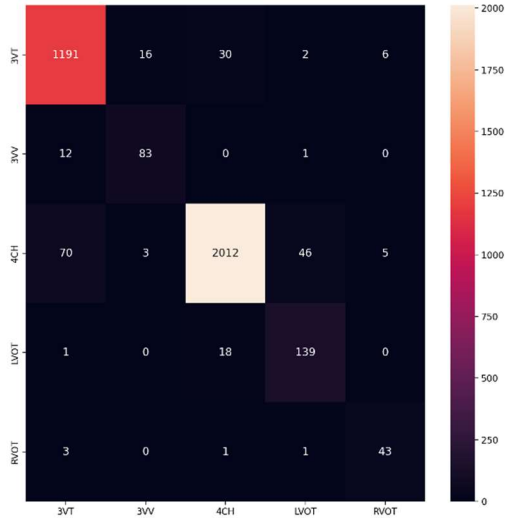

Fig. 11 Confusion Matrix after rotation and brightness augmentation

Finally, we can see accuracy and loss converging and a great leap in the model performance as seen in Table III. All the less prevalent classes have been learned by the model and the main view (4CH) has also increased to an astonishing F1-score of 0.94.

IV. Conclusions

Recapping, we have proposed in this paper that enhancing the quality of a small and unbalanced dataset by use of preprocessing and augmentation methods could reduce class imbalance and improve the model performance. Through many experiments and setbacks, we were able to analyze the impact of these methods on the dataset, observing the model go from a very poor classification to a remarkable F1-Score of 0.94 with a confusion matrix with few false positives and false negatives.

We can conclude that, if we take the time to understand better the data being used and apply the right methods for improvement of the dataset, like reducing redundancy, increasing diversity, and augmenting the images, it is possible to bring balance to a small, unbalanced dataset. Also, using a proven, efficient model is not enough to obtain good performance if your dataset is bad or too raw for use.

Exploration of the quality of the dataset has a lot of potentials, especially in medical imaging. Some promising subjects that we are already discussing and researching for future work are using transfer learning in known models trained with computer vision datasets, for feature extraction and fine-tuning of our model [19].

Another possibility is to explore a weighted loss function in conjunction with the methods present here, as this loss would punish the network more accordingly weight defined for each class [20]. We already have some crude implementations of this technique but was not used in this paper.

Also, many professionals in the medical field feel uneasy with the neural networks' black box nature and would give more credit for these solutions if they could understand how they have taken decisions. Explainable Artificial Intelligence (XAI) aims to solve these issues by bringing more transparency to the understanding of the model's bias, decisions impact and, as a result, generating better metrics [21].

References

[1] Luis Perez and Jason Wang. The Effectiveness of Data Augmentation in Image Classification using Deep Learning. *arXiv:1712.04621 [cs]*, December 2017. arXiv: 1712.04621.

[2] S. Kevin Zhou, Hayit Greenspan, Christos Davatzikos, James S. Duncan, Bram Van Ginneken, Anant Madabhushi, Jerry L. Prince, Daniel Rueckert, and Ronald M. Summers. A Review of Deep Learning in Medical Imaging: Imaging Traits, Technology Trends, Case Studies With Progress Highlights, and Future Promises. *Proceedings of the IEEE*, 109(5):820– 838, May 2021, doi:10.1109/JPROC.2021.3054390.

[3] Andre Esteva, Katherine Chou, Serena Yeung, Nikhil Naik, Ali Madani, Ali Mottaghi, Yun Liu, Eric Topol, Jeff Dean, and Richard Socher. Deep learning-enabled medical computer vision. *npj Digital Medicine*, 4(1):5, December 2021, doi:10.1038/s41746-020-00376-2.

[4] Swati Rai, Jignesh S. Bhatt, and S. K. Patra. Augmented Noise Learning Framework for Enhancing Medical Image Denoising. *IEEE Access*, 9:117153–117168, 2021,doi:10.1109/ACCESS.2021.3106707.

Table III.
Rotation and Brightness Augmentation added Test Report

Class	Precision	Recall	F1-score	Number of Samples
3VT	0.93	0.96	0.94	1245
3VV	0.81	0.86	0.84	96
4CH	0.98	0.94	0.96	2136
LVOT	0.74	0.88	0.80	158
RVOT	0.80	0.90	0.84	48
Weighted Acc	0.94	0.94	0.94	3683

[5] Jing Wang, Xiaofeng Liu, Fangyun Wang, Lin Zheng, Fengqiao Gao, Hanwen Zhang, Xin Zhang, Wanqing Xie, and Binbin Wang. Automated interpretation of congenital heart disease from multi-view echocardiograms. *Medical Image Analysis*, 69:101942, April 2021, doi:10.1016/j.media.2020.101942.

[6] Amirata Ghorbani, David Ouyang, Abubakar Abid, Bryan He, Jonathan H. Chen, Robert A. Harrington, David H. Liang, Euan A. Ashley, and James Y. Zou. Deep learning interpretation of echocardiograms. *npj Digital Medicine*, 3(1):10, December 2020, doi:10.1038/s41746-019-0216-8.

[7] Day, T.G.; Kainz, B.; Hajnal, J.; Razavi, R.; Simpson, J.M. Artificial Intelligence, Fetal Echocardiography, and Congenital Heart Disease. *Prenatal Diagnosis* 2021, 41, 733–742, doi:10.1002/pd.5892.

[8] Nurmaini, S.; Rachmatullah, M.N.; Sapitri, A.I.; Darmawahyuni, A.; Tutuko, B.; Firdaus, F.; Partan, R.U.; Bernolian, N. Deep Learning-Based Computer-Aided Fetal Echocardiography: Application to Heart Standard View Segmentation for Congenital Heart Defects Detection. *Sensors* 2021, *21*, 8007, doi:10.3390/s21238007.

[9] Fiorentino, M.C.; Villani, F.P.; Di Cosmo, M.; Frontoni, E.; Moccia, S. A Review on Deep-Learning Algorithms for Fetal Ultrasound-Image Analysis. arXiv:2201.12260 [cs, eess] 2022.

[10] Nisselrooij, A.E.L.; Teunissen, A.K.K.; Clur, S.A.; Rozendaal, L.; Pajkrt, E.; Linskens, I.H.; Rammeloo, L.; Lith, J.M.M.; Blom, N.A.; Haak, M.C., "Why are congenital heart defects being missed?", Ultrasound Obstet Gynecol, vol. 55, nº 6, p. 747–757, jun. 2020, doi: 10.1002/uog.20358.

[11] Dablain, D.; Krawczyk, B.; Chawla, N.V. DeepSMOTE: Fusing Deep Learning and SMOTE for Imbalanced Data. *IEEE Transactions on Neural Networks and Learning Systems* 2022, 1–15, doi:10.1109/TNNLS.2021.3136503.

[12] Mullick, S.S.; Datta, S.; Das, S. Generative Adversarial Minority Oversampling. *In Proceedings of the Proceedings of the IEEE/CVF International Conference on Computer Vision (ICCV)*; October 2019.

[13] Bellinger, C.; Corizzo, R.; Japkowicz, N. Calibrated Resampling for Imbalanced and Long-Tails in Deep Learning. *In Proceedings of the Discovery Science*; Soares, C., Torgo, L., Eds.; Springer International Publishing: Cham, 2021; pp. 242–252, doi: 10.1007/978-3-030-88942-5_19.

[14] Lin, T.-Y.; Goyal, P.; Girshick, R.; He, K.; Dollár, P. Focal Loss for Dense Object Detection. *In Proceedings of the 2017 IEEE International Conference on Computer Vision (ICCV)*; 2017; pp. 2999–3007, doi: 10.1109/ICCV.2017.324.

[15] Chollet, Francois. 2017. *Deep Learning with Python*. New York, NY: Manning Publications.

[16] Mingxing Tan and Quoc V. Le. "Efficientnet: Rethinking model scaling for convolutional neural networks", 2020.

[17] Vaseli, H.; Liao, Z.; Abdi, A.H.; Girgis, H.; Behnami, D.; Luong, C.; Taheri Dezaki, F.; Dhungel, N.; Rohling, R.; Gin, K.; et al. "Designing Lightweight Deep Learning Models for Echocardiography View Classification. In Proceedings of the Medical Imaging 2019: Image-Guided Procedures, Robotic Interventions, and Modeling"; Fei, B., Linte, C.A., Eds.; SPIE: San Diego, United States, March 8 2019; p. 14.

[18] Scikit-image library documentation, https://scikit-image.org/docs/stable/

[19] Long Teng, Zhong, Liang Fu, Qian Ma, Yu Yao, Bing Zhang, Kai Zhu, and Ping Li. Interactive Echocardiography Translation Using Few-Shot GAN Transfer Learning. *Computational and Mathematical Methods in Medicine*, 2020:1–9, March 2020.

[20] K. R. M. Fernando and C. P. Tsokos, "Dynamically Weighted Balanced Loss: Class Imbalanced Learning and Confidence Calibration of Deep Neural Networks," *IEEE Transactions on Neural Networks and Learning Systems*, vol. 33, no. 7, pp. 2940–2951, 2022, doi: 10.1109/TNNLS.2020.3047335..

[21] Qiao, S.; Pang, S.; Luo, G.; Pan, S.; Yu, Z.; Chen, T.; Lv, Z. "RLDS: An Explainable Residual Learning Diagnosis System for Fetal Congenital Heart Disease". Future Generation Computer Systems 2022, 128, 205–218, doi:10.1016/j.future.2021.10.001.

Communication Papers of the of the 17th Conference on Computer Science and Intelligence Systems pp. 11–20
DOI: 10.15439/2022F25
ISSN 2300-5963 ACSIS, Vol. 32

Towards Automatic Facility Layout Design Using Reinforcement Learning

Hikaru Ikeda, Hiroyuki Nakagawa, Tatsuhiro Tsuchiya
Graduate School of Information Science and Technology
Osaka University, Japan
{h-ikeda, nakagawa, t-tutiya}@ist.osaka-u.ac.jp

***Abstract*—The accuracy and perfection of layout designing significantly depend on the designer's ability. Quick and near-optimal designs are very difficult to create. In this study, we propose an automatic design mechanism that can more easily design layouts for various unit groups and sites using reinforcement learning. Specifically, we devised a mechanism to deploy units to be able to fill the largest rectangular space in the current site. We aim to successfully deploy given units within a given site by filling a part of the site. We apply the mechanism to the three sets of units in benchmark problems. The performance was evaluated by changing the learning parameters and iteration count. Consequently, it was possible to produce a layout that successfully deployed units within a given one-floor site.**

***Index Terms*—reinforcement learning, machine learning, layout design, facility layout problem**

I. Introduction

THE FACILITY layout problem (FLP) [1], [2] is an optimization problem of deploying equipment and machines in a facility. The solution to this problem depends on the designer's ability. Therefore, various methods and procedures have been proposed to solve the FLP. For example, Genetic Algorithm (GA), Genetic Programming (GP), and deep learning are used. In this study, we propose a layout design support mechanism using reinforcement learning. Reinforcement learning is a machine learning method in which learning is performed without training data. An agent learns through trial and error. It makes it possible to obtain layouts for different conditions from training ones. We make learning agent possible to create a layout in various environment by predetermining the maximum layout area, and generating layouts for the sites that are less than that. The object of this study is to clarify whether reinforcement learning is effective for solving the FLP.

The structure of this paper proceeds as follows. Section 2 explains the layout design, current problems, and reinforcement learning as the background of this study. Section 3 explains the layout design mechanism using reinforcement learning. Section 4 describes the results of the experiments conducted to demonstrate the effectiveness of the proposed mechanism and performance. Section 5 describes the discussion based on the experiments presented in Section 4. Section 6 describes the prospects, such as the problems found and future issues, and Section 7 concludes the paper.

II. Background

A. Layout design

The FLP is a well studied combinatorial optimization problem which arises in a variety of problems such as layout design of the deployment and flow lines of equipment, materials, parts, work-in-process, workers, circuit board design, warehouses, backboard wiring problems [3]. An efficient and rational layout is desirable for the layout design process. The purpose of layout design is to obtain a layout that is close to optimal under the specified conditions.

Facility layout design has been studied for a long time [4]. Many of them use GA [5] and GP [6]. GA is a programming technique which forms its basis from the biological evolution. GA uses the principles of selection and evolution to produce several solutions to a given problem. GP is considered to be a variant of GA, and used to evolve abstractions of knowledge, like mathematical expressions or rule-based systems. Venkatesh and Jim [7] use GA to reduce the sum of the product of the three factors of material handling cost, which are: the volume of material handling (frequency of journeys); the cost of material handling, and the distance travelled. José et al. [8] introduced biased random-key GA for the unequal area facility layout problem where a set of rectangular facilities with given area requirements has to be placed, without overlapping, on a rectangular floor space. The role of GA is to evolve the encoded parameters that represent the facility placement sequence, the vector of facility aspect ratios, and the position of the first facility. Stanislas [9] introduced to apply AI to floor plans analysis and generation. His ultimate goal is threefold: (1) to generate floor plans. (2) to qualify floor plans. (3) to allow users to browse through generated design options. He have chosen nested Generative Adversarial Neural Networks or GANs. Luisa et al. [10] introduced Firefly algorithm (FA), which was designed to solve continuous optimization problems. From the map of the layout that contains the (x, y) coordinates corresponding to the location of each of the nodes or workstations that are distributed on the plant, and paths between nodes are defined, the system solves layout problem as traveling salesman problem (TSP). Jing et al. [11] introduced the ant colony optimization (ACO) algorithm, which is a bio-inspired optimization algorithm based on the behavior of natural ants that succeed in finding the shortest

paths from their nest to food sources by communicating via pheromone trails. Singh et al. [12] introduced a layout generating method using the space-filling curve. The space-filling curve [13] describes plane spaces based on the trajectory of an individual curve. The layout was created by allocating the required area based on the space-filling curve of the site. In these current layout design, the techniques and methods are not standardized.

B. Reinforcement learning

Reinforcement learning [14] is a machine learning method that implement optimal system control through trial and error by the system itself. Machine learning methods are generally classified into five types: supervised learning, unsupervised learning, self-supervised learning, semi-supervised learning, and reinforcement learning. While supervised, unsupervised self-supervised and semi-supervised learning require training data for learning, reinforcement learning obtain the data generated from its own experience. A reinforcement learning program developer creates a high learning efficiency model instead of preparing learning data. An agent in reinforcement learning learns the behavior to maximize the score set for the objective in an environment.

Reinforcement learning uses the following concepts.

- *agent*: subject of learning.
- *environment*: virtual space in which the agent acts.
- *state*: situation which the agent is located.
- *action*: what the agent does in a state.
- *reward*: value obtained by an action of the agent.
- *return*: sum of rewards that can be earned in the future.
- *policy*: guidelines for choosing actions.
- *episode*: the entire sequence of learning.
- *trial*: a learning step of an episode.
- *action-value function*: a function that represents the value of actions in the current state.

In reinforcement learning, *rewards* and *returns* are similar but different concepts. Reward is the invariant value given as a score for an action that causes a transition to the next state. Return, on the other hand, is the expected total value of the reward that will be finally obtained. In reinforcement learning, an agent is created that does not simply select an action with a large immediate reward but evolves to choose the action toward the one with the highest return. Fig. 1 shows a flow of reinforcement learning. The agent acts according to the *policy* in the environment. This *action* causes a transition from the current state to the next state. The *reward* is obtained based on the results of the action. The learning proceeds by updating the *action-value function* [15]and changing the state based on this reward. *Returns* is calculated by *rewards* and *action-value function* is calculated by *returns*. The agent continues the *trial* several times and creates an *episode*. The series of actions follow the Markov decision process [16]. The Markov decision process has the characteristic that the probability distribution of the future state depends only on the current state and not on all past states. This is called the Markov property.

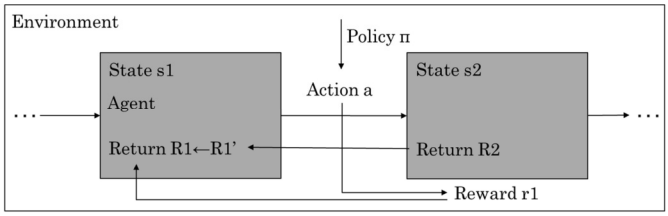

Fig. 1. Flow of reinforcement learning.

There are three main learning methods for reinforcement learning: dynamic programming (DP) method [17], Monte Carlo (MC) method [18], and time difference (TD) method [19]. The DP method is a method of obtaining optimal behavior by solving the Bellman equation when each parameter of the system is known. The MC method was used to obtain the optimal behavior from the real reward obtained by repeating the trial. The TD method combines DP and MC methods to obtain the optimal behavior by solving the Bellman equation [20], [21] from the obtained reward. Currently, many learning methods have been developed based on these three methods. For example, DQN [22], SARSA [23], SAC [24] and Policy Gradients [25]. In particular, DQN using the TD method is currently a major part of reinforcement learning [14].

The Bellman equation is expressed as below:

$$V(S_t) = r(S_{t+1}) + \gamma V(s_{t+1}) \tag{1}$$

- S_t: t-th states.
- $V(S_t)$: return in S_t,
- $r(S_{t+1})$: reward obtained when transitioning to state S_{t+1}
- γ: discount factor

The return is expressed by the obtained reward in the current state and the return in the future state. This means the sum of the discounted rewards from all future states until the end of the trial. The discount factor γ is used to express the influence on the return and is set from 0 to 1. The closer the value is to 0, the less is the influence on the past states.

This Bellman equation is the basis of many reinforcement learning methods, and the above mentioned three methods can also be expressed using this equation.

Several studies have been conducted on reinforcement learning and space control, including layout problems. Xinhan et al. [26] introduced a method of searching for an appropriate arrangement while moving furniture in a room using a deep Q-Network (DQN) [27]. While this method can be arranged so as not to interfere with the function of the room, it can be arranged according to any policy. However it can only learn one piece of furniture at a time, which means that it is not possible to assume the arrangement of multiple units. Matthias et al. [28] study the layout for four functional units next to the logistic lane where the material is transported by vehicles using reinforcement learning. Their layout is generated to

be optimized regarding a single planning objective, i.e., the transportation time. Richa et al [29] introduced reinforcement learning framework for selecting and sequencing containers to load onto ships in ports. The goal is to minimize the number of crane movements required to load a given ship. We can regard the problem as an assignment problem in which the order of assignments is important and therefore the reward is dependent of the order. Azalia et al [31] introduced a new graph placement method based on reinforcement learning, and demonstrate state-of-the-art results on chip floorplanning. They show that their method can generate chip floorplans that are comparable or superior to human experts in under six hours, whereas humans take months to produce acceptable floorplans for modern accelerators. Ruizhen et al. [30] introduced the transport-and-pack (TAP) problem, a frequently encountered instance of real-world packing. They developed a neural optimization solution based on reinforcement learning. Given an initial spatial configuration of boxes, they seek an efficient method to iteratively transport and pack the boxes compactly into a target container. Xinhan et al. [32] explore the interior graphics scenes design task as a Markov decision process, which is solved by deep reinforcement learning. Their goal is to generate an accurate layout for the furniture in the indoor graphics scenes simulation. Peter et al. [33] described the recent surge of research interest in Artificial Intelligence. They regard machine learning techniques including reinforcement learning as the most promising approach to facility layout research. López et al. [34] developed a virtual reality application that creates a production line for electric drills in a virtual space using deep reinforcement learning. Their PCG method can reduce the resources required for development and can personalize the 3-Dimentional virtual environments. Amine et al. [35] developed a Mixed Integer Programming (MIP) robust model for a form of Multi-floor layout problem. In the experiment, they created facility layouts reflecting the relationship between the cellar containing main storages and upper floors in which departments will be located in predetermined locations.

III. The Proposed Mechanism

We propose a layout-deployment mechanism using a reinforcement learning technique to deploy given units within a given site as a solution for FLP. An agent in our mechanism arranges the units on a flat site and proposes an efficient layout. This section explains the specific environment settings and algorithms of the proposed mechanism.

A. The mechanism specifications

Our mechanism assumes the following constraints.

1) Each functional space of the facility is modeled as a unit.
2) All of the units are represented as rectangles. In this study, a three-dimensional structure is not considered, that is, only one-floor layouts are considered.
3) The condition of the site is managed as shown in Fig. 2. Let the upper left block be (0, 0) and associate the two-dimensional array with the block whose right and bottom directions are positive.
4) If the width and the depth of a unit are different, we should consider a 90-degree-rotated deployment.

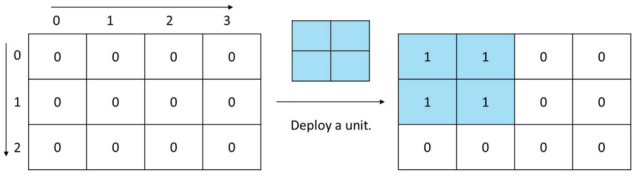

Fig. 2. Unit deployment.

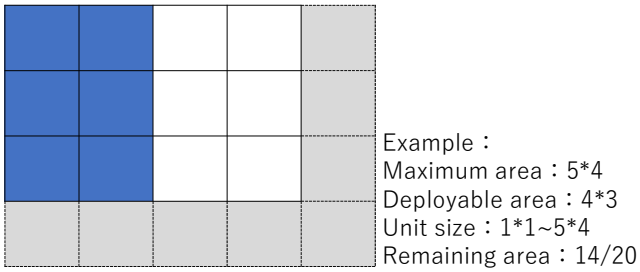

Fig. 3. An example site setting.

B. Layout design mechanism

Site setting

As shown in Fig. 2, the top-left block of the site is the origin, the rightward direction is the x-axis plus direction, and the downward direction is the y-axis plus direction. The site is managed as a two-dimensional array of integers, which is assigned as zero when a unit is not deployed on it. When the agent deployed a unit, the array value of the corresponding location was updated to the number of units deployed. In the layout method, the agent can only create a layout that matches the site size initially set. In this mechanism, we set the maximum depth and width of the site, separately from the depth and width of the site used for layout. Since the states are determined based on remaining area in the maximum site, the agent can use the learning results for sites of other sizes. In Fig. 3, the entire grid is the maximum extent of the site, and the maximum area minus the gray area is the area used for the layout.

Deployment mechanism

Unlike Go or Shogi, it is difficult to determine the placement of units on a site because there are various sizes of units. To solve this problem, a starting point was introduced. The starting point is set according to the current conditions of the site, and the units are deployed based on the starting point. The agent searches the site and defines the next starting point as the point that forms the largest rectangle with no units

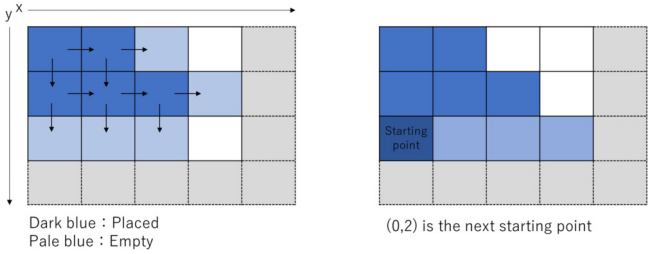

Fig. 4. Movement of the start point.

located. Fig. 4 shows an example of the starting point change. The first starting point was set to the origin. The dark blue area is already deployed, and the pale blue area is empty. In Fig. 4 the block at (0,2) is chosen as the next starting point.

Learning process

The problem to be dealt with in this study is the successful deployment of units within a given site. It may be difficult to completely evaluate the quality of unit deployment deployed in the middle of the trial. Therefore, the MC method, which allows learning to proceed by trying to achieve the end state and then evaluating each arrangement, is used in this study. The MC method requires longer time for learning but can generate a reliable solution. From the same reason, the MC method was also used in Mahjong [36], Chess [37], Shogi [38], and Go [39]. Since these game agents must evaluate solutions in tree structures, they use MC trees [40]. In our study, a table of *action-value-function* (Fig. 5) is created first. This function is called the action-value table and managed as a two-dimensional array, as shown in Fig. 5. One index of the array is state which is represented by the size and the maximum rectangular in the remaining area. Another index is action which is represented by the size of the unit that fits the site. All the values in the table were initialized to zero. The value in action-value-function is expressed as the average of the return in the state obtained in each trial.

One trial involved creating a layout for a set of units. The unit sets are randomly generated with the same number as the size of the site. The ϵ-greedy method [41], [42] was used to select the unit. The agent selects a random unit with a probability of ϵ (Exploration) and selects a unit with the highest action-value with a probability of 1 - ϵ (Exploitation). The ϵ-greedy method can choose unlearned actions in exploration that will never choose in exploitation. This method is commonly used with reinforcement learning. When selecting a unit, the agents consider whether units with different vertical and horizontal lengths can be arranged as units with interchanged lengths.

Fig. 6 shows the calculation of return. When the mechanism finds that none of the units can be deployed, the mechanism finishes the current trial and regards the number of blocks located by units as the reward value of the trial (Reward N in Fig. 6). The score of the final state N is 0 (Score N in Fig. 6). Return was calculated using these values and the Bellman equation. The values of Score N-1 in Fig. 6 (return at state N)

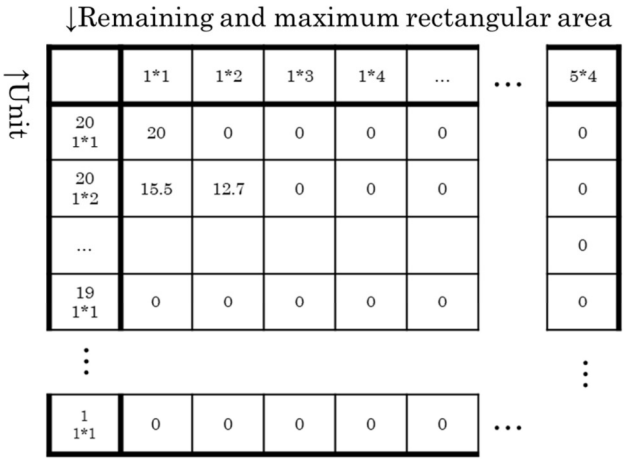

Fig. 5. Action-value table.

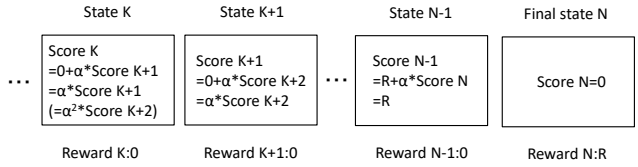

Fig. 6. Calculation of learning value.

were calculated as the sum of the reward N and the product of the score N and discount factor γ. The values of Score K in Fig. 6 (return at state K) are calculated as the sum of the reward K+1 and the product of the score K+1 and the discount factor γ. Returns are updated by returning to the first state in the trial. According to the above process, the return value of a trial is calculated using the following formula:

$$\begin{aligned} Score_k &= R_{k+1} + \gamma * Score_{k+1} \\ &= \gamma^{N-k-1} * R_N \end{aligned} \tag{2}$$

- N: Number of deployed units until final state.
- Score$_k$: the return in k-th state.
- R$_N$: the reward in k-th state.
- γ: discount factor.

Each value in the action-value table (Fig. 5) is calculated by the average of each return. The agent updates the action-value table for each trial and adjust the unit selection criteria.

learning mechanism

Fig. 7 shows the flow of one trial in an episode. First, the agent generates a set of units. Second, the agent selects a unit using ϵ-greedy method. Third, the agent deploys the unit based on the present starting point. Finally, the agent changes the staring point according to the site situation. The agent continues this procedure for as many units and calculates each value in the action-value table.

The agent learns the procedure to select the best from the set of units for the current site by repeating the trial.

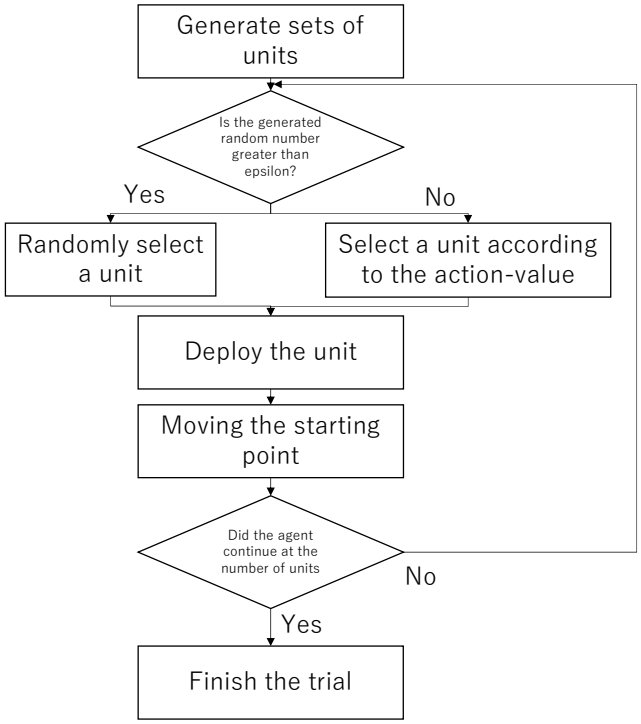

Fig. 7. Flow of one trial in our mechanism.

IV. EXPERIMENT

This section represents the contents and results of the experiment. Two experiments were conducted to demonstrate the effectiveness and efficiency of the proposed mechanism. First, the proposed mechanism was applied to the three sets of units in the benchmark problems [12] to affirm whether the proposed mechanism can appropriately obtain a layout that satisfies these conditions. A one-floor plan is considered. Thereafter, we measure whether the learning will become faster by executing learning multiple times for each set of units to affirm the possibility to deep learning for the combinations of existing units. Learning was conducted according to the learning process described in Section III-B. The variables ϵ used in the ϵ-greedy method and the variables γ used in the learning value calculation are $\epsilon = 0.9$ and $\gamma = 0.9$, respectively.

A. Experiment 1 : Effectiveness of the proposed mechanism

In this experiment, the proposed mechanism was applied to the benchmark problems to demonstrate the effectiveness. The site has 7 x 5 blocks, with a total size of 35 blocks. Learning was performed for 50,000,000-unit sets, and each unit set randomly generated the same number of units as the site and the size that fits in the site for each trial. The study [12], which describes the benchmark problems, illustrates layouts that deploy units using a space-filling curve (Fig. 8). Because the proposed mechanism handles rectangular units, the L-shaped units that appear in the layout of the benchmark problem are handled by dividing them as appropriate.

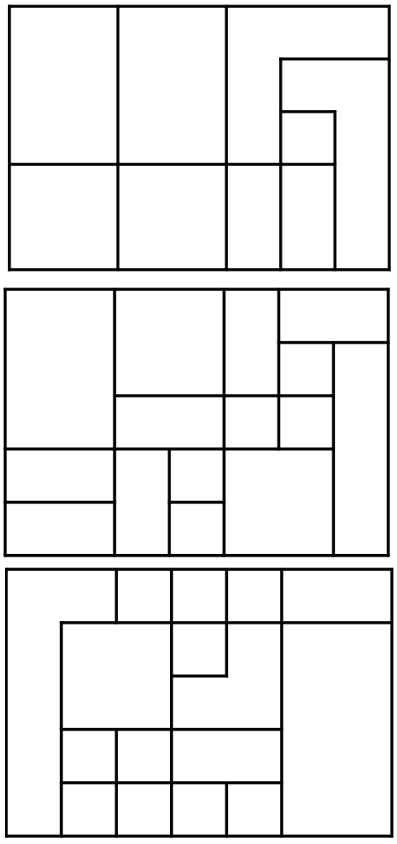

Fig. 8. Layouts of the benchmark problem illustrated in [12].

The results of the generation are presented in Fig. 9. It was observed that the layout in which all the units on each floor fit in the site could be generated. The maximum change in learning value is shown in Fig. 10. These change of the values decrease with learning and converge to a constant value as the learning stabilizes. In Experiment 1, the maximum change decreased from 35 to approximately 25. The decrease of the graph started at approximately 20,000,000 times. The execution time was about 12 h for learning with the learning model for 50,000,000 times used this time, while the generation time was less than 0.1 s.

B. Experiment 2 : Changing the iteration count

In this experiment, the efficiency of repeated learning was examined for one set of units. It is ensured that the layout can be generated when the iteration counts of one set of units are changed. The agent is trained to repeat 100 times and 1,000 times for one set of units, and the layout is derived in the same way as in Experiment 1. Learning is performed for 500,000-unit sets were repeated 100 times, and for 50,000-unit sets were repeated 1,000 times. First, the case of continuous learning of one set of units is examined. Second, the case of repeated learning for all prepared sets of units is examined.

1) Experiment 2 Result 1: The generation result in the case of learning one set of units continuously is shown in Fig.

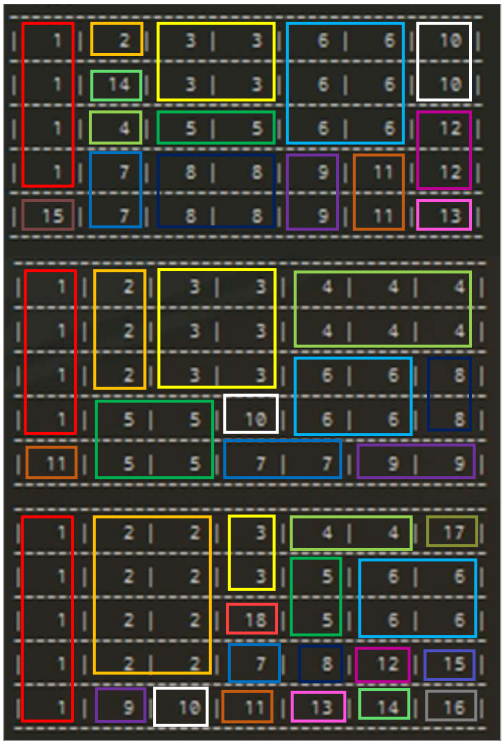

Fig. 9. Unit layout when learning 1 * 50,000,000 times.

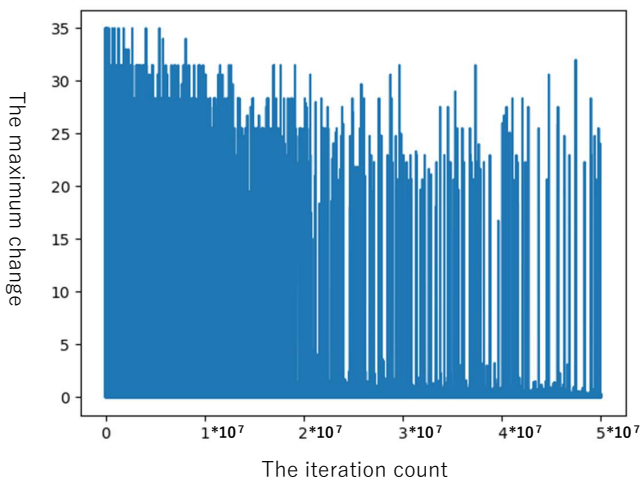

Fig. 10. Amount of change in learning value for 1*50,000,000 learning. Horizontal axis represents the iterarion count of learnings and Vertical axis represents the maximum change of the learning value.

11. The results were derived using a layout that could be completely satisfied at all iterations. The maximum change in the action-value function is shown in Fig. 12. This graph is similar to the graph shown in Fig. 10.

2) Experiment 2 Result 2: The generation result in the case of repeating learning prepared sets of units is shown in Fig. 13. In this case, a layout that was completely satisfied was derived for all the repeated numbers. The maximum change

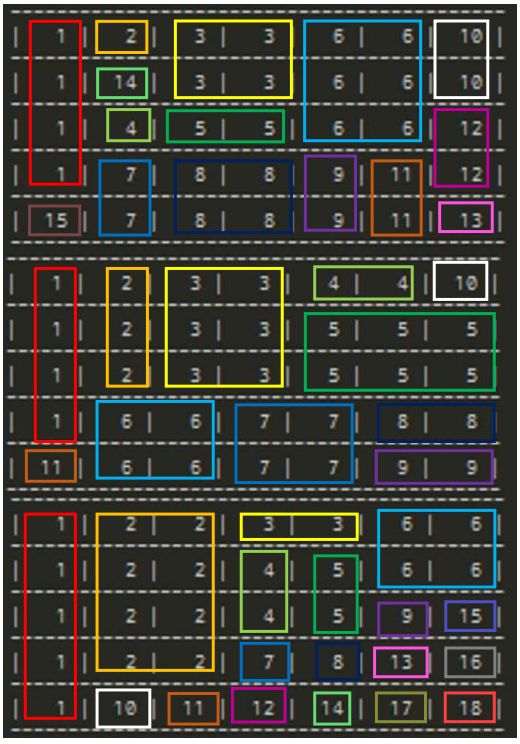

Fig. 11. Unit layout when learning 100*500,000 times.

in the action-value function is shown in Fig. 14. This graph is similar to the graph illustrated in Fig. 10 and 12.

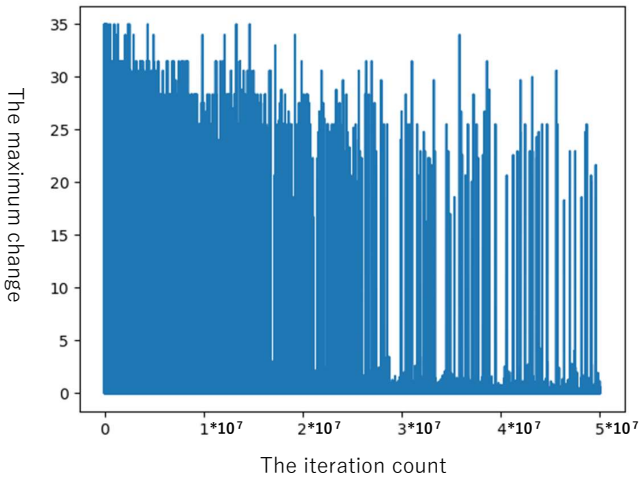

Fig. 12. Maximum change of action-value for 100* 500,000 learning.

V. Discussion

A. Unit Deployment

According to Experiments 1 and 2, large units tend to be deployed earlier in the trial, and one-block-size units tend to be deployed later in the layout generated by the proposed mechanism (Fig. 9, Fig. 11, Fig. 13). The agent learns to

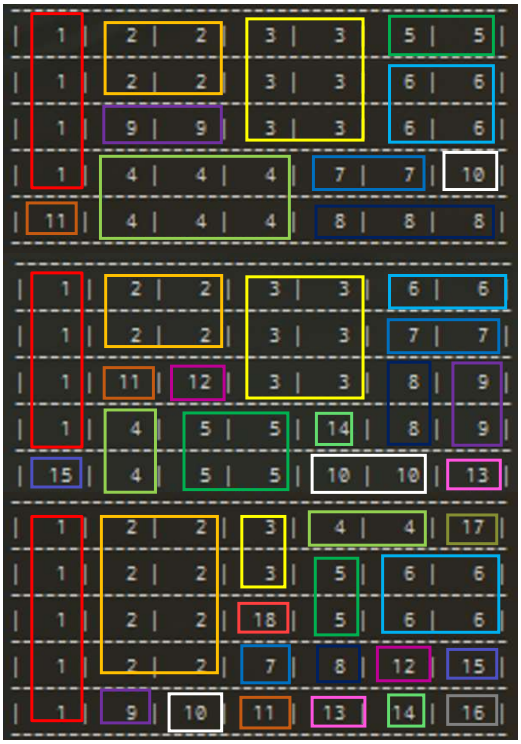

Fig. 13. Unit layout when learning 500,000*100 times.

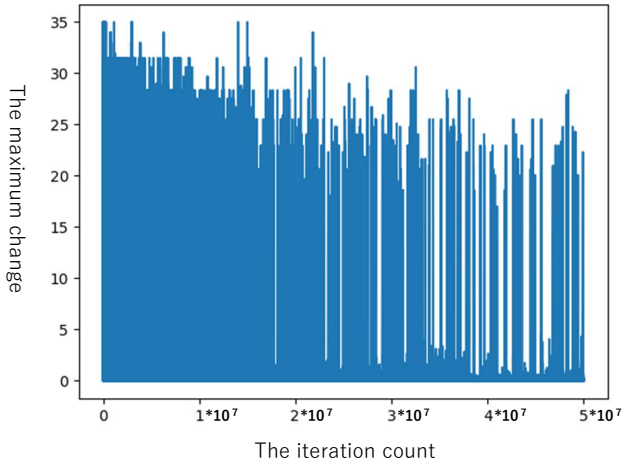

Fig. 14. Maximum change of action-value for 500,000*100 learning.

get more rewards and changes the starting point that forms the largest rectangle in which no units are located. The agent regards the number of blocks located by units as the reward value of the trial. Therefore, the agent's priority is to try to deploy larger units. This tendency reflects the proposed mechanism. Additionally, proposed mechanism is superior to some methods because the mechanism can specify the shape of units. For example, in JLAV model [43] units are approximated by a circle to determine the positions. Each unit can specify

TABLE I
FASTEST GENERATION COUNT AND AVERAGE.

	1*	2*	3*	10*
Avg. number	54587	94497.33	50315	54104
	20*	100*	200*	300*
Avg. number	120883.33	83282.5	66385.33	74313066
	400*	500*	1000*	*100
Avg. number	196713.833	153687.166	217674	175466.66
	*1000			
Avg. number	229450			

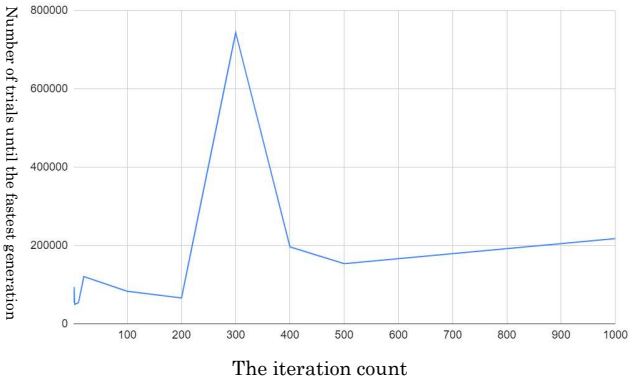

Fig. 15. Correlation between the number of the iteration counts and the number of trials until the fastest layout generations.Horizontal axis represents the iterarion count of learnings and Vertical axis represents number of trials until the fastest generation.

the size but can not specify the shape. From these viewpoints, reinforcement learning is effective to the FLP.

B. Repeated learning effect

Although Experiment 2 obtained the result when the iteration count was changed, we did not observe the large differences in the maximum change of action-value. Therefore, an additional experiment was conducted to demonstrate the differences of the number of iteration counts. To measure the learning ability of the agent, we measured how many learning trials were repeated before the fastest fulfilled layout could be generated for the three sets of units. A graph of the average trial times is shown in Fig. 15. As shown in Fig. 15, an outlier is generated when repeated 300 times. However the other parts of the graph tended to increase monotonically. It is considered that such a result was obtained because it takes time to simply encounter an unknown combination of units as the number of iterations counts increases. As the number of iterations increases, the possibility that the unit common to the desired unit set does not appear in learning increases. Therefore, it is better not to repeat learning using the same set of units.

C. Degree of learning

We conduct 50,000,000-iteration learning to perform sufficient learning in Experiment2 1 and 2. The layouts can be

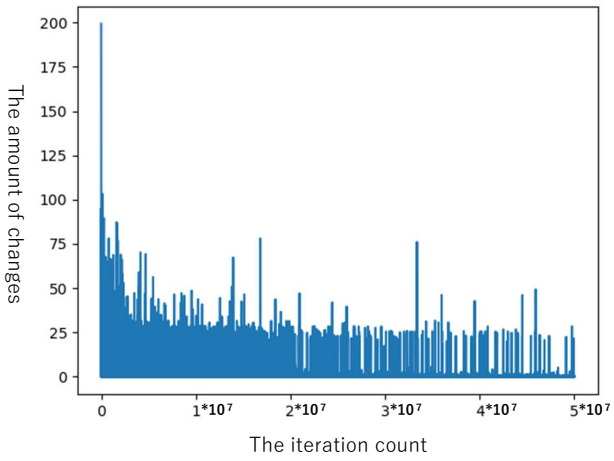

Fig. 16. Total amount of changes of 50,000,000-iteration learning.

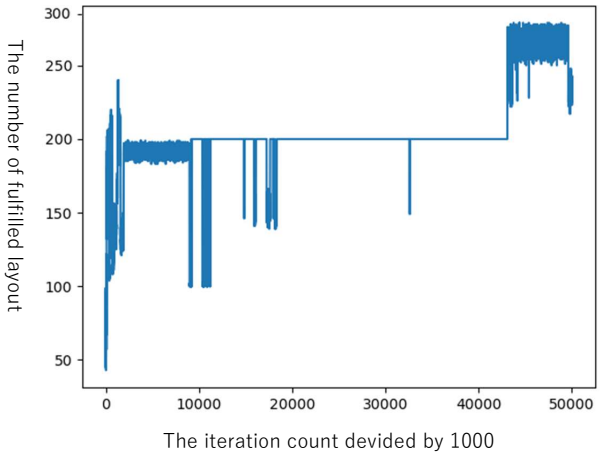

Fig. 17. Number of fulfilled layout using 100 orders of units.

generated by at most 2,000,000-iteration learning in Table I. According to Fig. 10, Fig. 12, and Fig. 14, the maximum change in the action-value decreased a few numbers from 35. Because the maximum change in the action-value is taken from all the changes in the action-value table, large changes are frequently observed in the graphs. Therefore, to avoid the effect of large changes, the total number of changes was graphed. Fig 16 shows a graph of the total amount of change of 50,000,000-iteration learning. According to Fig. 16, the number of changes is decreased from 200 and converged to around 25 when the agent learned about 10,000,000 times. The investigation shows that the approximate degree of learning can be measured by observing the total number of changes.

D. Unit order

Layouts were only generated with the same order sets of units in Experiment2 1 and 2. Therefore, an additional experiment was conducted to examine whether the agent can generate layouts when the order of the set of units is changed. Hundred different orders of units were prepared, and the agents were made to generate their layouts at each time step of learning. The experimental results are presented in Fig. 17. 50,000,000-iteration learning was conducted and check the layout of each order of sets of units for every 1000 learnings finished. The figure shows the total number of fulfilled layouts in three floors. From the figure, we could demonstrate that the learning with the proposed mechanism gradually increase the possibility of successful layout generation.

VI. Outlook

The problems and functions that we would like to implement in future studies are described below.

Enlarged table

The action-value table is created by the number of blocks that has no unit and the units that can be deployed at the site as the index. Therefore, the size of the table is the product of the number of each index. Because the number of units increases in response to the site area, the size of the table increases exponentially. Therefore, if the site area becomes too large, it may not be possible to secure the memory area. The study by Seongwoo [44] describes the efficiency of memory in deep Q-learning, and it is mentioned as one solution to this problem. Therefore, we will have to use deep Q-learning to tackle the problem of not only reducing calculation time, but also memory shortage.

Extension in three-dimensional direction

Most studies on layout creation are for flat sites, similar to the proposed mechanism. However, many facilities have a three-dimensional structure to make functions and activities efficient. This is a common practice in the areas with high land cost or concerns of the available land [45]. In the future, we would like to expand on the creation of a three-dimensional site layout. Helbor et al. [46] and Hahn et al. [47] studied the layout of the facility over multiple layers and stated that it is required to multi-floor layout the functions and activities of the facility at a lower cost.

Correlation between units

The proposed mechanism creates a layout that successfully deploys the given units within a given site. In actual facilities, each unit has a function and meaning, and each unit must be adjacent or should not be close. Therefore, we would like to set the relationship between the units and modify that the agent can learn that the units can be deployed close to each other. Yifei et al. [48], [49] completed the warehouse layout based on the current situation of comprehensive related relationships and warehouse problems using the SLP method. When the SLP method is used to analyze the non-logistics relationship between the operation units, it depends on several evaluation indicators. In the process of determining the degree of correlation, the subjective idea of the designer must be

mixed. Therefore, introducing correlation between units is a very time-consuming modification.

Accelerate learning

In the learning of this mechanism, it took approximately 12 h to learn 50,000,000 times. This result is evidently slow. For example, deep reinforcement learning, which uses a neural network to represent a table of learning values as an approximate function and performs learning, can reduce the time required for table reference and creation. Simultaneously, it is possible to speed up and reduce the load on the memory area of the learning table. Zhiang et al. [50] proposed a whole-building-energy-model-based deep reinforcement learning control framework. The building energy model (BEM), which is a detailed physics-based model used to predict a building's thermal and energy behaviors, has been widely used for building design decision support. Therefore, a deep neural network is expected to contribute to higher speeds.

Utilization of learned agents

To use the learned agent for generating the layout in other size sites, the maximum deployable site is set, and the remaining site is calculated from it. Therefore, its effectiveness was not affirmed in the experiments. If the same agent can generate layouts at different sites, the time and cost can be significantly reduced. Felipe et al. [51], [52] stated that learning a task from scratch every time is impractical because of the huge sample complexity of reinforcement learning algorithms.

VII. CONCLUSION

A mechanism that generates a facility layout using reinforcement learning was proposed. The proposed mechanism generates a layout plan that can successfully deploy the given units within a given site. Based on the results, reinforcement learning was considered to be effective to FLP. In addition, training the agent by providing additional information on the maximum rectangle in which no units are located, the agent can generate the layout for a set of various sets of units, and the effectiveness of learning when the iteration counts are changed was examined. Consequently, it was discovered that the agent tends to learn faster by providing new learning data for each trial without repetition. However, some situations could not be tested in the experiment. First, we could not examine whether the agent could learn and generate layouts at the multi-floor site. Second, we could not examine the layout generation with interrelationship among the units. The problem with generating the layout at the multi-floor site is one of the most important points to be examined for efficiency in the layout of warehouses and distribution facilities in the real world. In addition, speeding up learning using multi-agent [53], [54] or parallelization [55], [56], and comparing the MC method with other reinforcement learning methods, such as Q-learning, are future challenges. We would like to focus on these problems in future studies.

VIII. ACKNOWLEDGEMENTS

Kajima Corporation supported this work. We would like to thank Hiromasa Akagi and Fumi Sekimoto, who work with Kajima Corporation, for helpful discussions. We gratefully thank three anonymous referees for their constructive comments that helped improve the paper.

REFERENCES

[1] Andrew Kusiak, Sunderesh S.Heragu, 1987,The facility layout problem, European Journal of Operational Research 29, 229-251, https://doi.org/10.1016/0377-2217(87)90238-4
[2] Sunderesh S.Heragu, AndrewKusiak, 1991, Efficient models for the facility layout problem, European Journal of Operational Research, https://doi.org/10.1016/0377-2217(91)90088-D
[3] S.P.Singh, R.R.K.Sharma, 2006, A review of different approaches to the facility layout problems, The International Journal of Advanced Manufacturing Technology volume 30, pages 425–433, https://doi.org/10.1007/s00170-005-0087-9
[4] Kar Yan Tam, 1992, Genetic algorithms, function optimization, and facility layout design, European Journal of Operational Research Volume 63 issue 2, https://doi.org/10.1016/0377-2217(92)90034-7
[5] Anita Thengade, Rucha Dondal, 2012, Genetic Algorithm – Survey Paper, MPGI National Multi Conference 2012, ISSN: 0975 - 8887
[6] Pedro G. Espejo, Sebastian Ventura, Francisco Herrera, 2010, A Survey on the Application of Genetic Programming to Classification, IEEE Transactions on Systems, Man, and Cybernetics, Part C (Applications and Reviews, Volume 40, Issue 2, 10.1109/TSMCC.2009.2033566
[7] Venkatesh Dixit, Jim Lawlor, 2019, Modified genetic algorithm for automated facility layout design, International Journal of Advance Research, Ideas and Innovations in Technology, Volume 5, Issue 3, ISSN: 2454-132X
[8] José Fernando Gonçalvesa, Mauricio G.C.Resende, 2015, A biased random-key genetic algorithm for the unequal area facility layout problem, European Journal of Operational Research, Volume 246, https://doi.org/10.1016/j.ejor.2015.04.029
[9] Stanislas Chaillou, 2019, AI and Architecture An Experimental Perspective, The Routledge Companion to Artificial Intelligence in Architecture, ISBN:9780367824259
[10] Luisa Fernanda Vargas-Pardo, Frank Nixon Giraldo-Ramos, 2021, Firefly algorithm for facility layout problemoptimization, Visión electrónica, https://doi.org/10.14483/issn.2248-4728
[11] Jing fa, Liuab JunLiu, 2019, Applying multi-objective ant colony optimization algorithm for solving the unequal area facility layout problems, Applied Soft Computing, Volume 74, https://doi.org/10.1016/j.asoc.2018.10.012
[12] Russell D.Meller, Yavuz A.Bozer, 1997, Alternative Approaches to Solve the Multi-Floor Facility Layout Problem, Journal of Manufacturing Systems, Volume 16, Issue 3, https://doi.org/10.1016/S0278-6125(97)88887-5,
[13] Arthur R.Butz, 1969, Convergence with Hilbert's Space Filling Curve, Journal of Computer and System Sciences, https://doi.org/10.1016/S0022-0000(69)80010-3
[14] L.P.Kaelbling, M.L.Littman, A.W.Moore, 1996, Reinforcement Learning: A Survey, JAIR, https://doi.org/10.1613/jair.301
[15] Volodymyr Mnih, Koray Kavukcuoglu, David Silver, Alex Graves, Ioannis Antonoglou, Daan Wierstra, Martin Riedmiller, 2013, Playing Atari with Deep Reinforcement Learning, NIPS Deep Learning Workshop, https://doi.org/10.48550/arXiv.1312.5602
[16] Yu-Jui Liu, Shin-Ming Cheng, Yu-Lin Hsueh, 2017, eNB Selection for Machine Type Communications Using Reinforcement Learning Based Markov Decision Process, /url10.1109/TVT.2017.2730230
[17] Frank L. Lewis, Draguna Vrabie, 2009, Reinforcement learning and adaptive dynamic programming for feedback control, IEEE Circuits and Systems Magazine Volume9 Issue3, 10.1109/MCAS.2009.933854
[18] F. Llorente, L. Martino, J. Read, D. Delgado, 2021, A survey of Monte Carlo methods for noisy and costly densities with application to reinforcement learning, https://doi.org/10.48550/arXiv.2108.00490
[19] P. Cichosz, 1995, Truncating Temporal Differences: On the Efficient Implementation of TD(lambda) for Reinforcement Learning, 2017, JournalofArti cialIntelligenceResearch2, IEEE Transactions on Vehicular Technology, Volume 66, No. 12, https://doi.org/10.1613/jair.135

[20] Harmon, Mance E., Harmon, Stephanie S., 1997, Reinforcement Learning: A Tutorial., January,

[21] E. N. Barron, H. Ishii, 1989, The Bellman equation for minimizing the maximum cost, Nonlinear Analysis, Theory, Methods and Applocations, https://doi.org/10.1016/0362-546X(89)90096-5

[22] Christopher J. C. H. Watkins, Peter Dayan, 1992, Q-Learning, https://doi.org/10.1007/BF00992698 Machine Learning, 8, 279-292

[23] Ali Asghari, Mohammad Karim Sohrabi, Farzin Yaghmaee, 2021, Task scheduling, resource provisioning, and load balancing on scientifc workfows using parallel SARSA reinforcement learning agents and genetic algorithm, The Journal of Supercomputing, https://doi.org/10.1007/s11227-020-03364-1

[24] Feng Ding, Guanfeng Ma, Zhikui Chen, Jing Gao, Peng Li, 2021, Averaged Soft Actor-Critic for Deep Reinforcement Learning, Complexity, vol.2021, https://doi.org/10.1155/2021/6658724

[25] Seyed Sajad Mousavi, Michael Schukat1, Enda Howley, 2017, Traffic light control using deep policy-gradient and value-function-basedreinforcement learning, IET Intelligent Transport Systems, https://doi.org/10.1049/iet-its.2017.0153

[26] Xinhan Di, Pengqian Yu, IHome Company, IBM Research, 2021, Deep Reinforcement Learning for Producing Furniture Layout in Indoor Scenes, Cornell University, https://doi.org/10.48550/arXiv.2101.07462

[27] Vincent Francois-Lavet, Peter Henderson, Riashat Islam, Marc G. Bellemare, Joelle Pineau, 2018, An Introduction to Deep Reinforcement Learning, Foundations and Trends in Machine Learning, Volume 11, https://doi.org/10.1561/2200000071

[28] Matthias Klar, Moritz Glatt, Jan C. Aurich, 2021, An implementation of a reinforcement learning based algorithm for factory layout planning, Manufacturing Letters, Volume 30, October, https://doi.org/10.1016/j.mfglet.2021.08.,

[29] Richa Verma, Sarmimala Saikia, Harshad Khadilkar, Puneet Agarwal, Gautam Shrof, Ashwin Srinivasan, 2019, A Reinforcement Learning Framework for Container Selection and Ship Load Sequencing in Ports, Autonomous Agents and Multiagent Systems,

[30] Ruizhen Hu, Juzhan Xu, Bin Chen, Minglun Gong, Hao Zhang, Hui Huang, 2020, TAP-Net: Transport-and-Pack using Reinforcement Learning, ACM Transactions on Graphics, Volume 39, December, https://doi.org/10.1145/3414685.3417796

[31] Azalia Mirhoseini, Anna Goldie, Mustafa Yazgan, Joe Wenjie Jiang, Ebrahim Songhori, Shen Wang, Young-Joon Lee, Eric Johnson, Omkar Pathak, Azade Nazi, Jiwoo Pak, Andy Tong, Kavya Srinivasa, William Hang, Emre Tuncer, Quoc V. Le, James Laudon, Richard Ho, Roger Carpenter, Jeff Dean, 2021, A graph placement methodology for fast chip design, Nature, volume 594, pages207–212, https://doi.org/10.1038/s41586-021-03544-w

[32] Xinhan Di, Pengqian Yu, 2021, Multi-Agent Reinforcement Learning of 3D Furniture Layout Simulation in Indoor Graphics Scenes, ICLR SimDL Workshop, https://doi.org/10.48550/arXiv.2102.09137

[33] Peter Burggraf, Johannes Wagner, Benjamin Heinbach, 2021, Bibliometric Study on the Use of Machine Learning as Resolution Technique for Facility Layout Problems, IEEE Access, Volume 9, 10.1109/ACCESS.2021.3054563

[34] Christian E. López, James Cunningham, Omar Ashour, Conrad S. Tucker, 2020, Deep Reinforcement Learning for Procedural Content Generation of 3D Virtual Environments, Journal of Computing and Information Science in Engineering, https://doi.org/10.1115/1.4046293

[35] Niloufar Izadinia, Kourosh Eshghi, Mohammad Hassan Salmani, A robust model for multi-floor layout problem, 2014, Computers and Industrial Engineering 78, http://dx.doi.org/10.1016/j.cie.2014.09.023

[36] Junjie Li, Sotetsu Koyamada, Qiwei Ye, Guoqing Liu, Chao Wang, Ruihan Yang, Li Zhao, Tao Qin, Tie-Yan Liu, Hsiao-Wuen Hon, 2020, Suphx: Mastering Mahjong with Deep Reinforcement Learning, Cornell University, https://doi.org/10.48550/arXiv.2003.13590

[37] Matthew Lai, 2015, Giraffe: Using Deep Reinforcement Learning to Play Chess, partial fulfilment of the requirements for the MSc Degree in Advanced Computing of Imperial College, https://doi.org/10.48550/arXiv.1509.01549

[38] Adrian Goldwaser, Michael Thielscher, 2020, Deep Reinforcement Learning for General Game Playing, The Thirty-Fourth AAAI Conference on Artificial Intelligence (AAAI-20), https://doi.org/10.1609/aaai.v34i02.5533

[39] David Silver, Thomas Hubert, Julian Schrittwieser, Ioannis Antonoglou, Matthew Lai, Arthur Guez, Marc Lanctot, Laurent Sifre, Dharshan Kumaran, Thore Graepel, Timothy Lillicrap, Karen Simonyan, Demis Hassabis, 2018, A general reinforcement learning algorithm that masters chess, shogi, and Go through self-play, Science, 10.1126/science.aar6404,

[40] Guillaume Chaslot, Sander Bakkes, Istvan Szita, Pieter Spronck, 2008, Monte-Carlo Tree Search: A New Framework for Game AI, Proceedings of the Fourth Artificial Intelligence and Interactive Digital Entertainment Conference, https://ojs.aaai.org/index.php/AIIDE/article/view/18700

[41] Yahui Liu, Buyang Cao, Hehua Li, Improving ant colony optimization algorithm with epsilon greedy and Levy flight, 2021, Complex and Intelligent Systems 17111722,https://doi.org/10.1007/s40747-020-00138-3

[42] Tailong Yang, Shuyan Zhang, Cuixia Li, 2021, A multi-objective hyper-heuristic algorithm based on adaptive epsilon-greedy selection, Complex and Intelligent Systems, https://doi.org/10.1007/s40747-020-00230-8

[43] Abbas Ahmadi, Mohammad Reza Akbari Jokar, 2016, An efficient multiple-stage mathematical programming method for advanced single and multi-floor facility layout problems, Applied Mathematical Modelling, Volume 40, Issues 9–10, Pages 5605-5620, https://doi.org/10.1016/j.apm.2016.01.014

[44] Seongwoo Lee, Joonho Seon, Chanuk Kyeong, Soohyun Kim, Younghyu Sun, Jinyoung Kim, 2021, Novel Energy Trading System Based on Deep-Reinforcement Learning in Microgrids, https://doi.org/10.3390/en14175515,

[45] Amine Drira, Henri Pierreval, SoniaHajri-Gabouj, 2007, Facility layout problems: A survey, Annual Reviews in Control, Volume 31, Issue 2, https://doi.org/10.1016/j.arcontrol.2007.04.001

[46] Stefan Helber, Daniel Bohme, Farid Oucherif, Svenja Lagershausen, Steffen Kasper, 2015, A hierarchical facility layout planning approach for large and complex hospitals, Flexible Services and Manufacturing Journal, pp 5-29, https://doi.org/10.1007/s10696-015-9214-6

[47] Peter Hahn, J.MacGregor Smith, Yi-Rong Zhu, 2008, The Multi-Story Space Assignment Problem, Annals of Operations Research,pp77-103, https://doi.org/10.1007/s10479-008-0474-3

[48] Yifei Zhang, 2021, The design of the warehouse layout based on the non-logistics analysis of SLP, E3S Web of Conferences 253, https://doi.org/10.1051/e3sconf/202125303035

[49] Yifei Zhang, 2020, Research on layout planning of disinfection tableware distribution center based on SLP method, MATEC Web of Conferences 325, https://doi.org/10.1051/matecconf/202032503004

[50] Zhiang Zhang, Adrian Chongb, Yuqi Panc, Chenlu Zhanga, Khee Poh Lam, 2019, Whole building energy model for HVAC optimal control: A practical framework based on deep reinforcement learning, Energy and Buildings, Volume 199, Pages 472-490, https://doi.org/10.1016/j.enbuild.2019.07.029

[51] Felipe Leno Da Silva, Anna Helena Reali Costa, 2019, A Survey on Transfer Learning for MultiagentReinforcement Learning Systems, Journal of Artificial Intelligence Research 64, https://doi.org/10.1613/jair.1.11396

[52] Felipe Leno Da Silva, Matthew E. Taylor, Anna Helena Reali Costa, 2018, Autonomously Reusing Knowledge in Multiagent Reinforcement Learning, Proceedings of the Twenty-Seventh International Joint Conference on Artificial Intelligence (IJCAI-18),

[53] Wei Du, Shifei Ding, 2020, A survey on multi-agent deep reinforcement learning: from the perspective of challenges and applications, Artificial Intelligence Review, https://doi.org/10.1007/s10462-020-09938-y

[54] Ingy Elsayed-Aly, Suda Bharadwaj, Christopher Amato, Rüdiger Ehlers, Ufuk Topcu, Lu Feng, 2021, Safe Multi-Agent Reinforcement Learning via Shielding, Autonomous Agents and Multiagent Systems, https://doi.org/10.48550/arXiv.2101.11196

[55] Alfredo V. Clemente, Humberto N. Castejon, Arjun Chandra, 2017, EFFICIENT PARALLEL METHODS FOR DEEP REINFORCEMENT LEARNING, Cornell University, https://doi.org/10.48550/arXiv.1705.04862

[56] Arun Nair, Praveen Srinivasan, Sam Blackwell, Cagdas Alcicek, Rory Fearon, Alessandro De Maria, Vedavyas, Panneershelvam, Mustafa Suleyman, Charles Beattie, Stig Petersen, Shane Legg, Volodymyr Mnih, Koray Kavukcuoglu, David Silver, 2015, Massively Parallel Methods for Deep Reinforcement Learning, the Deep Learning Workshop, International Conference on Machine Learning, https://doi.org/10.48550/arXiv.1507.04296

1st Workshop on Artificial Intelligence for Next-Generation Diagnostic Imaging

THE application of artificial intelligence (AI) becomes nowadays one of the most promising areas of health innovation. Among the most promising clinical applications of AI is diagnostic imaging, where AI algorithms can boost processing power of huge, heterogeneous medical image resources and therefore uncover disease characteristics that fail to be found by the naked eyes. AI can optimize radiologists' workflows and facilitate quantitative assessments of radiographic characteristics using radiomics approach. Nowadays refinement of AI imaging studies is required by consistent selection of clinically meaningful and patient-related endpoints.

The workshop on Artificial Intelligence for Next-Generation Health and Medical Applications – AI4NextGenHMA'22— provides an interdisciplinary forum for researchers, developers, radiologist and clinicians to present and discuss latest advances in research work related to theoretical and practical applications of AI in diagnostic imaging and related areas. The workshop aims to bring together specialists for exchanging ideas and promote fruitful discussions.

TOPICS

The list of topics includes, but is not limited to:

- AI for diagnostic imaging and digital pathology
- DL models and architectures for medical image analysis
- Explainable AI (XAI) for diagnostic imaging
- Radiomics and quantitative image analysis
- Structured reporting in radiology
- Standardization of data annotation for AI
- Clinical decision support systems, especially integrating results of image analysis
- Clinical pathways based on image analysis and integration of clinical data
- Biomedical ontologies, terminologies, standards and clinical guidelines
- Data mining and knowledge discovery in radiology
- Domain knowledge representation and integration into DL/ML models in medical tasks
- Precision medicine and personalized medicine based on diagnostic imaging
- Natural language processing for radiological report analysis
- Medical signal processing and analysis
- Social and ethical aspects of AI in radiology

TECHNICAL SESSION CHAIRS

- **Jóźwiak, Rafał,** Warsaw University of Technology, Poland
- **Pancerz, Krzysztof,** Academy of Zamość, Poland

Communication Papers of the of the 17th Conference on Computer Science and Intelligence Systems pp. 23–30
DOI: 10.15439/2022F128
ISSN 2300-5963 ACSIS, Vol. 32

Detecting Cancerous Regions in DCE MRI using Functional Data, XGboost and Neural Networks

Povilas Treigys, Jolita Bernatavičienė
Vilnius University
Institute of Data Science and Digital Technologies
Akademijos st. 4, Vilnius, Lithuania
Email: {povilas.treigys, jolita.bernataviciene}@mif.vu.lt

Aleksas Vaitulevičius
Vilnius University
Institute of Data Science and Digital Technologies
Akademijos st. 4, Vilnius, Lithuania
Email: aleksas.vaitulevicius@mif.stud.vu.lt

Jurgita Markevičiūtė
Vilnius University
Institute of Applied Mathematics
Naugarduko st. 24, Vilnius, Lithuania
Email: jurgita.markeviciute@mif.vu.lt

Ieva Naruševičiūtė, Mantas Trakymas
Vilnius University
National Cancer Institute
Santariškių st. 1, Vilnius, Lithuania
Email: {ieva.naruseviciute, mantas.trakymas}@nvi.lt

***Abstract*—Cancerous region detection in the prostate is performed using different imaging sequences by multiparametric magnetic resonance imaging. One of those modalities is dynamic contrast enhancement. The authors of this paper are testing possible modifications of workflow which use this modality for more accurate cancerous region detection in the prostate. The introduced changes are timestamp mapping in the segmentation step, proportionate Simple Linear Iterative Clustering region number to prostate region size in each slice, a new definition of labels and new extracted features. Furthermore, experiments are performed for segmentation in a single timestamp only. The experiments test the effect of modification on curve classification by using XGBoost classification and flat neural network approaches. Lastly, the authors perform hyper-parameter tuning of both approaches and evaluates obtained results statistically.**

I. Introduction

One of the most lethal cancer globally is prostate cancer. According to the research by Bray et al. in paper [6], it has the second highest incidence rate among males after lung cancer. Successful prostate cancer treatment requires early diagnosis. Preliminary identification of cancer is related to a higher concentration of a protein produced by the prostate called Prostate-Specific Antigen (PSA), as it is described in paper [17] by Hayes and Barry. However, PSA testing has a high level of false-positive and false-negative cases. Therefore, in addition to PSA testing, many biopsies are taken, which is a highly invasive testing method. As an alternative to this method, PI-RADS is introduced in paper [2]. It is a structured reporting scheme for multiparametric (mp) prostate Magnetic Resonance Imaging (MRI). Literature evidence of the same paper and the expert opinion consensus indicate better interpretation and performance of prostate cancer evaluation when using PI-RADS rather than PSA testing. Examples of MRI modalities used for cancer evaluation are T2 weighted images (T2W), Diffusion Weighted Images (DWI), Apparent Diffusion Coefficients (ADC), and Dynamic Contrast-Enhanced (DCE) images.

This work was not supported by any organization

Vaitulevicius et al. introduce in paper [27] the workflow for detecting cancerous regions in the prostate by using DCE sequences together with preliminary research. This modality is acquired by capturing a sequence of MRI scans during intravenous injection of a contrast agent. Typically gadolinium is used, and the scans are performed every few seconds for several minutes. As described by Low et al. in paper [23], during this period, tumours attract a higher amount of contrast medium due to their typically higher vascular permeability and density caused by angiogenesis. This data can detect, characterize, and monitor tumours using Functional Data Analysis (FDA) and machine learning methods. The approach tested in the experiments described by Vaitulevičius et al. in paper [27] performs the following steps. Firstly, these DCE sequences' cross-sectional images are segmented using image segmentation algorithms such as the Simple Linear Iterative Clustering (SLIC) algorithm. Secondly, the regions are aggregated to values representative of regions by calculating such metrics as mean or median. Thirdly, for each region x function $f_x : T \to I$ are created by fitting aggregated values of region x. In the definition of these functions T is the set of timestamps while I is the set of aggregated values at the timestamps T. Finally, the preliminary research is performed on the K-nearest neighbours algorithm (KNN) using functional data and the support vector machine (SVM) algorithm using extracted features from functional data.

In this paper, several adjustments to the workflow are tested. Firstly, instead of a fixed number of SLIC regions, using a proportionate number of SLIC regions in each slice is proposed and compared to the workflow described in paper [27]. Secondly, the experiments are done to determine if using landmark registration on data improves or worsens the classification accuracy metrics. Moreover, the experiments are repeated on thirteen patients separately instead of one.

Furthermore, this paper focuses entirely on segmenting each timestamp individually and does not introduce any experiments on the temporal variance matrix calculated between all timestamps. This paper chooses only a single timestamp for each patient for segmentation. Finally, two new algorithms, flat neural network and XGBoost classification introduced in paper [11], are tested using features extracted from functional data as these algorithms are more advanced and highly tunable. Therefore, the hyperparameters of those algorithms are tuned. The data used for experiments is the same as in the experiments introduced in paper [27]. The data for the investigation, under the terms of the bioethical agreement, was provided by Lithuanian National Cancer Institute.

A lot of prostate cancer research with MRI data is already done. Many examples of machine learning applications on MRI modalities are given in paper [13]. Papers [19] and [1] conducted research tests the possibility of using T2W sequences for cancer localization. Another examples are usage of DWI sequences to solve prostate cancer segmentation and severity evaluation problems presented in papers [26], [18], [29] and [4]. Moreover, in paper [14] research was conducted which tested the capability of various adaptations of U-net to detect and grade cancerous tissue by using T2-weighted and DWI modalities. Lastly, technological improvements such as the ones presented in paper [10] in DCE MRI modality data acquisition creates a demand to research DCE MRI sequences. One of the research on DCE MRI sequences was performed in paper [20]. However, the paper [20] focuses purely on machine learning and does not use FDA approach.

To summarize, authors of this paper introduced and tested adjustments to the workflow described in article [27] by Vaitulevičius et al. The changes are segmentation timestamp mapping, using a proportionate number of SLIC regions to prostate size in each slice, label definition, extracted features and new classification models.

II. Experiment setup

As mentioned in the introduction, several adjustments to the workflow described in paper [27] was introduced. The experiments are performed according to a new workflow. Data used in the experiments is the same as in the experiment of previously published author's investigation. However, investigations of this paper, differently from the experiment described in article [27], are performed on 13 patients instead of one by performing model training and validation for each patient separately. The example of a single patient's single slice in 3 different timestamps is visualized in Fig. 1. The left shows the DCE image taken at the timestamp at which the contrast agent has not yet reached the prostate region. The middle shows the DCE image is taken at the timestamp the contrast agent is flowing through arteries, and the right DCE MRI image is taken at the timestamp when the contrast agent is accumulating in the prostate. Meanwhile, in Fig. 2 cancerous and prostate masks are displayed. Lastly, each patient's data is split into a training set of 70% of the patient's dataset and a validation set of 30% of the patient's dataset. The ratio of classes in training and validation data sets is equal.

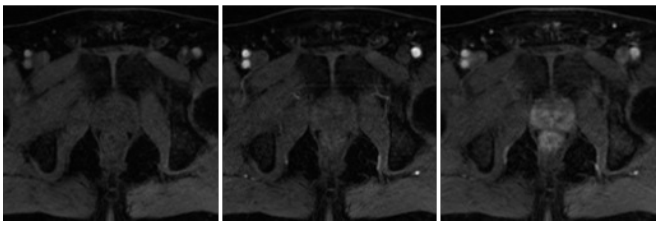

Fig. 1. Example of the DCE images of a single slice at 3 different timestamps.

Flat neural network and XGBoost algorithms are tested in the experiments presented in this paper. Authors test only the simple flat neural network, consisting of only dense layers and compare it to another machine learning algorithm - XGBoost. Flat neural network is chosen as a baseline as deep neural networks are highly scalable group of machine learning methods and flat neural network is the most simple one. Meanwhile, XGBoost is a relatively new algorithm which has already proven to be effective in solving various tasks in the medical field. For example, the experiment provided in paper [9] indicates that XGBoost achieves the most accurate results when predicting the outcome of hypertension. The other example is the experiment provided in article [16]. Authors show that XGBoost excels in the pathway analysis, which is used to determine the role of the tested protein task. One more example is the experiment provided in paper [21], which indicates that XGBoost accurately predicts mortality from acute kidney injury.

A. Chose of timestamps for each patient

Each patient's data is acquired at different timestamps and do not correspond to each other. For example, if patient A has 31 timestamps while patient B has 20 timestamps, then the patient's A timestamp five will not conform to patient's B timestamp five. Meanwhile, chosen timestamp for segmentation for each patient has to be conforming in order to not introduce the effect of the timestamp choice. To overcome this problem, each patient's timestamps are mapped to 25 timestamps. An illustrative scheme of mapping is displayed in Fig. 3 where columns Patient A timestamps and Patient B timestamps correspond to original timestamps. Firstly, the timestamps of the patients are normalized to the interval

Fig. 2. The left image is a cancerous region mask and the right image is the prostate mask of a single slice.

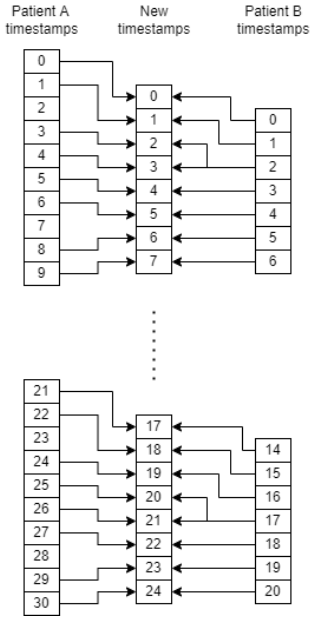

Fig. 3. Example of the timestamp mapping for Patient A data having 31 timestamps and Patient B data having 20 timestamps.

[0, 24]. Secondly, normalized timestamps are rounded to the whole numbers. The resulting new timestamps are displayed in the column New timestamps. However, after this step, patients with more than 25 timestamps have multiple DCE images at a single timestamp, while patients with less than 25 timestamps have none at specific timestamps. Therefore, if more than one patient's timestamp is mapped to a new timestamp, then the latest timestamp of those timestamps is selected for a new timestamp. Suppose none of the patient's timestamps gets mapped to a new timestamp. In that case, patient's normalized rounded timestamp, which has a minor absolute difference with a new timestamp, is mapped to a new timestamp. If more than one of such timestamps exists, then the earliest timestamp is mapped to a new timestamp. As mentioned in the introduction, a single timestamp is used for experiments when performing segmentation. The chosen timestamp was the 5th.

B. Segmentation

In the original segmentation described in article [27], each patient's slice is segmented into a fixed number of zones, 50. However, it seems it is biased towards SLIC regions of slices in which prostate regions are smaller as they have a smaller area, but the number of regions produced from them is the same.

This paper investigates the ability to select the number of SLIC regions proportionate to the size of the slice. Firstly, the slice with the largest prostate region is chosen. For that slice, 50 of SLIC regions are obtained. Secondly, number of SLIC regions in other slices are calculated by using formula $n_i = n_{max} \times s_i / max(S)$ where n_{max} is number of SLIC regions to which the slice with largest prostate region is segmented, s_i - prostate size in the slice, S - list of prostate region sizes across slices. The results are rounded to whole numbers. These results are the amount of SLIC regions for each slice. The difference between the original and modified approaches is illustrated in Fig. 4.

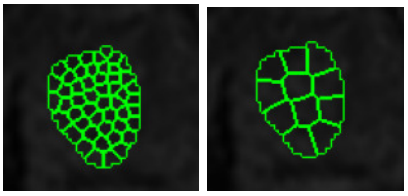

Fig. 4. Example of the slice segmentation. On the left the result of modified segmentation approach, on the right - the original segmentation is displayed.

C. SLIC region labels

In paper [27], positive class was assigned to the SLIC regions, which had an overlap of $\geq 50\%$ with cancer mask and with malignant biopsy mask. However, this definition resulted in a very small amount of samples of regions with positive class labels resulting in an imbalanced class problem. Therefore in this paper, a new description of positive class label is applied, which results in less accurate labels, but it increased the data sample amount for positive class labels.

In the research described in this paper, positive class is assigned to SLIC regions with the overlap of $\geq 50\%$ with cancer mask, which has overlap with at least one malignant biopsy mask and no overlap with benign biopsy masks. SLIC regions to which negative label 0 is assigned remain the same as in paper [27]. The rest of the SLIC regions are not used in training or validation. These SLIC regions include regions that either have:

- Overlap of $< 50\%$ with cancer masks, which overlap with at least one malignant biopsy mask and has no overlap with benign biopsy masks.
- Overlap with cancer mask, which has no overlap with malignant biopsy mask.

The example of SLIC region labels defined in this paper is displayed in Fig. 5.

D. Features from functional data

A different set of features are chosen for the training and validation in the experiments described in this paper than in the experiments described by Vaitulevičius et al. in paper [27]. Firstly, the number of uniformly spaced discrete values is increased from 10 to 100. Such adjustment results in the longer training process and increased accuracy of functional data representation. Secondly, the maximal value's timestamp normalized to the interval [0, 1] is not used for the experiments as it is the same for the registered functional data. After registering the data, this feature becomes equal for all regions. Therefore, it does not carry any valuable information for experiments conducted with functional data registration. Thus, extracted features in the investigations of this paper are:

- uniformly spaced discrete values - $f(x_i)$ where f is a single function from functional data and $x_i \in [0, 1]$, $x_i - x_{i-1} = x_j - x_{j-1}$ with $i \in [0, 100]$ and $j \in [0, 100]$.
- max value of the function - $\sup_{x\in[0,1]} f(x)$.
- modified band depth - functional depth described in paper [22].
- integral depth - functional depth described in paper [15].

Lastly, two types of experiments are conducted. First experiment uses only discrete FDA values. Second - discrete values obtained from FDA and the features such as: modified band depth, integral depth and max value of the function. If the second experiment will not bear significant results, then that would indicate that no additional information is needed than the discrete values of the functional data itself

E. Software used for experiments

All experiments are performed by using Python 3.8 programming language with latest packages:

- scikit-fda - smoothing time series into functional data and functional data transformations.
- xgboost - XGBoost classification model training. The library is introduced in paper [11]
- hyperopt - XGBoost classification model's hyperparameter tuning. The library is introduced in paper [8].
- keras - flat neural network model's training with tensorflow framework. The library is published in [12].
- keras_tuner - flat neural network model's hyperparameter tuning. The library is published in [24].
- scikit-learn - data splitting and metric calculation. The library is introduced in paper [25].
- scipy - statistical tests.

III. Hyperparameter tuning

Hyperparameter tuning of both algorithms is performed using each patient's data separately. Tuning allows the investigation of possible hyperparameters for a more general model. Persistent values of hyperparameters indicate that those values can be used in a more general model. However, non-persistent values suggest that the model is too simple and hardly can be generalized.The dataset is split into stratified training and validation sets for hyperparameter tuning. The validation set contains 30% of the dataset while the training set - 70%. Each feature of the training set is scaled by normalizing it to the interval [0, 1], while validation set features are scaled by dividing each by the maximum value of the training set.

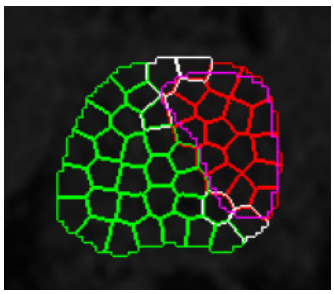

Fig. 5. Example of SLIC region labels. The regions with a red contour are regions representing the positive class label. The regions with a green outline are regions representing the negative class label. The labels with white contours are not used in the training or validation. The purple contour is the cancerous region mask which has overlap with malignant biopsy mask and no overlap with benign biopsy masks

Moreover, due to the high class imbalance, additional class weights are assigned. For positive class weight is calculated by using formula $w_p = 1 - (n_p/n_a)$ and for negative class - $w_n = 1 - (n_n/n_a)$ where n_p is the number of SLIC regions with a positive class in the training set, n_n is the number of SLIC regions with a negative class in the training set, n_a - size of the training set.

Lastly, early stopping is used for XGBoost classification and flat neural network algorithms to avoid overfitting. For XGBoost, if after iterating through the training set ten times F1 score of the validation set does not improve, then the training is stopped. For a flat neural network, if after ten epochs F1 score of the validation set does not improve, then the training is stopped, and the model with the highest F1 score of the validation set is chosen.

A. XGBoost algorithm hyperparameter tuning

Hyperparameters of the XGBoost classification algorithm are tuned by using Tree of Parzen Estimators (TPE) described by Bergstra et al. in paper [7]. The training for each patient is repeated at least 400 times in hyper-parameter tuning. Hyperparameters are tuned by maximizing the F1 score on the validation data set. The space of tuned hyperparameters is taken from Kagle competition [3]. Tuned hyperparameters are:

- Subsample ratio of columns when constructing each tree. The search space of this hyperparameter is in interval [0.4, 0.8].
- Minimum loss reduction required to make a further partition on a leaf node of the tree. The search space of this hyperparameter is in interval [0, 1].
- Maximal depth of the XGBoost ensemble tree. The search space of this hyperparameter is in an interval of natural numbers [3, 18].
- Minimum sum of instance weight (Hessian) needed in a child. The search space of this hyperparameter is in an interval of natural numbers [0, 10].
- L1 regularization term on weights. The search space of this hyperparameter is in interval [0, 1].

Number of gradient boosted trees. This hyperparameter is a constant and set to 180 and each training is performed by minimizing the logistic regression loss function.

B. Flat neural network algorithm hyperparameter tuning

Hyperparameters of the flat neural network algorithm are tuned by using the Bayesian tuning algorithm described by Barsce et al. in paper [5]. The training for each patient is repeated at least 25 times. Each training is performed in 100 epochs or less (if the early stop is triggered). Due to the non-deterministic behaviour of the flat neural network training

algorithm, each hyperparameter tuning procedure has been repeated ten times. Hyperparameters are tuned by maximizing the mean of the F1 score on the validation data set. The architecture of the tuned flat neural network is:

- Input layer
- First hidden layer is a dense layer with a ReLU activation function and the number of neurons equal to a number of input dimensions.
- Search the number of hidden dense layers (depth of neural network). The search space of this hyperparameter is in an interval of natural numbers [1, 10]. Each layer's activation function is ReLU. A number of neurons are also tuned and is set to repetitive numbers of 32 in the interval of natural numbers [32, 1024].
- Last layer of the neural network contains only a single neuron. The activation function of this layer is tuned by testing activation functions - sigmoid, softmax and ReLU.

IV. Results

In the experiments provided in this paper, hyperparameter tuning and training are done on each patient's data separately. The collected accuracy metrics of the resulting models are calculated on the validation set. Accuracy metrics are precision, recall, F1, balanced accuracy and specificity. Experiments with the flat neural network are repeated ten times with each patient's dataset. Collected accuracy metrics of flat neural network's model are aggregated on a patient and configuration basis by calculating the mean and the standard deviation. Those metrics can be used to choose a more stable model as mean is heavily affected by outliers and standard deviation indicates how much do the outliers affect the mean. Lastly, the median value of each accuracy metric is calculated on configuration basis as median have lesser effect of outliers and represent the sample distribution better than mean. Those configurations are registered, unregistered functional data, only discrete and not only discrete extracted features from functional data, proportionate and fixed number of SLIC regions in the slice and lastly selected model - XGBoost or flat neural network.

Tables I and III contain medians of validation dataset classification accuracy metrics of flat neural network and XGBoost model respectively. Tables II and III contain hyperparameters acquired by hyperparameter tuning on dataset of single patient for flat neural network and XGBoost model respectively. The shown hyperparameter tuning result is acquired from the patient's validation dataset, which is classified with the highest balanced accuracy.

In the tables I, II, and III is registered column denotes if functional data in the experiments is registered (registered) or not (unregistered). Column extracted features denotes if only discrete values of functional data are used (only discrete) or discrete values, maximal values, integral depth, or modified band depth (not only discrete). Column number of SLIC regions denotes if, in the experiments, segmentations in each slice are performed with a fixed number of SLIC regions (fixed SLIC) or not (proportionate SLIC).

Table III indicates that the highest median of balanced accuracy - 0.855 is achieved by using non-registered functional data, a proportionate number of SLIC regions to prostate size and extracted features: discrete values, modified band depth, integrated depth and maximal values. For this configuration, tuned hyperparameters on the patient's dataset with the best balanced accuracy were achieved is:

- Subsample ratio of columns when constructing each tree - 0.412 (column colsample bytree)
- Minimum loss reduction required to make a further partition on a leaf node of the tree - 0.005 (column gamma)
- Maximum tree depth for base learners - 6 (column max depth)
- Minimum sum of instance weight(hessian) needed in a child - 0 (column min child weight)
- L1 regularization term on weights - 0.53 (column reg alpha)

Table I indicates that the highest median of mean balanced accuracy - 0.831 is achieved using non-registered functional data, a fixed number of SLIC regions and extracted features: discrete values, modified band depth, integrated depth and

TABLE I
MEDIANS OF FLAT NEURAL NETWORK MODEL'S CLASSIFICATION ACCURACY METRICS ON VALIDATION DATASET

is registered	extracted features	number of SLIC regions	precision mean	precision std	recall mean	recall std	f1 mean	f1 std	**balanced accuracy mean**	balanced accuracy std	specificity mean	specificity std
unregistered	not only discrete	proportionate SLIC	0.369	0.061	0.650	0.071	0.442	0.046	0.772	0.031	0.923	0.036
		fixed SLIC	0.279	0.052	0.733	0.084	0.391	0.040	**0.831**	0.037	0.943	0.028
	only discrete	proportionate SLIC	0.353	0.074	0.633	0.091	0.413	0.059	0.784	0.044	0.936	0.037
		fixed SLIC	0.332	0.041	0.738	0.114	0.395	0.043	0.812	0.056	0.942	0.016
registered	not only discrete	proportionate SLIC	0.332	0.087	0.642	0.145	0.393	0.077	0.775	0.060	0.928	0.030
		fixed SLIC	0.181	0.061	0.660	0.141	0.270	0.044	0.772	0.067	0.935	0.036
	only discrete	proportionate SLIC	0.282	0.078	0.686	0.113	0.364	0.077	0.782	0.052	0.911	0.036
		fixed SLIC	0.186	0.047	0.667	0.076	0.268	0.038	0.801	0.021	0.933	0.017

TABLE II
RESULTS OF FLAT NEURAL NETWORK MODEL'S TUNING (DISPLAYED HYPERPARAMETERS ARE ONLY OF ONE PATIENT FOR WHICH BALANCED ACCURACY ON THE VALIDATION SET IS THE HIGHEST)

is registered	extracted features	number of SLIC regions	activation function	0	1	2	3	4	5	6	7	8	9	10
unregistered	not only discrete	proportionate SLIC	sigmoid	864	416									
		fixed SLIC	sigmoid	1024										
	only discrete	proportionate SLIC	sigmoid	1024										
		fixed SLIC	sigmoid	1024										
registered	not only discrete	proportionate SLIC	sigmoid	1024	384	320								
		fixed SLIC	sigmoid	1024										
	only discrete	proportionate SLIC	sigmoid	1024	32	32	32	32	32	32	32	480	32	1024
		fixed SLIC	sigmoid	672	32	32	32	32	32	32	32	32		

maximal values. Table II indicates that for this configuration, tuned hyperparameters on the patient's dataset with the best balanced accuracy were achieved using the activation function of the last layer - Sigmoid (column activation function) and one layer with 1024 neurons.

The table IV accuracy metrics are aggregated to a single configuration basis by calculating medians. Those configurations are:

- if functional data used in the experiment is registered (registered) or not (unregistered).
- if only discrete values extracted from functional data are used (only discrete), or the addition of discrete values such as modified band depth, integral depth and max values (not only discrete) increases accuracy.
- if in the experiments, segmentations in each slice are performed with a fixed number of SLIC regions (fixed SLIC) or proportionate number of SLIC regions to prostate size (proportional SLIC).
- if the experiments are performed with XGBoost classification (XGBoost) or flat neural network (flat neural network).

Table IV indicates that using unregistered function data (balanced accuracy - 0.804) gives more accurate results than using registered functional data (balanced accuracy - 0.773). Furthermore, it also indicates that using only extracted discrete values from functional data (balanced accuracy - 0.789) gives slightly more accurate results than using maximal values, integrated depth and modified band depth (balanced accuracy - 0.78). However, that contradicts the one made from tables I and III. This contradiction indicates that other configurations have effect on how well do extracted features perform or that the effect of this configuration is very small. Moreover, table IV indicates that using a fixed number of SLIC regions (balanced accuracy - 0.792) gives more accurate results than using a proportionate number of SLIC regions to prostate size (balanced accuracy - 0.783). However, tables I and III indicate that this configuration is dependent on which machine learning algorithm is used. Lastly, the table IV indicates that XGBoost classification algorithm (balanced accuracy - 0.792) is better than Flat neural network (balanced accuracy - 0.785).

Finally, statistical tests are performed on acquired balanced accuracy values. A single sample is formed for each configuration by taking all balanced accuracies that use that exact configuration. Further paired statistical tests are performed on sample pairs of configurations which are compared in the experiments of this paper. As samples are relatively small, the chosen tests are Wilcoxon tests introduced in paper [28]. The resulting p-values acquired by performing statistical tests on samples of balanced accuracies are as follows:

- Using a flat neural network and using XGBoost model -

TABLE III
MEDIANS OF XGBOOST MODEL'S CLASSIFICATION ACCURACY METRICS ON VALIDATION DATASET AND RESULTS OF XGBOOST MODEL'S TUNING (DISPLAYED HYPERPARAMETERS ARE ONLY OF ONE PATIENT FOR WHICH BALANCED ACCURACY ON THE VALIDATION SET IS THE HIGHEST

is registered	extracted features	number of SLIC regions	precision	recall	f1	**balanced accuracy**	specificity	colsample bytree	gamma	max depth	min child weight	reg alpha
unregistered	not only discrete	proportionate SLIC	0.400	0.750	0.471	**0.855**	0.959	0.412	0.005	6	0	0.530
		fixed SLIC	0.500	0.600	0.540	0.794	0.985	0.458	0.002	15	0	0.636
	only discrete	proportionate SLIC	0.455	0.667	0.462	0.810	0.964	0.420	0.000	8	0	0.596
		fixed SLIC	0.500	0.640	0.514	0.793	0.971	0.457	0.247	13	0	0.008
registered	not only discrete	proportionate SLIC	0.571	0.650	0.533	0.780	0.971	0.727	0.019	16	0	0.825
		fixed SLIC	0.450	0.560	0.483	0.748	0.976	0.665	0.080	13	1	0.446
	only discrete	proportionate SLIC	0.500	0.625	0.429	0.752	0.977	0.586	0.020	6	0	0.046
		fixed SLIC	0.500	0.667	0.465	0.750	0.980	0.698	0.007	10	0	0.505

TABLE IV
MEDIANS OF ACCURACY METRICS OBTAINED ON THE VALIDATION DATASET. THIS AGGREGATION IS PERFORMED ON CONFIGURATION BASIS (THE CONFIGURATION IS DENOTED WITH COLUMN EXPERIMENTS DONE WITH)

configuration	precision	recall	f1	**balanced accuracy**	specificity
unregistered	0.382	0.675	0.446	0.804	0.951
registered	0.361	0.657	0.431	0.773	0.948
not only discrete	0.389	0.667	0.457	0.780	0.948
only discrete	0.356	0.667	0.426	0.789	0.951
proportionate SLIC	0.394	0.667	0.450	0.783	0.948
fixed SLIC	0.355	0.667	0.431	0.792	0.953
XGBoost	0.500	0.652	0.502	0.792	0.973
flat NN	0.303	0.675	0.366	0.785	0.934

0.289765.
- Using registered functional data and unregistered functional data - 0.000007.
- Using additional extracted features and using discrete values only - 0.203341.
- Using a fixed number of SLIC regions and a proportionate number of SLIC regions - 0.502053.

To summarize the obtained results, the following comparisons are performed:

- XGboost model's results are compared to flat neural network's results:
  - Median of all validation dataset classification balanced accuracy metrics by using XGBoost classification algorithm is 0.792, while using a flat neural network - 0.785.
  - The highest median of validation dataset balanced accuracy calculated for each configuration separately with XGBoost classification algorithm is 0.855 while with the flat neural network - 0.831.
  - P-value of statistical test performed between these balanced accuracies is 0.289765.
- Using unregistered functional data is compared with registered functional data usage:
  - Median of all validation dataset classification balanced accuracy metrics using non-registered functional data is 0.804, while registered functional data is 0.773.
  - The highest median of validation dataset balanced accuracy calculated for each configuration separately with non-registered functional data is 0.855 while with registered functional data - 0.801.
  - P-value of statistical test performed between these balanced accuracies is 0.000007.
- Using additional extracted features from functional data is compared with using a dataset which represents functional data itself only:
  - Median of all validation dataset classification balanced accuracy metrics by using additional extracted features from functional data is 0.780, while dataset which represents functional data itself only - 0.789.
  - The highest median of validation dataset balanced accuracy calculated for each configuration separately with additional extracted features from functional data is 0.855 while with a dataset representing functional data itself only - 0.812.
  - P-value of statistical test performed between these balanced accuracies is 0.203341.
- Using a proportionate number of SLIC regions to prostate size is compared with using a fixed number of SLIC regions:
  - The highest median of validation dataset balanced accuracy calculated for each configuration separately by using a proportionate number of SLIC zones to prostate size is 0.855 while a fixed number of SLIC zones - 0.794.
  - Using flat neural network algorithm as the highest median of validation dataset balanced accuracy calculated for each configuration separately by using a proportionate number of SLIC zones to prostate size is 0.784 while a fixed number of SLIC zones - 0.831.
  - P-value of statistical test performed between these balanced accuracies is 0.502053.

V. CONCLUSION

The results obtained by this research that:

- XGBoost classification algorithm gives slightly more accurate results (in configuration investigation as well) than the flat neural network. However, the obtained better performance is insignificant as the p-value of the statistical test performed between obtained results is 0.29.
- Unregistered functional data gives significantly more accurate results than registered (in configuration investigation as well). The median of classification balanced accuracy metrics using non-registered functional data is 0.804, while registered functional data - 0.773. The result difference is statistically significant as the p-value of the statistical test performed between these balanced accuracies is less than 0.05.
- There is no significant difference in classification results between using additional extracted features from functional data and using a dataset which represents functional data only (in configuration investigation as well). The median of classification balanced accuracy metrics using additional extracted features from functional data is 0.78, while dataset which represents functional data only - 0.789. However, this comparison is insignificant as the

p-value of the statistical test performed between these balanced accuracies is 0.203.

- Application of proportionate number of SLIC zones to prostate size gives more accurate results than a fixed number of SLIC zones when using XGBoost classification algorithm. The highest median of balanced accuracy calculated for each configuration by using a proportionate number of SLIC zones to prostate size is 0.855 while a fixed number of SLIC zones - 0.794. In opposite, the flat neural network algorithm performs better with fixed number of SLIC zones - 0.831, that proportionate - 0.784 (in terms of balanced accuracy and configuration investigation). This comparison is insignificant as the p-value of the statistical test performed between these balanced accuracies is 0.502.

Results obtained indicate further research directions:

- The experiments should be repeated on higher data variability from more patients. The data variability could be used to explain the proportionate number SLIC zones performance with flat neural networks.
- The search of ensemble classifier that merge the proposed scheme of processing DCE modality with processing other prostate MRI modalities could improve the results.

ACKNOWLEDGMENT

The authors are thankful for the high performance computing resources provided by the Information Technology Research Center of Vilnius University.

REFERENCES

[1] R. Alkadi, F. Taher, A. El-Baz, and N. Werghi, "A deep learning-based approach for the detection and localization of prostate cancer in T2 magnetic resonance images," *Journal of digital imaging*. 32(5), (2019):793-807.

[2] S. Alqahtani and et al, "Prediction of prostate cancer Gleason score upgrading from biopsy to radical prostatectomy using pre-biopsy multiparametric MRI PIRADS scoring system," *Scientific reports 10.1* (2020): 1-9.

[3] P. Banerjee, "A Guide on XGBoost hyperparameters tuning," *Kaggle*. (2020)

[4] T. Barrett and et al, "Ratio of Tumor to Normal Prostate Tissue Apparent Diffusion Coefficient as a Method for Quantifying DWI of the Prostate," *American Journal of Roentgenology* vol 205, (2015): 585-593. Doi: 10.2214/AJR.15.14338.

[5] J. C. Barsce, J. A. Palombarini and E. C. Martínez, "Automatic tuning of hyper-parameters of reinforcement learning algorithms using Bayesian optimization with behavioral cloning," *CoRR* vol abs/2112.08094, (2021)

[6] J. F. F. Bray, I. Soerjomataram, R. L. Siegel, L. A. Torre, and A. Jemal, "Global cancer statistics 2018: GLOBOCAN estimates of incidence and mortality worldwide for 36 cancers in 185 countries," *CA: a cancer journal for clinicians 68.6* (2018): 394-424.

[7] J. Bergstra, R. Bardenet, Y. Bengio, and B. Kégl, "Algorithms for hyper-parameter optimization," *Advances in neural information processing systems* vol. 24 (2011): 394-424.

[8] J. Bergstra, B. Komer, C. Eliasmith, D. Yamins and D. D. Cox, "Hyperopt: a python library for model selection and hyperparameter optimization," *Computational Science & Discovery, 8(1)* p.014008 (2015).

[9] W. Chang and et al, "Prediction of Hypertension Outcomes Based on Gain Sequence Forward Tabu Search Feature Selection and XGBoost," *Diagnostics*, 11(5) (2021) p.792

[10] A. Chatterjee and et al, "Performance of ultrafast DCE-MRI for diagnosis of prostate cancer," *Academic radiology, 25(3)* (2018): 349-358.

[11] T. Chen, and C.Guestrin, "XGBoost: A Scalable Tree Boosting System," *In Proceedings of the 22nd ACM SIGKDD International Conference on Knowledge Discovery and Data Mining*. New York, NY, USA: ACM (2016): 785–794

[12] F. Chollet, and et al, "Keras," *GitHub*. (2015).

[13] R. Cuocolo and et al, "Machine learning applications in prostate cancer magnetic resonance imaging," *European radiology experimental*. 3(1), (2019):1-8.

[14] C. De Vente, P. Vos, M. Hosseinzadeh, J. Pluim, and M. Veta, "Deep learning regression for prostate cancer detection and grading in bi-parametric MRI," *IEEE Transactions on Biomedical Engineering*. 68(2), (2020):374-383.

[15] R. Fraiman and G. Muniz, "Trimmed means for functional data," *Test 10*. (2001): 419–440. doi:10.1007/BF02595706.

[16] G. N. Dimitrakopoulos, A. G. Vrahatis, V. Plagianakos, and K. Sgarbas, "Pathway analysis using XGBoost classification in Biomedical Data," *In Proceedings of the 10th Hellenic Conference on Artificial Intelligence* (2018): 1-6

[17] J. H. Hayes, and M. J. Barry, "Screening for prostate cancer with the prostate-specific antigen test: a review of current evidence," *Jama* 311(11) (2014): pp.1143-1149.

[18] A. M. Hotker and et al, "Assessment of Prostate Cancer Aggressiveness by Use of the Combination of Quantitative DWI and Dynamic Contrast-Enhanced MRI. AJR," *American journal of roentgenology* vol. 206,4 (2016): 756-63. doi:10.2214/AJR.15.14912.

[19] J. Jucevičius and et al, "Automated 2D Segmentation of Prostate in T2-weighted MRI Scans," *International journal of computers communication & control*, [S.l.], v. 12, n. 1, (2016): 53-60. ISSN 1841-9844.

[20] B. Liu and et al, "Prediction of prostate cancer aggressiveness with a combination of radiomics and machine learning-based analysis of dynamic contrast-enhanced MRI," *Clinical radiology*, 74(11) (2019): 896-e1.

[21] J. Liu and et al, "Predicting mortality of patients with acute kidney injury in the ICU using XGBoost model," *Plos one*. (2021);16(2):e0246306.

[22] S. López-Pintado and J. Romo, "On the Concept of Depth for Functional Data" *Journal of the American Statistical Association* v. 104, n. 486 (2009): 718-734. doi:10.1198/jasa.2009.0108.

[23] R. N. Low, D. B. Fuller, and N. Muradyan, "Dynamic gadolinium-enhanced perfusion MRI of prostate cancer: assessment of response to hypofractionated robotic stereotactic body radiation therapy," *American Journal of Roentgenology 197.4* (2011): 907-915.

[24] T. O'Malley and et al, "Keras Tuner," https://github.com/keras-team/keras-tuner (2019).

[25] F. Pedregosa and et al, "Scikit-learn: Machine learning in Python," *Journal of machine learning research* vol. 12, (2011): 2825-2830.

[26] I. Reda and et al, "Deep learning role in early diagnosis of prostate cancer," *Technology in cancer research & treatment*, 17, (2018) p.1533034618775530.

[27] A. Vaitulevičius and et al, "DCE MRI Modality Investigation for Cancerous Prostate Region Detection: Case Analysis ," unpublished.

[28] F. Wilcoxon, "Individual Comparisons by Ranking Methods," *Biometrics Bulletin* vol. 1, (1945): 80-83. doi:10.2307/3001968.

[29] C. J. Wu and et al, "DWI-associated entire-tumor histogram analysis for the differentiation of low-grade prostate cancer from intermediate-high-grade prostate cancer," *Abdom Imaging 40*, 3214-3221 (2015).

4th International Workshop on Artificial Intelligence in Machine Vision and Graphics

THE main objective of the 4th Workshop on Artificial Intelligence in Machine Vision and Graphics (AIMaViG'22) is to provide an interdisciplinary forum for researchers and developers to present and discuss the latest advances of artificial intelligence in the context of machine vision and computer graphics. Recent advancements in artificial intelligence resulted in the rapid growth of both methods and applications of machine learning approaches in computer vision, image processing, and analysis. The development of parallel computing capabilities in the first decade of the 21st century that boosted the development of deep neural networks became a real gamechanger in machine vision. The workshop covers the whole range of AI-based theories, methods, algorithms, technologies, and systems for diversified and heterogeneous areas related to digital images and computer graphics.

TOPICS

The topics and areas include but are not limited to:

- image processing and analysis:
  - image enhancement,
  - linear and non-linear filtering,
  - object detection and segmentation,
  - shape analysis,
  - scene analysis and modeling,
  - scene understanding,
- machine learning for vision and graphics:
  - pattern recognition,
  - deep neural models,
  - convolutional networks,
  - recurrent networks,
  - graph networks,
  - generative adversarial networks,
  - neural style transfer,
  - deep reinforcement learning,
- machine vision:
  - image acquisition,
  - stereo and multispectral imaging,
  - embedded vision,
  - robotic vision,
- image theory:
  - computational geometry,
  - image models and transforms,
  - modeling of human visual perception,
  - visual knowledge representation and reasoning,
- visualization and computer graphics:
  - data-driven image synthesis,
  - graphical data presentation,
  - computer-aided graphic arts and animation,
- applications:
  - innovative uses of graphic and vision systems,
  - image retrieval,
  - autonomous driving systems,
  - remote sensing,
  - digital microscopy,
  - security and surveyance systems,
  - document analysis,
  - OCR systems.

TECHNICAL SESSION CHAIRS

- **Iwanowski, Marcin,** Warsaw University of Technology, Poland
- **Kwaśnicka, Halina,** Wrocław University of Science and Technology, Poland
- **Śluzek, Andrzej,** Khalifa University, United Arab Emirates

PROGRAM COMMITTEE

- **Andrysiak, Tomasz,** Bydgoszcz University of Science and Technology, Poland
- **Angulo, Jesús,** Mines ParisTech, France
- **Cyganek, Bogusław,** AGH University of Science and Technology, Poland
- **Kasprzak, Włodzimierz,** Warsaw University of Technology, Poland
- **Kwolek, Bogdan,** AGH University of Science and Technology, Poland
- **Okarma, Krzysztof,** West Pomeranian University of Technology, Poland
- **Olszewski, Dominik,** Warsaw University of Technology, Poland
- **Palus, Henryk,** Silesian University of Technology, Poland
- **Subbotin, Sergey,** Zaporozhye National Technical University, Ukraine
- **Tomczyk, Arkadiusz,** Lodz University of Technology, Poland

Communication Papers of the of the 17th Conference on Computer Science and Intelligence Systems pp. 33–38
DOI: 10.15439/2022F8
ISSN 2300-5963 ACSIS, Vol. 32

Neural Network Enhanced Automatic Garment Measurement System

Paweł Kowaleczko*[1,2], Przemysław Rokita[1], Marcin Szczuka[3,4]
[1] Institute of Computer Science, Warsaw University of Technology
ul. Nowowiejska 15/19, 00-665 Warsaw, Poland
[2] QED Software sp. z o.o.
ul.Miedziana 3A/18, 00-814 Warsaw, Poland
[3] Institute of Informatics, University of Warsaw
Banacha 2, 02-097 Warsaw, Poland
[3] BAKERS sp. z o.o.
ul. Branickiego 11/154, 02-972 Warsaw, Poland
Email: pawel.kowaleczko.dokt@pw.edu.pl, pro@ii.pw.edu.pl, szczuka@mimuw.edu.pl

***Abstract*—The measurement of garments is most often a very laborious task. Automatic garment measurement systems may be thus a great convenience in fashion e-commerce cataloguing issues. In this paper, we propose an automatic garment measurement system that uses classical computer vision algorithms, as well as an error correction neural network, which reduces the overall error. We make use of data collected by our partner, which contains photographs of garments with ArUco markers. Using such data, we estimate the coordinates of feature points, which are used to calculate a specific size of a garment. We apply the error correction neural network to this measured size to minimize the error. The conducted experiments show, that our method is a useful tool that meets the requirements of practicality and its results are comparable with the current state of the art methods. Additionally, our error correction neural network is a novelty in the field of automatic garment measurement and there is no need for the garments templates, which are used in the previous solutions.**

I. Introduction

IN RECENT years, a huge increase of interest in online shopping can be observed. Since 2017, the global e-commerce market almost doubled its value [1]. Because of its convenience, more and more people do their shopping online. However, shopping for garments may very often be problematic because of the inconsistency in sizes grading. The same piece of cloth may be tagged as size S by one producer, and as size M by another. This inconsistency is the cause of many returns of orders, which is one of the main problems and unnecessary expenses of running a fashion retail business online. To reduce the risk of return it is beneficial to additionally provide the specific dimensions, like sleeve length, waist width etc., in one of the common metrics - centimetres or inches.

The accurate measurement technique is particularly useful in the case of the online second-hand shops. The clothes sold there come from different suppliers and producers, whose size tables may be varied and inconsistent. In some cases, the clothes may have no indication of size whatsoever.

The solutions proposed in this paper are an answer to real-life challenges encountered during the commercial R&D project. The Kidihub (kidihub.com) online second-hand shop specialises in gathering, listing and selling used children's clothes. In Kidihub's business model the clothes are being sent to the company's warehouse by parents, and then assessed and qualified by the staff. The assessment process not only involves verification of quality and state (new, like new, small defect, ...) of the particular piece of clothing, but also leads to more extensive labelling of items. This labelling (tagging) is indeed the main focus of the R&D project. Once a piece of clothing is qualified as worthy listing, it is being ironed and arranged for picture taking. Then, the items need to be tagged with a number of feature values such as sex, colour, pattern, type, and – most crucially – size. The strive to increase the automation of measurement process and reduce the human involvement in the arrangement of clothes and picture-taking is what drives this research.

We propose a method for automatic garment measurement which uses as an input a photograph of a piece of cloth. This photograph includes ArUco marker [2] for the sake of the need to determine the pixel to centimetre ratio to calculate the dimensions in centimetres. However, any marker, even a piece of cardboard, can be used for this task if the detection algorithm of this marker is implemented.

We extract the contours of the garment and find the key feature points essential to determine the specific dimensions, such as points where sleeves end, hips edge points of pants etc. We calculate the Euclidean distance between those points and correct the error using a neural network. The main task of this network is to reduce the calibration error - the photos were taken in different camera to plane distances setups and only a single ArUco marker was provided, so the calibration was not possible. This neural network is also the main novelty of our work, one that makes it possible to reduce the error

This research was co-funded by Smart Growth Operational Programme 2014-2020, financed by European Regional Development Fund, in frame of project POIR.01.01.01-00-0420/20, operated by National Centre for Research and Development in Poland.
*Corresponding author

by roughly 30%. This paper is organized as follows - in Section 2. we shortly describe all related works available in the public domain. In the next section, we describe the dataset collected by our partner and the methods of filtering that we applied, as well as preprocessing methods and implementation details. In Section 4. we explain implemented measurement algorithms in detail for each of the garment types separately. In the next section, we introduce the main novelty of our work, error correction neural network - we explain the purpose of this network, input data preparation methods and architecture. In Section 6. we present the performance of our system, especially laying emphasis on the improvement that the error correction neural network introduces. In the last section, we summarize our work and suggest potential ways of future development and improvement of our system and, in general, the whole area of automatic garment measurement.

II. Related Work

Even though many automatic garment measurement systems exist, most of them are based on determining the physical features of the clothes, where special devices need to be dressed and often photographs from multiple views have to be taken. The most comprehensive overview at all of the methods is presented in [3].

There are only a few works [4], [5], [6] of automatic measurement systems based on the computer vision algorithms. All of them (as in the case of our system) focus on determining the key points based on the corner detection algorithm. Those works then focus on matching the contour of the photographed garment with the predefined template of the garment type contour. Those key points are then matched with the points that are marked on the template contour. We decided to use a different approach, where we do not use any template.

Our automatic measurement module will be a part of a bigger system of automatic garment tagging, part of which will be a garment type classifier. Assuming that we have the garment type information, we defined four measurement algorithms, each for one type of garment. Those types include pants, skirts, sleeveless dresses and top garments with sleeves (t-shirts, jackets, sweaters etc.). To our surprise, none of the previously developed methods make use of deep neural networks, which currently outperform classic algorithms in most computer vision tasks. The main limitation in applying deep neural networks to the automatic garment measurement may be the fact, that they need large amounts of tagged data to train.

III. Dataset and Preprocessing

A. Dataset

We use a dataset collected by Bakers company (the owner of Kidihub store). This dataset consists of 900 images of near HD resolution with various height to width ratios (see Fig. 1). There are nine different types of garments (coats, dresses, jackets, jerseys, shirts, shorts, skirts, tops, trousers). These nine types are later grouped into four groups - tops (coats, jackets, jerseys, shirts, tops), skirts, pants (shorts, trousers) and dresses. To increase the contrast, photos of dark garments were taken on a white background. For the same purpose, bright garments were photographed on black background.

Unfortunately, some parts of the dataset did not meet our contrast requirements so those photos had to be removed. The other cause of rejection was the improper orientation of the photos - some pictures were flipped by 90 degrees. We were unable to rotate them back automatically using the ArUco marker orientation, because in many cases the marker itself was also rotated by some angle. Those requirements resulted in a rejection of 76 pictures, leaving 824 pictures for further processing. All ground truth labels for each picture, such as garment type, color, material and dimensions were annotated by the human operator during the collection process.

B. Preprocessing

Extracting the contour of the garment is essential for the feature points extraction task. We reduce the size of each image so the width of the image is 500 pixels and the height is properly adjusted to the width so the original proportions of images are retained. We apply gamma correction with $\gamma = 0.4$ and increase the contrast of the image multiplying all pixel values by two (adjusted to the maximum 8-bit pixel value). Next, the Canny filter is applied to detect the edges and we dilate the image twice to avoid the situations where there are some gaps in the contour which makes it impossible to detect.

Using such preprocessing methods, the maximal outer contour (which, as we assume, belongs to the garment) is found. Additionally, we detect the ArUco marker (using the function from OpenCV library) and calculate the pixel to cm ratio (real, measured by human operator, ArUco marker size is 10cm) which we then use to adjust the value of the distance between two feature points to be given in centimetres. The general flowchart of our algorithm is outlined in Fig 2.

C. Implementation Details

We decided to use the Python programming language for implementation purposes. Python is known for its syntax simplicity which is the cause that it is currently one of the most popular programming languages. Because Python uses an interpreter, not a compiler, it is considerably slower than other programming languages, like C, C++ or Java. However, in our task the inference time (if it is in reasonable range) is not that important.

We make use of computer vision algorithms implemented in the OpenCV library [7]. For training deep neural networks task we use PyTorch library [8] with its wrapper called PyTorch Lightning [9]. If not stated otherwise we use all functions from those libraries with default parameters values.

IV. Baseline Measurement Model

A. Corner points detection

To find the specific dimensions of a garment, we have to determine the coordinates of feature points, which are usually the corner points of the contour. We focus on analysing the variability of the coordinates of points that are part of the

(a) (b) (c) (d)

Fig. 1: Example pictures from the dataset: dress (a), jacket (b), skirt (c) and trousers (d)

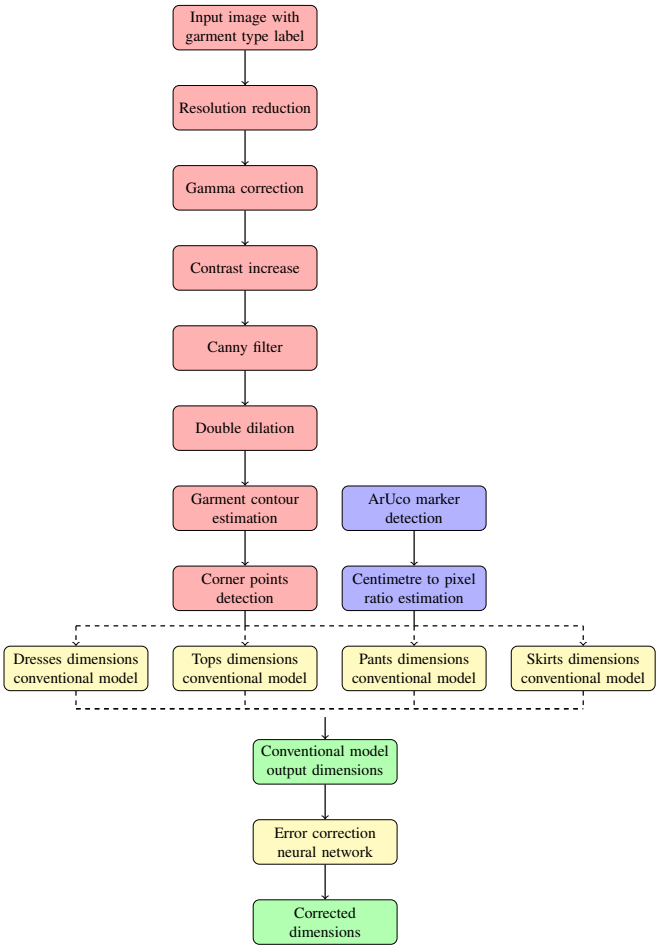

Fig. 2: The flowchart of our proposed measurement method. Preprocessing steps are outlined as red blocks, blue blocks are associated with AruCo marker operations, yellow blocks correspond to dimensioning models' blocks and green block are estimated dimensions blocks. Dashed lines are used in cases where only one processing path is possible.

found contour. Those contour points are ordered counterclockwise in a Python array. If x's or y's derivative with respect to point index in array ($\frac{dx}{d(idx)}$, $\frac{dy}{d(idx)}$) changes its value rapidly (it is discontinuous) we can suspect, that this point is a corner point. We decided to use the index step (step used in calculating the derivatives) equal to five (based on empirical testing) to make the derivative smoother. After calculating the derivatives we calculate the absolute differences between the following derivatives (also using step value equal to five), which should result in a plot of peaks visible in Figure 3. We sum up those differences calculated for the x and y coordinates and find the most distinctive peaks. The whole process is presented in Figure 3. We use those corner points as candidates for the extreme points selection, which are described in the following section, as well as candidates for some of the feature points.

B. Pants Measurement

In the pants measurement task, we need to find the length of pant legs and waist width. We assume that the waist section of the photographed pants is not heavily curved, because we calculate the distance only between two extreme waist points. In this case, we call the feature points that we need to find the extreme points - the outer ends of pant legs and waist points are the four points that are the furthest points of contour with respect to top left, top right, bottom left and bottom right corners of the image. These points are selected from the set of detected corner points. To find the waist width, we calculate the euclidean distance between the top left and top right points of the contour. Pantlegs length is the average of distances between the top left - bottom left and top right - bottom right points.

C. Skirts Measurement

In this task, we need to determine the waist width and total length of the garment. Waist width is found in the same way as it was in the case of pants. To find total length we calculate an approximate middle vertical axis value (the mean value of the x coordinates of the top left and top right points of the contour). Then we find two intersection points of this axis with

the contour points - one in the top part of the contour and one in the bottom.

D. Sleeveless Dresses Measurement

In the sleeveless dresses measurement task we need to determine the total length (which is done the same ways as in the case of skirts) and width in the chest. To find chest width we first define the chest area which is the range of y values included in the subjectively selected range (0.3h, 0.85h) where h is the vertical span of the contour of the garment. We once again define the middle vertical axis the same way, as it was defined in the measurement of the skirts. Then for each y from range (0.3h, 0.85h) and constant value of x vertical axis (point (x_v, y_n)) we find the points from the left and right part of the contour (contour is divided by vertical axis), which distances to those (x_v, y_n) points are the smallest. This way we obtain pairs of points from the left and right parts of the contour, and chest width is the pair which distance is the smallest.

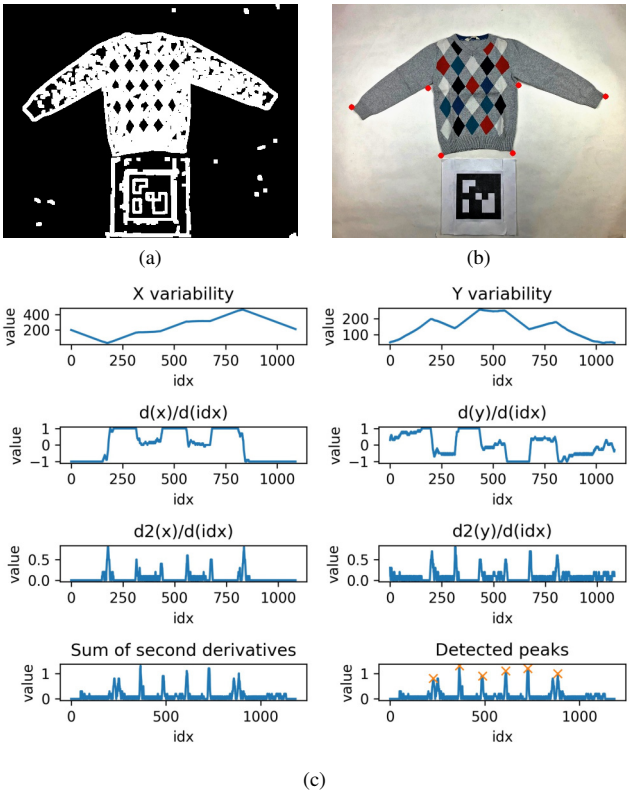

Fig. 3: Corner detection algorithm. (a) image with Canny filter applied, (b) image with marked corner points, (c) plots of variabilities of x and y coordinates of the contour with potential corner points marked with orange crosses on peaks plot.

E. Tops Measurement

Tops measurement was the most challenging task. We need to find bottom width, chest width, sleeves lengths and total length.

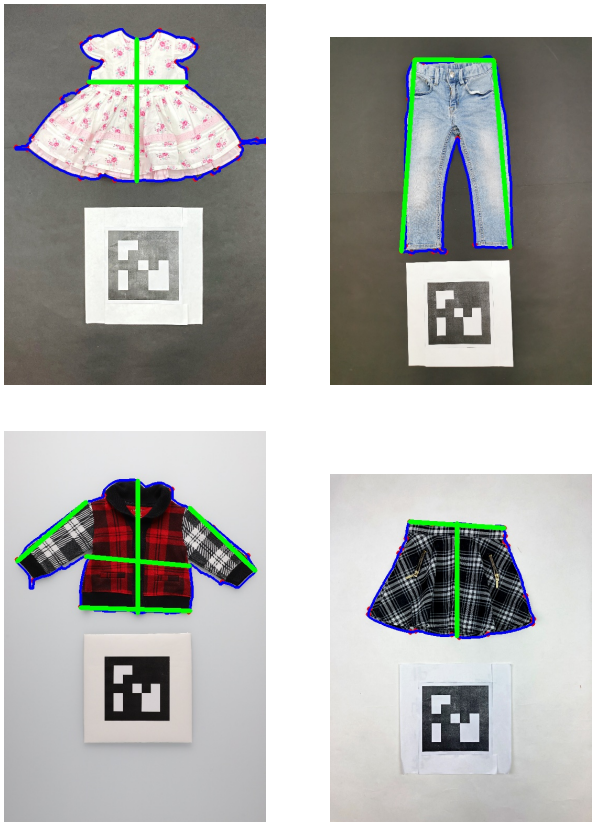

Fig. 4: Output from our automatic measurement system. Measurement dimensions are marked as green lines. Garments are cased in blue contours.

To find the bottom (waist) width we once again use the vertical axis to split the contour into two parts and specify the minimal y value over which (counting from the top of the image, where $y = 0$) the bottom line should be. We arbitrarily choose this value to be in the 0.85 of the vertical span of the garment (difference between top and bottom point of the contour). We divide the contour using the vertical axis and minimal y into the bottom left and bottom right parts. Those parts may include not only the bottom part of the contour, which is our area of interest but also parts of the sleeves. However, those sleeves parts of the contour are separated from our area of interest - the bottom part of the contour. To filter out those sleeve parts we investigate the variability of the values of the x coordinates of these parts - if the distance from the vertical axis increases or decreases rapidly (there is a big gap betwen the x coordinates of the contour points) we reject those points. Then we find the maximal distance between the vertical axis and points of contour left after applying the filtering procedure. The maximal distance for the left and right parts of the contour is equal to the sought bottom width.

We select chest points out of all corner points of the contour. To find chest feature points we firstly restrict the area where

TABLE I: Experimental results of our measurement module on the test dataset. Mean percentage errors and standard deviations of errors are presented for the results from the baseline model and error correction neural network model. In the last column the shares of corrected dimensions in relation to all dimensions are presented.

	Mean percentage error [%]	Error SD [%]	Reduced mean percentage error [%]	Reduced error SD [%]	Percentage corrected [%]
Tops	6.36	5.24	4.10	3.30	66.4
Skirts	4.56	3.30	4.20	3.44	69.2
Pants	7.13	5.29	4.01	2.91	76.7
Dresses	6.08	4.82	3.92	2.66	63.6
All	6.45	5.14	4.07	3.16	69.2

the corner points may be in the $x_b \pm 0.15 \cdot I_{width}$ area, where x_b is the x coordinate of one of the bottom points and I_{width} is the width of the image. We also reject all the feature points for which y coordinates are greater than $y_b - 0.1 \cdot I_{height}$. This way we propose candidates for the potential left and right chest points out of which we select the pair which distance is the smallest.

We determine shoulders points (which are used to find the sleeve lengths and are not corner points, because the curvature of the contour is too small) by choosing the points from the top part of the contour which intersects with two vertical axes. Those axes are x coordinates of the chest points. To get total sleeve lengths we apply contour corner detection algorithms starting from the left shoulder point and going counterclockwise on the contour for the left sleeve and starting from the right shoulder point going clockwise for the right sleeve. The first corner point found is identified as the sleeves feature point. We make sure that the monotonicity changed permanently to reject "local" corner points, which may be a result of some distortions in the contour.

After obtaining all feature points in the way described above we calculate Euclidean distances between them. Sleeve length is the average of right and left sleeve lengths, similarly to the pantlegs lengths.

V. Error Correction Neural Network

After obtaining the dimensions of a measured garment and recounting it into centimetres (using the ArUco marker of known size), there are still possible sources of errors. The main source of errors may be the lack of camera calibration which is essential to reduce the impact of lenses distortions errors. There may be also some imperfections in determining the coordinates of the feature points and we do not take into account the curvature of the contours.

To overcome those issues (especially to simulate the camera calibration) we propose the error correction neural network. This network takes as an input a 14 element vector which includes x and y coordinates of all four ArUco marker corners and two feature points used in the specific measurement process. The two remaining elements of the input are image width and height. The task of this network is to predict the normalized residual, which is the difference between target dimension value (measured by human operator and taken from the dataset) and baseline model prediction (measured by our model) in relation to baseline model prediction (relative percentage error). Such prediction may reduce the total error of our baseline model.

The model itself consists of four fully connected layers with 64, 128, 64, 32 nodes respectively and returns single value - relative percentage error - which may be both positive and negative number. Each layer is followed by batch normalization layer, leaky ReLU activation and dropout (with the probability of dropout of 0.3) layers. We use Adam optimizer and MSE loss function. We did not focus our efforts on finding the most optimal values of network parameters or architecture. This model is trained on the dataset of all independent dimensions evaluated by our base model where the predicted dimensions error is no greater than the 20% of the target dimension. We apply this constraint to reject the predictions which were obvious errors, however, it is not guaranteed that all dataset elements left are correct. Such a dataset have 2369 elements. 90% of the dataset is then used for training and 10% for testing. The final measurement of our system $Dim_{corrected}$ is obtained by applying the simple equation:

$$Dim_{corrected} = (1 + ECNN_{out}) \cdot Dim \tag{1}$$

where $ECNN_{out}$ is the output of the error correction neural network, and Dim is the output dimension from the conventional model.

VI. Experimental Results

As it was stated in the previous section, we reject those measurements for which the error is greater than 20%. We assume that such errors will be easy to notice on the output image (Figure 4) and those images will be rejected by a human operator after just taking a look at the result of our baseline model measurement. All ground truth values are measured by the employees of Kidihub during the process of photographing. In Table I, we present the experimental results per each category of our baseline automatic measurement system tested on test dataset. Each of our measurements is a Euclidean distance between two specific key points (which are described in detail in the previous section). We do not consider the curvature of the cloth, hence our requirement that the garment should be tiled on a photograph. The mean percentage relative error (relative error of measured size in centimetres in relation to ground truth size) varies from 4.56% for skirts to 7.13% for pants and is 6.45% on average for all garments (row All). The standard deviation of error for all categories is also quite high - 5.14%. After applying the error correction neural network

the mean percentage error is significantly reduced for each category, and on average by almost 30%. The average error for all categories is reduced to 4.07%. For each category, the majority of measurement results errors were reduced (on average for 69.2% of data). Target data resolution, which is 1cm, also have a significant impact on the final error value. The value of the average error of which the source is the measurement resolution is 3.16%. One should also have in mind that the process of measuring the garments may also produce some kind of human-related error - the measured piece of cloth may be partially folded or the human annotator may read the result of measurement incorrectly. Because of this quite significant level of measurement resolution error, as well as potential human annotator errors, it is hard to tell if our method outperforms state of the art solutions, of which errors are about 2-3%.

VII. Conclusions

We proposed a set of fast automatic measuring algorithms for four different categories of garments. We designed those algorithms with the quality and characteristics of the dataset from our partner, as well as their requirements in mind. The pictures must contain tiled garments on a contrasting background with the specific ArUco marker. We also must know the category of the garment, however, this step will be automated in our system by applying garment classification neural network in the future. We introduced the error correction neural network, which reduces the error on average by 2.38%. This neural network does not need any additional information as an input, it uses only information extracted from the images by classic computer vision algorithms. Application of this neural network reduces the mean average error to about 4%, however very significant is the fact, that the resolution of the ground truth dimensions that we compare to is rather low (1cm) which results in large measurement resolution error of 3.16% on average. Taking this into account our method is very close to the state of the art methods (about 2-3% of relative error) and do not need a special shooting setup, camera calibration and garment category template as the previous methods did.

There are still many areas of our system, that can be improved. We especially have in mind our baseline algorithm in this regard. We pin our hope on involving more neural network solutions. In our opinion, if a dataset of images and all feature points would be provided, the neural network trained on such dataset would easily outperform state of the art methods. However, collecting such a dataset is a laborious task. Our solution also would surely benefit from filtering the output data from our baseline model on which we train the error correction neural network. We also think that it would be beneficial to check how our solution works if the calibration pattern was present on the images. The reason for this is that we are not entirely sure what types of errors and to what extent the error correction neural network reduces. If those errors were orthogonal to the calibration error, such a system would probably outperform current state of the art methods without the additional constraints.

References

[1] S. Chevalier, Retail e-commerce sales worldwide from 2014 to 2024.
URL https://www.statista.com/statistics/379046/worldwide-retail-e-commerce-sales/

[2] A. Rosebrock, Detecting ArUco markers with OpenCV and Python - an online tutorial.
URL https://www.pyimagesearch.com/2020/12/21/detecting-aruco-markers-with-opencv-and-python/

[3] J. Juvonen, Study of the automatic garment measurement, report prepared for ROBOCOAST EU network by Aarila Dots Oy. (2019).
URL https://new.robocoast.eu/wp-content/uploads/2020/09/Feasibility-study-Automatic-garment-measurement_Aarila-Dots.pdf

[4] L. Cao, Y. Jiang, M. Jiang, Automatic measurement of garment dimensions using machine vision, in: 2010 International Conference on Computer Application and System Modeling (ICCASM 2010), Vol. 9, 2010, pp. V9–30–V9–33. doi:10.1109/ICCASM.2010.5623093.

[5] K. Chen, Image analysis technology in the automatic measurement of garment dimensions., Asian Journal of Information Technology 4 (9) (2005) 832–834.
URL https://medwelljournals.com/abstract/?doi=ajit.2005.832.834

[6] C. Li, Y. Xu, Y. Xiao, H. Liu, M. Feng, D. Zhang, Automatic measurement of garment sizes using image recognition, in: Proceedings of the International Conference on Graphics and Signal Processing, ACM, 2017, pp. 30–34. doi:10.1145/3121360.3121382.

[7] G. Bradski, A. Kaehler, The OpenCV Library, Dr. Dobb's Journal of Software Tools 3 (2000).

[8] A. Paszke, S. Gross, F. Massa, A. Lerer, J. Bradbury, G. Chanan, T. Killeen, Z. Lin, N. Gimelshein, L. Antiga, A. Desmaison, A. Kopf, E. Yang, Z. DeVito, M. Raison, A. Tejani, S. Chilamkurthy, B. Steiner, L. Fang, J. Bai, S. Chintala, Pytorch: An imperative style, high-performance deep learning library, in: H. Wallach, H. Larochelle, A. Beygelzimer, F. d'Alché-Buc, E. Fox, R. Garnett (Eds.), Advances in Neural Information Processing Systems (NeurIPS 2019), Vol. 32, Curran Associates, Inc., 2019. doi:10.48550/arXiv.1912.01703.
URL https://arxiv.org/abs/1912.01703

[9] W. Falcon, et al., PyTorch Lightning, gitHub repository. (2019).
URL https://github.com/PyTorchLightning/pytorch-lightning

Communication Papers of the of the 17th Conference on Computer Science and Intelligence Systems pp. 39–43
DOI: 10.15439/2022F98
ISSN 2300-5963 ACSIS, Vol. 32

Face and silhouette based age estimation for child detection system.

Tomasz Lehmann*, Andrzej Pacut† and Piotr Paziewski‡
Research and Academic Computer Network (NASK), Warsaw, Poland
Email: *tomasz.lehmann@nask.pl, †andrzej.pacut@nask.pl, ‡piotr.paziewski@nask.pl

***Abstract*—The problem of age estimation based on facial images is a well-known computer vision task that is widely applied in identification systems. With help of the special *Dyzurnet.pl* unit detecting Internet content, related to sexual abuse of children we slightly redefined a problem. Our *Convolutional Neural Network (CNN)* solution is focused on infants and prepubescents recognition and in the particular age ranges can be considered as *the-state-of-the-art* in children detection.**

Silhouette-based age estimation is often concentrated on the human gait or body proportions analysis. Single image age estimations on the dressed (fully or partly) body are not typically researched because of a lack of properly labeled data. In our work, we present the method used to train image preparation and the final effectiveness of age estimation of that kind.

The proposed solution is a part of the system for responding to threats to children's safety in cyberspace with particular emphasis on child pornography

I. Introduction

CHILD pornography is a form of child sexual exploitation. European law defines child pornography as any visual depiction of sexually explicit conduct involving a minor (persons younger than an age adopted in the resolution of the particular country). The advancement of artificial intelligence technology, particularly in image classification and object detection, could be applied to overcome the current flaws of child sexual abuse material. The problem of the age estimation of people detected on the single image is considered one of the most important tasks in this project. In the following paper, we show methods for face-based and silhouette-based age estimation. The author's main contributions to the age estimation problem are a novel child categorization based on their sexual maturity and the untypical methodology of database creation.

The presented approach is based on convolutional neural network *CNN* classification. *CNNs* are regularized versions of multilayer perceptions where they take advantage of the hierarchical pattern in data and assemble patterns of increasing complexity using smaller and simpler patterns embossed in their filters. This kind of artificial neural network has become dominant in various computer vision tasks.

To implement face age estimation in the wild, age estimation must be combined with face detection. Figure 1 illustrates face age estimation combined with face detection. In this paper, we analyze the usefulness of publicly available datasets. Also, we address the issue of the head pose in the context of face-based age estimation.

Fig. 1: Face age estimation vizualization.

A. Related Works

Age estimation based on face images is an object of many scientific papers and projects [1], [2], [3]. Most often, it is defined as an estimation of accurate age (with 1-year precision). Exception of this rule is the *oui-adience* project [4], where authors defined 8 age ranges. In our paper, we define age estimation as classification into one of 4 age ranges: 0-2, 3-12, 13-17, and 18+. These ranges were proposed by the *Dyżurnet.pl* team. The team responds to anonymous reports received from Internet users about potentially illegal material, mainly related to the sexual abuse of children. Age ranges have been established according to sexual maturity stages.

Silhouette-based age estimation is much less popular in scientific papers. Age prediction from human body images was presented in [5] where authors used their training dataset which contained just 1500 elements. In the context of child detection, the method based on the ratio between head and body heights was also proposed in [6]. The greatest number of researches touched an area of gait-based human age classification ([7], [8], [9]) but to our newest knowledge, there is any application for a single image age classification based on still body images. In this paper, we present our method of database collecting and our results achieved on the test dataset.

II. Experimental setup

A. Datasets

1) Face based age estimation: As there are many papers and projects addressing face age estimation, there are also many datasets for this task. However, the distribution of age in the majority of available datasets does not fit our purposes. Table I shows the number of samples for each class for different datasets. Publicly available datasets differ not only in sample quantity and age distribution but also in label quality. *Imdb* [1], *wiki* [1], *magaage* [14], and *adience* [4] datasets have relatively many samples but labels quality is low while *appa* [10] and *fgnet* [11] datasets have relatively few samples

but labels quality is high. *Appa* dataset is often used as a benchmark for face age estimation solutions. For every image, it contains 2 labels. One label corresponds to real age and the second label corresponds to apparent age that is estimated by a group of experts. In our research, we decided to use the apparent labels as they had fewer outliers than real-age labels. For research purposes, we also created an in-house dataset based on part of images from *AFW* dataset [12] and *HELEN* dataset [13].

TABLE I: Number of samples for each class for different datasets.

Dataset	**Number of samples**			
	0-2	**3-12**	**13-17**	**18+**
imdb	14	1552	4215	177235
wiki	6	107	738	43373
megaage	0	4986	9239	27326
adience	1817	3174	1122	6151
appa	108	533	284	5947
fgnet	70	372	159	362
in-house	82	207	89	407

One of the most important characteristics of face age estimation datasets is head pose distribution. To examine head pose in publicly available datasets, we used *WHENet* estimator [15]. Figure 2 shows head poses distribution on publicly available datasets. Results show that the great majority of faces in publicly available datasets have a frontal pose. This is a serious problem if the trained model is supposed to be used on *in-the-wild* photos. To address this issue, we propose the usage of the dataset used in one of the face alignment problem projects [16] (later referred as face alignment dataset). In the referring dataset, for every face image, there are several images with artificially rotated heads. An example of an original image with several artificially rotated heads is shown in Figure 3. As images from face alignment dataset come among others from *AFW* and *HELEN* datasets, we were able to easily match images from our in-house dataset (which also contains images *AFW* and *HELEN* datasets) with images from *face_alignment* dataset.

Fig. 3: Examples of artificial head rotations.

2) Silhouette based age estimation: Because of the lack of databases dedicated to silhouettes based age estimation as a base for our research, we used *imdb* database [1]. Age distribution and image diversity were not satisfying and we decided to exploit a web crawler that downloaded extra images of people mostly younger than 15 years old (photos were examined by downloaded content). Single silhouette images were obtained with *YOLOv3* algorithm [17]. We used *Dlib-ml* [18] software for face detection and we removed images that contained none or more than a single one. Detected faces were used to label our non-label part of the database with the face-based age estimation model which predicted an accurate age on a scale 0-99 [3]. In this way, we received a database containing 794567 labeled images.

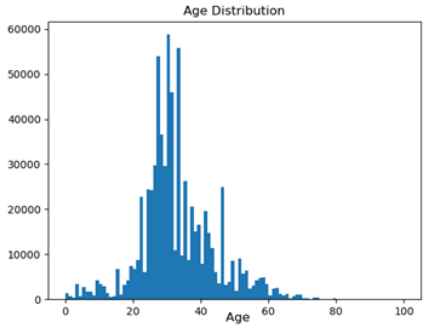

Fig. 4: Age distribution of received silhouette based database.

Figure 5 depicts few examples of images included to the final database.

Fig. 5: Silhouette-based age estimation database examples.

B. Proposed methods

1) Face based age estimation: For face based age estimation we decided to use *resnet* [21] architecture with 4 neurons in the output layer. It is a convolutional neural network that can be utilized as a *state-of-the-art* image classification model. During tests, we used *resnet* networks with different depths (*resnet50*, *resnet101*) in order to keep optimal model size compared to training data size. Similar implementation techniques were presented in [20]. For the loss function, we used cross-entropy presented in Figure 6. As a metric, we used *Balanced Mean Absolute Error (BMAE)* and for the training algorithm, we used ADAM [24]. To level the distribution of labels during training, we decided to use an undersampling technique. Undersampling is a popular method used for balancing uneven datasets by keeping all of the data in the minority class and decreasing the size of the majority class. For data augmentation we used *autoAgment* [19] transformations. During tests, every training configuration was run 5 times with different data split for training, validation, and test sets. It is a popular technique for assessing how the results of a statistical analysis will generalize to an independent data set.

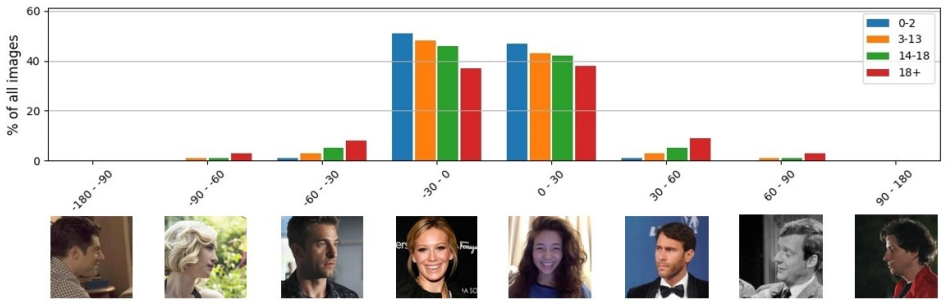

Fig. 2: Head poses distribution on publicly available datasets.

$$Loss = -\sum_{c=1}^{M} y_{o,c} \log(p_{o,c})$$

M number of classes

y binary indicator (0 or 1)

if class label c is the correct classification for observation o

p predicted probability observation o is of class c

Fig. 6: Cross-Entropy loss function.

2) Silhouette based age estimation: For silhouette based age estimation we proposed pretrained on *ImageNet* [22] dataset *senet154* [23] architecture with added *perceptron* to in the final layer. The mentioned fully connected neural network changes size of output to 100 elements which corresponds to age classes. *SENet* architectures generalise extremely well across challenging datasets which made results slightly better than using *resnet*. As a loss function we chose *Mean Squared Error (MSE)* defined as:

$$MSE = \frac{1}{n}\sum_{n}(x_n - y_n)^2$$

n number of tensors

x_n tensor ground truth

y_n tensor prediction

Fig. 7: MSE formula.

ADAM [24] was chosen as the optimizer.

We decided to split the dataset into three parts: train, test and validation subsets, with proportions 80:15:5. Validation process was supposed to determine optimal training parameters.

C. Results

1) Face based age estimation:

a) Dataset selection: Due to the high number of available datasets and their different characteristics, datasets selection is not obvious. To analyze which datasets increase the accuracy (*BMAE*) of the model, we run multiple tests with the usage of different datasets. We started using only *appa* dataset and with every next test, we expanded the used datasets. For every configuration, we tested accuracy on in-house dataset for *resnet50* and *resnet101* architectures. Table II shows results of described tests. Even though some of the datasets had low-quality labels, they still improved the accuracy of the model. Usage of deeper networks did not improve model performance.

b) Model optimization for wide range of head poses: To prepare the model for in-the-wild images with a wide range of head poses, we produced an in-house dataset with artificially rotated heads as described in the "datasets" section. For research purposes, we split images from in-house datasets to train, valid, and test. Then, for every image from the in-house dataset, we took 3 corresponding images from *face_alignment* dataset with different rotations: R0 (head without rotation), R1 (heads with 45 degrees rotation), and R2 (heads with 90 degrees rotation). Finally, we compared the performance of the model with and without rotated head samples in train/valid sets. We tested the performance of models on images with different head poses (R0, R1, R2) and on *appa* images to make sure that additional data do not decrease model performance on *appa* dataset. Results of the described experiment are shown in Table III. Results show that age estimation accuracy decreases with head rotation. That is a highly not desirable situation that could be problematic during age identification on the real sexual abuse images. The addition of images from the face_alignment dataset has significantly increased model accuracy on images with head rotation.

c) Model performance on appa dataset: Appa dataset is widely used as benchmark for age estimation problem. In order to obtain optimal performance on refereed dataset, we split training into two phases. Inspiration for this technique comes from [1]. In first phase, model is trained on *imdb*, *appa*, *adience*, *megaage* and *fgnet* dataset. In second phase, model is trained only on *appa* dataset. Model performance on *appa* test data (10% of appa dataset) is shown on table IV and V.

TABLE II: BMAE for different datasets sets and different network depths.

appa	fgnet	adience	megaage	imdb	wiki	BMAE	
						resnet50	resnet101
✓	X	X	X	X	X	0.374 +/- 0.042	0.403 +/- 0.046
✓	✓	X	X	X	X	0.358 +/- 0.024	0.381 +/- 0.034
✓	✓	✓	X	X	X	0.337 +/- 0.024	0.366 +/- 0.043
✓	✓	✓	✓	X	X	0.302 +/- 0.047	0.303 +/- 0.017
✓	✓	✓	✓	✓	✓	0.221 +/- 0.021	0.232 +/- 0.027

TABLE III: BMAE for different models and different test data.

usage of face_alignment dataset during training	BMAE			
	R0	R1	R2	appa
yes	0.244 +/- 0.054	0.285 +/- 0.03	0.616 +/- 0.094	0.256 +/- 0.016
no	0.221 +/- 0.023	0.242 +/- 0.03	0.383 +/- 0.039	0.255 +/- 0.028

TABLE IV: MAE score on *appa* for age range classification for different age ranges for face based age estimation.

Age range	MAE
0-2	0.134 (+/-0.055)
3-12	0.175 (+/-0.048)
13-17	0.217 (+/-0.1)
18+	0.401 (+/-0.079)

TABLE V: Confusion matrix for age range classification for different age ranges for face based age estimation.

Label age range	Predicted age range			
	0-2	3-12	13-17	18+
0-2	86%	14%	<1%	<1%
3-12	10%	81%	8%	1%
13-17	<1%	8%	77%	15%
18+	<1%	1%	14%	85%

Depicted results should be interpreted as promising, however, because of untypical age ranges and labeling procedures they cannot be compared with other *state-of-the-art* solutions. The innovation of the method makes it incomparable.

2) Silhouette based age estimation: We assessed results by analyzing two main criteria: *Mean Absolute Error (MAE)* in the given age range and confusion matrix for the processed output where age was grouped in the same way as it was during face-based age estimation.

TABLE VI: MAE score for different age ranges.

Age range	MAE
0-2	3.42 +/- 0.15
3-12	3.68 +/- 0.17
13-17	2.17 +/- 0.10
18+	7.77 +/- 1.20

TABLE VII: Confusion matrix for output processed data.

Confusion matrix	Age range predicitons			
Age range labels	0-2	3-12	13-17	18+
0-2	65%	25%	8%	3%
3-12	<1%	68%	20%	11%
13-17	<1%	9%	65%	26%
18+	<1%	3%	9%	88%

We can observe that *MAE* scores are the best for categories that include images of children and teenagers. It is what we have expected because of the tightest age ranges. From the point of an ongoing project that is an important feature. Otherwise, the confusion matrix shows us that adults' predictions are more accurate than in the other age categories. It might be an effect of unbalanced data or human body biological attributes which indicates sexual maturity. Presented results are much less correct than in face-based age estimation. This is the result of the worse quality of images and accumulating approximation which is the consequence of database collecting and labeling procedures.

III. Conclusions

Achieved results will be evaluated on the database specially constructed for *the APAKT* project. The database will include real images of child sexual exploitation as well as adult pornography. Face-based age estimation results can be considered the best solution dedicated to the detection of infants, prepubescent and pubescent children. Untypical age ranges and labeling procedures make our models incomparable with other *state-of-the-art* solutions. Silhouette-based age estimation delivers relatively worse results but requires the construction of a new database. It is a new perspective on the case of age estimation. The next part of the research will be optimizing results for a given database which will also contain illegal and sensitive content with minor nudity.

IV. Acknowledgement

Presented work is a part of the *System for responding to threats to children's safety in cyberspace with partic-*

ular emphasis on child pornography (APAKT) CYBERSECIDENT/455132/III/NCBR/2020 project financed by *Polish National Center for Research and Development*.

REFERENCES

[1] R. Rothe, R. Timofte, L. Van Gool. 2015. "DEX: Deep EXpectation of Apparent Age from a Single Image". 2015 IEEE International Conference on Computer Vision Workshop (ICCVW), pp. 252-257. doi: 10.1109/ICCVW.2015.41.

[2] H. Pan, H. Han, S. Shan, X. Chen. 2018. "Mean-Variance Loss for Deep Age Estimation from a Face". 2018 IEEE/CVF Conference on Computer Vision and Pattern Recognition, pp. 5285-5294. doi: 10.1109/CVPR.2018.00554.

[3] Y. Tingting, W. Junqian, W. Lintai, X. Yong. 2019. "Three-stage network for age estimation". 2019. CAAI Transactions on Intelligence Technology. doi: 10.1049/trit.2019.0017

[4] G. Levi, T. Hassner. 2015. "Age and Gender Classification Using Convolutional Neural Networks". IEEE Workshop on Analysis and Modeling of Faces and Gestures (AMFG) at the IEEE Conf. on Computer Vision and Pattern Recognition (CVPR). doi: 10.1109/cvprw.2015.7301352

[5] Y. Ge, J. Lu, W. Fan and D. Yang. 2013. "Age estimation from human body images". 2013 IEEE Conference on Acoustics. Seech and Signal Processing. doi: 10.1109/ICASSP.2013.6638072

[6] O. F. Ince, J. Park, J. Song, B. Yoon. 2014. "Child and Adult Classification Using Ratio of Head and Body Heights in Images". International Journal of Computer and Communication Engineering. doi: 10.7763/IJCCE.2014.V3.3042

[7] O. F. Ince, J. Park, J. Song, B. Yoon. 2021. "Real-Time Gait-Based Age Estimation and Gender Classification from a Single Image". Proceedings of the IEEE/CVF Winter Conference on Applications of Computer Vision (WACV). doi: 10.1109/WACV48630.2021.00350

[8] N. Mansouri, M. Aouled Issa, Y. B. Ben Jemaa. 2017. "Gait-based Human Age Classification Using a Silhouette Model". IET Biometrics. doi: 10.1049/iet-bmt.2016.0176

[9] H. Zhu, Y. Zhang, G. Li, J. Zhang, H. Shan. 2019. "Ordinal Distribution Regression for Gait-based Age Estimation". SCIENCE CHINA Information Sciences. doi: 10.1007/s11432-019-2733-4

[10] E. Agustsson, R. Timofte, S. Escalera, X. Baro, I. Guyon, R. Rothe, 2017. "Apparent and Real Age Estimation in Still Images with Deep Residual Regressors on Appa-Real Database". 2017 12th IEEE International Conference on Automatic Face & Gesture Recognition (FG 2017), pp. 87-94. doi: 10.1109/FG.2017.20.

[11] Y. Fu, T. M. Hospedales, T. Xiang, J. Xiong, S. Gong, Y. Wang, Y. Yao. 2016. "Robust Subjective Visual Property Prediction from Crowdsourced Pairwise Labels". IEEE Transactions on Pattern Analysis and Machine Intelligence, 38(3). 563–577. doi: 10.1109/tpami.2015.2456887

[12] X. Zhu, D. Ramanan. 2012. "Face detection, pose estimation, and landmark localization in the wild". 2012 IEEE Conference on Computer Vision and Pattern Recognition. pp. 2879-2886. doi: 10.1109/CVPR.2012.6248014.

[13] V. Le, J. Brandt, Z. Lin, L. Bourdev, T. S. Huang. 2012. "Interactive Facial Feature Localization". Lecture Notes in Computer Science. 679–692. doi:10.1007/978-3-642-33712-3_49

[14] Y. Zhang, L. Liu, C. Li, C.-C. Loy, Chen Change. 2017. "Quantifying Facial Age by Posterior of Age Comparisons". Proceedings of the British Machine Vision Conference (BMVC). doi: 10.5244/C.31.108

[15] Zhou, Yijun, Gregson, James. 2020. "WHENet: Real-time Fine-Grained Estimation for Wide Range Head Pose". arXiv. doi: 10.48550/arXiv.2005.10353

[16] X. Zhu, Z. Lei, X. Liu, H. Shi, S. Li. 2016. "Face Alignment Across Large Poses: A 3D Solution". 2016 IEEE Conference on Computer Vision and Pattern Recognition (CVPR). pp. 146-155. doi: 10.1109/CVPR.2016.23

[17] J. Redmon, A. Farhadi. 2018. "YOLOv3: An Incremental Improvement". arXiv:1804.02767. doi: 10.48550/arXiv.1804.02767

[18] D. King, A. Farhadi. 2009. "Dlib-ml: A machine learning toolkit". Journal of Machine Learning Research

[19] Cubuk, E. D., Zoph, B., Mane, D., Vasudevan, V., Le, Q. V. 2019. "AutoAugment: Learning Augmentation Strategies From Data". 2019 IEEE/CVF Conference on Computer Vision and Pattern Recognition (CVPR). doi:10.1109/cvpr.2019.00020

[20] M. Leppioja, P. Luuka, C. Lohrmann. 2021. "Image based classification of shipments using transfer learning". Recent Advances in Business Analytics. Selected papers of the 2021 KNOWCON-NSAIS workshop on Business Analytics. ACSIS, Vol. 29. pages 37–44 (2021), doi: 10.15439/2021B4

[21] K. He, X. Zhang, S. Ren, J. Sun. 2016. "Deep Residual Learning for Image Recognition". 2016 IEEE Conference on Computer Vision and Pattern Recognition (CVPR). pp. 770-778. doi: 10.1109/CVPR.2016.90.

[22] J. Deng, W. Dong, Socher, R., Li-Jia Li, Kai Li, Li Fei-Fei. 2009. "ImageNet: A large-scale hierarchical image database". 2009 IEEE Conference on Computer Vision and Pattern Recognition. doi:10.1109/cvprw.2009.5206848

[23] J. HU, L. Shen, G. sun. 2018. "Squeeze-and-Excitation Networks". IEEE Conference on Computer Vision and Pattern Recognition. doi: 10.1109/CVPR.2018.00745

[24] D. P. Kingma, J. Ba. 2014. "Adam: A Method for Stochastic Optimization". Proceedings of the 3rd International Conference on Learning Representations. doi: 10.48550/arXiv.1412.6980

1st Workshop on Personalization and Recommender Systems

RECOMMENDER Systems are present in our everyday life while we reading news, logging in to social media or buying something at e-shops. Thus, it is not suprising that this domain is getting more and more attention from researchers from academia as well as from industry practitioners. However, the way in which they look at the same problem differs a lot.

Personalization is an important element in novel recommendation techniques. Nonetheless, it is a wider topic that concerns also user modelling and representation, personalized systems, adaptive educational systems or intelligent user interfaces.

The objective of PeRS is to extend the state-of-the-art in Personalization and Recommender Systems by providing a platform at which industry practitioners and academic researchers can meet and learn from each other. We are interested in high quality submissions from both industry and academia on all topics related to Personalization and Recommender Systems.

TOPICS

The list of topics includes, but is not limited to:

- Personalization
  - User Profiles
  - Ontology-based user models
  - Personalized systems
  - Intelligent user interfaces
- Recommender Systems approaches
  - Collaborative Recommender Systems
  - Semantic-based Recommender Systems
  - Context-aware Recommender Systems
  - Cross-domain Recommender Systems
- Machine Learning techniques for Recommender Systems
  - Association Rules
  - Clustering methods
  - Neural Networks
  - Deep Learning
  - Reinforcement Learning
- Applications of Recommender Systems methods
  - News recommendations
  - Tourism recommendations
  - Fashion recommendations
  - Podcasts recommendations
  - Medical recommendations
  - Other domain-specific recommenders
- Evaluation of Recommender Systems
  - Metrics
  - Evaluation studies
  - Reproducibility of existing methods
  - Case studies of real-world implementations

TECHNICAL SESSION CHAIRS

- **Karpus, Aleksandra,** Gdańsk University of Technology, Poland
- **Przybyłek, Adam,** Gdańsk University of Technology, Poland

PROGRAM COMMITTEE

- **Anelli, Vito Walter,** Politechnic University of Bari, Italy
- **Aziz Butt, Shariq,** University of Lahore, Pakistan
- **Borg, Markus,** SICS Swedish ICT AB, Sweden
- **Brzeski, Adam,** Gdańsk University of Technology, Poland
- **Cellary, Wojciech,** WSB Universities in Poznan, Poland
- **Dedabrishvili, Mariam,** International Black Sea University, Georgia
- **de Gemmis, Marco,** University of Bari "Aldo Moro", Italy
- **Dutta, Arpita,** National University of Singapore, Singapore
- **Ghofrani, Javad,** University of Lübeck, Germany
- **Goczyła, Krzysztof,** Gdańsk University of Technology, Poland
- **Inayat, Irum,** National University of Computer and Emerging Sciences, Pakistan
- **Lops, Pasquale,** University of Bari "Aldo Moro", Italy
- **Madeyski, Lech,** Wroclaw University of Technology, Poland
- **Marcinkowski, Bartosz,** University of Gdańsk, Poland
- **Misra, Sanjay,** Ostfold University College, Halden, Norway
- **Mohapatra, Durga Prasad,** NIT Rourkela, India
- **Mukta, Saddam Hossain,** United International University, Bangladesh
- **Ng, Yen Ying,** Nicolaus Copernicus University, Poland
- **Nguyen, Phuong T.,** University of L'Aquila, Italy
- **Nocera, Francesco,** Politechnic University of Bari, Italy
- **di Noia, Tommaso,** Politechnic University of Bari, Italy
- **Orłowski, Cezary,** WSB University in Gdańsk, Poland
- **Polignano, Marco,** University of Bari "Aldo Moro", Italy
- **Poniszewska-Maranda, Aneta,** Lodz University of Technology, Poland

- **Szymański, Julian,** Gdańsk University of Technology, Poland
- **Taweel, Adel,** Birzeit University, Palestine
- **Theobald, Sven,** Fraunhofer IESE, Germany
- **Tkalcic, Marko,** University of Primorska, Slovenia
- **Vagliano, Iacopo,** Amsterdam University Medical Center, Netherlands
- **Wrycza, Stanisław,** University of Gdańsk, Poland

Communication Papers of the of the 17th Conference on Computer Science and Intelligence Systems pp. 47–54
DOI: 10.15439/2022F75
ISSN 2300-5963 ACSIS, Vol. 32

Evaluating Diversification in Group Recommender Systems*

Amanda Chagas de Oliveira
Institute of Computing
Federal University of Bahia

Frederico Araujo Durao
Institute of Computing
Federal University of Bahia

***Abstract*—The formation of groups is an ordinary event in our routines. For example, people used to lunch, travel, or hang out in groups. Conversely, getting a consensus over an item may be difficult for some groups as the number of digital information increases. Group Recommender Systems (GRS) rise to assist in this task, as they filter which items may be more relevant to the group. Although there are consensus techniques to help in this matter, recommendations to groups can become monotonous, and this opens space for applying diversification techniques to improve recommendations. In this paper, we expose a model for recommendation to groups using diversification techniques and present the results of the online experiment where the proposal obtained an increase in precision at all levels compared with baseline.**

I. Introduction

RECOMMENDER Systems (RS) are automated tools for locating the information that is pertinent to the user [1]. Although most RS are made to serve a single user, there are instances where a group of interests must be considered. Therefore a Group Recommender System (GRS) must consider each member's preferences.

A GRS has the role of finding what is relevant to a group rather than to individuals. Given that we live in communities participating in group activities is a usual behavior in everyday life. However, even straightforward tasks such as selecting a playlist for a group of friends can be challenging. All individual preferences must be considered when processing recommendations in a group scenario. The group size at least multiplies the recommendation problem. Therefore, it is necessary to use consensus techniques to identify the items that satisfy the group as a whole as well as each member. In the literature, GRS has been examined from a variety of angles. [1] investigate strategies for aggregating individual preferences, [2] study on effective group recommendation methods, and [3] use various strategies when recommending items to groups.

Group recommendations are based on a group profile that combines the members' preferences. Recommendations frequently fall into known scenarios without diversity if such a profile is not kept updated or modified. This issue, known as overspecialization, may negatively affect GRS since recommendations become increasingly repetitious and unappealing. Hence, GRS must exploit various approaches to diversify recommendations to improve the overall group satisfaction. Diversity in RS has been extensively researched in the literature in recent years. The first work to formally introduce the concept of diversity was [4], [5] explore diversity while evaluating RS, and [6] discuss the effects of diversity algorithms in group recommendations. By addressing the issue of overspecialization in diversity for group recommendation, this article seeks to contribute to this particular field of research.

Therefore, in addition to boosting diversity in the recommendation list, we suggest creating and evaluating a group recommendation model that employs a diversification algorithm to optimize consensus among members. The main objective therefore is to lessen the effects of overspecialization to maximize group members' satisfaction. This proposal is an extension of a previous work [7], on which the authors developed the preliminary version of the group recommendation model using diversification techniques. Unlike the previous work, this proposal provides a comprehensive user assessment that addresses crucial aspects involving group recommendations such as group size and group formation, besides discussing the results from real users. In particular, we perform a user trial in which 6 groups of users assess the recommendations generated by our model against a state-of-the-art baseline method. Because the groups differ in size, we also discuss how this attribute impacts the precision of recommendations.

The research questions that drive our study are i) Are the group recommendations still relevant even after diversification? and ii) How accurate are the predictions considering the error?

This paper is structured as follows. Section II presents related work. Section III provides important background on the area, Section IV depicts the overall approach. Section V presents the experimental evaluation. Section VI discusses the key achievements and points out the limitations of the work. Section VII concludes the paper and sets forth the future works.

II. Related Work

GRS generally suggests a group of individuals participating in a group activity. Group recommendation has received much study in the literature from a variety of angles, including aggregation techniques [1], [5], group consensus [3] and graph-based algorithms [8]. However, the use of diversity algorithms in GRS is yet a low explored field [6].

The authors would like to thank FAPESB and CAPES for the financial support. Grant Term: PPF0001/2021. Technical Cooperation Agreement 45/2021. CAPES Program: PDPG-FAP no. 88887.637752/2021-00.

Regarding GRS, [1] provide a thorough review and insightful explanations of a number of aggregation techniques, including *Least Misery*, *Most Pleasure* and *Average Without Misery*. [2] propose semantics that accounts for item relevance and group disagreements. Nonetheless, use three group building strategies to bring users together: first similar users, then dissimilar users, and finally, groups formed randomly. In our work, the users create groups as they wish, as detailed in Section IV-B. [9] propose to utilize the multi-criteria ratings to learn the group expectations to build their effective group recommendation models. The author presents a new dataset related to the educational field where group preferences are already collected, thus dispensing the use of group formation strategies. [8] focus on generating recommendations to massive groups, varying from 10 to 1000 members. The authors explore the group interest and the connection between group users to divide a big group into subgroups and generate an interest subgroup-based recommendation list. Thus, the generated lists are aggregated into the final one by a dynamic aggregation function considering the subgroup's contribution. In this work, we do not form groups based on their connections or similarity, and our experiments were conducted with real users rather than synthetic ones. [10] present a method for group recommendation in Telegram. Their method receives a set of users, analyses their groups, and recommends a list of ranked groups. Considering the membership graph and users record, the authors combine two previous pieces of research to achieve their proposed method. In contrast to this work, the author's proposal does not recommend items to the groups. They rather generate ranked groups using graph-based algorithms.

Diversity in RS is discussed by [5], which indicates significant concerns beyond RS accuracy. They highlight the advantages of diversification algorithms in particular and give numerous methods for re-ranking recommended lists. Similarly, we chose this course of action from a group standpoint. Diversity is a broad concept. The authors in [11] present a latent factor model that achieves the required accuracy level while maintaining a certain level of diversity in RS. The authors use elastic-net regression to regularize the model for accuracy and diversity in an optimization framework. However, in this work, we address the diversity topic from a group perspective and perform a greedy re-ranking in the final recommendation list. In addition, [12] suggest a method to re-rank the recommendation list by appearance frequency of items to recommend more range of items to improve diversity. Their appearance frequency score is calculated over the user's rating predictions. [6] also discuss the problem of diversity in GRS. However, their experiments ran over synthetic groups rather than real ones. However, it is also not clear how their preference matrix is set up.

III. Background

A. Aggregation Techniques

Aggregation techniques in a GRS are consensus functions capable of integrating different preferences into a single one or the group profile. The proposed method combines individual scores to create a collective profile. The aggregation techniques used in this proposal, the Average Without Misery (AWM), was inspired by [1].

The approaches of aggregation are [3]:

- **Average Without Misery (AWM).** This technique can be characterized as a synthesis of the Average and Least Misery strategies (LM). The Average determines the mean of each individual's ratings for each candidate item, taking the average into account as the group rating for that particular candidate item. The LM approach assumes that the group rating for that candidate item is the lowest individual rating, hence sparing group members from misery. The AWM was implemented in this study as follows: LM specifies the group rating for each candidate item if any individual rating for that candidate item is equal to or less than the threshold. However, the Average establishes the group rating for that candidate item if the individual ratings are above the threshold. We define the threshold as two based on the Likert Scale [13] when considering the dataset used in this study, in which ratings range from 0.5 to 5. In this instance, value 2 already conveys disapproval.

Most studies in the literature use the Average and Least Misery techniques. In this paper, we implement the AWM as a combination of both. From the results obtained in our previous work [7], the AWM technique performs better than the others analyzed.

B. Diversification Algorithms

Diversification can be defined for a list of items as a factor expressing how different pair items are on this list [4].

$$Similarity(x, y) = \frac{\sum_{i=1}^{n} w_i \cdot sim_i(x_i, y_i)}{\sum_{i=1}^{n} w_i} \tag{1}$$

Equation 1 defines the similarity between a pair of items, where n is the item attributes, w is the weight of the attribute, and $sim(x, y)$ is the comparison of attribute i from items x and y. The **title** and **genres** are attributes from the items that are used in the Cosine Similarity similarity calculus in this paper.

In particular, this proposal assessed two ways to diversification from the literature: Bounded Random Selection and Bounded Greedy Selection.

- **Bounded Random Selection.** On this algorithm, there is a list L with the rated items by the user, a list of candidate items C, and the final list with diversified recommendation R. For each item i_l in L, the algorithm searches for items in C similar to i_l and adds those items in a new list J, with a bounded length. Then, items are randomly chosen in J and included in R.
- **Bounded Greedy Selection.** This approach selects items greedily by taking the most diverse item on each turn and appending it to R. However, it is essential to define a greedy selection function. This greedy function needs

to consider similarity and diversity of the items. The flow of this algorithm is similar to the Random; however, the greedy function selects the items that maximize diversity while still taking similarity into account, rather than picking them at random from J.

$$Diversifying(x, R) = \alpha \cdot rel(x) + ... \\ ... + (1 - \alpha) \cdot \frac{1}{|R|} \sum_{y \in R} dist(x, y) \quad (2)$$

Equation 2 in this study presents the greedy function for weighting diversity and similarity [5], where α is used to balance the equation's factors, and $rel(x)$ is the relevance function for item x, which can be expressed on similarity. This equation represents the greedy approach for diversification covered in [14], [15], and [5].

IV. A Group Recommendation Model Using Diversification Techniques

A. Notations and Proposal Flow

The proposed model recommends a list of movies I to a group G composed of n users $u \in U$.

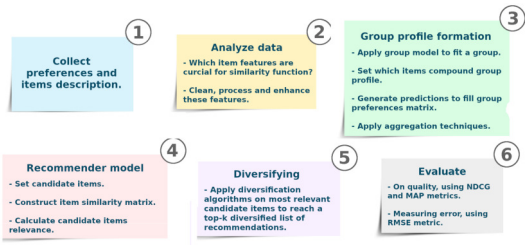

Fig. 1. Flow of proposed model defined in steps.

Figure 1 enumerates the recommendation flow. The 1st step is collecting item descriptions and user preferences from a given dataset. The 2nd step is about data prepossessing to reduce noise and redundancy. In the 3rd step, the group profile is created using aggregation techniques. In the 4th step, the group recommendations are generated. Diversification takes place in step 5. Finally, the group recommendations are evaluated in step 6. In the following, steps 3, 4, and 5 are depicted.

B. The Group Model

A group can be defined as a system of recurrent social relations or a reunion of people who share some characteristic, some idea, or some common interest [16]. Hence, it is crucial to define rules for group formation when recommending to groups. We divided the rules into two: group size and cohesion between members. **Group size:** The size of the group can vary drastically even in real life, from a couple having lunch to a crowd of thousands in a football stadium. In our experiments, we set the group size to 3 or 5, also inspired by recurrent use in the literature [17] and [6]. **Cohesion between members:** This aspect focuses on the relationship between members. Most of the datasets used in RS focus on modeling individual preferences rather than the relationship between those users. In our experiments, we asked participants to form groups as they wished.

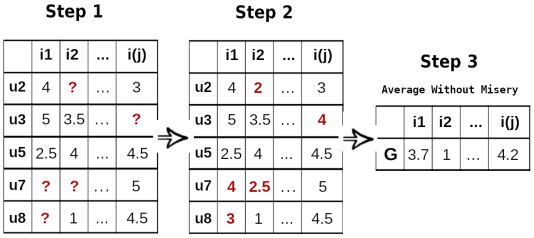

Fig. 2. Group profile generation flow.

Once the group is created, the next step is to define the group profile. In this phase, aggregation techniques are applied to individual preferences toward a single group profile G.

Figure 2 illustrates 5 members u_2, u_3, u_5, u_7, and u_8, and their respective ratings assigned to each item i_1 to $i_{(j)}$. The symbol ***?*** indicates no rating.

In order to apply aggregation techniques on the user preference matrix, the vacant slots (***?***) are predicted. We tested different prediction algorithms: Neighbourhood-based [18] i) *KnnWithMeans*, ii) *Knn*; and Matrix Factorization Based iii) Singular Value Decomposition (SVD) [19]. From our empirical observations, we selected the SVD algorithm which performed more accurately. Figure 2 - Step 2 illustrates the dense user preference matrix after employing the SVD algorithm. Once the user preference matrix is dense, the aggregation techniques are applied. Figure 2 illustrates the aggregation technique used in this paper $AverageWithoutMisery$, thus producing the group profile $G = \{3.7, 1, ..., 4.2\}$.

C. Recommendation Model

To generate group recommendations, we compare each movie's title and genres against candidate items. We only used these two features because information like director or cast were not available in the dataset. Therefore we employ a Content-Based (CB) approach [20] that recommends unknown items that are similar to the better-rated items in the group profile (see Algorithm 1).

In Algorithm 1, pi and ci stands for profile items and candidate items respectively. GP is the group profile and it is sorted by ratings, bc refers to the best candidates and stores the most similar candidate items from profile items. The list R is the recommendations generated for the group, and DR is the final list with the recommendations diversified. Important structures in Algorithm 1 are detailed as follows:

.

Algorithm 1: Algorithm for Group Recommendation.

Data: n as the number of groups; $size$; $Users$ as all dataset users; $Items$ as items from dataset; sim as the similarity matrix of items.
Result: DR list of recommendations diversified.

```
1  while n > 0 do
2      G = random(Users, size)
3      pi, ci = splitDatasetItems(Items, G)
4      GP = generateGroupProfile(pi, G)
5      bc = getMostSimilarItems(GP, ci, sim)
6      for x ∈ bc do
7          for y ∈ GP do
8              r = relevance(x, y)
9              R = R + r
10         end
11     end
12     DR = diversifyRecommendations(R)
13     n = n - 1
14 end
```

1) **Set candidate items.** It is important to split the dataset out into candidate and profile items. As mentioned in Section IV-B, any item that is rated by a group member is classified as a profile item, otherwise, it is a candidate item. This step is viewed in line 3, where pi are the profile items and ci are the candidate items.
2) **Sorting the group profile.** Provided the group profile, we know which items the group enjoys at most. We sort this list in a descending order by ratings $r_{G,i}$ in order to keep the preferred items at the beginning of the list. This step is defined in line 4.
3) **Constructing the items similarity matrix.** The next step is to build up the similarity matrix between items, where each cell value (x, y) corresponds to the similarity score for items x and y. Particularly, we use Cosine Similarity [21] as it performs great with textual information. The experiment for weighing the cosine similarity was based on the returned items' relevance, i.e., which movies are more similar to the group profile. We performed several tests empirically until achieving the best relevance. Then we applied the following setting: 0.8 for the title and 0.2 for the genre. Algorithm 1 receives the similarity matrix as an input sim.
4) **Setting relevance.** At this stage of the model, we already have the group score over the profile items, and we know which candidate items are more similar to profile items bc. Therefore, it is crucial to quantify how relevant a candidate item is to a group. Thus, we elaborate the Equation 3 that combines similarity values with group preference to express the relevance of the item.

$$relevance(x, y) = \frac{a \cdot sim(x, y) + b \cdot \frac{r_{(G,y)}}{max(r)}}{a + b} \quad (3)$$

Equation 3 shows x as a candidate item from bc, and y as a preferred item from GP for group G. In the first factor of the equation, the similarity between items, $sim(x, y)$ is normalized as well as the second factor $r_{(G,y)}$. Then, the relevance of x is the result of the weighted mean of variables a and b over x and y similarity, and how preferred y was rated by G, respectively. The sum of variables a and b may never be less than 1. This step is defined in line 8 of the algorithm.

D. Diversifying Group Recommendations

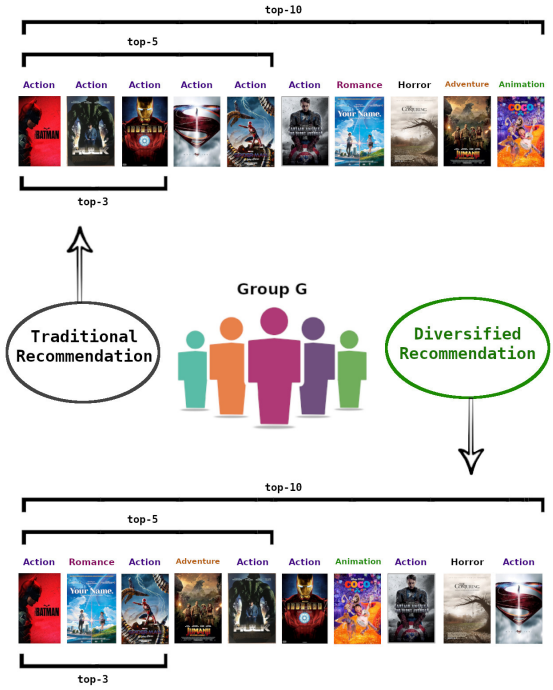

Fig. 3. Impact of diversification on top-k.

The outcome of the recommendation model is a list of recommended items R for the group. However, how diverse is R? In other words, how similar the top-k items are on this list? Considering k as 10, most items tend to have similar aspects. Therefore, we diversify the top-k to generate a relevant and diverse ranking for the group.

Most of the diversification algorithms are based on re-ranking items to improve diversity. Likewise, we implement the *Greedy Re-ranking Algorithm* [5]. This approach is used in Algorithm 1 at line 12. The entire implementation of this proposal is available at an online repository [1].

Figure 3 illustrates the recommendations for group G, using traditional recommendation techniques versus diversified recommendations. By observing the traditional recommendation set, up to the top-5 items, all movies belong to the same genre, i.e., action. A different genre is only observed in the item at the 7th position. In contrast, some diversity is already observed in the top-3 list using the diversification approach. It is important to outline that both lists are formed by the same items, the second an output from the diversification process.

V. Online Experimental Evaluation

In order to evaluate our model with real users, an online experiment was undertaken. This section depicts the method-

[1] https://github.com/amandachagas/GRSwithDiversity.git

TABLE I
DATA SAMPLE USED IN THE EXPERIMENT.

Id	Title	Genres	Year	ImdbLink	Cover	Youtube
1	Daybreakers	Action, Drama, Horror...	2010	...title/tt433362	...images-na.ssl...	.../watch?v=CtiLjvVwvY4
2	Jupiter Ascending	Action, Adventure, Sci-Fi	2015	...title/tt1617661	...images/MV5B...	.../watch?v=THVFkk-sEus
3	The Commuter	Crime, Drama, Mystery...	2018	...title/tt1590193	...images/Adh4F...	.../watch?v=aDshY43Ol2U

ology, dataset, metrics, and results obtained. In the end, we discuss the results and the overall achievements.

A. Methodology

The online experiment was conducted with 24 student volunteers at the University. Before participating in the experiment, they were introduced to the GRS concepts and the experiment's goals. We also ensured that all personal information was anonymized and used strictly for scientific purposes. All were informed about the two phases of the experiment: 1) collecting individual preferences and 2) evaluating the recommendations as a group.

*1) **Collecting user preferences**:* A Web System[2] was built for collecting the user preferences. The Web System (see Figure 4) was populated with movie data from the MovieLens dataset [22]. For each movie, we also provided complementary information including *cover*, *imdbLink* and *youtubeID*. The movie covers are listed along with their meta information and the rating option, ranging from 0.5 (dislike) to 5 (like at most). Once a movie is rated, the movie box background becomes green to signalize which movies are evaluated. Each user was asked to rate at least 20 movies so that we could evaluate the approach comprehensively. Worth mentioning that we do not address the cold start problem in this work, but the plans are set for future works.

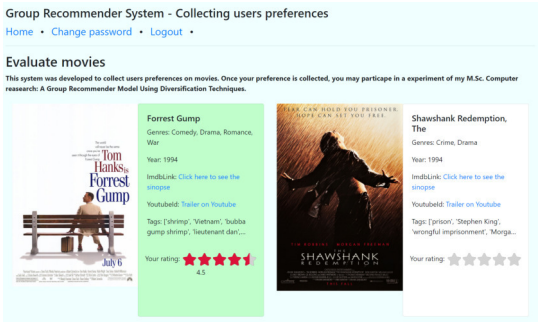

Fig. 4. Collecting users preferences from the Web System.

*2) **Generating recommendations to groups**:* Before generating the recommendations for the groups, we formed the groups. In this work, we did not experiment with any formation heuristics. We simply asked the participants to form groups based on their free will or affinity and only limited the group size to *3* or *5* members. Once the groups were formed, we calculated the group profiles and generated the recommendations. The final group setting was: $G31$, $G32$, $G33$, $G51$, $G52$ and $G53$. For the sake of clarity, we adopt the following terminology *GXY*, where G means *group*, X means the *size* of the group, and Y means the *ID* of the group.

[2]Collecting preferences - https://collectprefgrs.herokuapp.com/

B. Baseline experimental setup

This paper compares our model with the baseline [6]. In their article, baseline's author settled their experiment as the following configuration: 1) They used three datasets, MovieLens, TripAdvisor, and Amazon; 2) Their evaluation metrics were the *S-Recall* and the *Normalized utility*; 3) They formed synthetic groups randomly with $size = 10$ to performed recommendations; 4) They ran a user study were they asked real users to assessed which recommendation list is more diverse, theirs our the baseline ones. Also, they asked the actual users to express which list they preferred.

Therefore, for clarity, in this experiment, we exposed the baseline's algorithm to a new environment, where users are real instead of synthetic. They expressed their ratings for the recommended items. Also, the group size is different, and we assessed using other metrics at different levels.

C. Dataset

MovieLens [22], the dataset used in the experiment, contains 100,000 ratings over 9,000 movies evaluated by 600 users. The original dataset was enriched with data from another experiment with 24 new users and 686 new ratings. Moreover, to each movie, we added it a links to its *cover*, *imdbLink* and *youtubeLink*. We were capable of enhancing the dataset using the *imdbId* information, which is provided in a separate file from the movie's characteristics. This improvement covered approximately 93% of the entire dataset. Despite that, we had to reduce the movie titles' noise to improve the similarity calculations. Table I demonstrates the characteristics of the movie in the final dataset.

D. Metrics

The NDCG, AP, ILD and RMSE were used in the experiment:

*1) **Normalized Discounted Cumulative Gain (NDCG)**:* The NDCG is densely used in Information Retrieval field for measuring the quality of ranked items [23], [24]. The NDCG comprises the value of DCG divided by IDCG. Whereas we recommend the top-k items in a rank, the implementation of the Discounted Cumulative Gain (DCG) and the Ideal Discounted Cumulative Gain (IDCG). The list with top-k items is denoted as $R_k = \{r_1, r_2, ..., r_k\}$, the calculated relevance of an item at position i in the list is represented

by rel_i. The perfect ranking scores 1.0 in this metric. The $DCG@k = \sum_{i=1}^{|R_k|} \frac{rel_i}{log_2(i+1)}$. The $IDCG = max(DCG@k)$ is the maximum value of DCG, and $NDCG@k = \frac{DCG@k}{IDCG}$.

*2) **Average Precision (AP)**:* Precision is the percentage of relevant items recommended to the user [25]. Therefore, $Precision@k$ ($P@k$) represents the percentage of relevant items returned for the user at k level. The $P@k = \frac{RIK}{len(k)}$, where k is the size of the rank to evaluate, RIK stands for **R**elevant **I**tems in the list at **K**, and $len(k)$ is the size of the list at k. In order to observe precision related to the groups size, we implemented the Average Precision (AP) as $AP(G,k) = \frac{\sum_{i=1}^{|G|} P@k}{|G|}$, where G represents a list of groups, and for each group, $P@k$ is considered in the mean for a certain k level for each group in the list. The Precision metric compares the output items with a truth list to set relevance. However, we needed to adapt this metric to evaluate the baseline outputs since they provide no ground-truth list. Thus, inspirited by [17], we defined relevant recommendations as those with a score higher than the global mean of assessed movies.

*3) **Intra List Diversity (ILD)**:* Is a measure for comparing how diversified is a list. The result displays the diversity score, which ranges from 0 to 1, with 0 denoting no diversity and 1 denoting a fully diversified list. The ILD is the antithesis of the Intra List Similarity (ILS) metric, which measures similarity rather than distance between items [15]. We implemented the ILD score in a list of items R as $ILD(R) = \frac{\sum_{i \in R} \sum_{j \in R/\{i\}} Distance(i,j)}{2}$ where $Distance(i,j) = 1 - Similarity(i,j)$. This way, we calculate the mean of all distances from pairs *(i,j)* in list R.

*4) **Root Mean Squared Error (RMSE)**:* The RMSE is a metric used to model error and to help providing a picture of the error distribution [26], [27]. The error considered in this experiment is expressed as $error(r) = (r' - r'')^2$, where for each recommended item r, the truth value r' is subtracted from the predicted value r''. This error function in the RMSE is $RMSE(R) = \sqrt{\frac{1}{len(R)} \cdot \sum_{r \in R} error(r)}$.

E. Results

*1) **Density graph**:* Figure 5 illustrates the rating distribution from user participation. The most common rate is 5.0, with 233 ratings, representing 33.96% of the total assessment. The second most common rate is 4.0, with 134 ratings (19.53%). Worth mentioning that 14.13% of all ratings are under the rate of 3.0. Therefore, the density graph indicates that the group members were pleased with recommendations aligned with the group preference.

*2) **NDCG**:* Figure 6 shows the NDCG results achieved by our approach at positions 3 (nDCG@3), 5 (nDCG@5) and 10 (nDCG@10). On the one hand, the best NDCG result is observed in the group $G33$ with 0.86 at positions 3 and 5. On the other hand, the worst performance is witnessed in the group $G31$, which scored 0.57 at position 5. The other groups varied the NDCG results from 0.72 to 0.80,

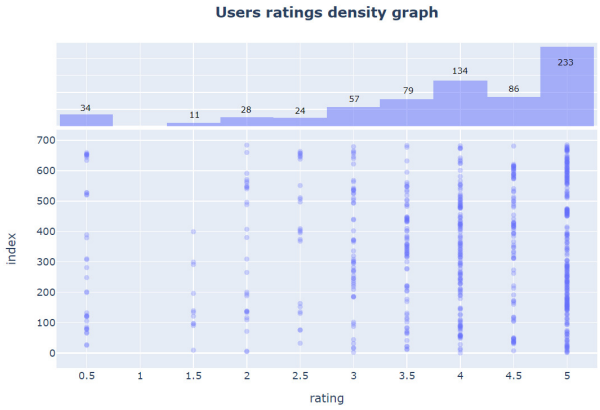

Fig. 5. Density graph of participants' ratings.

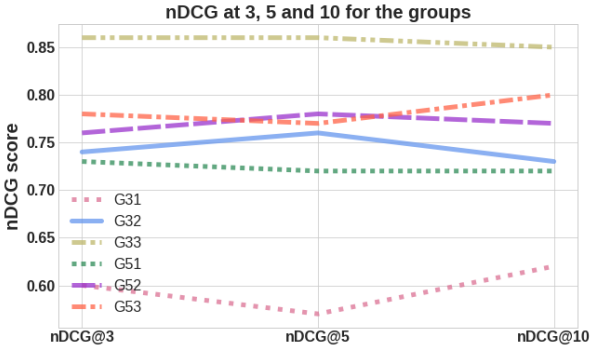

Fig. 6. NDCG for the groups at different levels.

indicating an up-and-coming recommendation list. Looking at the group size, we can observe that the groups with 5 members performed more consistently than the groups with 3 members, especially when we focus on the groups $G31$ (disliked most of the recommendations) and $G33$ (enjoyed most of the recommendations).

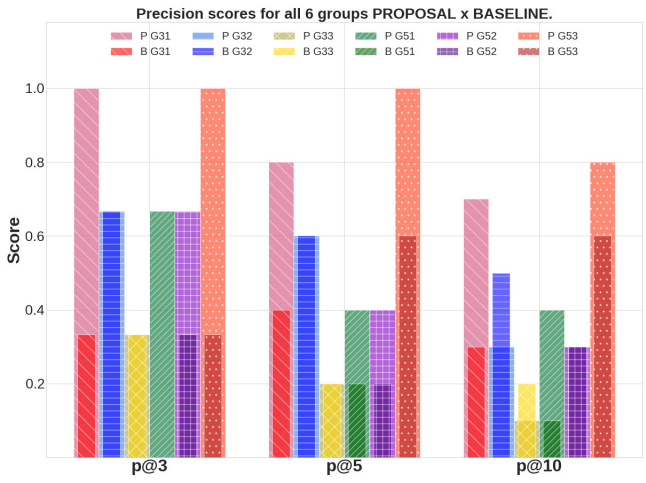

Fig. 7. Precision rates for the groups at different levels. Our proposed model is represented by P and the baseline method is represented by B.

TABLE II
METRICS MATRIX

		nDCG						Average Precision					RMSE
		@3	@5	@10	mean	median	std	@3	@5	@10	median	std	
n=3	G31	0.6	0.57	0.62	0.73	0.74	0.11	0.67	0.53	0.37	0.6	0.20	0.22
	G32	0.74	0.76	0.73									
	G33	0.86	0.86	0.85									
n=5	G51	0.73	0.72	0.72	0.76	0.77	0.03	0.78	0.6	0.5	0.4	0.15	0.20
	G52	0.76	0.78	0.77									
	G53	0.78	0.77	0.8									

3) ***Precision****:* Figure 7 shows the precision results achieved by our approach (P) versus the baseline (B) at positions 3 (p@3), 5 (p@5) and 10 (p@10), for all groups compared. When our approach generates the recommendations, the group $G53$ achieves the highest scores with a surprising precision average of 0.93. The group $G32$ achieves the highest scores with a precision average of 0.58, when the baseline generates the recommendations. As it shows, our approach overcomes the baseline in all compared groups, except for the group $G33$, with the lowest overall result, with an average score of 0.21.

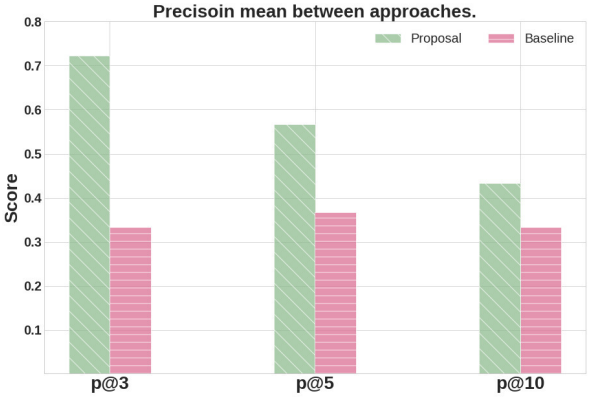

Fig. 8. Precision average between approaches.

4) ***Average Precision****:* Figure 8 shows the average precisions achieved by our approach versus the baseline at positions 3 (p@3), 5 (p@5) and 10 (p@10). The proposed approach overcomes the baseline in all levels, with an advantage of 0.4 points at $p@3$, 0.2 points at $p@5$, and a slight advantage of 0.1 point at $p@10$. In addition, we can observe that as the position increases, the precision means of our approach tend to fall, whereas the baseline seems steady. It is important to point out that the lowest average precision achieved by our approach is 0.44 at position 10, still higher than the highest average precision achieved by the baseline approach, 0.35 at position 5.

5) ***Diversification****:* Figure 9 express the diversity score obtained by the proposal and the baseline. The proposal scores 0.94 with std equals to 0.02, however, the baseline performs better, scoring 0.96 with std equals to 0.01. The baseline method exceeds the proposed one with advantage around 2%.

6) ***Group Size x Metrics****:* Table II summarizes the NDCG, AP, and RMSE results achieved by our approach; however, they are separated by the group size (3 and 5). We can observe

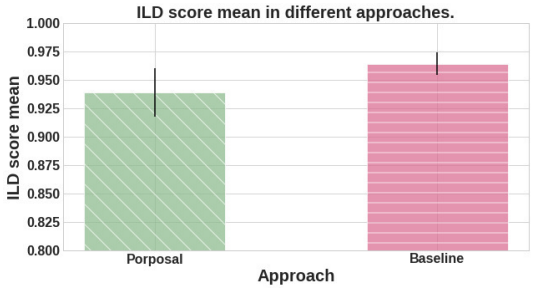

Fig. 9. ILD average score between approaches.

that the groups with 5 members perform better than those with 3 groups for all compared metrics. It is essential to highlight that in the NDCG metric, the std result for the groups with 5 members achieves lower variance than those with 3 members (0.03 against 0.11). In contrast, the opposite occurs for the Average Precision median (0.6 against 0.4). Finally, we evaluated the error rate (RMSE) when filling the sparse matrices. In addition, The RMSE for groups with 3 and 5 members are nearly the same (0.22 against 0.20), achieving a meager error rate.

VI. DISCUSSION AND LIMITATIONS

Despite the promissory results observed, some limitations must be discussed. As to the first research question posed in Section V *i) Are the group recommendations still relevant even after diversification?* The answer is positive, as our approach overcomes the baseline regarding precision. In particular, our approach's lowest Average Precision result overcomes the best Average Precision outcome of the baseline approach. As to the group size, all groups appear to have enjoyed the recommendations, even though the higher variance is observed in groups with 3 members. As to the second research question, *ii) How accurate are the predictions considering the error?* The answer is also positive as the RMSE error rate is approximately 20%, thus leading to relevant group recommendations despite the diversification and group size.

As a limitation, the cold start problem is not treated when no evaluation is observed. A solution can be a hybrid content-based filtering RS. Hence, other metadata such as the actors and director can be compared so that preferences are predicted, and the user matrix is filled out.

Contextual information is another critical aspect that must be carefully incorporated into the proposed model. The motivation that drives a group of people to watch a movie may vary

depending on the occasion and degree of intimacy with the group members, among other aspects. Such an improvement will require designing a more elaborated user and group model that consider such a piece of information.

The diversification addressed in this paper is based on the dissimilarity of key movie features: title and genres. Nevertheless, several other movie characteristics still can be processed, including cast, synopsis, and direction. All these features can be analyzed those can impact diversity.

VII. Conclusion

This paper proposes a group recommendation model that suggests relevant movies for groups based using diversification. The diversification algorithm re-ranks the recommendation list taking into account the relevance of an item and the dissimilarity among them. For evaluating the proposal, a user trial with 24 participants divided into 6 groups was undertaken to assess the proposal. The results show satisfactory results over a baseline method. The proposed approach overcame the compared baseline in all levels of AP evaluation. Moreover, the results point out that the performance for groups of size 5 has a lower variance in std rather than 3.

As for future work, we look forward to performing a deeper study regarding the impact of group size on the recommendations. Also, another online experiment with more participants will help validate the proposal. Additionally, the similarity function can be improved by adding more features related to movies, like directors, cast, or summary. Heuristics for group formation must also be investigated as they impact the acceptance of recommendations. We also plan to test several variations for the diversification algorithm using related metrics MSE and NRMSE. Last but not least, we plan to explain the recommendations to group members. It is already proved that justification serves as essential means to help users to make better decisions among the suggested items.

References

[1] J. Masthoff, *Group Recommender Systems: Combining Individual Models*. Boston, MA: Springer US, 2011, pp. 677–702.

[2] S. Amer-Yahia, S. B. Roy, A. Chawlat, G. Das, and C. Yu, "Group recommendation: Semantics and efficiency," *Proc. VLDB Endow.*, vol. 2, no. 1, pp. 754–765, Aug. 2009. doi: 10.14778/1687627.1687713

[3] A. Jameson and B. Smyth, *Recommendation to Groups*. Berlin, Heidelberg: Springer Berlin Heidelberg, 2007, pp. 596–627.

[4] K. Bradley and B. Smyth, "Improving recommendation diversity," in *Proceedings of the Twelfth Irish Conference on Artificial Intelligence and Cognitive Science, Maynooth, Ireland*. Citeseer, 2001, pp. 85–94.

[5] M. Kaminskas and D. Bridge, "Diversity, serendipity, novelty, and coverage: A survey and empirical analysis of beyond-accuracy objectives in recommender systems," *ACM Trans. Interact. Intell. Syst.*, vol. 7, no. 1, pp. 2:1–2:42, Dec. 2016. doi: 10.1145/2926720

[6] N. T. Toan, P. T. Cong, N. T. Tam, N. Q. V. Hung, and B. Stantic, "Diversifying group recommendation," *IEEE Access*, vol. 6, pp. 17 776–17 786, 2018. doi: 10.1109/ACCESS.2018.2815740

[7] A. Oliveira and F. Durao, "A group recommendation model using diversification techniques," in *Proceedings of the 54th Hawaii International Conference on System Sciences*, Hawaii, HI, USA, 2021. doi: 10.24251/HICSS.2021.326 p. 2669.

[8] D. Qin, X. Zhou, L. Chen, G. Huang, and Y. Zhang, "Dynamic connection-based social group recommendation," *IEEE Transactions on Knowledge and Data Engineering*, vol. 32, no. 3, pp. 453–467, 2020. doi: 10.1109/TKDE.2018.2879658

[9] Y. Zheng, "Educational group recommendations by learning group expectations," in *2019 IEEE International Conference on Engineering, Technology and Education (TALE)*, 2019. doi: 10.1109/TALE48000.2019.9225968 pp. 1–7.

[10] D. Karimpour, M. A. Z. Chahooki, and A. Hashemi, "Grouprec: Group recommendation by numerical characteristics of groups in telegram," in *2021 11th International Conference on Computer Engineering and Knowledge (ICCKE)*, 2021. doi: 10.1109/ICCKE54056.2021.9721494 pp. 115–120.

[11] S. Raza and C. Ding, "A regularized model to trade-off between accuracy and diversity in a news recommender system," in *2020 IEEE International Conference on Big Data (Big Data)*, 2020. doi: 10.1109/BigData50022.2020.9378340 pp. 551–560.

[12] S. Miyamoto, T. Zamami, and H. Yamana, "Improving recommendation diversity across users by reducing frequently recommended items," in *2018 IEEE International Conference on Big Data (Big Data)*, 2018. doi: 10.1109/BigData.2018.8622314 pp. 5392–5394.

[13] D. Bertram, "Likert scales," *Retrieved November*, vol. 2, p. 2013, 2007.

[14] B. Smyth and P. McClave, "Similarity vs. diversity," in *Case-Based Reasoning Research and Development*, D. W. Aha and I. Watson, Eds. Berlin, Heidelberg: Springer Berlin Heidelberg, 2001. doi: 10.1007/3-540-44593-5_25 pp. 347–361.

[15] C.-N. Ziegler, S. M. McNee, J. A. Konstan, and G. Lausen, "Improving recommendation lists through topic diversification," in *Proceedings of the 14th International Conference on World Wide Web*, ser. WWW '05. New York, NY, USA: ACM, 2005. doi: 10.1145/1060745.1060754 p. 22–32.

[16] A. G. Galliano, Ed., *Introdução à sociologia*. Harper e Row do Brasil, 1981.

[17] O. Kaššák, M. Kompan, and M. Bieliková, "Personalized hybrid recommendation for group of users: Top-n multimedia recommender," *Information Processing and Management*, vol. 52, no. 3, pp. 459 – 477, 2016. doi: 10.1016/j.ipm.2015.10.001

[18] R. Ahuja, A. Solanki, and A. Nayyar, "Movie recommender system using k-means clustering and k-nearest neighbor," in *2019 9th International Conference on Cloud Computing, Data Science Engineering (Confluence)*, 2019. doi: 10.1109/CONFLUENCE.2019.8776969 pp. 263–268.

[19] S. Girase, D. Mukhopadhyay *et al.*, "Role of matrix factorization model in collaborative filtering algorithm: A survey," *arXiv preprint arXiv:1503.07475*, 2015. doi: 10.48550/arXiv.1503.07475

[20] P. Lops, M. de Gemmis, and G. Semeraro, "Content-based recommender systems: State of the art and trends," in *Recommender Systems Handbook*, F. Ricci, L. Rokach, B. Shapira, and P. B. Kantor, Eds. Springer US, 2011, pp. 73–105.

[21] G. Adomavicius, Tuzhilin, and Alexander, "Toward the next generation of recommender systems: a survey of the state-of-the-art and possible extensions," *IEEE Transactions on Knowledge and Data Engineering*, vol. 17, no. 6, pp. 734–749, jun 2005. doi: 10.1109/TKDE.2005.99

[22] F. M. Harper and J. A. Konstan, "The movielens datasets: History and context," *ACM Trans. Interact. Intell. Syst.*, vol. 5, no. 4, Dec. 2015. doi: 10.1145/2827872

[23] L. Baltrunas, T. Makcinskas, and F. Ricci, "Group recommendations with rank aggregation and collaborative filtering," in *Proceedings of the fourth ACM conference on Recommender systems*. Barcelona, Spain: ACM, 2010. doi: 10.1145/1864708.1864733 pp. 119–126.

[24] K. Järvelin and J. Kekäläinen, "Cumulated gain-based evaluation of ir techniques," *Transactions on Information Systems (TOIS)*, vol. 20, no. 4, pp. 422–446, 2002. doi: 10.1145/582415.582418

[25] C. D. Manning, P. Raghavan, and H. Schütze, *Introduction to Information Retrieval*. New York, NY, USA: Cambridge University Press, 2008. ISBN 0521865719, 9780521865715

[26] T. Chai and R. R. Draxler, "Root mean square error (rmse) or mean absolute error (mae)? – arguments against avoiding rmse in the literature," *Geoscientific Model Development*, vol. 7, no. 3, pp. 1247–1250, 2014. doi: 10.5194/gmd-7-1247-2014

[27] E. J. Gilroy, R. M. Hirsch, and T. A. Cohn, "Mean square error of regression-based constituent transport estimates," *Water Resources Research*, vol. 26, no. 9, pp. 2069–2077, 1990. doi: 10.1029/WR026i009p02069

Communication Papers of the of the 17th Conference on Computer Science and Intelligence Systems pp. 55–62
DOI: 10.15439/2022F39
ISSN 2300-5963 ACSIS, Vol. 32

Exploiting Social Capital for Recommendation in Social Networks*

Paulo Roberto de Souza
Federal University of Bahia
Institute of Computing

Frederico Araujo Durao
Federal University of Bahia
Institute of Computing

João Paulo Dias de Almeida
Federal Institute of Sergipe

***Abstract*—Many computational techniques have been proposed by social networks to analyze the users' behaviors to recommend relevant content for them. Social networks generate a huge volume of information, which users cannot consume, generating a problem known as information overload. This way, filtering relevant information to help users with this problem becomes necessary. Social networks have many available features, such as relationships and interactions, which can be used to investigate the users' behaviors regarding news on their feed. The value of news can be defined as Social Capital, which is used by this work to model the user's preferences. This paper aims to investigate, model, and quantify interactions on social networks by exploiting social capital to develop a recommender system. Hence, in order to evaluate recommendations, an experiment was conducted with real users. Results show that our proposal was able to generate relevant recommendations on at least 62% of the scenarios.**

I. Introduction

THE EXPONENTIAL growth of Web 2.0 has been driven by key innovations such as Online Social Networks (OSN), in which users have become the information drivers on the Web. Online Social Networks provide a virtual environment in which people can share information, experiences, opinions, interests and specially make connections [1]. For example, on the microblogging social network Twitter, more than 300 million users post 140 million of tweets every day, generating a huge amount of information which is shared and consumed by millions of others users.

Although online social networks are primarily used to communicate and relate with others, over the last few years OSNs have become important tools of mass communication, particularly as a way to disseminate news and influence others. The energy emanating from social interactions and available resources has been investigated in literature as Social Capital (SC). [2] formalizes Social Capital as an aggregated value of resources that are available on relations' networks. [3] claim that these social networks features can be analyzed to model user preferences. The underlying assumption of SC is that individuals benefit from various norms and values that a social network fosters and produces, such as trust, reciprocity, information, and cooperation [4], [5]. All these observations aim to solve one of the most challenging problems of online social networks: the Information Overload, which is the natural human incapacity to process the huge amount of information produced in social networks [6]. Too much information can quickly cross users' cognitive limits in processing news and can make them feel overwhelmed and overloaded. [7] warn that 66% of users on Twitter felt overloaded when they received a lot of posts, and more than one-half reported needing a tool to filter irrelevant posts. After realizing this, Twitter developed a tool for marking comments as irrelevant or offensive, but not to analyze social capital as well. In this scenario, even users are able to mark posts as irrelevant or offensive, but there are no guarantees that similar posts will not come up in the future, or even that other posts that consider the social capital features will be recommended.

Recommender Systems (RS) therefore ascend as key tools to cope with the Information Overload problem by filtering relevant information according to the user's interest [8]. In literature, the problems about Information Overload (IO) have been discussed by many authors through analyses such as User's Influence [9], Interactions [10], and News Timeline [11], but none of them focus on the analysis of exploiting SC. [12] claims that RSs are more common among the generations of Web applications due to collaboration, interaction, and sharing of information. These systems use various piece of information to model each user's preferences such as clicks, website history, purchases, and items' evaluation. The term item, in general, describes what is used by RS to recommend to the user, like news or tweets on Twitter, or books on Amazon [13].

The power of SC in social networks is naturally affected by irrelevant information, which can overload users. This way, once the SC inherited from OSNs is neglected, RS perform an important role in content filtering on social networks. Given the complexity and resources offered by social networks, the value of the recommended item can consider other aspects, such as collaboration [14], interaction [15], and influence [16]. For instance, news can supposedly be more informative if there is good discussion on its comments. Different points of view can help the reader see that information from various perspectives. For example, a user can encounter solutions for a particular problem from others' opinions in social networks. In other words, the value of a recommendation item is associated with the social engagement behind it, beyond the traditional similarity metrics of interest.

This paper aims to investigate, model, and quantify interactions and available resources on social networks by exploiting SC, besides developing a RS through this exploitation. This

This work was partially funded by the Coordenacao de Aperfeicoamento de Pessoal de Nivel Superior - Brasil (CAPES) – Grant number 001

approach analyzes and values news that have more interactions or comments across a set of news, which are interesting for a user in order to suggest what is most relevant. We can point out that this paper does not consider misinformation or news published by bots yet.

The main contributions of this work are: i) *The Social Capital Recommendation Model* that calculates the value of news recommendations grounded from social interactions in a social network, ii) *The User Model* that comprises a user profile from user interactions and feedbacks from recommended news, and iii) *A Social Network Interaction Dataset* containing data from user activities in the social network.

The remaining aspects of this paper are structured as follows: Section II discusses related works. Section III introduces the proposed recommendation algorithm. Section IV presents the RecSocial application as well as the experiment setup and results. Section V discusses the results. Finally, Section VI concludes this paper and presents future work.

II. Related Works

Recommender systems on social networks have been attracting attention for a long time. These systems aim to aid users in decision-making, for example: which news to read [17], which account to follow [18], or which Wiki Pages to read [19]. In this context, many techniques are used to generate recommendations, such as machine learning, content-based and user-based filtering, besides collaborative filtering. Moreover, RS are widely used in literature, but both social capital and RS are rarely addressed working together. Nevertheless, we use similar studies to compare their techniques with our work such as: Text Analysis (TA), Topic Modeling (TM), Semantic Enrichment (SE), User Popularity (UP), Natural Language Processing (NLP), Sentiment Analysis (SA), Conceptual Relations (CR), Collaborative-Filtering (CF), Content-Based-Filtering (CB), Social Capital (SC), Empiric Analysis (EA), and Centrality Measure (CM).

[20] explore Twitter to analyze and recommend news through a CB algorithm, which has the goal to use different strategies (topic modeling, semantic enrichment, and temporal restrictions) to create a user's profile. Furthermore, they have developed a framework that models the user's preferences by adopting a semantic enrichment approach. So, this work depicts different techniques from our proposal, focusing more on semantic and topic modeling. Our proposal, on the other hand, focuses on the news' content, besides interactions and other features. Furthermore, [19] have developed a tag-based RS, which aims to recommend wiki pages used in corporate environments. In other words, pages are created for knowledge sharing about a particular subject within the organization. This way, they proposed a method called Wiki Page Collaborative Value (WPCV), which calculates the collaborative value of wiki pages. This approach analyzes the collaborative activities on a wiki page, such as edition, evaluation, tagging, or comments. Besides that, other features are adopted as a user experience about the subject and interaction among social ties. As a result, the score obtained through the WPC method is used to rank and recommend wiki pages. [19] employ features similar to those used in this paper. [21] have developed an analysis on how the user's personality is manifested through different features on Facebook. They use many features such as the user's actions, including the number of published photos, events, and groups he has uploaded or created and the amount of news that he has liked. In addition, they use aspects of the profile that depends on the actions of a user and their friends, including the number of times a user has been tagged in photos, and the size and density of their friendship network. Thereby, [21] present a feature analysis similar to the one in our work. [22] added a new strategy assigning weights to topics/concepts of user's interest. This approach helps specify to what extent the user is interested in a topic. In this manner, they observed that, by considering the change of interest for a long time, the recommendations' quality was improved. Regardless of how they approached different techniques when compared to this work, we have adopted a weighting sentiment analysis to improve the recommendations.

In turn, [23] have developed a CB RS called Lumi Social News, using a mobile approach, which aims to recommend extracted news from the active user's timeline in their social networks based on their geographic location. The news are ranked according to their popularity and local trending. In other words, they are measured according to the frequency of sharing and interactions (likes and sharing, for example) among individuals of the same geographic location as the active user on the system. [17] approach a RS called TGS-post in order to recommend tweets based on conceptual relations among interest topics of a target user. The main goal of TGS-post is to present a new timeline for a user, which is ranked according to their interest. [24] proposed a framework, which has the goal to analyze tweets and identify which are the criteria that make them popular. The basic idea is to analyze the tweets in order to find the basis of the popularity of a person and extract the reasons supporting the popularity. As a result, they claim that this analysis can be used to recommend a list of the most popular users according to the personal interests of each individual. [10] have developed a RS, which uses the interactions maintained among users on social networks, therefore recommending users with similar preferences. These three studies, approach similar features in our work, using them to measure popularity, influence, and others to identify the user's preferences and behavior.

[18] have developed a RS called ElRank, which aims to recommend Twitter users to be followed. They depict the importance of interactions among users from which they can be measured and integrated into a proximity metric that factors the relationships among users and the number of interactions. Furthermore, they consider influent users those that have a large number of followers and with a high frequency of interaction to recommend them. Hence, we can observe how the news shown in a user's timeline can contribute to overloading him/her or even reduce his/her engagement. In such manner, this study approaches features which are analyzed so as to construct our proposed social capital model.

III. The Proposal

A. Twitter Features

This paper uses Twitter for evaluation purposes. However, the recommendation model may be implemented by other platforms (i.e. Instagram, Facebook), as it implements the basic concepts of social networks. Twitter is a micro-blogging service that allows users to share messages, called tweets, which contain various resources and offer a glossary[1] with a wide list: **Timeline**: A list of tweets published by accounts that a user follows; **News (Tweet)**: It is a message which contains a max of 280 chars. The term news will be adopted to refer the content created by the user on Twitter; **Retweet**: It is the action to forward a tweet; **Favorite**: It is the user action of liking a tweet; **Lists**: It is a functionality that allows creating personalized lists of users or topics. For example, a user can create lists with users or topics that are most interesting for him/her such as "soccer players", "top 10 TV shows"; **Reply**: It is the users' action to comment on a tweet; and **(Un)Follow**: The act of un/following another account.

1) Twitter's API: Twitter provides an API to access information on its platform. This way, endpoints are available to extract the content of a timeline, post news, interact, or even follow any account. Moreover, the platform provides access plans that have limitations on extracting data in a range of time. As an example, we adopted a standard plan, which allows us to make 450 requests within a 15-minute window. So, if a high number of users makes requests in a short period of time, we will not be able to access that information.

B. Notation

In this section we present the mathematical notations that will be used along this proposal. **U**: The set of all users; **N**: The set of all extracted news; **TC**: The number of received likes; **TE**: The number of retweeted news; **TCP**: The number of comments that a news has; **TS**: The number of followers; **TLS**: The number of lists that a user belongs; **TNP**: The number of published news; **TXT**: The text of published piece of news; ps_n: The sentiment weight of a comment or news; **STM**: The reputation score of a mentioned user; and **STC**: The social capital score of a comment or a piece of news.

1) Users (U): Social networks are constituted of interlinked users that post, comment, mention or forward some news. Users are represented as $U = \{u_1, u_2, ..., u_n | 1 \leq n \leq \mathbb{N}\}$, where each $u \in U$ is defined as a tuple $u = \langle TC, TS, TLS, TNP, RN \rangle$ with four metadata, which are used to calculate the influence of users in the social network (see Section III-E). RN is the assigned rating for news when a user participates in an online experiment. This was created to demonstrate that the user's profile is updated constantly.

2) News (N): News are the recommended items for a given user, and they are formally represented as $N = \{n_1, n_2, ..., n_z | 1 \leq z \leq \mathbb{N}\}$, where each $n \in N$ is a tuple $n = \langle TC, TE, STM, STC, TCP, TXT \rangle$ with six metadata, which are also used to calculate the reputation and influence of users in the social network (see Section III-E).

[1]https://help.twitter.com/pt/glossary

C. News Pre-processing and Modeling

All extracted news are pre-processed and modeled according to the Fig. 1. As a result of the pre-processing, the news are represented as $NM_n = \{feat, (term, frequency | term \in BW, feat \in n\}$, where each $feat_i$ represents a news metric (i.e. amount of likes, retweets, comments, followers, followees), $term_i$ is a news' term (i.e. keywords from comments or posted news) and $frequency$ is a relevancy derived from TF-IDF calculation. Fig. 1 shows the news modeling scheme.

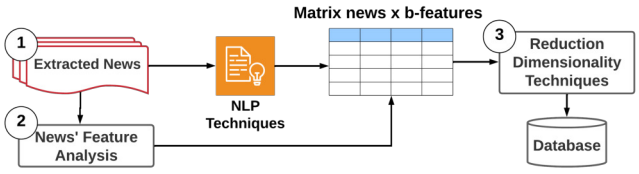

Fig. 1. Steps to model the news.

Extracted News: The news are extracted from the public timelines using the Twitter API. Besides the text itself, all interaction data (features) associated to the news is also withdrawn, including retweets, likes, comments, hyperlinks and hashtags; **News Feature Analysis**: Once the feature vector is created, the relevance of each term of the news is calculated using TF-IDF metric. Moreover, each extracted feature is added to the news model. and **Sparseness**: A multidimensional news matrix *news* $\times$ *b-features* is created containing all features of all extracted news. Principal Component Analysis technique is used to reduce the matrix dimension [25].

.

D. User's Influence

This work approaches a new influence metric represented by the Equation 3, which is a part of the Equation 4 to measure how influential a user is, considering their popularity and reputation, besides his activity according to post frequency and feedback received by his followers. The Equation 3 calculates a user's influence based on his popularity (Equation 1) [26],

$$PScore_u = 1 - e^{-\lambda . TS} \tag{1}$$

where $PScore_u$ represents the popularity score of a user u, λ is a constant that by default is 1, which helps provide a fine adjustment, and TS is the number of followers.

In addition, the Equation 3 employs the Equation 2 to measure the user's reputation considering the number of lists in which he/she is inserted [27]. The idea behind this metric is to identify the credibility, reputation, and reliability of a user compared to other users that shared similar interests. As a result, the Equation 2 shows that the lower the score, the better is a user's reputation:

$$RScore_u = \begin{cases} \frac{TS_u}{TLS_u}, \; if \; TLS_u \neq 0 \\ TS_u \; if \; TLS_u = 0 \end{cases} \tag{2}$$

where u is the active user, TS is the number of followers, and TLS is the number of lists that a user u is inserted in. In other words, if a user is popular and has high posting frequency and feedback on their network, their score will be high. However, it is necessary to observe other users that do not have a good reputation, as this metric factors the number of followers and lists. Hence, new users or even those with few followers can produce interesting content and should be taken into account.

$$IScore_u = \frac{PScore_u + TC_u + TNP_u}{RScore_u} \tag{3}$$

where TC is the number of likes that u received for the news that they posted, and TNP is the number of news published by the user u.

E. The Social Capital Metric

Every news impact on people, the position where it appears in the timeline represents relevance to the user. In other words, each social network adopts different methods to rank news with the goal of satisfying its users or even helping them in the decision-making process (e.g. finding a healthy restaurant nearby). [28] and [29] claim that an interesting approach is to exhibit news with a high number of comments, interactions, connections and positive sentiment at the top of the news' list. The rationale is that much attention is being focused on that particular set of news.

We try to calculate the Social Capital as the power of a news ($n \in N$) based on the amount of interaction and its impact on the network over a period of time. This way, Equation 4 sums up these interactions pondered by the sentiment classification expressed by the text and influence of a user, calculated by the $IScore_u$. The sentiment analysis is used to provide new insights to understand the user's preference. Moreover, this classification can be used to model news' comments to predict their relevance [30]. The Social Capital metric is shown as:

$$SCScore(n,u) = \begin{cases} (TC_n + TE_n + STM_n + STC_n + TCP_n) \\ \cdot ps_n \cdot IScore_u,\ if\ ps_n \neq 0 \\ (TC_n + TE_n + STM_n + STC_n + TCP_n) \\ \cdot IScore_u,\ if\ ps_n = 0 \end{cases} \tag{4}$$

where n is a news, u is a user who posted it, TC, TE, STM, STC, TCP are described in Section III-B, and ps_n is the sentiment score, which is calculated from the Algorithm 2. Our intuition behind this metric is that news with more repercussions within a context of the user's interest can be useful to provide information, reduction of the information overload problem, and improve the user's engagement

F. Recommendation Model

Besides the social capital, the recommendation model contemplates the user's reputation and the sentiment on the recommended news. Indeed, our intuition behind this approach is that news with more comments, interactions, etc. can be relevant according to the user's preferences. In this case, the following algorithms provide the recommendation model according to the aforementioned equations.

1) Reputation's Algorithm: The Algorithm 1 calculates the user's influence and has as an input a user ($u \in U$), who posts, comments, or was mentioned in news. It has as an output the user's influence score. Line 1 initializes variables according to each user's features. Line 2 verifies if a user has followers, if true, the max number of followers is assigned to TS. Line 5 verifies if the user has been inserted in any lists, if true, the constant β is assigned to TLS. The value used in this work was 1, once it is not less or equal to 0. Line 8 calculates the user's reputation. Line 9 verifies if a user is authentic, which is used to establish if the account is authentic, active, and remarkable. So, in case an account has those characteristics the score is increased, which is carried out by the constant θ in line 10, and the value used was 1. Finally, line 12 calculates the score.

Algorithm 1 User's influence pseudo-code.

Require: $User\ u \in U$
Ensure: $IScore_u$
$TS, TC, TLS, RNP \in u$
2: **if** $TS = 0$ **then**
$TS \leftarrow maxFollowers$
4: **end if**
if $TLS = 0$ **then**
6: $TLS \leftarrow \beta$
end if
8: $reputationScore \leftarrow RScore_u$
if $user$ is $verified_u$ **then**
10: $reputationScore \leftarrow reputationScore + \theta$
end if
12: **return** $\dfrac{PScore_u + TC + TNP}{reputationScore}$

2) Sentiment Analysis Algorithm: The Algorithm 2 shows how the text of the news is analyzed and processed in order to classify the user's sentiment while typing it.

Algorithm 2 Sentiment analysis of a text/comment.

Require: Text of a news/comment $text_n \mid n \in N$
Require: Classification of the news sentiment $label$
text $\leftarrow$ preProcess($text_n$)
2: **if** text $\neq$ null and text.size > 0 **then**
return nlp.classify(preProcessedText)
4: **end if**
return null

Thus, the Algorithm 2 has the news text as input and the classification of this text as an output. Line 1 processes the text removing irrelevant data. Line 2 verifies if a text is null and if its length is greater than zero. If true, line 3 uses the Amazon Comprehend service to classify the sentiment expressed by the text, which can be negative, positive, neutral, or mixed. This service has a set of available tools to analyze texts in natural language. We can point out that this service uses a

pre-trained model to gather insights about a document or a set of documents. Besides that, according to Amazon, this model is continuously trained on a large body of text so that there is no need to provide training data. Finally, in the same line mentioned above, the label is returned.

Algorithm 3 Pseudo-code of a recommendation model.

```
Require: News n ∈ N, User u ∈ U
Require: SCScore(n, u)
    URS ← influenceScore(u)
2:  TC, TE, TCP ∈ n
    STM, STC, score ← 0
4:  for user ∈ M_n do
        STM ← STM + influenceScore(user)
6:  end for
    for com ∈ C_n do
8:      STC ← STC + scScore(com, com.whoPosted)
    end for
10: score ← score + ( (TC+TE+STM+TCP+STC) · URS)
    sentimentWheight ← 0
12: if shouldAnalyzeSentiment then
        sentimentLabel ← sentimentAnalysis(text_n)
14:     if sentimentLabel is positive then
            sentimentWheight ← α
16:     else
            if sentimentLabel is negative then
18:             sentimentWheight ← θ
            else
20:             sentimentWheight ← β
            end if
22:     end if
        score ← score · sentimentWheight
24: end if
    return score + Similarity(u, n)
```

3) Recommendation Model With Social Capital: The Algorithm 3 calculates the social capital of news, which receives as an input a piece of news n and a user u, and generates the social capital score as an output. The Algorithm 3 employs techniques from both Algorithms 1 and 2. Lines 2 initializes variables according to each news features. Line 4 iterates each mentioned user of the news, so the algorithm calculates the user's influence. Line 7 iterates each comment, and line 8 calculates its social capital. Line 10 calculates the partial score, which is weighted by the user's influence. Line 12 verifies if the sentiment analysis should be considered, if so, the analysis is undertaken (line 13) as shown in Algorithm 2. Lines 13-22 verify each condition to assign the weight to the final score, in which α, θ, and β are the weights used on the social capital score. In this work, the values 1.5, 1, and 0.5 were used as alpha, omega, and beta, respectively. These values were adjusted empirically. Line 25 calculates the cosine similarity [31] between the user's profile and the current news. We consider a high similarity, scores greater than 0.7. In other words, we use the user's ratings from each recommended news in order to update his profile and then, recommend a set of news that is closest to his previous preferences. In this case, we increase the score of news with the user's profile similarity score. Finally, a set of news that will be presented to an active user is ranked by the social capital score in order to show news with the highest score at the top of the list.

IV. Experimental Evaluation

The proposed approach was evaluated in a user trial with the goal of assessing the quality of recommendations. To conduct the experiment, we developed the RecSocial web-based system, an application used for collecting the users' feedbacks and evaluating the generated recommendations using the approach proposed by this work.

A. The RecSocial Application

The RecSocial was created for evaluation purposes exclusively. All data collected from the user trial resulted in dataset[2], which is available freely online. For this, some steps are realized: 1) **News Extraction**: RecSocial is populated with news extracted from Twitter; 2) **Pre-processing**: Data is pre-processed in order to remove redundancies, inconsistencies, noises and irrelevant data. After that, we calculate the statistics about the data on the RecSocial including the number of followers, likes and comments in a news, etc; 3) **Social Capital Model**: The Social Capital score for each piece of news imported from Twitter is calculated; and 4) **Recommendation Model**: Finally, the recommendations are generated so that users are able to evaluate them.

1) Using RecSocial: Initially, the user creates their account and logs in. After authentication, a set of topics and subtopics of interest (Sports, Trips, News, etc.) are shown so that user selects those which will form their timeline. Bear in mind that we are trying to simulate Twitter's timeline. After authentication, the system shows a set of topics, which have a set of subtopics associated with a set of extracted news.

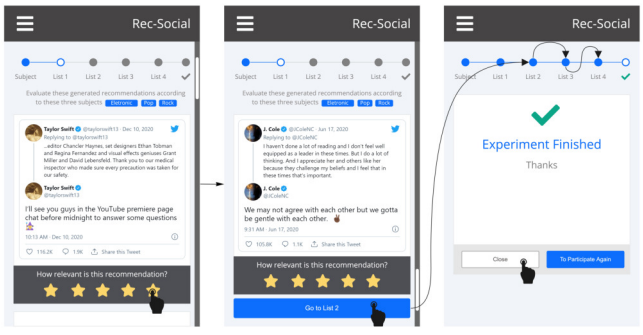

Fig. 2. Recommendations and user's feedback.

After selecting the topics of interest, recommendations are generated as shown in Fig. 2. In this step, the user evaluates each generated recommendation providing his/her feedback by a 5-point Likert scale. A "Go To List x" button appears at the bottom guiding the user to the next round of recommendations.

[2]shorturl.at/qBJQ3

For these experiments in particular, four rounds were undertaken. Finally, the logged user can close the app or participate again for a new round of recommendations. This app code is available on https://github.com/pauloprsdesouza/recsocial-api.

B. Methodology

For the online experiment, 80 volunteers took part in the experiment from 3/15/21 to 6/6/21. They were 20 to 40 years old and all very familiar with social networks, using them for various purposes including work, family and friendship. Before the experiment, the participants were introduced about the RecSocial application and received the two major instructions: 1) Select three subcategories from their interests; and 2) Evaluate four lists of recommendations, each with 10 items (tweets about news). In summary, 40 recommendations were evaluated by each participant using the 5-point Likert scale [32] (see Fig. 2). In total, there were 80 volunteers, 3.030 recommendations evaluated, 12.185 Twitter accounts used, 9.533 (78%) users mentioned and 32.252 news extracted.

C. Simulation of User's Timeline

In general, the participants do not feel comfortable in giving access to their Twitter personal accounts, once their behaviors on the microblogging can show a lot about them. In other words, they do not want to expose themselves in order to allow that an experiment can analyze their interactions and produced content over time. For this reason, we decided to simulate the user's timeline (on RecSocial) by allowing them to make up a timeline with Tweets from a wide range of categories such as music and news, for example. These categories represent the user interests and were used to retrieve Twitter accounts associated with them. For instance, if one chooses "Sports/-Football", then @FIFAcom is an eligible account from which its tweets will compose that user's timeline. In this case, our intuition behind this approach is to construct a user's timeline more as diversified as possible. In other words, the number of news was defined considering the diversity criteria for the RS.

Our approach was compared against other methods: i) Social Capital (SC); ii) Social Capital with Sentiment Analysis (SC+SA); iii) Cosine Similarity (CS-Plus); and iv) Baseline (B1) [33]. Inspired by [34], who uses an approach of incremental evaluation, called Prequential Evaluation, this experiment methodology updates the user's profile according to his preferences after every recommendation round. The following metricks were used: Mean Reciprocal Rank (MRR) [22], Precision@N [22], Mean Average Precision (MAP) [17], and Normalized Discounted Cumulative Gain (NDCG) [35].

D. Results

The experiment results are organized by the metrics analyzed. The MRR results are SC (0.75), SC+SA (0.68), CS+PLUS (0.67) and B1 (0.68). The SC algorithm achieves the highest MRR scores. The SC MRR score is 7% higher than both B1 and SC+SA MRR scores. The lowest MRR results are observed by the CS-PLUS algorithm. From these results, we can observe that SC algorithm was effective to generate relevant recommendations at the top of the list. In other words, users evaluated recommendations between ratings 4-5.

Fig. 3 shows the precision results. We can observe that the SC algorithm achieves higher scores than the other approaches. In other words, the proposed approach was able to generate relevant recommendations up to the fifth evaluated time. The compared methods present slight variations among them. We can point out that SC algorithm generates relevant recommendations in at least 60% of cases, demonstrating that SC approach can be useful to generate recommendations.

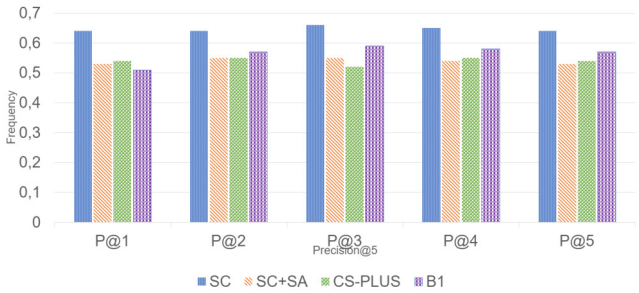

Fig. 3. Results of Precision@N metric.

The MAP results are SC (0.62), SC+SA (0.53), CS+PLUS (0.52) and B1 (0.55). The SC algorithm achieves the highest MAP scores. The SC MAP score is 7% and 9% higher than B1 and SC+SA MAP scores respectively. The lowest MAP results are observed by the CS-PLUS algorithm. In this case, we can observe that SC algorithm was able to generate the most interesting recommendations at the top of the list, in other words, MAP metric rewards first-loaded relevant recommendations.

The NDCG results are SC (0.85), SC+SA (0.81), CS+PLUS (0.79) and B1 (0.79). The SC algorithm achieves the highest NDCG scores. The SC NDCG score is 4% and 6% higher than SC+SA and B1 scores respectively. The CS-PLUS presents a score equal to B1. In this case, once the NDCG metric considers the order of recommended items versus the ideal order of recommended items, we observe that the SC algorithm was able to generate relevant recommendations in 85% of cases at least. We notice that the SC+SA algorithm has the second-best results when compared to the others, generating relevant recommendations in 81% of cases.

Fig. 4 shows the rate frequency by each comparison method. We can observe that the algorithm SC is the most frequently top rated (5 stars), and the least frequent for lower ratings (1-3). The top rating at SC is 3% higher than the B1 method, the second best observed. The other methods do not present relevant results when compared with SC.

Fig. 5 shows the correlation between evaluated recommendations and the news features. We calculate the average of all features of each news recommended and correlate it with ratings. We can observe that the SC algorithm achieves the highest scores. The SC score is 24% higher than B1, the second best observed. The other methods do not present relevant results when compared to SC. Therefore, we could

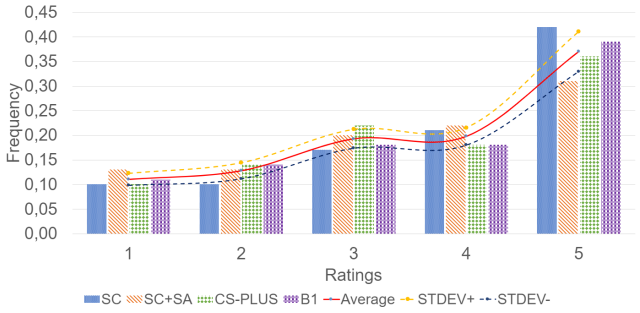

Fig. 4. Evaluation's rating frequency.

state that we have the intuition that users may prefer reading news with more interactions and with more features.

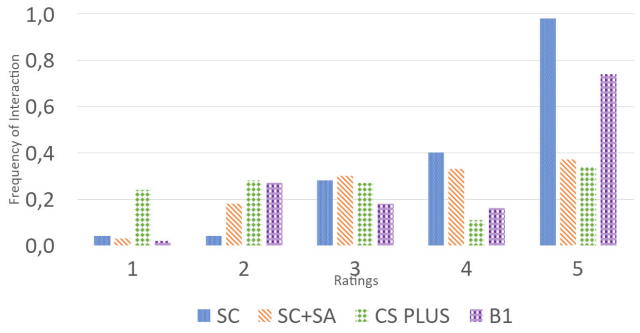

Fig. 5. Evaluated recommendations X news features.

Fig. 6 presents the correlation between recommendations evaluated with the IScore (see Section 3) metric. We can observe that SC is the most frequently top rated (4-5), and the least frequent for lower rating 3. Besides, the SC+AS achieves the SC rates (4 stars). In other words, recommendations published by influential users received better evaluations according to the proposed algorithms. These results can be expressed from the fact that the user's influence in the social capital approach can generate relevant recommendations according to the user's interests.

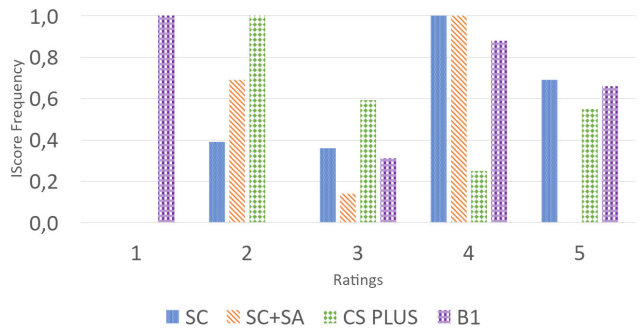

Fig. 6. Evaluated recommendations X news features.

V. Discussion

Personalization methods aim to provide the construction of the user's profile according to their interests. In this case, [11] discuss how the timeline order influences what a user sees, and they take many interactions and features of news into account to analyze it. Our work has found empiric results that the proposed social capital algorithm, besides the user influence metric can better order the user's timeline by providing relevant news. An example of this can be seen through Fig. 6, which demonstrates that users liked (ratings 4-5) news recommended through popular accounts. Besides that, both proposed metrics IScore and SCScore when used together have the capacity to measure the value of news, which provides a score that can be used to rank a user's timeline, as we can see from the previously aforementioned ranking metrics. In other words, taking interactions, relationships and other news features into account can be useful to generate relevant recommendations.

We can see that results from the other algorithms were more similar, indicating that the incremental approach adopted by this work updates the user's profile according to the last evaluation. Moreover, we observed that our second SC+SA algorithm does not present relevant results when compared with other implementations. This occurs because weights employed in sentiment analysis need other adjustments through empiric tests to perform online and offline experiments. In addition, texts with few words may be biased, which influences the weighting step.

Finally, this work does not deal with misinformation problems or even bots. Moreover, we know that these problems mentioned before may have a high social capital score if they present a high number of interactions, comments, etc. We must also point out yet that users can be overwhelmed or even overloaded with news that talks about the same context, but we need to consider the scope of this work, which is exploiting the social capital on social networks as a method to generate news recommendations.

VI. Conclusion

This work proposes a social capital metric to measure the news value used in generating personalized recommendations, according to the individual's profile. Thus, the results show that exploiting social capital on social networks can be useful to cope with the information overload problem. The hypothesis raised by this proposal is to have a timeline that contains the most interesting and relevant news at the top of the list, presenting a significant gain on the knowledge and on information overload reduction.

As future work, we intend to test our proposal with other approaches in order to measure how misinformation impacts the news with high social capital. Besides that, we plan to implement other techniques to cope with the synonymy and polysemy problem using WordNet, as well as to construct a bigger dataset in order to improve the user's profile. After that, we plan to conduct a long-term experiment using linear regression techniques to learn about user's behavior and further

improve their profile. Finally, we plan to resort to certain strategies in order to deal with misinformation and bots as previously mentioned by using available datasets in literature, and applying other available metrics in literature so as to compare the results with our proposed method.

REFERENCES

[1] K. K. Kapoor, K. Tamilmani, N. P. Rana, P. Patil, Y. K. Dwivedi, and S. Nerur, "Advances in social media research: Past, present and future," *Information Systems Frontiers*, vol. 20, no. 3, pp. 531–558, Nov. 2017. doi: 10.1007/s10796-017-9810-y

[2] P. Bourdieu, "The forms of capital," in *Readings in Economic Sociology*. Blackwell Publishers Ltd, 2002, pp. 280–291.

[3] J. Nahapiet and S. Ghoshal, "Social capital, intellectual capital, and the organizational advantage," *Academy of Management Review*, vol. 23, no. 2, pp. 242–266, Apr. 1998. doi: 10.5465/amr.1998.533225

[4] C. Spratt, J. Hong, K. McAreavey, and W. Liu, "Community-based measures for social capital," in *Studies in Computational Intelligence*. Springer International Publishing, Dec. 2018, pp. 327–338.

[5] J. Coleman, *Foundations of social theory*. Cambridge, Mass: Belknap Press of Harvard University Press, 1990.

[6] G. Pijpers, *Information Overload: A System for Better Managing Everyday Data*, ser. Microsoft executive leadership series. John Wiley and Sons Ltd, 2010.

[7] K. Bontcheva, G. Gorrell, and B. Wessels, "Social media and information overload: Survey results," 06 2013.

[8] F. Ricci, L. Rokach, and B. Shapira, *Recommender Systems: Introduction and Challenges*. Springer US, 2015, ch. 1, pp. 1–34.

[9] S. Forouzandeh, A. Sheikhahmadi, A. R. Aghdam, and S. Xu, "New centrality measure for nodes based on user social status and behavior on facebook," *International Journal of Web Information Systems*, vol. 14, no. 2, pp. 158–176, Jun. 2018. doi: 10.1108/ijwis-07-2017-0053

[10] Y. Li, J. Liu, and J. Ren, "Social recommendation model based on user interaction in complex social networks," *PLOS ONE*, vol. 14, no. 7, p. e0218957, Jul. 2019. doi: 10.1371/journal.pone.0218957

[11] N. Bartley, A. Abeliuk, E. Ferrara, and K. Lerman, "Auditing algorithmic bias on twitter," in *13th ACM Web Science Conference 2021*. ACM, Jun. 2021. [Online]. Available: https://doi.org/10.1145/3447535.3462491

[12] T. O'Reilly, "What is web 2.0," Sep 2005. [Online]. Available: https://www.oreilly.com/pub/a/web2/archive/what-is-web-20.html

[13] F. Ricci, L. Rokach, B. Shapira, and P. B. Kantor, *Recommender Systems Handbook*, F. Ricci, L. Rokach, B. Shapira, and P. B. Kantor, Eds. Springer, 2011.

[14] S. Berkovsky, J. Freyne, and G. Smith, "Personalized network updates: Increasing social interactions and contributions in social networks," in *User Modeling, Adaptation, and Personalization*. Springer Berlin Heidelberg, 2012, pp. 1–13.

[15] W. Feng and J. Wang, "Retweet or not?" in *Proceedings of the sixth ACM international conference on Web search and data mining - WSDM '13*. ACM Press, 2013. doi: 10.1145/2433396.2433470

[16] C. Li and F. Xiong, "Social recommendation with multiple influence from direct user interactions," *IEEE Access*, vol. 5, pp. 16 288–16 296, 2017. doi: 10.1109/ACCESS.2017.2739752

[17] D. P. Karidi, Y. Stavrakas, and Y. Vassiliou, "Tweet and followee personalized recommendations based on knowledge graphs," *Journal of Ambient Intelligence and Humanized Computing*, vol. 9, no. 6, pp. 2035–2049, Apr. 2017.

[18] H. Bo, R. McConville, J. Hong, and W. Liu, "Social network influence ranking via embedding network interactions for user recommendation," in *Companion Proceedings of the Web Conference 2020*. ACM, Apr. 2020. doi: 10.1145/3366424.3383299

[19] F. Durao and P. Dolog, "Improving tag-based recommendation with the collaborative value of wiki pages for knowledge sharing," *Journal of Ambient Intelligence and Humanized Computing*, vol. 5, no. 1, pp. 21–38, Apr. 2012. doi: 10.1007/s12652-012-0119-x

[20] F. Abel, Q. Gao, G.-J. Houben, and K. Tao, "Analyzing user modeling on twitter for personalized news recommendations," in *User Modeling, Adaption and Personalization*. Springer Berlin Heidelberg, 2011, pp. 1–12.

[21] Y. Bachrach, M. Kosinski, T. Graepel, P. Kohli, and D. Stillwell, "Personality and patterns of facebook usage," in *Proceedings of the 3rd Annual ACM Web Science Conference on - WebSci '12*. ACM Press, 2012. doi: 10.1145/2380718.2380722

[22] F. Abel, Q. Gao, G.-J. Houben, and K. Tao, "Twitter-based user modeling for news recommendations," in *Proceedings of the Twenty-Third International Joint Conference on Artificial Intelligence*, ser. IJCAI '13. AAAI Press, 2013. doi: 10.5555/2540128.2540558 p. 2962–2966.

[23] G. Kazai, I. Yusof, and D. Clarke, "Personalised news and blog recommendations based on user location, facebook and twitter user profiling," in *Proceedings of the 39th International ACM SIGIR conference on Research and Development in Information Retrieval*. ACM, Jul. 2016. doi: 10.1145/2911451.2911464

[24] R. K. Mudgal, R. Niyogi, A. Milani, and V. Franzoni, "Analysis of tweets to find the basis of popularity based on events semantic similarity," *International Journal of Web Information Systems*, vol. 14, no. 4, pp. 438–452, Nov. 2018. doi: 10.1108/ijwis-11-2017-0080

[25] M. E. Timmerman, "Principal component analysis," *Journal of the American Statistical Association*, vol. 98, no. 464, pp. 1082–1083, dec 2003. doi: 10.1198/jasa.2003.s308

[26] A. Aleahmad, P. Karisani, M. Rahgozar, and F. Oroumchian, "OLFinder: Finding opinion leaders in online social networks," *Journal of Information Science*, vol. 42, no. 5, pp. 659–674, Jul. 2016. doi: 10.1177/0165551515605217

[27] J. Bullas, "What is your twitter reputation?" 2011. [Online]. Available: https://www.jeffbullas.com/what-is-your-twitter-reputation/

[28] T. H. P. Silva, A. H. F. Laender, and P. O. S. V. de Melo, "On knowledge-transfer characterization in dynamic attributed networks," *Social Network Analysis and Mining*, vol. 10, no. 1, Jun. 2020.

[29] L. Camacho, J. Faria, S. Alves-Souza, and L. Filgueiras, "Social tracks: Recommender system for multiple individuals using social influence," in *Proceedings of the 11th International Joint Conference on Knowledge Discovery, Knowledge Engineering and Knowledge Management*. SCITEPRESS - Science and Technology Publications, 2019. doi: 10.5220/0008166503630371

[30] Y. Bae and H. Lee, "Sentiment analysis of twitter audiences: Measuring the positive or negative influence of popular twitterers," *Journal of the American Society for Information Science and Technology*, vol. 63, no. 12, pp. 2521–2535, Nov. 2012. doi: 10.1002/asi.22768

[31] F. Isinkaye, Y. Folajimi, and B. Ojokoh, "Recommendation systems: Principles, methods and evaluation," *Egyptian Informatics Journal*, vol. 16, no. 3, pp. 261–273, nov 2015. doi: https://doi.org/10.1016/j.eij.2015.06.005

[32] D. Jannach, M. Zanker, A. Felfernig, and G. Friedrich, *Recommender Systems: An Introduction. Cambridge*. Cambridge University Press, 2010.

[33] E. Lee, Y. J. Kim, and J. Ahn, "How do people use facebook features to manage social capital?" *Computers in Human Behavior*, vol. 36, pp. 440–445, Jul. 2014. doi: 10.1016/j.chb.2014.04.007

[34] J. Vinagre, A. M. Jorge, and J. Gama, "Evaluation of recommender systems in streaming environments," 2014. doi: 10.13140/2.1.4381.5367

[35] R. Zhang, H. Bao, H. Sun, Y. Wang, and X. Liu, "Recommender systems based on ranking performance optimization," *Frontiers of Computer Science*, vol. 10, no. 2, pp. 270–280, Jul. 2015. doi: 10.1007/s11704-015-4584-1

4th International Symposium on Rough Sets: Theory and Applications

THE RSTA symposium is devoted to the state-of-the-art and future perspectives of rough sets considered from both a theoretical standpoint and real-world applications. Rough set theory is a highly developed discipline with a large number of mechanisms potentially useful in intelligent data analysis. In our special session, we aim to invite deep research papers that address the practical problem of modeling artificial intelligence processes using techniques derived from rough sets. We also encourage scientists from other research fields to participate to initiate discussions and collaborations on other methods of data exploration and approximate computations.

TOPICS

The list of topics includes, but is not limited to:

- Artificial Intelligence
- Algebraic Logic
- Logics from Rough Sets
- Approximate Reasoning
- Clustering and Rough Sets
- Dominance-based rough sets
- Distributed Cognition
- Granular Computing
- Rough mereology
- Near sets and Proximity
- Fuzzy-rough hybrid methods
- Hybrid techniques
- Rough neural computing
- Evolutionary computation and rough set
- Image and Video Processing
- Rough Sets in Education Research
- Knowledge discovery from Databases
- Missing values
- Big data
- Bio-informatics
- Three-Way Decision Making
- Data security
- Intelligent Robotics
- Knowledge engineering
- Multimedia applications
- AHP and Decision Making
- Assistive technology and adaptive sensing systems

TECHNICAL SESSION CHAIRS

- **Artiemjew, Piotr,** Faculty of Mathematics and Computer Science, University of Warmia and Mazury in Olsztyn, Poland
- **Chelly Dagdia. Zaineb, UVSQ,** Paris-Saclay, France
- **Mani, A.,** Machine Intelligence Unit, Indian Statistical Institute, Kolkata, India

PROGRAM COMMITTEE

- **Bhattacharya, Malay,** Indian Statistical Institute, India
- **Chakraborty, Debarati,** Indian Statistical Institute, India
- **Chiru, Costin-Gabriel,** Politehnica University of Bucharest, Romania
- **Ciucci, Davide,** Università di Milano-Bicocca, Italy
- **Das, Monidipa,** Nanyang Technological University, Singapore
- **Dutta, Soma,** University of Warmia and Mazury in Olsztyn, Poland
- **Düntsch, Ivo,** Brock University, Canada
- **Gomolinska, Anna,** University of Bialystok, Poland
- **Henry, Christopher,** University of Winnipeg, Canada
- **Jana, Purbita,** Indian Institute of Technology, India
- **Janicki, Ryszard,** McMaster University, Canada
- **Li, Tianrui,** Southwest Jiaotong University, China
- **Lin, Zhe,** Department of Philosophy Xiamen University Xiamen, China
- **Ma, Minghui,** Sun Yat-Sen University, China
- **Matson, Eric,** Purdue University, USA
- **Matwin, Stan,** Dalhousie University, Canada
- **Mihálydeák, Tamás,** University of Debrecen, Hungary
- **Palmigiano, Alessandra,** The Vrije Universiteit Amsterdam, Netherlands
- **Pancerz, Krzysztof,** University of Rzeszow, Poland
- **Skowron, Andrzej,** Systems Research Institute, Polish Academy of Sciences and Cardinal Stefan Wyszynski University, Warsaw, Poland
- **Stell, John,** University of Leeds, United Kingdom
- **Suraj, Zbigniew,** Rzeszów University, Poland
- **Szczuka, Marcin,** Institute of Informatics, The University of Warsaw, Poland
- **Yao, Yiyu,** University of Regina, Canada
- **Zhu, William,** University of Science and Technology of China

Communication Papers of the of the 17th Conference on Computer Science and Intelligence Systems pp. 65–72
DOI: 10.15439/2022F282
ISSN 2300-5963 ACSIS, Vol. 32

Towards a Granular Computing Framework for Multiple Aspect Trajectory Representation and Privacy Preservation: Research Challenges and Opportunities

Zaineb Chelly Dagdia
Université Paris-Saclay, UVSQ, DAVID, France
LARODEC, ISG, Université de Tunis,Tunis, Tunisia
Email: zaineb.chelly-dagdia@uvsq.fr

Vania Bogorny
Programa de Pós-Graduação em Ciência da Computação,
Departamento de Informática e Estatística (INE),
Universidade Federal de Santa Catarina (UFSC),
Florianópolis, SC, Brasil
Email: vania.bogorny@ufsc.br

***Abstract*—In recent years, there has been a lot of research on trajectory data analysis and mining. Despite the fact that trajectories are multidimensional data characterized by the spatial, the temporal, as well as the semantic aspect, few are the studies that have taken into account all of these three dimensions. Apart from these dimensions that should be considered all together for an efficient trajectory data analysis and mining, it should be also made feasible to represent trajectories from several points of view, which is called *multiple aspect representation*. State-of-the-art works are typically restricted to a single trajectory representation, which limits the identification of a variety of key patterns. These multiple aspect trajectories are quite rich that they reveal sensitive information, making the user's privacy vulnerable; hence, raising several challenges when it comes to privacy preservation. In this paper, we show that there is a need to consider granular computing for multiple aspect trajectory representation and privacy preservation, and present new research challenges and opportunities in this concern.**

I. Introduction and motivation

TODAY, we are living the era of movement monitoring and mining where large volumes of mobility data are being captured about our everyday lives and routines. The collected data is characterized not only but its volume and velocity but also by its heterogeneity (variety) and uncertainty, and most importantly by its sensitive aspect. The collection and enrichment of this tremendous amount of mobility data with information from several sources is made possible by the popularization and frequent use of mobile devices [1], applications, sensors, internet channels, social networks, among many other services and instruments.

For instance, via the use of social networks such as Facebook and Twitter and navigation applications such as Google Maps, detailed information about our routines can be collected including the places that we have visited, the time that we have spent at each visited place, our emotions at a specific time and place, our means of transportation, etc. These are referred to as *"semantic trajectories"* which are characterized by their different aspects or dimensions, and their complex nature [2]. With this explosion of enriched trajectory data, emerged the problem of data privacy. The more information that is linked to mobility data, the more sensitive is the user privacy. Therefore, it became critical and essential to protect users' privacy.

When it comes to trajectory representation, the same semantic trajectory can be represented with respect to different aspects [2]. As an example, a raw trajectory can be represented as a sequence of stops and moves, or as a sequence of transportation means, or as a sequence of weather conditions, of activities performed during the movement, and so on. This led to the *"Multiple Aspect Trajectory"* (MAT) concept.

Multiple aspect trajectory representation is a hot topic and it is very recently that the MASTER model was proposed in [3]. The MASTER model allows the representation of the trajectory with space, time and several aspects, any of which might violate the user privacy. Therefore, there is a need to consider a novel structure that permits the representation of multiple aspect trajectories while considering privacy preservation.

The aim of this paper is to highlight the perspectives of applying Granular Computing (GrC) formal settings (e.g., rough set theory, rough set theory, set theory, etc.) to multiple aspect trajectory representation. We present a representation based on granular computation that we named $GrC - MAT$. The paper, also, presents the important aspects of granular computation that can be considered for privacy preservation. It is to be noted that the objective of this paper is not to make a survey of the state-of-art methods that deal with MAT representation and privacy preservation, nor to discuss their limitations.

The rest of the paper is organized as follows: Section II introduces the main concepts and fundamentals of multiple aspects trajectories and granular computation. Section III highlights the representation of multiple aspect trajectory. Section IV, introduces the proposed granular computing framework, $GrC - MAT$, for multiple aspect trajectory representation

This work has received funding from the European Commission's Horizon 2020 research and innovation programme under the Marie Sklodowska-Curie grant agreement N. 777695.

as well as covering its evolving aspect. In Section V, we discuss our vision of the future research challenges and opportunities in multiple aspect trajectory representation and privacy preservation from a granular computing perspective. Finally, Section VI concludes the paper.

II. Background

In this section, we introduce the main concepts and fundamentals of multiple aspects trajectories and granular computation.

A. Trajectory data models

When an individual or an object is moving, his/her/its location data is collected over time via mobile devices or applications or any other collection instruments. This data is in the form of a sequential spatiotemporal points, called *raw trajectory*, and is denoted as $Seq =< p_1, p_2, \ldots, p_n >$, where each $p_i = (x_i, y_i, t_i)$, with $p_i \in Seq$, x_i and y_i are the spatial position of the moving individual/object in space at a specific time frame t_i.

Several data models have been presented in the last decade to represent and augment trajectories with semantic information. These can be categorized into three main time frames. For instance, the work proposed in [4] initiated trajectory modelling via the use of sequences of events in space and over a specific time window. These are typically raw trajectories which represent the first category of trajectory data models, and are the simplest. Later on, and during the period of 2008 and 2018 which is characterized by the explosion of social networks and navigation applications, works have been around enriching trajectories with semantic information. In this concern, in [5], authors proposed the integration of geographic information while distinguishing stops and moves. The segments of a trajectory where the moving individual/object has stayed for a minimal amount of time define the stops, whereas the movement between stops define the moves. In this work, semantic trajectories can have each stop linked to Points of Interest (POI), which are usually a place name, reflecting semantic information; which are added as a third dimension to space and time. In 2014, a semantic trajectory data model called CONSTANT was proposed in [2]. The model associates the moving individual/object trajectories to a set of other information such as the visited POIs, the activities performed at a specific POI, and the transportation means. Also, within this second category, the BAQUARA framework was proposed in [6]. The semantic model enriches trajectories with ontologies and linked open data.

Very recently, in [3] and within the third category, authors introduced the MASTER model, which introduces the multiple aspect trajectory concept. Multiple aspect trajectories can be defined as the enhancement of the basic view of semantic trajectories with the notion of multiple heterogeneous aspects, characterizing different semantic dimensions related to the pure movement data. MASTER allows the augmentation of trajectories with any type of information, dubbed aspects. The model addresses the issue raised by [7], in which different aspects were taken into account independently. The model permits the representation of a trajectory in terms of space, time, and a variety of other aspects. Figure 1 depicts a multiple aspect trajectory with aspects that differ along the trajectory, as defined by [3].

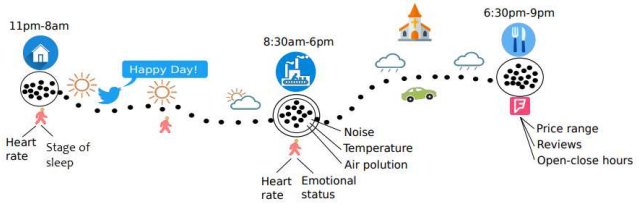

Fig. 1. Example of a multiple aspect trajectory as defined in [3].

As shown in Figure 1, the trajectory contains a wealth of information, aspects, about the moving individual, including: (1) the heart rate and the sleeping stage which are collected by a smartwatch, at home, from 11pm to 8am; (2) the humor is provided by a tweet when the individual walks to work; (3) the environmental information such as noise, temperature, and pollution are collected by sensors at a smart office; and (4) from 6:30pm to 9pm, the characteristics of the places visited by the individual, such as price, reviews, and open-close hours of a restaurant are collected as well [8].

This recent category of trajectory displays a person's very precise daily routine in depth than earlier models, while revealing lots of sensitive information. Hence, raising privacy concerns.

B. Granular computing models

Granular Computing (GrC) [9] is an emerging information processing computing paradigm that focuses on representing and processing complex entities, known as *"granules"*, which are produced from the process of data abstraction and knowledge extraction from information or data. The roots of GrC can be traced back to the works of Zadeh [10] defining a granule as a clump of points (objects) drawn together by indistinguishability or indiscernibility, similarity, proximity, or functionality.

Granules can be decomposed into a set of smaller and finer granules which are known as *"subgranules"*. Levels, hierarchies, and granular structures can all be used to organize granules and subgranules. Granulation is a procedure or a process which is needed for constructing or decomposing granules. In [11], author provides a comprehensive overview of the unified principals of granular computing along with its comprehensive algorithm framework and design practices.

The origins of the granular computing ideology are to be found in the rough sets and fuzzy sets literature [12], [13], but they can also be found in some other formal settings for GrC such as interval calculus, set theory, shadowing sets, and probabilistic granules [9]. The concept of granules and granulation are defined differently in each of these settings, and the work of [14] offers a preliminary way to uncover commonality and bridge the gap across these settings.

All of these formal settings, allow, in general, the formation of granular structures. Space and temporal aspects are naturally represented via multi-level structures in which high-level granules reflect more abstract notions and low-level granules represent more particular and more specific concepts. Such granular structures are critical to our predefined goals. GrC is based on a large set of interactions and relationships as defined in [15]. These may be used to organize granules in several structures such as hierarchies, trees, and networks. A granule g is a refinement of G (or G is a coarsening of g), denoted by $g \preceq G$, if all of g's data or subgranules are contained in some subgranules of G. When just some data or subgranules of g are contained in some subgranules of G, refinement (coarsening) can be partial, and is denoted as $g \sqsubseteq G$.

Structuring and forming the granules in the correct and most appropriate manner is an open research question that has been inspected by numerous researchers and is rather dependent on the application's requirements. The principle of justified granularity was developed in [16], [17] as a way to evaluate the performance of informational granules. The principle of justified granularity is based on a trade-off between the coverage and specificity measures, which do not exclusively depend on the application. Formally, coverage refers to the ability to cover data, while specificity refers to the granule prototype's level of abstraction as measured by its size. The proper expression of these two measures is dependent on the nature of the set formed.

For crisp sets, a measure of coverage may be $Cov(P) = \frac{1}{N} card\{X_k | x_k \in P\}$, but for fuzzy sets, the sum of the degree of memberships of the elements can be used $Cov(P) = \frac{1}{N}\sum_{k=1}^{N} \mu_p(X_k)$. $Cov(P)$ should, ideally, be equal to 1, indicating that the prototype covers all data. The intervals must be as narrow (specific) as feasible to achieve specificity. An interval's specificity can be assessed in a variety of ways. A specificity measure must meet two criteria: it must achieve a maximum value for a single element, and the larger the interval, the lower the specificity measure. The two concepts of coverage and specificity are at odds. To visualize their relationship, consider arranging them in the form of a coverage-specificity plot, which may also be parameterized, and calculating the area under the curve to derive a global measure of quality.

Another criterion for granule design is the principal of uncertainty level preservation as defined in [18], [19], which is primarily concerned with assessing the quality of the granulation itself.

This principle considers the quantification of uncertainty as an invariant property to be retained during the granulation process by considering information granulation as a mapping between some input and output. The discrepancy between the input and output entropy is considered as an error that must be decreased in order to achieve optimal information granulation [20].

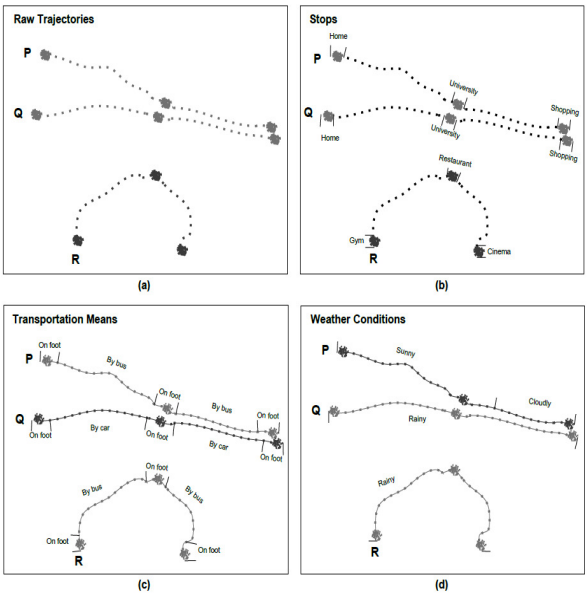

Fig. 2. Multiple trajectory representation [7]

III. Multiple Aspect Trajectory Representation

In this Section, we replicate the example given in [7], illustrated in Figure 2, to show the challenge in representing multiple aspect trajectories.

Figure 2 shows three trajectories, P, Q, and R, which are represented using four different aspects: (1) as raw trajectories (Figure 2(a)); (2) as stops and moves (Figure 2(b)), where the labeled parts are the stops; (3) as transportation means (Figure 2(c)); and (4) according to weather conditions (Figure 2(d)).

If every aspect is considered separately, and by considering only the space and semantic dimensions, excluding time for simplification, the three trajectories would be analyzed as follows:

- If $Aspect = raw\ trajectory$ then P and Q are spatially closer than P and R or Q and R.
- If $Aspect = stops$ then P and Q are the most similar.
- If $Aspect = transportation\ means$ then P and R are the most similar.
- If $Aspect = weather\ condition$ then Q and R are the most similar.

Two issues can be reported from the standpoint of similarity analysis: (1) the trajectories must consider multiple aspects, such as raw data, stops, transportation means, activities, weather conditions, and others; (2) existing similarity measures only consider a single representation (aspect). Now from a mining view point, the following important issue can be reported: multiple aspect trajectory data analysis can lead to new types of trajectory patterns that cannot be detected so far by existing data mining methods. More details about the illustration of these issues via examples can be found in [7].

Now in terms of representation, one would wonder why not simply combine all relevant data into a single trajectory

representation. When evaluating the stops representation, for example, one may claim that it is straightforward to enrich the trajectory with all relevant information such as weather, transportation means, activities, and so on. The issue is not as straightforward as it appears.

Let us assume the moving individual is walking and the weather changes from sunny to rainy during one stop. In the activity aspect, the moving individual changed his/her activity from meeting to coaching when the weather is rainy. All of these changes happen at a single stop (POI); labelled office.

It would be very hard to correctly split and annotate the stop into two weather conditions, each one having a different start and end time, splitting it in different activities [7]. The same stop would have multiple semantic labels for weather, transportation modes, stop names, activity names, and so on, as well as multiple time intervals associated with each semantic label, such as the start and end times of a stop, the duration of a transportation mode, the distance traveled by one transportation mode, and possibly different space information [7].

As it can be noted, the issues reported from the standpoint of similarity analysis and from a mining view point, are connected to the challenges linked to the multiple aspect trajectory representation. This leads to the ultimate challenge of how to efficiently represent trajectories with all this information while offering an appropriate why to conduct similarity analysis and mining tasks.

IV. A Granular Computing Framework for Multiple Aspect Trajectory Representation

The concept of "multiple aspect" trajectories can be modeled using the hierarchical structure of granular computing. Data granules are formal entities that aid in the organization of data and relationship knowledge. The use of data granules to represent the different aspects of MAT and the characteristics of each aspect can help to detect hidden patterns, as well as increase the logicality, systematicity, and efficiency of decision-making [21], [22]

In this section, we present a tentative representation of multiple aspect trajectory using granular computation, called $GrC - MAT$. In this representation, we consider that every aspect (or dimension) can be seen as a granule, and each granule can be, in its turn, represented using sub-granules. All of these granules are connected between each other to ensure an overall representation of the multiple aspect trajectory.

A. Definitions

Introducing GrC into multiple aspect trajectory generates the following related concepts:

*Definition 1 (**MAT Data Granule**):* Multiple aspect trajectory data granule, denoted as $Mat - Gr$, refers to a mobility data chunk defined via a set of mobility data elements drawn together by space, time, proximity, or indistinguishability [23].

*Definition 2 (**MAT Data Granulation**):* Multiple aspect trajectory data granulation refers to the process that partitions the mobility rich data into fine grained and semantically clear mobility data granules with respect to a set of criteria which are associated with spatial and temporal scale features together with other considered aspects.

*Definition 3 (**MAT Data Granular Layer**):* Multiple aspect trajectory data granular layer, denoted as $Mat - Lay$, is composed of a set of mobility data granules with respect to a certain set of granulation criteria.

*Definition 4 (**MAT Data Granular Structure**):* Multiple aspect trajectory data granular structure, denoted as $Mat-GrS$, refers to the relational structure generated by the links between several mobility data granules corresponding to various granulation criteria.

*Definition 5 (**MAT Granular Computing**):* Multiple aspect trajectory granular computing refers to the process that uses mobility data granules to describe, analyze, and solve multiple aspect trajectory data mining problems from different scales and perspectives.

B. A granular representation of multiple aspect trajectories: a tentative representation

Multiple aspect trajectory data granule is a complete entity with multiple dimensions, such as space, time, weather, transportation means, emotion status, and activity. As all of these dimensions are related to the spatial and temporal scales, then the granular representation of multiple aspect trajectories should consider the spatiotemporal aspect. This can be guaranteed by integrating the time and space dimensions, as attributes of data granules, into a single systematic model.

Figure 3 represents the multiple aspect trajectory data granule structure. Every considered data granule $Mat-Gr$ is represented via a layer $Mat-Lay_l$, where $l \in \{1, \ldots, L\}$, and L is the maximum number of layers for the different considered dimensions. With respect to this structure, every $Mat - Gr$ can be defined in different scales; denoted as $Mat-Gr_l$. The data granules in each upper scale $Mat-Gr_l$ are transformed into those in the lower scale $Mat-Gr_{l+1}$ using a granulation criteria (rule) GCr_i, where $i \in \{1, \ldots, L-1\}$. The data granules decrease (increase) as the scale decreases (increases). A correlation, representing the connection between the different aspects of the multiple aspect trajectory, is reflected by the different edges between the various $Mat-Gr_l$. All $Mat-Gr_l$ are connected between each other as well as between their corresponding granules. For a simplified view, in Figure 3, only few edge are represented.

*Example 4.1 (**Example of a granular representation of a multiple aspect trajectory**):* Let us suppose that during one stop the object is moving on foot and the weather condition changes from Sunny to Rainy. Figure 4 represents a simplified view of a type-2 granular structure of such representation. The edges represent the different correlations between the different granules; i.e., temporal-spacial, temporal-activity, space-weather, ..., and space-temporal-weather-activity.

With respect to this granular structure, we can define the following roots:

- At POI, Weather = "Sunny" during "Start-time" and "End-time", and Activity = "Foot"

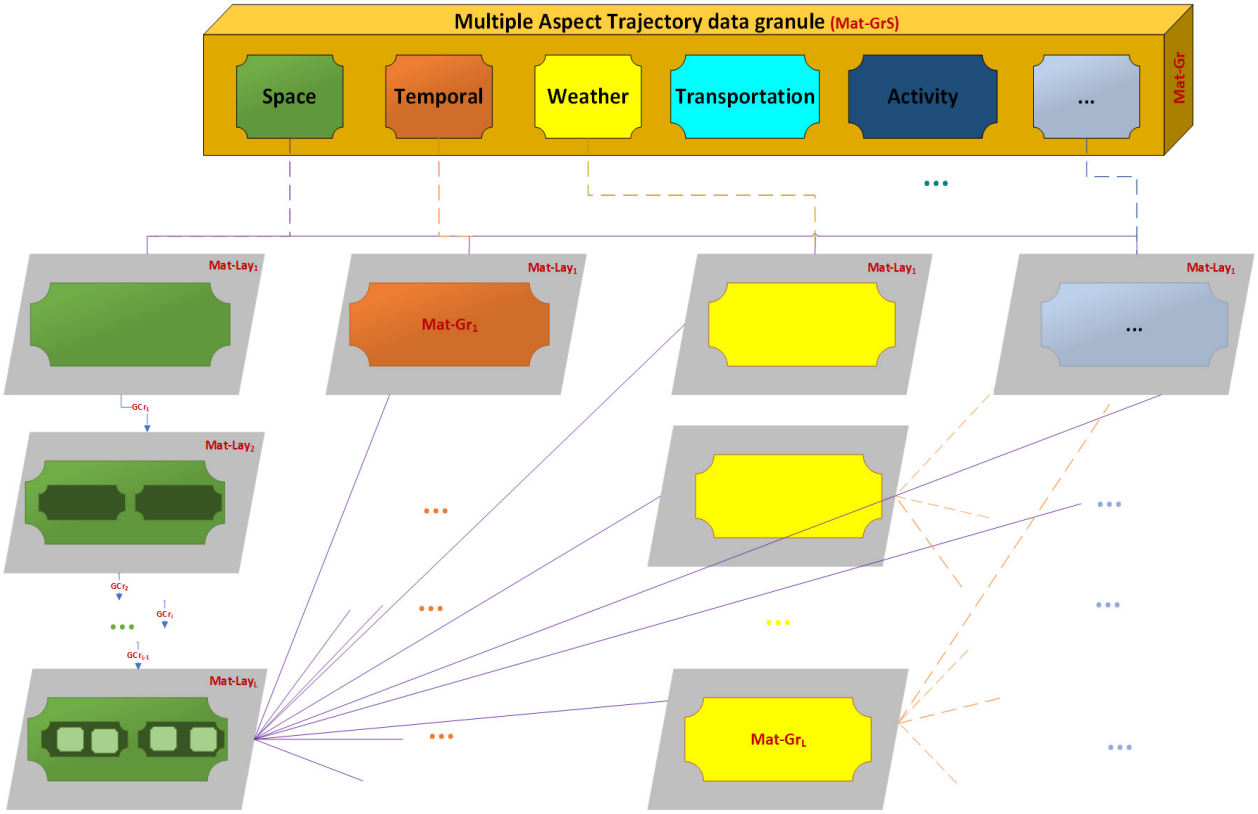

Fig. 3. A granular representation of multiple aspect trajectories (inspired by [24])

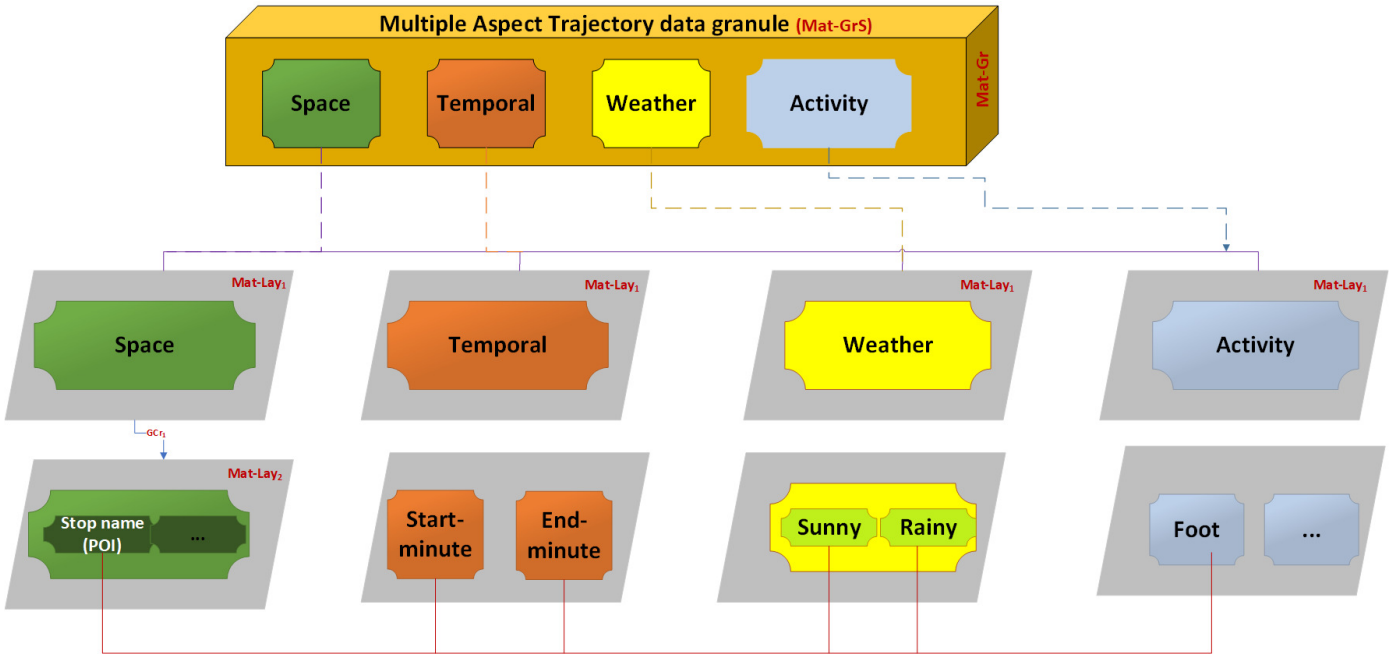

Fig. 4. Example of a granular representation of a multiple aspect trajectory

- At POI, Weather = "Rainy" during "Start-time" and "End-time", and Activity = "Foot"

With respect to the need of representing different aspects at a time, sub-granular structures can be extracted from Figure 3. This is to achieve landscape law mining at a specific scale for different granules.

*Example 4.2 (**Example of reasoning**):* The *"Weather"* granule can be considered as a *"localized or a particular view or aspect"* of the MAT presented in Figure 4. *"Sunny"* and *"Rainy"* are examples of granules of the sub-layer ($Mat - Lay_2$) of the *"Weather"* granular layer ($Mat - Lay_1$). Data granules in $Mat - Lay_2$, for instance, can be viewed as an *"information table"*, with a binary values representation, and different granules can be further generated from it. For example, if we consider *"Rough Set Theory"* as a GrC theory, we can generate three disjoint regions (granules) by applying the *"lower approximation"* and *"upper approximation"*; namely, the ‘‘positive region" which comprises those data objects certainly related with the decision class, the *"negative region"* which comprises those objects certainly not related with the decision class, and the *"boundary region"* which comprises those objects possibly related with the decision class. The connections and relationships between the granules may be interpreted by the rough set *"dependency degree"*. All granules of the different granular layers provide a collective description of the MAT.

C. An evolving granular representation

So far we have created a hierarchical granular structure resembling the hierarchies existing between the different aspects that can be considered in multiple aspect trajectories. To accommodate other aspects that can be further considered in multiple aspect trajectories, either in $Mat - Gr$ or/and in $Mat - Lay_l$, we can leverage on the concept of evolvable granules [25], [26].

In [26], the behavior of evolving granules is reported via Figure 5, and explained as follows, when considering only time and space: the time window shows different objects registered by sensors in three time slices, t, $2t$, and $3t$. The top of the figure shows three granular structures, where granules denote the position of the objects in the space dimension. During $time = t$, singleton granular structures are created comprising $\{a\}$, $\{b\}$ and $\{c\}$. During $time = 2t$, two additional objects, $\{d\}$ and $\{e\}$, are recognized and merged with the existing granules to form higher level granules $\{a, d\}$, $\{b, e\}$, and $\{c\}$. This process continues to iterate in the next time windows, and, as output, granular structures evolve with granules that can be either merged, split, removed or new granules formed. In [26], a complete formalism to deal with splitting and merging criteria in the case of granules created with Fuzzy c-means can be found.

To accommodate other aspects in $Mat-Gr$ or/and $May-Lay_l$, we should reason on the evolution of granular structures. To do so, the transitions between $May - Lay_l$ and $May - Lay_{l+1}$ should be considered with respect to the applied granulation criteria GCr_i. This can be achieved depending on previous knowledge about the rules (GCr_i) that govern the evolution of phenomena under observations and/or the actions that can enable situations transitions.

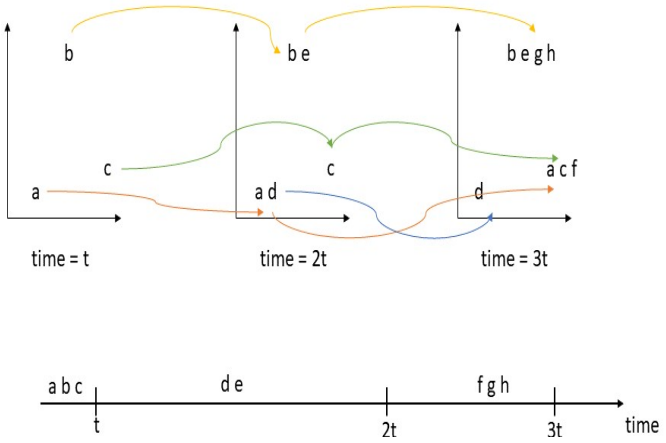

Fig. 5. Behavior of evolving granules by granulating time and space [20]

V. Research Challenges and Opportunities

In [7], authors presented a set of challenges and opportunities tied to multiple aspect trajectory data analysis. These include multiple aspect representation, feature extraction, data storage, similarity analysis and data mining, visualization, and privacy protection. The later challenge was further detailed in [8] where authors presented a survey of the state-of-the-art trajectory anonymization methods for privacy preservation, together with a description of a set of challenges for anonymizing multiple aspect trajectories. Therefore, in this section, we mainly focus on presenting the main challenges tied to multiple aspect trajectory representation and privacy preservation from a granular computing perspective.

Representing multiple aspect trajectories reveals many challenges when it comes to defining the concrete structure and connections, between the different considered aspects. Among these challenges, we mention the uncertainty and the imprecision that can be found in mobility data. Let us consider a basic scenario in which people wander around a city and reveal their locations twice an hour. To avoid stalking, the disclosed location is chosen at random from within a one-kilometer radius circle that contains the user's location. Not being conscious of uncertainty may lead to erroneous deductions. For example, we could mistakenly believe that a group of individuals have met or that someone has stayed at a a privacy-sensitive location. If we take uncertainty in account, such erroneous conclusions can be avoided. For instance, if an individual was more than one kilometer away from the location of an accident, we may safely assume that that individual was not involved in that accident [27].

By considering a granular computing representation, our $GrC-MAT$ model car efficiently handle such type of uncertainty in mobility data. Settings related to GrC implementation, including fuzzy sets, rough sets, and inclusion degree theory,

contain all the results of uncertain reasoning (e.g., inclusion degree [28] based on conditional probability as is a form of uncertain reasoning).

A resulting challenge from the above is how to formally define the granular computing model based on the formal setting used to implement GrC.

Now from a building point of view, the definition of the granules, the construction of the granule layers in an optimized way using the granulation criteria – which also needs to be defined–, the definition of the edges between the different granules as well as the strength (degree) of these edges, present all major challenges.

Now when it comes to the privacy preservation challenge, the hierarchical or tree or network structure adopted to build the $GrC - MAT$ model can be use to hide sensitive/private information. This can be achieved by several means such as moving from a granular layer to another to avoid specificity and ensure generality and vice-versa, by ignoring/not reporting some edges (correlations) connecting the different granules, or by switching a granule by another. Also, the fact of using the fundamentals of the GrC theories to report some granules instead of the actual granules that need to be reported can deal with the privacy issues. For instance, when referring to rough set theory, we can report the *"boundary region"*, as a granule, comprising those objects *possibly* related with the decision class, instead of reporting the ''positive region" which comprises those data objects *certainly* related with the decision class or instead of the *"negative region"* which comprises those objects *certainly* not related with the decision class. The challenge, in this concern, is to formally study the feasibility of these assumptions.

The GrC structure can still lead to a privacy leak as the deductive route from non-sensitive to sensitive features can be mined; which is another challenge to be considered. The sensitive features can be defined as the set of features that should be hidden using algorithms in such a way that they cannot be reasonably approximated using the set of non-sensitive features. This is quite a challenge since the non-sensitive features may contain concepts on which sensitive features inferentially depend; these are known as *"quasi-identifiers"*. To cut the deductive route to any potential privacy leak, these quasi-identifiers must be appropriately hidden. However, they must be uncovered first. In this concern, rough set theory as a GrC example, seemed to be one among the right tools to be used to undermine the deductive route from non-sensitive to sensitive features by modelling and analyzing the dependency "non-sensitive $\longrightarrow$ sensitive" [29]. Rough set theory provides numerical quantities that measure the degree of dependency of attributes. This study was presented in [30], where authors have learned the quasi-identifiers, computed a granulation of the information system that maximizes the distribution of sensitive features in each granule, and masked the deductive route from non-sensitive to sensitive attributes. This rises the challenge of how to undermine this deductive route within a multiple aspect scenario. It would be also interesting to investigate this challenge when coupling it with the evolving structure of the GrC model.

Another challenge is how to defined similarity in multiple aspect trajectories based on granular computation. As previously mentioned, in the era of big data, large amounts of semantically rich mobility data became available. This called for the need for new trajectory similarity metrics in the context of multiple-aspect trajectories. Existing techniques have several constraints concerning the links between characteristics and their semantics. These techniques are too rigid, demanding a match on all features, or too lenient, treating all features as unrelated. Granular computing formal settings can be used to represent the appropriate dependencies between the features and hence new similarity measures dedicated to multiple aspect trajectories can be defined.

Granular computing methods offer plenty of opportunities to handle the challenges tied to multiple aspect trajectory representation and privacy preservation. This will present a considerable addendum to the mobility data management, analytic and privacy communities and fields.

VI. Conclusion

In this paper, we presented a granular computing view for multiple aspect trajectory representation. Such representation will allow a more natural, a flexible, and a complete representation of multiple aspect trajectories. Additionally, by using the fundamentals of some granular formal settings such as fuzzy sets and rough sets, there are several opportunities and possibilities to deal with the privacy aspect and hence, ensure multiple aspect trajectory privacy preservation.

From a practical and applied perspectives, the potential advantages of this $GrC - MAT$ approach can be reflected by the following aspects: (i) a good semantic scalability ensured by data granularization based on the extendable granulation criteria which cover not only the spatiotemporal scales but also the other aspects of mobility data with clear semantics; (ii) the adaptation to vertical dynamic changes in the data. This implies when introducing modifications to granular layers. This dynamic adaptation is ensured by the independency of the granulation criteria of each layer, which implies that the only required change will be the update of the granulation criteria between the affected adjacent granular layers; hence, not affecting other granular layers; and last but not least (iii) the adaptation to horizontal dynamic changes in the data. The granular structure of the $GrC - MAT$ model allows dynamic incremental data expansion in a specific granular layer without affecting other adjacent layers. As previously mentioned, granular computing will present a considerable addendum to the mobility data management, mobility data mining, analytic and privacy communities and fields.

As future works, we will focus on the discussed challenges of the multiple aspect trajectory representation and privacy preservation from a granular computing perspective, to find efficient approaches that handle all these aspects.

ACKNOWLEDGMENT

This work has received funding from the European Commission's Horizon 2020 research and innovation programme under the Marie Sklodowska-Curie grant agreement N. 777695.

REFERENCES

[1] P. Kucharski, D. Sielski, T. Jaworski, A. Romanowski, and J. Kucharski, "Use of fuzzy cognitive maps for enhanced interaction with multiple mobile devices." in *FedCSIS (Communication Papers)*, 2018, pp. 217–222.

[2] V. Bogorny, C. Renso, A. R. de Aquino, F. de Lucca Siqueira, and L. O. Alvares, "Constant–a conceptual data model for semantic trajectories of moving objects," *Transactions in GIS*, vol. 18, no. 1, pp. 66–88, 2014.

[3] R. d. S. Mello, V. Bogorny, L. O. Alvares, L. H. Z. Santana, C. A. Ferrero, A. A. Frozza, G. A. Schreiner, and C. Renso, "Master: A multiple aspect view on trajectories," *Transactions in GIS*, vol. 23, no. 4, pp. 805–822, 2019.

[4] K. S. Hornsby and S. Cole, "Modeling moving geospatial objects from an event-based perspective," *Transactions in GIS*, vol. 11, no. 4, pp. 555–573, 2007.

[5] S. Spaccapietra, C. Parent, M. L. Damiani, J. A. de Macedo, F. Porto, and C. Vangenot, "A conceptual view on trajectories," *Data & knowledge engineering*, vol. 65, no. 1, pp. 126–146, 2008.

[6] R. Fileto, C. May, C. Renso, N. Pelekis, D. Klein, and Y. Theodoridis, "The baquara2 knowledge-based framework for semantic enrichment and analysis of movement data," *Data & Knowledge Engineering*, vol. 98, pp. 104–122, 2015.

[7] C. A. Ferrero, L. O. Alvares, and V. Bogorny, "Multiple aspect trajectory data analysis: research challenges and opportunities." in *GeoInfo*, 2016, pp. 56–67.

[8] T. T. Portela, F. Vicenzi, and V. Bogorny, "Trajectory data privacy: Research challenges and opportunities." in *GEOINFO*, 2019, pp. 99–110.

[9] W. Pedrycz, A. Skowron, and V. Kreinovich, *Handbook of granular computing*. John Wiley & Sons, 2008.

[10] L. A. Zadeh, "Toward a theory of fuzzy information granulation and its centrality in human reasoning and fuzzy logic," *Fuzzy sets and systems*, vol. 90, no. 2, pp. 111–127, 1997.

[11] W. Pedrycz, *Granular computing: analysis and design of intelligent systems*. CRC press, 2018.

[12] G. Wang, Q. Liu, Y. Yao, and A. Skowron, "Rough sets, fuzzy sets, data mining, and granular computing," *RSFDGrC, Springer 2003, Chongqing, China*, pp. 41–48, 2003.

[13] Z. Pawlak, "Granularity of knowledge, indiscernibility and rough sets," in *1998 IEEE International Conference on Fuzzy Systems Proceedings. IEEE World Congress on Computational Intelligence (Cat. No. 98CH36228)*, vol. 1. IEEE, 1998, pp. 106–110.

[14] D. Dubois and H. Prade, "Bridging gaps between several forms of granular computing," *Granular Computing*, vol. 1, no. 2, pp. 115–126, 2016.

[15] Y. Yao, "A triarchic theory of granular computing," *Granular Computing*, vol. 1, no. 2, pp. 145–157, 2016.

[16] W. Pedrycz and W. Homenda, "Building the fundamentals of granular computing: A principle of justifiable granularity," *Applied Soft Computing*, vol. 13, no. 10, pp. 4209–4218, 2013.

[17] W. Pedrycz, A. Gacek, and X. Wang, "Clustering in augmented space of granular constraints: a study in knowledge-based clustering," *Pattern Recognition Letters*, vol. 67, pp. 122–129, 2015.

[18] L. Livi and A. Sadeghian, "Data granulation by the principles of uncertainty," *Pattern Recognition Letters*, vol. 67, pp. 113–121, 2015.

[19] ——, "Granular computing, computational intelligence, and the analysis of non-geometric input spaces," *Granular Computing*, vol. 1, no. 1, pp. 13–20, 2016.

[20] G. D'Aniello, A. Gaeta, V. Loia, and F. Orciuoli, "A granular computing framework for approximate reasoning in situation awareness," *Granular Computing*, vol. 2, no. 3, pp. 141–158, 2017.

[21] K. Zhou, Z. Tian, and Y. Yang, "Periodic pattern detection algorithms for personal trajectory data based on spatiotemporal multi-granularity," *IEEE Access*, vol. 7, pp. 99 683–99 693, 2019.

[22] F. J. Cabrerizo, J. A. Morente-Molinera, S. Alonso, W. Pedrycz, and E. Herrera-Viedma, "Improving consensus in group decision making with intuitionistic reciprocal preference relations: A granular computing approach," in *2018 IEEE International Conference on Systems, Man, and Cybernetics (SMC)*. IEEE, 2018, pp. 1471–1476.

[23] L. A. Zadeh, "Some reflections on soft computing, granular computing and their roles in the conception, design and utilization of information/intelligent systems," *Soft computing*, vol. 2, no. 1, pp. 23–25, 1998.

[24] C. Yunxian, L. Renjie, Z. Shuliang, and G. Fenghua, "Correction: Measuring multi-spatiotemporal scale tourist destination popularity based on text granular computing," *PloS one*, vol. 15, no. 5, p. e0233068, 2020.

[25] M. Antonelli, P. Ducange, B. Lazzerini, and F. Marcelloni, "Multi-objective evolutionary design of granular rule-based classifiers," *Granular Computing*, vol. 1, no. 1, pp. 37–58, 2016.

[26] W. Pedrycz, "Evolvable fuzzy systems: some insights and challenges," *Evolving Systems*, vol. 1, no. 2, pp. 73–82, 2010.

[27] C. Silvestri and A. Vaisman, *Mobility and Uncertainty*. Cambridge University Press, 2013, p. 83–102.

[28] W. Xu, J. Mi, and W. Wu, "Granular computing methods and applications based on inclusion degree," *Beijing: Science Press*, 2017.

[29] M. Bishop, J. Cummins, S. Peisert, A. Singh, B. Bhumiratana, D. Agarwal, D. Frincke, and M. Hogarth, "Relationships and data sanitization: A study in scarlet," in *Proceedings of the 2010 New Security Paradigms Workshop*, 2010, pp. 151–164.

[30] C. Wafo Soh, L. Njilla, K. Kwiat, and C. Kamhoua, "Learning quasi-identifiers for privacy-preserving exchanges: A rough set theory approach," *Granular Computing*, vol. 5, no. 1, pp. 71–84, 2020.

Communication Papers of the of the 17th Conference on Computer Science and Intelligence Systems pp. 73–77
DOI: 10.15439/2022F90
ISSN 2300-5963 ACSIS, Vol. 32

Algebraic structures gained from rough approximation in incomplete information systems

Carolin Hannusch, Tamás Mihálydeák

***Abstract*—We give an algebraic approach for defining rough sets on incomplete information systems. The constructed approximation sets are based on objects. Given several attributes, the value of each attribute can be known or unknown for each object. In the current paper, we introduce four different approaches, a real value, a binary, a ternary and a likelihood approach. Furthermore, we define operations on the elements of the introduced approximation sets. For all three cases we can show that the achieved structure is a quasi-Brouwer-Zadeh distributive lattice with the defined operations. We also show that the introduced lower and upper approximations build up commutative monoids with the introduced operations.**

I. Introduction

DIFFERENT systems of rough set theory were created in the last forty years: Pawlak's original theory of rough sets (see in e.g. [1]–[3]), covering systems relying on tolerance relations [4], general covering systems [5], [6], decision-theoretic rough set theory [7], general partial approximation spaces [8], similarity based approximation spaces [9]. There is a very important common property:

- all systems rely on given background knowledge represented by the system of base sets;
- one cannot say more about an arbitrary set (representing a 'new' property) or about its members than the lower and upper approximations of the set make possible.

The members of a base set have to be treated in the same way

- absolutely in the Pawlak's original theory,
- relatively in the systems with non pairwise disjoint base sets.

It means generally that if something holds for a given object, then it holds for all objects belonging to at least one same base set containing the given object. Several researchers have been considering algebraic structures of rough sets, e.g. [10], [11], [12].

In real practice there is a huge amount of objects, and the background knowledge corresponds to an information system. The framework of an information system is given by attributes, and their possible attribute values. An object can be embedded in an information system by giving the attribute values of the attributes of the information system. In many practical cases some attribute values of an object are unknown and so these values are missing, therefore the information system is not complete. Recently researchers constructed partial approximation spaces for rough sets based on an incomplete information system [13]. In the current paper we aim to give an approach for rough sets based on

- an incomplete information system, especially on objects whose properties of certain attributes can be known or not known;
- taking into consideration all possible systems of attribute values (not only those for which there is an object in the information system with a system of attribute values).

We characterize a set by the approximation of its members but we focus on their systems of attribute values, which is a new idea in Rough Set Theory. The lower and upper approximations are given with the help of possible systems of attribute values (and not by the objects appearing in the information system).

The paper is organized as follows. In Section II we introduce all necessary definitions. In Section III we introduce operations and in Section IV we show that the defined sets build a quasi-BZ distributive lattice. In Section V we show some arithmetics of the introduced lower and upper approximation sets according to the introduced operations. Finally, in Section VI we draw a first conclusion of the new definitions and proven propositions and give some ideas for further research.

II. Approximation by rough sets

Given a set of objects Ω, we assume that each object $\omega \in \Omega$ can be characterized by n attributes. We map a set of values Σ to each attribute. For our purposes, we assume that the elements of Σ are numbers, but the reader should be aware of the fact that Σ can be any nonempty set. Each attribute assigns a value of Σ for each object. Thus each object can be represented by a vector of length n, each coordinate representing the value of one attribute.

Definition 2.1: Let U be non-empty universe of objects, $(P_1, \ldots, P_n)$ be a system of attributes $(n \in \mathbb{N}, n > 0)$, Σ be a set of values, ϵ be a fixed distinguished member of Σ and $f : U \Rightarrow \Sigma^n$ be a function which maps each object to a vector of length n. Then $I = (U, P, \Sigma, f)$ is an *information system*. If for each $i(1 \leq i \leq n)$ and $o \in U$ we have $f(o)_i \neq \epsilon$, then we say that I is *complete*, else I is said to be an *incomplete information system*.

At this point, we need to remark that this representation is not injective, which means that there can be two different objects with the same vector of attributes. (The reader can think for example of two people with the same hair colour and height.) Our purpose is to give several different approaches for a rough set approximation, depending on Σ. It depends strongly on the given problem which of the following approaches is the most suitable. Therefore we give a small motivating example for each approach.

A. The real value approximation

Let Ω be a set of objects, $\omega \in \Omega$ and $\Sigma = [0,1]$ the closed interval between 0 and 1. Further, let ν_ω be the vector belonging to the object ω,

$$\nu_\omega = (\nu_1, \ldots, \nu_n)$$

where ν_i denotes the value of the i^{th} attribute of the object ω and $\nu_i \in \Sigma$, $\forall i \in \{1, \ldots, n\}$. We determine

$$\nu_i = 0 \Leftrightarrow \text{ we know nothing about the } i^{th} \text{ attribute of } \omega,$$

i.e. 0 is the fixed distinguished member of Σ. In the following, for the convenience of the reader we write ν instead of ν_ω.

Now we can define two sets for each object ω : In one set we collect all those n-long vectors which have the same "known information" and in the other set we collect all those vectors which have the same "unknown information".

Definition 2.2: Let $\nu = (\nu_1, \ldots, \nu_n)$ be a string of length n, such that $\nu_i \in \Sigma$ and $\nu_i = 0 \Leftrightarrow$ the information about the i^{th} attribute is not known - for all $i \in \{1, \ldots, n\}$. Then we define

$$\varphi_\omega = \{v = (v_1, \ldots, v_n) \in \Sigma^n |$$

$$v_j = \nu_j \Leftrightarrow \nu_j \neq 0 \text{ and } 0 < v_i \leq 1 \Leftrightarrow \nu_i = 0\}$$

and

$$\delta_\omega = \{v = (v_1, \ldots, v_n) \in \Sigma^n |$$

$$0 < v_i \leq \nu_i \Leftrightarrow \nu_i \neq 0 \text{ and } v_i = 0 \Leftrightarrow \nu_i = 0\}.$$

Remark 1: With this definition, the sets φ_ω and δ_ω are infinite. For a set of objects Ω, we can then define the following sets ϕ and Δ, build up on φ and δ respectively, which means we collect "all possible known information" and search for the "unknown" in each object.

Definition 2.3: Let U be the universe of objects and $\Omega \subseteq U$. Then each element of Ω can be represented by an n-long vector in Σ^n. We define

$$\phi(\Omega) = \bigcup_{\omega \in \Omega} \varphi_\omega$$

and

$$\Delta(\Omega) = \bigcap_{\omega \in \Omega} \delta_\omega.$$

Remark 2: We have $(0, 0, \ldots, 0) \in \Delta(\Omega)$.

Definition 2.4: Let Ω be a set of objects. Then we say that $\mathcal{U}$ is an upper approximation of Ω if $\mathcal{U} \subseteq \phi(\Omega)$ and $\mathcal{L}$ is a lower approximation of Ω if $\mathcal{L} \subseteq \Delta(\Omega)$.

Remark 3: It is clear that there are several objects, or subsets of objects which can have the same upper and/or lower approximation.

Remark 4: The pair $(\mathcal{L}, \mathcal{U})$ can be considered as a rough set.

Example 1:

Let $\nu = (0, 0.1, 0.2, 0.3, 0)$. Each ν_i denotes the value of a medical indicator, such as bloodsugar, hemoglobin, etc. Then we have

$$\varphi_\nu = \{v = (v_1, \ldots, v_5) \mid v_1, v_5 \in \Sigma,$$

$$v_2 = \nu_2, v_3 = \nu_3, v_4 = \nu_4\}$$

and

$$\delta_\nu = \{v = (v_1, \ldots, v_5) \mid v_1 = 0, v_5 = 0, v_2 = 0$$

$$\text{or } \nu_2, v_3 = 0 \text{ or } \nu_3, v_4 = 0 \text{ or } \nu_4\}.$$

B. The binary approach

Let I be a complete information system. Further, let $\Sigma = \{0, 1\}$ and ν be the vector belonging to one object,

$$\nu = (\nu_1, \ldots, \nu_n)$$

where

$$\nu_i = 0 \Leftrightarrow \text{the object does not fulfill the } i^{th} \text{ attribute}$$

and

$$\nu_i = 1 \Leftrightarrow \text{ the object fulfills the } i^{th} \text{ attribute .}$$

Definition 2.5: Let $\nu = (\nu_1, \ldots, \nu_n)$ be a string of length n, such that $\nu_i \in \{0, 1\}$ and $\nu_i = 1 \Leftrightarrow$ the information about the i^{th} attribute is fulfilled. Then we define φ_ν and δ_ν in the following way

$$\varphi_\nu = \{v = (v_1, \ldots, v_n) | v_j = 1 \Leftrightarrow \nu_j = 1 \text{ and}$$

$$v_i \in \{0, 1\} \Leftrightarrow \nu_i = 0\}$$

and

$$\delta_\nu = \{v = (v_1, \ldots, v_n) | v_j \in \{0, 1\} \Leftrightarrow \nu_j = 1 \text{ and}$$

$$v_i = 0 \Leftrightarrow \nu_i = 0\}.$$

Definition 2.6: Let Ω be a set of objects, each element is represented by an n-long vector in Σ^n. Then we define

$$\phi(\Omega) = \{(v_1, \ldots, v_n) \mid \text{if } \exists \omega \in \Omega : \nu_\omega[i] = 0 \Rightarrow v_i = 0 \text{ or } 1,$$

$$\text{otherwise } v_i = 1\}$$

and

$$\Delta(\Omega) = \{(v_1, \ldots, v_n) \mid \text{if } \exists \omega \in \Omega : \nu_\omega[i] = 1 \Rightarrow v_i = 0 \text{ or } 1,$$

$$\text{otherwise } v_i = 0\}.$$

Remark 5: In this case $\phi(\Omega)$ and $\Delta(\Omega)$ are finite sets, since $\mid \phi(\Omega) \mid \leq 2^n$ and $\mid \Delta(\Omega) \mid \leq 2^n$.

Of course, in this case we can also use the definitions of upper and lower approximations as in Definition 2.4, thus we get a similar rough set as in Remark 4.

Example 2: Let $\nu = (\nu_1, \nu_2)$, where ν_1 denotes if Disease X test is positive and ν_2 denotes if Disease X antigen is positive. Thus $\nu = (0, 1)$ means that current Disease X infection is not fulfilled, and antigen exists. Then $\varphi = \{(0, 1), (1, 1)\}$ and $\delta = \{(0, 1), (0, 0)\}$.

C. The ternary approach

If we want to use the simplicity of a binary approach for an incomplete information system, then we collide with the problem that "no" and "not known" would be the same. Thus it is advisable to include a third symbol for "not known" and therefore we come to a ternary approach.
Let I be an incomplete information system, Further, let $\Sigma = \{0, \frac{1}{2}, 1\}$ and ν be the vector belonging to one object,

$$\nu = (\nu_1, \ldots, \nu_n)$$

where

$$\nu_i = 0 \Leftrightarrow \text{the object does not fulfill the } i^{th} \text{ attribute of } \nu$$

and

$$\nu_i = 1 \Leftrightarrow \text{ the object fulfills the } i^{th} \text{ attribute}$$

and

$$\nu_i = \frac{1}{2} \Leftrightarrow \text{ we don't know if the } i^{th} \text{ attribute is fulfilled.}$$

Definition 2.7: Let $\nu = (\nu_1, \ldots, \nu_n)$ be a string of length n, such that $\nu_i \in \{0, \frac{1}{2}, 1\}$ and $\nu_i = 1 \Leftrightarrow$ the information about the i^{th} attribute is fulfilled. Then we define φ_ν and δ_ν in the following way

$$\varphi_\nu = \{v = (v_1, \ldots, v_n) | v_j \geq \nu_j\}$$

and

$$\delta_\nu = \{v = (v_1, \ldots, v_n) | v_j \leq \nu_j\}.$$

Example 3: Let $\nu = (\nu_1, \nu_2, \nu_3)$, where ν_1 denotes if Disease X test is positive, ν_2 denotes if Disease Y test is positive and ν_3 denotes if Disease Z test is positive. Let $\nu = (1, 0, \frac{1}{2})$. Then

$$\varphi = \left\{ \left(1, 0, \frac{1}{2}\right), \left(1, \frac{1}{2}, \frac{1}{2}\right), \left(1, 1, \frac{1}{2}\right), (1, 0, 1), \right.$$

$$\left. \left(1, \frac{1}{2}, 1\right), \left(1, 1, \frac{1}{2}\right), (1, 1, 1) \right\}$$

and

$$\delta = \left\{ \left(1, 0, \frac{1}{2}\right), \left(\frac{1}{2}, 0, \frac{1}{2}\right), \left(0, 0, \frac{1}{2}\right), (0, 0, 0), (1, 0, 0) \right\}.$$

Remark 6: The ternary approach enables us to investigate objects or a set of objects through attributes which can be known or unknown. For example, we can draw consequences of the relation between the infections with two or more diseases, although we do not have the exact information about each infection for every member of the set.

D. The likelihood approach

Let $\Sigma = [0, 1]$ and ν be the vector belonging to one object, $\nu = (\nu_1, \ldots, \nu_n)$ where ν_i denotes the likelihood of ν fulfilling the i^{th} attribute. In this case $\nu \in \Sigma^n$.
Since the likelihood is a real value between 0 and 1, this case is mathematically the same as in Section II-A. The likelihood approach is for example useful if the value of an attribute is binary and we know that an object has value 1 for an attribute with the likelihood p, where $p \in \Sigma$.
Example 4: Let $\nu = (\nu_1, \nu_2)$, where ν_1 denotes if Disease X antigen exists, ν_2 denotes if Disease X test is positive. Then $a = (0.4, 0.2)$ means that the object a has Covid antigen with 40% probability and has active Covid infection with 20% probability. If $b = (0.2, 0.2)$, then $\mathcal{L} = \{(x, y) \mid 0.1 \leq x \leq 0.2 \text{ and } 0.01 \leq y \leq 0.2\}$ is a lower approximation set for both, a and b.
All of our approaches have in common that the sets $\phi(\Omega)$ and $\Delta(\Omega)$ contain information about Ω without containing Ω itself. Therefore we are able to say something about a set without knowing its elements, which is a good achievement with many applications in real-life-problems.

III. Operations

In this section we introduce four operations on vectors. These operations can be applied to any two vectors of the same length, which implies they can be applied to our representation of objects for any attribute set Σ.
Definition 3.1: Let a and b be two objects, each can be represented by a vector of length n : $a = (a_1, \ldots, a_n)$ and $b = (b_1, \ldots, b_n)$, where $a_i, b_i \in \Sigma$ for some nonempty set Σ. Then we define the following operations:

$$a \vee b := (\max\{a_1, b_1\}, \ldots, \max\{a_n, b_n\})$$

and

$$a \wedge b := (\min\{a_1, b_1\}, \ldots, \min\{a_n, b_n\}).$$

Definition 3.2: For any $a = (a_1, \ldots, a_n) \in \Sigma^n$ we define the following Kleene complementation:

$$' : \Sigma^n \to \Sigma^n, \ a' = (1 - a_1, \ldots, 1 - a_n)$$

and the following Brouwer complementation:

$$^{\sim} : \Sigma^n \to \Sigma^n, \ a_i^{\sim} = \begin{cases} 0, & \text{if } a_i \neq 0 \\ 1, & \text{if } a_i = 0 \end{cases}.$$

IV. Quasi-Brouwer-Zadeh distributive lattice

In [10] quasi-Brouwer-Zadeh (BZ) distributive lattices were introduced. In this section we show that the set of objects which we introduced in Section II is a quasi-BZ lattice under the operations defined in Section III.
Proposition 4.1: $\langle \Sigma^n, \vee, \wedge, ', ^{\sim}, 0, 1 \rangle$ is a quasi-Brouwer-Zadeh distributive lattice in both cases $\Sigma = [0, 1]$ and $\Sigma = \{0, 1\}$.
Proof. We show that all properties of a quasi-BZ distributive lattice listed in ([10], Section 3) are fulfilled. For the convenience of the reader, we use the same notations for the

fulfilled points as the authors in Definition 7 in [10]. All steps can be achieved by direct computation. Σ is a distributive lattice with respect to $\vee$ and $\wedge$, since $\min\{a_i, \max\{b_i, c_i\}\} = \max\{\min\{a_i, b_i\}, \min\{a_i, c_i\}\}$ (see Table I).

TABLE I
VERIFICATION TABLE 1

case	$\min\{a_i, \max\{b_i, c_i\}\}$	$\max\{\min\{a_i, b_i\}, \min\{a_i, c_i\}\}$
$a_i \leq b_i \leq c_i$	a_i	a_i
$a_i \leq c_i \leq b_i$	a_i	a_i
$b_i \leq a_i \leq c_i$	a_i	a_i
$b_i \leq c_i \leq a_i$	c_i	c_i
$c_i \leq a_i \leq b_i$	a_i	a_i
$c_i \leq b_i \leq a_i$	b_i	b_i

The property (K1) is fulfilled, since $1 - (1 - a_i) = a_i$. We verify (K2) by II. (K2) $(a \vee b)' = a' \wedge b'$ means in our case $1 - \max\{a_i, b_i\} = \min\{(1 - a_i), (1 - b_i)\}$ must be fulfilled in all possible cases (see Table II).

TABLE II
VERIFICATION TABLE 2

	$1 - \max\{a_i, b_i\}$	$\min\{(1 - a_i), (1 - b_i)\}$
$a_i \leq b_i \leq c_i$	$1 - b_i$	$1 - b_i$
$a_i \leq c_i \leq b_i$	$1 - b_i$	$1 - b_i$
$b_i \leq a_i \leq c_i$	$1 - a_i$	$1 - a_i$
$b_i \leq c_i \leq a_i$	$1 - a_i$	$1 - a_i$
$c_i \leq a_i \leq b_i$	$1 - b_i$	$1 - b_i$
$c_i \leq b_i \leq a_i$	$1 - a_i$	$1 - a_i$

Further, property (K3) $a \wedge a' \leq b \vee b'$ is fulfilled if and only if $\min\{a_i, 1 - a_i\} \leq \max\{b_i, 1 - b_i\}$ in all possible cases. This is clear since $\min\{a_i, 1 - a_i\} \leq 0.5 \leq \max\{b_i, 1 - b_i\}$. Furthermore, the property (B1) $a \wedge a^{\sim\sim} = a$ is fulfilled since $\min\{a_i, 1\} = a_i$ and the property (B2) $(a \vee b)^{\sim} = a^{\sim} \wedge b^{\sim}$ is fulfilled since $(a \vee b)^{\sim}[i] = 1 \Leftrightarrow a_i = b_i = 0$ and $(a^{\sim} \wedge b^{\sim})[i] = 1 \Leftrightarrow a_i = b_i = 0$. Finally, (B3) $a \wedge a^{\sim} = 0$ holds since either $a_i = 0$ or $a_i^{\sim} = 0$. □

We can even say more about this quasi-BZ lattice, which the next proposition will show.

Proposition 4.2: $\langle \Sigma^n, \vee, \wedge, ', ^{\sim}, 0, 1\rangle$ is a de Morgan BZ (BZ^{dM}) distributive lattice.

Proof. We have

$$(a \wedge b)_i^{\sim} = \begin{cases} 0 \Leftrightarrow a_i \wedge b_i \neq 0 \Leftrightarrow \min(a_i, b_i) \neq 0 \\ 1 \Leftrightarrow a_i \wedge b_i = 0 \Leftrightarrow \min(a_i, b_i) = 0 \end{cases}$$

and

$$(a^{\sim} \vee b^{\sim})_i = \begin{cases} 0 \Leftrightarrow \max(a_i^{\sim}, b_i^{\sim}) = 0 \Leftrightarrow \\ a_i^{\sim} \wedge b_i^{\sim} = 0 \Leftrightarrow a_i \neq 0, b_i \neq 0 \\ 1 \Leftrightarrow \max(a_i^{\sim}, b_i^{\sim}) \neq 0 \Leftrightarrow \\ a_i^{\sim} \wedge b_i^{\sim} \neq 0 \Leftrightarrow a_i = 0, b_i = 0 \end{cases}.$$

Thus $\langle \Sigma^n, \vee, \wedge, ', ^{\sim}, 0, 1\rangle$ fulfills the $\vee$ de Morgan property (B2a). □

V. ARITHMETICS OF APPROXIMATION SETS

In this section we investigate the connection between the operations related to objects and the approximations introduced in Section II.

Proposition 5.1: Let Ω be a set of objects, $\omega_1, \omega_2 \in \Omega$. Then

1) $\delta_{\omega_1} \cap \delta_{\omega_2} = \delta_{\nu_{\omega_1} \wedge \nu_{\omega_2}}$
2) $\delta_{\omega_1} \cup \delta_{\omega_2} = \delta_{\nu_{\omega_1} \vee \nu_{\omega_2}}$

Proof. We denote $v = (v_1, \ldots, v_n)$ and v_i denotes the i^{th} coordinate of v for each $i = 1, \ldots, n$. For the convenience of the reader, we denote the i^{th} coordinate of ν_{ω_1} by $\nu_{\omega_1}[i]$ and the i^{th} coordinate of ν_{ω_2} by $\nu_{\omega_2}[i]$.

1) By definition we have $\delta_{\omega_1} \cap \delta_{\omega_2} = \{v \mid 0 \leq v_i \leq \nu_{\omega_1}[i] \Leftrightarrow \nu_{\omega_1}[i] \neq 0; v_i = 0 \Leftrightarrow \nu_{\omega_1}[i] = 0\} \cap \{v \mid 0 \leq v_i \leq \nu_{\omega_2}[i] \Leftrightarrow \nu_{\omega_2}[i] \neq 0; v_i = 0 \Leftrightarrow \nu_{\omega_2}[i] = 0\} = \{v \mid 0 \leq v_i \leq \min\{\nu_{\omega_1}[i], \nu_{\omega_2}[i]\} \Leftrightarrow \nu_{\omega_1}[i] \neq 0$ and $\nu_{\omega_2}[i] \neq 0; v_i = 0 \Leftrightarrow \nu_{\omega_1}[i] = 0$ or $\nu_{\omega_2}[i] = 0\}$ and since the latter case is included in the first case this is equal to $\{v \mid 0 \leq v_i \leq \min\{\nu_{\omega_1}[i], \nu_{\omega_2}[i]\}\}$, which is $\delta_{\nu_{\omega_1} \wedge \nu_{\omega_2}}$ by definition.
2) Similarly to the previous case we have $\delta_{\omega_1} \cup \delta_{\omega_2} = \{v \mid 0 \leq v_i \leq \max\{\nu_{\omega_1}[i], \nu_{\omega_2}[i]\}\} = \delta_{\nu_{\omega_1} \vee \nu_{\omega_2}}$.

□

Proposition 5.2: Let Ω be a set of objects, $\omega_1, \omega_2 \in \Omega$. Then

1) $\varphi_{\omega_1} \cap \varphi_{\omega_2} \neq \emptyset \Leftrightarrow \varphi_{\omega_1} \subseteq \varphi_{\omega_2}$ or $\varphi_{\omega_2} \subseteq \varphi_{\omega_1}$
2) $\varphi_{\nu_{\omega_1} \wedge \nu_{\omega_2}} \subseteq \varphi_{\omega_1} \cup \varphi_{\omega_2}$

Proof. We denote $v = (v_1, \ldots, v_n)$ and v_i denotes the i^{th} coordinate of v for each $i = 1, \ldots, n$. For the convenience of the reader, we denote the i^{th} coordinate of ν_{ω_1} by $\nu_{\omega_1}[i]$ and the i^{th} coordinate of ν_{ω_2} by $\nu_{\omega_2}[i]$.

1) We have $\varphi_{\omega_1} \cap \varphi_{\omega_2} = \{v \mid 0 \leq v_i \leq 1 \Leftrightarrow \nu_{\omega_1}[i] = 0$ and $\nu_{\omega_2}[i] = 0; v_i = \nu_{\omega_1}[i] = \nu_{\omega_2}[i]($ if $\nu_{\omega_1}[i] = \nu_{\omega_2}[i])\}$.
2) The statement is true since $\varphi_{\nu_{\omega_1} \wedge \nu_{\omega_2}} = \{v \mid 0 \leq v_i \leq 1 \Leftrightarrow \min\{\nu_{\omega_1}[i], \nu_{\omega_2}[i]\} = 0; v_i = \min\{\nu_{\omega_1}[i], \nu_{\omega_2}[i]\}\}$.

□

Let $\mathcal{L}$ and $\mathcal{U}$ be a lower and upper approximation of a set Ω as defined in Definition 2.4. We denote the algebraic closure of $\mathcal{L}$ by $\overline{\mathcal{L}}$ and the algebraic closure of $\mathcal{U}$ by $\overline{\mathcal{U}}$. Then we gain a commutative monoid for these algebraic closures with the operations defined in Definition 3.1. Thus we can prove the following propositions.

Proposition 5.3: Let Ω be a set of objects and $\omega \in \Omega$. If $\underbrace{(1, \ldots, 1)}_{n} \in \overline{\mathcal{L}}$, then $\langle \overline{\mathcal{L}}, \wedge\rangle$ is a commutative monoid.

Proof. The operation $\wedge$ is associative since $\min\{a, \min\{b, c\}\} = \min\{\min\{a, b\}c\}$. Further we have a unit element $e = \underbrace{(1, \ldots, 1)}_{n}$ since $\min\{a, 1\} = a$ for all $a \in [0, 1]$. By assumption we have $e \in \overline{\mathcal{L}}$. Finally, the operation is commutative since $\min\{a, b\} = \min\{b, a\}$.

□

Proposition 5.4: Let Ω be a set of objects and $\omega \in \Omega$. If $\underbrace{(0, \ldots, 0)}_{n} \in \overline{\mathcal{L}}$, then $\langle \overline{\mathcal{L}}, \vee\rangle$ is a commutative monoid.

Proof. The operation $\vee$ is associative since $\max\{a, \max\{b, c\}\} = \max\{\max\{a, b\}c\}$. Further we have a unit element $e = \underbrace{(0, \ldots, 0)}_{n}$ since $\max\{a, 0\} = a$ for all $a \in [0, 1]$. By assumption we have $e \in \overline{\mathcal{L}}$. Finally, the operation is commutative since $\max\{a, b\} = \max\{b, a\}$. □

Proposition 5.5: Let Ω be a set of objects and $\omega \in \Omega$. If $\underbrace{(1, \ldots, 1)}_{n} \in \overline{\mathcal{U}}$, then $\langle \overline{\mathcal{U}}, \wedge \rangle$ is a commutative monoid.

Proof. The operation $\wedge$ is associative since $\min\{a, \min\{b, c\}\} = \min\{\min\{a, b\}c\}$. Further we have a unit element $e = \underbrace{(1, \ldots, 1)}_{n}$ since $\min\{a, 1\} = a$ for all $a \in [0, 1]$. By assumption we have $e \in \overline{\mathcal{U}}$. Finally, the operation is commutative since $\min\{a, b\} = \min\{b, a\}$. □

Proposition 5.6: Let Ω be a set of objects and $\omega \in \Omega$. If $\underbrace{(0, \ldots, 0)}_{n} \in \overline{\mathcal{U}}$, then $\langle \overline{\mathcal{U}}, \vee \rangle$ is a commutative monoid.

Proof. The operation $\vee$ is associative since $\max\{a, \max\{b, c\}\} = \max\{\max\{a, b\}c\}$. Further we have a unit element $e = \underbrace{(0, \ldots, 0)}_{n}$ since $\max\{a, 0\} = a$ for all $a \in [0, 1]$. By assumption we have $e \in \overline{\mathcal{U}}$. Finally, the operation is commutative since $\max\{a, b\} = \max\{b, a\}$. □

VI. Conclusion

In the current paper, we introduce a representation for objects of an incomplete information system and we introduce operations which make the gained structure a BZ-distributive lattice. Since in ([10] Proposition 14) a complete information system is associated to a BZ-distributive lattice, this opens the door to several possibilities for investigating rough sets based on incomplete information systems. From a certain point of view, an incomplete information system can be handled mathematically similarly as a complete information system. The literature of rough set theory is extremely large for complete information systems, e.g. [10], [12], [14]. Given a quasi-BZ lattice, a whole rough approximation space can be constructed (see for example Proposition 8 and Definition 8 in [10]). Therefore the current paper can be considered as a new idea how to represent an incomplete information system in such a way that known algebraic structures will be achieved. In this way, we can use good properties of algebraic structures in order to handle sets of objects, even if we do not have all important information. It seems to be surprising that we find the algebraic structure of monoids when we investigate rough sets, but actually monoids also appear in algebraic approaches for complete information systems, see for example [15] and [16]. Therefore it seems to be worthwhile to investigate monoids when we investigate rough sets. A research problem for the future is to find applications which can help to solve problems representing and working with information systems based on the algebraic structures gained from the approaches which were represented in the current paper.

Acknowledgement

The author was partially supported by the construction EFOP-3.6.3-VEKOP-16-2017-00002. This project is supported by the European Union, co-financed by the European Social Fund.

References

[1] Z. Pawlak, "Rough sets," *International Journal of Parallel Programming*, vol. 11, no. 5, pp. 341–356, 1982.
[2] Z. Pawlak and A. Skowron, "Rough sets and boolean reasoning," *Information sciences*, vol. 177, no. 1, pp. 41–73, 2007.
[3] Z. Pawlak *et al.*, "Rough sets: Theoretical aspects of reasoning about data," *System Theory, Knowledge Engineering and Problem Solving, Kluwer Academic Publishers, Dordrecht, 199l*, vol. 9, 1991.
[4] A. Skowron and J. Stepaniuk, "Tolerance approximation spaces," *Fundamenta Informaticae*, vol. 27, no. 2, pp. 245–253, 1996.
[5] Y. Yao and B. Yao, "Covering based rough set approximations," *Information Sciences*, vol. 200, pp. 91 – 107, 2012.
[6] Z. Pawlak and A. Skowron, "Rudiments of rough sets," *Information sciences*, vol. 177, no. 1, pp. 3–27, 2007.
[7] J. Yao, Y. Yao, and W. Ziarko, "Probabilistic rough sets: Approximations, decision-makings, and applications," *International Journal of Approximate Reasoning*, vol. 49, no. 2, pp. 253–254, 2008.
[8] Z. Csajbók and T. Mihálydeák, "A general set theoretic approximation framework," in *Advances on Computational Intelligence* (S. Greco, B. Bouchon-Meunier, G. Coletti, M. Fedrizzi, B. Matarazzo, and R. R. Yager, eds.), (Berlin, Heidelberg), pp. 604–612, Springer Berlin Heidelberg, 2012.
[9] D. Nagy, T. Mihálydeák, and L. Aszalós, "Similarity based rough sets," in *Rough Sets* (L. Polkowski, Y. Yao, P. Artiemjew, D. Ciucci, D. Liu, D. Ślęzak, and B. Zielosko, eds.), (Cham), pp. 94–107, Springer International Publishing, 2017.
[10] G. Cattaneo and D. Ciucci, "Algebraic structures for rough sets," in *Transactions on Rough sets II*, pp. 208–252, Springer, 2004.
[11] G. Liu and W. Zhu, "The algebraic structures of generalized rough set theory," *Information Sciences*, vol. 178, no. 21, pp. 4105–4113, 2008.
[12] A. Mani, G. Cattaneo, and I. Düntsch, *Algebraic methods in general rough sets*. Springer, 2018.
[13] D. Ciucci, T. Mihálydeák, and Z. E. Csajbók, "On definability and approximations in partial approximation spaces," in *International Conference on Rough Sets and Knowledge Technology*, pp. 15–26, Springer, 2014.
[14] L. Polkowski, *Rough sets*. Springer, 2002.
[15] T. Murai, S. Miyamoto, M. Inuiguchi, Y. Kudo, and S. Akama, "Fuzzy multisets in granular hierarchical structures generated from free monoids," *Journal of Advanced Computational Intelligence and Intelligent Informatics*, vol. 19, no. 1, pp. 43–50, 2015.
[16] B. Praba, V. Chandrasekaran, and A. Manimaran, "A commutative regular monoid on rough sets," *Italian Journal of Pure and Applied Mathematics*, vol. 31, pp. 307–318, 2013.

15th International Workshop on Computational Optimization

MANY real world problems arising in engineering, economics, medicine and other domains can be formulated as optimization tasks. These problems are frequently characterized by non-convex, non-differentiable, discontinuous, noisy or dynamic objective functions and constraints which ask for adequate computational methods.

The aim of this workshop is to stimulate the communication between researchers working on different fields of optimization and practitioners who need reliable and efficient computational optimization methods.

TOPICS

The list of topics includes, but is not limited to:

- combinatorial and continuous global optimization
- unconstrained and constrained optimization
- multiobjective and robust optimization
- optimization in dynamic and/or noisy environments
- optimization on graphs
- large-scale optimization, in parallel and distributed computational environments
- meta-heuristics for optimization, nature-inspired approaches and any other derivative-free methods
- exact/heuristic hybrid methods, involving natural computing techniques and other global and local optimization methods
- numerical and heuristic methods for modeling

The applications of interest are included in the list below, but are not limited to:

- classical operational research problems (knapsack, traveling salesman, etc)
- computational biology and distance geometry
- data mining and knowledge discovery
- human motion simulations; crowd simulations
- industrial applications
- optimization in statistics, econometrics, finance, physics, chemistry, biology, medicine, and engineering
- environment modeling and optimization

BEST PAPER AWARD

The best WCO'22 paper will be awarded during the social dinner of FedCSIS 2022.

The best paper will be selected by WCO'22 co-Chairs by taking into consideration the scores suggested by the reviewers, as well as the quality of the given oral presentation.

TECHNICAL SESSION CHAIRS

- **Fidanova, Stefka,** Bulgarian Academy of Sciences, Bulgaria
- **Mucherino, Antonio,** INRIA, France
- **Zaharie, Daniela,** West University of Timisoara, Romania

Communication Papers of the of the 17th Conference on Computer Science and Intelligence Systems pp. 81–84
DOI: 10.15439/2022F224
ISSN 2300-5963 ACSIS, Vol. 32

Performance and Scalability Experiments with a Large-scale Air Pollution Model on the EuroHPC Petascale Supercomputer DISCOVERER

Tzvetan Ostromsky
Institute of Information and Communication Technologies (IICT),
Bulgarian Academy of Sciences (BAS), Sofia, Bulgaria
Email: ceco@parallel.bas.bg

***Abstract*—The basic parallel versions of the Danish Eulerian Model (UNI-DEM) has been implemented on the new petascale supercomputer DISCOVERER, installed last year in Sofia, Bulgaria by the company Atos. DISCOVERER is part of the European High Performance Computing Joint Undertaking (EuroHPC), which is building a network of 8 powerful supercomputers across the European Union (3 pre-exascale and 5 petascale).**

The results of some scalability experiments with the basic MPI and a hybrid MPI-OpenMP parallel implementations of UNI-DEM on the new Bulgarian petascale supercomputer DISCOVERER (in EuroHPC network) are presented here. They are compared with similar earlier experiments performed on the Mare Nostrum III supercomputer (petascale too) at Barcelona Supercomputing Centre – the most powerful supercomputer in Spain by that time, upgraded currently to the pre-exascale Mare Nostrum V, also part of the EuroHPC JU infrastructure.

***Index Terms*—air pollution, numerical model, supercomputer, parallel computing, algorithm, scalability, MPI, OpenMP**

I. Introduction

THE environmental modelling and air pollution modelling in particular is one of the toughest problems of computational mathematics (together with the meteorological modelling). All relevant physical and chemical processes in the atmosphere should be taken into account, which are mathematically represented by a complex PDE system. To simplify it a proper splitting procedure is applied. As a result the initial system is replaced by several simpler systems (submodels), connected with the main physical and chemical processes. These systems should be calculated in a large spatial domain, as the pollutants migrate quickly on long distances, driven by the atmosphere dynamics, especially on high altitude. Here they are exposed to temperature, light and other condition changes in extremely wide range, so does the speed of most chemical reactions. One of the major sources of difficulty is the dynamics of the atmospheric processes, which require small time-step to be used (at least, for the chemistry submodel) in order to get a stable numerical solution of the corresponding system. All this makes the treatment of large-scale air pollution models a tuff and heavy computational task. It has always been a serious challenge, even for the fastest and most powerful state-of-the-art supercomputers.

The first crucial point on the way to this goal is domain decomposition technique. This is a natural way to achieve distributed memory parallelization of any numerical problem over a large spatial domain. For some of them however, like the advection-diffusion equations in our case, there is always certain overhead due to the boundary conditions. Minimizing this overhead is a key point towards efficient optimization. On the other hand, optimization should not restrict the portability of the parallel implementation, as the intensive development in the computer technology inevitably leads to regular updates or complete replacement of the outdated hardware. Standard parallel programming tools as MPI and OpenMP (for distributed / shared memory models) are used in order to preserve portability of the code. Another important parallel optimization issue is the load-balance. MPI barriers, used to force synchronization between the processes in data transfer commands, often do not allow good load-balance. This obstacle can be avoided to some extent by using non-blocking communication routines from the MPI standard library.

II. Description and parallel implementations of the Danish Eulerian Model

DEM is a powerful and sophisticated large scale air pollution model, with some 30-year development history [8], [5], [6], [9]. Over the years it was successfully applied in different long-term environmental studies in various areas (including environment protection, human health care, agricultural production, forestry, wildlife, culture heritage protection, etc.). By processing a huge amount of data (most of it - for the quickly changing meteorological conditions), the model is able to calculate the variable concentrations of a number of pollutants and other chemically active species interacting with them (precursors), over a long time period. Moreover, various accumulative quantities (AOT40, AOT60, etc.) are calculated on yearly basis.

A. Mathematical representation of UNI-DEM

An air pollution model can be described by a system of partial differential equations for calculating the concentrations of a number of pollutants (and other chemical species that interact with the pollutants) in the atmosphere above the

studied geographical region. The main physical and chemical processes (horizontal and vertical wind, diffusion, chemical reactions, emissions and deposition) should be adequately represented in the system. In particular, the Danish Eulerian Model (DEM) [7], [8] is mathematically represented by the following system of partial differential equations:

$$\frac{\partial c_s}{\partial t} = -\frac{\partial(uc_s)}{\partial x} - \frac{\partial(vc_s)}{\partial y} - \frac{\partial(wc_s)}{\partial z} + \quad (1)$$

$$+\frac{\partial}{\partial x}\left(K_x\frac{\partial c_s}{\partial x}\right) + \frac{\partial}{\partial y}\left(K_y\frac{\partial c_s}{\partial y}\right) + \quad (2)$$

$$+\frac{\partial}{\partial z}\left(K_z\frac{\partial c_s}{\partial z}\right) + \quad (3)$$

$$+E_s + Q_s(c_1, c_2, \ldots, c_q) - (k_{1s} + k_{2s})c_s \; ; \quad (4)$$

$$s = 1, 2, \ldots, q \; ; \quad (5)$$

where the following notation is used:

q - number of equations = number of chemical species,
c_s - concentrations of the chemical species considered,
u, v, w - components of the wind along the coordinate axes,
K_x, K_y, K_z - diffusion coefficients,
E_s - emissions in the space domain,
k_{1s}, k_{2s} - coefficients of dry and wet deposition respectively ($s = 1, \ldots, q$),
$Q_s(c_1, c_2, \ldots, c_q)$ - non-linear functions that describe the chemical reactions between the species.

B. Splitting into submodels

The above rather complex system is split into three subsystems (submodels), according to the major physical and chemical processes as well as the numerical methods applied in their solution (marked by different colors in the right-hand-side of the system). These are horizontal advection and diffusion chemistry, emissions and deposition and vertical exchange submodels, respectively. The discretization of the spatial derivatives in these sub-models results in forming three large systems of ordinary differential equations. More details about the numerical methods, applied to solve these systems, can be found in [1], [3], [8].

C. Parallelization strategy

The MPI standard library is used as a main parallelization tool. The MPI (Message Passing Interface) was initially developed as a standard communication library for distributed memory computers. Later, proving to be efficient, portable and easy to use, it became one of the most popular parallelization tools for application programming. Now it can be used on much wider class of parallel systems, including shared-memory computers and clustered systems (each node of the cluster being a separate shared-memory machine). Thus it provides high level of portability of the code.

In the case of DEM, MPI parallelization is based on the space domain partitioning [5], [6]. The space domain is divided into sub-domains (the number of the sub-domains is equal to the number of MPI tasks). Each MPI task works on its own sub-domain. On each time step there is no data dependency between the MPI tasks on both the chemistry and the vertical exchange stages. This is not so with the advection-diffusion stage. Spatial grid partitioning between the MPI tasks requires overlapping of the inner boundaries and exchange of certain boundary values on the neighboring subgrids for proper treatment of the boundary conditions. The subdomains are usually too large to fit into the fastest cache memory of the corresponding CPU. In order to achieve good data locality, the smaller calculation tasks are grouped in chunks (if appropriate) for more efficient cache utilization. An input parameter CHUNKSIZE is provided, which controls the amount of short-term reusable data in order to reduce the transfer between the cache and the main (slower access) memory. It should be tuned with respect to the cache size of the target machine.

More detailed description of the main computational stages of DEM and the parallelization techniques used in each of them can be found in [1], [5], [6], [8].

III. Numerical experiments with UNI-DEM on two petascale supercomputers (IBM MareNostrum III in Barcelona, Spain and Atos DISCOVERER EuroHPC in Sofia, Bulgaria)

Results of scalability experiments with the 2-D fine-resolution grid version of UNI-DEM on two of the most powerful supercomputers in Europe will be shown in Tables I and II in this section.

A. Numerical experiments on the IBM MareNostrum III supercomputer at BSC - Barcelona, Spain

Characteristics of the system IBM MareNostrum III

- 3028 nodes IBM dx360 M4, 16-core, 32 GB RAM per node;
- 48488 cores in total (Intel SandyBridge-EP E5-2670, 2600 MHz);
- Total RAM $>$ 94 TB; Disk storage 1,9 PB;
- Interconnection networks: Infiniband / Gigabit Ethernet;
- Theoretical peak performance $\sim$ 1 PFLOPS.

Some values of the user-defined parameters of UNI-DEM used in the experiments are given below:

- Grid-version: $(480 \times 480 \times 1)$;
- Time period of modelling: 1 year;
- Time step: 90 sec. (both in advection and chemistry stages);
- Cache utilization parameter: `NSIZE` = 32 .

B. Numerical experiments on the EuroHPC JU supercomputer DISCOVERER in Bulgaria

Characteristics of the DISCOVERER supercomputer

- Based on the Atos' platform BullSequana XH2000

TABLE I
TIME (T) IN SECONDS AND SPEED-UP (*Sp*) OF UNI-DEM ON IBM MARENOSTRUM III AT BSC - BARCELONA, SPAIN

Time (T) in seconds and speed-up (*Sp*) of UNI-DEM (MPI basic version) on IBM MareNostrum III								
NP	#	Advection		Chemistry		TOTAL		
(MPI)	NODES	T [s]	(*Sp*)	T [s]	(*Sp*)	T [s]	(*Sp*)	*E* [%]
4	1	33340	(*4.0*)	29050	(*4.0*)	69378	(*4.0*)	100 %
8	1	16927	(*7.9*)	15508	(*7.5*)	38162	(*7.3*)	91 %
16	1	9000	(*14.8*)	7739	(*15.0*)	22072	(*12.6*)	79 %
32	2	4929	(*27.1*)	4120	(*28.2*)	14113	(*19.7*)	61 %
64	4	2569	(*51.9*)	2176	(*53.4*)	9235	(*30.1*)	47 %
96	6	2067	(*64.5*)	1409	(*82.5*)	6985	(*39.7*)	41 %
160	10	1471	(*90.6*)	845	(*137.5*)	5638	(*49.2*)	31 %

TABLE II
TIME (T) IN SECONDS AND SPEED-UP (*Sp*) OF UNI-DEM ON THE EUROHPC JU SUPERCOMPUTER DISCOVERER IN SOFIA, BULGARIA

Time (T) in seconds and speed-up (*Sp*) of UNI-DEM (MPI basic version) on DISCOVERER								
NP	#	Advection		Chemistry		TOTAL		
(MPI)	NODES	T [s]	(*Sp*)	T [s]	(*Sp*)	T [s]	(*Sp*)	*E* [%]
4	1	23408	(*4.0*)	21615	(*4.0*)	48604	(*4.0*)	100 %
8	1	11830	(*7.9*)	11072	(*7.8*)	25045	(*7.8*)	97 %
12	1	7785	(*12.0*)	7112	(*12.2*)	17036	(*11.4*)	95 %
16	1	6023	(*15.5*)	5438	(*15.3*)	13061	(*14.9*)	93 %
24	2	4075	(*23.0*)	3630	(*23.8*)	9148	(*21.3*)	89 %
36	3	2786	(*33.6*)	2314	(*37.4*)	6248	(*31.1*)	86 %
48	4	2216	(*42.3*)	1845	(*46.9*)	4805	(*40.5*)	84 %
60	4	1790	(*52.3*)	1358	(*61.3*)	3638	(*53.4*)	89 %
80	5	1420	(*65.9*)	978	(*85.2*)	3050	(*63.7*)	80 %
96	6	1243	(*75.3*)	824	(*101.1*)	2701	(*72.0*)	75 %
120	8	1072	(*87.3*)	662	(*125.8*)	2394	(*81.2*)	68 %
160	10	895	(*104.6*)	498	(*167.3*)	2052	(*94.7*)	59 %

- CPU type: AMD EPYC 7H12 (code name Rome), frequency 2.6GHz, power consumption 280W
- 12 racks, 376 blades, 1128 nodes, 144384 cores in total
- 128 cores per node, RAM: 128 GB per node
- Total RAM 300 TB; Disk storage 2 PB
- Interconnection: Dragonfly+ with 200Gbps (IB HDR) bandwidth per link
- Sustained performance: 4.518 petaflops
- Theoretical peak performance: 6 petaflops
- TOP500 ranking: # 91 in the world; # 27 in EU (June 2021)

DEM code parallelization and optimization details

- AMD compilers for MPI code (mpifort, mpicc)
- Automatic compiler optimization level: -O3 (mostly)
- Additional parallelism by OpenMP directives of the performance-critical parts of the code, if appropriate (with -fopemp argument for invoking the proper version (extension) of the compiler and linking the necessary libraries)

IV. CONCLUSIONS

- The parallel MPI implementation of DEM is well balanced, portable and proved to run efficiently on some of the most powerful parallel supercomputers in Europe, including the Bulgarian Petascale supercomputer DISCOVERER, part of the EuroHPC JU network.
- The efficiency and speed-up is higher in the computationally-intensive stages. In particular, the chemistry stage (which does not need any communication between the tasks) has almost linear overall speed-up. The advection stage scales pretty well too, taking into account that there is some unavoidable computational overhead due to overlapping boundaries of the partitioning.
- The time for the computationally-intensive stages is additionally reduced in relation with the number of threads in the hybrid MPI-OpenMP code with the OpenMP lower level of parallelism switched on, which can be exploited on core level within a node.
- For the sake of comparability the size of chunks at the chemistry-deposition stage `NSIZE`=32 has been set in all experiments. This might not be the optimal value in all cases. When the number of MPI tasks is large, better results can be expected with a lower value of `NSIZE`, especially when the OpenMP level of parallelism is switched on.

V. PLANS FOR FUTURE WORK

For some environmental applications it is highly desirable to simplify the model as much as possible, keeping the reliability of its output results. A careful sensitivity analysis is needed in order to decide how to do such simplifications. On the other hand, it is important to analyze the influence of variations of

the initial conditions, the boundary conditions, the rates of some chemical reactions, etc. on the model results in order to make right assumptions about the possible simplifications, which could be done. Such analysis can give valuable information about the performance of reliable and reasonable simplifications. It can also help in identifying the accuracy-critical parameters. Thus the sensitivity analysis version of DEM SA-DEM was created [2], [4]. Its complexity is of higher order, a real challenge for the top performance supercomputers nowadays. Its implementation on DISCOVERER and obtaining results - data for further research in various important scientific, social and economic areas is our goal for the future.

ACKNOWLEDGMENTS

This research was supported in part by the Bulgarian NSF project "Efficient methods for modelling, optimization and decision making" (contract # KP-06-N52/5), and by the European High-Performance Computing Joint Undertaking via the Discoverer Fast Track & Benchmark Access project Installing, benchmarking, performance and scalability analysis of the UNI-DEM package for air pollution modelling.

REFERENCES

[1] V. Alexandrov, A. Sameh, Y. Siddique and Z. Zlatev, Numerical integration of chemical ODE problems arising in air pollution models, *Env. Modeling and Assessment*, 2 (1997) 365–377.

[2] I. Dimov, R. Georgieva, S. Ivanovska, Tz. Ostromsky, Z. Zlatev, Studying the sensitivity of pollutants' concentrations caused by variations of chemical rates, *J. Comput. Appl. Math., Vol. 235 (2010), pp. 391–402.*

[3] Ø. Hov, Z. Zlatev, R. Berkowicz, A. Eliassen and L. P. Prahm, Comparison of numerical techniques for use in air pollution models with non-linear chemical reactions, Atmospheric Environment, Vol. 23 (1988), pp. 967–983.

[4] Tz. Ostromsky, I. Dimov, R. Georgieva, Z. Zlatev, Air pollution modelling, sensitivity analysis and parallel implementation, Int. Journal of Environment and Pollution, Vol. 46 (1-2), (2011), pp. 83–96.

[5] Tz. Ostromsky, Z. Zlatev, Parallel Implementation of a Large-scale 3-D Air Pollution Model, in: Large Scale Scientific Computing (S. Margenov, J. Wasniewski, P. Yalamov, Eds.), LNCS-2179, Springer, 2001, pp. 309–316.

[6] Tz. Ostromsky, Z. Zlatev, Flexible Two-level Parallel Implementations of a Large Air Pollution Model, in: Numerical Methods and Applications (I.Dimov, I.Lirkov, S. Margenov, Z. Zlatev - eds.), LNCS-2542, Springer (2002), pp. 545–554.

[7] WEB-site of the Danish Eulerian Model, available at: http://www.dmu.dk/AtmosphericEnvironment/DEM

[8] Z. Zlatev, Computer treatment of large air pollution models, Kluwer (1995).

[9] Z. Zlatev, I. Dimov, Computational and Numerical Challenges in Environmental Modelling, Elsevier, Amsterdam (2006).

Communication Papers of the of the 17th Conference on Computer Science and Intelligence Systems pp. 85–92
DOI: 10.15439/2022F19
ISSN 2300-5963 ACSIS, Vol. 32

Surrogate Estimators for Complex Bi-Level Energy Management

Fatiha Bendali, Jean Mailfert
LIMOS Lab. CNRS/UCA
Clermont-Ferrand, France

Eloise Mole Kamga
Labex IMOBS3, LIMOS Lab
CNRS/UCA, Clermont-Ferrand,
France

Alejandro Olivas Gonzalez,
Alain Quilliot,
Labex IMOBS3,
LIMOS Lab, UCA/CNRS
Clermont-Ferrand, France
Email: {alain.quilliot@uca.fr}

Hélène Toussaint
LIMOS UCA/CNRS
Clermont-Ferrand, France

***Abstract*—We deal here with the routing of vehicles in charge of performing internal logistics tasks inside some protected area. Those vehicles are provided in energy by a local solar hydrogen production facility, with limited storage and time-dependent production capacities. One wants to synchronize energy production and consumption in order to minimize both production and routing costs. Because of the complexity of resulting bi-level model, we deal with it by short-cutting the production scheduling level with the help of surrogate estimators, whose values are estimated through fast dynamic programming algorithms and through machine learning.**

I. Introduction

THE notion of multi-level decisional [1, 5, 6] model arises when decision is shared between several players. Solving such a model aims at providing a scenario which would be the best (or almost the best) in case all the players accept to submit themselves to a common authority (centralized paradigm), or, if it is not the case (collaborative paradigm), at helping them into the search for a compromise solution [14].

Solving a multi-level model is a difficult task and standard approaches involve decomposition schemes, which may be hierarchical (Benders decomposition of ILP models, …) or transversal (Lagrangean relaxation,…). Still, in both case, a major difficult remains, related to the sensitivity issue, that means about the way one may retrieve information from the handling of the different levels in order to make them interact. So a trend, boosted by the rise of machine learning technology [12, 15], is to bypass some levels of the global model through surrogate constraints or functions, likely to behave as an approximation of the values induced inside the model by optimal decisions taken at those levels.

It is this point of view which we adopt here while dealing with a problem related to the synchronization between local solar energy (hydrogen, PV, [9]) production and its consumption by a fleet of autonomous vehicles. This problem arose in the context of the activities of IMOBS3 (*Innovative Mobility*) Labex in Clermont-Ferrand of the national PGMO program promoted by power company EDF. On one side, the production manager schedules the activity of the micro-plant, which includes not only energy production, but also energy purchase and sale on the market, taking into account that both production costs and production capacities are time-dependent. On the other side, the fleet manager schedules and routes the vehicles in such a way they efficiently achieve a set internal logistic tasks. Both meet in order to perform *refueling transactions*, when the vehicle moves toward the micro-plant in order to refuel. Limited storage capacities impose to synchronize time dependent energy production and consumption. Though many searchers have recently showed interests into the emerging decisional models which are related to the management of renewable energy, they most often focused either on production control and scheduling [1, 10] or one the issues related to consumption [2, 3, 7, 11, 13], without dealing with the synchronized interaction between both levels. We do it here by shortcutting the part of the process related to production scheduling and using a surrogate formulation of the cost related to production. We try two kind of such surrogate formulations: the first one is based upon the fact that, a routing decision Γ being given, an optimal refueling decision may be obtained in polynomial time by solving a simple parametric auxiliary *Refuel*(Γ, β) problem, where β is a cost parameter; the second formulation relies on an approximation by a neural network of the optimal value of the production sub-problem which results from fixing both route decision Γ and related refueling strategy. Though in practice part of the difficulty here is due to uncertainty [8), we suppose, for the sake of simplicity, that all our system behaves in a deterministic way.

So the paper is organized as follows. We first (Section II) describe the problem and its ILP formulation. While doing it, we introduce *strong no_sub-tour* constraints, which may be separated in polynomial time in order to make possible the implementation of a *Branch and Cut* algorithm. Next (Section III) describes an auxiliary parametric problem *Refuel*(Γ, β), which may be solved in polynomial time through dynamic programming. We use it as a surrogate quality estimator, which computes *ad hoc* vehicle routes while bypassing the production part of the problem. In Section IV, we apply machine learning in order to get a fast approximation of the optimal value for the production sub-problem. Section V is devoted to numerical experiments.

II. The SVREP: SynchroniZed Vehicle Routing/Energy Production Problem

We consider a fleet of autonomous hydrogen powered vehicles, initially located at a depot 0, and which are required to perform a VRP: *Vehicle Routing Problem* tour, that means to visit a set of stations {0,…, *M*} within a time horizon [0, *TMax*]. Moving from station *j* to station *k* requires $\Delta_{j,k}$ time units and an amount $E_{j,k}$ of energy. Those vehicles are constrained by a same fuel storage capacity C^{Veh}, they all start their journey with a same fuel load E_0, and are required to end it loaded with at least E_0 energy units. For the sake of simplicity, we restrict here ourselves to the case when only one vehicle is involved.

Because of this hypothesis about the fuel load of the vehicle at the beginning and at the end of its tour, this vehicle must refuel at least once. It does it while moving to a micro-plant – 1, provided with a storage facility (a tank) with capacity C^{Prod}, filled with hydrogen which may be either produced *in situ*, or bought, or, in case of excess, sold. We restrict ourselves to the case when hydrogen may neither be bought from outside nor sold. Hydrogen is produced from period to period through a combination of photolysis and electrolysis, which makes both its production rate (the amount of energy produced in one period if the micro-plant is activated) and its production cost (the cost of the electricity for the electrolysis) be time dependent. Periods are labeled from 1 to *N*, and every period has a same duration *p* in such a way that *TMax* = *p.N*. The production rate at period *i* is denoted by R_i and related production cost is denoted by $Cost_i$. Activating the micro-plant requires some human intervention, whose cost is fixed and denoted by *C_Act*. Refueling the vehicle takes a full period, and safety forbids the micro-plant to be at the same time producing and refueling. A consequence is that the vehicle may not be served as soon as it arrives to the micro-plant, but must wait until the micro-plant achieves its production target. At time 0, the micro-plant is loaded with H_0 energy units, and it should be loaded with at least H_0 at the end of the process. Though in true life uncertainty is part of the problem, we suppose here that production rates are deterministic. An example of cost and production rates is provided by figure 1.

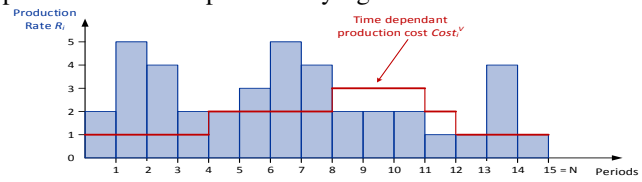

Figure 1. *Time dependent production rates costs for the micro-plant*

Then, resulting **SVREP**: *Synchronized Vehicle Routing and Energy Production* problem is about the computation of the route Γ, of the production schedule and of the *refueling transactions* (*j*, *k*, *L*, *T**) which will tell us the stations *j* such that the vehicle deviates its route while moving from *j* to its successor *k* in Γ in order to go to the micro-plant, related load *L* and related time *T**. The goal is to minimize a mixed cost *G_Cost* + α.*T*, where *G_Cost* is the global economic cost induced by the production process, *T* is the time when the vehicle achieves its journey, and α is a time versus money conversion coefficient. Figure 2 below shows an example of synchronization between a route 0, 1, …, *M*, 0 followed by the vehicle and the production of hydrogen by the micro-plant during periods 1,…, *N*, in case *p* = 2, E_0 = 8, H_0 = 4, *TMax* = 30, *C_Act* = 7, C^{Prod} = 15, C^{Veh} = 15, α = 1. In such a case, the vehicle refuels twice: the first transaction, performed at period 5 between stations 1 and 2, involves 13 fuel units, and the second one, performed at period 13 between stations 3 and 4, involves 12 fuel units. Resulting tour ends at time 30 and production cost is 3.7 + 2 + 6 + 1 = 30. It comes that resulting global cost is 30 + 30 = 60.

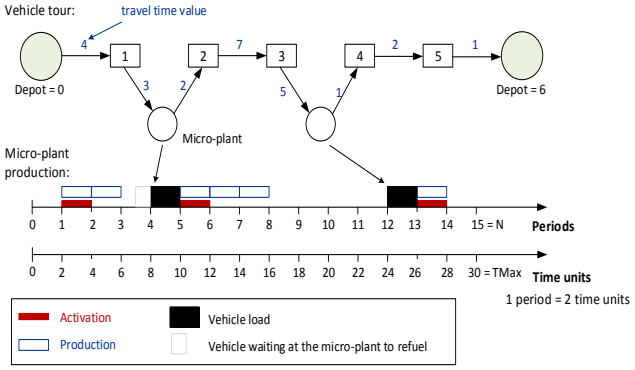

Figure 2. *A **SVREP** feasible solution.*

A. An ILP Formulation ILP_SVREP of SVREP

SVREP is does not fit the ILP machinery. Still, it is interesting to set such a model **ILP-SVREP**, since it will help us in benchmarking and also since part of this model will play a role inside our surrogate quality estimator oriented approach. We introduce fictitious period 0, a fictitious station *M*+1 identified with *Depot* = 0, and the following variables:

- **Production variables**:
  - $z = (z_i, i = 0,\ldots, N)$, with {0, 1} values: $z_i = 1$ ~ the micro-plant is active during period *i*.
  - $y = (y_i, i = 1,\ldots, N)$, with {0, 1} values: $y_i = 1$ ~ the micro-plant is activated at time (*p*-1).*i*.
  - $V^{Prod} = (V^{Prod_i}, i = 0,\ldots, N) \geq 0$: V^{Prod_i} is the load of the *micro-plant* tank at the end of period *i*.
  - $\delta = (\delta_i, i = 1,\ldots, N)$, with {0, 1} values: $\delta_i = 1$ ~ a refueling transaction takes place during period *i*.
  - $L^* = (L^*_i, i = 1,\ldots, N) \geq 0$: f $\delta_i = 1$, then L^*_i is the hydrogen transferred to the vehicle during period *i*.
- **Vehicle variables**:
  - $Z = (Z_{j,k}\ k \neq j$ in -1, 0,…, *M*+1, with {0, 1} values: $Z_{j,k} = 1$ iff the vehicle moves from *j* to *k*.
  - $X = (X_{j,k},\ k \neq j$ in 0,…, *M*+1), with {0, 1} values: *X* means the restriction to stations {0,…, *M*} of the vehicle route.
  - $L = (L_j, j = 0,\ldots, M) \geq 0$: if $Z_{j,-1} = 1$ then L_j = quantity of hydrogen loaded by the vehicle at the micro-plant.

- $T = (T_j, j = 0,\ldots, M+1) \geq 0$: T_j = time when the vehicle arrives at j.
- $T^* = (T^*_j, j = 0,\ldots, M+1) \geq 0$: if $Z_{j,-1} = 1$, then T^*_j = time when the vehicle starts refueling.
- $V^{Veh} = (V^{Veh}_j, j = 0,\ldots, M+1) \geq 0$: V^{Veh}_j = hydrogen load of the vehicle when it arrives in j.

- **Synchronization variables**: $U = (U_{i,j}, i = 1,\ldots, N, j = 0,..., M)$ with {0, 1} values: $U_{i,j} = 1$ ~ the vehicle refuels during period i after traveling from j to the micro-plant.

Then, α being a time vs money coefficient, the *cost* function comes as follows: $\boldsymbol{Cost} = \Sigma_{i=1,\ldots,N} (C\_Act.y_i + Cost_i.z_i) + \alpha.T_{M+1}$.

We must now explicit the constraints, while distinguishing those related to production, to routing and to synchronization.

- **Production constraints**:
  - For any $i = 1,\ldots, N$: $y_i \geq z_i - z_{i-1}$. (E1)
  - For any $i = 1,\ldots, N$: $z_i + \delta_i \leq 1$. (E2)
  - $z_0 = 0$; $V^{Prod}_0 = H_0$; $V^{Prod}_N \geq H_0$. (E3)
  - For any $i = 1,\ldots, N$: $V^{Prod}_i = V^{Prod}_{i-1} + z_i.R_i - L^*_i$. (E4)
  - For any $i = 1,\ldots, N$: $L^*_i \leq V^{Prod}_{i-1} \leq C^{Prod}$ and $L^*_i \leq \delta_i.C^{Veh}$. (E5)

  Explanation: (E1) expresses the fact that activating the micro-plant at period i means that it was idle at period i-1 and that it becomes active at period i. (E2) means that simultaneously producing and refueling is forbidden. (E3) reflects the initial and final requirements. (E4, E5) express the way the load micro-plant's tank evolves throughout the periods and set bounds on the amount of hydrogen transferred by the micro-plant to the vehicle.

- **Vehicle constraints**:
  - $Z_{M+1,0} = 1$; For any j, $Z_{j,j} = 0$; For any $j \neq M+1$, $Z_{j,0} = 0$ and $Z_{M+1,j} = 0$. (F1)
  - For any $j = 0,\ldots, M+1$, $\Sigma_k Z_{j,k} = 1 = \Sigma_k Z_{k,j}$. (F2)
  - $\Sigma_j Z_{-1,j} = \Sigma_j Z_{j,-1} \geq 1$. (F2Bis)
  - For any k, j, $X_{k,j} \geq Z_{k,j}$. (F3)
  - For any $j = 0,\ldots, M$, $\Sigma_k X_{j,k} = 1 = \Sigma_k X_{k,j}$. (F3Bis)
  - $V^{Veh}_0 = E_0$; $V^{Veh}_{M+1} \geq E_0$. (F4)
  - For any $j = 0,\ldots, M+1$: $E_{j,-1} \leq V^{Veh}_j \leq C^{Veh}$. (F4Bis)
  - For any $j, k = 0,\ldots, M+1$: $Z_{j,k} + (V^{Veh}_k - V^{Veh}_j + E_{j,k})/C^{Veh} \leq 1$. (F5)
  - For any $j,k = 0,\ldots, M$: $(X_{j,k} - Z_{j,k}) + (V^{Veh}_k - V^{Veh}_j + E_{j,-1} + E_{-1,k} - L_j)/C^{Veh} \leq 1$. (F6)
  - For any $j = 0,\ldots, M$: $L_j \leq C^{Veh} + E_{j,-1} - V^{Veh}_j$. (F7)
  - For any $j = 0,\ldots, M$: $L_j \leq (\Sigma_k (X_{j,k} - Z_{j,k})).C^{Veh}$. (F7Bis)
  - $T_0 = 0$; $T_{M+1} \leq TMax$. (F8)
  - For any $j, k = 0, \ldots, M$: $Z_{j,k} + (T_j + \Delta_{j,k} - T_k)/TMax \leq 1$. (F9)
  - For any $j, k = 0, \ldots, M$: $(X_{j,k} - Z_{j,k}) + (T^*_j + p + \Delta_{-1,k} - T_k)/TMax \leq 1$. (F10)
  - For any $j = 0,\ldots, M$: $(\Sigma_k (X_{j,k} - Z_{j,k})) + (T_j + \Delta_{j,-1} - T^*_j)/TMax \leq 1$ (F10Bis)

  Explanation: (F1, F2, F2Bis) mean that the vehicle follows a circular route which visits exactly once every station j and refuels at least once. (F3, F3Bis) mean that vector X describes the route followed by the vehicle when bypassing the micro-plant. Notice that if $X_{j,k} = 1$ and $Z_{j,k} = 0$ then (F3, F3Bis) also implies that $Z_{j,-1} = Z_{-1,k} = 1$. (F4, F4Bis) express the initial and final constraints on the vehicle's tank, as well as the fact that the vehicle must be able to return to the micro-plant as soon as it needs. (F5) expresses the way the load of the vehicle evolves when the vehicle moves from station j to station k without refueling and (F6) expresses what happens when the vehicle refuels between j and k. (F7, F7Bis) set bounds on the fuel amount that the vehicle may receive while moving from station j to its successor k according to X. (F8) sets the initial and final conditions related to the time values. (F9) expresses the evolution of time value T when the vehicle moves from station j to station k without refueling. (F10, F10Bis) express this evolution when the vehicle refuels while moving from j to k, taking into account refueling and waiting times.

- **Synchronization constraints**:
  - For any $j = 0,\ldots, M$: $\Sigma_{i=1,\ldots,N} U_{i,j} = Z_{j,-1}$. (G1)
  - For any $i = 1,\ldots, N$, $\delta_i = \Sigma_{j=0,\ldots,M} U_{i,j}$ (G2)
  - For any $j = 0,\ldots, M$, $T^*_j = \Sigma_{i=1,\ldots,N} p.(i-1).U_{i,j}$. (G3)
  - For any $i = 1,\ldots, N$, $j = 0, \ldots, M$: $U_{i,j} + (L_j - L^*_i)/C^{Veh} \leq 1$. (G4)

  Explanation: (G1, G2) mean that refueling transactions induce a matching between the refueling periods and the stations j such that the vehicle moves from j to *micro-plant* = - 1 during its trip. (G3) fixes the time when such a refueling transaction involving station j starts. (G4) means that, when a refueling transaction takes place which involves both station j and period i, then received load L_j is equal to (does not exceed) transferred load L^*_i.

B. Enhancing SVREP: Strong No_Sub_Tour Constraints

Above ILP formulation may be enhanced by additional constraints (*Cuts*). The first one tells us that the capacity of the micro-plant imposes at least $(\Sigma_{i=1,\ldots,N} R_i.z_i)/C^{Prod} - 1$ refueling transactions and so at least $(\Sigma_{i=1,\ldots,N} R_i.z_i)/C^{Prod}$ activations of the production. It may be formulated as follows: $\Sigma_{1 \leq i \leq N} y_i \geq (\Sigma_{i=1,\ldots,N} R_i.z_i)/C^{Prod}$. (E6)

Also, we get a lower bound for time value T_{M+1} by setting:

- $T_0 = 0$; $T_{M+1} \geq \Sigma_{j,k=-1,\ldots,M+1} \Delta_{j,k}.Z_{j,k}$. (F11)

Finally, we notice that, if the vehicle spends an amount W of energy while moving inside or at the boarder of some station subset A, which does contain the micro-plant – 1 but may possibly contain 0, M+1 or both, then it must move at least

$\lceil W/C^{Veh} \rceil$ times toward the micro-plant in order to refuel. In order to formalize resulting constraint, we denote by J the set $\{-1, 0, \ldots, M+1\}$ and set, for any such a subset A of J:

- $Cl(A) = \{$arcs $e = (j, k)$ s.t at least j or k is in $A\}$;
- $\delta(A) = \{$arcs $e = (j, k)$, s.t $j \notin A$ and $k \in A\}$;

Also, for any arc $e = (j, k)$, we set:

- $\Pi_{j,k} = E_0$ if $(j, k) = (M+1, 0)$ and $\Pi_{j,k} = C^{Veh}$ else.
- $\Pi^*_{j,k} = C^{Veh} - E_0$ if $(j, k) = (M+1, 0)$ and $\Pi_{j,k} = C^{Veh}$ else.

This leads us to the following *Strong No_Subour* constraint:

- For any subset A of $\{0, \ldots, M+1\}$,
  $\Sigma_{(j,k) \in \delta(A)} \Pi_{j,k} .Z_{j,k} \geq \Sigma_{(j,k) \in Cl(A)} E_{j,k}.Z_{j,k}$ (F12)
- For any subset A of $\{0, \ldots, M+1\}$,
- $\Sigma_{(j,k) \in \delta(J\text{-}A)} \Pi^*_{j,k} .Z_{j,k} \geq \Sigma_{(j,k) \in Cl(A)} E_{j,k}.Z_{j,k}$ (F12Bis)

Theorem 1: *If {0, 1} vector Z satisfies (F1, F2, 2Bis, F12, F12Bis) if and only if arcs (j, k) such that $Z_{j,k} = 1$ define a collection γ of sub-tours $\gamma_0, \gamma_1, \ldots, \gamma_s, .., \gamma_S$, such that:*

- *γ_0 starts from Depot = 0, ends into micro-plant = - 1, and spend less than E_0 energy; (I1)*
- *γ_1 starts from micro-plant = - 1, ends into Depot = 0, and spend less than $C^{Veh} - E_0$ energy; (I2)*
- *Routes $\gamma_2, \ldots, \gamma_S$ start from – , end into -1and do not require more than C^{Veh} energy units. (I3)*

Sketch of the Proof: (F1, F2, F2Bis) implies that F gives rise to a collection γ of sub-tours $\gamma_0, \ldots, \gamma_S$, which satisfy (I1, I2, I3) above but for the energy consumption conditions. Then one checks that if some tour γ_s spends more energy than related upper bound, then a subset A of $\{0, \ldots, M+1\}$ exists which makes Z violate either (F12) or (F12Bis). □

Notice that (F12) contains the standard *no_subtour* constraint for VRP as soon as $E_{j,k} = 0$ implies $j = k$.

C. Separating the Strong No_Sub_Tour Constraints.

Given a rational vector Z solution of the linear program obtained by relaxing the integrality constraints from **ILP-SVREP**, separating (F12) means checking (*separation* process), whether there exists $A \subseteq \{0, 1, \ldots, M+1\}$ which violates this constraint. Once provided with such an efficient separation procedure, we may perform a *Branch and Cut* process, while using the *callback* mechanisms as implemented in libraries, like CPLEX, GUROBI, … It happens to be the case here:

Theorem 2: *(F12, F12Bis) may be separated in polynomial time through application of a max flow (min cut) procedure on some auxiliary network.*

Sketch of the proof. Let us first deal with (F12). Some vector Z, being given, separating (F12) means searching for $A \subseteq \{0, 1, \ldots, M+1\}$ which violates (F12), and so for $B = \{-1, 0, 1, \ldots, M+1\} - A$, such that $\Sigma_{j,k \in B} Z_{j,k}.E_{j,k} + \Sigma_{(j,k) \in \delta(B)} \Pi_{j,k} .Z_{j,k} < \Lambda = \Sigma_{j,k} Z_{j,k}.E_{j,k}$. (*)

In order to do it, we construct a network G^{Aux}, whose node set is $\{-1, 0, 1, \ldots, M+1, M+2\}$ and whose arc set U^{Aux} may be written $U^{Aux} = U \cup Copy(U)$, with:

- $U = \{$all pairs (j, k), $j, k = -1, 0, \ldots, M+1\}$ such that $Z_{j,k} \neq 0$: such an arc $u = (j, k)$ is provided with a capacity $w_u = Z_{j,k}.(\Pi_{j,k} - E_{j,k})$;
- With any arc $e = (j, k)$ in U, we associate an arc $u = Copy(e) = (j, M+2)$: such an arc $u = Copy(e)$ $(j, M+2)$ is provided with a capacity $w_u = Z_{j,k}.E_{j,k}$. Then arc set $Copy(U)$ is the set of all arcs $Copy(e)$, $e \in U$.

In order to conclude, we only need to check that: Searching for B such that (*) holds is equivalent to searching for $B \subseteq \{-1, 0, 1, \ldots, M+1\}$, such that: $\Sigma_{u \in UAux,\ \text{s.t}\ (origin(u) \in B) \wedge (destination(u) \notin B)} w_u < \Lambda$. It is known that, in case B exists, it may be retrieved through application of the standard *Min Cut* algorithm. We proceed the same way with (F12Bis). □

III. A First Surrogate Estimator approach for SVREP

Since **SVREP** is a bi-level problem the idea here is to focus on the routing level: If vehicle route Γ is fixed, which may be represented by a vector X as in **SVERP** ILP formulation, then the quality $Q\_SVREP(\Gamma)$ of Γ derives from the resolution of **SVREP** with X fixed. Though such a resolution can be performed in pseudo-polynomial time (see [4]), it remains too time costly to be achieved all along an iterative process. So we replace $Q\_SVREP(\Gamma)$ by a surrogate estimator $Q\_Surr(\Gamma)$, easy to compute and likely to provide us with sensitivity information. Let us discuss this estimator.

A. A Parametric P_Refuel Auxiliary Problem

Intuitively, a good route Γ requires little time and few energy. So we define the following auxiliary parametric problem **P_Refuel**(Γ, β), whose optimal value $Refuel(\Gamma, \beta)$ is going to become our estimator $Q\_Surr(\Gamma)$:

P_Refuel(Γ, β): {β being a production price parameter, compute the refueling stations j in Γ, together with load values L_j in such a way that:

- Resulting values V_j meet constraints (F4,…, F7) of the **SVREP ILP** model;
- $\alpha.TIME + \beta.FUEL$ is the smallest possible, where $TIME$ ($FUEL$) is the time (energy) required by Γ augmented with the refueling transactions}.

Explanation: Parameter β means a price for energy, Because of this interpretation of β as a price of energy, we consider the mean unit price $\beta_0 = (\Sigma_i Cost_i./R_i)/N$ as reference value.

B. Solving P_Refuel(Γ, β).

Given Γ and β. Let us define the following *refuel* acyclic graph $G\_Refuel = (N, A)$: (see Fig. 3)

- The node set N of G_Refuel is the set of all pairs (j, V),

$j = 0, 1, \ldots, M, 0 \leq V \leq C^{Veh}$.

- A *standard* arc from node (j, V) to node (j', V'), $j < j$', means that the vehicle moves along Γ from j to j', while refueling immediately before arriving to j'. Then V' is equal to $C^{Veh} - E_{-1,j'}$. If we denote by $j°$ the predecessor of j' in Γ, then the cost of such an arc is equal to $\alpha.TIME(j, j') + \beta.FUEL(j, j')$, where:
  - $TIME(j, j')$ is the time required by moving from j to j' along Γ, augmented with the detour $\Delta_{-1,j'} + \Delta_{j°,-1} + p - \Delta_{j,j°}$.
  - $FUEL(j, j')$, is the energy required by moving from j to j' along Γ, augmented with the detour $E_{-1,j'} + E_{j°,-1} - E_{j,j°}$.

  An *end* arc from node (j, V) to node (M+1, $V' \geq E_0$), means that the vehicle moves from j to M+1 without performing any refueling transaction. We get the cost of such an arc as well as the relationship between V and V' in a straightforward way.

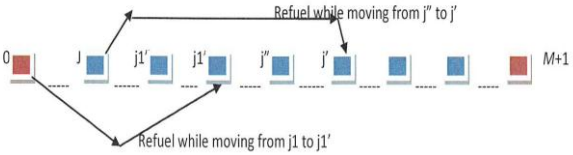

Figure 3: *The G_Refuel Acyclic Graph.*

Theorem 3: *For any β, solving **P_Refuel**(Γ, β) means computing a shortest path from (0, E_0) until (M+1, $V \geq E_0$) and can be solved in polynomial time. Besides, parametric resolution of **P_Refuel**(Γ, β) may be achieved in polynomial time, providing value Refuel(Γ, β) and related tour Γ for all values β.*

Sketch of the proof: The first part of above statement is pure routine. The second part is obtained by observing that the number of values V involved in the path search process does not exceed M.(M+1)/2. The last part is obtained by noticing that, for any node in the graph H, Bellman induction process makes appear a polynomial bounded number of frontier values β and related cost values. We get values L_j are obtained by making the vehicle arrive to the micro-plant with the smallest possible load. □

It comes that all values *Refuel*(Γ, β) may be obtained through a unique dynamic programming ***DP_Refuel***(β), together with related refueling stations.

C. Solving SVREP through the use of SURROGATE estimator Refuel(Γ, β)}.

Above sub-sections lead us to introduce the following parametric problem: **SVREP-SURROGATE**(β):{Compute Γ which minimizes *Refuel*(Γ, β)}.

This formulation suggests us to handle any **SVREP** instance according to the following parametric process:

First *Surrogate Estimator SVREP* Resolution Scheme:

1) Initialize (greedy VRP heuristic);
2) Perform a parametric resolution of ***P_Refuel***(Γ, β) and extract related set Ω of critical β values;
3) For every value β in Ω do
   Solve **SVREP_SURROGATE**(β) and get related tour Γ(β), together with vectors Z(β), X(β) and L(β);
   Solve **SVREP** while setting $Z = Z(\beta)$, $X = X(\beta)$ and $L = L(\beta)$ and using the exact algorithm of [4];
4) Keep the best **SVREP** solution obtained this way.

D. Two ways for solving SVREP_SURROGATE

Ler us first introduce the following ILP model:

ILP_SVREP_SURROGATE: {Compute {0, 1} valued vector $Z = (Z_{j,k}\ k \neq j$ in -1, 0,…, M+1: $Z_{j,k} = 1$ iff the vehicle moves from j to k) in such a way that:

- Constraints (F1, F2, F2Bis, F12, F12Bis) are satisfied;
- $\Sigma_{j,k} Z_{j,k}.(\alpha.T_{j,k} + \beta.E_{j,k})$ be the smallest possible}.

Theorem 4: *For any β, solving SVREP_SURROGATE(β) is equivalent to solving ILP_SVREP_SURROGATE.*

Sketch of the proof: F12 and F12Bis ensures us that Z computed this way defines a collection γ of sub-tours $\gamma_0, \gamma_1, \ldots, \gamma_s, .., \gamma_S$, such that (I1), (I2), (I3) of Theorem 1 are satisfied. This collection may be turned into a route Γ, optimal solution of **SVREP_SURROGATE**(β). □

So we may solve **SVREP_SURROGATE**(β) is to apply the branch and cut algorithm which derives from Theorem 1

Another approach (heuristic) consists in implementing a LNS (*Large Neighborhood Search*) algorithm to the route Γ:

***LNS_SVREP_SURROGATE(β)* Algorithmic Scheme**:

- Current Γ being given, apply ***DP_Refuel***(β) and decompose Γ into a collection γ of sub-tours $\gamma_0, \gamma_1, \ldots, \gamma_s, .., \gamma_S$, which meets (I1, I2, I3);
- Apply an *Insertion/Removal* operator, (see Fig. 4):
  - *Removal* step: It removes a set R of q stations (between 5% to 30% of stations in 1,…, M) from Γ. Several strategies are tried:*Random*; *Poor*: Focus on poorly inserted station; *Shaw*: Focus on stations close to each others.
  - *Insertion* step: Reinserts stations of R while making in such a way that (I1,…, I3) remain satisfied. Best insertion strategy is applied.
  - *Permutation* step: It randomly reorders sub-tours $\gamma_2, \ldots, \gamma_S$ in the decomposition γ.

- Retrieve resulting route Γ* from resulting collection γ*, applies ***DP_Refuel***(β)and get the value *Refuel*(Γ*, β).
- If *Refuel*(Γ*, β) is smaller than current value *Refuel*(Γ, β) then replace Γ by Γ*and keep on else try (no more that *Trial* times) again above *Insertion/Removal* operator or decide to stop,

Taken as a whole, the ***LNS_SVREP-Surrogate*** algorithm works as a GRASP process: It randomly builds (through some greedy VRP algorithm) initial routes $\Gamma_1,\ldots, \Gamma_{Init}$, and applies above descent process to every Γ_k, .

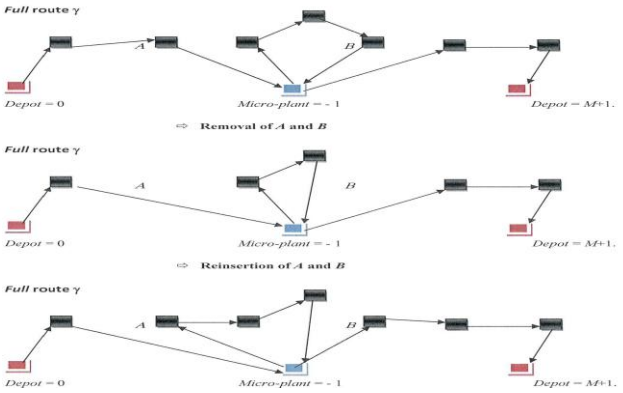

Figure 4: *Insertion/Removal Operator*.

IV. A MACHINE LEARNING ORIENTED APPROACH

We choose here to learn the optimal value *Fuel_Cost*(γ) of the problem **Fuel_Cost**(γ) induced by imposing Z and X and L in the **SVREP** model. In order to do it, we design a neural network *N_Fuel_Cost* which we implement with the *TensorFlow* software and which we train with a large number (6000) of **Fuel_Cost**(γ). Our surrogate problem becomes: **SVREP-ML_SURROGATE**{Compute γ which minimizes *N_Fuel_Cost*(γ)}. We derive:

ML_Surrogate_ *SVREP* Resolution Scheme:

1) Initialize *Init* collections γ;
2) For every γ obtained this way do
   a) Apply the previous LNS descent scheme in order to minimize *N_Fuel_Cost*(γ);
   b) Solve **Fuel_Cost**(γ) while using the dynamic programming algorithm described in [4];
3) Keep the best **SVREP** solution obtained this way.

Description of the *N_Fuel_Cost* neural network.

- The input layer of *N_Fuel_Cost* is 2-sided:
  - On one side, we consider the *production* data, which means production rates R_i and production costs $Cost_i$, $i = 1,\ldots, N$, together with capacity C^{Prod}, fixed activation cost *C_Act* and initial load H_0. In order to control the size of the network, we compress those data as soon as $Q.20 \leq N < (Q+1),20$, by merging consecutive periods $i = Q.q,\ldots., (Q+1),i - 1$ into one macro-period with *ad hoc* production cost and rate.
  - On another side, we consider the *vehicle* data related to γ, which are the number S of refueling transaction, the time (periods) windows for those transactions, and related loads $\mu_1,\ldots\mu_S$. So we fix an upper bound equal to 10, and implement a fusion mechanism for the case $S \geq 10$ in order to fix size of those data.
- The 2 first hidden layers involve synaptic arcs which connects periods and transactions to a small number of neighbor periods. Those arcs transport impulsions which take rational values in [0, 1] and so tend to emulate Boolean calculus. They are filtered by standard sigmoid functions and they aim at making appear, as outputs of the third layers:
  - the probability that production takes place at period (macro-period) i in case of the *left* side (see Fig. 5) of the network;
  - the probability that the last refueling transaction takes place at period i in case of the *right* (according to Fig. 5) side of the network.
  - They involve synaptic arcs which connects periods and transactions to a small number of neighbor periods.
- The last hidden layer derives (*left* side) the production cost from the above mentioned probability vector and (*right* side) the expected period for the latest refueling transaction, and involve RELU activation functions (smooth functions, null when the input is negative, and linear when the inputs are positive).
- Finally the output layer retrieves the final cost $\Sigma_{i = 1,\ldots,N} (C\_Act.y_i + Cost_i.z_i) + \alpha.T_{M+1}$ from both quantities computed by the last hidden layer.

The following figure 5 illustrates the construction of *N_Fuel_Cost*, which contains 986 synaptic arcs.

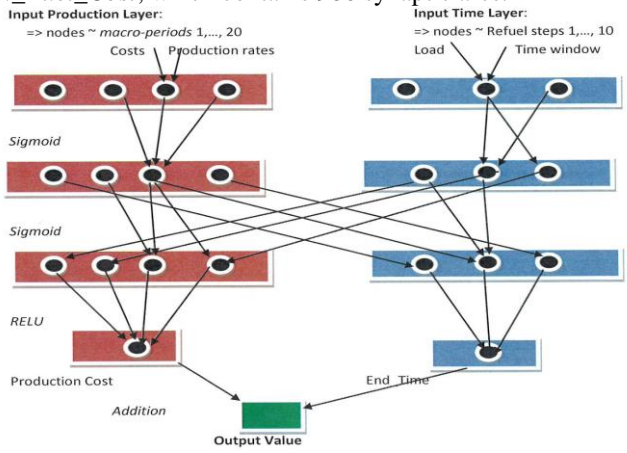

Figure 5: *The Neural Network N_Fuel_Cost*.

V. NUMERICAL EXPERIMENTS

Goal: Evaluate the behavior of surrogate estimators into the resolution of the **SVREP** problem.

Technical Context: We use a processor IntelCore i56700@3.20 GHz, with 16 Go RAM, together with a C++ compiler and libraries CPLEX12 (for ILP models) and TensorFlow/Keras (for machine lerning).

Instances: As for the vehicle part, we generate M (between 6 and 50) stations as points with integral coordinates in a 2-dimensional square, and derive Δ, E values according to a rounding of the Euclidean and Manhattan distances. We introduce a parameter $Q = V\_TSP/C^{Veh}$ between 3 and 10, where V_TSP is an estimation of the energy required by the production, we split the period set into $K = 2, \ldots, 5$ intervals, corresponding to different qualities of the weather and randomly generate rates R_i for every such interval.

Activation cost C_Act is generated in such a way that expected activation cost be equal to R time the expected production cost, with R between 0.2 and 2. The capacity of the micro-plant is generated as equal to $H.C^{Veh}$, with H between 1 and 3. Finally, mean production rates are updated in such a way that the maximal production capacity of the micro-plant does not exceed $S.V\_TSP$, where S is a control parameter between 2 and 4. We use here 10 instances:

TABLE I. CHARACTERISTICS OF THE INSTANCES

Instance	*N*	*M*	*Q*	*K*	*R*	*S*	*H*	*α*
1	45	6	3	3	1	3	2	8
2	45	6	3	3	0.3	2	1	8.5
3	30	8	3	5	0.5	2	3	11
4	40	8	3	2	0.3	2	3	5
5	140	10	3	4	0.25	4	1	6.5
6	140	10	5	4	0.25	4	1	6.5
7	120	15	6	3	2	2.5	2	8
8	120	15	6	5	2	2.5	2	15.5
9	200	20	9	5	0.7	3.5	1	14
10	200	20	9	5	0.25	2	2	18

Outputs: For every instance:

- We apply (Table II) the general **SVREP** ILP model, and get (in less than 1 CPU h), a lower bound LB_G, an upper bound UB_G, CPU time T_G, the value $Relax$ of the rational relaxation at the root, and the number C_G of *strong no_sub_tour* cuts which were generated.
- We solve (Table 3) **ILP_SVREP_SURROGATE**(β) with $\beta = (\Sigma_i\ Cost_i./R_i)/N$, while using the branch and cut algorithm of III.*D*. We keep memory of resulting lower and upper bounds LB_S1 and UB_S1, as well as CPU time T_S1 and the number C_S1 of generated cuts (F12, F12Bis). We also try to **ILP_SVREP_SURROGATE** without using *strong no_sub-tour* constraints and get lower and upper bounds LB_W and UB_W.
- We apply (Table 4) ***LNS_SVREP_SURROGATE***(β_0) with $Trial = 2.M$; $Init = 10$; $\tau = 15\%$ to **SVREP_SURROGATE,** and keep resulting value V_Heur, CPU time T_Heur, as well as the number Try of trials per iterations the mean number $Iter$ of iterations of performed during the descent process. We do the same thing (Table 5) with the procedure **SVREP_ML_SURROGATE**, which involves machine learning. We keep resulting value V_ML, CPU time T_ML, as well as values Try and $Iter$.
- We apply (Table 6) the global First SVREP resolution scheme of Section III.*C* with $\beta = \beta_0$ and denote by W_ILP the value of **ILP_SVREP_SURROGATE** and by W_Heur the value obtained with ***LNS_SVREP_SURROGATE***. We do the same with the resolution scheme involving machine learning and denote by W_ML resulting value, and with 5 values β ranging from $\beta_0/4$ until 4. β_0. W_ILP5 and W_Heur5 denote the values obtained by applying the global scheme of Section III.*C*, with respectively ***ILP_VREP_SURROGATE*** and ***LNS_SVREP_SURROGATE***.

Those results may be summarized into the following tables:

TABLE 2: BEHAVIOR OF THE GLOBAL ILP MODEL

Inst.	*LB_G*	*UB_G*	*T_G*	*Relax*	*C_G*
1	735.3	735.3	628.4	344.5	6
2	951.3	951.3	265.3	312.0	25
3	709.2	709.2	159.7	413.5	72
4	322.1	508.2	3600	208.7	146
5	969.0	969.0	1819.3	611.7	188
6	1153.4	1486.3	3600	764.5	286
7	1972.7	3065.5	3600	1652.3	330
8	3386.9	4211.8	3600	3008.2	518
9	4923.0	9594.3	3600	4021.2	646
10	5956.6	8560.3	3600	5365.4	601

Comments: As expected, the global ILP model of Section II is in trouble, even on small instances. Still Table 6 will make appear the upper bound UB_G is close to optimality.

TABLE 3: BEHAVIOR OF ILP_ SVREP_SURROGATE

Inst.	*LB_S1*	*UB_S1*	*T_S1*	*C_S1*	*LB_W*	*UB_W*
1	684.4	684.4	0.02	2	684.4	684.4
2	835.3	835.3	0.04	6	835.3	835.3
3	705.9	705.9	0.07	7	705.9	705.9
4	474.6	474.6	0.85	50	474.6	474.6
5	916.2	916.2	4.7	46	762.1	916.2
6	1386.3	1386.3	6.97	143	1038.0	1387.0
7	2891.7	2891.7	243.7	296	2220.6	2902.8
8	4020.3	4020.3	522.05	412	2808.2	4022.6
9	9023.6	9077.2	3600	468	3702.5	9077.2
10	7773.0	7773.9	1602.5	286	2891.9	7812.3

Comments: *Strong no_sub_tour* constraints significantly increase our ability to manage **ILP_SVREP_SURROGATE**. Also, we notice that the optimal value of **ILP_SVREP_SURROGATE** provides us, when $\beta = \beta_0$ = mean unitary production cost, with a kind of approximation (10% in average) of the optimal **SVREP** value.

TABLE 4:
BEHAVIOR OF THE HEURISTICFOR SVREP_SURROGATE

Inst.	*V_Heur*	*T-Heur*	*Iter*	*Try*
1	684.4	0.01	4.4	8.1
2	835.3	0.01	2.9	6.3
3	705.9	0.01	5.3	4.9
4	474.6	0.02	7.5	6.6
5	916.2	0.02	4.4	10.3
6	1386.3	0.04	5.2	10.6
7	2891.7	0.05	10.3	6.5
8	4047.2	0.07	6.6	9.8
9	9077.2	0.17	11.3	14.5
10	7802.0	0.15	16.5	22.4

Comments: Our Removal/Insertion heuristic provides very good approximations under low computational costs.

TABLE 5.
BEHAVIOR OF THE HEURISTIC FOR SVREP_ML__SURROGATE

Inst.	*V_ML*	*T-ML*	*Iter*	*Try*
1	786.2	0.01	7.2	4.1
2	994.4	0.01	3.7	7.4
3	700.5	0.01	7.1	8.0
4	543.6	0.01	6.4	5.4
5	936.3	0.02	10.6	7.5
6	1627.8	0.02	10.8	9.2
7	3280.9	0.02	8.1	13.1
8	4458.3	0.02	12.7	10.8
9	1046.0	0.03	18.5	11.9
10	9322.7	0.03	10.0	13.5

Comments: The gap between the optimal SVREP value and its approximation through the neural network *N_Fuel_Cost* is rather important, in average around 7%, with a peak at 10%.

TABLE 6: SVREP VALUE OBTAINED WITH $\beta = \beta_0$, AND 5 VALUES β.

Inst.	*W_ILP*	*W_Heur*	*W_ML*	*W_ILP5*	*W_Heur5*
1	735.3	735.3	735.3	735.3	735.3
2	956.3	956.3	951.3	956.3	956.3
3	709.2	709.2	709.2	709.2	709.2
4	535.2	535.2	568.2	508.2	508.2
5	969.2	969.2	990.0	969.0	969.0
6	1493.4	1492.3	1566.3	1486.3	1486.3
7	3003.5	3025.7	3065.5	3003.5	3025.7
8	4274.4	4211.8	4388.0	4211.8	4211.8
9	9342.5	9397.5	9794.7	9248.4	9365.0
10	8473.1	8465.1	8560.3	8420.8	8465.1

Comments: Computing tour Γ while estimating its quality as the optimal value of **SVREP_SURROGATE**(β) is efficient, with a low sensitivity to parameter β. The second approach involving machine learning, though more generic and better fitted to the management of uncertainty, unfortunately happens here to be less efficient.

VI. CONCLUSION

We dealt here with a complex energy management problem, while shortcutting the production sub-problem. We tried 2 approaches: the first consisted in estimating the quality of a routing strategy as the parametric increase of energy and time consumption by the vehicle; the second one consisted in learning, through a neural network, the value of the production sub-problem. Numerical experiments made appear, at least in our case, a better efficiency of the first approach. Still, because the machine learning oriented approach is far more generic, it would be worthwhile to go deeper with it, and make the value learned by a neural network more sensitive to the application of local search operators. It could also help us in managing this uncertainty through a joint estimation of both the expected value of a production cost and of the risk of failing in meeting production requirements according to this cost.

ACKNOWLEDGMENT

Present work was funded by French ANR Labex IMOBS3, and by PGMO Program..

REFERENCES

[1] Y. Adulyasak, J.F. Cordeau, R.Jans :The production routing problem: A review. *Computers & Operations Research*, 55, p 141-152, (2015). doi:10.1016/J.COR.2014.01.011

[2] A.Albrecht, P. Pudney: Pickup and delivery with a solar-recharged vehicle. *Ph.D. thesis Australian Society for O.R* (2013).

[3] C.Artigues, E.Hébrard, A.Quilliot, H.Toussaint: "Models and algorithms for natural disaster evacuation problems". *Proceedings of the 2019 FEDCSIS WCO Conference*, p 143-146, (2019). DOI: http://dx.doi.org/10.15439/978-83-952357-8-8

[4] F.Bendali, J.Mailfert, E.Mole-Kamga, A.Quilliot, H.Toussaint : Pipe-lining dynamic programming procsses in order to synchronize energy production and consumption, *2020 FEDCSIS WCO Conf.*, p 303-306, (2020). DOI: http://dx.doi.org/10.15439/978-83-955416-7-4.

[5] A.Caprara, M.Carvalho, A.Lodi, G.J.Woeinger: A study on the computational complexity of the bilevel knapsack problem; *SIAM Journal on Optimization* 24 (2), p 823-838, (2014).

[6] L.Chen, G.Zhang: Approximation algorithms for a bi-level Knapsack problem; *Theoretical Computer Sciences* 497, p 1-12, (2013).

[7] T. Erdelic, T. Caric: (2019). A survey on the electric vehicle routing problem: Variants and solution approaches. *Journal of Advanced Transportation*, (2019). doi:10.1155/2019/5075671.

[8] S.Fidanova, O.Roeva, M.Ganzha: " Ant colony optimization algorithm for fuzzy transport modelling ". *Proceedings of the 2020 FEDCSIS WCO Conference*, p 237-240, (2020). DOI: http://dx.doi.org/10.15439/978-83-955416-7-4

[9] C.Grimes, O.Varghese, S.Ranjan. Light, water, hydrogen:Solar generation by photoelectrolysis. *Springer-Verlag US*, (2008).

[10] S.Irani, K.Pruhs: Algorithmic problems in power management. *SIGACT News*, 36, 2, p 63-76, (2003).

[11] C.Koc, O.Jabali, J.Mendoza, G.Laporte: The electric vehicle routing problem with shared charging stations. *ITOR*, 26 , p 1211-1243, (2019). doi:https://doi.org/10.1111/itor.12620.

[12] M.Krzyszton: "Adapative supervison: method of reinforcement learning fault elimination by application of supervised learning". *Proceedings of the 2018 FEDCSIS AI Conference*, p 139-149, (2018). DOI: http://dx.doi.org/10.15439/978-83-949419-5-6

[13] G. Macrina, L.D. Pugliese, F. Guerriero: (2020). The green-vehicle routing problem: A survey. In *Modeling and Optimization in Green Logistics, Cham: Springer International Publishing*. p. 1-26, (2020). doi:10.1007/978-3-030-45308-4_1

[14] K.Stoilova, T.Stoilov: "Bi-level optimization application for urban traffic management". *2020 FEDCSIS WCO Conference*, p 327-336, (2020). DOI: http://dx.doi.org/10.15439/978-83-949419-5-6

[15] J. Wojtuziak, T. Warden, O. Herzog: "Machine learning in agent based stochastic simulation: Evaluation in transportation logistics"; *Computer and Mathematics with Applications 64, p 3658-3665, (2012).* https://doi.org/10.1016/j.camwa.2012.01.079.

Communication Papers of the of the 17th Conference on Computer Science and Intelligence Systems pp. 93–96
DOI: 10.15439/2022F170
ISSN 2300-5963 ACSIS, Vol. 32

An Optimization Technique for Estimating Sobol Sensitivity Indices

Venelin Todorov
Institute of Mathematics and Informatics
Bulgarian Academy of Sciences
8 Acad. G. Bonchev Str., 1113 Sofia, Bulgaria
Institute of Information and Communication Technologies
Bulgarian Academy of Sciences
25A Acad. G. Bonchev Str., 1113 Sofia, Bulgaria
Email: vtodorov@math.bas.bg, venelin@parallel.bas.bg

Slavi Georgiev
Institute of Mathematics and Informatics
Bulgarian Academy of Sciences
8 Acad. G. Bonchev Str., 1113 Sofia, Bulgaria
Department of Applied Mathematics and Statistics
Angel Kanchev University of Ruse
8 Studentska Str., 7004 Ruse, Bulgaria
Email: sggeorgiev@math.bas.bg, sggeorgiev@uni-ruse.bg

***Abstract*—In this paper we proposed an optimization technique for improving the Monte Carlo approaches based on Halton and Sobol algorithms. The proposed technique is novel in the sense that the optimization of the Halton and Sobol sequences is applied for the first time and essentially improves the results by the original sequences. The results will be of great importance for the environment protection and the trustability of forecasts.**

I. Introduction

WHEN it comes to decision making, the reliability of the large-scale mathematical models is questioned [9], [10], [8], [18]. To improve the reliability, the sensitivity of model outputs to variations of model inputs due to natural variability is studied and analyzed. By definition [4], [15], [17] *sensitivity analysis* is a procedure to measure how sensitive are the mathematical model outputs are to some variations of the input data. The input data in this paper for sensitivity analysis is derived through runs of the large-scale mathematical model for large-distance transportation of air pollution – **Uni**fied **D**anish **E**ulerian **M**odel (UNI-DEM). The model is created at the Danish National Environmental Research Institute (http://www2.dmu.dk/AtmosphericEnvironment/DEM/, [19], [20], [21]).

This model considers large geographical region (4800 × 4800 km), including Europe and the Mediterranean in full and Asia and Africa in part. It also describes the primary chemical, photochemical and physical processes between the considered species and the emissions in the environment of rapidly changing meteorological conditions. It is that model which is chosen for a case study in the paper since the chemical processes are regarded with great precision amongst the other atmospheric chemistry models [3].

Slavi Georgiev is supported by the Bulgarian National Science Fund (BNSF) under Project KP-06-M32/2 - 17.12.2019 "Advanced Stochastic and Deterministic Approaches for Large-Scale Problems of Computational Mathematics" and Scientific Research Fund of University of Ruse under FNSE-03. Venelin Todorov is supported by BNSF under Project KP-06-N52/5 "Efficient methods for modeling, optimization and decision making" and BNSF under Project KP-06-N52/2 "Perspective Methods for Quality Prediction in the Next Generation Smart Informational Service Networks". The work is also supported by BNSF under Bilateral Project KP-06-Russia/17 "New Highly Efficient Stochastic Simulation Methods and Applications".

II. Global Sensitivity Analysis – Sobol Approach

The mathematical model is assumed to be represented by a model function

$$\mathrm{u} = f(\mathrm{x}), \tag{1}$$

where $\mathrm{x} = (x_1, x_2, \ldots, x_d) \in U^d \equiv [0;1]^d$ is the vector of input parameters with a joint **p**robability **d**ensity **f**unction (p.d.f.) $p(\mathrm{x}) = p(x_1, \ldots, x_d)$.

The Sobol approach idea is based on a decomposition of the integrable model function f into terms of increasing dimensionality [15], [17]:

$$f(\mathrm{x}) = f_0 + \sum_{\nu=1}^{d} \sum_{l_1<\ldots<l_\nu} f_{l_1\ldots l_\nu}(x_{l_1}, x_{l_2}, \ldots, x_{l_\nu}), \tag{2}$$

where f_0 is some constant.

The representation (2) is called the ANOVA-representation of the model function $f(\mathrm{x})$ in case each term is chosen to satisfy the following condition [16]:

$$\int_0^1 f_{l_1\ldots l_\nu}(x_{l_1}, x_{l_2}, \ldots, x_{l_\nu})\mathrm{d}x_{l_k} = 0, 1 \le k \le \nu, \nu = 1, \ldots, d.$$

This condition guarantees that the functions in the right hand-side of (2) are uniquely defined, and $f_0 = \int_{U^d} f(\mathrm{x})\mathrm{dx}$. The quantities

$$\mathbf{D} = \int_{U^d} f^2(\mathrm{x})\mathrm{dx} - f_0^2, \quad \mathbf{D}_{l_1\ \ldots\ l_\nu} = \int f^2_{l_1\ \ldots\ l_\nu} \mathrm{d}x_{l_1} \ldots \mathrm{d}x_{l_\nu} \tag{3}$$

are referred to as total and partial variances, respectively. An analogous decomposition holds for the total variance which is represented by the corresponding partial variances: $\mathbf{D} = \sum_{\nu=1}^{d} \sum_{l_1<\ldots<l_\nu} \mathbf{D}_{l_1\ldots l_\nu}$. The primary sensitivity measures following the Sobol approach are defined as Sobol global sensitivity indices [16], [14]:

$$S_{l_1\ \ldots\ l_\nu} = \frac{\mathbf{D}_{l_1\ \ldots\ l_\nu}}{\mathbf{D}}, \quad \nu \in \{1, \ldots, d\}, \tag{4}$$

and the **t**otal **s**ensitivity **i**ndex (TSI) of an input parameter $x_i, i \in \{1, \ldots, d\}$ defined by [16], [14]:

$$S_i^{tot} = S_i + \sum_{l_1 \neq i} S_{il_1} + \sum_{l_1, l_2 \neq i, l_1 < l_2} S_{il_1 l_2} + \ldots + S_{il_1 \ldots l_{d-1}}, \quad (5)$$

where S_i is named *the main effect (first-order sensitivity index)* of x_i and $S_{il_1 \ldots l_{j-1}}$ is the j^{th} order sensitivity index. The higher-order terms characterize the interaction effects between the unknown input parameters $x_{i_1}, \ldots, x_{i_\nu}, \nu \in \{2, \ldots, d\}$ on the output variance. It is obvious that the rigourous mathematical treatment of the problem of supplying global sensitivity analysis includes evaluating total sensitivity indices (5) of corresponding order that, based on the formulae (3)-(4), results in computing multidimensional integrals.

III. Sobol and Halton Sequences and Their Optimizations

Quasirandom or low discrepancy sequences, which vivid representatives are the Halton and Sobol sequences, are "less random" than a pseudorandom number sequence, but they are much more useful for numerical calculation of integrals in higher dimensions, since the low discrepancy sequences tend to sample space "more uniformly" than random numbers [2].

Let $\mathrm{x}_i = (x_i^{(1)}, x_i^{(2)}, \ldots, x_i^{(s)})$ for $i = 1, 2, \ldots$ and $n = \ldots a_3(n), a_2(n), a_1(n)$ be the representation of n in base b. The respective multidimensional quasirandom sequence is defined as follows: $X_n = (\phi_{b_1}(n), \phi_{b_2}(n), \ldots, \phi_{b_s}(n))$, where the bases b_i are relatively prime numbers.

Halton sequence [5], [6] is defined as:

$$s_n^{(k)} = \sum_{i=0}^{\infty} \sigma_{i+1}^{(k)} a_{i+1}^{(k)}(n) b_k^{-(i+1)},$$

where $(b_1, b_2, \ldots, b_s) \equiv (2, 3, 5, \ldots, p_s)$, and p_i designates the i-th prime, and $\sigma_i^{(k)}$, $i \geq 1$ denotes the set of permutations on $(0, 1, 2, \ldots, p_k - 1)$.

Sobol sequence [1], [7] is defined by:

$$\mathrm{x}_k \in \overline{\sigma}_i{}^{(k)}, k = 0, 1, 2, \ldots$$

where $\overline{\sigma}_i{}^{(k)}$, $i \geq 1$ are the set of permutations on every $2^k, k = 0, 1, 2, \ldots$ subsequent points of the Van der Corput sequence, defined by $n = \sum_{i=0}^{\infty} a_{i+1}(n) b^i$, $\phi_b(n) = \sum_{i=0}^{\infty} a_{i+1}(n) b^{-(i+1)}$ when $b = 2$.

In binary for the Sobol sequence we have that: $x_n^{(k)} = \bigoplus_{i \geq 0} a_{i+1}(n) v_i$, where v_i, $i = 1, \ldots, s$ is the set of direction numbers [7].

IV. Optimization by Scrambling

The fundamental motivation of optimization targets at obtaining more uniform quasirandom sequences, especially in high dimensions. The proved convergence rate for the Scrambling Algorithms improves drastically the rate for the unscrambled nets [13], which is $n^{-1}(\log\ n)^{d-1}$. The idea of scrambling is founded on randomization of a single digit at each iteration. Let

$$x^{(i)} = (x_{i,1}, x_{i,2}, \ldots, x_{i,s}),\ i = 1, \ldots, n \quad (6)$$

be quasirandom numbers in $[0, 1)^s$, and let

$$z^{(i)} = (z_{i,1}, z_{i,2}, \ldots, z_{i,s}) \quad (7)$$

be the respecive scrambled version of the point $x^{(i)}$. Suppose now that every $x_{i,j}$ could be represented in base b as

$$x_{i,j} = (0.x_{i1,j}\ x_{i2,j} \ldots x_{iK,j} \ldots)_b \quad (8)$$

with K being the number of digits for scrambling. To scramble the Halton sequence, we use a permutation of the radical inverse coefficients obtained by applying a reverse-radix operation to each of the possible coefficient values [11]. To scramble the Sobol sequence, we use random linear scramble blended with a random digital shift [12].

V. Sensitivity Studies with Respect to Emission Levels

In this section we give the outcomes for the sensitivity of UNI-DEM output (particularly the monthly ammonia mean concentrations) with respect to the data variation of anthropogenic emissions as input. The input itself comprises 4 different constituents
$\mathbf{E} = (\mathbf{E^A}, \mathbf{E^N}, \mathbf{E^S}, \mathbf{E^C})$:

- $\mathbf{E^A}$ – ammonia (NH_3);
- $\mathbf{E^S}$ – sulphur dioxide (SO_2);
- $\mathbf{E^N}$ – nitrogen oxides $(NO\ +\ NO_2)$;
- $\mathbf{E^C}$ – anthropogenic hydrocarbons.

The domain into consideration is the 4-dimensional hypercube $[0.5, 1]^4$.

Results regarding the relative error estimation for the quantities f_0, the total variance $\mathbf{D}$, the first-order (S_i) and the total (S_i^{tot}) sensitivity indices are presented in Tables I, II, III, respectively. f_0 is represented by a 4-dimensional integral, while the rest of the above quantities are represented by 8-dimensional integrals, following the ideas of the *correlated sampling* technique to compute sensitivity measures in a robust way (see [8], [17]). Four different stochastic approaches employed for numerical integration are given in separate columns in the tables.

For $n = 2^{24}$ for the model function f_0 the best algorithm is the Halton scrambled sequence, followed by the Halton sequence – see the results in Tables I for the maximum number of samples. For number of samples $n = 2^{24}$ for the total variance D the best algorithm is the Sobol sequence, followed by the Halton scrambled sequence – see the results in Tables II for the maximum number of samples. The performance of te algorithms can be seen on Fig. 1.

It can be seen in Table III that the optimized SOBOPT and HALOPT improve the results in most of the cases, and most importantly for the small in value sensitivity indices S_2, S_4, S_2^{tot}, S_4^{tot}. These are the most important cases because they determine the reliability of the model results.

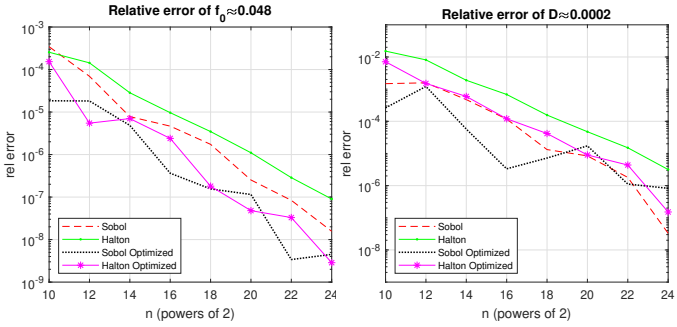

Fig. 1. Relative errors for the calculation of $f_0 \approx 0.048$ (left) and $\mathbf{D} \approx 0.0002$ (right)

TABLE I
RELATIVE ERROR FOR THE EVALUATION OF $f_0 \approx 0.048$.

# n	SOBOL Relative error	HALTON Relative error	SOBOPT Relative error	HALOPT Relative error
2^{16}	4.6585e-06	9.6538e-06	**3.6422e-07**	2.3992e-06
2^{20}	2.5234e-07	1.1020e-06	1.1501e-07	**4.7965e-08**
2^{24}	1.5669e-08	9.0096e-08	4.4868e-09	**2.8637e-09**

VI. SENSITIVITY STUDIES WITH RESPECT TO CHEMICAL REACTIONS RATES

In this section we explore the sensitivity of the ozone concentration values in the air over Genova with respect to the rate variation of some chemical reactions of the condensed CBM-IV scheme ([19]), in particular: # $1, 3, 7, 22$ (time-dependent) and # $27, 28$ (time independent). The reduced equations of the chemical reactions follow:

$$
\begin{aligned}
&[\#\mathbf{1}] \quad NO_2 + h\nu \Longrightarrow NO + O;\\
&[\#\mathbf{3}] \quad O_3 + NO \Longrightarrow NO_2;\\
&[\#\mathbf{7}] \quad NO_2 + O_3 \Longrightarrow NO_3;\\
&[\#\mathbf{22}] \quad HO_2 + NO \Longrightarrow OH + NO_2;\\
&[\#\mathbf{27}] \quad HO_2 + HO_2 \Longrightarrow H_2O_2;\\
&[\#\mathbf{28}] \quad OH + CO \Longrightarrow HO_2.
\end{aligned}
$$

The domain into consideration is the 6-dimensional hypercube $[0.6, 1.4]^6$).

The authors of [8] argue which formulation of

$$f_0^2 = \left(\int_{U^d} f(\mathrm{x}) \mathrm{dx} \right)^2 \tag{9}$$

is better when expressing the total variance and the Sobol global sensitivity measures. The first formula is

$$f_0^2 \approx \frac{1}{n} \sum_{i=1}^{n} f(\mathrm{x}_{i,1}, \ldots, \mathrm{x}_{i,d}) \; f(\mathrm{x}'_{i,1}, \ldots, \mathrm{x}'_{i,d}) \tag{10}$$

and the second one is

$$f_0^2 \approx \left\{ \frac{1}{n} \sum_{i=1}^{n} f(\mathrm{x}_{i,1}, \ldots, \mathrm{x}_{i,d}) \right\}^2 \tag{11}$$

where x and x' are two independent sample vectors. If one estimates sensitivity indices of a fixed order, the expression (10) is better (as it is recommended in [8]), and this is why we apply it here as well.

The relative error estimation for the quantities f_0, the total variance $\mathbf{D}$ and a part of the sensitivity indices are provided in Tables IV, V and VI, respectively.

The quantity f_0 is represented by 6-dimensional integral, while the rest are represented by 12-dimensional integrals, following the concept of *correlated sampling*.

TABLE II
RELATIVE ERROR FOR THE EVALUATION OF THE TOTAL VARIANCE $\mathbf{D} \approx 0.0002$.

# n	SOBOL Relative error	HALTON Relative error	SOBOPT Relative error	HALOPT Relative error
2^{16}	1.1726e-04	6.8346e-04	**3.3306e-06**	1.2015e-04
2^{20}	**8.4017e-06**	4.7374e-05	1.7242e-05	8.9747e-06
2^{24}	**3.2922e-08**	3.1611e-06	8.2382e-07	1.5148e-07

TABLE III
RELATIVE ERROR FOR ESTIMATION OF SENSITIVITY INDICES OF INPUT PARAMETERS USING DIFFERENT QUASI-MONTE CARLO APPROACHES ($n \approx 2^{16}$).

EQ	RV	SOBOL	HALTON	SOBOPT	HALOPT
S_1	9e-01	**5.4870e-06**	2.9981e-04	2.3006e-05	7.7156e-05
S_2	2e-04	4.2469e-03	3.2104e-02	**2.2210e-03**	1.1998e-02
S_3	1e-01	**1.3725e-04**	2.3291e-03	3.2724e-04	4.7869e-04
S_4	4e-05	4.5620e-02	1.1969e-01	**1.7836e-02**	7.2187e-02
S_1^{tot}	9e-01	**1.8865e-05**	2.9900e-04	4.2060e-05	6.1643e-05
S_2^{tot}	2e-04	5.1886e-03	3.1544e-02	1.3834e-03	**1.2575e-04**
S_3^{tot}	1e-01	**1.5898e-05**	2.2959e-03	1.8409e-04	6.2183e-04
S_4^{tot}	5e-05	5.5960e-02	1.1911e-01	**3.9446e-02**	4.3995e-02

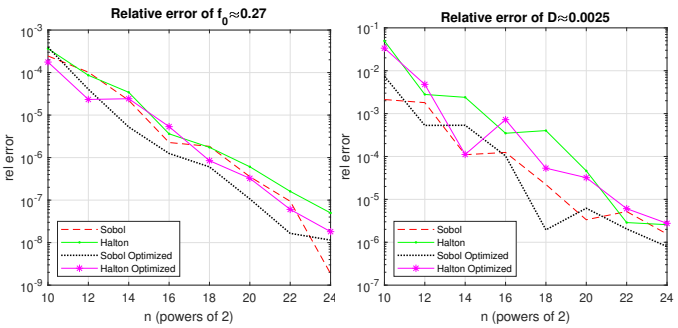

Fig. 2. Relative errors for the calculation of $f_0 \approx 0.27$ (left) and $\mathbf{D} \approx 0.0025$ (right)

For $n = 2^{24}$ for the model function f_0 the best algorithm is the Sobol scrambled sequence, followed by the Sobol sequence – see the results in Tables IV for the maximum number of samples. For number of samples $n = 2^{24}$ for the total variance D the best algorithm is again the Sobol scrambled sequence, followed again by the Sobol sequence – see the results in Tables V for the maximum number of samples. The behaviour of the algorithms can be seen on Fig. 2.

TABLE IV
RELATIVE ERROR FOR THE EVALUATION OF $f_0 \approx 0.27$.

	SOBOL	**HALTON**	**SOBOPT**	**HALOPT**
n	Relative error	Relative error	Relative error	Relative error
2^{16}	2.2604e-06	3.6220e-06	**1.2498e-06**	5.3505e-06
2^{20}	3.5561e-07	6.0821e-07	**1.0645e-07**	3.2548e-07
2^{24}	**1.8639e-09**	4.9903e-08	1.1468e-09	1.8102e-08

TABLE V
RELATIVE ERROR FOR THE EVALUATION OF THE TOTAL VARIANCE $\mathbf{D} \approx 0.0025$.

	SOBOL	**HALTON**	**SOBOPT**	**HALOPT**
n	Relative error	Relative error	Relative error	Relative error
2^{16}	1.2418e-04	3.4838e-04	**1.0328e-04**	7.2396e-04
2^{20}	**3.3461e-06**	4.6222e-05	6.2125e-06	3.2061e-05
2^{24}	1.5526e-06	2.5678e-06	**7.9422e-07**	2.7586e-06

It can be seen in Table VI that the optimized SOBOPT and HALOPT improve the results in most of the cases, and for very important small in value sensitivity indices S_5. The basic algorithm is better for the two way interaction sensitivity indices, but for the most important first order sensitivity indices our optimization methods produce the best results.

TABLE VI
RELATIVE ERROR FOR ESTIMATION OF SENSITIVITY INDICES OF INPUT PARAMETERS USING DIFFERENT QUASI-MONTE CARLO APPROACHES ($n \approx 2^{16}$).

EQ	RV	**SOBOL**	**HALTON**	**SOBOPT**	**HALOPT**
S_1	4e-01	3.2231e-04	2.8340e-03	**9.5066e-05**	4.0386e-04
S_2	3e-01	3.8337e-04	3.7322e-03	**2.2260e-04**	4.6835e-04
S_3	5e-02	**6.5037e-04**	7.5211e-03	9.6837e-04	8.1435e-04
S_4	3e-01	4.3936e-04	2.2956e-03	3.3630e-04	**2.3527e-04**
S_5	4e-07	9.8860e+00	4.5383e+01	**9.4627e+00**	6.9084e+01
S_6	2e-02	1.7170e-03	1.3009e-02	2.3921e-04	**1.4770e-04**
S_1^{tot}	4e-01	2.6837e-04	2.7466e-03	**1.3978e-04**	2.8687e-04
S_2^{tot}	3e-01	5.6342e-04	3.2551e-03	**6.7337e-05**	5.6446e-04
S_3^{tot}	5e-02	8.6595e-04	6.6357e-03	9.9762e-04	**4.3254e-04**
S_4^{tot}	3e-01	2.1786e-04	2.1826e-03	5.9956e-04	**9.0355e-05**
S_5^{tot}	2e-04	1.3627e-01	**2.5437e-02**	6.6954e-02	3.3439e-02
S_6^{tot}	2e-02	2.5998e-03	1.0451e-02	**5.3173e-04**	3.0023e-03
S_{12}	6e-03	**1.4614e-03**	7.5509e-03	6.6880e-03	6.2554e-03
S_{14}	5e-03	**1.3828e-03**	9.7965e-03	3.3325e-03	8.0309e-03
S_{24}	3e-03	**3.3757e-03**	1.6310e-02	1.8226e-02	7.6253e-03
S_{45}	1e-05	**4.3069e-01**	8.2357e-01	6.2288e-01	5.1080e-01

VII. CONCLUSION

We have investigated the computational efficiency of several stochastic algorithms for multidimensional numerical integration in terms of relative error and computational effort. The case study is the sensitivity analysis of the UNI-DEM model output to variation of the input emissions of the anthropogenic pollutants and of the rates of a couple of chemical reactions. It is considered the influence of emission levels over very important air pollutants, in particular ammonia, ozone, ammonium sulphate and ammonium nitrate.

The numerical experiments show that the obtained optimization methods are one of the best available stochastic approaches for computing sensitivity indices and especially the most difficult task – the smallest in value sensitivity indices which are very important for the model results reliability. The results will be of great importance for the environment protection and the trustability of forecasts.

REFERENCES

[1] I. Antonov, V. Saleev, An economic method of computing LP_τ-sequences, USSR Comput. Math. Phys. 19, (1979), 252–256.

[2] I. Dimov, Monte Carlo Methods for Applied Scientists, New Jersey, London, Singapore, World Scientific, (2008).

[3] I.T. Dimov, R. Georgieva, Tz. Ostromsky, Z. Zlatev, Advanced algorithms for multidimensional sensitivity studies of large-scale air pollution models based on Sobol sequences, Computers and Mathematics with Applications 65(3), "Efficient Numerical Methods for Scientific Applications", Elsevier, (2013), 338–351.

[4] F. Ferretti, A. Saltelli, S. Tarantola, Trends in sensitivity analysis practice in the last decade, Journal of Science of the Total Environment 568, (2016), 666–670.

[5] J. Halton, On the efficiency of certain quasi-random sequences of points in evaluating multi-dimensional integrals, Numerische Mathematik 2, (1960), 84–90.

[6] J. Halton, G.B. Smith, Algorithm 247: radical-inverse quasi-random point sequence, Communications of the ACM 7, (1964), 701–702.

[7] S. Joe, F. Kuo, Remark on algorithm 659: implementing Sobol's quasirandom sequence generator, ACM Transactions on Mathematical Software 29(1), (2003), 49–57.

[8] T. Homma, A. Saltelli, Importance measures in global sensitivity analysis of nonlinear models, Reliability Engineering and System Safety 52, (1996), 1–17.

[9] A. Karaivanova, E. Atanassov, T. Gurov, R. Stevanovic, K. Skala, Variance reduction MCMs with application in eEnvironmental studies: sensitivity analysis. AIP Conference Proceedings 1067(1), (2008), 549–558.

[10] A Karaivanova, I. Dimov, S. Ivanovska, A quasi-Monte Carlo method for integration with improved convergence, In International Conference on Large-Scale Scientific Computing, Springer, Berlin, Heidelberg, (2001), 158–165.

[11] L. Kocis, W. J. Whiten, Computational investigations of low-discrepancy sequences, ACM Transactions on Mathematical Software 23(2), (1997), 266–294.

[12] J. Matousek, On the L2-discrepancy for anchored boxes, Journal of Complexity 14(4), (1998), 527–556.

[13] G. Ökten, A. Göncüb, Generating low-discrepancy sequences from the normal distribution: Box–Muller or inverse transform?, Mathematical and Computer Modelling 53, (2011), 1268–1281.

[14] A. Saltelli, S. Tarantola, F. Campolongo, M. Ratto, Sensitivity Analysis in Practice: A Guide to Assessing Scientific Models, Halsted Press, New York, (2004).

[15] I. Sobol, Numerical methods Monte Carlo, Nauka, Moscow, (1973).

[16] I.M. Sobol, Sensitivity estimates for nonlinear mathematical models, Mathematical Modeling and Computational Experiment 1(4), (1993), 407–414.

[17] I.M. Sobol, S. Tarantola, D. Gatelli, S. Kucherenko, W. Mauntz, Estimating the approximation error when fixing unessential factors in global sensitivity analysis, Reliability Engineering & System Safety 92, (2007), 957–960.

[18] S.L. Zaharieva, I.R. Georgiev, V.A. Mutkov, Y.B. Neikov, Arima approach for forecasting temperature in a residential premises part 2, in 2021 20th International Symposium INFOTEH-JAHORINA (INFOTEH), IEEE, (2021), 1–5.

[19] Z. Zlatev, Computer Treatment of Large Air Pollution Models, KLUWER Academic Publishers, Dorsrecht-Boston-London, (1995).

[20] Z. Zlatev, I.T. Dimov, K. Georgiev, Three-dimensional version of the Danish Eulerian model, Z. Angew. Math. Mech. 76(S4), (1996), 473–476.

[21] Z. Zlatev, I.T. Dimov, Computational and Numerical Challenges in Environmental Modelling, Elsevier, Amsterdam, (2006).

Communication Papers of the of the 17th Conference on Computer Science and Intelligence Systems pp. 97–100
DOI: 10.15439/2022F164
ISSN 2300-5963 ACSIS, Vol. 32

A Stochastic Optimization Method for European Option Pricing

Venelin Todorov
Institute of Mathematics and Informatics
Bulgarian Academy of Sciences
8 Acad. G. Bonchev Str., 1113 Sofia, Bulgaria
Institute of Information and Communication Technologies
Bulgarian Academy of Sciences
25A Acad. G. Bonchev Str., 1113 Sofia, Bulgaria
Email: vtodorov@math.bas.bg, venelin@parallel.bas.bg

Slavi Georgiev
Institute of Mathematics and Informatics
Bulgarian Academy of Sciences
8 Acad. G. Bonchev Str., 1113 Sofia, Bulgaria
Department of Applied Mathematics and Statistics
Angel Kanchev University of Ruse
8 Studentska Str., 7004 Ruse, Bulgaria
Email: sggeorgiev@math.bas.bg, sggeorgiev@uni-ruse.bg

***Abstract*—In the contemporary finance the Monte Carlo and quasi-Monte Carlo methods are solid instruments to solve various problems. In the paper the problem of deriving the fair value of European style options is considered. Regarding the option pricing problems, Monte Carlo methods are extremely efficient and useful, especially in higher dimensions. In this paper we show simulation optimization methods which essentially improve the accuracy of the standard approaches for European style options.**

I. INTRODUCTION

THE Monte Carlo approach has become a popular computational tool to solve problems in quantitative finance [3]. New approaches have been designed to outperform classical Monte Carlo ones in terms of numerical efficiency. It is observed that there could be efficiency gains in using special optimization stochastic approaches instead of the random sequences distinctive for standard Monte Carlo [10]. The basic definitions are taken form [5], [6], [8], [23], [25].

A European call option provides its holder with the right, but not the obligation, to byu some quantity of a prescribed asset (underlying) S at a prescribed price (strike or exercise price) E at a prescribed time (maturity or expiry date) T.

A European put option has the same features as its call counterpart, except that holder could sell the underlying rather than buying it.

Risk neutrality is a feature of an investor who is indifferent to the quantity of risk. This definition takes part in the formation of the risk-neutral evaluation formula. A more rigourous approach, based on an appropriately defined probability space of random variables could be found in [9], [17].

Slavi Georgiev is supported by the Bulgarian National Science Fund (BNSF) under Project KP-06-M32/2 - 17.12.2019 "Advanced Stochastic and Deterministic Approaches for Large-Scale Problems of Computational Mathematics" and Scientific Research Fund of University of Ruse under FNSE-03. Venelin Todorov is supported by BNSF under Project KP-06-N52/5 "Efficient methods for modeling, optimization and decision making" and BNSF under Project KP-06-N52/2 "Perspective Methods for Quality Prediction in the Next Generation Smart Informational Service Networks". The work is also supported by BNSF under Bilateral Project KP-06-Russia/17 "New Highly Efficient Stochastic Simulation Methods and Applications".

The risk-free interest rate r is an abstract interest rate, used to borrow or lend money at, which is sometimes implied from the yields of T-bonds.

The Wiener process $\mathrm{d}X$ is a special type of Markov stochastic process with the respective properties: $\mathrm{d}X \sim \mathrm{N}(0, \sqrt{\mathrm{d}t})$, where $\mathrm{N}(\mu, \sigma)$ is the Gaussian distribution with mean μ and variance σ^2.

The most fundamental problem in option pricing is obtaining a "fair" value of the option contract $V(S,t)$, if the following parameters are given: the exercise price E, the asset price $S(t)$, the expiry time T, the risk-free interest rate r and the assumption on the dynamics model of S:

$$\mathrm{d}S = \mu S \mathrm{d}t + \sigma S \mathrm{d}X, \tag{1}$$

where $\mathrm{d}X$ is the increment of a Wiener process, μ is the drift rate and σ is the volatility of the asset price, measuring the average growth and level of fluctuations, respectively.

The celebrated Black-Scholes pricing formula for a European call option can be written ([2] or [25]) using the following parabolic partial differential equation:

$$\frac{\partial V}{\partial t} + \frac{1}{2}\sigma^2 S^2 \frac{\partial^2 V}{\partial S^2} + rS\frac{\partial V}{\partial S} - rV = 0, \tag{2}$$

with final condition

$$V(S,T) = \max(S - E, 0)$$

and Dirichlet boundary conditions

$$V(0,t) = 0, V(S,t) \sim S - Ee^{-r(T-t)}, S \to \infty.$$

The European put option price is governed by the same equation as (2), but with terminal condition

$$V(S,T) = \max(E - S, 0),$$

and boundary conditions

$$V(0,t) = Ee^{-r(T-t)}, V(S,t) \sim 0, S \to \infty.$$

Fortunately, there exist explicit closed form solutions. The call option is described by

$$V(S,t) := C(S,t) = S\mathrm{N}(d_1) - Ee^{-r(T-t)}\mathrm{N}(d_2),$$

where

$$d_1 = \frac{\ln(\frac{S}{E}) + (r + \frac{\sigma^2}{2})(T-t)}{\sigma\sqrt{T-t}}$$

and

$$d_2 = \frac{\ln(\frac{S}{E}) + (r - \frac{\sigma^2}{2})(T-t)}{\sigma\sqrt{T-t}}$$

and $\mathrm{N}(z)$ is the cumulative distribution function of the standard normal distribution. Considering put option,

$$V(S,t) := P(S,t) = Ee^{-r(T-t)}\mathrm{N}(-d_2) - S\mathrm{N}(-d_1),$$

where d_1, d_2, and $\mathrm{N}(z)$ remain the same.

There are two general approaches in Monte Carlo modelling [7]. The first one is *Monte Carlo simulation*, where the algorithms are used for direct simulation of the underlying phenomena of the model. Thus Monte Carlo serves as a tool to choose from the many possible outcomes in a particular circumstance, and it solves probabilistic problems simulating random variables and processes. The other direction is *Monte Carlo numerical* methods, where the algorithms are used to solve deterministic methods by manufacturing random variables. In the context of option pricing, the basic idea is to represent the option premium as mathematical expectation of the random variable (European option risk-neutral valuation formula [17]):

$$V(S,t) = \mathbb{E}_{\mathbb{Q}}(e^{-r(T-t)}h(S(T)) \mid S(t) = S, \mu = r)$$

where $\mathbb{E}_{\mathbb{Q}}(\cdot)$ is the expectation operator, $h(S)$ is the payoff function, in particular $h(S) = \max(S-E, 0)$ for a call and $h(S) = \max(E-S, 0)$ for a put.

In this paper, we employ the first approach of Monte Carlo simulation (of the Geometric Brownian motion (1)).

II. Stochastic methods

One of the basic problems of the methods belonging to Monte Carlo family is the fact that one realization which is close to other ones does not bring a lot of new information for the underlying problem. This could be solved by applying variance-reduction techniques, one of which is the stratified sampling. It splits the original integration domain in several subdomains. It could be shown that the variance of stratified sampling is never greater that the crude method sampling [24].

Latin Hypercube Sampling (LHS) is one of most pronounced types of stratified sampling, originating from [20]. Similar procedure is described in [11]. An improved version of LHS is proposed by [21], [22]. We briefly describe the method in terms of numerical integration. The whole domain $[0,1]^d$ is split into m^d disjoint subdomains of volume m^{-d}, and then a single point is sampled from each subdomain. Let the point x_k, $k = 1, \ldots, m^d$ has coordinates $\mathrm{x}_{k,j}$, $j = 1, \ldots, d$. One of the advantages of LHS is that it does not require more samples in case of more dimensions. A sample scheme of random, stratified and LHS in case of sixteen points is given on Fig. 1 [15].

We supply a weaker variant of the theorem from [20]:

Theorem 1: If $f(\mathrm{x}_1, \mathrm{x}_2, \ldots \mathrm{x}_d)$ is a monotonic function w. r. t. each of its arguments, then $\mathrm{Var}(T_L) \leq \mathrm{Var}(T_R)$, where T_L is the approximation of $\int_{U^d} f(\mathbf{x})\mathrm{d}\mathbf{x}$ derived by the LHS method and T_R is the approximation of the latter integral derived by random sampling.

Let $\mathrm{x}_i = (x_i^{(1)}, x_i^{(2)}, \ldots, x_i^{(s)})$, $i = 1, 2, \ldots$. Then the discrepancy (star discrepancy) of the set is provided by the formula:

$$D_N^* = D_N^*(\mathrm{x}_1, \ldots, \mathrm{x}_N) = \sup_{\Omega \subset \mathrm{E}^s} \left| \frac{\#\{\mathrm{x}_n \in \Omega\}}{N} - V(\Omega) \right|,$$

where $\mathrm{E}^s = [0,1)^s$.

Let the base b representation of n be given by the expression [18]: $n = \ldots a_3(n), a_2(n), a_1(n)$, $n > 0, n \in \mathbb{Z}$.

Let the radical inverse sequence be defined as [19]: $n = \sum_{i=0}^{\infty} a_{i+1}(n)b^i$, $\phi_b(n) = \sum_{i=0}^{\infty} a_{i+1}(n)b^{-(i+1)}$ and its discrepancy satisfy: $D_N^* = \mathcal{O}\left(\frac{logN}{N}\right)$. If $b = 2$, then the Van der Corput sequence [19] is derived.

Halton sequence [13], [14] is defined as:

$$s_n^{(k)} = \sum_{i=0}^{\infty} \sigma_{i+1}^{(k)} a_{i+1}^{(k)}(n) b_k^{-(i+1)},$$

where $(b_1, b_2, \ldots, b_s) \equiv (2, 3, 5, \ldots, p_s)$, where p_i designates the i-th prime, and $\sigma_i^{(k)}$, $i \geq 1$ is the set of permutations on $(0, 1, 2, \ldots, p_k - 1)$.

Sobol sequence [1], [4], [12] is defined as:

$$\mathrm{x}_k \in \overline{\sigma}_i{}^{(k)}, k = 0, 1, 2, \ldots,$$

where $\overline{\sigma}_i{}^{(k)}$, $i \geq 1$ is the set of permutations on each $2^k (k = 0, 1, 2, \ldots)$ subsequent points of the Van der Corput sequence. In case of binary we arrive on:

$x_n^{(k)} = \bigoplus_{i \geq 0} a_{i+1}(n) v_i$, where v_i, $i = 1, \ldots, s$ is a set of direction numbers [16].

The following discrepancy estimate is valid for the ***Halton, Sobol, Faure*** -based QMC algorithms:

$$D_N^* = \mathcal{O}\left(\frac{log^s N}{N}\right).$$

The used implementation of the Sobol sequence (SOB) in this paper is an adaptation of the idea of [1] and further modifies the INSOBL and GOSOBL procedures in ACM TOMS Algorithm 647 [12] and ACM TOMS Algorithm 659 [4], [16].

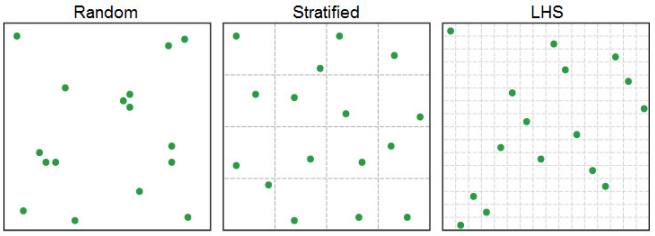

Fig. 1. Example of random, stratified and LHS with sixteen points (d = 2, m = 4).

The standard M-dimensional Halton sequence (HAL) [13], [14] comprises M 1-dimensional van der Corput sequences and uses first M primes as bases.

Another variance reduction techniques consist of manipulating the (quasi-)random sequence in such a way to improve its desired probabilistic properties.

In a simple Monte Carlo simulation, the samples are independent and identically distributed. The idea of **antithetic variates** is to reduce the variance by introducing samples that are negatively correlated.

The concept of **moment matching** Monte Carlo follows the idea that the generated samples from the Monte Carlo method are expected to obey the same statistical properties as the theoretical distribution. This simply means that the empirical moments of the sample should equal their theoretical counterparts. It may seem appealing at first glance, but it raises concerns as well, the primary of which is that the distribution is no longer the same.

III. Numerical examples and results

In this section we will present some computational experiments and simulations in order to demonstrate the effectiveness of the proposed approach. We consider a European call option with $r = 0.05$, $\sigma = 0.2$, $K = 220$ and $T = 1$ year time to maturity. We assume that $S_0 = 200$.

For reference values, we provide the results with the crude / plain Monte Carlo method (Table I).

TABLE I
CRUDE MONTE CARLO METHOD

N	V_{exact}	V	Error	Time (sec)
1e2	12.0801762594485	11.395	0.68508	0.009731
1e3	12.0801762594485	11.54	0.54011	0.001870
1e4	12.0801762594485	12.045	0.034958	0.002909
1e5	12.0801762594485	12.159	0.078974	0.006350
1e6	12.0801762594485	12.114	0.033989	0.043681
1e7	12.0801762594485	12.089	0.0092241	0.326507
1e8	12.0801762594485	12.082	0.0016232	3.922560

A. Latin hypercube sampling

First we give the results with the LHS quasirandom sequence. For different number of random points, distributed logequally from $N = 1e2$ to $N = 1e8$, we display the results from the application of the sole LHS and consecutively combined with antithetic variates and moment matching techniques, see Tables II, III and IV.

TABLE II
LHS WITHOUT OTHER VARIANCE REDUCTION

N	V_{exact}	V	Error	Time (sec)
1e2	12.0801762594485	12.01	0.070212	0.001102
1e3	12.0801762594485	12.064	0.01657	0.001364
1e4	12.0801762594485	12.083	0.0026497	0.002349
1e5	12.0801762594485	12.08	5.5395e-05	0.010674
1e6	12.0801762594485	12.08	6.7257e-06	0.097699
1e7	12.0801762594485	12.08	2.7833e-08	0.992030
1e8	12.0801762594485	12.08	1.6933e-07	12.402776

TABLE III
LHS WITH ANTITHETIC VARIATES

N	V_{exact}	V	Error	Time (sec)
1e2	12.0801762594485	12.029	0.051276	0.001545
1e3	12.0801762594485	12.077	0.0031408	0.001317
1e4	12.0801762594485	12.08	0.00021551	0.002592
1e5	12.0801762594485	12.08	4.762e-05	0.011522
1e6	12.0801762594485	12.08	1.4455e-05	0.107597
1e7	12.0801762594485	12.08	1.975e-07	1.083230
1e8	12.0801762594485	12.08	9.3442e-08	14.027701

TABLE IV
LHS WITH MOMENT MATCHING

N	V_{exact}	V	Error	Time (sec)
1e2	12.0801762594485	12.027	0.052906	0.002450
1e3	12.0801762594485	12.067	0.01366	0.001866
1e4	12.0801762594485	12.08	0.00027461	0.003071
1e5	12.0801762594485	12.08	6.2304e-05	0.010709
1e6	12.0801762594485	12.08	6.9669e-06	0.102625
1e7	12.0801762594485	12.08	1.2712e-06	1.034859
1e8	12.0801762594485	12.08	1.2036e-07	14.027701

In general, the application of variance reduction techniques takes 10%-15% more computational time. For small values of N, the combined approach gives more accurate results that the plain Halton sequence. For bigger values of N, this advantage is not that pronounced, as the antithetic variates technique appears to perform better than the moment matching one.

B. Halton sequence

We continue the simulations with the Halton sequence. The results concerning the sole Halton and the additionally applied antithetic variates and moment matching techniques are presented on Tables V, VI and VII.

TABLE V
HALTON WITHOUT OTHER VARIANCE REDUCTION

N	V_{exact}	V	Error	Time (sec)
1e2	12.0801762594485	11.111	0.96902	0.004395
1e3	12.0801762594485	12.099	0.01904	0.005186
1e4	12.0801762594485	12.073	0.0068783	0.010478
1e5	12.0801762594485	12.081	0.00043392	0.064871
1e6	12.0801762594485	12.08	0.00010187	0.628980
1e7	12.0801762594485	12.08	2.9878e-05	6.310790
1e8	12.0801762594485	12.08	5.5002e-06	65.628562

TABLE VI
HALTON WITH ANTITHETIC VARIATES

N	V_{exact}	V	Error	Time (sec)
1e2	12.0801762594485	12.298	0.21807	0.002178
1e3	12.0801762594485	12.056	0.024416	0.003771
1e4	12.0801762594485	12.082	0.0021855	0.009744
1e5	12.0801762594485	12.08	0.00034855	0.065575
1e6	12.0801762594485	12.08	3.5754e-05	0.627989
1e7	12.0801762594485	12.08	2.9969e-05	6.493375
1e8	12.0801762594485	12.08	7.532e-06	67.408394

The conclusions about the Halton sequence are similar to these of the LHS. For lower values of N, the results are relatively bad. For higher, however, the accuracy improves

TABLE VII
HALTON WITH MOMENT MATCHING

N	V_{exact}	V	Error	Time (sec)
1e2	12.0801762594485	11.669	0.41132	0.002109
1e3	12.0801762594485	12.084	0.0037734	0.003770
1e4	12.0801762594485	12.081	0.00079293	0.010174
1e5	12.0801762594485	12.08	3.4485e-05	0.064448
1e6	12.0801762594485	12.08	1.5061e-05	0.636945
1e7	12.0801762594485	12.08	4.5434e-07	6.388943
1e8	12.0801762594485	12.08	1.3984e-06	66.411237

significantly and the moment matching technique performs best.

C. Sobol sequence

We conclude the experiments with tests with the Sobol quasirandom sequence. The simulations follow the previous pattern and the results are given in Tables VIII, IX and X.

TABLE VIII
SOBOL WITHOUT OTHER VARIANCE REDUCTION

N	V_{exact}	V	Error	Time (sec)
1e2	12.0801762594485	11.171	0.90959	0.003620
1e3	12.0801762594485	12.062	0.018076	0.006366
1e4	12.0801762594485	12.095	0.015131	0.008283
1e5	12.0801762594485	12.083	0.002552	0.051577
1e6	12.0801762594485	12.082	0.0015908	0.447782
1e7	12.0801762594485	12.08	0.00017189	4.461646
1e8	12.0801762594485	12.08	6.1323e-05	44.393839

TABLE IX
SOBOL WITH ANTITHETIC VARIATES

N	V_{exact}	V	Error	Time (sec)
1e2	12.0801762594485	11.021	1.0594	0.002160
1e3	12.0801762594485	12.125	0.044527	0.002771
1e4	12.0801762594485	12.091	0.010636	0.008956
1e5	12.0801762594485	12.083	0.0030839	0.050479
1e6	12.0801762594485	12.082	0.0016988	0.451211
1e7	12.0801762594485	12.08	0.00015271	4.522295
1e8	12.0801762594485	12.08	5.9658e-05	45.655215

TABLE X
SOBOL WITH MOMENT MATCHING

N	V_{exact}	V	Error	Time (sec)
1e2	12.0801762594485	12.05	0.030024	0.002263
1e3	12.0801762594485	12.001	0.079036	0.003115
1e4	12.0801762594485	12.093	0.012791	0.007114
1e5	12.0801762594485	12.08	0.0001421	0.049672
1e6	12.0801762594485	12.08	0.00012572	0.467593
1e7	12.0801762594485	12.08	5.1817e-05	4.473896
1e8	12.0801762594485	12.08	1.0556e-05	45.425531

Again the general implications remain valid. The antithetic variates performance does not differ significantly from the plain Sobol one, while they are outperformed by the moment matching technique.

Finally, the best results are obtained by the combination of Latin hypercube sampling with the antithetic variates.

IV. CONCLUSION

An efficient optimization technique for Monte Carlo methods has been presented. The proposed approach shows an essential advantage over the well known stochastic approaches based on the standard sequences. The improved accuracy will be crucial for more reliable results for European option pricing. What is more, the suggested approach could be used in situations where the other deterministic methods fail – e. g. in case of high dimensions, complex contract specifications, etc.

REFERENCES

[1] I. Antonov, V. Saleev, An economic method of computing LP_τ-sequences, USSR Comput. Math. Phys. 19, 252-256, 1979.
[2] F. Black, M. Scholes, The pricing of pptions and corporate liabilities, J. Pol. Econ. 81, 637-659, 1973.
[3] P. P. Boyle, Options: a Monte Carlo approach, J. Finan. Econ. 4, 323-338, 1977.
[4] P. Bratley, B. Fox, Algorithm 659: Implementing Sobol's quasirandom sequence generator, ACM Transactions on Mathematical Software, 14 (1), 88-100, 1988.
[5] D. M. Chance, An Introduction to Derivatives (third edition), The Dryden Press, 1995.
[6] J. C. Cox, S. A. Ross, M. Rubinstein, Option Pricing: a simplified approach, J. Fin. Econ. 7, 229-263, 1979.
[7] I. Dimov, Monte Carlo Methods for Applied Scientists, New Jersey, London, Singapore, World Scientific, 2008.
[8] D. Duffie, Dynamic Asset Pricing Theory, Princeton, 1992.
[9] D. Duffie, Security Markets: Stochastic Models, Academic Press, Inc. 1988.
[10] R. Eckhardt, Stan Ulam, John von Neumann and the Monte Carlo Method, 1987.
[11] V. Eglajs, P. Audze, New approach to the design of multifactor experiments. Problems of Dynamics and Strengths, 35 (in Russian), Riga, Zinatne Publishing House, 104-107, 1977.
[12] B. Fox, Algorithm 647: Implementation and relative efficiency of quasirandom sequence generators, ACM Transactions on Mathematical Software, 12(4), 362-376, 1986.
[13] J. Halton, On the efficiency of certain quasi-random sequences of points in evaluating multi-dimensional integrals, Numerische Mathematik, 2, 84-90, 1960.
[14] J. Halton, G.B. Smith, Algorithm 247: Radical-inverse quasi-random point sequence, Communications of the ACM, 7, 701-702, 1964.
[15] W. Jarosz, Efficient Monte Carlo Methods for Light Transport in Scattering Media, PhD dissertation, UCSD, 2008.
[16] S. Joe, F. Kuo, Remark on Algorithm 659: Implementing Sobol's quasirandom sequence generator, ACM Transactions on Mathematical Software, 29(1), 49-57, 2003.
[17] M. Broadie, P. Glasserman, Pricing American-style securities using simulation, J. of Economic Dynamics and Control 21, 1323-1352, 1997.
[18] H. Niederreiter, Random Number Generation and Quasi-Monte Carlo Methods CBSM 63, 1992.
[19] H. Niederreiter, Monatsh. Math. 86, 203-219, 1978.
[20] M.D. McKay, R.J. Beckman, W.J. Conover, A comparison of three methods for selecting values of input variables in the analysis of output from a computer code, Technometrics 21(2), 239-245, 1979.
[21] B. Minasny, B. McBratney, A conditioned Latin hypercube method for sampling in the presence of ancillary information, Journal Computers and Geosciences archive, 32(9), 1378-1388, 2006.
[22] B. Minasny, B. McBratney, Conditioned Latin Hypercube Sampling for Calibrating Soil Sensor Data to Soil Properties, Chapter: Proximal Soil Sensing, Progress in Soil Science, 111-119, 2010.
[23] Y. Lai, J. Spanier, Applications of Monte Carlo/Quasi-Monte Carlo Methods in Finance: Option Pricing, Proceedings of a conference held at the Claremont Graduate University, 1998.
[24] I. Sobol, Numerical methods Monte Carlo, Nauka, Moscow, 1973.
[25] P. Wilmott, J. Dewynne, S. Howison, Option Pricing: Mathematical Models and Computation, Oxford University Press, 1995.

Communication Papers of the of the 17th Conference on Computer Science and Intelligence Systems pp. 101–104
DOI: 10.15439/2022F84
ISSN 2300-5963 ACSIS, Vol. 32

An Optimized Monte Carlo Approach for Multidimensional Integrals Related to Intelligent Systems

Venelin Todorov*†, Ivan Dimov†, Stefka Fidanova†, Rayna Georgieva†, Tzvetan Ostromsky†, Stoyan Poryazov*
*Institute of Mathematics and Informatics
Bulgarian Academy of Sciences
8 Acad. G. Bonchev Str., 1113 Sofia, Bulgaria
†Institute of Information and Communication Technologies
Bulgarian Academy of Sciences
25A Acad. G. Bonchev Str., 1113 Sofia, Bulgaria
Email: vtodorov@math.bas.bg, venelin@parallel.bas.bg, ivdimov@bas.bg, stefka@parallel.bas.bg, rayna@parallel.bas.bg, ceco@parallel.bas.bg, stoyan@math.bas.bg

***Abstract*—We study an optimized Monte Carlo algorithm for solving multidimensional integrals related to intelligent systems. Recently Shaowei Lin consider the difficult task of evaluating multidimensional integrals with very high dimensions which are important to machine learning for intelligent systems. Lin multidimensional integrals with 3 to 30 dimensions, related to applications in machine learning, will be evaluated with the presented optimized Monte Carlo algorithm and some advantages of the method will be analyzed.**

I. Introduction

TEN YEARS ago Shaowei Lin in his works [4], [5] consider the important problem of evaluating multidimensional integrals used in intelligent systems. The first multidimensional Lin integrals are of the form

$$\int_{\Omega} p_1^{u_1}(x)\dots p_s^{u_s}(x)dx, \tag{1}$$

and the second Lin integrals are of the form

$$\int_{\Omega} e^{-Nf(x)}\phi(x)dx, \tag{2}$$

where $f(x)$ and $\phi(x)$ are multidimensional polynomials with an integer N. Up to now multidimensional Lin integrals (1) and (2) are computed unsatisfactory with deterministic [10] and algebraic methods [9], and it is known that the Monte Carlo (MC) methods [3], [7], [8] outperforms the deterministic methods which suffer from the so called ,,curse of dimensionality" [3] especially for higher dimensions.

Venelin Todorov is supported by the Bulgarian National Science Fund under Project KP-06-M32/2 - 17.12.2019 "Advanced Stochastic and Deterministic Approaches for Large-Scale Problems of Computational Mathematics" and Project KP-06-N52/5 "Efficient methods for modeling, optimization and decision making". The work is also supported by the Bulgarian National Science Fund under Project KP-06-N52/2 "Perspective Methods for Quality Prediction in the Next Generation Smart Informational Service Networks" and by the Bilateral Project KP-06-Russia/17 "New Highly Efficient Stochastic Simulation Methods and Applications".

The paper is organised as follows. The description of the optimal stochastic approach is given in Section II. The numerical study with Lin multidimensional integrals is given in Section III. Finally some concluding remarks are given in Section IV.

II. The optimal stochastic approach

We adapt the idea of the original MC method developed by Atanassov and Dimov twenty years ago [1].

Let d and k be integers, $d, k \geq 1$. We consider the class

$$F_0 \equiv \mathbf{W}^k(\|f\|; U^d) \tag{3}$$

(sometimes abbreviated to $\mathbf{W}^k$) of real functions f defined over the unit cube $U^d = [0,1)^d$, possessing all the partial derivatives

$$\frac{\partial^r f(\mathbf{x})}{\partial x_1^{\alpha_1}\dots\partial x_d^{\alpha_d}},\ \ \alpha_1+\dots+\alpha_d = r \leq k, \tag{4}$$

which are continuous when $r < k$ and bounded in sup norm when $r = k$. The semi-norm $\|\cdot\|$ on $\mathbf{W}^k$ is defined as

$$\|f\| = \sup\left\{\left|\frac{\partial^k f(\mathbf{x})}{\partial x_1^{\alpha_1}\dots\partial x_d^{\alpha_d}}\right|,\ \ \alpha_1+\dots+\alpha_d = k,\ \mathbf{x}\equiv(x_1,\dots,x_d)\in U^d\right\}. \tag{5}$$

Now for $n, s, k \geq 1$ we construct a MC integration formula depending on $m \geq 1$ and $\binom{s+k-1}{s}$ points in $[0,1]^s$. Points $x^{(r)}$ are exactly $\binom{s+k-1}{s}$ and if for $P(x)$ for the degree of the polynom $\deg P \leq k$ is fulfilled $P(x^{(r)}) = 0$, then $P \equiv 0$. If $N = n^s$ for $n \geq 1$ we divide $[0,1]^s$ into n^s *endless undercubes* K_j, i.e.

$$[0,1]^s = c_{i=1}^{n^s} K_j$$

and

$$K_j = \prod_{i=1}^{s}[a_i^j, b_i^j),$$

$$b_i^j - a_i^j = \frac{1}{n},$$

$i = 1, \ldots, s$. For every cube K_j we evaluate the coordinates of $\binom{s+k-1}{s}$ points $y^{(r)}$, determined by

$$y_i^{(r)} = a_i^r + \frac{1}{n} x_i^{(r)}.$$

We choose m random points $\xi_i(j,s) = (\xi_1(j,p), \ldots, \xi_s(j,p))$ from every cube K_j, so all $\xi_i(j,p)$ are independent uniformly distributed random points, and calculate $f(y^{(r)})$ and $f(\xi_i(j,p))$, and the Lagrange polynom of f in z to obtain $L_k(f,z)$.. Now for every P of max degree $k-1$ we have $L_k(f,z) \equiv z$. For every $j = 1, \ldots, N$ we sum and obtain:

$$\int_{K_j} f(x)dx \approx \frac{1}{mn^s} \sum_{s=1}^{m} [(\xi(j,p)) - L_k(f, \xi(j,p))] + \int_{K_j} L_k(f,x)dx.$$

$$I(f) \approx \frac{1}{mn^s} \sum_{j=1}^{N} \sum_{s=1}^{m} [(\xi(j,p)) - L_k(f, \xi(j,p))] + \sum_{j=1}^{N} \int_{K_j} L_k(f,x)dx.$$

$$\int_{K_j} f(x)dx \approx \frac{1}{mn^s} \sum_{s=1}^{m} [(\xi(j,p)) - L_k(f, \xi(j,p))] + \int_{K_j} L_k(f,x)dx.$$

$$I(f) \approx \frac{1}{mn^s} \sum_{j=1}^{N} \sum_{s=1}^{m} [(\xi(j,p)) - L_k(f, \xi(j,p))] + \sum_{j=1}^{N} \int_{K_j} L_k(f,x)dx.$$

Thus an optimal MC approximation with an optimal order of convergence $\mathcal{O}\left(N^{-\frac{1}{2}-\frac{k}{d}}\right)$ for d-dimensional functions from the class W^k is derived.

III. Numerical results

We will use the following notations: LHSM=Latin Hypercube sampling *method* [6], SOBOLS=Sobol quasi-random *sequence* [2], OPTIMAL=*optimal* approach under consideration. In the Tables below the relative errors (RELERR) obtained with the three approaches are given for the corresponding multidimensional integral (MI).

We study the following Lin multidimensional integrals (1) and (2): Example 1. s=3.

$$\int_{[0,1]^3} \exp(x_1 x_2 x_3) \approx 1.14649907. \tag{6}$$

Example 2. s= 4.

$$\int_{[0,1]^4} x_1 x_2^2 e^{x_1 x_2} \sin(x_3)\cos(x_4) \approx 0.1089748630. \tag{7}$$

Example 3. s= 5.

$$\int_{[0,1]^5} \exp(-100 x_1 x_2 x_3)(\sin(x_4) + \cos(x_5)) \approx 0.1854297367. \tag{8}$$

Example 4. s= 7.

$$\int_{[0,1]^7} e^{1-\sum_{i=1}^{3} sin(\frac{\pi}{2}.x_i)}.arcsin(sin(1) + \frac{\sum_{j=1}^{7} x_j}{200}) \approx 0.75151101. \tag{9}$$

Example 5. s= 15.

$$\int_{[0,1]^{15}} (\sum_{i=1}^{10} x_i^2)(x_{11} - x_{12}^2 - x_{13}^3 - x_{14}^4 - x_{15}^5)^2 \approx 1.96440666. \tag{10}$$

Example 6. s= 25.

$$\int_{[0,1]^{25}} \frac{4x_1 x_3^2 e^{2x_1 x_3}}{(1+x_2+x_4)^2} e^{x_5+\cdots+x_{20}} x_{21} \ldots x_{25} \approx 108.808. \tag{11}$$

Example 7. s= 30.

$$\int_{[0,1]^{30}} \frac{4x_1 x_3^2 e^{2x_1 x_3}}{(1+x_2+x_4)^2} e^{x_5+\cdots+x_{20}} x_{21} \ldots x_{30} \approx 3.244540. \tag{12}$$

Table I
RELERR FOR THE 3-MI.

N	SOBQMC	t	LHSM	t	OPTMC	t
10^3	4.87e-4	0.47	6.14e-3	0.004	3.12e-5	0.81
10^4	1.56e-4	1.88	6.56e-4	0.06	2.05e-6	4.13
10^5	2.51e-5	15.6	1.34e-4	0.51	4.58e-7	31.62
10^6	7.43e-6	105.80	6.84e-5	5.22	6.72e-8	155
10^7	1.58e-6	934	1.73e-5	17	5.34e-9	1053

Table II
RELERR FOR THE 3-MI FOR A FIXED TIME.

time(s)	SOBOLS	LHSM	OPTIMAL
1	2.93e-4	5.11e-4	1.21e-5
5	8.01e-5	7.32e-5	1.12e-6
10	4.71e-5	4.32e-5	7.21e-7
100	7.68e-6	5.32e-6	8.61e-8

Table III
RELERR FOR THE 4-MI.

N	SOBOLS	t,s	LHSM	t,s	OPTIMAL	t,s
10^4	2.61e-5	2.14	5.29e-4	0.07	1.52e-5	4.81
10^5	5.93e-6	17.6	3.56e-4	0.60	7.96e-6	45.1
10^6	1.51e-6	193	4.36e-5	4.97	2.31e-7	352.6
10^7	8.30e-7	1121	8.12e-6	47.1	8.16e-9	2651

For the 3-dimensional integrals for a number of samples $N = 10^7$ the best approach is OPTIMAL - it gives a relative error $5.34e-9$ -see Table I and for a preliminary given time in seconds the best approach for 100s is OPTIMAL- the relative error is $8.61e-8$ in Table II. For the 4-dimensional integrals for a number of samples $N = 10^7$ the best approach is OPTIMAL - it gives a relative error $8.16e-9$ -see Table III and for a preliminary given time in seconds the best approach for 20s is OPTIMAL- the relative error is $6.54e-7$

Table IV
RELERR FOR THE 4-MI FOR A FIXED TIME.

time,s	SOBOLS	LHSM	OPTIMAL
0.1	4.07e-4	4.18e-4	4.22e-5
1	3.54e-5	3.32e-4	2.31e-5
5	5.26e-5	4.23e-5	1.12e-5
10	6.50e-6	3.48e-5	7.53e-6
20	4.55e-6	2.16e-5	6.54e-7

Table V
RELERR FOR THE 5-MI.

N	SOBOLS	t,s	LHSM	t,s	OPTIMAL	t,s
10^3	5.29e-4	0.03	9.38e-3	0.007	2.75e-5	2.1
10^4	1.43e-4	0.3	3.44e-3	0.07	7.22e-6	2.3
10^5	2.36e-5	2.77	2.01e-3	0.69	2.36e-6	6.2
10^6	6.07e-6	24.2	1.80e-4	6.17	5.46e-7	20.0
10^7	2.30e-6	245	2.46e-5	60.5	7.01e-8	105.1

Table VI
RELERR FOR THE 5-MI FOR A FIXED TIME.

time,s	SOBOLS	LHSM	OPTIMAL
0.1	1.34e-4	3.21e-3	1.09e-4
1	7.21e-5	8.54e-4	5.58e-5
5	1.54e-5	3.25e-4	1.71e-6
10	9.32e-6	8.65e-5	8.15e-7
20	7.39e-6	5.02e-5	5.46e-7

Table VII
RELERR FOR THE 7-MI.

N	SOBOLS	t,s	LHSM	t,s	OPTIMAL	t,s
10^4	2.27e-4	0.76	1.79e-3	0.13	2.13e-4	10.2
10^5	1.22e-4	7.45	2.53e-4	1.15	4.41e-5	40.2
10^6	4.71e-5	72.3	8.27e-5	10.32	1.27e-6	167.1
10^7	9.45e-6	697	1.69e-5	101.2	1.45e-7	595.1

Table VIII
RELERR FOR THE 7-MI FOR A FIXED TIME.

time,s	SOBOLS	LHSM	OPTIMAL
0.1	2.38e-3	1.85e-3	2.37e-3
1	6.19e-4	1.85e-4	3.37e-4
5	8.81e-5	9.79e-5	1.38e-4
10	1.88e-5	8.36e-5	8.78e-5
20	3.87e-6	5.46e-5	6.87e-5

in Table IV. For the 5-dimensional integrals for a number of samples $N = 10^7$ the best approach is again OPTIMAL - it gives a relative error $7.01e-8$ -see Table V and for a preliminary given time in seconds the best approach for 20s is again the optimal approach - the RELERR is $8.37e-8$ in Table VI. For the 7-dimensional integrals for a number of samples $N = 10^7$ the best approach is again OPTIMAL -

Table IX
RELERR FOR THE 15-MI.

N	SOBOLS	t,s	LHSM	t,s	OPTIMAL	t,s
10^3	2.04e-3	0.98	1.06e-2	0.12	7.54e-3	27.4
10^4	2.89e-4	9.3	7.33e-3	1.07	6.51e-4	81.5
10^5	1.13e-4	93.8	1.54e-3	10.11	7.29e-5	242.1
10^6	1.93e-5	935	1.14e-4	99.6	8.29e-6	720.2

Table X
RELERR FOR THE 15-MI FOR A FIXED TIME.

time,s	SOBOLS	LHSM	OPTIMAL
1	1.10e-3	3.64e-3	3.51e-2
5	2.45e-4	7.32e-4	1.23e-2
10	9.48e-5	1.94e-4	9.63e-3
20	9.87e-6	4.05e-5	7.51e-3
100	8.17e-7	4.03e-6	9.51e-5

Table XI
RELERR FOR THE 25-MI.

N	SOBOLS	t,s	LHSM	t,s	OPTIMAL	t,s
10^3	1.47e-1	0.4	7.54e-1	0.02	3.77e-3	2.03
10^4	5.68e-2	5.64	5.39e-2	0.15	3.18e-3	19.52
10^5	7.21e-3	33.4	2.11e-2	1.07	5.33e-5	181
10^63	2.89e-3	161	1.71e-4	8.21	3.11e-5	1234

Table XII
RELERR FOR THE 25-MI FOR A FIXED TIME.

time,s	SOBOLS	LHSM	OPTIMAL
1	9.51e-2	2.11e-2	7.24e-2
5	5.76e-2	1.61e-2	8.16e-3
10	2.71e-2	9.58e-3	5.18e-3
20	8.28e-3	7.87e-3	3.13e-3

Table XIII
RELERR FOR THE 30-MI.

N	SOBOLS	t,s	LHSM	t,s	OPTIMAL	t,s
10^3	1.18e-1	0.42	8.81e-1	0.02	2.01e-2	5.4
10^4	8.40e-2	4.5	6.19e-2	0.14	6.53e-3	14.5
10^5	1.18e-2	30.2	2.78e-2	1.16	1.35e-3	145
10^6	9.20e-3	168	9.86e-3	8.61	2.11e-4	1290

Table XIV
RELERR FOR THE 30-MI FOR A FIXED TIME.

time,s	SOBOLS	LHSM	OPTIMAL
1	1.01e-1	2.38e-2	4.38e-1
5	7.76e-2	1.81e-2	1.16e-2
10	5.71e-2	9.48e-3	8.11e-3
20	1.28e-2	7.87e-3	4.63e-3

it gives a relative error $1.45e-7$ -see Table VII and for a preliminary given time in seconds the best approach for 20s is now the Sobol approach SOBOLS - the relative error is $3.87e-6$ in Table VIII. For the 15-dimensional integrals for a number of samples $N = 10^6$ the best approach is again OPTIMAL - it gives a relative error $8.29e-6$ -see Table IX and for a preliminary given time in seconds the best approach for 100s is again the Sobol approach - the relative error is $8.17e-7$ in Table X. For the 25-dimensional integrals for a number of samples $N = 10^6$ the best approach is again OPTIMAL - it gives a relative error $3.11e-5$ -see Table XI and for a preliminary given time in seconds the best approach for 20s is now the optimal approach - the relative error is $3.13e-3$ in Table XII. For the 30-dimensional integrals for a number of samples $N = 10^6$ the best approach is again OPTIMAL - it gives a relative error $2.11e-4$ -see Table XIII and for a preliminary given time in seconds the best approach for 20s is the optimal approach - the relative error is $4.63e-3$ in Table XIV. From all the results we can conclude that for a preliminary given number of samples the optimal approach OPTIMAL always outperforms the Sobol approach SOBOLS, but the optimal approach is a computationally expensive algorithm, and sometimes for a preliminary given time in seconds the Sobol approach SOBOLS or even the Latin hypercube sampling approach LHSM outperforms the optimal approach OPTIMAL.

IV. Conclusion

In this paper an optimal Monte Carlo approach for computing Lin multidimensional integrals (1) and (2) which are important for machine learning in intelligent systems has been presented. This is the first time a specific optimal approach is used for evaluating multidimensional integrals in intelligent systems and also the comparison between the three methods has never been performed before. In our case study the Sobol sequence, the Latin hypercube sampling algorithm and the optimal Monte Carlo approach have been compared on some important Lin multidimensional integrals. The optimal Monte Carlo is one of the best available algorithms for high dimensional integrals and one of the few possible methods, because the deterministic methods are impractical for higher dimensions. At the same time the optimal method is suitable to deal with 30-dimensional problems for less than a minute on a laptop. It is an important element since this may be crucial in some control test examples in intelligent systems. In the future the scope of our work will be develop other optimal Monte Carlo approaches based on other techniques.

References

[1] Atanassov E. and Dimov I.T., A new optimal monte carlo method for calculating integrals of smooth functions, Journal of Monte Carlo Methods and Applications 5 (1999), no. 2, 149–167, https://doi.org/10.1515/mcma.1999.5.2.149.

[2] Bratley P., Fox B., Algorithm 659: Implementing Sobol's Quasirandom Sequence Generator, ACM Transactions on Mathematical Software, 14 (1), 1988, 88–100.

[3] Dimov I., Monte Carlo Methods for Applied Scientists, New Jersey, London, Singapore, World Scientific, 2008, 291p.

[4] Lin S., "Algebraic Methods for Evaluating Integrals in Bayesian Statistics," Ph.D. dissertation, UC Berkeley, May 2011.

[5] Lin, S., Sturmfels B., Xu Z.: Marginal Likelihood Integrals for Mixtures of Independence Models, Journal of Machine Learning Research, Vol. 10, pp. 1611-1631, 2009.

[6] Minasny B., McBratney B.: A conditioned Latin hypercube method for sampling in the presence of ancillary information Journal Computers and Geosciences archive, Volume 32 Issue 9, November, 2006, Pages 1378-1388.

[7] Paskov S.H., *Computing high dimensional integrals with applications to finance*, Technical report CUCS-023-94, Columbia University (1994).

[8] Pencheva, V., Georgiev, I., & Asenov, A. (2021, February). Evaluation of passenger waiting time in public transport by using the Monte Carlo method. In AIP Conference Proceedings (Vol. 2321, No. 1, p. 030028). AIP Publishing LLC.

[9] Song, J., Zhao, S., Ermon, S., A-nice-mc: Adversarial training for mcmc. In Advances in Neural Information Processing Systems, pp. 5140-5150, 2017.

[10] Watanabe S., Algebraic analysis for nonidentifiable learning machines. NeuralComput.(13), pp. 899—933, April 2001.

Communication Papers of the of the 17th Conference on Computer Science and Intelligence Systems pp. 105–112
DOI: 10.15439/2022F230
ISSN 2300-5963 ACSIS, Vol. 32

Development of Software Tool for Optimization and Evaluation of Cycling Routes by Characterizing Cyclist Exposure to Air Pollution

Petar Zhivkov
Inst. of I&C Tech., Bulgarian Academy of Sciences
Sofia, Bulgaria
Email: pzhivkov@iit.bas.bg

Alexander Simidchiev
Medical Institute of Ministry of Interior.
Sofia, Bulgaria
Email: alex@simidchiev.net

***Abstract*—In modern cities, poor air quality has contributed to replacing motorized cars with active modes of transportation such as cycling. However, when designing and building bike infrastructure, officials neglect to consider air quality concerns connected to cyclists, and most cycling lanes are developed next to heavy-traffic roadways. This poses additional health risks to cyclists, due to their increased ventilation rate. To preserve a sustainable quality of life for a city's residents, it's critical to understand how to detect and quantify PM exposure, especially in potentially hazardous locations. This study offers a software tool based on experimental data to optimize and evaluate cycling routes by calculating the overall amount of particulate matter intake in terms of the physiological response of cyclists.**

I. Introduction

AIR POLLUTION is a significant public health problem that has long been a source of anxiety for citizens. An air pollutant is described as any substance that can affect humans, animals, plants, or materials. In the case of humans, an air pollutant may cause or lead to an increase in mortality or serious illness, as well as pose a current or potential health risk [1]. Measurements of air emissions are critical for epidemiology and air quality control, but the scope of ground-based air pollution observations has limitations [2]. Somatic symptoms of asthma in adults and children have been linked to moderate increases in vehicular exhaust such as fine particulate matter (PM2.5), nitrogen dioxide (NO2), ozone, carbon monoxide, and traffic-related air pollution (TRAP) [3].

The presence of PM (Particulate Matter) is one of the key causes of increased morbidity and mortality in modern cities. It is a suspended combination of solid and liquid particles that vary in quantity, size, shape, surface area, chemical composition, solubility, and origin. Total suspended particles (TSPs) have a trimodal size distribution in the ambient air, including coarse particles (PM10), fine particles (PM2.5), and ultrafine particles (PM1) [4]. PM size-selective sampling refers to the collection of particles that are below, above, or within a defined aerodynamic range of sizes, which is commonly chosen to be relevant to inhalation and deposition, causes, or toxicity [5].

Poor air quality in large cities has contributed to the substitution of motorized vehicles with an active means of transportation, such as cycling [6]. This method has been extensively adopted by multiple communities due to reduced congestion [7] and the numerous health benefits of physical exercise. Cycling infrastructure near roadways, on the other hand, has been identified as a harmful scenario for cyclists owing to air pollution exposure [8]. Although this has piqued the scientific community's interest [9], there have been few studies conducted in European cities where many individuals are continually exposed to PM from anthropogenic sources, such as automobile traffic.

Estimates of air pollution exposure for research projects are frequently based on measurements obtained by stationary regulatory monitors, such as those operated by the European Environmental Agency (EEA). While these monitors are highly precise and well-suited to assuring compliance with federal air quality requirements, their utility for recording individual-level pollution exposure is limited for many reasons: 1) Firstly because monitor locations rarely coincide with exposure locations (e.g., home, work, or school), an individual's exposure to air pollution can only be measured indirectly through spatial interpolation techniques such as inverse distance weighted interpolation and kriging, or statistical methods such as land-use regression modeling. [10] 2) Secondly, regulatory monitors offer limited temporal resolution (e.g., hourly averages in the case of particulate matter monitors), which may lead them to miss transient spikes in pollution levels; 3) Thirdly, indirect methods of exposure assessment typically estimate exposure for a single location per individual, such as their location of residence, place of work [11], or school [12], which does not capture exposures that occur while people are at different locations or during regular activities like commuting and errands.

The majority of dedicated bicycle lanes in cities are close to heavy-traffic roadways, this can lead to a substantial health risk to cyclists due to their high pollutant intake via higher ventilation rates [13], [14] and high levels of physical activity [8], [15]. Researchers have concentrated on assessing actual exposure levels of cyclists on pre-selected routes using personal samplers [16] or inferring personal exposure from measurements of street-level pollution using mobile labs or

fixed-site ambient air monitoring stations [17]. Many studies have also sought to connect particular physiological responses with cyclists' exposure to air pollution and discovered evidence that short-term exposure can result in harmful health effects [18]. One research even found that cyclists absorbed a greater proportion of fine PM2.5 particles and black carbon than drivers of motorized forms of transportation [19].

Despite the discussed findings, municipal authorities in Sofia and other Bulgarian cities fail to take air quality concerns into account when developing and building bike infrastructure. Most of the dedicated cycling lanes in the cities are built on heavy traffic roadways. As a result, more scientific information is needed to describe the air pollution exposure on cyclists and optimize bike routes. This study reviews the development and the evaluation of a tool that proposes optimized cycling routes by calculating the intake dosage of ambient PM. We also emphasized the effects of transportation on air quality and that bike paths should be prioritized on small streets instead of building cycling infrastructure near high-traffic roadways.

After the introduction the rest of the paper is designed as follows. In section 2 we give a brief overview of the methodology used in this study. There is discussed how the software is built, how study routes are selected, who are the participants of this study and how mobile and fixed sensors are used. In addition, it is shown how the inhalation rate and the intake dosage are calculated. In Section 3 we introduce the computational results, analysis, and discussion. Finally, Section 4 presents the conclusions and recommendations for future research.

II. Methodology and instruments

Cities are notorious for their high levels of air pollution and sickness. Transportation, household heating, and industry are considered to be the main sources of air pollution in urban areas. Sofia is situated in a valley, where the two main sources of air pollution are household heating and transportation. The city is one of the most polluted ones in the European Union with high concentrations of particulate matter, especially during the winter season due to household heating during low temperatures and low ventilation as a result of temperature inversions.

Sofia is the capital of Bulgaria with nearly 1.5 million inhabitants. The city has a relatively small bicycle infrastructure with nearly 60 km of cycling paths. This paper describes the development of a software tool that optimizes biking routes by evaluating cyclist air pollution exposure.

A. Study design

An increase in morbidity in Sofia after days of high air pollution was investigated in recent research [20], [21]. On fig. 1 is illustrated the exposure-health effect model on which this study is based. Air pollution concentrations lead to different doses of inhaled polluted air. The doze leads to different health effects. Generally speaking, the higher the dose - the bigger the risk for health effects.

Fig. 1. Exposure - Health effect development

This study discusses the creation of a software tool that aims to select an optimized cycling route that provides the least PM inhalation dose for a cyclist trying to go from point A to point B.

Inhalation Dose (ID) depends on pollutant concentrations, the time, and the Ventilation Rate (VR) [min]. We calculate the inhalation dose by incorporating into the model the PM exposure for each cyclist with biomarkers such as heart rate, and time needed to take each route. The next subsection will provide more depth into the formulas used in the calculation model.

B. Method for calculating ventilation rate and inhalation dose

To calculate cyclist's VR (in L/min), we utilize [22]'s model equation that is based on the Heart Rate (HR) [min] (Eq. (1)).

$$VR = 0.00070724 \times HR^{2.17008537} \tag{1}$$

To determine the amounts of particular matter that are impacting cyclists, we use Eq. (2) [22] to compute the PM inhalation dose for each stretch:

$$PM_{inh} = PM_{conc} \times VR \times time \tag{2}$$

where PM_{inh} (μg) is the mass of pollutants entering cyclists' respiratory tracts over the course of the journey (round trip); PM_{conc} ($\mu g/m^3$) is the median pollutant exposure.

The following formulas (Eq. (1) and Eq. (2)) lead to the following hypothesis: if we want to build a tool that reduces the inhaled dose of PM it should select a track that is:
(1) Fast and short. The lesser the time, the lesser PM_{inh}
(2) Requires less effort. HR is increased during ascending and high speed. Looking for routes with denivelation.
(3) Go through less PM concentrations. Heavy-traffic roads should be skipped. Small streets and parks are preferred.

These formulas (Eq. (1) and Eq. (2)) are also used in the validation of the tool, which will be later discussed. In the next section we examine the path finding algorithms.

C. Path finding algorithms

Path finding algorithms are built on top of graph search algorithms and examine connections between nodes by starting at one node and moving via relationships until they reach their target. These algorithms determine the cheapest route in terms of weight or hops. Weights may be everything that can be measured, including capacity, cost, time, and distance.

As discussed in the previous section, for the purposes of this software, it is required to not enough to compute the shortest path in linear time [23], [24]. In addition, it should present

options that are longer than the shortest way but have different desired characteristics, such as less vehicle traffic and small denivelation. The k-Shortest Paths problem is a straightforward method for calculating alternative routes [25].

In this study, we use an alternative routing, and in particular the k-Shortest Paths with Limited Overlap (k-SPwLO), previously introduced in [26]. The k-SPwLO query seeks paths that are (a) sufficiently distinct from each other and (b) as short as possible. Although the method performs better than a baseline solution that lists pathways in order of increasing length, OnePass is not useful even for medium-sized road networks [27]. For this purpose, we use MultiPass, a more accurate method that, by adding second pruning criteria, expands and enhances OnePass. MultiPass travels the network k-1 times but only evaluates and extends the most promising pathways, in contrast to OnePass, which traverses the road network once and expands only those paths that satisfy the similarity criterion. Pruning is done on any path that cannot lead to a solution.

Let P specifically be a collection of routes on a road network G that connect nodes s and t. A path p' (s→t) is referred to as an "alternative" in P when p' is enough dissimilar to every path p ∈ P. Formally, the overlap ratio between p' and p determines how similar they are:

$$Sim(p', p) = \frac{\sum_{(n_x, n_y) \in p' \cap p} w_{xy}}{l(p)}, \tag{3}$$

where $p' \cap p$ indicates the group of edges that both are shared by p' and p. Given the similarity threshold θ route p' is alternative to set P if $Sim(p', p) \leq \theta$.

Given a source node s and a target node t, a k-SPwLO query provides a collection of k routes from s to t, ordered in increasing length order, such that:
(1) the shortest route p'(s→t) is always included,
(2) all k routes are pairwise dissimilar with regard to the similarity threshold θ, and
(3) all k routes are as short as possible.

This paper uses a new approach to the k-SPwLO. Most of the applications use alternative paths, leaving the final route choice to the user. While in this software we add weights in order to choose the shortest alternative route with the least traffic and smallest denivelation. The following subsection is revealing insights into the software's development.

D. Development of the software tool

The software is developed on a cloud infrastructure and for its development is used free software Python, Django, and GraphQL (for the database). It is connected to gis data providers such as Google maps, Strava, and the route is rendered on Openstreet map.

Firstly, using the pathfinding algorithm described in the previous section, the software is programmed to search for a route that: (1) is the shortest; (2) has the smallest denivelation; and (3) skips heavy-traffic roadways when possible. The calculation model is based on previously mentioned formulas (Eq. (1) and Eq. (2)), which were used for developing the weights for the search algorithm.

After the calculation is done, the software renders the optimized path. To evaluate the model and further improve its search algorithms we designed a tool that combines air quality data from fixed sensors and gis data from the Strava app.

The software uses an aggregation tool that extracts air quality data both from standard instruments and low-cost sensor networks such as Luftdaten, Smog, Openaqi, and many others. It receives, records, cleans, and calibrates the air quality data from fixed low-cost sensors.

Traditionally, concentrations of air emissions have been monitored by air monitoring stations equipped with standard equipment, allowing for highly reliable monitoring results. However, the high costs of equipment and servicing make meeting the demands of high-resolution surveillance and assessing the extent of personal exposure impossible [28], [29]. As the need for more condensed monitoring is gradually increasing, low-cost air quality sensors have been widely used in air monitoring in recent years due to the benefits of low cost, low power usage, quick operation, and rapid response [30]. As a result, environmental monitoring stations are often sparsely dispersed, resulting in observations with inadequate geographical resolution. Low-cost air quality monitors have recently been developed as an option that can increase monitoring granularity. However, using low-cost air quality monitors comes with a number of drawbacks: They are impacted by cross-sensitivities between different ambient contaminants, as well as external variables such as traffic, weather fluctuations, and human activity, and their accuracy declines with time.

To mitigate the above-mentioned drawbacks of fixed low-cost sensors we calibrate the data from them. We examine both the data from environmental monitoring stations and the Luftdaten network of low-cost sensors. To calibrate the data from low-cost sensors and increase its reliability we use the [31]'s two-step calibration method that utilizes artificial neural networks and anomaly detection.

After the selection, the two study routes are evaluated through mobile and fixed sensors.

E. Study routes

The two study routes start from the national stadium Vasil Levski and end up at Pette kiosheta, two spots in the center of Sofia with active cycling flow.

The two study routes are in the center of Sofia and are picked so they can meet the following criteria:

(1) should have the same start and end points;

(2) one of the routes to be on the dedicated bike lane, while the other is the proposed from the software (short; low denivelation; follows small streets);

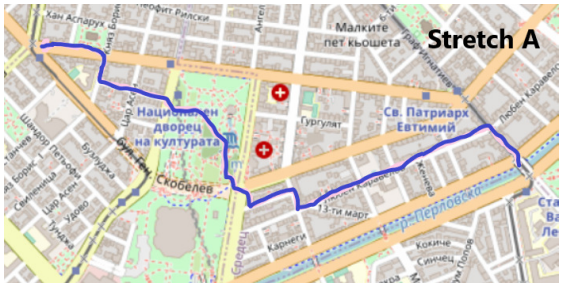

Fig. 2. Stretch A - suggested by our software as it searches the least inhalation dose

Fig. 3. Stretch B - suggested by the majority of navigation softwares as it is on a dedicated bike lane

(3) the routes should be actively used by cyclists;

(4) both routes pass nearby fixed sensors from the Luftdaten network;

Stretch A (fig.2) is the optimized cycling route that is suggested by the software tool and software point that goes on the shortest path through small central streets and parks, while Stretch B (fig.3) uses the developed cycling infrastructure (that mainly includes cycling near heavy-traffic roadways), it is longer in distance and is suggested by the navigation software due to the dedicated bike lanes.

The tool also evaluates the routes using mobile and fixed sensors for gathering air quality data. In the next section is described the implication of mobile sensors.

F. Measuring PM exposure with wearable mobile devices

Low-cost wearable pollution sensors are inexpensive environmental monitoring devices that people can carry or wear while going about their daily activities. Because they detect pollution levels directly and in real time, they may allow health providers and researchers to monitor individual-level exposures and empower citizens to manage their personal exposure to pollutants beyond what regulatory monitors can do [32].

For this study, PM1, PM2.5, temperature, and relative humidity are measured by AirBeam2. To quantify particle matter, AirBeam2 employs a light scattering approach. Light from a laser scatters off particles in the airstream as air is pulled through a sensor chamber. A detector registers the light scatter and converts it into a value that estimates the number of particles in the air. When recording a mobile session, these measures are sent to the AirCasting Android app via Bluetooth once per second.

The tests are conducted by 10 study participants. The mobile equipment was connected to the front of each bicycle, allowing the sampling lines to catch pollutants without being obstructed; it was also braced at the bottom to reduce vibration. Round trips were made on working days in the morning during High Traffic (HT) hours (8:00–9:30 h) and Low Traffic (LT) hours (10:30–12:00 h) and during the Non-Working Days (NWD): weekends and holidays.

G. Participants

We recruited 10 people (ages 27–41) by word of mouth and contact with a local cycling network (8 males and 2 females). Prior to study enrolment, subjects completed a preliminary screening survey. Exclusion criteria included respiratory (including asthma), cardiovascular, or other chronic illnesses, as well as smoking (current or recent). We only enrolled those who were already frequent riders in Sofia.

These factors were utilized to reduce the risk of harm from unfamiliarity with streets in Sofia or inexperience with riding, as well as adverse acute health effects. Further, the participants were asked to restraint from alcohol and caffeine for 48 hours before the tests. The 10 participants performed round trips on the two stretches during the HT, LT, and NWD.A certified pulmonologist (one of the coauthors) taught the project participants how to identify their Heart Rate (HR) [HB]/min using a pulse oximeter. In addition, the HR was tracked during cycling by a smart wrist.

III. Results

A. PM1 and PM2.5 concentrations from Mobile measurements

Table 1 shows the minimum, maximum, and median of PM1 and PM2.5 concentrations for the two examined stretches on working days during HT. The concentrations for ultrafine particles with a diameter below 1 micron (PM1) were measured in a range between 8 and 24 μg /m3 (mean 11 μg /m3) for Stretch A and between 8 and 41 μg /m3 (mean 14 μg /m3) for Stretch B. The concentrations for fine particles under 2.5 microns (PM2.5) are between 12 and 29 μg /m3 (mean 15 μg /m3) for Stretch A and between 12 and 45 μg /m3 (mean 19 μg /m3) for Stretch B.

Table 2 are presented the PM1 and PM2.5 concentrations for Stretch A and B on working days during LT. Measurements from Stretch A show lower concentration levels both for PM1 and PM2.5. The concentrations for ultrafine particles with diameter below 1 micron (PM1) was measured between 6 and 19 μg /m3 (mean 10 μg /m3) for Stretch A and between 5 and 34 μg /m3 (mean 12 μg /m3) for Stretch B. The concentrations for fine particles under 2.5 microns (PM2.5) are between 10 and 24 μg /m3 (mean 13 μg /m3) for Stretch A and between 9 and 38 μg /m3 (mean 15 μg /m3) for Stretch B.

Table 3 illustrates the minimum, maximum, and median of PM1 and PM2.5 concentrations for the two examined stretches during weekends and holidays. Measurements for Stretch A

TABLE I
PM1 AND PM2.5 CONCENTRATIONS FROM MOBILE MEASUREMENTS ON WORKING DAYS DURING HT

Routes	**PM1**			**PM2.5**		
	min	max	mean	min	max	mean
Stretch A	8	24	11	12	29	15
Stretch B	8	41	14	12	45	19

TABLE II
PM1 AND PM2.5 CONCENTRATIONS FROM MOBILE MEASUREMENTS ON WORKING DAYS DURING LT

Routes	**PM1**			**PM2.5**		
	min	max	mean	min	max	mean
Stretch A	6	19	10	10	24	13
Stretch B	5	34	12	9	38	15

TABLE III
PM1 AND PM2.5 CONCENTRATIONS FROM MOBILE MEASUREMENTS DURING WEEKENDS AND HOLIDAYS

Routes	**PM1**			**PM2.5**		
	min	max	mean	min	max	mean
Stretch A	3	7	4	4	11	7
Stretch B	3	8	4	5	11	7

show nearly the same lower concentration levels for PM1 and PM2.5. The concentrations for PM1 are between 3 and 7 μg /m3 (mean 4 μg /m3) for Stretch A and between 3 and 8 μg /m3 (mean 4 μg /m3) for Stretch B. The concentrations for PM2.5 are between 4 and 11 μg /m3 (mean 7 μg /m3) for Stretch A and between 5 and 11 μg /m3 (mean 7 μg /m3) for Stretch B.

Despite the fact that the dedicated cycling route is rather open, the high volume of cars, buses, and trucks in this corridor is the primary cause of elevated pollution concentrations. As a result, PM2.5 concentrations were similar during weekends, but with nearly 20% higher concentrations between the two routes during working days.

B. Ventilation rate

To measure the Ventilation Rate (VR), we took measurements of the Heart Rate (HR), oxygen saturation (SpO2), and Respiratory Rate (RR) of each project participant. Each parameter's mean has a modest level of variability and the final results for the VR are presented in Table 4. There were no differences observed in these three factors on whether the route was taken on a working day or a non-working day, as they are not affected directly by traffic or different levels of short-term air pollution exposure. The speed and denivelation data are shown in the table were taken from the developed software tool thanks to the Strava API integration.

Despite the same start and end points different distances and Stretch A was shorter 3.8 km compared to 4.4 km of Stretch B and was faster 15:52 min compared to 18:04 of Stretch B. The values were rather constant during working and non-working days. The dedicated cycling route had longer straight corridors with fewer intersections and crossroads that lead to higher maximum and average speeds. Also, Stretch B has a higher denivelation - 15m compared to 3m in Stretch A. All these data findings lead to an increased the VR of the cyclists on Stretch B - 11.06 L/min, compared to 10.14 L/min for Stretch A.

Table 5 are shown the results of the cyclists' inhalation doze for PM1 and PM2.5. They are calculated based on the mean value of PM exposure during the round trip, measured by mobile sensors, together with the time needed to take it and the VR for each cyclist.

Stretch B shows an increased inhalation as it takes a longer time to complete the round trip, takes more effort, and the cyclist is exposed to higher PM concentrations due to vehicle exhausts. Even during the weekends when PM concentrations were similar on the two routes - Stretch B showed higher inhalation dozes due to the prolonged time and higher ventilation rate (higher denivelation, higher average speed).

The measurements for SpO2 and RR did not show any particular short-term health effects. This was expected as participants in the study, due to safety reasons, were non-smokers, without chronic illnesses, and regular cyclists. This does not mean that people with chronic illnesses and sensitivity to air pollution might not receive some symptoms or irritations as some studies observe [2], [3].

C. Rendering cycling routes and incorporating data from fixed sensors

To demonstrate the technology for our fixed sensors that we developed, in this study we are using Luftdaten fixed low-cost sensors. It is a citizen science project in which the air stations are adopted and maintained by citizens and situated on their balconies. Sofia has a dense mesh of over 300 low-cost air

TABLE IV
FIELD MEASUREMENTS

	Stretch A	**Stretch B**
VR (L/min)	10.14	11.06
HR (beats/min)	82.30	85.66
Denivelation gained (m)	3	15
Avg. Speed (km/h)	14.3	14.7

TABLE V
PM1 AND PM2.5 INHALATION DOZE DURING THE ROUNDS

Period	**Pollutant**	**Stretch A (optimized)**	**Stretch B (cycling lanes)**
High Traffic	$PM1_{inh}$	29.74	46.45 (↑56%)
	$PM2.5_{inh}$	40.56	63.04 (↑55%)
Low Traffic	$PM1_{inh}$	27.04	39.82 (↑47%)
	$PM2.5_{inh}$	35.15	49.77 (↑42%)
Non-Working Days	$PM1_{inh}$	10.82	13.27 (↑23%)
	$PM2.5_{inh}$	18.93	23.23 (↑23%)

Fig. 4. Cycling route exposure from fixed sensors

quality stations from the Luftdaten network providing spatial and temporal resolution for PM2.5 and PM10 concentrations.

On fig.4 can be seen the concentrations for stretch B during LT where measurements from fixed sensors in a vicinity of 200m or closer to the route are applied on the stretch. The rendered route shows exactly where the participants in the survey have passed thanks to the gis integration of Strava and Openstreetmap APIs. The black colored line means that there is no fixed sensor in this part of the route that is closer than 200m, while the green and yellow colored lines represent the concentrations measured by the fixed sensors nearby. For concentration values of PM2.5 between 0 and 12 - green color is used, while yellow color stands for values of PM2.5 between 12 and 35. These color categories are inspired by the EPA's air quality index and are the same for visualizing the Aircasting routes measured with the wearable sensors.

Thanks to Sofia's dense mesh of low-cost sensors, 5 fixed sensors are used for stretch A and 6 sensors for stretch B as they pass the selection criteria. By comparing data from mobile sensors, we investigated that (1) Luftdaten's fixed sensors, especially if not located exactly on the route, cannot find ultralocal peaks in PM and failed to identify the zone with the most heavy-traffic and PM concentration; and (2) the sensors also cannot identify temporal exposure such as passing next to a bus, a truck, or a moped, while mobile sensors detect it very successfully. The main reason for these two findings is that Luftdaten's sensors are situated on quiet streets and are not transmitting air quality data every second.

The authors suggest a more dense mesh of air quality sensors on heavy-traffic roads in cities to mitigate the above-mentioned issues. They could be attached or integrated next to traffic lights or street lamps. This will bring accuracy in quantifying PM exposure, especially in potentially hazardous locations.

The created tool can dynamically change values for air pollution and can render the same route in different time frames and respectively different air pollution concentrations. The software can find implementation for selecting pedestrian routes as well, yet it will have more impact on finding bike routes due to cyclists' higher ventilation and often proximity to vehicle exhaust.

IV. CONCLUSION AND FUTURE RESEARCH

This study presented the development of a software tool that optimizes cycling paths based on algorithms that predict the least harmful air pollutants. The algorithm is a new implementation of alternative routing and in particular the k-Shortest Paths with Limited Overlap. It is based on experimental data and equations that calculate the total inhaled dose of pollutants by a cyclist. Together with this, in the study was evaluated through two cycling routes: Stretch A - suggested by the newly developed software; that goes through small streets in Sofia, and Stretch B - suggested by navigation apps; that goes along a designated bicycle lane. Ten cyclists are making round trips on the two routes during 3 periods: (1) high traffic and (2) low traffic on working days and (3) during non-working days. Based on the data gathered in the study are calculated the cyclists' exposure and potential inhalation dose to PM1 and PM2.5 pollution on the two routes.

Exposure concentrations on bicycle lanes happened to be higher than the optimized track's exposure levels, especially on working days. Even in cases when the mean concentrations were nearly equal, the inhalation dose for the cyclist was always greater on the bike lane route as it is longer in time and distance, with higher denivelation, and requires more intensive cycling. By choosing the optimized cycle track, the inhalation dose of PM1 is reduced with 23% on non-working days to 56% (55% for PM2.5) during high traffic on working days. The results show that there is an enhanced risk to the health of cyclists using the studied bicycle paths during working days when traffic-related pollutants.

The outcomes of this study and the developed tool are useful to medical experts, cyclists, and pedestrians. They prove that optimization of mobility and taking data-driven decisions can reduce air pollution exposure. In addition, the research implications can be useful to policymakers and environmental specialists. The results of this study build on previous findings [33] that suggest that redesigning streets for low-speed multimodal traffic without barriers is a more sustainable and pragmatic approach than building cycling infrastructure on high-traffic roadways. In the studied bicycle lanes, cyclist exposure to PM was closely linked to vehicular traffic because the study is not performed during the heating season and there is a significant difference between low-traffic and high-traffic tests. Bicycle lanes with no physical barriers between the bicycle route and the road have higher exposure, a conclusion which is found in another study [34]. Our findings contribute to a better understanding of Sofia's traffic-related pollution issues and emphasize the importance of taking air quality into account when developing and constructing cycle paths in Bulgarian cities.

This study focused on the most problematic urban polluters - fine and ultrafine PM. Further studies will be beneficial in including data for other vehicle-related pollutants such as black carbon and NO2 emissions. In addition, it is useful to analyze the particulate matter from automotive emissions with chemical analysis and further detect the various metals in PM. The integration of more mobile and fixed sensors on high-traffic roadways and using of the software tool from this study will further improve the understanding of transport-related air pollution and reduce exposure.

ACKNOWLEDGMENT

The authors would like to thank air.bg, luftdaten.info, LL-Cloud, AirLief, Aircasting, Air for Health, and Air Solutions for cooperating with data for this research. The work is supported by the National Scientific Fund of Bulgaria under the grant DFNI KP-06-N52/5.

REFERENCES

[1] M. Kampa and E. Castanas, "Human health effects of air pollution," *Environmental pollution*, vol. 151, no. 2, pp. 362–367, 2008.

[2] X. Qin, L. Hou, J. Gao, and S. Si, "The evaluation and optimization of calibration methods for low-cost particulate matter sensors: Inter-comparison between fixed and mobile methods," *Science of The Total Environment*, vol. 715, p. 136791, 2020.

[3] A. J. Cohen, M. Brauer, R. Burnett, H. R. Anderson, J. Frostad, K. Estep, K. Balakrishnan, B. Brunekreef, L. Dandona, R. Dandona *et al.*, "Estimates and 25-year trends of the global burden of disease attributable to ambient air pollution: an analysis of data from the global burden of diseases study 2015," *The Lancet*, vol. 389, no. 10082, pp. 1907–1918, 2017.

[4] C. A. Pope III and D. W. Dockery, "Health effects of fine particulate air pollution: lines that connect," *Journal of the air & waste management association*, vol. 56, no. 6, pp. 709–742, 2006.

[5] J. C. Chow, "Measurement methods to determine compliance with ambient air quality standards for suspended particles," *Journal of the Air & Waste Management Association*, vol. 45, no. 5, pp. 320–382, 1995.

[6] M. Pratt, O. L. Sarmiento, F. Montes, D. Ogilvie, B. H. Marcus, L. G. Perez, R. C. Brownson, L. P. A. S. W. Group *et al.*, "The implications of megatrends in information and communication technology and transportation for changes in global physical activity," *The Lancet*, vol. 380, no. 9838, pp. 282–293, 2012.

[7] C. M. de Chardon, "The contradictions of bike-share benefits, purposes and outcomes," *Transportation research part A: policy and practice*, vol. 121, pp. 401–419, 2019.

[8] A. Y. Bigazzi and M. A. Figliozzi, "Review of urban bicyclists' intake and uptake of traffic-related air pollution," *Transport Reviews*, vol. 34, no. 2, pp. 221–245, 2014.

[9] A. De Nazelle, O. Bode, and J. P. Orjuela, "Comparison of air pollution exposures in active vs. passive travel modes in european cities: A quantitative review," *Environment international*, vol. 99, pp. 151–160, 2017.

[10] S. Xie, J. R. Meeker, L. Perez, W. Eriksen, A. Localio, H. Park, A. Jen, M. Goldstein, A. F. Temeng, S. M. Morales *et al.*, "Feasibility and acceptability of monitoring personal air pollution exposure with sensors for asthma self-management," *Asthma research and practice*, vol. 7, no. 1, pp. 1–11, 2021.

[11] S. Reis, T. Liška, M. Vieno, E. J. Carnell, R. Beck, T. Clemens, U. Dragosits, S. J. Tomlinson, D. Leaver, and M. R. Heal, "The influence of residential and workday population mobility on exposure to air pollution in the uk," *Environment international*, vol. 121, pp. 803–813, 2018.

[12] M. Hauptman, J. M. Gaffin, C. R. Petty, W. J. Sheehan, P. S. Lai, B. Coull, D. R. Gold, and W. Phipatanakul, "Proximity to major roadways and asthma symptoms in the school inner-city asthma study," *Journal of Allergy and Clinical Immunology*, vol. 145, no. 1, pp. 119–126, 2020.

[13] M. Zuurbier, G. Hoek, M. Oldenwening, V. Lenters, K. Meliefste, P. Van Den Hazel, and B. Brunekreef, "Commuters' exposure to particulate matter air pollution is affected by mode of transport, fuel type, and route," *Environmental health perspectives*, vol. 118, no. 6, pp. 783–789, 2010.

[14] W. Ham, A. Vijayan, N. Schulte, and J. D. Herner, "Commuter exposure to pm2. 5, bc, and ufp in six common transport microenvironments in sacramento, california," *Atmospheric Environment*, vol. 167, pp. 335–345, 2017.

[15] H.-Y. Park, S. Gilbreath, and E. Barakatt, "Respiratory outcomes of ultrafine particulate matter (ufpm) as a surrogate measure of near-roadway exposures among bicyclists," *Environmental Health*, vol. 16, no. 1, pp. 1–7, 2017.

[16] A. De Nazelle, M. J. Nieuwenhuijsen, J. M. Antó, M. Brauer, D. Briggs, C. Braun-Fahrlander, N. Cavill, A. R. Cooper, H. Desqueyroux, S. Fruin *et al.*, "Improving health through policies that promote active travel: a review of evidence to support integrated health impact assessment," *Environment international*, vol. 37, no. 4, pp. 766–777, 2011.

[17] L. I. Panis, B. de Geus, G. Vandenbulcke, H. Willems, B. Degraeuwe, N. Bleux, V. Mishra, I. Thomas, and R. Meeusen, "Exposure to particulate matter in traffic: a comparison of cyclists and car passengers," *Atmospheric Environment*, vol. 44, no. 19, pp. 2263–2270, 2010.

[18] S. Weichenthal, R. Kulka, A. Dubeau, C. Martin, D. Wang, and R. Dales, "Traffic-related air pollution and acute changes in heart rate variability and respiratory function in urban cyclists," *Environmental health perspectives*, vol. 119, no. 10, pp. 1373–1378, 2011.

[19] M. A. Hernández, O. Ramírez, J. A. Benavides, and J. F. Franco, "Urban cycling and air quality: Characterizing cyclist exposure to particulate-related pollution," *Urban Climate*, vol. 36, p. 100767, 2021.

[20] S. Fidanova, P. Zhivkov, and O. Roeva, "Intercriteria analysis applied

on air pollution influence on morbidity," *Mathematics*, vol. 10, no. 7, p. 1195, 2022.

[21] P. Zhivkov and A. Simidchiev, "Quantitative relationship between particulate matter and morbidity," in *International Conference on Large-Scale Scientific Computing*. Springer, 2021, pp. 275–283.

[22] I. D. Do Vale, A. S. Vasconcelos, and G. O. Duarte, "Inhalation of particulate matter in three different routes for the same od pair: A case study with pedestrians in the city of lisbon," *Journal of Transport & Health*, vol. 2, no. 4, pp. 474–482, 2015.

[23] H. Bast, D. Delling, A. Goldberg, M. Müller-Hannemann, T. Pajor, P. Sanders, D. Wagner, and R. F. Werneck, "Route planning in transportation networks," in *Algorithm engineering*. Springer, 2016, pp. 19–80.

[24] L. Wu, X. Xiao, D. Deng, G. Cong, A. D. Zhu, and S. Zhou, "Shortest path and distance queries on road networks: An experimental evaluation," *arXiv preprint arXiv:1201.6564*, 2012.

[25] E. Q. Martins and M. Pascoal, "A new implementation of yen's ranking loopless paths algorithm," *Quarterly Journal of the Belgian, French and Italian Operations Research Societies*, vol. 1, no. 2, pp. 121–133, 2003.

[26] T. Chondrogiannis, P. Bouros, J. Gamper, and U. Leser, "Alternative routing: k-shortest paths with limited overlap," in *Proceedings of the 23rd SIGSPATIAL International Conference on Advances in Geographic Information Systems*, 2015, pp. 1–4.

[27] ——, "Exact and approximate algorithms for finding k-shortest paths with limited overlap," in *20th International Conference on Extending Database Technology: EDBT 2017*, 2017, pp. 414–425.

[28] P. Mouzourides, P. Kumar, and M. K.-A. Neophytou, "Assessment of long-term measurements of particulate matter and gaseous pollutants in south-east mediterranean," *Atmospheric Environment*, vol. 107, pp. 148–165, 2015.

[29] J. Y. Chin, T. Steinle, T. Wehlus, D. Dregely, T. Weiss, V. I. Belotelov, B. Stritzker, and H. Giessen, "Nonreciprocal plasmonics enables giant enhancement of thin-film faraday rotation," *Nature communications*, vol. 4, no. 1, pp. 1–6, 2013.

[30] Y. Wang, J. Li, H. Jing, Q. Zhang, J. Jiang, and P. Biswas, "Laboratory evaluation and calibration of three low-cost particle sensors for particulate matter measurement," *Aerosol Science and Technology*, vol. 49, no. 11, pp. 1063–1077, 2015.

[31] P. Zhivkov, "Optimization and evaluation of calibration for low-cost air quality sensors: Supervised and unsupervised machine learning models," in *2021 16th Conference on Computer Science and Intelligence Systems (FedCSIS)*. IEEE, 2021, pp. 255–258.

[32] S. Xie and B. E. Himes, "Personal environmental monitoring," in *Precision in Pulmonary, Critical Care, and Sleep Medicine*. Springer, 2020, pp. 305–320.

[33] E. Barnes and M. Schlossberg, "Improving cyclist and pedestrian environment while maintaining vehicle throughput: Before-and after-construction analysis," *Transportation research record*, vol. 2393, no. 1, pp. 85–94, 2013.

[34] C. M. Kendrick, A. Moore, A. Haire, A. Bigazzi, M. Figliozzi, C. M. Monsere, and L. George, "Impact of bicycle lane characteristics on exposure of bicyclists to traffic-related particulate matter," *Transportation research record*, vol. 2247, no. 1, pp. 24–32, 2011.

Communication Papers of the of the 17th Conference on Computer Science and Intelligence Systems pp. 113–116
DOI: 10.15439/2022F221
ISSN 2300-5963 ACSIS, Vol. 32

Dirichlet's principle revisited: An inverse Dirichlet's principle definition and its bound estimation improvement using stochastic combinatorics

Lubomír Štěpánek
Department of Statistics and Probability
Faculty of Informatics and Statistics
Prague University of Economics and Business
nám. W. Churchilla 4, 130 67 Prague, Czech Republic
lubomir.stepanek@vse.cz

Filip Habarta
Department of Statistics and Probability
Faculty of Informatics and Statistics
Prague University of Economics and Business
nám. W. Churchilla 4, 130 67 Prague, Czech Republic
filip.habarta@vse.cz

Ivana Malá
Department of Statistics and Probability
Faculty of Informatics and Statistics
Prague University of Economics and Business
nám. W. Churchilla 4, 130 67 Prague, Czech Republic
malai@vse.cz

Luboš Marek
Department of Statistics and Probability
Faculty of Informatics and Statistics
Prague University of Economics and Business
nám. W. Churchilla 4, 130 67 Prague, Czech Republic
marek@vse.cz

***Abstract*—Dirichlet's principle, also known as a pigeonhole principle, claims that if $n \in \mathbb{N}$ item are put into $m \in \mathbb{N}$ containers, with $n > m$, then there is a container that contains more than one item. In this work, we focus rather on an inverse Dirichlet's principle (by switching items and containers), which is as follows: considering $n \in \mathbb{N}$ items put in $m \in \mathbb{N}$ containers, when $n < m$, then there is at least one container with no item inside. Furthermore, we refine Dirichlet's principle using discrete combinatorics within a probabilistic framework. Applying stochastic fashion on the principle, we derive the number of items n may be even greater than or equal to m, still very likely having one container without an item. The inverse definition of the problem rather than the original one may have some practical applications, particularly considering derived effective upper bound estimates for the items number, as demonstrated using some applied mini-studies.**

I. Introduction

WHILE the Dirichlet's principle is applied in various fields such as number theory and calculus [1], data compression [2], quantum mechanics [3] and many others, in this work, we focus only on the original definition in a pure discrete fashion, and mainly on a derived, inverse form. The original version of the Dirichlet's principle [4] claims that if there are more items than containers so that the items are put into the containers, then there is at least one container containing two or more items. Thus, due to the idea's relative simplicity, applications of the original Dirichlet's principle are usually limited to rather fancy problems coming from recreational mathematics.

Within the paper, going further, we refine the original Dirichlet's principle in an inverse form: when there are fewer items than containers and put inside them, there is at least one container with no items inside.

The estimate of a maximum number of items lower than the number of containers is relatively poor in a stochastic fashion, though. The inverse definition enables applying the pigeonhole principle to some real-world situations and helps solve them effectively. We demonstrate how the stochastic approach to inverse Dirichlet's principle, together with combinatorial calculations of probabilities, helps to get more effective estimates for selected problem parameters, as indicated above. To be more specific, we applied stochastic-based inverse Dirichlet's principle to a real-world situation called *an unoccupied doubleseat problem*, originated by the paper's authors, where an individual wants to know a probability of an unoccupied doubleseat in a row of doubleseats when booking their seat. The inverse Dirichlet's principle would return a relatively poor estimate of a maximum number of individuals who booked their seats so far, ensuring there should be at least one unoccupied doubleseat. However, the probabilistic approach can show a substantially significant probability of an unoccupied doubleseat even for more already booking individuals than estimated using the pigeonhole principle.

II. An inverse Dirichlet's principle definition and stochastic combinatorial approach to selected applications of the principle

A. An inverse Dirichlet's principle definition

Assuming there are $n \in \mathbb{N}$ items put into $m \in \mathbb{N}$ containers, with $n < m$, then there is for sure at least one container with no items inside it.

A *proof*, built by contradiction, is clear and as follows. Suppose that each of $m \in \mathbb{N}$ containers contains at least one of all $n \in \mathbb{N}$ items inside, with $n < m$. Then there is minimally

$m \cdot 1 = m$ items, which is in contradiction with the assumption of $n < m$ items. □

We apply the inverse version of Dirichlet's principle to a real-world inspired problem called *an unoccupied doubleseat problem*, where an individual wants to know how likely there is an unoccupied doubleseat in a row of k of them (*containers*) when n individuals (*items*) randomly occupied the seats before him. Moreover, we show that Dirichlet's principle can be replaced by a stochastic approach, estimating the same output as the inverse pigeonhole principle, i. e. a maximum number of items so that there is (likely) an unoccupied container[1].

B. An unoccupied doubleseat problem

Let us assume we have a row of $k \in \mathbb{N}$ doubleseats[2] as in Fig. 1 and $n \in \mathbb{N} \cup \{0\}$ individuals who have randomly occupied n of the seats, one seat per individual, with $0 \leq n \leq 2k$. If there is a newcomer who would like to sit down on one of the seats not occupied so far, what is the probability that there is at least one unoccupied[3] doubleseat in the row[4]?

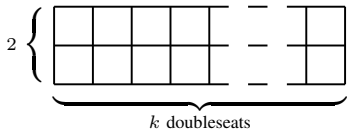

Fig. 1. A row of $k \in \mathbb{N}$ doubleseats, used in the *unoccupied doubleseat problem*.

1) A solution by the inverse Dirichlet's principle: The pigeonhole principle is limited to offering only a discrete solution. When the newcomer wants to know how likely there are one or more unoccupied doubleseats, assuming there are $2k$ seats in total, arranged as k doubleseats (*containers*), and n seats are already occupied (*items*). Applying the Dirichlet's principle, when there are $n < k$ individuals taking the seats, there must be at least one unoccupied doubleseat. Otherwise, if there are $n \geq k$ individuals occupying the seats, no one can assure whether there are one or more free doubleseats. For $n > 2k-2$ sitting individuals, there is for sure no unoccupied doubleseat.

2) A solution by a combinatorial stochastic approach: Let us mark as p a probability there is at least one unoccupied doubleseat, assuming a row of k doubleseats and n randomly sitting individuals at the moment, $0 \leq n \leq 2k$. When $0 \leq n \leq k-1$, then obviously, as claimed above, $p = 1$. For $k \leq n \leq 2k$, we get

$$\begin{aligned} p &= P(\geq 1 \text{ unoccupied doubleseat} \mid k \leq n \leq 2k) = \\ &= 1 - P(0 \text{ unoccupied doubleseat} \mid k \leq n \leq 2k). \end{aligned} \quad (1)$$

[1]Somewhat similar problem, bur using rather the original Dirichlet's principle, not the inverse one, is so-called birthday problem, [5].

[2]For example, in a bus, a train, or a plane.

[3]I. e., both seats of such a doubleseat are unoccupied.

[4]Newcomers, particularly when alone, prefer to sit down on an unoccupied doubleseat to not sitting next to someone other.

The term $P(0 \text{ unoccupied doubleseat} \mid k \leq n \leq 2k)$ in formula (1) could be estimated as follows – since the first n individuals take their seats randomly, we may assume

$$\begin{aligned} p &= P(\geq 1 \text{ unoccupied doubleseat} \mid k \leq n \leq 2k) = \\ &= 1 - P(0 \text{ unoccupied doubleseat} \mid k \leq n \leq 2k) = \\ &= 1 - \frac{N}{M}. \end{aligned} \quad (2)$$

While the denominator M of the term $1-p$ is straightforward, since a number of all ways how $2k$ seats can by taken by n individuals is equal to $M = \binom{2k}{n}$, the numerator N is tricky.

Assuming there is no unoccupied doubleseat, each of k doubleseats is occupied by one or two of n individuals. Thus $n-k$ doubleseats must be fully occupied, while $k-(n-k) = 2k-n$ doubleseats are occupied only by one individual. The number of ways $n-k$ doubleseats of k in total are fully occupied, is equal to $\binom{k}{n-k}$, while the number of ways $2k-n$ doubleseats are occupied only by one individual is 2^{2k-n}. In total, the numerator N of the $1-p$ term, i. e. number of ways how one or both seats per each of k doubleseats are taken by n individuals, is equal to $N = \binom{k}{n-k} \cdot 2^{2k-n}$. Putting things together, we improve formula (2) as

$$\begin{aligned} p &= P(\geq 1 \text{ unoccupied doubleseat} \mid k \leq n \leq 2k) = \\ &= 1 - P(0 \text{ unoccupied doubleseat} \mid k \leq n \leq 2k) = \\ &= 1 - \frac{N}{M} = \\ &= 1 - \frac{\binom{k}{n-k} \cdot 2^{2k-n}}{\binom{2k}{n}}. \end{aligned} \quad (3)$$

What is worth mentioning is the probability p, i. e., there are one or more unoccupied doubleseats for n already sitting individuals, is close to 1.0 even for values $n > k-1$, as we can see in Table I and Fig. 2.

TABLE I
MAXIMUM NUMBERS n OF ALREADY SITTING INDIVIDUALS THAT STILL ENSURE THERE IS ONE OR MORE UNOCCUPIED DOUBLESEAT WITH THE PROBABILITY p FOR GIVEN TOTAL NUMBER k OF DOUBLESEATS.

$k = 10$		$k = 20$		$k = 30$	
p	n	p	n	p	n
1.00	9	1.00	19	1.00	29
> 0.99	10	> 0.99	24	> 0.99	40
> 0.95	11	> 0.95	26	> 0.95	43
> 0.90	12	> 0.90	28	> 0.90	45
> 0.80	13	> 0.80	29	> 0.80	47

3) A lower bound for the probability estimate coming from the combinatorial stochastic approach: Considering formula (3), one may try to derive a lower bound for the probability there are one or more unoccupied doubleseats in a row of $k \in \mathbb{N}$ doubleseats, assuming $n \in \mathbb{N} \cup \{0\}$ seats are already occupied. However, before the lower bound construction, we introduce some lemmas to be applied.

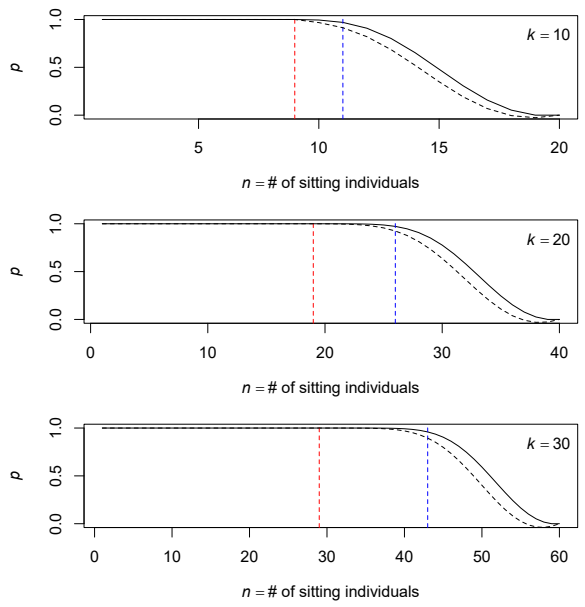

Fig. 2. Maximum numbers n of already sitting individuals that still ensure there is one or more unoccupied doubleseats with the probability p for given total number k of doubleseats. There are estimates of maximum n ensuring ≥ 1 unoccupied doubleseat by the inverse Dirichlet's principle (the red dashed line) and by the stochastic refining of the Dirichlet's principle (the blue dashed line, with $p > 0.95$). The black dashed line stands for the lower bound of the probability estimate.

Lemma. Assuming real numbers $0 < d < r \leq s$, a fraction $\frac{r}{s}$ is greater than or equal to a fraction $\frac{r-d}{s-d}$, i. e. $\frac{r}{s} \geq \frac{r-d}{s-d}$.

Proof. Since $r \leq s$, it is also $rd \leq sd$ and $-rd \geq -sd$, and, eventually, $rs - rd \geq rs - sd$. Thus, if $rs - rd \geq rs - sd$, it is also $r(s-d) \geq s(r-d)$, and since $r - d > 0$ and $s - d > 0$, it is also $\frac{r}{s} \geq \frac{r-d}{s-d}$. □

Lemma. Assuming real numbers $0 < d_i < r \leq s$ for $\forall i \in \{1, 2, \ldots, m\}$, it is

$$\prod_{i=1}^{m} \frac{(r-d_i)(r+d_i)}{(s-d_i)(s+d_i)} \leq \left(\frac{r}{s}\right)^{2m}. \tag{4}$$

Proof. Considering the previous lemma, it is obviously $\frac{r^2-d_i^2}{s^2-d_i^2} \leq \frac{r^2}{s^2}$ for $\forall i \in \{1, 2, \ldots, m\}$, thus, it is also $\prod_{i=1}^{m} \frac{r^2-d_i^2}{s^2-d_i^2} \leq \left(\frac{r^2}{s^2}\right)^m = \left(\frac{r}{s}\right)^{2m}$, and, finally, by reformulation, it is $\prod_{i=1}^{m} \frac{(r-d_i)(r+d_i)}{(s-d_i)(s+d_i)} \leq \left(\frac{r}{s}\right)^{2m}$. □

Let us now derive a lower bound for the probability in formula (3). We get

$$\begin{aligned}
p &= 1 - P(0 \text{ unoccupied doubleseat} \mid k \leq n \leq 2k) = \\
&= 1 - \frac{\binom{k}{n-k} \cdot 2^{2k-n}}{\binom{2k}{n}} = \\
&= 1 - \frac{\frac{k!}{(n-k)!(2k-n)!}}{\frac{(2k)!}{n!(2k-n)!}} \cdot 2^{2k-n} = \\
&= 1 - \frac{n!k!}{(n-k)!(2k)!} \cdot 2^{2k-n} = \\
&= 1 - \frac{n!}{(n-k)!} \frac{k!}{(2k)!} \cdot 2^{2k-n} = \\
&= 1 - \underbrace{\frac{n(n-1)\cdots(n-k+1)}{2k(2k-1)\cdots(2k-k+1)}}_{k \text{ terms}} \cdot 2^{2k-n} = \\
&= 1 - \frac{(\eta+\lambda)(\eta+\lambda-1)\cdots\eta\cdots(\eta-\lambda+1)(\eta-\lambda)}{(\kappa+\lambda)(\kappa+\lambda-1)\cdots\kappa\cdots(\kappa-\lambda+1)(\kappa-\lambda)} \cdot 2^{2k-n},
\end{aligned}$$

where $\eta = n - \frac{k-1}{2}$, $\kappa = 2k - \frac{k-1}{2}$ and $\lambda = \frac{k-1}{2}$. Applying the formula (4), we get

$$\prod_{i=0}^{(k-1)/2} \frac{(\eta - (\lambda - i))\,(\eta + (\lambda - i))}{(\kappa - (\lambda - i))\,(\kappa + (\lambda - i))} \leq \left(\frac{\eta}{\kappa}\right)^k,$$

so,

$$\begin{aligned}
p &= 1 - P(0 \text{ unoccupied doubleseat} \mid k \leq n \leq 2k) = \\
&= 1 - \frac{(\eta+\lambda)(\eta+\lambda-1)\cdots\eta\cdots(\eta+\lambda-1)(\eta+\lambda)}{(\kappa+\lambda)(\kappa+\lambda-1)\cdots\kappa\cdots(\kappa+\lambda-1)(\kappa+\lambda)} \cdot 2^{2k-n} \geq \\
&\geq 1 - \left(\frac{\eta}{\kappa}\right)^k = \\
&= 1 - \left(\frac{n - \frac{k-1}{2}}{2k - \frac{k-1}{2}}\right)^k \cdot 2^{2k-n},
\end{aligned} \tag{5}$$

which is the lower bound of the probability p. Counting up all arithmetic operations in formulas (3) and (5), we get asymptotic time complexity $\Theta(8k - n)$ for the precisely calculated probability p while only $\Theta(3k - n + 7)$ for the probability lower bound. Moreover, the lower bound formula (5) minimizes the risk of over- or underfloating due to avoiding terms with combinatorial coefficients of $\binom{a}{b}$ type. Checking the Fig. 2, we see the probability lower bound (the black dashed line) is quite effective with limited possibility to be improved.

C. An unoccupied l-seat problem

Now, we generalize the *unoccupied doubleseat problem* in terms of changing the doubleseats to l-seats for $l \in \mathbb{N}$. Let us assume we have a row of $k \in \mathbb{N}$ consecutive l-seats as in Fig. 3 and $n \in \mathbb{N} \cup \{0\}$ individuals who randomly sitting on n of the seats, one seat per individual, with $0 \leq n \leq lk$. What is the probability there is an unoccupied[5] l-seat?

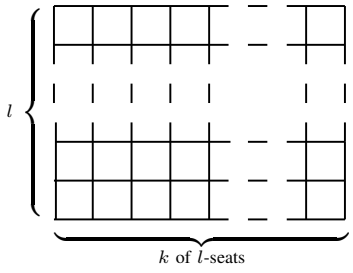

Fig. 3. A row of $k \in \mathbb{N}$ consecutive l-seats, used in the *unoccupied l-seat problem*.

[5]I. e., all l seats of such an l-seat are unoccupied.

1) A solution by the inverse Dirichlet's principle: Obviously, by applying the pigeonhole principle, assuming there are k of l-seats (*containers*), and n seats are already occupied (of lk in total) (*items*), if and only if there are $n < k$ sitting individuals, there is for sure one or more unoccupied l-seats. On the other hand, for $n > lk - l$ sitting individuals, there is surely no unoccupied l-seat.

2) A solution by a combinatorial stochastic approach: Again, by reformulation the probability p estimating there is at least one unoccupied l-seat using formula (1), assuming k of l-seats and n randomly sitting individuals at the moment, $k \leq n \leq lk$ (as far as for $0 \leq n \leq k-1$ is the problem solved using the Dirichlet's principle), we get

$$\begin{aligned} p &= P(\geq 1 \text{ unoccupied } l\text{-seat} \mid k \leq n \leq lk) = \\ &= 1 - P(0 \text{ unoccupied } l\text{-seat} \mid k \leq n \leq lk) = \\ &= 1 - \frac{N}{M} = 1 - \frac{N}{\binom{lk}{n}}, \end{aligned} \tag{6}$$

where the denominator M is how lk seats can be taken by n individuals, i. e. $M = \binom{lk}{n}$; however, the numerator N is analytically nontrivial and is calculated exhaustively using Algorithm 1 with asymptotic time complexity roughly $\Theta\left(2n(2l+k)\right)$.

Algorithm 1: Calculating a total number N of ways all k of l-seats are occupied by n individuals, so that there is at least one sitting individual on each l-seat

Data: $k \in \mathbb{N}$ of l-seats for $l \in \mathbb{N}$, n individuals with $k \leq n \leq lk$

Result: A total number N of ways all k of l-seats are occupied by n individuals, so that there is at least one sitting individual on each l-seat

$N = 0$;
for $\forall\ [d_1, d_2, \ldots, d_k] \in \mathbb{N}^k : \sum_{i=1}^{k} d_i = n$ **do**
  if $\forall i \in \{1, 2, \ldots, k\} : 1 \leq d_i \leq l$ **then**
    $N \leftarrow N + \prod_{i=1}^{k} \binom{l}{d_i}$
  end
end

Checking the Table II and Fig. 4, compared to Dirichlet's principle results, the stochastic approach still returns larger estimates of the maximum number n of sitting individuals ensuring (likely) an unoccupied l-seat; however, stochastically-based maximum n's seem closer to Dirichlet-based estimates for the l-seats problem than for the doubleseat one.

III. Conclusion remarks

Refining the Dirichlet's principle using a stochastic combinatorial approach enables us to improve estimates of the upper number n of items randomly placed in k of l-containers, still likely ensuring there is at least one l-container with no item in it. On a more practical note, whenever someone books a seat in a row of l-seats, even if the number of already booked seats is higher than the number of the l-seats, there is still a high probability of an unoccupied l-seat, unexpectedly according to the discrete inverse Dirichlet's principle, though.

TABLE II
Maximum numbers n of already sitting individuals that still ensure there is one or more unoccupied l-seats with the probability p for given total number k of l-seats.

$k=6, l=3$		$k=9, l=3$	
p	n	p	n
1.00	5	1.00	8
> 0.99	5	> 0.99	9
> 0.95	6	> 0.95	10
> 0.90	6	> 0.90	11
> 0.80	7	> 0.80	12

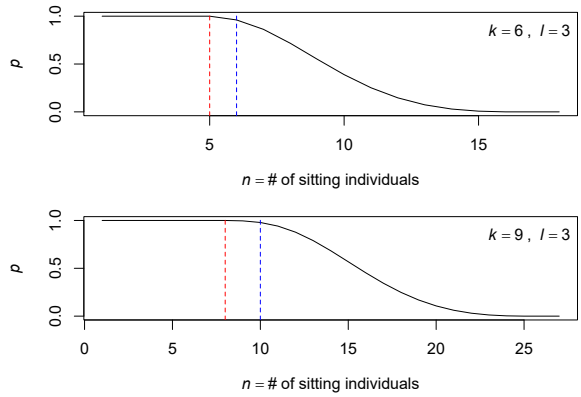

Fig. 4. Maximum numbers n of already sitting individuals that still ensure there is one or more unoccupied l-seats with the probability p for given total number k of l-seats. There are estimates of maximum n ensuring ≥ 1 unoccupied l-seat by the inverse Dirichlet's principle (the red dashed line) and by the stochastic refining of the Dirichlet's principle (the blue dashed line, with $p > 0.95$).

IV. Acknowledgement

This paper is supported by the grant OP VVV IGA/A, CZ.02.2.69/0.0/0.0/19_073/0016936 by the Internal Grant Agency of the Prague University of Economics and Business.

References

[1] Lynn Loomis and Shlomo Sternberg. "Potential theory in $\mathbb{E}^n$". In: *Advanced Calculus*. World Scientific, Mar. 2014, pp. 474–508. DOI: 10.1142/9789814583947_0013.

[2] Giridhar D. Mandyam, Nasir U. Ahmed, and Neeraj Magotra. "DCT-based scheme for lossless image compression". In: *SPIE Proceedings*. SPIE, Apr. 1995. DOI: 10.1117/12.206386.

[3] Yakir Aharonov, Fabrizio Colombo, Sandu Popescu, et al. "Quantum violation of the pigeonhole principle and the nature of quantum correlations". In: *Proceedings of the National Academy of Sciences* 113.3 (Jan. 2016), pp. 532–535. DOI: 10.1073/pnas.1522411112.

[4] Benoit Rittaud and Albrecht Heeffer. "The Pigeonhole Principle, Two Centuries Before Dirichlet". In: *The Mathematical Intelligencer* 36.2 (Aug. 2013), pp. 27–29. DOI: 10.1007/s00283-013-9389-1.

[5] Mario Cortina Borja and John Haigh. "The birthday problem". In: *Significance* 4.3 (Aug. 2007), pp. 124–127. DOI: 10.1111/j.1740-9713.2007.00246.x.

Computer Science and Systems

CSS is a FedCSIS track aiming at integrating and creating synergy between FedCSIS technical sessions which thematically subscribe to more technical (or applicable) aspects of computer science and related disciplines. The CSS track spans themes ranging from hardware issues close to the discipline of computer engineering via software issues tackled by the theory and applications of computer science, and to communication issues of interest to distributed, smart, multimedia and network systems.

The track is oriented on the research where the computer science meets the real world problems, real constraints, model objectives, etc. However the scope is not limited to applications, we all know that all of them were born from the innovative theory developed in laboratory. We want to show the fusion of these two worlds. Therefore one of the goals for the track is to show how the idea is transformed into application, since the history of modern science show that most of successful research experiments had their continuation in real world. CSS track is going to give an international panel where researchers will have a chance to promote their recent advances in applied computer science both from theoretical and practical side.

SCOPE

- Applied parallel and distributed computing and systems
- Applied system architectures and paradigms
- Problem-oriented simulations and modelling
- Applied methods of multimodal, constrained and heuristic optimization
- Applied computer systems in technology, medicine, ecology, environment, economy, etc.
- Theoretical fundamentals of the above computer sciences developed into the practical use
- Hardware engineering

Track includes technical sessions:

- Actors, Agents, Assistants, Avatars (1st Workshop 4A'22)
- Computer Aspects of Numerical Algorithms (15th Workshop CANA'22)
- Concurrency, Specification and Programming (30^{th} International Symposium CS&P'22)
- Multimedia Applications and Processing (15th International Symposium MMAP'22)
- Scalable Computing (12th Workshop WSC'22)

TRACK CHAIRS

- **Dimov, Ivan,** Bulgarian Academy of Sciences, Institute of Information and Communication Technologies, Bulgaria
  relax
- **Wasielewska-Michniewska, Katarzyna,** Systems Research Institute, Polish Academy of Sciences, Poland

PROGRAM CHAIRS

- **Dimov, Ivan,** Bulgarian Academy of Sciences, Institute of Information and Communication Technologies, Bulgaria
- **Wasielewska-Michniewska. Katarzyna, Systems Research Institute,** Polish Academy of Sciences, Poland

PROGRAM COMMITTEE

- **Barbosa, Jorge,** University of Porto, Portugal
- **Braubach, Lars,** University of Hamburg, Germany
- **Cabri, Giacomo,** Università di Modena e Reggio Emilia, Italy
- **Georgiev, Krassimir,** Institute of Information and Communication Technologies, Bulgarian Academy of Sciences, Bulgaria
- **Homles, Violeta,** University of Huddersfield, United Kingdom
- **Jezic, Gordan,** University of Zagreb, Croatia
- **Lirkov, Ivan,** Institute of Information and Communication Technologies, Bulgarian Academy of Sciences, Bulgaria
- **Mangioni, Giuseppe,** Dipartimento di Ingegneria Elettrica Elettronica e Informatica (DIEEI) - University of Catania, Italy
- **Millham, Richard,** Durban University of Technology, South Africa
- **Modoni, Gianfranco,** STIIMA-CNR, Italy
- **Pandey, Rajiv,** Amity University, India
- **Petcu, Dana,** West University of Timisoara, Romania
- **Roszczyk, Radosław,** Warsaw University of Technology, Poland
- **Rycerz, Katarzyna,** AGH University of Science and Technology, Poland
- **Schreiner, Wolfgang,** Research Institute for Symbolic Computation (RISC), Austria
- **Tanwar, Sudeep,** Nirma University, Ahmedabad (Gujarat), India
- **Tudoroiu, Nicolae,** John Abbott College, Canada
- **Vardanega, Tullio,** University of Padua, Italy
- **V Vinoth Kumar, MVJ College of Engineering,** India

15th Workshop on Computer Aspects of Numerical Algorithms

NUMERICAL algorithms are widely used by scientists engaged in various areas. There is a special need of highly efficient and easy-to-use scalable tools for solving large scale problems. The workshop is devoted to numerical algorithms with the particular attention to the latest scientific trends in this area and to problems related to implementation of libraries of efficient numerical algorithms. The goal of the workshop is meeting of researchers from various institutes and exchanging of their experience, and integrations of scientific centers.

TOPICS

- Parallel numerical algorithms
- Novel data formats for dense and sparse matrices
- Libraries for numerical computations
- Numerical algorithms testing and benchmarking
- Analysis of rounding errors of numerical algorithms
- Languages, tools and environments for programming numerical algorithms
- Numerical algorithms on coprocesors (GPU, Intel Xeon Phi, etc.)
- Paradigms of programming numerical algorithms
- Contemporary computer architectures
- Heterogeneous numerical algorithms
- Applications of numerical algorithms in science and technology

TECHNICAL SESSION CHAIRS

- **Bylina, Beata,** Maria Curie-Sklodowska University, Poland
- **Bylina, Jaroslaw,** Maria Curie-Sklodowska University, Poland
- **Stpiczyński, Przemysław,** Maria Curie-Sklodowska University, Poland

PROGRAM COMMITTEE

- **Anastassi, Zacharias,** ASPETE School of Pedagogical and Technological Education, Greece
- **Brugnano, Luigi,** Università di Firenze, Italy
- **Burczynski, Tadeusz,** Polish Academy of Sciences, Poland
- **Czachórski, Tadeusz,** Institute of Theoretical and Applied Informatics, Polish Academy of Sciences, Gliwice, Poland
- **Czarnul, Pawel,** Faculty of Electronics, Telecommunications and Informatics, Gdansk University of Technology, Poland
- **Domanska, Joanna,** Institute of Theoretical and Applied Informatics, Polish Academy of Sciences, Poland
- **Fialko, Sergiy,** Cracow University of Technology, Poland
- **Georgiev, Krassimir,** Institute of Information and Communication Technologies, Bulgarian Academy of Sciences, Bulgaria
- **Gepner, Paweł,** PAWEŁ GEPNER AI, Poland
- **Giannoutakis, Konstantinos,** Department of Applied Informatics, University of Macedonia, Greece
- **Grochla, Krzysztof,** Institute of Theoretical and Applied Informatics of PAS, Poland
- **Kozielski, Stanislaw,** Institute of Informatics, Silesian University of Technology, Poland
- **Laccetti, Giuliano,** University of Naples Federico II and INFN, Italy
- **Lirkov, Ivan,** Institute of Information and Communication Technologies, Bulgarian Academy of Sciences, Bulgaria
- **Luszczek, Piotr,** University of Tennessee Knoxville, USA
- **Marowka, Ami,** Bar-Ilan University, Israel
- **Mehmood, Rashid,** King Abdulaziz University, Saudi Arabia
- **Mrozek, Dariusz,** Silesian University of Technology, Institute of Informatics, Poland
- **Petcu, Dana,** West University of Timisoara, Romania
- **Rojek, Krzysztof,** Czestochowa University of Technology, Poland
- **Sawerwain, Marek,** University of Zielona Góra, Poland
- **Shaska, Tony,** Oakland University, USA
- **Sidje, Roger B.,** University of Alabama, USA
- **Siminski, Krzysztof,** Silesian University of Technology, Poland
- **Skubalska-Rafajłowicz, Ewa,** Wrocław University of Science and Technology, Poland
- **Szyld, Daniel,** Temple University, USA
- **Telek, Miklos,** Budapest University of Technology and Economics, Hungary
- **Tomov, Stanimire,** University of Tennessee Knoxville, USA
- **Ustimenko, Vasyl,** University of Maria Curie Sklodowska in Lublin, Poland

Communication Papers of the of the 17th Conference on Computer Science and Intelligence Systems pp. 121–128
DOI: 10.15439/2022F132
ISSN 2300-5963 ACSIS, Vol. 32

Intel Iris Xe-LP as a platform for scientific computing

Filip Krużel
Cracow University of Technology
ul. Warszawska 24, 31-155 Kraków, Poland
Email: filip.kruzel@pk.edu.pl

Mateusz Nytko
Cracow University of Technology
ul. Warszawska 24, 31-155 Kraków, Poland
Email: mateusz.nytko@pk.edu.pl

***Abstract*—In the present article, we describe the implementation of the finite element numerical integration algorithm for the Intel Iris Xe-LP Graphics Processing Unit. This GPU is a direct successor of a Xeon Phi accelerator architecture. Although it is used in integrated circuits and does not offer substantial performance, its test should be treated as a preview of the estimated performance for the Intel HPG Graphics Cards that are announced to be released in 2022. In the article, we use our previously developed auto-tuning Finite Element numerical integration OpenCL code on the Intel Iris Xe-LP GPU integrated into the Intel i7 11370H CPU and compare the results with the Nvidia GeForce RTX 3060 GPU. This article brings the answer to the question of whether the new Intel architecture can be a direct competitor to the more classic GPU architecture. It also allows showing if the new architecture can be used for the computation of complex engineering tasks.**

I. Introduction

DURING the evolution of computer architectures used in scientific computing, we can observe two main trends. The first is connected to the increasing number of computing cores and wide register units in CPUs. The second coincides with the use of specialized accelerators used to speed up the most demanding fragments of code. In the development of the modern computing accelerators, most of the architectures were based on GPUs, which occur with the SIMD manner of calculation with the use of the thousands of threads operating simultaneously. Since the presentation of the first Nvidia Tesla in 2007 [1], the architecture of the most of the accelerators used in high-performance systems is based on the Nvidia GPUs. According to the top500 list in November 2021, almost 30% of the supercomputers have Nvidia GPU-based accelerators (Fig. 1).

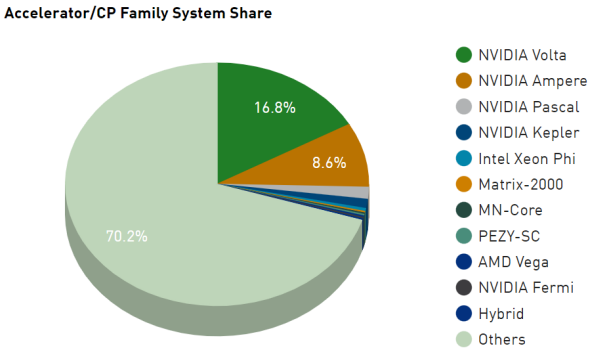

Fig. 1. Top500 Accelerators [2]

Despite these trends, there have also been attempts to find a middle ground between the high computational power provided by GPU-based accelerators and the relative ease of programming and versatility of CPUs. This type of accelerator combines both - the relatively large amount of computing cores with the extensive registers. As an example of such an architecture, the CELL Broadband Engine developed by IBM can be chosen. This architecture consists of one general processing core and eight smaller specialistic cores (Synergistic Processor Elements) equipped with wide 128-bit vector registers and AL units. These two types of accelerators, developed by Nvidia and IBM, inspired Intel, their main competitor, to search for its solution in the area of computing accelerators. Based on the wide vector registers which characterise the Cell/BE architecture, Intel started to create Larabee's graphics card architecture. With this architecture, the company attempted to overcome the main barrier to wider adoption of accelerators programming techniques, which was the complex model and programming method. The main advantages of the designed architecture were extensive (512-bit) vector registers, specialised texture units, coherent memory hierarchy and compatibility with x86 architecture [3]. At the same time, Intel was working on the Single-Chip Computer and Teraflops Research Chip projects characterised by a huge multi-core structure. Based on these designs, the Intel MIC (Many Integrated Core) architecture was developed and used in the Intel Xeon Phi coprocessors codenamed Knights Corner(KNC) [4]. The MIC architecture was advertised as an architecture that could combine the power of GPU accelerators with the ease of programming that characterizes processors. The next generation of the MIC architecture, Knights Landing, was offered as a separate PCI-express card and a stand-alone CPU. Intel Xeon Phi was a significant part of the most powerful computer systems in the world and in June 2015 the usage of this type of accelerator reached 34% of all systems [2]. Even though Intel Xeon Phi architecture was officially discontinued [5], its evolution led to the Intel Xe graphics cards, which were announced in November 2019 [6]. The new architecture was mentioned

not to repeat the Xeon Phi's mistakes, provide a unified programming model (oneAPI), and outstanding performance [7]. Intel Xe has different variants of microarchitectures, from integrated/low power consumption (Xe-LP) to enthusiast/high-performance gaming (Xe-HPG), data centre/high performance (Xe-HP) and high-performance computing (Xe-HPC) [8]. Due to the continuous unavailability of more advanced solutions (Xe-HPG/HPC), the authors decided to test the only available version of Intel's new architecture - Xe-LP. To do this, we try to port the numerical integration algorithm on the Intel Iris Xe GPU. Our previous study includes the development of the algorithm for modern GPUs [9], [10], CPUs [11], Hybrid systems [12] as well as Intel Xeon Phi [13], [14], [15]. Extending previous research into the new architecture may provide clues as to whether Intel's direction will allow it to compete with solutions currently dominating the market.

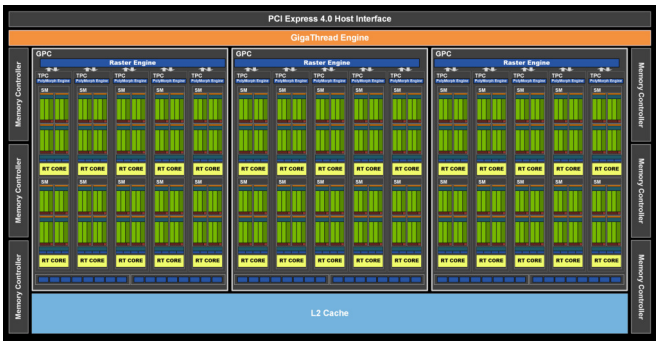

Fig. 2. GeForce RTX 3060 Laptop [16]

II. Graphic Processor Unit (GPU)

To perform the tests, the authors used a mobile version of the GeForce RTX 3060 graphics card as the reference chip, and the Intel i7 11370H processor's integrated graphics chip, Intel Iris XE-LP. Both chips tested were built into the one laptop. The GeForce RTX 3060 graphics card is based on the Ampere architecture [16]. As we can see on the figure 2 the GPU is divided into 3 GPC (Graphics Processing Clusters), which consist of 5 TPC (Texture Processing Clusters). Each TPC cluster contains 2 blocks of streaming multiprocessors (SM), which adds up to 30 SM blocks. The applied GigaThread Engine acts as a scheduler distributing work among streaming multiprocessors.

Each streaming multiprocessor contains 64 cores running at single precision, giving a total of 3840 cores. Additionally, each SM contains 4 Tensor cores, one Ray Tracing core, a 256kb register file, four texture units, and 128KB of L1 Cache/Shared memory [16].

The research used the Intel i7 11370 processor - a quad-core and eight-threaded unit with a base core clock frequency of 3.3 GHz. Built on the Tiger Lake architecture, it was first unveiled in autumn 2020. The processor is equipped with a graphics chip based on the Intel XE-LP architecture. Compared to previous generations, the aforementioned graphics chip architecture can reach a computing power of 2.2 teraflop.

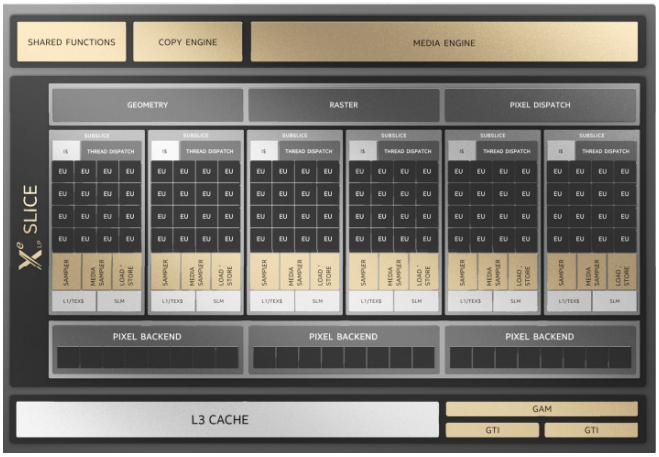

Fig. 3. Intel Iris XE-LP architecture [17]

The architecture of the Intel XE-LP chip is divided into 6 blocks (Fig. 3). There are 16 Execution Units in each of them, which makes 96 of them in total. The execution unit is the smallest block in the architecture which is multithreaded itself - it can execute 7 threads [18]. The computing unit consists of 8 SIMD units (single instruction multiple data) used to perform single and double-precision operations, and 2 SIMD units for extended match operations [17]. The executing units are combined in pairs in which the work is divided using the Thread Controler.

III. Numerical Integration

One of the most challenging engineering tasks in the use of accelerators has proven to be Finite Element Method procedures. One of the fundamental parts of FEM is numerical integration, used to prepare elementary stiffness matrices for the system solver. Most research on the use of accelerator computing power has focused on the use of GPUs to accelerate the solution of the final system of linear equations [19], [20]. Often the solution procedure is optimised first, as it is the most time-consuming part of FEM. However, once the procedure mentioned above is optimised, the earlier computational steps, such as numerical integration or assembling the whole matrix, also significantly affect the execution time [21].

Early research on transferring numerical integration to GPUs for specific FEM applications has been presented for, among others, linear elasticity with higher-order approximation [22], [23], nonlinear elasticity [24] and electromagnetism [25], [26]. A comprehensive study of the finite element assembly process on GPUs is described in [27], [28]. A separate set of papers dealt with attempts to develop tools for the automatic generation of finite element codes [29] in the context of GPU computing described in [30], [31]. Recent publications have extended the scope of research to include energetic aspects of numerical integration and assembly [32] and modern approximations such as isogeometric analysis [33]. Previous Intel architecture, Xeon Phi was also very widely used in finite element method procedures. It included

solving a differential equation using numerical integration in TVD Methods [34], the elastodynamic finite integration technique [35], using the shifted boundary method to solve a FEM problem [36] or solving partial differential equations using hybridised discontinuous Galerkin discretisation [37]. The research presented in this paper is part of a trend to exploit the possibilities of accelerating FEM calculations with modern accelerators.

A. Finite Element Method

The finite element method is used to compute an approximate solution of partial differential equations defined for a given, usually three-dimensional computational area Ω along with given boundary conditions $\partial\Omega$ [38], [39], [40], [41]. The computational area is divided into several elements with simple geometry (tetrahedrons, cubes or prisms). Computations are performed using a so-called weak formulation that defines the problem to be solved.

The approach chosen in this paper is based on the most commonly used assumption that each element in the computational domain is integrated only once. The integration results in a small elementary stiffness matrix whose single element is calculated in the form:

$$(A^e)^{rs} = \int_{\Omega_e} \left(\sum_i \sum_j \boldsymbol{C}^{i;j} \frac{\partial \boldsymbol{\phi}^r}{\partial \boldsymbol{x}_i} \frac{\partial \boldsymbol{\phi}^s}{\partial \boldsymbol{x}_j} + \sum_i \boldsymbol{C}^{i;0} \frac{\partial \boldsymbol{\phi}^r}{\partial \boldsymbol{x}_i} \boldsymbol{\phi}^s + \right. \\ \left. + \sum_i \boldsymbol{C}^{0;i} \boldsymbol{\phi}^r \frac{\partial \boldsymbol{\phi}^s}{\partial \boldsymbol{x}_i} + \boldsymbol{C}^{0;0} \boldsymbol{\phi}^r \boldsymbol{\phi}^s \right) d\Omega + \mathrm{BCL}, \tag{1}$$

where r and s are local indices from 1 to N_S - the number of shape functions for a given element.

Similarly, the vector on the right-hand side is calculated from the formula:

$$(b^e)^r = \int_{\Omega_e} \left(\sum_i \boldsymbol{D}^i \frac{\partial \boldsymbol{\phi}^r}{\partial \boldsymbol{x}_i} + \boldsymbol{D}^0 \boldsymbol{\phi}^r \right) d\Omega + \mathrm{BCR}, \tag{2}$$

BCL and BCR denote words related to boundary conditions defined for a single element and its shape function.

B. Numerical Integration Algorithm

The numerical integration in the Finite Element Method is correlated with the geometry used and the type of approximation by given elementary shape functions. Therefore, an appropriate geometric transformation must be applied to the mesh geometry used for the calculations. Denoting the physical coordinates in the mesh as $\boldsymbol{x}$, the transformation from the reference element with coordinates $\boldsymbol{\xi}$ is denoted as $\boldsymbol{x}(\boldsymbol{\xi})$. It is usually obtained by the general form of a linear, multilinear, quadratic, cubic or other transformation of the geometric basis functions and the set of degrees of freedom. The use of the Jacobian matrix $J = \frac{\partial \boldsymbol{x}}{\partial \boldsymbol{\xi}}$ is required to transform the coordinates from the reference to the real element, and the whole process is the distinguishing part of numerical integration in the Finite Element Method. This significantly contrasts this algorithm from other integration and matrix multiplication algorithms. A numerical quadrature transforms an analytic integral into a sum over integration points in the reference domain. Of the various possible quadratures, we will focus on the most popular Gauss quadrature [42]. The coordinates in the reference element are denoted as $\boldsymbol{\xi}^Q$ and the weights as $\boldsymbol{w}^Q$ where $Q = 1, ..., N_Q$ (N_Q - the number of Gauss points depending on the type of element and the approximation degree used). In the final numerical integration formula used in our calculations, we use the determinant of the Jacobian matrix $det\boldsymbol{J} = det(\frac{\partial \boldsymbol{x}}{\partial \boldsymbol{\xi}})$ and obtain:

$$\int_{\Omega_e} \sum_i \sum_j \boldsymbol{C}^{i;j} \frac{\partial \boldsymbol{\phi}^r}{\partial \boldsymbol{x}_i} \frac{\partial \boldsymbol{\phi}^s}{\partial \boldsymbol{x}_j} d\Omega \approx \\ \approx \sum_{Q=1}^{N_Q} \left(\sum_i \sum_j \boldsymbol{C}^{i;j} \frac{\partial \boldsymbol{\phi}^r}{\partial \boldsymbol{x}_i} \frac{\partial \boldsymbol{\phi}^s}{\partial \boldsymbol{x}_j} \det \boldsymbol{J} \right) \Bigg|_{\boldsymbol{\xi}^Q} \boldsymbol{w}^Q \tag{3}$$

In order to unify and describe the algorithm from the point of view of mathematical computation for the most efficient implementation on hardware, some modifications have been made to the above formulas by introducing the following indices:

- $\boldsymbol{\xi}^Q[i_Q]$, $\boldsymbol{w}^Q[i_Q]$ – tables with local coordinates of integration points (Gauss points) and weights assigned to them, $i_Q = 1, 2, ..., N_Q$, where N_Q – number of Gauss points depending on geometry and type and the chosen approximation degree,
- $\boldsymbol{G}^e$ – element geometry data table (related to the transformation from reference element to real element),
- $\mathbf{vol}^Q[i_Q]$ – table with volumetric elements $\mathbf{vol}^Q[i_Q] = det\left(\frac{\partial \boldsymbol{x}}{\partial \boldsymbol{\xi}}\right) \times \boldsymbol{w}^Q[i_Q]$,
- $\boldsymbol{\phi}[i_Q][i_S][i_D]$, $\boldsymbol{\phi}[i_Q][j_S][j_D]$ – tables with the values of consecutive locally shaped functions and their derivatives relative to global ($\frac{\partial \phi^{i_S}}{\partial x_{i_D}}$) and local coordinates ($\frac{\partial \hat{\phi}^{i_S}}{\partial \xi_{i_D}}$) at subsequent integration points i_Q,
  - $i_S, j_S = 1, 2, ..., N_S$, where N_S – the number of shape functions depending on the chosen geometry and the degree of approximation,
  - $i_D, j_D = 0, 1, ..., N_D$, where N_D – dimension of space. For i_D, j_D different from zero, the tables refer to derivatives with respect to the coordinate with index i_D, and for $i_D = 0$ to the shape function, so $i_D, j_D = 0, 1, 2, 3$,
- $\boldsymbol{C}[i_Q][i_D][j_D]$ – table with values of the problem coefficients (material data, values of degrees of freedom in previous nonlinear iterations and time steps, etc.) at successive Gauss points,
- $\boldsymbol{D}[i_Q][i_D]$ – table with the values of the coefficients d^i at subsequent Gauss points,
- $\boldsymbol{A}^e[i_S][j_S]$ – an array storing the local, elementary stiffness matrix,
- $\boldsymbol{b}^e[i_S]$ – array storing the local, elementary right-hand side vector.

Using the notation presented, general formula for the elementary stiffness matrix was created:

$$\boldsymbol{A}^e[i_S][j_S] = \sum_{i_Q}^{N_Q} \sum_{i_D,j_D}^{N_D} \boldsymbol{C}[i_Q][i_D][j_D]\times \\ \times\boldsymbol{\phi}[i_Q][i_S][i_D] \times \boldsymbol{\phi}[i_Q][j_S][j_D] \times \mathbf{vol}^Q[i_Q], \tag{4}$$

A right-handed vector formula was created analogously:

$$\boldsymbol{b}^e[i_S] = \sum_{i_Q}^{N_Q} \sum_{i_D}^{N_D} \boldsymbol{D}[i_Q][i_D]\times \\ \times\boldsymbol{\phi}[i_Q][i_S][i_D] \times \mathbf{vol}^Q[i_Q]. \tag{5}$$

Through the notation introduced, we create a general numerical integration algorithm for finite elements of the same type and approximation degree (Alg. 1).

The optimal structure of the algorithm must take into account the capabilities of the hardware for which the algorithm should be developed. For external accelerators usually connected through some limiting interface, the cost of transferring data to and from the accelerator can be very high and should be hidden by a sufficiently large number of calculations. This situation is favoured by the designed form of the algorithm 1, where the outer loop is a loop over all elements. Also, the general form of the algorithm 1, which does not take into account the location of the data at different memory levels, allows us to treat each inner loop as independent and to change its order for optimal performance. We can also achieve this because all the necessary data can be calculated in advance and used when needed. This allows us to create different variations of the algorithm depending on the hardware used. We further reference these versions of the algorithm as SQS and SSQ in opposite to the reference QSS type presented on algorithm 1. In this notation, the letters indicate the order of the loops, where Q denotes the loop over Gauss points, and S represent the loop over shape functions.

Algorithm 1: Generalised numerical integration algorithm for elements of the same type and degree of approximation

- determine the algorithm parameters – N_{EL}, N_Q, N_S;
- load tables $\boldsymbol{\xi}^Q$ and $\boldsymbol{w}^Q$ with numerical integration data;
- load the values of all shape functions and their derivatives relative to local coordinates at all integration points in the reference element;
- **for** $e = 1$ *to* N_{EL} **do**
  - load problem coefficients common for all integration points (Array $\boldsymbol{C}^e$);
  - load the necessary data about the element geometry (Array $\boldsymbol{G}^e$);
  - initialize element stiffness matrix $\boldsymbol{A}^e$ and element right-hand side vector $\boldsymbol{b}^e$;
  - **for** $i_Q = 1$ *to* N_Q **do**
    - calculate the data needed for Jacobian transformations ($\frac{\partial \boldsymbol{x}}{\partial \boldsymbol{\xi}}$, $\frac{\partial \boldsymbol{\xi}}{\partial \boldsymbol{x}}$, **vol**);
    - calculate the derivatives of the shape function relative to global coordinates using the Jacobian matrix;
    - calculate the coefficients $\boldsymbol{C}[i_Q]$ and $\boldsymbol{D}[i_Q]$ at the integration point;
    - **for** $i_S = 1$ *to* N_S **do**
      - **for** $j_S = 1$ *to* N_S **do**
        - **for** $i_D = 0$ *to* N_D **do**
          - **for** $j_D = 0$ *to* N_D **do**
            - $\boldsymbol{A}^e[i_S][j_S] += \boldsymbol{C}[i_Q[[i_D][j_D]\times \times\boldsymbol{\phi}[i_Q][i_S][i_D]\times\boldsymbol{\phi}[i_Q][j_S][j_D]\times \times\mathbf{vol}$
            - **if** $i_S = j_S$ **and** $i_D = j_D$ **then**
              - $\boldsymbol{b}^e[i_S] += \boldsymbol{D}[i_Q][i_D]\times \times\boldsymbol{\phi}[i_Q][i_S][i_D]\times$ **vol**
            - **end**
          - **end**
        - **end**
      - **end**
    - **end**
  - **end**
  - write the entire matrix $\boldsymbol{A}^e$ and vector $\boldsymbol{b}^e$;
- **end**

IV. Problems solved

To test the algorithm for both low and high-intensity tasks, the Poisson and convection-diffusion problems were chosen. The former task is characterised by the fact that its exact solution is known so that its correctness can be tested. It also requires relatively few resources, allowing fine-grained algorithms performing a large number of relatively small tasks to be tested. In contrast to Poisson, the convection-diffusion-reaction problem is resource-intensive, allowing testing of a coarse-grained implementation with fewer large elements to compute. Selecting these two tasks allows in-depth testing of the hardware for tasks commonly encountered in FEM and scientific and engineering computing.

A. Poisson equation

The first of the studied problems - Poisson equation can f.e. describe stationary temperature distribution (6).

$$\nabla^2 u = f \tag{6}$$

For the Poisson task, the matrices of the coefficients of the convection-diffusion-reaction $\boldsymbol{C}[i_Q]$ are of the form (7), for all integration points.

$$\boldsymbol{C}[i_Q] = \begin{bmatrix} 1 & 0 & 0 & 0 \\ 0 & 1 & 0 & 0 \\ 0 & 0 & 1 & 0 \\ 0 & 0 & 0 & 0 \end{bmatrix} \tag{7}$$

This allows the individual words of the stiffness matrix to be obtained according to a simplified formula (8).

$$(A^e)^{rs} = \int_{\Omega_e} \sum_i \sum_j \frac{\partial \phi^r}{\partial \boldsymbol{x}_i} \frac{\partial \phi^s}{\partial \boldsymbol{x}_j} d\Omega \tag{8}$$

The $\boldsymbol{D}[i_Q]$ coefficients vector has the form (9).

$$\boldsymbol{D}[i_Q] = \begin{bmatrix} 0 & 0 & 0 & S_v \end{bmatrix} \tag{9}$$

where S_v is a right-hand-side coefficient, different for each integration point.

B. Generalized convection-diffusion-reaction problem

Another of the tasks studied was the generalised convection-diffusion-reaction problem. In order to maximise the use of resources, it was assumed that the array $\boldsymbol{C}[i_Q]$ and the coefficients of the vector $\boldsymbol{D}[i_Q]$ would be fully filled with values different than 0. Arrays of this type appear, for example, in the convective heat transfer problem, after SUPG stabilisation has been applied.

For the studied convection-diffusion-reaction problem, the coefficients $\boldsymbol{C}[i_Q]$ and $\boldsymbol{D}[i_Q]$ are constant for the whole element. This allows us to generalise the solved problem by freeing it from the details of specific applications while maintaining the increased computational intensity of the algorithm.

C. Approximation

The finite element method is based on discretising the considered continuous area into a specified number of elements. These elements are usually simple geometry elements such as tetrahedrons, cubes or prisms. In the cases considered in this work, prismatic elements were used.

With this type of elements, it is possible to reproduce even the most complex geometry of the computational area Ω [43].

For the standard first-order linear approximation, the degrees of freedom of an element are related to its vertices. The basic shape functions for a reference prismatic element are in the form of a combination of 2D function that depends on x and y coordinations of the given vertice, with the function dependent on coordinate z.

V. Development tools

A. ModFEM

A modular software platform for finite element engineering calculations, ModFEM [44], was used as the primary tool used in the research. Thanks to its modular design, it allows modifying individual parts of FEM calculations, such as approximation, mesh handling and solution solvers.

The program consists of several levels on which the different modules are located. The main module managed by the user is the problems module, which defines the FEM weak formulation and determines which other modules the user uses. The most important modules are the mesh module, the approximation module and the solver module. The rest of the modules in the ModFEM code are used for different kinds of division of labour over several types of hardware. Thanks to its structure, this framework allows working in a distributed environment, which makes it an excellent tool for FEM computations both on accelerators and single computers, as well as in high-performance computing environments such as clusters or specialised supercomputers. In the course of the research, an extension to the approximation module was developed with appropriate accelerator support. The problem modules of the investigated tasks were also modified in order to properly prepare data structures and to comparatively test the numerical integration algorithm in the OpenCL environment.

B. OpenCL

The OpenCL language was used to test different types of accelerators. OpenCL allows programming of virtually any multi-core and vector machines - from modern CPUs to GPUs, through hybrid PowerXCell units, APUs and Intel Xeon Phi accelerators. The OpenCL specification includes a C99-based programming language for programming accelerators and an application programming interface (API) for platform support (defined as a given combination of available computing hardware and system software) and execution on processors [45]. Due to the portability of OpenCL code between devices of different types, each memory area can be physically mapped differently depending on the available hardware resources. OpenCL includes routines to preserve the portability of the code between different hardware platforms by adapting the memory and execution models to a given architecture [46]. Direct implementation on a given machine depends on the OpenCL development platform provider and the corresponding drivers.

With OpenCL technology, it has become possible to write programs on many types of accelerators. However, this has not solved the problem of performance portability, as each architecture requires separate optimizations [15]. For our work, we have developed a system for automatic tuning of the numerical integration algorithm [9].

C. Auto-tuning

Due to the different possibilities of using memory in accelerators based on graphics cards, eight parameters of the numerical integration algorithm affecting its final performance have been extracted:

1) WORKGROUP_SIZE - related to the minimum number of threads possible to launch on the accelerator - in the case of tests on the GPU, it was set to 64 due to the recommendation of the manufacturers of the tested cards.
2) USE_WORKSPACE_FOR_PDE_COEFF - a factor that determines whether problem data should be stored in threads' shared memory or registers (line 5 of the 1 algorithm).
3) USE_WORKSPACE_FOR_GEO_DATA - geometric data stored in threads' shared memory or registers (line 6 of algorithm 1).

4) USE_WORKSPACE_FOR_SHAPE_FUN - data of shape functions and their derivatives stored in the shared memory or registers (lines 3 and 10 of algorithm 1).
5) USE_WORKSPACE_FOR_STIFF_MAT - algorithm's local stiffness matrices and right-hand-side vectors stored in the threads' shared memory or registers (lines 7, 16, and 18 of the 1 algorithm).
6) COMPUTE_ALL_SHAPE_FUN_DER - algorithm computes the values of all shape functions and their derivatives before entering the double loop after the shape functions (line 10 of algorithm 1).
7) COAL_READ - memory readout in a continuous manner.
8) COAL_WRITE - continuously writing to memory.

The last two parameters of the numerical integration algorithm, concern the way of writing and reading data from the accelerator memory. Due to the physical design of this type of device and the operation of threads in groups, how memory is accessed can have a significant impact on the performance of the algorithm. Optimal access to memory should be grouped concerning threads, so that writes and reads are done in a continuous (coalesced) manner - whole vectors of data from memory. The list of parameters in the auto-tuning system is mostly concerned with the way memory is handled in the OpenCL model, which is based on the architecture of graphics cards. Arrays passed as arguments to the numerical integration procedure (e.g., geometric data and problem coefficients) can be used directly in calculations, or previously downloaded to local arrays, stored in registers or shared memory. By using shared memory as a temporary data read buffer, data is read continuously - a single thread reads the next memory cell and writes to the shared buffer. The read data can be stored in the buffer and used at a later time for calculation, or can be written into registers, freeing up the buffer for further use. How this data is stored in appropriate buffers is defined by the USE_WORKSPACE_FOR_* parameters. The total number of combinations of these parameters for any architecture is 40. Since there are 3 variants of the algorithm for each architecture (QSS, SQS, and SSQ), and we have 2 tasks, the total number of combinations per architecture is 240. The developed system consists of a set of scripts and code fragments responsible for compiling the kernel with the appropriate options. Due to the different compilation options available from various software vendors, it was necessary to implement different options depending on the installed accelerator and version of the OpenCL framework.

VI. Results

A. Poisson problem

During testing, it turned out that the QSS version of the numerical integration algorithm achieved the best results for both accelerators tested. Therefore, we have prepared the comparison graph (Fig. 4). The tuning options are arranged in the following order:

1) COAL_READ (CR)
2) COAL_WRITE (CW)
3) COMPUTE_ALL_SHAPE_FUN_DER (CASFD)
4) USE_WORKSPACE_FOR_PDE_COEFF (PDE)
5) USE_WORKSPACE_FOR_GEO_DATA (GEO)
6) USE_WORKSPACE_FOR_SHAPE_FUN (SHP)
7) USE_WORKSPACE_FOR_STIFF_MAT (STIFF)

In comparison with the results for GeForce RTX 3060 we can observe that the results for Intel Xe are more chaotic.

Fig. 4. Automatic tuning on tested GPUs in QSS version of the numerical integration algorithm for Poisson problem

On this graph, we see that the results for Nvidia GPU are very regular and connected with the use of only one option - CW. On Intel Xe, we can observe more chaotic results but with the best results in the same cases - with the CW option enabled. The use of shared memory in GeForce plays almost no role at all - it can be connected with the fact that in the Nvidia GPU all data are cached in L1 and L2 caches which results in no differences in the less resource-consuming cases. In the Iris Xe case, we can observe more memory dependent results - especially with the combination of the coalesced read/write and the use of the shared memory for SHP or GEO data. Although the OpenCL routine returns the presence of 64 kB of Shared Memory on Intel Xe (in opposition to 48 kB in Nvidia), it seems like this memory is mapped to the internal L3 cache memory which is slower than the classical SM used in external GPUs.

TABLE I
Results (in *ns*) of calculation for one element in Poisson problem

	QSS	*SQS*	*SSQ*
Intel Iris Xe-LP	9,185791	16,17432	49,23503
Nvidia GeForce 3060 RTX	0,992839	1,798503	8,390299

TABLE II
Options combination for the best times for Poisson problem

	QSS	*SQS*	*SSQ*
Intel Iris Xe-LP	0100010	1100001	0100000
Nvidia GeForce 3060 RTX	1101000	1110010	0100010

The best results obtained are shown in the table I. We can see that in the QSS and SQS cases GeForce is 9 times

faster than Intel Iris Xe. In SQS case GeForce is almost 6 times faster than Iris. Table II show the combination of options for the best results. As it was observed on the graphs earlier, all best results are connected with the use of coalesced writing of data. It indicates that both devices prefer vectorized organization of data in the memory what is characteristic for modern computing devices (both CPU and GPU).

B. Convection-diffusion-reaction problem

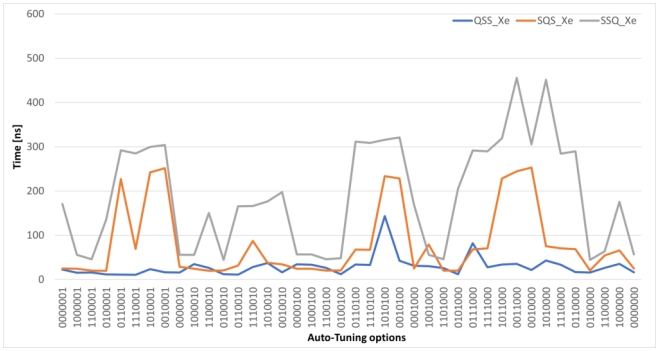

Fig. 5. Automatic tuning on Intel Iris Xe GPU for convection-diffusion problem

In the case of the more resource-consuming convection problem for Intel Iris Xe, we have observed more diversified results, and in some cases, the SQS version of the numerical integration algorithm was better than the QSS version (Fig. 5). The QSS version shows a more even level, only with a peak when the extensive use of shared memory is observed (GEO+CASFD+CR). In the Nvidia case, the results are similar to the Poisson case and are very regular in shape and the QSS version was the best in all the cases.

As in the Poisson problem, when we compare the results for the QSS algorithm for both GPUs, we can observe more chaotic results for the Intels' GPU (Fig. 6).

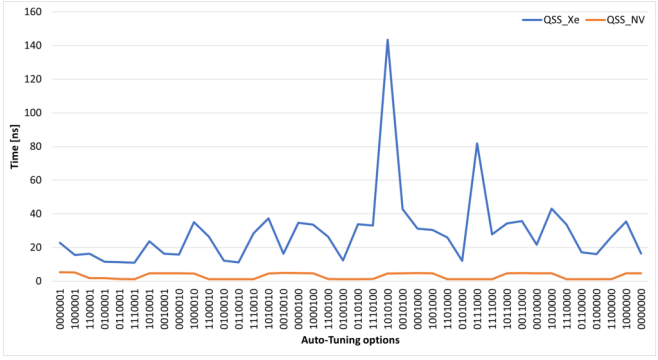

Fig. 6. Automatic tuning on tested GPUs in QSS version of the numerical integration algorithm for convection-diffusion problem

The best results presented in table III also show the same differences between the Nvidia and Intel GPUs, reaching out ten times faster execution on the GeForce RTX 3060. From the best options analysis (Tab. IV) we can still observe the great role of the coalesced writing in all variants of the algorithm. The other options show a more chaotic nature, but in the Nvidia case, we can observe that more resource-demanding types of an algorithm (SQS and SSQ) are making good use of the possibility of storing data in the shared memory.

TABLE III
RESULTS (IN *ns*) OF CALCULATION FOR ONE ELEMENT IN CONVECTION-DIFFUSION PROBLEM

	QSS	*SQS*	*SSQ*
Intel Iris Xe-LP	10,98633	19,90763	44,42342
Nvidia GeForce RTX 3060	1,196289	1,904297	9,090169

TABLE IV
OPTIONS COMBINATION FOR THE BEST TIMES FOR CONVECTION-DIFFUSION PROBLEM

	QSS	*SQS*	*SSQ*
Intel Iris Xe-LP	1110001	1100010	0100000
Nvidia GeForce 3060 RTX	1100000	0110010	0100100

VII. CONCLUSIONS

Intel Xe seems to have a more chaotic nature of execution and its parametric tuning graphs are more reminiscent of CPU graphs or the Xeon Phi we researched earlier [11], [47]. This may be due to its more complex design and different memory organisation than classic GPUs. Despite this, the results indicate a quite high potential of the discussed architecture and give hope that its versions intended for scientific and technical computing equipped with additional levels of memory [17] will be able to take an equal fight with the existing players that is Nvidia and AMD. In our future work, we are planning to test Intel Xe-LP architecture with the more time-consuming discontinuous Galerkin approximation for the Finite Element Method numerical integration and test the OpenCL 3.0 features connected with the use of the shared memory buffer between CPU and GPU cores in the integrated heterogeneous architectures. After this study, the authors hope that moving to the Intel Xe-HPC units will be easier to perform and provide the High-Performance Computing community with the answer if the new Intels' architecture can be competitive with existing solutions.

VIII. REFERENCES

[1] "NVIDIA Tesla C870 Professional Graphics Card," tech. rep., VideoCardz, 2015.
[2] E. Strohmaier, J. Dongarra, H. Simon, M. Meuer, and H. Meuer, *Top500 The List*, 2020.
[3] L. Seiler, D. Carmean, E. Sprangle, T. Forsyth, M. Abrash, and P. Dubey, "Larrabee: a many-core x86 architecture for visual computing," *SIGGRAPH 08: ACM SIGGRAPH 2008 papers*, pp. 1–15, 2008.
[4] R. Goodwins, "Intel unveils many-core Knights platform for HPC," *ZdNet*, 2010. Accessed on 27th November 2015.
[5] Intel, "Product change notification 116378 - 00," July 23, 2018.
[6] Intel, "Intel Unveils New GPU Architecture with High-Performance Computing and AI Acceleration, and oneAPI Software Stack with Unified and Scalable Abstraction for Heterogeneous Architectures," *Intel Newsroom*, 2019.
[7] I. Cutress, "Intel's Xe for HPC: Ponte Vecchio with Chiplets, EMIB, and Foveros on 7nm, Coming 2021," *AnandTech*, 2019.

[8] R. Smith, "The Intel Xe-LP GPU Architecture Deep Dive: Building Up The Next Generation," *AnandTech*, 2020.

[9] K. Banaś, F. Krużel, and J. Bielański, "Optimal kernel design for finite element numerical integration on GPUs," *Computing in Science and Engineering*, vol. Volume 22, no. Issue 6, pp. 61–74, 2020.

[10] K. Banaś, F. Krużel, J. Bielański, and K. Chłoń, "A comparison of performance tuning process for different generations of NVIDIA GPUs and an example scientific computing algorithm," in *Parallel Processing and Applied Mathematics* (R. Wyrzykowski, J. Dongarra, E. Deelman, and K. Karczewski, eds.), (Cham), pp. 232–242, Springer International Publishing, 2018.

[11] F. Krużel, "Vectorized implementation of the FEM numerical integration algorithm on a modern CPU," in *European Conference for Modelling and Simulation*, vol. Volume 33, pp. 414–420, 2019.

[12] F. Krużel and K. Banaś, "AMD APU systems as a platform for scientific computing," *Computer Methods in Materials Science*, vol. 15, no. 2, pp. 362–369, 2015.

[13] K. Banaś and F. Krużel, "Comparison of Xeon Phi and Kepler GPU performance for finite element numerical integration," in *High Performance Computing and Communications, 2014 IEEE 6th Intl Symp on Cyberspace Safety and Security, 2014 IEEE 11th Intl Conf on Embedded Software and Syst (HPCC,CSS,ICESS), 2014 IEEE Intl Conf on*, pp. 145–148, Aug 2014.

[14] F. Krużel and K. Banaś, "Finite element numerical integration on Xeon Phi coprocessor," *Annals of Computer Science and Information Systems*, pp. 603–612, 10 2014.

[15] K. Banaś and F. Krużel, "OpenCL performance portability for Xeon Phi coprocessor and NVIDIA GPUs: A case study of finite element numerical integration," in *Euro-Par 2014: Parallel Processing Workshops*, vol. 8806 of *Lecture Notes in Computer Science*, pp. 158–169, Springer International Publishing, 2014.

[16] Nvidia Corporation, *NVIDIA AMPERE GA102 GPU ARCHITECTURE: Ampere GA10x*, 2021. Whitepaper.

[17] Intel Corporation, *Intel Architecture Day 2020 Presentation Slides*, 2020. Whitepaper.

[18] Intel Corporation, *oneAPI GPU Optimization Guide*, 2022. Intel Developer Guide.

[19] M. Geveler, D. Ribbrock, D. Göddeke, P. Zajac, and S. Turek, "Towards a complete FEM-based simulation toolkit on GPUs: Unstructured grid finite element geometric multigrid solvers with strong smoothers based on sparse approximate inverses," *Computers & Fluids*, vol. 80, pp. 327 – 332, 2013. Selected contributions of the 23rd International Conference on Parallel Fluid Dynamics ParCFD2011.

[20] L. Buatois, G. Caumon, and B. Levy, "Concurrent number cruncher: A GPU implementation of a general sparse linear solver," *Int. J. Parallel Emerg. Distrib. Syst.*, vol. 24, no. 3, pp. 205–223, 2009.

[21] J. Mamza, P. Makyla, A. Dziekoński, A. Lamecki, and M. Mrozowski, "Multi-core and multiprocessor implementation of numerical integration in Finite Element Method," in *Microwave Radar and Wireless Communications (MIKON), 2012 19th International Conference on*, vol. 2, pp. 457 – 461, 2012.

[22] P. Plaszewski, P. Maciol, and K. Banas, "Finite element numerical integration on GPUs.," in *PPAM'09: Proceedings of the 8th international conference on Parallel processing and applied mathematics*, (Berlin, Heidelberg), pp. 411–420, Springer-Verlag, 2010.

[23] P. Macioł, P. Płaszewski, and K. Banaś, "3D finite element numerical integration on GPUs," in *Proceedings of the International Conference on Computational Science, ICCS 2010, University of Amsterdam, The Netherlands, May 31 - June 2, 2010* (P. M. A. Sloot, G. D. van Albada, and J. Dongarra, eds.), vol. 1 of *Procedia Computer Science*, pp. 1093–1100, Elsevier, 2010.

[24] J. Filipovic, I. Peterlík, and J. Fousek, "GPU acceleration of equations assembly in finite elements method-preliminary results," in *SAAHPC: Symposium on Application Accelerators in HPC*, 2009.

[25] A. Dziekoński, P. Sypek, A. Lamecki, and M. Mrozowski, "Finite element matrix generation on a GPU," *Progress In Electromagnetics Research*, vol. 128, pp. 249–265, 2012.

[26] A. Dziekoński, P. Sypek, A. Lamecki, and M. Mrozowski, "Generation of large finite-element matrices on multiple graphics processors," *International Journal for Numerical Methods in Engineering*, vol. 94, no. 2, pp. 204–220, 2013.

[27] C. Cecka, A. J. Lew, and E. Darve, "Application of assembly of finite element methods on graphics processors for real-time elastodynamics," in *GPU Computing Gems. Jade edition*, pp. 187–205, Morgan Kaufmann, 2011.

[28] C. Cecka, A. J. Lew, and E. Darve, "Assembly of finite element methods on graphics processors," *International Journal for Numerical Methods in Engineering*, vol. 85, no. 5, pp. 640–669, 2011.

[29] A. Logg, K.-A. Mardal, G. N. Wells, *et al.*, *Automated Solution of Differential Equations by the Finite Element Method*. Springer, 2012.

[30] G. R. Markall, D. A. Ham, and P. H. Kelly, "Towards generating optimised finite element solvers for GPUs from high-level specifications," *Procedia Computer Science*, vol. 1, no. 1, pp. 1815 – 1823, 2010. ICCS 2010.

[31] G. R. Markall, A. Slemmer, D. A. Ham, P. H. J. Kelly, C. D. Cantwell, and S. J. Sherwin, "Finite element assembly strategies on multi-core and many-core architectures," *International Journal for Numerical Methods in Fluids*, vol. 71, no. 1, pp. 80–97, 2013.

[32] L. Tang, X. Hu, D. Chen, M. Niemier, R. Barrett, S. Hammond, and G. Hsieh, "GPU acceleration of data assembly in finite element methods and its energy implications," in *Application-Specific Systems, Architectures and Processors (ASAP), 2013 IEEE 24th International Conference on*, pp. 321–328, June 2013.

[33] A. Karatarakis, P. Karakitsios, and M. Papadrakakis, "Gpu accelerated computation of the isogeometric analysis stiffness matrix," *Computer Methods in Applied Mechanics and Engineering*, vol. 269, pp. 334–355, 2014.

[34] F. Cabral, C. Osthoff, G. Costa, D. Brandao, M. Kischinhevsky, and S. Gonzaga de Oliveira, "Tuning Up TVD HOPMOC Method on Intel MIC Xeon Phi Architectures with Intel Parallel Studio Tools," *2017 International Symposium on Computer Architecture and High Performance Computing Workshops (SBAC-PADW), Computer Architecture and High Performance Computing Workshops (SBAC-PADW), 2017 International Symposium on, SBAC-PADW*, pp. 19 – 24, 2017.

[35] I. W. C. Schneck, E. D. Gregory, and C. A. Leckey, "Optimization of elastodynamic finite integration technique on intel xeon phi knights landing processors.," *Journal of Computational Physics*, vol. 374, pp. 550 – 562, 2018.

[36] N. M. Atallah, C. Canuto, and G. Scovazzi, "The second-generation shifted boundary method and its numerical analysis.," *Computer Methods in Applied Mechanics and Engineering*, vol. 372, 2020.

[37] S. Muralikrishnan, M.-B. Tran, and T. Bui-Thanh, "An improved iterative hdg approach for partial differential equations.," *Journal of Computational Physics*, vol. 367, pp. 295 – 321, 2018.

[38] O. Zienkiewicz and R. Taylor, *Finite element method. Vol 1-3*. London: Butterworth Heinemann, 2000.

[39] C. Johnson, *Numerical Solution of Partial Differential Equations by the Finite Element Method*. Cambridge University Press, 1987.

[40] E. Becker, G. Carey, and J. Oden, *Finite Elements. An Introduction*. Englewood Cliffs: Prentice Hall, 1981.

[41] L. Demkowicz, J. Kurtz, D. Pardo, M. Paszyński, W. Rachowicz, and A. Zdunek, *Computing with Hp-Adaptive Finite Elements, Vol. 2: Frontiers Three Dimensional Elliptic and Maxwell Problems with Applications*. Chapman & Hall/CRC, 2007.

[42] J. N. Lyness, "Quadrature methods based on complex function values," *Mathematics of Computation*, vol. 23, no. 107, pp. 601–619, 1969.

[43] Y. Kallinderis, "Adaptive hybrid prismatic-tetrahedral grids," *International Journal for Numerical Methods in Fluids*, vol. 20, pp. 1023–1037, 1995.

[44] K. Michalik, K. Banaś, P. Płaszewski, and P. Cybułka, "ModFEM – a computational framework for parallel adaptive finite element simulations," *Computer Methods in Materials Science*, vol. 13, no. 1, pp. 3–8, 2013.

[45] A. Howes, L.; Munshi, *The OpenCL Specification*. Khronos OpenCL Working Group, 2014. version 2.0, revision 26.

[46] S. Rul, H. Vandierendonck, J. D'Haene, and K. De Bosschere, "An experimental study on performance portability of OpenCL kernels," in *Application Accelerators in High Performance Computing, 2010 Symposium, Papers*, (Knoxville, TN, USA), p. 3, 2010.

[47] K. Banaś, F. Krużel, and J. Bielański, "Finite element numerical integration for first order approximations on multi- and many-core architectures," *Computer Methods in Applied Mechanics and Engineering*, vol. 305, pp. 827 – 848, 2016.

30th International Symposium on Concurrency, Specification and Programming

THE symposium on Concurrency, Specification, and Programming is the series of meeting formerly organized every even year by Humboldt University of Berlin and every odd year by Warsaw University. It deals with formal specification of concurrent and parallel systems, mathematical models for describing such systems, and programming and verification concepts for their implementation. The symposium has a tradition dating back to the mid-seventies; since 1993 it was named CS&P. During the past 30 years, CS&P has become an important forum for researchers from European and Asian countries.

TOPICS

The list of topics includes, but is not limited to:

- Mathematical models of concurrency
- Formal specification languages
- Theory of programming
- Model checking and testing
- Multi-agent systems
- Rough sets
- Verification
- Formal aspects of knowledge management
- Knowledge discovery and data mining
- Soft computing
- Applications, e.g. in Robotics

TECHNICAL SESSION CHAIRS

- **Czaja, Ludwik,** Vistula University, Poland
- **Nguyen, Hung Son,** University of Warsaw, Poland
- **Schlingloff, Holger,** Humboldt University, Germany
- **Vogel, Thomas,** Humboldt University, Germany

PROGRAM COMMITTEE

- **Artiemjew, Piotr,** University of Warmia and Mazury, Poland
- **Dutta, Soma,** University of Warmia and Mazury in Olsztyn, Poland
- **Gomolinska, Anna,** University of Bialystok, Institute of Informatics, Poland
- **Redziejowski, Roman,** Poland
- **Senyurek, Edip,** Vistula University, Poland
- **Skowron, Andrzej,** Systems Research Institute, Polish Academy of Sciences and Cardinal Stefan Wyszynski University, Warsaw, Poland
- **Stepaniuk, Jaroslaw,** Bialystok University of Technology, Poland
- **Suraj, Zbigniew,** Institute of Computer Science, College of Natural Sciences, University of Rzeszów, Poland
- **Szczuka, Marcin,** Institute of Informatics, University of Warsaw, Poland
- **Wasilewski, Piotr,** University of Warsaw, Poland
- **Werner, Matthias,** TU Chemnitz, Germany
- **Wolf, Karsten,** Universität Rostock, Germany

Communication Papers of the of the 17th Conference on Computer Science and Intelligence Systems pp. 131–138
DOI: 10.15439/2022F135
ISSN 2300-5963 ACSIS, Vol. 32

Type System of Anemone Functional Language

Paweł Batko, Marcin Kuta
AGH University of Science and Technology,
Al. Mickiewicza 30, 30-059 Krakow, Poland,
Institute of Computer Science,
Faculty of Computer Science, Electronics and Telecommunications
Email: mkuta@agh.edu.pl

***Abstract*—Anemone is a functional language, which provides an actor system as its model of concurrency. This paper describes type system of the Anemone language. The type system is the strong point of Anemone. In comparison to a dynamic type system, the static type system of Anemone guarantees more exact error detection. The full type inference disposes the programmer from explicit specification of type labels. As the type system of Anemone is polymorphic, code conciseness, rich data structures and pattern matching are provided in Anemone.**

I. Introduction

ANEMONE language is a functional language [1], [2] inspired by Scala, Erlang, Haskell, and ML. It supports a wide range of features including actors communicating via messages, tight integration with the LLVM infrastructure, interoperability with the C language, and automatic memory management with garbage collector.

Anemone language is equipped with a static, polymorphic type system, with full type inference based on let-polymorphism. The static type system guarantees that more errors are detected than using a dynamic type system. Error detection is also performed earlier – at the compile time rather than the run time. The full type inference disposes the programmer from explicit specification of type labels in a program. As the type system of Anemone is polymorphic, the code is concise and algebraic data types enable rich data structures and pattern matching.

In this paper, we show the design and implementation of the type system adopted in Anemone and the inference algorithm. Type inference has been based on the Hindley-Milner algorithm. The Hindley-Milner inference has been implemented with algorithm W. In particular, we present the extension of algorithm W introduced for the purpose of the Anemone language. We also show data structures which are the basis for above algorithms, including representations of type variables and type schemes.

II. Type Systems in Functional Languages

The choice of a type system is an important decision which determines many aspects of compiler architecture. The two main options are dynamic typing and static typing.

Contrary to no typing, with dynamic typing each value is ascribed a particular type. The type correctness of a program is performed during the run time. Dynamic typing offers the programmer flexibility because he does not have to adjust his program to a static type system. The drawback of this approach is the reduced amount of static information about a compiled program. This reduces the range of applicable optimisations and imposes a generation of the additional code which verifies the program correctness with respect to its types. Dynamic typing introduces an additional overhead during the run time. Scheme and Clojure are examples of functional languages which use this approach. Anemone is not typed dynamically as lack of accurate error detection at the compile time is an important drawback of this approach.

Static typing associates a label denoting its type with each variable. The current type systems originate from the simply typed lambda-calculus [3]. The set of operations that may be performed on a given variable are limited by the type of variable that it is. Static typing offers several advantages:

- an early and exact error detection,
- increased opportunities for code optimizations due to additional static information,
- type information is a form of code documentation,
- better support for programming environments.

Type systems based on dependent typing can express types which depend not only on other types, but also on values of variables. For example, they can guarantee that a function taking number n will return a list of length n. Epigram [4] and Agda [5] implement such a type system.

III. Polymorphic Type Systems

The core concept of a polymorphic type system is to create within a language abstractions of values which are independent from type. Functions and data types are examples of such abstractions. Parametric polymorphism enables generic code typing and uses type variables, which are replaced with concrete types when needed. Other kinds of polymorphism include:

- *ad-hoc* polymorphism, which associates many implementations with a single function identifier. The proper function is chosen on the basis of passed parameters.
- subtype polymorphism, the examples of which are subtypes present in object-oriented languages.

In Figure 1, the function `map` can take a list of elements of type *int* as well as a list of elements of type *string*. In a polymorphic type system, the function only needs to be defined once. In languages which do not support polymorphism, the programmer would have to implement a distinct function

```
map :: (a -> b) -> [a] -> [b]
map _ [] = []
map f (x:xs) = f x : map f xs

map id ["1", "2"]
map id [1, 2]
```

Fig. 1: Example of a polymorphic type system

The function `map` takes two parameters. The first parameter is function `f` mapping any type `a` to any type `b`. The second parameter is a list of elements of type `a`. The function `map` returns a list of elements of type `b`. Example from *Haskell*

for each of types or would have to typecast to `void*` type, sacrificing type safety, as is usually done in *C*.

Parametric polymorphic type systems further divide into predicative polymorphism and impredicative polymorphism [6].

Predicative polymorphism distinguishes monotypes from polytypes. A monotype does not have type variables, e.g., *int*, *int* $\mapsto$ *bool*. A polytype can be parametrised with a type variable, e.g. $\forall a.a$, where a is a type variable rather than a concrete type. A type variable can be substituted with any monotype.

Let us temporarily assume that a constructor of function type, $\rightarrow$, is the only available constructor of type. In rank-1 (prenex) polymorphism, a polytype may contain a universal quantifier located only at the leftmost position. This means that the quantified variable can be only substituted with a monotype, and a polytype containing universal quantifier cannot be on the left hand side of $\rightarrow$ constructor, provided that the given type is encoded as a tree.

Rank-2 polymorphism forbids the presence of a universal quantifier in the encoding of a type as a tree at positions passing through two arrows. This rule can be applied to define polymorphisms of higher ranks. For example, $\forall a.a \rightarrow a$ is both rank-1 and rank-2 type (and higher), while $(\forall a.a \rightarrow a) \rightarrow$ *bool* is only rank-2 type (and higher). The crucial caveat of rank-3 polymorphism (or higher) is undecidability of its full type reconstruction [7].

Impredicative polymorphism is the strongest form of parametric polymorphism. It can express types where a type variable can be substituted with any type or type variable. For example, given type $z = \forall a\ list[a]$, type variable, a, can by substituted with z. *Haskell* is a prominent example of a language implementing such a type system.

An example of a rank-1 polymorphic type system is let-polymorphism – this is characterised by its restriction of type generalisation to the syntactic *let* construct. Let-polymorphism is used in some versions of *ML*, and it has been implemented in Anemone. An advantage of languages which implement rank-1 polymorphism is the possibility of performing global type inference without type annotations in the source code.

Anemone language is equipped with a static type system with let-polymorphism and global type inference. This solution is much more complicated than dynamic typing. This has been chosen due to additional static guarantees of program correctness, avoiding overhead linked to type annotations (achieved with type inference) and flexibility in creating abstractions which use the polymorphism mechanism.

Table I summarizes type systems of few functional languages.

TABLE I: Type systems of different functional languages

Type system	Language
Dynamic typing	Scheme, Closure
Impredicative polymorphism	Haskell
Dependent typing	Epigram, Agda
Let-polymorphism	ML, Anemone

IV. Implementation of the Type System

Implementation of the static, polymorphic type system is based on the unification algorithm and algorithm W [8].

A. Unification algorithm

The type inference algorithm in Anemone applies the unification algorithm [9]. Unification searches for substitutions of values for variables, such that two unified expressions become equal.

Let us consider expressions $f(a, x)$ and $f(y, f(y, b))$, where a and b denote values, and x and y are variables. To unify them, substitution $S = [a/y, f(a, b)/x]$ should be applied, which denotes that y should be substituted with a, and x should be substituted with $f(a, b)$. The application of a substitution to an expression is written as: $[a/y, f(a, b)/x]f(a, x)$. Substitution S is a composition of two substitutions, $S = [f(y, b)/x] \circ [a/y]$. Substitution S is called a unifier of $f(a, x)$ and $f(y, f(y, b))$, because after its application, these expressions become equal. In the context of the implemented type inference, variables refer to type variables, values refer to types, and functions refer to type constructors.

The idea of the unification algorithm is to find the principal unifier (the most general unifier) of two expressions. This is such a unifier U, that any unifier S of two expressions can be constructed by the composition of some unifier T with the principal unifier U, written as $S = U \circ T$.

The Anemone compiler implements the unification algorithm (Fig. 2) which operates on type variables and types. Figure 3 presents data types which are defined in the Anemone compiler and are needed by the unification algorithm. Type *TypeVar* represents type variables, and type *TypeApp* represents simple and complex types. For example, variable x would be represented as `TypeVar("x")`, and type constructor $f(x, a)$ (where a is a type) as `TypeApp("f", TypeVar("x"), TypeApp("a"))`.

B. Hindley-Milner type inference

Hindley-Milner type inference [8] [10] is defined for two languages: the language of expressions L_e and the language of types L_t. The language of expressions, defined with grammar in Fig. 4a, contains variables x, expressions e, function definitions, function calls and *let* expressions.

The language of types, generated by grammar in Fig. 4b, defines types of these expressions. It defines primitive types ι,

function `Unify(`s, t`)`**:**
  if $t = x$ ***and*** $s = y$ **then**
    $[x/y]$
  else if $s = x$ ***and not*** `Occurs` *(x, t)* **then**
    $[t/x]$
  else if $t = x$ ***and not*** `Occurs` *(x, s)* **then**
    $[s/x]$
  else if $s = f(p_1, p_2, .., p_n)$ ***and*** $t = f(p'_1, p'_2, .., p'_n)$ **then**
    $U_1 =$ `Unify(`p_1, p'_1`)`
    `Unify(`$f(U_1p_2, .., U_1p_n)$, $f(U_1p'_2, .., U_1p'_n)$`)` $\circ\ U_1$
  else
    `Fail`
  end
function `Occurs(`x, t`)`**:**
  if $t = f(p_1, p_2, .., p_n)$ **then**
    if $\exists i.\ x = p_i$ **then**
      true
    else
      $\exists i.$ `Occurs(`x,p_i`)`
    end
  else
    false
  end

Fig. 2: Unification algorithm presented with function *Unify*

Function *Unify* takes two type schemes, *s*, *t*, (i.e., types, which may contain a universal quantifier) as its parameters and returns their principal unifier, if it exists. Function *Occurs* takes type variable x and type scheme t as its parameters, and checks, whether variable x occurs in the definition of type scheme *t*.

```
sealed trait TypeTerm

case class TypeVar(name: String)
extends TypeTerm

case class TypeApp(name: String,
                   typeTerms: Seq[TypeTerm]
                              = Seq.empty)
extends TypeTerm
```

Fig. 3: Implementation of variables and types values in the Anemone compiler

type variables α, type expressions τ, and type schemes σ. Type expressions τ describe types without a universal quantifier, whereas type scheme σ also describes types with a universal quantifier. Universally quantified type variables are referred to as generic type variables. The remaining type variables are free variables.

Inference rules are written as:

$$A \vdash e : \sigma\,,$$

which means that under assumption A, expression e has a type defined with type scheme σ. Symbol A_x denotes the set of hypotheses concerning types from A without hypotheses concerning x.

$$e ::= x \mid ee' \mid \lambda x.e \mid \text{let } x = e \text{ in } e'$$

(a) Grammar of the language of expressions L_e

$$\sigma ::= \tau \mid \forall\alpha\sigma$$
$$\tau ::= \alpha \mid \iota \mid \tau \to \tau$$

(b) Grammar of the language of types L_t

$$\begin{aligned} e ::= {} & x \\ & \mid e(e_1, e_2, .., e_n) \\ & \mid \lambda(x_1, x_2, .., x_n).e \\ & \mid \text{let } x = e \text{ in } e' \\ & \mid \mathit{fix}(x, e) \\ & \mid \mathit{noarg}(e) \end{aligned}$$

(c) Grammar of the language of expressions used in the compiler of *Anemone*

Fig. 4: Grammar of languages used in the Hindley-Milner inference

Type schemes can be ordered w.r.t. their generality. For example, type $\sigma_1 = \forall x.(y \to x) \to x$ is more general than type $\sigma_2 = \forall x.(x \to x) \to x$, because type σ_1 can be transformed to type σ_2 with substitution $[x/y]$. Type $\sigma_0 = \forall x.z \to x$ is even more general than σ_1 and σ_2. With respect to generality, type schemes can be ordered from the most specific type to the most general type with relation $<$ (more general), denoted as $\sigma_2 < \sigma_1 < \sigma_0$.

Figure 5 presents the implementation of type schemes in the Anemone compiler, realised with classes *Forall* and *Type*. Polymorphic type $\forall a.a$ would be implemented as `Forall("a", TypeApp("a"))`.

Hindley-Milner type inference is performed with six inference rules:

$$TAUT: \frac{}{A \vdash e : \sigma}\ (x : \sigma \in A) \tag{R1}$$

$$INST: \frac{A \vdash e : \sigma}{A \vdash e : \sigma'}\ (\sigma > \sigma') \tag{R2}$$

$$GEN: \frac{A \vdash e : \sigma}{A \vdash e : \forall\alpha\sigma}\ (\alpha \text{ is not free in } A) \tag{R3}$$

$$COMB: \frac{A \vdash e : \tau' \to \tau \quad A \vdash e' : \tau'}{A \vdash (ee') : \tau} \tag{R4}$$

$$ABS: \frac{A_x \cup \{x : \tau'\} \vdash e : \tau}{A \vdash (\lambda x.e) : \tau' \to \tau} \tag{R5}$$

$$LET: \frac{A \vdash e : \sigma \quad A_x \cup \{x : \sigma\} \vdash e' : \tau}{A \vdash (\text{let } x = e \text{ in } e') : \tau} \tag{R6}$$

Rule (R1) is a tautology which attributes type to an expression. Rule (R2) defines instantiating of a more specific type scheme. Rule (R3) enables type generalization w.r.t. a generic type variable. Rules (R4) and (R5) determine the type of function application and the type of function definition, respectively. Rule (R6) enables the typing of expressions wherever an introduced variable has been used.

According to the above rules, the only available types are simple types ι and function types, constructed with operator $\rightarrow$. In addition to simple types and function types, Anemone offers complex types (introduced with a type constructor, i.e., a function returning a new type). For example, a type representing a pair of values `Pair`: $a \times b$ can be defined with the following type constructors:

1) `PairConstructor`: $\forall ab.\ a \rightarrow b \rightarrow a \times b$
2) `GetFirst`: $\forall ab.\ a \times b \rightarrow a$
3) `GetSecond`: $\forall ab.\ a \times b \rightarrow b$

This approach is used in the compiler of Anemone. It introduces appropriate type constructors for each data structure defined in Anemone.

```
sealed trait TypeScheme

case class Forall(name: String,
                  typeScheme: TypeScheme)
     extends TypeScheme

case class Type(typeTerm: TypeTerm)
     extends TypeScheme
```

Fig. 5: Implementation of type schemes in the compiler of *Anemone*

C. Algorithm W

Algorithm *W* [8] implements Hindley-Milner type inference and is the basis for type reconstruction performed by the Anemone compiler. Algorithm *W* works according to formula $W(A, e) = (S, \tau)$, where A is a set of variables with known types and e is an expression, the type of which is reconstructed. The result of the algorithm is a pair (S, τ), where S is the principal unifier needed to find the type of expression e, and τ is the reconstructed type of expression e.

Within the algorithm *W* a closure $\overline{A}(\tau)$ of type τ at assumptions *A* is defined as

$$\overline{A}(\tau) = \forall \alpha_1, \alpha_2, .., \alpha_n.\ \tau\ ,$$

where $\alpha_1, \alpha_2, .., \alpha_n$ are free type variables in τ and do not occur in A.

Algorithm 1 presents the original form of algorithm *W*, which consists of four rules. Each rule corresponds to one of four production rules of grammar in Fig. 4a and inference rules (R1)–(R6).

- The first rule of algorithm *W* corresponds to inference rules *INST* preceded by rule *TAUT*;
- the second rule of algoritm *W* corresponds to inference rule *COMB*;
- the third rule corresponds to rule *ABS*;
- the fourth rule corresponds to rules *LET* and *GEN*.

1) **if** e is identifier x **and** hypothesis about its type belongs to the set of known hypotheses $x\colon \forall \delta_1, \delta_2, .., \delta_n.\ \tau'$ **then**
$$S = [\,] \quad \tau = [\gamma_i/\delta_i]\tau'\,,$$
where γ_i is a new type variable.
2) if e is function application $e_1 e_2$ **and**:
$$W(A, e_1) = (S_1, \tau_1)$$
$$W(S_1 A, e_2) = (S_2, \tau_2)$$
$$\mathit{Unify}(S_2\tau_1, \tau_2 \rightarrow \gamma) = V\,,$$
where γ is a new type variable **then**
$$S = VS_2S_1 \quad \tau = V\gamma\,.$$
3) **if** e is function abstraction $\lambda x.e_1$ **and**:
$$W(A_x \cup \{x\colon \gamma\}, e_1) = (S_1, \tau_1)\ ,$$
where γ is a new type variable **then**
$$S = S_1 \quad \tau = S_1\gamma \rightarrow \tau_1\,.$$
4) **if** e is expression `let` $x = e_1$ `in` e_2 **and**:
$$W(A, e_1) = (S_1, \tau_1)$$
$$W(S_1 A_x \cup \{x\colon \overline{S_1 A}(\tau_1)\}, e_2) = (S_2, \tau_2)\,,$$
then
$$S = S_2S_1 \quad \tau = \tau_2\,.$$

Algorithm 1: Algorithm *W*

D. Implementation of algorithm W

Figure 4c presents the grammar of the language of expressions used in the Anemone compiler. In comparison to the grammar of L_e (Fig. 4a), there are the following changes:

- replacing definitions and calls of a unary function with definitions and calls of n-ary function ($n > 0$)
- introduction of *fix* operator, which enables definitions of recursive functions
- introduction of *noarg* operator, representing definitions of functions with no arguments

As Anemone enables n-ary functions, appropriate constructs supporting n-ary functions have been introduced. Modelling n-ary functions with operators acting on unary functions would imply that a call of a binary function with only one argument provided is correct as (from the point of view of implementation of algorithm *W*) a function would always take only one parameter. Such an implementation of algorithm *W* was considered; however, it would impose implementation of partial parametrisation (currying) for each function in Anemone. While interesting, this approach would require significant modifications in the entire compiler. The solution

1) **if** e is identifier x **then** proceed according to the steps in Algortihm 1.
2) **if** e is of the form $\lambda(x_1, x_2, .., x_n).e$ **and**:

   $$W(A_{x_1 x_2 .. x_n} \cup \{x_1 : \gamma_1, x_2 : \gamma_2, .., x_n : \gamma_n\}, e) = (S_1, \tau_1) ,$$

   where $\gamma_1, \gamma_2, .., \gamma_n$ are new type variables, **then**:

   $$S = S_1 \quad \tau = (S_1\gamma_1, S_1\gamma_2, .., S_1\gamma_n) \to \tau_1 \ .$$

3) **if** e is a operator of zero-argument function, $noarg(e_1)$, **and**:

   $$W(A, e) = (S_1, \tau_1) \ ,$$

   then:

   $$S = S_1 \quad \tau = unit \to \tau_1 \ .$$

4) **if** e is a multiargument function call, $e_1(e_2, e_3, .., e_{n+1})$, **and**:

   $$W(A, e_1) = (S_1, \tau_1) \ ,$$

   $$\underset{2 \le i \le n+1}{\forall} : \quad W(S_1 A, e_i) = (S_i, \tau_i) \ ,$$

   $$Unify(S_{n+1} S_n .. S_2 \tau_1, (\tau_2, \tau_3, .., \tau_{n+1}) \to \gamma) = V \ ,$$

   where γ is a new type variable, **then**:

   $$S = V S_{n+1} S_n .. S_1 \quad \tau = V\gamma \ .$$

5) **if** e is expression `let` $x = e_1$ `in` e_2 **then** proceed according to the definition in Algorithm 1.
6) **if** e is a fixed point expression $fix(x, e_1)$ **and**:

   $$W(A_x \cup \{x : \gamma\}, e_1) = (S_1, \tau_1) \ ,$$

   $$Unify(S_1\gamma, \tau_1) = V \ ,$$

   where γ is a new type variable, **then**:

   $$S = V S_1 \quad \tau = V S_1 \gamma \ .$$

Algorithm 2: Extended version of algorithm *W* applied in *Anemone*

chosen for implementation introduces constructs which support representations of n-ary functions at the level of the algorithm *W* as it limits necessary reorganisations to the module of type reconstruction.

Algorithm 2 presents the extended version of algorithm *W* applied in Anemone, which takes into account new constructs and changes in grammar of L_e.

E. Implementation of let-polymorphism

Anemone is equipped with a kind of parametric polymorphism known as let-polymorphism. Its name stems from the syntactic construct present in *ML*, where this kind of polymorphism has been introduced. The *let* construct, also present in the definition of algorithm *W*, introduces generically typed expressions.

Anemone does not have keyword *let* which serves to introduce polymorphic functions, as is done in *ML*. Moreover, *AST* representing Anemone code is more extensive than the simple language of expressions, L_e (Fig. 4a), on which algorithm *W* is based. Also, the grammar of type expressions, presented in Fig. 4b, is much simpler than the set of types possible to express in Anemone, due to the possibility to construct types of structures.

When implementing algorithm *W* for Anemone, it was possible to choose between two approaches. The first approach extends the definition of algorithm *W* in Algorithm 1, in order that the implementation also comprises constructs expressed by particular *AST* nodes of Anemone. The second approach transforms *AST* to a simpler form corresponding to the language of expressions L_e.

In the Anemone compiler, the second approach has been chosen. In the phase of type reconstruction, *AST* is transformed to a simpler form used in the implementation of algorithm *W*, which we shall call *WAST*. The implemented version of algorithm *W* uses a slightly richer grammar of expressions, defined in Fig. 4c.

Usually, a structure containing many *WAST* nodes is created from each *AST* node, and extension of algorithm *W* for the purpose of Anemone facilitates this transformation with moderate complication of implementation of algorithm *W*.

In particular, the algorithm of type reconstruction in the Anemone compiler proceeds as follows:

1) Nodes introducing new types are separated from nodes which are a subject to type reconstruction. Nodes introducing new types are declarations of new data types and declarations of external functions.
2) Each external function and its type is added to the set of known assumptions about types.
3) For each declaration introducing a new data type, the new type and its name are added to the set of known assumptions about types.
4) The set of known assumptions about types is complemented with types corresponding to built-in operators and primitive data types,
5) The set of known types is converted to the form in Fig. 4b, i.e. type schemes, simple types and type constructors – similarly to type `Pair` in Sect. IV-B.
6) The remaining *AST* nodes are converted to subtrees of *WAST*. It is recorded which *AST* node corresponds to a given subtree of *WAST*.
7) Algorithm *W* is executed on *WAST* representation of a program, with assumptions about types gathered from structure declarations, external functions, and built-in operators and types.
8) The obtained principal unifier is applied to all *WAST* nodes in order to obtain the most general type for each node.
9) For each *WAST* node corresponding to *AST* node, its type is mapped to type representation used in *AST*.

As a result of using dedicated representation of *WAST* code during type reconstruction, the entire process of type reconstruction is independent from remaining modules of the implemented compiler. Moreover, the unification algorithm

and algorithm *W*, which are crucial for the process of type reconstruction, operate on relatively simple, abstract data types dedicated to this task. Above features guarantee strong resistance of the entire module to changes implemented in other modules of the compiler and enable its seamless extension in the future.

F. Code generation for polymorphic functions

Polymorphic functions must be compatible at the binary level. For example, mapping function *map* takes as its arguments a list of elements and a function to be executed on each element of the list. A parameter responsible for this function receives type $\forall x.\ x \to y$, where x and y are type variables. Without knowing concrete values of variables x and y, their representation for the target architecture should be chosen. Let be given a memory pointer. Let us define *minus* function taking a value of primitive type *double* and returning its negation. Type of function *minus* will be instantiated as *double* $\to$ *double*. Assembly code of this function must be independent from information, whether function argument is of floating-point type. During a function call in a given architecture, an argument of floating-point type may be passed differently (e.g., in a different register) than a value of a pointer. If we pass to function *map* function *minus*, implementation of *map* will call the passed function as if it would take a parameter being a pointer, whilst function *minus* expects a floating-point type. Such an incompatibility can easily lead to errors in a compiled program.

```
f:    # type::('a, 'b) -> unit
...
movq    %rdi, (%rsp)
movq    %rsi, 8(%rsp)
movq    %rdx, 16(%rsp)
...

g:    # type::(double, 'b) -> unit
    ...
movq    %rdi, (%rsp)
vmovsd  %xmm0, 8(%rsp)
movq    %rsi, 16(%rsp)
...
```

Fig. 6: Assembly code *x86_64* generated for functions *f* and *g*

Functions *f* and *g* have similar signatures (given after # sign). Consistently with the implemented in Anemone type system, usage of function *g* can be replaced with usage of function *f* because generic type variable *'a* can be unified with type *double*. If generated assembly code treats first argument of function *g* as a floating-point number, then value of this argument is obtained from register *xmm0*. In contrast, when first argument of function *f* is treated as a pointer, its value is obtained from register *rsi*.

Figure 6 presents different assembly codes of two functions, taking a pointer and a floating-point number, respectively, as a parameter. To avoid the problem of binary incompatibility between functions, Anemone compiles all the function parameters as pointers. This solution is known as boxed representation [11]. The potential drawback of this solution is reduced efficiency of generated code; however, it guarantees correctness of programs with polymorphic functions. An alternative approach for compiling polymorphism uses intentional type analysis [12].

V. Conclusions

The type system is one of the strongest points of the Anemone language. Full type inference disposes the programmer from manual defining of type labels. Moreover, let-polymorphism enables function definitions with respect to generic parameters of type. In this way, a separate function implementation for each type becomes redundant and code conciseness is promoted.

Support for algebraic data types and pattern matching enables rich data structures, and easy implementation of lists, trees or other data structures. The implemented type system guarantees static correctness of a program while preserving code conciseness and expressiveness.

Appendix

Figure 7 presents basic constructs of Anemone. The example defines functions `fib` and `factorial` of type `double -> double` which use conditional expressions `if-else`. Function `factorial` defines nested function `helper` inside its body.

```
type:: (double) -> double
fun fib(n) {
    if(n == 0) {
        1
    } else {
        if(n == 1) {
            1
        } else {
            fib(n-1) + fib(n-2)
        }
    }
}

type:: (double) -> double
fun factorial(m) {
    type:: (double, double) -> double
    fun helper(ax, n) {
        if(n == 0){
            ax
        } else {
            var n2 = n - 1 in {
                helper(ax*n, n2)
            }
        }
    }
    helper(1,m)
}
```

Fig. 7: Basic constructs of the Anemone language

Functions in Anemone are first-class citizens, as they can be: assigned to a variable (Fig. 8), passed as function arguments (Fig. 9), returned from a function (Fig. 10), and handled as a closure with a non-empty environment (Fig. 11).

```
fun foo(){
        fun bar(){
                1
        }
        bar
}
```

Fig. 10: Returning function from a function

```
fun buildAdder(n){
        fun adder(x){
                x + n
        }
        adder
}
```

Fig. 11: Function being a closure with non-emtpy environment

```
data BoolList = BoolCons {
    value :: boolean,
    next :: BoolList
} | BoolNil { }
```

Fig. 12: Definition of new multi-variant data type

```
data List 'a = Cons 'a {
    value :: 'a,
    next :: List 'a
} | CNil { }
```

Fig. 13: Definition of polymorphic data type. Variable `a` is a type variable

```
fun foo(l) {
        match l {
                | Cons(v, n) => {
                        bar(v, n)
                }
                | cnil :: CNil => {
                        baz()
            }
        }
}
```

Fig. 14: Usage of pattern matching mechanism

```
fun bar(x){
        var f = foo in {
                f(x)
        }
}
```

Fig. 8: Assignment of a function `foo` to a variable

```
fun apply(f, x){
        f(x)
}
```

Fig. 9: Passing a function as a parameter

Anemone defines three primitive types: `boolean`, `double` and `string`. Examples in Figs. 12 and 13 define a multi-variant data type `BoolList` and polymorphic data type `List`.

Anemone also offers pattern matching, as shown in Fig. 14. There are two kinds of patterns. Pattern `| Cons(v, n) =>` is similar to deconstructive assignment, pattern `| cnil :: CNil =>` is similar to declaration of a variant field.

Concurrency in Anemone is implemented with actors [1], [2]. Actor model of *Anemone* has the following features:

- asynchronous communication with message passing, which is clearer and less error-prone than thread model and makes manual synchronization redundant
- actors modelled as functions (similarly to Erlang) and actor function called for each new message (similarly to the Akka library).
- possibility of creating many actors in one thread
- possibility of dynamic creation of new actors
- identification of received messages through pattern matching
- message passing model implemented with shared memory
- complete integration with the garbage collector

An example of creating an actor system with two actors communicating with each other via messages is given in Fig. 15.

ACKNOWLEDGMENTS

The research presented in this paper was supported by the funds of Polish Ministry of Education and Science assigned to AGH University of Science and Technology.

REFERENCES

[1] P. Batko and M. Kuta, "Actor Model of a New Functional Language - Anemone," in *Proceedings of the 12th International Conference on Parallel Processing and Applied Mathematics, PPAM 2017*, ser. Lecture Notes in Computer Science, vol. 10778, 2018. doi: 10.1007/978-3-319-78054-2_20 pp. 213–223.

[2] ——, "Actor model of Anemone functional language," *Journal of Supercomputing*, vol. 74, no. 4, pp. 1485–1496, 2018. doi: 10.1007/s11227-017-2233-1

[3] A. Church, "A Formulation of the Simple Theory of Types," *Journal of Symbolic Logic*, vol. 5, no. 2, pp. 56–68, 1940. doi: 10.2307/2266170

[4] J. McKinna, "Why Dependent Types Matter," *SIGPLAN Notes*, vol. 41, no. 1, pp. 1–1, 2006. doi: 10.1145/1111320.1111038

[5] A. Bove, P. Dybjer, and U. Norell, "A Brief Overview of Agda — A Functional Language with Dependent Types," in *22nd International Conference on Theorem Proving in Higher Order Logics, TPHOLs 2009*, 2009. doi: 10.1007/978-3-642-03359-9_6 pp. 73–78.

[6] B. C. Pierce, *Types and Programming Languages*. MIT Press, 2002. ISBN 978-0-262-16209-8

[7] A. J. Kfoury and J. B. Wells, "Principality and Decidable Type Inference for Finite-Rank Intersection Types." in *Proceedings of the 26th ACM SIGPLAN-SIGACT Symposium on Principles of Programming Languages, POPL'99*, 1999. doi: 10.1145/292540.292556 pp. 161–174.

[8] L. Damas and R. Milner, "Principal Type-schemes for Functional Programs," in *Proceedings of the 9th ACM SIGPLAN-SIGACT Symposium on Principles of Programming Languages, POPL'82*, 1982. doi: 10.1145/582153.582176 pp. 207–212.

[9] J. A. Robinson, "A Machine-Oriented Logic Based on the Resolution Principle," *Journal of the ACM*, vol. 12, no. 1, pp. 23–41, 1965. doi: 10.1145/321250.321253

[10] R. Hindley, "The principal type-scheme of an object in combinatory logic," *Transactions of the American Mathematical Society*, vol. 146, pp. 29–60, 1969. doi: 10.2307/1995158

[11] M. Hicks, "Types and Intermediate Representations," Department of Computer and Information Science, University of Pennsylvania, Technical Report MS-CIS-98-05, 1998.

```
fun ping(state, msg) {
  var otherActorId = state in {
    match msg {
      | s :: String => {
          printStr(s)
          sendMsg(otherActorId, "fromPing")
          nap(1)
          state
      }
      | otherActorId :: ActorId => {
          sendMsg(otherActorId, "fromPing - first")
          otherActorId
} } } }

fun pong(state, msg) {
  var otherActorId = state in {
    match msg {
      | s :: String => {
          printStr(s)
          sendMsg(otherActorId, "fromPong")
          nap(1)
          state
} } } }

fun main_fun() {
  createActorSystem(2)
  var pingActorRef = createActor(ping, 0),
      pongActorRef = createActor(pong, pingActorRef) in {
        sendFromOutside(pingActorRef, pongActorRef)
} }
```

Fig. 15: Creating and starting an actor system

[12] R. Harper and G. Morrisett, “Compiling polymorphism using intensional type analysis,” in *Proceedings of the 22nd ACM SIGPLAN-SIGACT Symposium on Principles of Programming Languages, POPL’95*, 1995. doi: 10.1145/199448.199475 pp. 130–141.

Communication Papers of the of the 17th Conference on Computer Science and Intelligence Systems pp. 139–142
DOI: 10.15439/2022F257
ISSN 2300-5963 ACSIS, Vol. 32

Heuristic algorithm for periodic patterns discovery in a database workload reconstruction

Marcin Zimniak, Bogdan Franczyk
Information Systems Institute
Leipzig University
Germany
Email: {zimniak, franczyk}@wifa.uni-leipzig.de

Marta Burzańska, Piotr Wiśniewski
Faculty of Mathematics and Computer Science
Nicolaus Copernicus University in Toruń
Poland
Email: {quintria, pikonrad}@mat.umk.pl

***Abstract*—Information about the existence of periodic patterns in a database workload can play a big part in the process of database tuning. However, full analysis of audit trails can be cumbersome and time-consuming. This paper discusses a heuristic algorithm that focuses on workload reconstruction based on pattern discovery in a simplified workload notation. This notation is based on multisets representing database actions (such as user queries) requiring access to specific persistent objects, but without the access cost analysis. Each action in this notation is a multiset of accessed objects, which can be tables, system files, views, etc. The theoretical model for such an approach has been discussed in detail in the authors' previous work [1] This work is mostly proof-of-a-concept for the theoretical approach. Additionally, in order to test the performance of the proposed algorithm, a test-data generator has been constructed. Both the previous and the current papers are parts of a research project dealing with the application of periodic pattern theory to the field of database optimization and tuning [2], [3], [4], [5].**

I. Introduction

THE WORKLOAD reconstruction for an SQL database is a non-trivial task. However it can be very important when considering tuning options. Because in a typical relational database queries tend to be repetitive to a point, discovering recurring patterns may lead to the improvement of DBMS performance. This paper is part of a research project tackling the application of the periodic pattern theory to the database workload reconstruction and prediction [5] This paper follows the research discussed theoretically in [1], and provides a heuristic reconstruction algorithm utilising a recursive periodic pattern discovery process. This work on the workload reconstruction strays from the research on the prediction of the n-th database state based on the retrospective analysis of the n-1 previous states (actions) [6]. Instead we focus on the global system usage estimation and prediction with the help of the reconstruction methods working with a simplified workload dump. In order to verify and evaluate the researched algorithm we have also developed a parameterized test-data generator. It is capable of generating a list of random multisets with a hidden periodicity feature. It is not predetermined but rather the construction of the generator ensures the existence of some non-trivial periodic patterns. The generated test-data is used to firstly verify the correctness of the main heuristic algorithm when it comes to the recognition of periodic patterns when searching for the optimal workload reconstruction. The second task was to aid the research on the reconstruction quality measure and time-efficiency of the reconstruction algorithm. The overall goal was to develop a fast, statistically stable algorithm that works with an optimal time and space complexity. The conducted tests have confirmed these assumptions. The programming language used for the development of the algorithm and the generator was Python 3.

The reconstruction problem touches on the possibility of the reconstruction (lossy or lossless) of a given system based on partial data obtained from the earlier (or current) behaviour of the system. The problem of reconstruction, as well as the current research on it, work with the concept of reconstructability (non-reconstructability) of affine functions [7], [8] and the reconstruction of multisets over grupoids as well. Apart from some open problems for multisets over groupoids, the concept of reconstructing the sequence of multisets (in general) is a new concept and has not been studied so far. In the proposed approach, we reduce the presentations of multisets in sequences to increasing sequences. Such a simplification for the presentation of multisets is related to the homogeneous treatment of elements (subtrees) that are implementations of algebra expressions, including entity instances sets (tables), which are a part of the output relational algebra. Such assumptions for multisets made it possible to tackle the problem of the reconstruction of the sequences of multisets without considering the problem of coverage of multisets, which takes place in the case of the reconstruction of the mutliset over grupoids. The aim of this work is to provide efficient algorithms for the reconstruction of the considered system and to provide qualitative information on the degree of its reconstruction. The algorithm can be applied to complex systems, such as database systems, whose log interpretations can be written in the form of a sequence of multisets, etc. The degree of reconstruction allows to evaluate the predictions of the whole system; the methodology of the algorithm takes into account the simultaneous inclusion of the time and frequency domains in each step of the reconstruction algorithm, for all periodic patterns included in the reconstruction. The problem of workload predicting has already been discussed by the author [2] in terms of another concept of the periodic pattern. The methods of signal analysis or wavelets are based on the assumption (in short) that points in time have been assigned

values (real numbers), including the use of appropriate reconstruction methods[9], [10]. In our data model, first, we do not consider the points in time, but the time periods (pulled down to points) and sets of elements (including elements allowed multiple times), not to mention the nesting interpenetration of events considered on such structures etc. Therefore, the methodology of time series, Fast Fourier Transform (FFT) in discrete form (DFT), spectra, etc., does not work for events in the context of the data under consideration. In addition, we do not consider the independent behavior of individual elements, but we study and take into account (periodic) behavior of multiple sets of elements and their subsets, taking into account the interactions of one on another (in various proportions) as well as the entire system on individual elements, etc.

The paper is organised as follows. In Section II we focus on methodology. Section III provides our recursive reconstruction algorithm. Section IV specifies test data generator. Section V concludes effectiveness of the algorithm, possible future works end this section.

II. Methodology

The methodology used in the workload reconstruction process is based on the concept of intelligent extraction of periodic patterns in the workload defined below. The methods used in the author's previous works are standard bottom-up methods. The methods used in the current work use a recursive approach in combination with the heuristic method(s), much more efficient than the previous ones.

The theory and applications of the concept of periodic patterns to the workload prediction problem were discussed in the previous works of one of the authors [5], [2]. The theory of periodic patterns is well known. It grew out of, among others, the periodic sets [11] as well as periodic events [12]

Let recall terminology defined in previous considerations [1]. Let the workload W_L and the sequence of time units U be given. The non empty subsequences $C, C' \subseteq W_L$ of the same length and consecutive coordinates are called *equivalent* if $C = C'$ occurs for all corresponding coordinates.

A *periodic pattern* in a workload W_L is a tuple $<C,\ f,\ t,\ p,>$ where:

1) the *carrier* C determines a non empty subsequence $C \subseteq W_L$
2) f is a number of time unit in U where the repetitions of C start
3) t is a total number of occurrences of equivalent sequences $C \subseteq W_L$, such that p denotes the number of consecutive time unit elements after which the t pairs of neighbouring sequences are equivalent.
4) Parameters f, t, p satisfy the following inequality: $f, t \geq 1,\ p \geq 0,\ f + (t-1) * p + |C| - 1 \leq |U|$

Also, if $t = 1$ then $p = 0$ and the pattern $<C,f,1,0>$ is called the *trivial periodic pattern* (*trivial* pattern)

Let $<C,\ f,\ t,\ p,>$ be a periodic patterns in W_L with a given U.

A *trace of a carrier* C is a subsequence $C \subseteq W_L$, denoted $tr(C, f, n)$, in which the first $f - 1$ elements are the empty multisets.

A *trace of a periodic pattern* $<C,\ f,\ t,\ p,>$ over the time unit sequence U, under the condition $f+(t-1)*p+|C|-1 \leq n$, is a subsequence $TR(< C, f, t, p >, n)$ of a sequence W_L such, that $TR(< C, f, t, p >, n) = tr(C, f, n) \uplus tr(C, f + p, n) \uplus \ldots \uplus tr(C, f + (t-1) * p, n)$

Let R be a non-empty set of periodic pattens in a W_L given time unit sequence $U(n)$. In the current approach , we say that R is a *reconstruction of the workload* W_L in $U(n)$ if:

i. $\uplus_{s=1}^{|R|} TR(< C_S, f_S, p_S >, n) = W_L$
ii. all TRs implementing connect-disconnect processes remain consistent in relation to each other. We allow duplication of database connect/disconnect processes in case of hypothetical processes, assuming that logging in and logging out does not involve costs.

As a *quality measure of the reconstruction* R is a real value $0 \leq m_R < 1$ defined as:
$m_R = 1 - (1/\sum_{i=1}^{|R|}(\|C_i\| * t_i))^{1/|R|}$
where $\|C_i\|$ is the length of the carrier C_i, $|R|$ is the cardinality of R. When $R = R_0 = \{< W_L, 1, 1, 0 >\}$ we assume that $m_{R_0} = 0$.

The test data generator, described in Section IV, is to provide synthetic data in the form of a sequence of multisets representing the sequence of database queries expressed in the evaluation representation obtained thanks to the `EXPLAIN PLAN` operation. This internal representation is then encoded using the syntax tree table [2]. The task of the presented test data generator is to generate hypothetical periodic patterns, but the generator does not determine the occurrence of a specific periodicity.

III. Workload reconstruction algorithm

With reference to the algorithm of [1], the algorithm presented in this paper has undergone some modifications and, as noted in the introduction, the simplification does not consider workload costs (in general). The pseudocode for the maximum relative frequency heuristic reconstructive algorithm is presented below. The heuristic is based on the local selection of the maximum relative frequency of the elements.

IV. Test data generator

In order to verify and evaluate the researched algorithm we have also developed a parameterized test-data generator. It is capable of generating a list of random multisets with a hidden periodicity feature. It is not predetermined but rather the construction of the generator ensures the existence of some non-trivial periodic patterns. The generator has been implemented in Python 3 language.

The basic building block of the result set is the list of lists:

```
[[object_number, number of occurrences], ...]

e.g. [[1.2], [2.2], [4.1], [6.3]]
```

Algorithm 1 Reconstruction algorithm

INPUT : W_L, list e

OUTPUT: optimal reconstruction R with the optimal value m_R

1) e= [e1, e2, e3,..] sorted (or not: in case of greedy heuristic), R : = < W_L,f,t,0 >, m_R:=0 , C:= W_L, R: = $\emptyset$, |R|: = 1,
2) While |C| <> 0:
   a) C : = C $\setminus$ TR (pp) ; for the current element e, starting from a minimum f value until all possibilities for f have been analyzed, search for such p and t that pp : = < e_i ,f,t,p > is a periodic pattern in W_L
   b) R : = R $\cup$ < C, f, 1,0> $\cup$ pp ; |R|++, Determination of min f and max t when selecting an element from the W_L sequence, i.e. identifying systems matching: f + (t - 1) * p $\leq$ n, pp = < C_{pp}, f, t, p >
   c) For the following elements, accept the last used t and p (start with the minimum value of f for which there is pp with parameters t and p, skipping the cases: t=1, p > [n/2]), always proceed until the possibility of a non-trivial periodic pattern with the given parameters t and p is exhausted. If no patterns are found for the current t and p, do the same as in the previous step, starting with the current element (if there is one, otherwise the next one). In the absence of the current element e, sort the array e (based on the relative frequency) for the current elements. Normalisation Rule + Decomposition Rule [1] : < C, f, 1,0> in each step is a (trivial) periodic pattern in W_L. Use the Decomposition Rules for periodic patterns found for elements for which patterns with t and p parameters were found. Create periodic patterns: pp_i, pp_j in W_L with C_i, p_i, t_i and C_j, p_j, t_j respectively, such that: p_i= p_j = p and t_i= t_j = t, in order to pair (reduce) periodic patterns to the form: pp_{ij} = < tr (C_i , 1, f_j - f_i + |C_j |) $\uplus$ tr (C_j , f_j - f_i, f_j - f_i + | C_j |), f_i , t, p > in W_L , and pair in such a way as to maximise the value of m_R, |R| $-$ $-$, use ($--$) as many times as the number of reduced pairs (reduction associative). As a results from method used above we consider only those cases in which the very last step of the recursion consists of non-trivial patterns. Otherwise, the interruption and output of the algorithm with the output as reconstruction of W_L not possible.
   d) Return and possibly replace (depending on the value of the previous scenario of the previous "recursive paths") the maximum m_R and associated set R

The full multiset list may then take the form:

```
WL=[[1,8], [2,4], [ [1,7], [2,3] ] , [1,6],
[3,2], [[1,7],[2,1]], [[1,1],[2,1]],
 [[1,7],[2,1]] ,  [[1,1][2,1]] , [[1,3],
[2,1],[3,2]],  [[1,1],[2,1]] ],
[2,1],[3,2]],  [[1,1],[2,1]] ]
```

The generator randomly sets the number of occurrences with a set decreasing probability of a number (from 1 to maxOcc parameter) being chosen.

The generator has a number of parameters that can be set to modify its performance. The most important are:

1) N - the size of the generated set; by default 1000
2) maxObj - the maximum number of "objects" (tables, indexes, lob files ertc.) - 20 by default
3) maxOcc - the maximum number of object occurrences in an element - by default 10

In the above example, the maxObj has been set to 3, therefore e=[1, 2, 3] is a set of all object appearing in WL

The generator starts by randomly selecting a number of objects that are to appear in a generated multiset. It then randomly (but according to a specified distribution parameter) select objects and their occurrence numbers. Then the generator proceeds with this procedure to generate following multisets. However, there is a chance (parametrized) that a multiset, that is to be generated, will be chosen from previously generated once. If such possibility is to happen, another parameter specifies how many following multisets should also be copied. Of course the mentioned parameter only specifies the maximum amount of copied elements, but the actual amount is randomly selected. We proceed in such manner until all N multisets have been generated.

The generator is equipped in a high amount of parameters influencing the pseudo-randomness. Therefore it is possible to estimate the number of potential periodic patterns present in the generated data

V. Conclusions and further works

Testing procedures for the algorithm included the analysis of the query series transformation to their multiset representation. Such representation was generated form the obtained database traces and resulted in a multiset sequence of a type described in chapter IV. Then followed the tests of the performance of the designed algorithm on the test data. The generated test-data was used to firstly verify the correctness of the main heuristic algorithm when it comes to the recognition of periodic patterns when searching for the optimal workload reconstruction. The second task was to aid the research on the reconstruction quality measure and time-efficiency of the reconstruction algorithm. The overall goal was to develop a fast, statistically stable algorithm that works with an optimal time and space complexity. The algorithm has been implemented in Python 3 and the tests were not meant to evaluate the actual time performance, but rather they focused on testing

the statistical stability and correctness of the results. Therefore, the performed tests were used for empirical verification of the correctness and stability of the algorithm's operation and have confirmed that not only is the algorithm stable but also optimal in its performance. Future work on the subject may include working on new heuristics combined with reconstruction algorithms' efficiency comparative analysis. Another aspect worth researching is the extended implementation of the reconstruction algorithm that takes into account the cost analysis derived from both the DBMS statistics and the relational algebra operators; the analysis of parallelization possibilities for periodic pattern discovery algorithms with the help of the GPU processing capabilities. Also it may be interesting to additionally enhance the heuristics with the computation of the reconstruction significance rate.

REFERENCES

[1] M. Zimniak, M. Burzanska, and B. Franczyk, "On some heuristic method for optimal workload reconstruction," in *Proceedings of the 27th International Workshop on Concurrency, Specification and Programming, Berlin, Germany, September 24-26, 2018*, ser. CEUR Workshop Proceedings, B. Schlingloff and S. Akili, Eds., vol. 2240. CEUR-WS.org, 2018. [Online]. Available: http://ceur-ws.org/Vol-2240/paper5.pdf

[2] M. Zimniak, J. R. Getta, and W. Benn, "Predicting database workloads through mining periodic patterns in database audit trails," *Vietnam Journal of Computer Science*, vol. 2, no. 4, pp. 201–211, 2015.

[3] M. Zimniak and J. R. Getta, "On systematic approach to discovering periodic patterns in event logs," in *Computational Collective Intelligence - 8th International Conference, ICCCI 2016, Halkidiki, Greece, September 28-30, 2016, Proceedings, Part I*, ser. Lecture Notes in Computer Science, N. T. Nguyen, Y. Manolopoulos, L. S. Iliadis, and B. Trawinski, Eds., vol. 9875. Springer, 2016, pp. 249–259. [Online]. Available: https://doi.org/10.1007/978-3-319-45243-2_23

[4] M. Zimniak, J. R. Getta, and W. Benn, "Discovering periodic patterns in system logs," in *Proceedings of the LWA 2014 Workshops: KDML, IR, FGWM, Aachen*, 2014, pp. 156–161.

[5] ——, "Deriving composite periodic patterns from database audit trails," in *Asian Conference on Intelligent Information and Database Systems*. Springer, 2014, pp. 310–321.

[6] K. Pommerening, "Cryptology part i: Classic ciphers (mathematical version)," 2014.

[7] E. LEHTONEN, "Reconstructing multisets over commutative groupoids and affine functions over nonassociative semirings," *International Journal of Algebra and Computation*, vol. 24, no. 01, pp. 11–31, 2014. [Online]. Available: https://doi.org/10.1142/S0218196714500027

[8] E. Lehtonen, "Totally symmetric functions are reconstructible from identification minors," *The Electronic Journal of Combinatorics*, vol. 21, no. 2, Apr. 2014. [Online]. Available: https://doi.org/10.37236/2863

[9] P. Wojtaszczyk, *A Mathematical Introduction to Wavelets*. Cambridge University Press, Feb. 1997. [Online]. Available: https://doi.org/10.1017/cbo9780511623790

[10] C. K. Chui, "Wavelets: A mathematical tool for signal analysis," 1997.

[11] A. B. Matos, "Periodic sets of integers," *Theoretical Computer Science*, vol. 127, no. 2, pp. 287–312, 1994.

[12] P. Serafini and W. Ukovich, "A mathematical model for periodic scheduling problems," *SIAM Journal on Discrete Mathematics*, vol. 2, no. 4, pp. 550–581, 1989.

15th International Symposium on Multimedia Applications and Processing

SOFTWARE Engineering Department, Faculty of Automation, Computers and Electronics, University of Craiova, Romania "Multimedia Applications Development" Research Centre

Background and Goals

Multimedia and information have become ubiquitous on the web and communication services, creating new challenges for detection, recognition, indexing, access, search, retrieval, automated understanding, processing and generation of several applications which are using image, signal or various multimedia technologies.

Recent advances in pervasive computers, networks, telecommunications, and information technology, along with the proliferation of multimedia mobile devices—such as laptops, iPods, personal digital assistants (PDA), and smartphones—have stimulated the rapid development of intelligent applications. These key technologies by using Virtual Reality, Augmented Reality and Computational Intelligenceare creating a recent multimedia revolution which will have significant impact across a wide spectrum of consumer, business, healthcare, educational and governmental domains. Yet many challenges remain.

We welcome papers covering innovative applications, practical usage but also theoretical aspects of the above mentioned trends. The key objective of this session is to gather results from academia and industry partners working in all subfields of multimedia and language: content design, development, authoring and evaluation, systems/tools oriented research and development. We are also interested in looking at service architectures, protocols, and standards for multimedia communications—including middleware—along with the related security issues. Finally, we encourage submissions describing work on novel applications that exploit the unique set of advantages including home-networked entertainment and games. However, innovative contributions which don't exactly fit into these areas are also welcomed to this session.

The Multimedia Applications and Processing (MMAP) will provide an opportunity for researchers and professionals to discuss present and future challenges as well as potential collaboration for future progress in the field. The MMAP Symposium welcomes submissions of original papers concerning all aspects of multimedia domain ranging from concepts and theoretical developments to advanced technologies and innovative applications. MMAP invites original previously unpublished contributions that are not submitted concurrently to a journal or another conference. Papers acceptance and publication will be judged based on their relevance to the symposium theme, clarity of presentation, originality and accuracy of results and proposed solutions.

Call for Papers

MMAP 2022 is a major forum for researchers and practitioners from academia, industry, and government to present, discuss, and exchange ideas that address real-world problems with real-world solutions.

The MMAP 2022 Symposium welcomes submissions of original papers concerning all aspects of multimedia domain ranging from concepts and theoretical developments to advanced technologies and innovative applications. MMAP 2022 invites original previously unpublished contributions that are not submitted concurrently to a journal or another conference. Papers acceptance and publication will be judged based on their relevance to the symposium theme, clarity of presentation, originality and accuracy of results and proposed solutions.

Topics

- Audio, Image and Video Processing
- Animation, Virtual Reality, 3D and Stereo Imaging
- Big Data Science and Multimedia Systems
- Cloud Computing and Multimedia Applications
- Machine Learning, Fuzzy Systems, Neural Networks and Computational Intelligence for Information Retrieval in Multimedia Applications
- Data Mining, Warehousing and Knowledge Extraction
- Multimedia File Systems and Databases: Indexing, Recognition and Retrieval
- Multimedia in Internet and Web Based Systems
- E-Learning, E-Commerce and E-Society Applications
- Human Computer Interaction and Interfaces in Multimedia Applications
- Multimedia in Medical Applications and Computational biology
- Entertainment, Personalized Systems and Games
- Security in Multimedia Applications: Authentication and Watermarking
- Distributed Multimedia Systems
- Network and Operating System Support for Multimedia
- Mobile Network Architecture and Fuzzy Logic Systems
- Intelligent Multimedia Network Applications
- Future Trends in Computing System Technologies and Applications
- Trends in Processing Multimedia Information

- Multimedia Ontology and Perception for Multimedia Users

Best Paper Award

A best paper award will be made for work of high quality presented at the MMAP Symposium. Award comprises a certificate for the authors and will be announced on time of conference. Selected papers will be invited to high IF journals organized for the participants of MMAP.

- Authors should submit draft papers (as Postscript, PDF or MSWord file).
- The total length of a paper should not exceed 10 pages IEEE style (including tables, figures and references). IEEE style templates are available here.
- Papers will be refereed and accepted on the basis of their scientific merit and relevance to the workshop.
- Preprints containing accepted papers will be published on a USB memory stick provided to the FedCSIS participants.
- Only papers presented at the conference will be published in Conference Proceedings and submitted for inclusion in the IEEE Xplore®database.
- Conference proceedings will be published in a volume with ISBN, ISSN and DOI numbers and posted at the conference WWW site.
- Conference proceedings will be submitted for indexation according to information here.
- Extended versions of selected papers presented during the conference will be published as Special Issue(s).
- Organizers reserve right to move accepted papers between FedCSIS events.

Winners of MMAP 2019 Best Paper Award

- Depth Map Improvements for Stereo-based Depth Cameras on Drones. Authors: Daniel Pohl (Intel Corporation), Sergey Dorodnicov (Intel Corporation).
- Information theoretical secure key sharing protocol for noiseless public constant parameter channels without cryptographic assumptions. Authors: Valery Korzhik, Vladimir Starostin, Muaed Kabardov, Aleksandr Gerasimovich, Victor Yakovlev, Aleksey Zhuvikin (The Bonch-Bruevich Saint-Petersburg State University of Telecommunications), Guillermo Morales-Luna (Computer Science Department CINVESTAV-IPIV, Mexico City, Mexico).

Advisory Board

- **Neustein, Amy,** Boston University, USA
- **Jain, Lakhmi C.,** University of South Australia and University of Canberra, Australia
- **Zurada, Jacek,** University of Louisville, United States
- **Ioannis, Pitas,** University of Thessaloniki, Greece
- **Badica, Costin,** University of Craiova, Romania
- **Borko, Furht,** Florida Atlantic University, USA
- **Kosch, Harald,** University of Passau, Germany
- **Uskov, Vladimir,** Bradley University, USA
- **Deserno, Thomas M.,** Aachen University, Germany
- **Burdescu, Dumitru Dan,** University of Craiova, Romania

Technical Session Chair

- **Schiopoiu Burlea, Adriana,** University of Craiova, Romania

Communication Papers of the of the 17th Conference on Computer Science and Intelligence Systems pp. 145–151
DOI: 10.15439/2022F51
ISSN 2300-5963 ACSIS, Vol. 32

Replication of first click eye tracking A/B test of webpage interactive elements

Julia Falkowska
Department of Computer Science and Systems Engineering
Wrocław University of Science and Technology
Wrocław, Poland
julia.falkowska@pwr.edu.pl

Janusz Sobecki
Department of Computer Science and Systems Engineering
Wrocław University of Science and Technology
Wrocław, Poland
janusz.sobecki@pwr.edu.pl

***Abstract*—In this paper, we present a replication of our experiments of first click eye tracking A/B test of interactive website elements [13]. The main difference between these two experiments is the equipment used; the first study was done using Tobi X-60 eye-tracker, while the replication described in this paper was conducted using Tobii TX 300, a higher frequency eye tracker. Eye tracking metrics used to evaluate the user experience of websites were almost identical. This paper presents the results of an experiment in which seven commercial websites were tested with the A/B first click test. This work examines the validity of a specific set of eye tracking metrics for their broad application in user experience research on websites.**

***Index Terms*—eye tracking, user experience, eye tracking metrics, A/B tests**

I. Introduction

TODAY, user experience (UX) plays a crucial role in webpage design, which is exhibited, for example, in increasing the amount of money allocated for this aspect in web development projects. The ISO 9241-210 standard defines UX as "a person's perceptions and responses that result from the use or anticipated use of a product, system, or service." Therefore, UX should include user's emotions, beliefs, preferences, perceptions, physical and psychological responses, behavior, and accomplishments that the user experiences interacting with a given product, system, or service. User experience and usability are often used as synonyms, however, many authors [1-3] indicate that these two terms should not be conflated. The main difference is that user experience (UX) refers to how the user feels when interacting with the system, while usability is just an aspect of the user experience that mainly relates to efficiency of the interface. Additionally, UX extends usability by taking into account a holistic perspective of user's feelings and attitudes towards the product, system, or service. In addition to usability, there are other factors that significantly contribute to UX such as ergonomics, design/aesthetics, accessibility, human factors and system performance. A complete conceptual framework of UX that takes into account usability and user perception is presented in the work of Hellweger and Wang [4].

To monitor the user's behavior during an interacrion with a webpage, researchers use different devices, such as web cams [5], EEG headsets [6], touch screens [7], thermal cameras [8], and eye trackers. The latter are especially popular in user experience research [9]. For example, the work of Schall et al., Horsley et al., and Bojko [10-12] presents many effective eye tracking methodologies applied to UX and usability testing of webpages. These eye tracking methodologies can be applied, among other research efforts, in different stages of A/B tests of website design [13]. In principle, eye tracking UX research is based on the assumption that the fixation point determines the elements of the user interface that attract user's attention and that the rest of the areas are invisible or incomprehensible during completion of the task on a tested webpage [14].

Testing with users is the most effective when such tests are conducted throughout the project lifecycle to enable the design to be improved interactively. Therefore, tests should be performed already at the earliest phase of the design process, using static or interactive mock-ups. At this stage, any changes need to be applied only to the design of the mock-up and do not require code modifications, which would be significantly more time and effort consuming. With this approach, we can ensure early in the process that the outcome is congruent with users' needs to a large extent, thus avoiding the high cost of changes during the development stage. In our research, we used the first click testing method (task ends with user's first click) on static representations of webpages. In every trial, the participant is asked to click on an element or a location that would contain the information they were asked to find. As an example, we may want to test findability of an element that links a subpage where all products are displayed. The task here might be phrased as: 'Try to find out what this company has in offer.' The task ends when the user makes the first click, no matter if it was on the expected element or not.

With first click testing, we can correlate eye tracking metrics with a click of a mouse over an element of the website. User clicking a mouse click on an element is understood as finding the item and recognizing it as meeting the user's needs. Our previous studies have shown that eye tracking analysis is a valid method to evaluate interface design and interactive web elements [15-17]. In these research, the analyses showed statistically significant differences between different webpage projects and selected metrics.

Inspired by NNGroup research [18] our study was carried out on two variants of each tested website: with a well-

designed target element (user-friendly) and a poorly designed target element (harder for the user). Webpage designs selected for the experiment represent some of the most popular types of websites and do not require specialized knowledge to use them. The websites used in our study fall into one of the following categories: e-commerce, travel or restaurant websites.

In this paper, we present a replication of the research by Falkowska et al. [13] using a Tobii TX 300 eye tracker, which produces better quality data than Tobii X-60 eye tracker used in the study described in work [13]. In the summary of the original paper, we pointed out that the low frequency (60Hz) of Tobii X-60 eye tracking data registration resulted in the lack of precise fixation on small interface elements and in numerous shifts. In the experiment replication, we also used a bigger, 23" screen (instead of 17" screen) to more precisely monitor differences in fixation on the interface elements. This in turn resulted in fewer samples than registrations and had an impact on the significance calculations. For five designs in the study [13], none of the metrics showed a significant difference between design versions A and B. However, we have noticed that in most cases the average values of the used measures showed a trend indicating that improved designs (variant A) were better than less user-friendly versions (variant B). Nevertheless, most of these results were not statistically significant. Additionally, most of the participants were experienced web users and it is very likely that they were simply used to various layouts and designs, both good and bad, from the user experience point of view.

In our previous work [13], we have presented an experiment that verifies the usability of nine common commercial websites of hotels, e-shops, restaurants, fitness clubs, energy providers, social networks and insurance companies. Participants have been presented with static representations of these websites on a screen and asked to perform certain tasks on them. In the current experiment, the number of tasks has been reduced to seven because we previously found that one task was too difficult for the participants. The experiment was constructed as a standard A/B test, with version A designed as a more user friendly variant and version B as a less user friendly variant of the same interface. Versions A of all websites have been designed to increase visibility and/or readability by modifying size, contrast, or adding supporting graphic elements [19], [20]. Different versions of the same website have been presented to separate groups of users. For each task we measured seven eye tracking metrics to investigate whether the differences in selected metrics values for design versions A and B are significant [21], [22].

The paper is organized as follows. The first part of this paper introduces eye tracking studies and eye tracking measures. This is followed by the presentation of the stimuli used in the experiment. The experimental setup and corresponding methodology are described in section three. Section four presents the results. In section five, we present the discussion and finally in the section six we present our conclusions.

II. Eye tracking studies and eye tracking metrics

Eye tracking studies began in the nineteenth century and over the years many different technologies and methods have been established and introduced into various disciplines [23]. Already from the early 90s of the last century, eye trackers were used in usability studies [22]. Since then, eye tracking has been applied in many varieties of usability studies:

- usefulness of web or desktop applications [24-28],
- perception of information (graphics or texts) [29-34],
- correlation between declarative data and eye tracking measures [25-36],
- comparative studies of the effectiveness of system interfaces [37],
- correlation of eye tracking data with the strategy of searching for information in web systems [38],
- correlation of eye tracking data with users' behavior in the system, e.g. purchase decisions [39],
- method and speed of user interaction with information elements depending on their parameters, e.g. size or location [40-44],
- exploring potential new applications and use cases, e.g. for mobile applications [45],
- comparing the eye tracking registration method with other research methods [46].

In these studies, several implementations of methodologies have been used, in particular:

- users perform several prepared tasks in the system [24], [26], [37], [46],
- users perform tasks on specially prepared materials according to research purposes (i.e. different pages or graphic interface designs) [26], [29], [32], [33], [34], [36], [40], [41], [42], [47], [48],
- supplemented with declarative methods (questionnaires, interviews) [25], [35], [49].

Finally, the data that have been gathered during the studies needs to be analyzed. The rough eye tracking data in the form of gaze coordinates on a plane, together with time stamps, are usually transformed into metrics that can be interpreted as results:

- the characteristics of the gaze path to identify usability problems, mainly by identifying elements on which users focus or which are omitted [24-27], [37],
- the number of fixations: information whether the user saw / did not see, read / did not read the presented information [24, 31], the amount of visual attention [29], the difficulty of completing the task [36], processing and understanding the information [32], [50] frequency of attracting attention understood as attractiveness [42],
- time to the first fixation: how quickly the user notices the information [26], [29], [40], [41], identification of the elements that attract attention [30].
- fixation time: the amount of visual attention [30], [33], [35], [40], [47], the time spent processing given content, evaluating the object as

attractive [32], [38], [41], evaluating an object as difficult to understand or read [43],
- duration of the first fixation: the effectiveness of focusing visual attention [30],
- time from noticing to clicking on an element: indication of an element that is problematic for the user [48].

Most of the eye tracking metrics used in UX studies are based on fixations. In eye tracking studies [23], fixation is defined as a functional component: what purposes does the eye movement (or lack thereof) serve? Fixation usually ranges from 100 to 500 ms. The average duration of a human eye fixation during reading is 200-250 ms and 280-330 ms for scene viewing [12]. The functional definition of fixation means stabilizing a target relative to the fovea, that is, being stationary or moving with respect to the head. Saccades, on the other hand, are defined as the interfixation interval. Holmqvist et al. [23] distinguished the following eye-tracking measure types:

- movement measures that concentrate on the whole variety of eye movements,
- position measure, which corresponds only to where the participant has or has not looked,
- numerosity measures that pertain to the whole spectrum of the number or rate of any countable eye movement event,
- latency measures, which give the values of the onset between two events.

We may also find other typologies of eye tracking measures, for example those proposed by Bojko [21]. These measures have been validated in many UX research to show cognitive processes of the user with which they are linked. The are also relatively easy to extract from the rough gaze data. According to Bojko [21], we can distinguish the following types of measures:

- mental workload measures,
- cognitive processing measures,
- target findability measures,
- target recognizability measures.

In addition to fixation, the notion of area of interest (AOI) is of great importance in eye tracking analysis. AOIs are the selected elements on a webpage for which a metric is calculated. In our research, we distinguished only one AOI on a webpage, which is typical for first click experiments . In our case it was a specific button.

For the analysis of our study, we have selected from the metrics related to cognitive overload described by Bojko in his book [21]. These metrics were selected as the most relevant for UX and their analysis is available in the Tobii Studio software we have used.

To date, more than one hundred eye tracking metrics have been established. In this paper, however, we only describe the metrics we have used in our research, which are [21]:

- time to first fixation belongs to attraction measures, which is a superclass of area noticeability measures that are useful for visibility assessment of an object or area by describing how many people noticed or how quickly something was noticed,
- the number of fixations prior to the first fixation on an AOI, similarly to the previous metric, it belongs to the attraction metric,
- first fixation duration on AOI belongs to cognitive processing measures and evaluates cognitive processing difficulty; longer fixation usually indicates deeper cognitive processing caused, for example, by more effortful extraction of information,
- fixation count over AOI is usually used when presenting results in the form of a heatmap; each fixation over AOI adds to the fixation count and is later presented on a heatmap as an appropriate color in the fixation area,
- visit count over AOI is a metric indicating the total count of all fixations and saccades over AOI,
- time from the first fixation on AOI to the mouse click within this area belongs to target recognizability measures - the faster the AOI is recognized as a task solution, the shorter it is,
- fixation duration in AOI measures the time spent observing the specific area by the participant, which usually indicates the participant's motivation and attention; higher values of this measure for a specific AOI indicate more interest on this AOI than for AOI's with lower values.

III. Experiment stimuli

Different versions of stimuli have been created by adding or changing visually one of the elements, or a group of elements of the websites' design. A task was prepared for each pair of design versions and the correct solution was to click on the modified/tested element. Ten webpage designs in two versions have been prepared for the study, however only seven of them have been analyzed, because three task instructions have been reported as difficult to understand by the participants in the interview after the study.

Interview after the study contained two questions, one closed and one open: "Did you have any doubts what you should in this task? (yes/ no/ can't tell)?" and "Please, explain/tell me more in your own words how you understood the task/instruction". For two tasks, all respondents declared the some problems occurrence of weakness, and in response to the open-ended question, they presented different ways of understanding the instruction. Due to the fact that the viewing paths are strongly dependent on the goal / performed task, we decided not to take into account these eye tracking data.

Table I presents the stimuli (webpage URL), along with the type of design modification, as well as the corresponding task. These websites were accessed between 1st and 15th November 2019.

Offline versions of these pages have been the basis for preparation of the stimuli used in the experiment. Modifications were made to specific elements to create a user interface that is more (A) or less (B) user friendly. The correct solution for each task was determined as clicking on a specific button on a given webpage.

TABLE I
EXPERIMENT DESCRIPTION DETAILS [6].

Name	Source page URL	Version A (more user friendly)	Version B (less user friendly)	Task
C21	//www.c21stores.com/ Germany	Main menu tab 'Stores and Events' with appropriate iconographic	Main menu tab 'Stores and Events' without appropriate iconographic	You will see a bookshop website with a particular book presented. You want to know what other readers think about that book. Click where you would look for information about that.
LS	http://www.loursinseattle.com	All caps main menu tabs	Sentence case main menu tab	You will see a restaurant website. That restaurant sometimes organizes food presentation days. Imagine you want to find more details about that. Click where you would look for information about that.
PP	http://www.peachpit.com/store/adobe-photoshop-elements-2019-classroom-in-a-book-9780135298633	(Shop best sellers >) under the product picture Gray and underlined link (Shop best sellers >) under the product picture	Submenu tabs (About, Description, Reviews, Sample, Content, Updates) at the bottom with white background	You will see a restaurant website. That restaurant sometimes organizes food presentation days. Imagine you want to find more details about that. Click where you would look for information about that.
POPO	www.poopourri.com	Black and underlined links (Shop best sellers >) under the product picture	Gray and underlined link (Shop best sellers >) under the product picture	You will see a cosmetic shop website. Imagine that someone recommended you this shop and you do not know any of their products, so you want to see the products that people buy the most. Click where you would look for information about that.
SS	www.swissotel.com	Gray background of button with language changed (English)	White background of the button with language changed (English)	You will see a hotel website. Imagine you want to change the website language. Click where you would look for information about that.
RM	www.rockymountainsoap.com /products/beech-tree-bud-eye-cream	Orange submenu elements (ingredients, how to use, shipping)	Gray submenu elements (ingredients, how to use, shipping)	You will see a page from an e-shop with a product presentation. Imagine you want to buy this product and you want to know more about delivery. Click where you would look for information about that.
FB	www.fitnessblender.com	White submenu font in the center of the website. Submenu elements: Workout Videos, Workout Programs, Meal Plans, FB Plus with descriptions.	Gray submenu font in the center of the website. Submenu elements: Workout Videos, Workout Programs, Meal Plans, FB Plus descriptions	You will see a fitness website. Imagine you have a specific training program and now you want to change your eating habits. Click where you would look for information about that.

IV. EXPERIMENT METHODOLOGY

In the experiment, two methods have been applied: first click testing recorded with eye tracking and one-on-one interviewing [14]. Each participant was asked to sit in front of the computer monitor and interact with each webpage by clicking the selected button. Each respondent was asked to complete seven tasks, which were later analyzed and presented in Table I. We finished the task when the participant clicked on a webpage element, which is also named as a first click testing [51]. We have used an eye tracking system to record participants' gaze activity. Using this system, the fixation path has been recorded together with screen and mouse activity. After finishing all tasks, all users have participated in a one-to-one sound recorded interview with the aim to verify their understanding of tasks, as well as confirm they have not seen any of these webpages before. With twenty participants and seven websites with two versions each (user-friendly and not), every webpage variant has been seen by ten participants. The webpages have been presented on a 23" LCD screen connected to a TX 300 eye tracker. The sessions have been recorded using Tobii Eye Tracker TX 300 and Tobii Studio software.

The experiment has been conducted at the Wrocław University of Science and Technology, Poland (WUST) from 28.06.2021 to 6.07.2021. Out of twenty participants, five were students, five were working and ten declared to be working students. Exactly half of the group was women and half men.

V. EXPERIMENT RESULTS

In this section, the experiment results are presented. The statistical significance was verified by two-tailed t-tests [52]. In our experiment each user interacted with only one version (A or B) and the number of users working with each version differs because of data quality issues encountered during eye tracking data collection. Therefore, we used the two-sample t-test [51], which specifies the degrees of freedom of t-test as

equal to (nA+nB-2), where nA and nB are numbers of users using version A or B accordingly. The results are presented in Tables II-VIII with statistically significant results (p=0.05) in bold face. For all tables, results for user-friendly variants of websites are shown in row A and results for less user-friendly variants can be found in row B.

Table II shows the time to first fixation for two versions of seven designs. Time to first fixation is defined as the time from the start of the stimulus display until the the participant fixated on the AOI [21].

In four out of seven designs, the average time to first fixation was longer for design B than design A, however the difference was not statistically significant. Table III presents average number of fixations prior to first fixation on an AOI. There were no significant results for this measure.

Table IV presents the average duration of first fixation on AOI, for the A and B versions of each website. There were no significant results for this measure.

Table V presents average number of fixations over AOI for the A and B versions of each website. There was only one significant difference in the scores for RM website version A (M=2, SD=0,84) and version B (M=2, SD=0,54), t(11)=2.42, p=.033.

Table VI presents the results for the average number of visits over AOI, for the A and B versions of design. There were two significant differences in the scores. Version A of the C21 website had a significantly lower average number of visits over AOI (M=2,5, SD=1,64) than version B (M=4, SD=1,77), t(14)= -2,48, p= .026 while version A of the RM website had a significantly higher average number of visits over AOI (M=2, SD=0,52) than version B (M=1, SD=0,53), t(11)=-3,08, p=. 01.

Table VII presents the results for the average time between the first fixation on AOI and the mouse click within this area for the A and B versions of each website. There were no significant results for this measure.

Table VIII presents the results for the average duration of fixation on AOI for the A and B versions of design. There were no significant results for this measure.

VI. Discussion

The experiment that we conducted and presented here is a replication of the experiment that was described in our previous work [13]. In the conclusion of that article, we hypothesized that an eye tracker with higher frequency should provide more precise experimental data that would potentially provide statistically significant results. In our replication we used Tobii TX 300, which has a five times higher frequency rate than Tobii X-60 used in the previous research. The second factor modified in the replication of the previous experiment was the participants' level of experience in using web systems. We expected that less experienced users would encounter more problems when using poorly designed web pages and, as a result, the differences between good and bad design would be more prominent, thus allowing us to obtain statistically significant results. Additionally, the statistical analysis was done using a two-tailed t-test for two samples [51]. This test is well suited for experiments with a small number of participants and may detect significant differences regardless of the small sample size [13]. Unfortunately, none of these measures have brought the expected results. Peculiarly, we observed even fewer significant results than in the previous work [13]. In this study we still observed differences in average values for many analyzed metrics and most of the designs, however, these differences have not reached the significance level due to the small number of participants. The differences that we observed in the data would be significant for a sample size of approximately one hundred participants. Unfortunately, due to lockdown measures it was impossible to recruit more people and conduct experiments.

Finally, we would like to address why, for certain measures, some websites have opposing results. E.g. for a particular measure, one website may have scored higher for user-friendly version A and another website had a higher result for its non user-friendly variant B. There may be at least two reasons for this. First is that the value of the metric depends not only on the design quality, but also on the webpage type and the content itself. The second is that the designs A and B do not produce great differences in usability.

VII. Conclusions

In this paper, we present a replication of a webpage first click experiment enhanced with eye tracking that was described in our previous work [13]. We designed the replication following the conclusions from that study, therefore we used better quality eye tracker. However, mainly because of insufficient differences between results for designs A and B, we did not received statistically significant results. We expect these kind of study would exhibit statistically significant results for greater number of participants of at least one hundred. For some metrics we obtained differences between their averages for design A and B with opposing results for different types of websites. Consequently, future eye tracking studies exploring the impact of good and bad webpage design should carefully consider the type and content of webpages used, as well as aim for a number of participants that provides a better chance to obtain statistically significant results.

Acknowledgment

We would like to thank the experiment participants for their kindness and patience, as well as for their volunteer participation.

References

[1] M. Thüring,S. Mahlke, "Usability, aesthetics and emotions in human–technology interaction", in International Journal of Psychology, vol. 42(4), 2007, pp. 253–264.

[2] V. Roto, E. C Law, A. P. Vermeeren, J. Hoonhout, "User experience white paper: Bringing clarity to the concept of user experience". 2011.

[3] B. Nigel, "What is the difference between the purpose of usability and user experience evaluation methods", in Proceedings of the Workshop UXEM, 2009, pp. 1–4.

[4] S. Hellweger, X. Wang, "What is user experience really: towards a UX conceptual framework", arXiv preprint arXiv:1503.01850, 2015.

TABLE II
MEAN TIME TO FIRST FIXATION ON THE A AND B VERSION OF EACH WEBSITE

	C21	**FB**	**GE**	**LS**	**POPO**	**PP**	**RM**	**SS**
A	3,8	5,58	17,81	2,98	6,7	5,59	4,64	2,12
B	3,47	5,53	17,31	3,81	9,57	10,95	5,57	1,99

TABLE III
AVERAGE NUMBER OF FIXATIONS BEFORE FIRST FIXATION ON AOI ON THE A AND B VERSION OF EACH WEBSITE

	C21	**FB**	**GE**	**LS**	**POPO**	**PP**	**RM**	**SS**
A	8	17	70	8,5	19,89	21,5	16,5	3,33
B	7,5	17,65	69,8	10,83	30,91	35,56	18,57	3,12

TABLE IV
AVERAGE DURATION OF FIRST FIXATION ON THE A AND B VERSION OF EACH WEBSITE

	C21	**FB**	**GE**	**LS**	**POPO**	**PP**	**RM**	**SS**
A	0,26	0,48	0,24	0,18	0,18	0,33	0,77	0,2
B	0,2	0,3	0,31	0,16	0,2	0,28	0,81	0,22

TABLE V
AVERAGE NUMBER OF FIXATIONS ON THE A AND B VERSION OF EACH WEBSITE

	C21	**FB**	**GE**	**LS**	**POPO**	**PP**	**RM**	**SS**
A	5,5	8,88	5,75	1,5	7,22	5,6	2,5	4,56
B	9,75	9,12	7,17	3	6,09	3,67	1,57	3,25

[5] M. Bratkowska, J. Falkowska, J. Sobecki, "Webcam eye tracking platforms for usability testing", in Proc. of 35th IBIMA Conference; 1–2 April 2020, Seville, Spain, pp. 3091–3099.

[6] P. Chynał, J. Sobecki, M. Rymarz, B. Kilijańska, "Shopping behaviour analysis using eyetracking and EEG", in 9th International Conference on Human System Interactions (HSI) July 2016, pp. 458–464, IEEE.

[7] K. Cichoń, J. Sobecki, J.M. Szymański, "Gesture tracking and recognition in touchscreens usability testing" in Proceedings of the International Conference on Multimedia, Interaction, Design and Innovation, June 2013, pp. 1–8.

[8] P. Chynał, J. Sobecki, "Application of thermal imaging camera in eye tracking evaluation", in 9th International Conference on 341 Human System Interactions (HSI) 2016, July. pp. 451–457. IEEE.

[9] P. Weichbroth, K. Redlarski, I. Garnik, " Eye-tracking web usability research", in 2016 Federated Conference on Computer Science and Information Systems (FedCSIS), pp. 1681–1684. IEEE.

[10] A. Schall, J. Bergstrom, "Introduction to eye tracking", Elsevier, 2014.

[11] M. Horsley, M. Eliot, B.A. Knight, "Current Trends in Eye tracking Research", Springer, 2014.

[12] A. Bojko, "Using Eye Tracking to Compare Web Page Designs: A Case Study", Journal of Usability Studies 2006. Issue 3, Vol. 1, pp. 112–120.

[13] J. Falkowska, J Sobecki, "First Click eye Tracking A/B Tests of Webpage Interactive Elements". in Proc. of 36th IBIMA Con-349 ference; Grenada, Spain 4–5 November 2020, pp. 12524–12530.

[14] B. Rogos-Turek, I. Moscichowska, "Research as a basis for User Experience design", (in Polish), PWN:Warszawa, Poland, 2015.

[15] P. Chynał, J. Falkowska, J.Sobecki, "Web page graphic design usability testing enhanced with eye tracking" in proceedings of the 1st International Conference on Intelligent Human Systems Integration (IHSI 2018), pp. 515–520.

[16] J. Falkowska, J. Sobecki, M. Pietrzak,"Eye tracking usability testing enhanced with EEG analysis", in proc. of 5th International Conference, held as Part of HCI International 2016, Toronto, Canada, July 17–22, 2016, pp. 399–411.

[17] J. Falkowska, B. Kilijańska, J. Sobecki, K. Zerka, "Microinteractions of forms in web based 360 systems usability and eye tracking metrics analysis", in proceedings of the AHFE 2018 International Conference on Human Factors and Systems Interaction, Springer, cop. 2019, pp. 164–174.

[18] "Flat UI Elements Attract Less Attention and Cause Uncertainty", available online: https://www.nngroup.com/articles/flat-ui-less-attention-cause-uncertainty (accessed on 1.09.2021)

[19] X. Kotval, J. Goldberg, "Eye Movements and Interface Component Grouping: An Evaluation Method", in Proceedings of the Human Factors and Ergonomics Society Annual Meeting 1998, 42, pp. 486–490.

[20] J. Goldberg, X. Kotval, "Computer interface evaluation using eye movements: Methods and constructs", International Journal of Industrial Ergonomics 1999, vol. 24, pp. 631–645.

[21] A. Bojko, "Eye tracking the user experience: A practical guide to research", Rosenfeld Media, 2013, pp. 121–143.

[22] J. Nielsen, K. Pernice, "Eye tracking Web Usability", New Riders: Berkley, CA, USA 2009.

[23] K Holmqvist, M. Nyström, R. Andersson, R. Dewhurst, H. Jarodzka, J. Van de Weijer, "Eye tracking: A comprehensive guide to methods and measures", OUP: Oxford, UK, 2011.

[24] P. Krehahn, V. Wohlgemuth, H.A. Meyer, "UxLab: Usability Optimization Case Study of a Environmental Management Information System (EMIS) Using Eyetracking Studies", in EnviroInfo 2010: Integration of Environmental Information in Europe, Shaker Verlag, Aachen, 2010, pp. 248–249.

[25] M.C. Pretorius, J. van Biljon, E. de Kock,"Added Value of Eye Tracking in Usability Studies: Expert and Non-expert Participants", in proc. of Human-Computer Interaction 2010, Vol. 332, pp. 110–121.

[26] C. Ehmke, S. Wilson, "Identifying Web Usability Problems from Eye-Tracking Data", in Proceedings of the 21st British HCI Group Annual Conference on People and Computers: HCI...but not as we know it, Volume 1; BCS 384 Learning & Development Ltd.: Swindon, GBR, September 3 2007; pp. 119–128.

[27] A. Çöltekin, B. Heil, S. Garlandini, S.I. Fabrikant, "Evaluating the Effectiveness of Interactive Map Interface Designs: A Case Study Integrating Usability Metrics with Eye-Movement Analysis", 2013.

[28] A. Çöltekin, B. Heil, S. Garlandini, S.I. Fabrikant, "Evaluating the Effectiveness of Interactive Map Interface Designs: A Case Study Integrating Usability Metrics with Eye-Movement Analysis", in Cartography and Geographic Information Science 2009, vol. 36, pp. 5–17.

TABLE VI
AVERAGE NUMBER OF VISITS OVER AOI FOR THE A AND B VERSION OF EACH WEBSITE

	C21	**FB**	**GE**	**LS**	**POPO**	**PP**	**RM**	**SS**
A	2,6	2,5	2,5	1,5	3,33	4,7	2,33	2,89
B	5	3	2,33	2,17	2,64	2,67	1,43	2,38

TABLE VII
MEAN TIME FROM FIRST FIXATION TO MOUSE CLICK ON THE A AND B VERSION OF DESIGN

	C21	**FB**	**GE**	**LS**	**POPO**	**PP**	**RM**	**SS**
A	8,35	3,09	4,08	3,15	4,92	7,34	3,64	2,42
B	14,15	4,1	2,97	4,34	4,71	5,88	1,86	2,21

TABLE VIII
MEAN FIXATION DURATION ON THE A AND B VERSION OF DESIGN

	C21	**FB**	**GE**	**LS**	**POPO**	**PP**	**RM**	**SS**
A	0,29	0,31	0,31	0,18	0,27	0,46	0,64	0,37
B	0,29	0,29	0,33	0,26	0,25	0,44	0,69	0,39

[29] H.-F. Ho, "The Effects of Controlling Visual Attention to Handbags for Women in Online Shops: Evidence from Eye Movements", in Computers in Human Behavior 2014, vol. 30, pp. 146–152.

[30] N. Steinfeld,"I Agree to the Terms and Conditions: (How) Do Users Read Privacy Policies Online? An Eye-Tracking Experiment", in Computers in Human Behavior 2016, 55, pp. 992–1000.

[31] H.-C. Liu, M.-L. Lai, H.-H. Chuang, "Using Eye-Tracking Technology to Investigate the Redundant Effect of Multimedia Web Pages on Viewers", in Cognitive Processes. Computers in Human Behavior 2011, vol. 27, pp. 2410–2417.

[32] C.-Y. Wang, M.-J. Tsai, C.-C. Tsai, "Multimedia Recipe Reading: Predicting Learning Outcomes and Diagnosing Cooking Interest Using Eye-Tracking Measures", in Computers in Human Behavior 2016, vol. 62, pp. 9–18.

[33] L. Grigg, A. Griffin, "A Role for Eye-Tracking Research in Accounting and Financial Reporting", in Current trends in eye tracking research Springer, Cham 2014; pp. 225–230.

[34] S. Djamasbi, M. Siegel, T. Tullis, "Can Fixation on Main Images Predict Visual Appeal of Homepages", in Proceedings of the 2014 47th Hawaii International Conference on System Sciences; IEEE: Waikoloa, HI, January 2014; pp. 371–375.

[35] Y. Habuchi, M. Kitajima, H. Takeuchi, "Comparison of Eye Movements in Searching for Easy-to-Find and Hard-to-Find Information in a Hierarchically Organized Information Structure", in the Proceedings of the the 2008 symposium on Eye tracking research & applications, Association for Computing Machinery: New York, NY, USA, March 26 2008; pp.131–134.

[36] A. Bojko, "Using Eye Tracking to Compare Web Page Designs: A ", inase Study", J. Usability Stu 2006, 1, pp. 112–120.

[37] J. Luan, Z. Yao, Z. F. Zhao, H. Liu, "Search Product and Experience Product Online Reviews: An Eye-Tracking Study on Consumers' Review Search Behavior", Computers in Human Behavior 2016, vol. 65, pp. 420–430.

[38] S.-F. Yang, "An Eye-Tracking Study of the Elaboration Likelihood Model in Online Shopping", in Electronic Commerce Research and Applications 2015, vol. 14, pp. 233–240.

[39] S. Djamasbi, M. Siegel, T. Tullis, "Designing Noticeable Bricklets by Tracking Users' Eye Movements", in Proceedings of the 2012 45th Hawaii International Conference on System Sciences; IEEE: Maui, HI, USA, January 2012; pp. 525–532.

[40] J. Hernández-Méndez, F. Muñoz-Leiva, "What Type of Online Advertising Is Most Effective for ETourism 2.0, An Eye Tracking Study Based on the Characteristics of Tourists", in Computers in Human Behavior 2015, vol. 50, pp. 618–625.

[41] H. Lin, Y.-C. Hsieh, F.-G. Wu, "A Study on the Relationships between Different Presentation Modes of Graphical Icons and Users' Attention", in Comput. Hum. Behav. 2016, vol. 63, pp. 218–228.

[42] Q. Wang, S. Yang, M. Liu, Z. Cao, Q. Ma, "An Eye-Tracking Study of Website Complexity from Cognitive Load Perspective", in Decision Support Systems 2014, vol. 62, pp. 1–10.

[43] S.P. Roth, A.N. Tuch, E.D. Mekler, J.A. Bargas-Avila, K. Opwis, "Location Matters, Especially for Non-Salient Features-An Eye-Tracking Study on the Effects of Web Object Placement on Different Types of Websites", in Int. J. Hum.-Comput. Stud. 2013, vol. 71, pp. 228–235.

[44] C. Cuadrat Seix, M.S. Veloso, J.J.R. Soler, "Towards the Validation of a Method for Quantitative Mobile Usability Testing 422 Based on Desktop Eyetracking", in Proceedings of the Proceedings of the 13th International Conference on Interacción Persona-Ordenador; Association for Computing Machinery: New York, NY, USA, October 3 2012; pp. 1–8.

[45] R. Bednarik, M. Tukiainen, "Validating the Restricted Focus Viewer: A Study Using Eye-Movement Tracking", in Behavior Research Methods 2007, 39, vol. pp. 274–282.

[46] Q. Wang, S. Yang, M. Liu, Z. Cao, Q. Ma, "An Eye-Tracking Study of Website Complexity from Cognitive Load Perspective", in Decision Support Systems 2014, vol. 62, pp. 1–10.

[47] A. Çöltekin, B. Heil, S. Garlandini, S.I. Fabrikant, "Evaluating the Effectiveness of Interactive Map Interface Designs: A Case Study Integrating Usability Metrics with Eye-Movement Analysis", in Cartography and Geographic Information Science 2009, vol. 36, pp. 5–17.

[48] C. Ehmke, S.G. Wilson, "Identifying Web Usability Problems from Eye-Tracking Data", September 1 2007; Vol. 1, pp. 119–128.

[49] J. Luan, Z. Yao, F. Zhao, H. Liu, "Search Product and Experience Product Online Reviews", in Comput. Hum. Behav. 2016, vol. 65, pp. 420–430.

[50] J. Falkowska, B. Kilijańska, J. Sobecki, K. Zerka, "Microinteractions of Forms in Web Based Systems Usability and Eye 436 Tracking Metrics Analysis" in International Conference on Applied Human Factors and Ergonomics. Springer, Cham, 2018, pp. 164–174.

[51] J. Sauro, J.R. Lewis, "Quantifying the User Experience: Practical Statistics for User Research", 2nd edition, Morgan Kaufmann: Amsterdam Boston Heidelberg, 2016.

Network Systems and Applications

MODERN network systems encompass a wide range of solutions and technologies, including wireless and wired networks, network systems, services, and applications. This results in numerous active research areas oriented towards various technical, scientific and social aspects of network systems and applications. The primary objective of Network Systems and Applications conference track is to group network-related technical sessions and promote synergy between different fields of network-related research.

The rapid development of computer networks including wired and wireless networks observed today is very evolving, dynamic, and multidimensional. On the one hand, network technologies are used in virtually several areas that make human life easier and more comfortable. On the other hand, the rapid need for network deployment brings new challenges in network management and network design, which are reflected in hardware, software, services, and security-related problems. Every day, a new solution in the field of technology and applications of computer networks is released. The NSA track is devoted to emphasizing up-to-date topics in networking systems and technologies by covering problems and challenges related to the intensive multidimensional network developments. This track covers not only the technological side but also the societal and social impacts of network developments. The track is inclusive and spans a wide spectrum of networking-related topics.

The NSA track is a great place to exchange ideas, conduct discussions, introduce new ideas and integrate scientists, practitioners, and scientific communities working in networking research themes.

TOPICS

- Networks architecture
- Networks management
- Quality-of-Service enhancement
- Performance modeling and analysis
- Fault-tolerant challenges and solutions
- 5G developments and applications
- Traffic identification and classification
- Switching and routing technologies
- Protocols design and implementation
- Wireless sensor networks
- Future Internet architectures
- Networked operating systems
- Industrial networks deployment
- Software-defined networks
- Self-organizing and self-healing networks
- Mulimedia in Computer Networks
- Communication quality and reliability
- Emerging aspects of networking systems

Track 3 includes technical sessions:

- Complex Networks—Theory and Application (1st Workshop CN-TA'22)
- Internet of Things—Enablers, Challenges and Applications (6th Workshop IoT-ECAW'22)
- Cyber Security, Privacy and Trust (3rd International Forum NEMESIS'22)

Communication Papers of the of the 17th Conference on Computer Science and Intelligence Systems pp. 155–159
DOI: 10.15439/2022F177
ISSN 2300-5963 ACSIS, Vol. 32

Ant Colony based Coverage Optimization in Wireless Sensor Networks

Mina Khoshrangbaf
International Computer Institute
Ege University
Izmir, Turkey
ma.khoshrang@gmail.com

Vahid Khalilpour Akram
International Computer Institute
Ege University
Izmir, Turkey
vahid.kkram@ege.edu.tr

Moharram Challenger
Department of Computer Science,
University of Antwerp and Flanders Make
Antwerp, Belgium
moharram.challenger@uantwerpen.be

***Abstract*— Maximizing the covered area of wireless sensor networks while keeping the connectivity between the nodes is one of the challenging tasks in wireless sensor networks deployment. In this paper, we propose an ant colony-based method for the problem of sensor nodes deployment to maximize the coverage area. We model sensor locations as a graph and use an adapted ant colony optimization-based method to find the best places for each sensor node. To keep the connectivity of the sensor network, every sensor must be covered by the other sensors; this is a hard constraint that is applied to the cost function as a penalty. The proposed algorithm is evaluated with different numbers of sensor nodes and sensing ranges. The simulation results showed that increasing the number of iterations in the algorithm generates a better coverage ratio with the same number of nodes.**

***Index Terms*—Wireless sensor networks, node deployment, coverage maximization, ant colony optimization.**

I. Introduction

IN RECENT years, the new generation of smart buildings, structures, vehicles, and factories are widely dependent on proper sensing and collecting of data from the environment. Wireless Sensor Networks (WSNs) are one the technologies that can be used to collect different kinds of information from various environments including harsh areas such as seabed, mountains, or urban areas [1]. Technically, a WSN is a set of small, low-energy sensor devices that can connect to the other nodes over wireless communication platforms. These devices may have different types of hardware and software capabilities such as processing units, sensing modules, and memories. Recent advances in electronic and hardware technologies allow the generation of a wide range of tiny, low-cost, low-energy devices that support local processing, sensing, and various communication methods. The diversity and capabilities of these devices grow exponentially which allows us to use them in different application areas. For example, collecting the status of patients and health care devices in hospitals, automation of activities and increasing the quality and efficiency of products in agriculture, monitoring the status and condition of devices in a factory, controlling the objects in smart homes, developing efficient rescue systems, real-time monitoring systems of critical infrastructures, and providing ad-hoc or mobile communication platforms are some applications of WSNs.

Maximizing the coverage area of WSNs and keeping the connectivity between the nodes are two essential necessities in these networks. Ideally, WSN should cover the maximum possible area and all available devices in the network should be able to communicate with other nodes. Generally, these two-requirement conflict with each other. Increasing the coverage area of a WSN needs to increase the distance between deployed nodes which weakens the connectivity. Placing the nodes far from each other reduces the possible alternate paths between the nodes and also weakens the strength of the wireless signals which may affect the connectivity between the nodes. To increase the connectivity robustness, we need to deploy more dense networks which allows to create alternative communication paths between the nodes. However, dense networks usually cover a limited area which is not acceptable in most applications. Some studies propose predefined deploying patterns that optimize both connectivity and coverage but most of the times placing the sensor nodes in the desired locations is not possible. Especially in harsh environments the nodes usually are distributed randomly which reduces the coverage area. In this paper, we propose an Ant Colony Optimization (ACO) based method to increase the coverage area of WSNs and preserve the connectivity between the nodes.

II. Related works

The importance of covering the maximum possible area in the region of interest has caused researchers to explore sensor deployment techniques to maximize the coverage in WSNs. The problem is considered in assorted conditions; some research projects take the communication or connectivity of the sensors into account while some do not, some papers try to find the minimum number of sensors while some take the number of sensors as a constraint and try to maximize the coverage for these sensors on the region of interest, some tries to cover just specified targets and some aim to cover the whole of the region of interest [2,3,4,5,6]. Various methods are used in this field but due to the good performance of the evolutionary algorithms in finding a solution for NP-hard optimization problems, these algorithms have been widely used to find the best deployment of nodes in order to maximize the coverage. Various swarm intelligence algorithms such as Genetic Algorithm and Particle Swarm Optimization algorithm are applied in literature [7,8,9,10,11].

Ant Colony Optimization algorithm is another evolutionary algorithm to solve the node deployment problem. In [12] an ACO based algorithm called ACO-Greedy is proposed to solve the Grid-based Coverage problem with Low-cost and Connectivity-guarantee (GCLC). The algorithm finds the minimum number of sensors with dynamic sensing and communication range that can provide full coverage, decrease deployment cost and prolong the lifetime of the network. [13] model the deployment problem as a multiple knapsack problem and use ant colony optimization algorithm to increase the coverage area. Network lifetime and coverage of the area are considered as objectives of the algorithm, which use the circle point concept. In [14] ACO-Discreet, a modification of Ant Colony Optimization is proposed which reduces the sensing cost with efficient deployment and

enhanced connectivity. The algorithm includes two phases: at the first phase, the ordinary ACO is used for the grid-based problem coverage with low cost and connectivity-guarantee. At this level to focus on points far from the ant's current location, a heuristic value is used. After obtaining a solution at the first phase, at the second phase, ACO operates on the solution to remove redundant sensors.

The authors of [15] propose an algorithm called Optimized Strategy Coverage Control (OSCC) which aims to maximize the coverage of the region of interest in three steps. At the first step they establish a relation mapping model of the sensors based on geometric figure and prepare the network model, then uses ACO to enhance the coverage with the minimum number of sensors, reducing the energy spending of the whole network and optimizing the routing path. The algorithm benefits from node moving path and direction to find the optimal subset of iterative optimization. An improved ACO called EasiDesign is proposed in [16] to solve connectivity guaranteed point k-coverage problem. The aim is to find the best minimum subset of locations for sensors. For this purpose, every ant chooses a point from all points which sensors can cover the critical points, to do this, ants apply stochastic local decision and then the pheromone is updated based on the quality of the solution to help the algorithm to find better solutions in the next iterations. Obstacle avoidance and unavailable points are taken into account to increase the practicality of the algorithm.

III. Proposed Approach

Ant colony optimization algorithm is a probabilistic technique inspired by the behavior of real ants. The basic idea of this member of the swarm intelligence methods family is the way that ants find the best route to go from a point to a target point using pheromone (Fig.1). After modeling the search space of the problem and initializing parameters, the algorithm starts with a set of random solutions and improve them until satisfying a predetermined stopping condition. Ants choose their path to construct a solution based on a probability that depends on pheromone and heuristic. At the end of each iteration, when all of the ants represent a solution for the problem, the pheromone matrix is updated based on the quality of the solution, that is the corresponding cost. The best ant, which is the ant with the lowest cost (for minimization problem) among all ants is cached when an iteration ends and the final solution is the best of the bests. We use ACO to find the best locations in the region of interest to deploy the sensors to achieve maximum coverage.

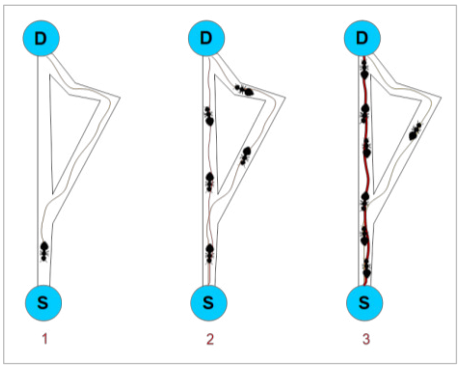

Fig. 1. Natural behavior of ants (Adapted from [17])

In order to formulate the problem, we assume the region of interest as a two-dimensional grid-based area. Sensors can locate at all points of the area. Each sensor can sense all points within its sensing radius and can communicate with all sensors within its communication radius. The purpose is to deploy the sensors so that they cover the maximum possible area in the region, considering each sensor must communicate with at least one other sensor. We denote the set of sensors with $S = \{s_1, s_2, \dots, s_n\}$ and location of sensor s_i and point p in the region of interest A is defined as (s_{i_x}, s_{i_y}) and (p_x, p_y) respectively. Euclidean distance between s_i and p is formulated as $d(s_i, p)$, shown in (1):

$$d(s_i, p) = \sqrt{(s_{i_x} - p_x)^2 + (s_{i_y} - p_y)^2} \quad (1)$$

If this Euclidean distance is equal to or lower than the sensing range r_s, the point can be sensed and is covered by the sensor si, otherwise, the point is not covered by s_i. This is the Boolean disk coverage model which is denoted as $c(s_i, p)$ in (2).

$$c(s_i, p) = \begin{cases} 1, & d(s_i, p) \le r_s \\ 0, & otherwise \end{cases} \quad (2)$$

So, the total covered points by the sensor s_i in area A is defined as (3). Considering $o(s_i, s_j)$ as the common points covered by s_i and s_j, the coverage function of the sensor set S on area A is shown in (4).

$$C(s_i, A) = \sum_{\forall p \in A} c(s_i, p) \quad (3)$$

$$coverage(S, A) = \sum_{i=1}^{n} C(s_i, A) - \sum_{i=1}^{n} \sum_{j=i+1}^{n} o(s_i, s_j) \quad (4)$$

We propose an ACO-based approach in which ants determine the coordinates of the sensors to deploy. For a $M \times M$ size area and n sensors, the solution space can be designed as a $(M \times M) \times n$ graph in which rows demonstrate all the possible coordinates that sensors can be placed, and each column represents one of the sensors. Fig. 2. shows the illustrated graph. An ant traverse on the graph and the path determines the coordinates of n sensors. For example, if the node on i'th row and j'th column of the graph is one of the nodes on the path of the ant, it means sensor number j must be located on the coordinate i. So, the path that every ant travels, can be shown as an $1 \times n$ array that each of its elements shows a location. Fig. 3. shows a sample ant path for 8 sensors problem in a 100×100 area. The first member 2580 means that the coordinates to locate sensor number 1 is (25,80), that is $(s_{1_x}, s_{1_y}) = (25,80)$.

All the original steps of ACO including creating the initial population and pheromone matrix, computing the probability matrix, pheromone updating and evaporation are the same in the proposed approach. To define the cost function of the algorithm, although the problem is maximizing the coverage, in order to include the communication condition, we reformulate the objective function as a minimization function. To do this, we use the total area of the region of interest, which means the area of the region of interest which is shown as *area(A)* is divided by the predefined function *coverage (S, A)*.

Each sensor must be covered by at least one other sensor, this is a hard constraint. We add this hard constraint as a penalty to the objective function. For each sensor s_i of the

sensor set S, which is not covered by any other sensor, a penalty equal to $p(s_i)$ is considered, which is defined in (5). The communication range of all sensors is equivalent and is shown with r_c. Sensor s_i is covered by sensor s_j if the Euclidean distance between these two sensors is equal or less than r_c. If there is no sensor inside the communication range of the sensor s_i, it means the sensor is not covered by any other sensor and must suffer a penalty. In order to delete the impact of the number of the sensors, the normalized total penalty for sensor set S can be formulated as (6):

$$p(s_i) = \begin{cases} 0, & \exists s_j \in S : d(s_i, s_j) \le r_c \\ 1, & otherwise \end{cases} \quad (5)$$

$$P(S) = \frac{\sum_{i=1}^{n} p(s_i)}{n} \quad (6)$$

In order to intensify the effect of the penalty on the objective function, we use κ as the coefficient of the penalty

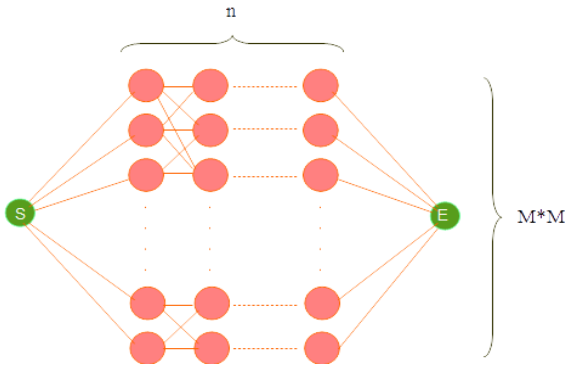

Fig. 2. Graph model of the proposed approach

S1	S2	S3	S4	S5	S6	S7	S8
2580	0265	1152	9804	7204	3288	1425	6206

Fig. 3. A sample ant path

which is a very large number. The final objective function of the proposed ACO algorithm is called *F(S)* and is shown in (7). The ant that has smaller *F* is the better ant and deposits more pheromone on the path.

$$F(S) = \left(\frac{area(A)}{coverage(S,A)}\right) + (\kappa \times P(S)) \quad (7)$$

All the ants travel based on the pheromone matrix and construct new paths and solutions. The algorithm continues until the stopping condition is satisfied, which is iteration in our case. At the end, the ant with the least cost that is maximum coverage and penalty equal to zero is the best ant which gives the best coordinates for n sensor on area A to be placed and have the most covered area.

IV. PERFORMANCE EVALUATION

To evaluate the performance of the algorithm, first we conduct experiments using various parameters in order to determine the optimum configuration of parameters for ACO-based deployment. We focus on the impact of ACO standard parameters as well as problem specialized parameters. The ACO parameters include the number of iterations, initial population size of ants, pheromone exponential weight, evaporation rate and parameters of the problem include sensing radius, number of sensors and penalty coefficient. The algorithm is implemented using MATLAB software with different values for the above parameters in a 100×100 grid-based sensing region, considering the maximum number of iterations as the stopping condition. Combinations of 50, 100, 200, 400, 500 and 1000 iterations with 20, 30, 40, 100, 200 population size, 10, 20, 50, 100 for penalty coefficient and 0.3, 0.5 evaporation rate are tested and the determined optimal parameters which have caused better results are listed in Table 1.

After the creation of a random population of ants at the first iteration, in which each member demonstrates a random deployment of the sensors, the algorithm proceeds to improve the solution and find the optimal deployment. At every iteration, based on the information of the past iterations is reflected on the pheromone matrix, the algorithm finds a better solution. That is, we get better cost as we progress. This can obviously be seen in Fig. 4. which shows that the coverage rate improves in each iteration for the deployment problem of 32 sensors with a sensing radius set to 10. It should be mentioned that considering the communication between sensors as a hard constraint and injecting it to the cost with a high impact, leads ants to focus on finding solutions with the least penalty. The implementation results show that the algorithm finds solutions with penalty equal to zero at even early steps. As consequence the outcome of the algorithm is a deployment with high coverage rate and zero penalty, which means all sensors are in communication with at least one other sensor.

TABLE I. OPTIMAL PARAMETERS

Parameter	Value
Number of Iterations	200
Population Size	100
Evaporation Rate	0.05
Penalty Coefficient	10

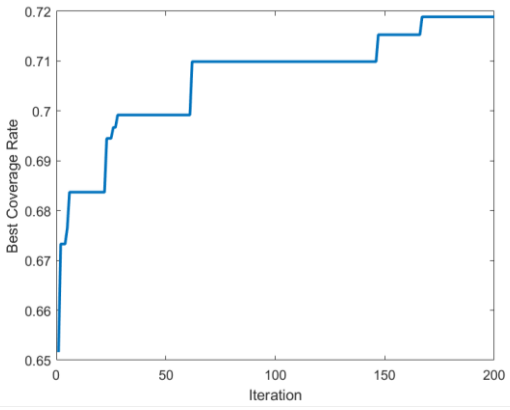

Fig. 4. Iterative process of the algorithm optimization

To evaluate the impact of the sensing range on coverage rate, we simulated the algorithm with three different sensing ranges: 5, 10 and 15 meters. We assume that all the sensors have the same sensing range and the communication range of the sensors is twice the sensing range. The algorithm tries to

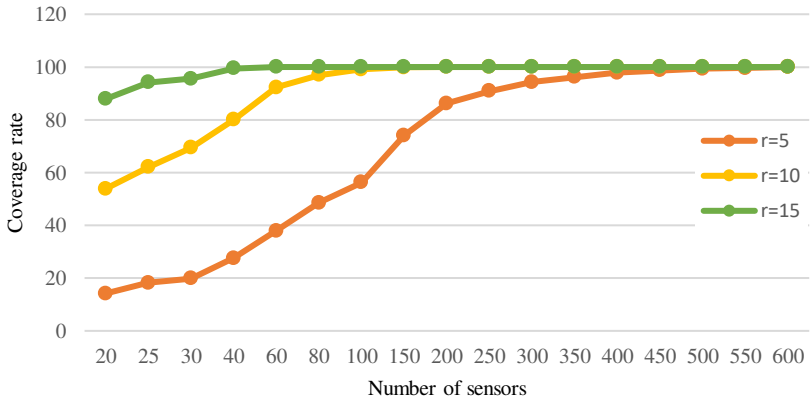

Fig. 5. Iterative process of the algorithm optimization

find the best coordinates to locate the sensors with the predetermined sensing range, such that they cover the maximum area, ensuring that every sensor is in the communication range of at least one other sensor.

One another determinative parameter in coverage rate is the number of sensors. As the region of interest gets larger more sensors are needed for full coverage of the area but not all time full coverage is the aim. Determining the number of sensors can be considered as the result of a trade-off between the cost of supply and maintenance and desired coverage rate.

To evaluate the impact of the number of sensors we simulated the algorithm with 18 different numbers in the range of [20 600]. In order to present the combinational effect of sensing range and number of sensors, we illustrated how coverage rate changes for different sensing ranges and number of sensors in Fig. 5. It can be seen that the coverage rate increases when the number of sensors becomes more. The sensing range has similar and even more effect, the larger

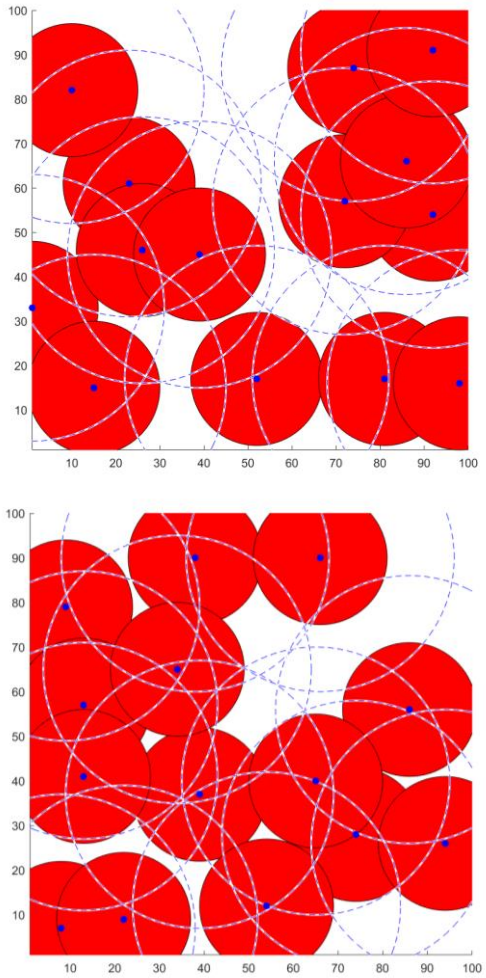

Fig. 6. Sensor Deployment of $n = 14$, $r_s = 15$ before(top) and after(bottom) optimization

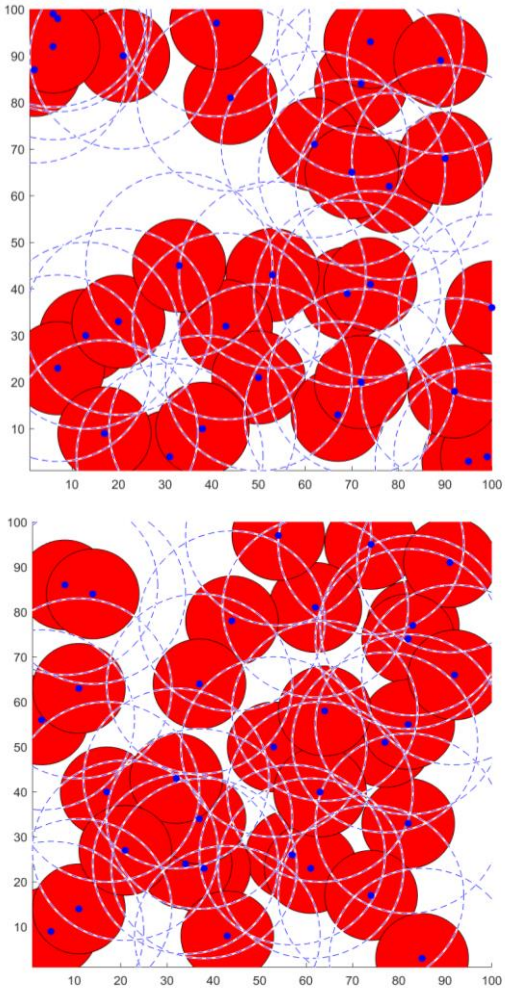

Fig. 7. Sensor Deployment of $n = 32$, $r_s = 10$ before(top) and after(bottom) optimization

range the more coverage rate. And obviously larger sensing range results in more coverage with fewer sensors compared to sensors with smaller range.

The algorithm processes on a random deployment and improves it to an approximate optimal solution. To compare the first situation of the sensors with the situation of the sensors which are located in the coordinates determined by the proposed algorithm, Fig. 6, Fig.7 and Fig. 8 show the region of interest covered by sensors before and after optimization for the number of sensors which have about 100% maximum possible coverage rate. The coverage rate of 14 sensors with a sensing range 15 m is 76.1% for 32 sensors with $r_s = 10$ m the rate is 72.6% and 128 sensors with a range of 5 m cover 67.3%, of the region of interest. As shown in the figures, all the deployments resulted from the algorithm ensuring the communication condition and all of the sensors are in communication with at least one other sensor.

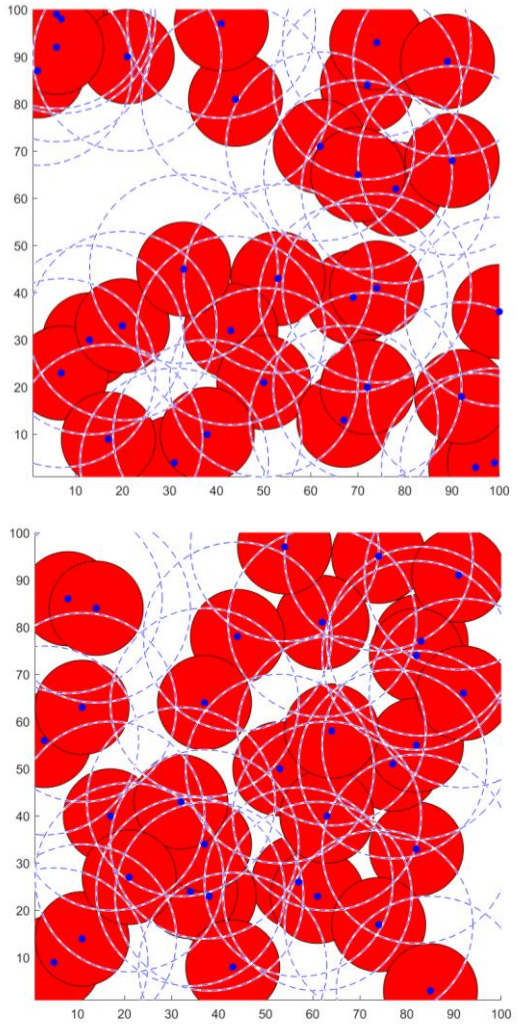

Fig. 8. Sensor Deployment of $n = 128$, $r_s = 5$ before(top) and after(bottom) optimization

CONCLUSION

In this work, we consider the problem of sensor nodes deployment to maximize the coverage area. We model sensor locations as a graph and use ACO to find the best places. Every sensor must be covered by other sensors; this is a hard constraint that is applied to the cost function as a penalty. The algorithm is evaluated with different numbers of sensors and sensing ranges. Better locations are found and the coverage rate increases as the algorithm iterates. Simulation results showed that our proposed sensor deployment approach improves the coverage rate of a set of sensors that are deployed randomly by finding new places to deploy. The simulation results showed that the prosed algorithm can increase the coverage ratio of the network to 76.1% with 14 sensor nodes where the sensing range of each node is 15 m. As future work, the proposed algorithm will be evaluated in a real testbed environment.

REFERENCES

[1] Sadik Arslan, Moharram Challenger, Orhan Dagdeviren, "Wireless sensor network based fire detection system for libraries", International Conference on Computer Science and Engineering (UBMK), IEEE, Antalya, Turkey, 05-08 October 2017.

[2] Harizan, Subash, and Pratyay Kuila. "Evolutionary algorithms for coverage and connectivity problems in wireless sensor networks: a study." Design frameworks for wireless networks. Springer, Singapore, 2020. 257-280.

[3] Al-Fuhaidi, Belal, et al. "An efficient deployment model for maximizing coverage of heterogeneous wireless sensor network based on harmony search algorithm." Journal of Sensors 2020 (2020).

[4] Wang, Lei, et al. "Wireless sensor network coverage optimization based on whale group algorithm." Computer Science and Information Systems 15.3 (2018): 569-583.

[5] Wang, Hui, et al. "A self-deployment algorithm for maintaining maximum coverage and connectivity in underwater acoustic sensor networks based on an ant colony optimization." Applied Sciences 9.7 (2019): 1479.

[6] Farsi, Mohammed, et al. "Deployment techniques in wireless sensor networks, coverage and connectivity: A survey." Ieee Access 7 (2019): 28940-28954.

[7] Yoon, Yourim, and Yong-Hyuk Kim. "An efficient genetic algorithm for maximum coverage deployment in wireless sensor networks." IEEE Transactions on Cybernetics 43.5 (2013): 1473-1483.

[8] Kong, Hongshan, and Bin Yu. "An improved method of WSN coverage based on enhanced PSO algorithm." 2019 IEEE 8th Joint International Information Technology and Artificial Intelligence Conference (ITAIC). IEEE, 2019.

[9] Tossa, Frantz, Wahabou Abdou, Eugène C. Ezin, and Pierre Gouton. "Improving coverage area in sensor deployment using genetic algorithm." International Conference on Computational Science. Springer, Cham, 2020.

[10] Zorlu, Ozan, and Ozgur Koray Sahingoz. "Increasing the coverage of homogeneous wireless sensor network by genetic algorithm based deployment." 2016 Sixth International Conference on Digital Information and Communication Technology and its Applications (DICTAP). IEEE, 2016.

[11] Zhu, Fang, and Wenhao Wang. "A coverage optimization method for WSNs based on the improved weed algorithm." Sensors 21.17 (2021): 5869.

[12] Liu, Xuxun, and Desi He. "Ant colony optimization with greedy migration mechanism for node deployment in wireless sensor networks." Journal of Network and Computer Applications 39 (2014): 310-318.

[13] Liao, Wen-Hwa, Yucheng Kao, and Ru-Ting Wu. "Ant colony optimization based sensor deployment protocol for wireless sensor networks." Expert Systems with Applications 38.6 (2011): 6599-6605.

[14] Qasim, Tehreem, et al. "ACO-Discreet: An efficient node deployment approach in wireless sensor networks." Information technology-new generations. Springer, Cham, (2018). 43-48.

[15] Sun, Zeyu, Weiguo Wu, Huanzhao Wang, Heng Chen, and Wei Wei. "An optimized strategy coverage control algorithm for WSN." International Journal of Distributed Sensor Networks 10.7 (2014): 976307.

[16] Li, Dong, Wei Liu, and Li Cui. "EasiDesign: an improved ant colony algorithm for sensor deployment in real sensor network system." 2010 IEEE Global Telecommunications Conference GLOBECOM 2010. IEEE, 2010.

[17] Fathima, K. Syed Ali, and K. Sindhanaiselvan. "Ant colony optimization based routing in wireless sensor networks." International Journal of Advanced Networking and Applications 4.4 (2013): 1686

1st Workshop on Complex Networks: Theory and Application

IN the nature and the world around us, we can observe many network structures that interconnect various elements such as cells, people, urban centers, network devices, companies, manufacturing machines, etc. Most of them have the nature of evolving networks whose structure changes over time. The analysis of such systems from the complex networks point of view allows for better understanding of the processes within them, which can be used to optimize their structure, improve their management methods, detect failures, improve their operating efficiency and plan their development and evolution.

The main goal of this event is to exchange knowledge and experience between specialists from different areas who in their research and design work use theories and solutions characteristic for complex systems. We believe that the meeting will create new ideas and concepts that will affect the development of contemporary methods of design, operation and analysis of network systems.

Topics

The list of topics includes, but is not limited to:

- Complex networks architecture
- Large scale networks analytics
- Mathematical and numerical analysis of networks
- Modeling of computer networks
- Cognitive networks
- Visualizations of network processes
- Dynamics on networks
- Biological and physical models on networks
- Dynamic modification of communication protocols parameters for enterprise and ISP systems
- Complex network management
- Performance modeling and analysis in complex networks
- Network function virtualization
- Social networks
- Graph theory and network algorithm application
- Evolving networks
- Detection of anomalies in the functioning of an enterprise-class computer network element
- Predictive maintenance
- Network technologies supporting society 5.0 and education 5.0
- Architecture for next-generation network applications
- Distributed complex systems for remote working and collaboration
- Algorithms for controlling and monitoring complex computer networks

Technical Session Chairs

- **Bolanowski, Marek,** Rzeszow University of Technology, Poland
- **Paszkiewicz, Andrzej,** Rzeszow University of Technology, Poland

Program Committee

- **Al-Naday, Mays,** University of Essex, United Kingdom
- **Ballas, Rüdiger G.,** Mobile University of Technology, Germany
- **Houssein, Essam H.,** Minia University, Egypt
- **Ignaciuk, Przemysław,** Lodz University of Technology, Poland
- **Kryvyi, Serhii,** Taras Shevchenko National University of Kyiv, Ukraine
- **Kuchanskyy, Vladislav,** Institute of Electrodynamics of the National Academy of Sciences of Ukraine
- **Palau, Carlos,** Universitat Politècnica de València, Spain
- **Provotar, Oleksandr,** Taras Shevchenko National University of Kyiv, Ukraine

Communication Papers of the of the 17th Conference on Computer Science and Intelligence Systems pp. 163–170
DOI: 10.15439/2022F43
ISSN 2300-5963 ACSIS, Vol. 32

Centrality Measures in multi-layer Knowledge Graphs

Jens Dörpinghaus*‡, Vera Weil†, Carsten Düing‡, Martin W. Sommer§
* Federal Institute for Vocational Education and Training (BIBB), Bonn, Germany,
Email: jens.doerpinghaus@bibb.de, https://orcid.org/0000-0003-0245-7752
† Department for Mathematics and Computer Science, University of Cologne, Germany
‡ University Koblenz-Landau, Koblenz, Germany
§ Argelander-Institut für Astronomie, Bonn, Germany

***Abstract*—Knowledge graphs play a central role for linking different data which leads to multiple layers. Thus, they are widely used in big data integration, especially for connecting data from different domains. Few studies have investigated the questions how multiple layers within graphs impact methods and algorithms developed for single-purpose networks, for example social networks. This manuscript investigates the impact on the centrality measures of graphs with multiple layers compared to a those measures in single-purpose graphs. In particular, (a) we develop an experimental environment to (b) evaluate two different centrality measures – degree and betweenness centrality – on random graphs inspired by social network analysis: small-world and scale-free networks. The presented approach (c) shows that the graph structures and topology has a great impact on its robustness for additional data stored. Although the experimental analysis of random graphs allows us to make some basic observations we will (d) make suggestions for additional research on particular graph structures that have a great impact on the stability of networks.**

I. Introduction

KNOWLEDGE graphs have been shown to play an important role in recent knowledge mining and discovery, for example in the fields of digital humanities, life sciences or bioinformatics. They also include single purpose networks (like social networks), but mostly they contain also additional information and data, see for example [1], [2], [3]. Thus, a knowledge graph can be seen as a multi-layer graph comprising different data layers, for example social data, spatial data, etc. In addition, scientists study network patterns and structures, for example paths, communities or other patterns within the data structure, see for example [4]. Very few studies have investigated the questions how multiple layers within graphs impact methods and algorithms developed for single-purpose networks, see [5]. This manuscript investigates the impact of a growing part of other layers on centrality measures in a single-purpose graph. In particular, we develop an experimental environment to evaluate two different centrality measures – degree and betweenness centrality – on random graphs inspired by social network analysis: small-world and scale-free networks.

This paper is divided into five sections. The first section gives a brief overview of the state of the art and related work. The second section describes the preliminaries and background. We will in particular introduce knowledge graphs and centrality measures. In the third section, we present the experimental setting and the methods used for this evaluation. The fourth section is dedicated to experimental results and the evaluation. Our conclusions are drawn in the final section.

II. Preliminaries

The term *knowledge graph* (sometimes also called a *semantic network*) is not clearly defined, see [6]. In [7], several definitions are compared, but the only formal definition was related to RDF graphs which does not cover labeled property graphs. As another example, [8] gives a definition of knowledge graphs limited to the definition of important features. Knowledge graphs were introduced by Google in 2012, when the Google Knowledge Graph was published on the use of semantic knowledge in web search, see https://blog.google/products/search/introducing-knowledge-graph-things-not/. This is a representation of general knowledge in graph format. Knowledge graphs also play an important role in the Semantic Web and are also called semantic networks in this context.

Thus, a *knowledge graph* is a systematic way to connect information and data to knowledge. It is thus a crucial concept on the way to generate knowledge and wisdom, to search within data, information and knowledge. Context is the most important topic to generate knowledge or even wisdom. Thus, connecting knowledge graphs with context is a crucial feature.

Definition 1 (Knowledge Graph)**.** *We define a knowledge graph as graph* $G = (E, R)$ *with entities* $e \in E = \{E_1, ..., E_n\}$ *coming from formal structures* E_i *like ontologies.*

The relations $r \in R$ can be ontology relations, thus in general we can say every ontology E_i which is part of the data model is a subgraph of G indicating $O \subseteq G$. In addition, we allow inter-ontology relations between two nodes e_1, e_2 with $e_1 \in E_1$, $e_2 \in E_2$ and $E_1 \neq E_2$. In more general terms, we define $R = \{R_1, ..., R_n\}$ as a list of either inter-ontology or inner-ontology relations. Both E as well as R are finite discrete spaces.

Every entity $e \in E$ may have some additional metainformation which needs to be defined with respect to the application of the knowledge graph. For instance, there may be several node sets (some ontologies, some actors (like employees or

stakeholders, for example), locations, ...) $E_1, ..., E_n$ so that $E_i \subset E$ and $E = \cup_{i=1,...,n} E_i$. The same holds for R when several context relations come together such as "is relative of", "has business affiliation", "has visited", etc.

By using formal structures within the graph, we are implicitly using the model of a labeled property graph, see [9] and [10]. Here, nodes and edges form a heterogeneous set. Nodes and edges can be identified by using a single or multiple labels, for example using $\lambda : E \to \Sigma$, where Σ denotes a set of labels. We need to mention that both concepts are equivalent, since graph databases use the concept of labeled property graphs.

Here, our experimental setting is – without loss of generality – settled in social network analysis (SNA). It is quite obvious that a social network containing actors may easily be extended with other data, for example spacial data (e.g. locations, rooms, towns, countries), or social groups (e.g. companies, clubs), or any other information (e.g. information data about actors). Once a social network is built, we may start to ask questions like "How many friends does actor X have?" or "To how many groups does actor Y belong?". The mathematical formulation of these questions would be "What is the degree of node X?" and "How many communities C_i can be found such that $Y \in C_i$?". The mathematical foundations in this and the following sections are based on the works of [11] and [12] unless otherwise noted.

In general, we define a *Graph* $G = (V, E)$ with a set of edges or vertices V – these are actors, locations or any other nodes in the network – and edges E, which describe the relations between nodes. The number of nodes $|V|$ is usually denoted with n. Given two nodes s =Simon and j =Jerusalem we may add an edge or relation (s, j) between both describing for example, that Simon is or was in Jerusalem. Then we say s and j are *connected* or they are *neighbors*. The *neighborhood* of a vertice v is denoted with $N(v)$ and describes all nodes connected to v. If we are interested in the size of this neighborhood we calculate the node *degree* given by $deg(v) = |N(v)|$.

The neighborhood thus gives information about the connectedness of an actor in the network. This can be useful to illustrate the direct influence of an actor within the complete network, especially for actors with a high node degree. But it is obvious that the amount of relations does not necessarily give a good idea on their quality or how we could use these relations. While the node degree is often used as a measure to create random graphs, it is in general not a good measure in order to analyze particular actors in networks, see [13].

Nevertheless, the *degree centrality* for a node $v \in V$ is given by

$$dc(v) = \frac{deg(v)}{n-1}$$

The output value ranges between 0 and 1 and gives a reference to the direct connections. As discussed, it omits all indirect relations and in particular the node's position in the network.

Definition 2 (Scale-Free Network)**.** *A network is scale-free if the fraction of nodes with degree k follows a power law $k^{-\alpha}$, where $\alpha > 1$.*

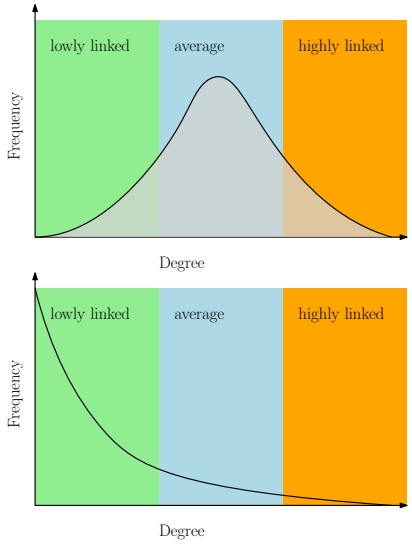

Fig. 1. Top: In random networks the degree distribution follows a given random distribution. Here, most nodes are average linked and an equal number of nodes is lowly and highly linked. Bottom: Real networks often follow other or even no standard random distribution. Here, a scale-free distribution is shown: Most nodes are lowly linked whereas only very few notes are highly linked.

Definition 3 (Small World Network [14])**.** *Let $G = (V, E)$ be a connected graph with n nodes and average node degree k. Then G is a small-world network if $k \ll n$ and $k \gg 1$.*

In any case, the *degree distribution* provides us with information about the network structure since we can distinguish between sparsely and densely connected networks. While [13] suggests statistical analysis to compute the correlation between attributes of the network and the density of nodes, this will not work for the small networks and the missing statistical values. In any case, although scale-free networks are not an universal characteristic for real-world networks, we might use this approach to get a first overview about the network itself. Random graphs, like the Erdős–Rényi networks, follow a Poisson distribution. Scale-free networks, inspired by real-world social networks, follow a power law. See Figure 1 for two examples of a random graph and a more common distribution in real word networks.

We will now discuss one more property to evaluate nodes and their position in the networks. These properties can be used to calculate statistical parameters, so-called *centrality measures*, cf. [15] and [16]. They answer the question "Which nodes in this network are particularly significant or important?".

Betweenness analyzes critical connections between nodes and thus gives an indication of individuals that can change the flow of information in a network. This measure is based on paths in a network:

> Much of the interest in networked relationships comes from the fact that individual nodes benefit (or suffer) from indirect relationships. Friends might provide access to favors from their friends, and

information might spread through the links of a network.[13]

A *path* p in a graph $G = (V, E)$ is a set of vertices $v_1, ..., v_t$, $t \in \mathbb{N}$, for example written as

$$p = [v_1, ..., v_t],$$

where $(v_i, v_{i+1}) \in E$ for $i \in \{1, \dots, t-1\}$. The length $|p|$ of the path p is the total number of edges – not nodes. Thus $|p| = t-1$. The path p links the starting node v_1 and an ending node v_t. In a path, no crossings are allowed, thus $v_i \neq v_j$ for all $i, j \in \{1, ..., t\}$. If all properties of a path are met except that the beginning and the end vertex are the same – that is, $v_1 = v_t$ – we denote this set as a *circle*.

Betweenness centrality was first introduced by [17][1] and considers other indirect connections, see [19]. Given a node v, it calculates the number $P_v(k, j)$, that is, the number of all shortest paths in a network for all beginning and ending nodes $k, j \in V$ that pass through v. If $P(k, j)$ denotes the total number of paths between k and j, the importance of v is given by the ratio of both values. Thus the betweenness centrality according to [13] is given by

$$bc(v) = \sum_{k \neq j, v \neq k, v \neq j} \frac{P_v(k, j)}{P(k, j)} \cdot \frac{2}{(n-1)(n-2)},$$

where n denotes the number of the vertices in the graph. This parameter allows an analysis of the critical links and how often a node lies on such a path. This centrality measure thus answers the questions whether a node can change the flow of information in a network or whether it is a bridge between other nodes, see [19].

While betweenness assumes network flows to be like packages flowing from a starting point to a destination, other measures consider multiple paths: For example, the so-called *eigenvector centrality* – introduced by [20] – measures the location of directly neighboring nodes in the network. For the eigenvector centrality, we "count walks, which assume that trajectories can not only be circuitous, but also revisit nodes and lines multiple times along the way."[21] This measure not only classifies the direct possibility to influence neighbors, but also ranks the indirect possibility to influence the whole network. For a detailed mathematical background we refer to [13].

Less popular measures are Katz prestige, and Bonacich's measure, see [13]. It has been shown that these measures are closely related, see [22].

III. Method

We evaluate the degree centrality and betweenness centrality on random graphs. First, we consider Scale-Free Networks with n nodes, see [13]. Moreover, [23] introduced a widely used graph model with three random parameters $\alpha+\beta+\gamma = 1$. These values define probabilities and thus define attachment rules to add new vertices between either existing or new nodes. This model allows loops and multiple edges, where a loop denotes one edge where the endvertices are identical, and multiple edges denote a finite number of edges that share the same endvertices. Thus, we convert the random graphs to undirected graphs. For testing purpose, we scale the number of nodes n and use $\alpha = 0.41$, $\beta = 0.54$, and $\gamma = 0.05$. We chose this random graph model since it is generic and feasible for computer simulations for measuring and evaluation purposes, see [24], [25].

[1]Initially introduced for symmetric relations – undirected graphs – it was extended to asymetric relations – directed graphs – by [18].

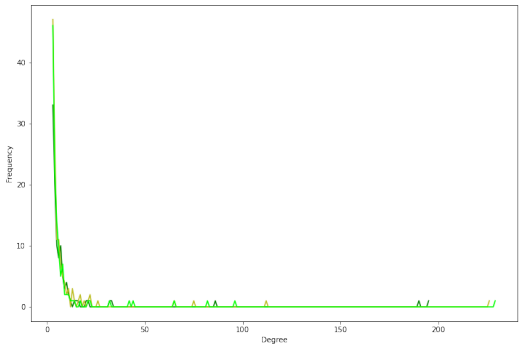

Fig. 2. Frequency of nodes with a given degree for three random Scale-Free Networks with $n = 150$ nodes.

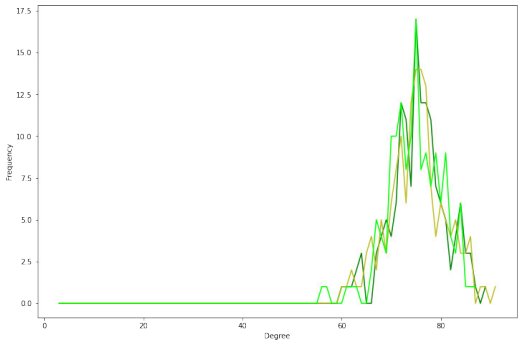

Fig. 3. Frequency of nodes with a given degree for three Newman-Watts-Strogatz small-world random graph with $n = 500$ nodes.

Figure 2 shows the frequency of nodes (y-axis) with a particular degree (x-axis) for three random networks with $n = 150$ nodes. Compared to Figure 2, Figure 1 clearly shows the scale-free distribution, in which many nodes have a small degree and only few nodes have a very large degree: most nodes are hence lowly linked. Thus these small-degree nodes lead to a few communities which are highly connected.

The second random graph uses a fixed degree distribution and is widely known as Newman-Watts-Strogatz small-world random graph [26]. The algorithm to create such as graph takes a number of nodes n, the number of k nearest neighbors that form a ring topology and the probability p for adding a new edge. A small-world graph contains only small average paths and thus has a small diameter, see [13]. Some studies like [27] study the relation between scale-free and small-world networks, in particular the relationship between the average

path length and local clusterings. In general, it is possible to generate scale-free networks with small-world attributes, see [28].

Figure 3 shows the frequency of nodes with a given degree for three random networks with $n = 500$ nodes. Compared to Figure 1, Figure 3 clearly shows the Poisson distribution with many nodes having an average degree. Together with Figure 2 it also illustrates the "long tail" of the scale-free distribution, see [13].

We will now evaluate how graph structures and in particular measures change when additional information are stored in extra layers. We partition a graph into an uncolored part that contains the 'original' data and into a part with blue nodes in which novel 'extra' data stored. These blue nodes simulate one or more new layers in the knowledge graph. One could imagine a graph in which every node represents a scientist in a social network, and two persons are connected whenever they are tied in the network (e.g. friends, collaborators, etc.). We now want to add more information to our graph by adding blue nodes. Every blue node represents a specific conference. Two blue nodes are connected whenever the conferences address - at least partly - the same community. A scientist is connected to a conference whenever they attended the workshop. The original graph is here the set of scientists, the blue nodes (the conferences) form a new layer, in which the extra data is stored.

Thus, given a random graph $G = (V, E)$, a next step comprises a probability p_b for blue nodes which leads to a graph G with blue nodes $B \subset V$. We first compute the centrality measures for all nodes in $V \setminus B$ in the graph $G = (V, E)$. Then we compute those measures for all nodes in $G \setminus B$, this time in the Graph $G \setminus B = (V \setminus B, E)$. Thus, we have two vectors $c_1, c_2 \in \mathbb{R}^n$ where here, n is the number of nodes in $V \setminus B$. We denote c_i by $c_i = \left(c_i^1, c_i^2, c_i^3, ...\right)$.

While comparing two vectors, we are interested in two values. The first one is the total number of misordered elements, that is, the total number of positions on which the elements differ from each other. The second value that we compute in order to compare two vectors is the number of moved elements. For this we count those elements that have a different predecessor and / or successor in the first vector compared to the second one.

Example III.1. *Let $c_1 = [1, 2, 3, 4, 5]$, $c_2 = [5, 3, 2, 1, 4]$ and $c_3 = [1, 5, 2, 3, 4]$. If c_1 is the original ordering, we see that c_2 has a totally different order. In c_3 the entry 5 is moved, but the rest of the list is unchanged, although still 4 elements are on the wrong location. Hence, the number of misordered elements in c_1 compared to c_2 is 5. The number of moved elements is 5 and 1.*

To identify both errors, we first define function e:

$$e(i, c_1, c_2) = \begin{cases} 0 & c_1^i = c_2^i \\ 1 & c_1^i \neq c_2^i \end{cases}$$

That is, $e(i, j, c_1, c_2) = 1$ if the element on the ith position of c_1 differs from the element on the jth position in c_2. To shorten notation, we write $e(i, c_1, c_2)$ whenever $i = j$.

Let x be an element contained in every c_u, $u \in \mathbb{N}$. Then $p(x, c_u)$ denotes the predecessor of element x in c_u and $s(x, c_u)$ denotes the successor of x in c_u. If x is the first element in c_u, then $p(x, c_u) = \emptyset$. If x is the last element of c_u, then $s(x, c_u) = \emptyset$. With these definitions, we define e_N:

$$e_N(x, c_1, c_2) = \begin{cases} 1 & \text{if } p(x, c_1) = \emptyset \text{ and } s(x, c_1) \neq s(x, c_2), \\ & \text{or } s(x, c_1) = \emptyset \text{ and } p(x, c_1) \neq p(x, c_2), \\ & \text{or } s(x, c_1) \neq s(x, c_2) \text{ and } p(x, c_1) \neq p(x, c_2), \\ 1/2 & \text{if } s(x, c_1) \neq s(x, c_2) \text{ and } p(x, c_1) = p(x, c_2), \\ & \text{or } s(x, c_1) = s(x, c_2) \text{ and } p(x, c_1) \neq p(x, c_2), \\ 0 & otherwise. \end{cases}$$

In other words, we consider the predecessor of an element in c_1 and check if this element is still a predecessor of this element in c_2, and analyse analoguously the successor of an element.

With this, we define two error measures ϵ and ϵ_N:

$$\epsilon(c_1, c_2) = \sum_{i=1}^{n} e(i, c_1, c_2)$$

$$\epsilon_N(c_1, c_2) = \sum_{x \in c_1} e_N(x, c_1, c_2)$$

Example III.2. *Let's reconsider Example III.1: Recall that $c_1 = [1, 2, 3, 4, 5]$, $c_2 = [5, 3, 2, 1, 4]$ and $c_3 = [1, 5, 2, 3, 4]$. Then, $\epsilon(c_1, c_2) = 5$ and $\epsilon_N(c_1, c_2) = 5$. Moreover, $\epsilon(c_1, c_3) = 4$ and $\epsilon_N(c_1, c_3) = 2.5$.*

We will now analyze different scenarios to evaluate the impact of additional blue nodes on a scale-free and a small-world network.

	ϵ	ϵ_N	ϵ	ϵ_N	ϵ	ϵ_N
Scale-Free	$n = 150$		$n = 300$		$n = 500$	
Mean	0.95	0.46	0.97	0.47	0.98	0.48
Small-World	$k = 4$		$k = 8$		$k = 50$	
Mean	0.97	0.97	0.97	0.96	0.95	0.96

TABLE I
MEAN VALUES FOR DEGREE CENTRALITY ERRORS.

IV. RESULTS

A. Degree Centrality

The Degree Centrality was evaluated with errors ϵ and ϵ_N for scale-free random graphs ($n = 150$, $n = 300$ and $n = 500$, see Figure 4) and Newman-Watts-Strogatz small-world random graphs ($n = 150$, $k \in \{4, 8, 50\}$, see Figure 5). The mean values are given in Table I.

Here, we see that the Small-World graph has a very high error rate for both ϵ and ϵ_N even for small p_B. In particular, the values are rather constant, no matter what value was chosen. In addition, the graph topology for different values of k has only very little impact on the error rate. Thus, even small changes

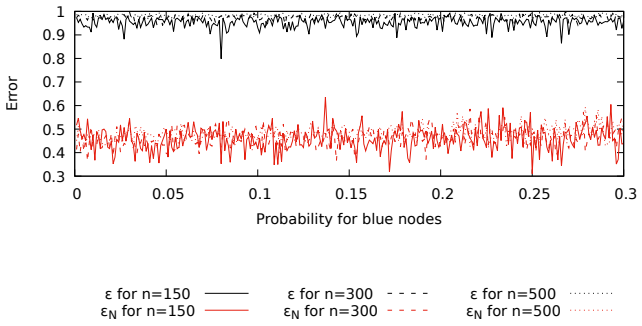

Fig. 4. Degree Centrality errors for scale-free random graphs ($n = 150$, $n = 300$ and $n = 500$) for different values of p_B between 0 and 0.3.

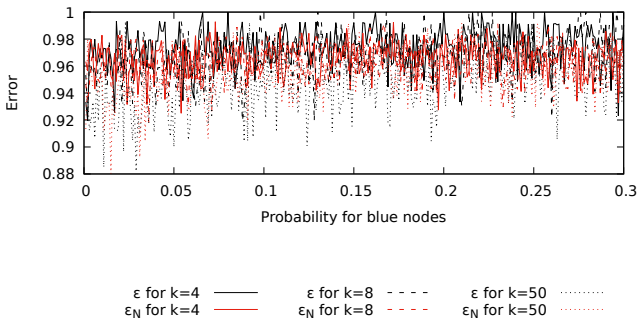

Fig. 5. Degree Centrality errors for Newman-Watts-Strogatz small-world random graph ($n = 150$, $k \in \{4, 8, 50\}$) for different values of p_B between 0 and 0.3.

in the graph structure (a very small value for p_B) have a great impact on the degree centrality. Since Small-World graphs have a high level of local clustering, the random exclusion of blue nodes will most likely effect not only one cluster, but also other clusters. This changes not only the position, but also the ordering of node degrees.

A different scenario occurs when considering Scale-Free graphs. Again we see a very high error rate for ϵ, even for small p_B. The values for ϵ_N are usually near to .5 (mean values 0.46, 0.47, 0.48). Neither the graph size n nor the value for p_B has an impact on these errors. Here, we see the scale-free distribution: the blue nodes do change the position of the degree centrality, but while they also change the ordering within clusters, they do not affect the complete ordering due to the longer distance between nodes.

B. Betweenness Centrality

The Betweenness Centrality was evaluated with errors ϵ and ϵ_N for scale-free random graphs ($n = 150$, $n = 300$ and $n = 500$, see Figure 6) and Newman-Watts-Strogatz small-world random graphs ($n = 150$, $k \in \{4, 8, 50\}$, see Figure 7). The mean values are given in Table II.

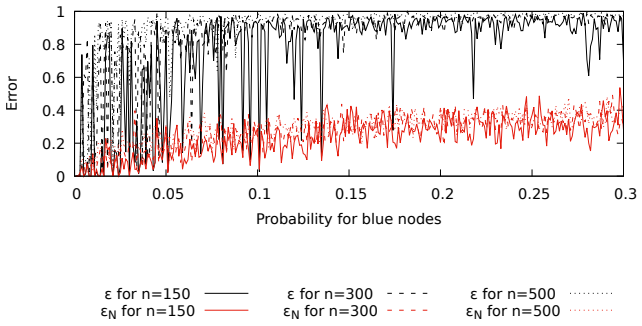

Fig. 6. Betweenness Centrality errors for scale-free random graphs ($n = 150$, $n = 300$ and $n = 500$) for different values of p_B between 0 and 0.3.

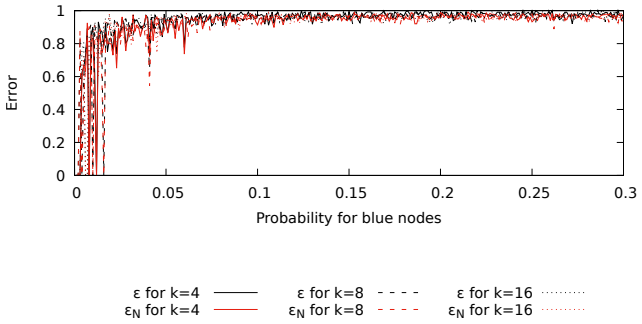

Fig. 7. Betweenness Centrality errors for Newman-Watts-Strogatz small-world random graph ($n = 150$, $k \in \{4, 8, 50\}$) for different values of p_B between 0 and 0.3.

	ϵ	ϵ_N	ϵ	ϵ_N	ϵ	ϵ_N
Scale-Free	$n = 150$		$n = 300$		$n = 500$	
Mean	0.77	0.23	0.87	0.27	0.91	0.29
Small-World	$k = 4$		$k = 8$		$k = 50$	
Mean	0.94	0.92	0.94	0.92	0.94	0.93

TABLE II
MEAN VALUES FOR BETWEENNESS CENTRALITY ERRORS.

Betweenness centrality (see Figure 6) in scale-free graphs is very much influenced by the choice for p_B. Again, the total error ϵ becomes very high although there are several outliers. More interesting is again the ordering error ϵ_N: although the error increases with a rising value of p_B, it remains very low. Again, the number of nodes n has only very little impact on the error measures.

Here, again, the Small-World graph has a very high error rate for both ϵ and ϵ_N although not for very small p_B, see Figure 7. In particular, we may find a boundary p'_B so that the values are rather constant for $p_B > p'_B$. Again, the graph topology for different values of k has only very little impact on the error rate. Thus, even small changes in the graph structure (a very small value for p_B) have a great impact on the betweenness centrality. Thus, the random choice of blue nodes again destroys the structures of local clustering which

will most likely effect not only one cluster, but also other clusters.

We will now consider two graph structures to take a closer look at their impact on the error measures.

C. Cliques

Let $G = (V, E)$ be a graph with $|V| = n$ and blue nodes $B \subset V$. The nodes in $G \setminus B = (V \setminus B, E)$ are denoted by $v_1, \ldots, v_{n-|B|}$ while the nodes in B are denoted by $v_{n-|B|+1}, \ldots, v_n$. We further assume that $G \setminus B$ is still connected. Let $dc(G)$ be the vector containing the degree centrality measures for all nodes v in G in descending order, where - after the computation of $dc(v)$ for all $v_1, \ldots, v_n \in V(G)$ - the values for all $v \in B$, that is, v_i with $i = n - |B| + 1, \ldots, n$, are deleted. Hence,

$$dc(G) = \big(dc(v_1), dc(v_2), ..., dc(v_{n-|B|})\big)$$

with $dc(v_j) \geq dc(v_{j+1})$ for all $j \in \{1, \ldots, n - |B|\}$.

Let $bc(G)$ be the vector containing the betweenness centrality measures for all nodes in G in descending order, where - after the computation of $bc(v)$ for all $v_1, \ldots, v_n \in V(G)$ - the values for all $v \in B$, that is, v_i with $i = n - |B| + 1, \ldots, n$, are deleted. That is,

$$bc(G) = (bc(v_1), bc(v_2), ..., bc(v_n - |B| + 1))$$

with $bc(v_j) \geq bc(v_{j+1})$ for all $j \in \{1, \ldots, n - |B|\}$. Let $p_{dc}(v)$ respectively $p_{bc}(v)$ be the position of node v in the vector $dc(G)$ respectively $bd(G)$. When it is clear from the context which vector is meant, we omit the index and simply write $p(v)$.

We may now prove some very basic observations on how a single blue node may influence the different error measures ϵ and ϵ_N, given that the blue node is part of a cluster in G. Here, with a cluster or a clique we denoate a complete subgraph of G.

Lemma IV.1. *Let $G = (V, E)$ be a graph with $|V| = n$ and blue nodes $B \subset V$ with $B = \{u\}$ where $G \setminus B$ is still connected. Let C_k be a clique in G with k nodes and let $u \in C_k$. Then*

$$\epsilon(dc(G), dc(G \setminus B)) \leq n - 1 - \min_{v \in N(u)} p_{dc}(v)$$

holds.

Proof. Let $a_1 = dc(G)$ and $a_2 = dc(G \setminus B)$. The only nodes which are affected by a decreasing degree centrality are those in the neighborhood $N(u)$ of the blue node u, since for $v \in N(u)$, only one node in the neighborhood of v is removed in $G \setminus B$ compared to G. Thus,

$$a_1^{p(v)} = a_2^{p(v)} - 1 \ \ \forall v \in N(u)$$

holds. Observe that $\min_{v \in N(u)} p_{dc}(v)$ denotes the smallest position in $dc(G)$ of a node in $N(u)$ (that is, the highest ranked neighbor of u in $dc(G)$). All nodes in $dc(G)$, that are higher ranked are not affected by the deletion of u. Recall that $dc(G)$ only has $n - |B| = n - 1$ entries. Thus, at most $n - 1 - \min_{v \in N(u)} p_{dc}(v)$ nodes change their position in $dc(G \setminus B)$ compared to $dc(G)$. □

We can rely on the same basic observations for the error measure ϵ_N:

Lemma IV.2. *Let $G = (V, E)$ be a graph with $|V| = n$ and blue nodes $B \subset V$ with $B = \{u\}$ where $G \setminus B$ is still connected. Let C_k be a clique in G with k nodes and let $u \in C_k$. Then*

$$\epsilon_N(dc(G), dc(G \setminus B)) \leq k - 1$$

holds.

Proof. Let $a_1 = dc(G)$ and $a_2 = dc(G \setminus B)$. Again, the only nodes which are affected by a decreasing degree centrality are those in the neighborhood of the blue node, that is the set $v \in N(u)$. Here, only one node in the neighborhood of these nodes is removed in $G \setminus B$. While the internal order of all nodes in $G \setminus \{C_k \setminus \{u\}\}$ does not change and the internal order of the $k - 1$ nodes in $C_k \setminus \{u\}$ remains untouched as well, at most the $k - 1$ nodes in $C_k \setminus \{u\}$ are shifted to a certain degree to the right, since their value in $dc(G \setminus B)$ decreased compared to $dc(G)$. Every vertex in $C_k \setminus \{u\}$ hence contributes at most 1 to the sum computed in $\epsilon_N(dc(G), dc(G \setminus B))$, which leads to the upper bound $k - 1$. □

The herefore stated lemma explains why this error increases for small-world networks: The node degree is high and a lot of local clusters exist.

Since betweenness centrality is also affected by the global structure of the graph, counting all shortest paths, the situation is slightly different.

Lemma IV.3. *Let $G = (V, E)$ be a graph with $|V| = n$ and blue nodes $B \subset V$ with $B = \{u\}$ where $G \setminus B$ is still connected. Let C_k be a clique in G with k nodes and let $u \in C_k$. Then*

$$\epsilon(bc(G), bc(G \setminus B)) \leq \begin{cases} 0 & if\ d(u) = k - 1 \\ \sum_{w \neq y} P_u(w, y) & otherwise. \end{cases}$$

Proof. **Case 1** $d(u) = k - 1$: In this case, u only lies on shortest paths between u and any node in $G \setminus \{u\}$, since $N(u) = C_k \setminus \{u\}$. That is, every shortest path through C_k ignores u, since u is only connected to nodes within $C_k \setminus \{u\}$, see Figure 8.

Thus, the number of shortest paths in G that include u is $n - 1$, that is,

$$\sum_{w \neq y, w \neq u, y \neq u} P_u(w, y) = n - 1$$

holds. Hence, for $v \in G \setminus B$,

$$\sum_{w \neq y, w \neq u, y \neq u} P_v^{G \setminus B}(w, y) = \sum_{w \neq y, w \neq u, y \neq u} P_v^{G}(w, y) - 1$$

where P^G denotes a shortest path in the graph G. In other words: There exists a value $b \in \mathbb{R}$ such that for every $v \in G \setminus B$,

$$bc(G)^{p(v)} = bc(G \setminus B)^{p(v)} - b.$$

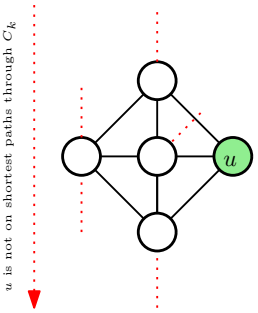

Fig. 8. If $d(u) = k - 1$, u lies only on shortest paths between u and any other node in $G \setminus \{v\}$. Any shortest path through C_k ignores u, since u is only connected to nodes within C_k.

Hence, the ordering of the values in $bc(G)$ compared to $bc(G \setminus B)$ does not change and the considered diffence is 0.

Case 2 $d(u) \geq k$: In this case, u lies on

$$s = \sum_{w \neq y, w \neq u, y \neq u} P_u(w, y)$$

shortest paths within the graph. Thus, removing this node will affect all these paths and thus the ordering of at most s nodes will be changed. Hence $\epsilon(bc(G), bc(G \setminus B)) \leq s$. □

Here, we considered highly connected blue nodes within clusters and their impact on the error measures. Usually, external data may not only be added to such dense structures but also to single nodes. Thus, we will now discuss the impact of nodes with degree 1.

D. Nodes with Degree 1

We now consider the special case in which the only existing blue node has degree 1.

Lemma IV.4. *Let $G = (V, E)$ be a graph with $|V| = n$ and blue nodes $B \subset V$ with $B = \{u\}$ where $G \setminus B$ is still connected. Let further $N(u) = \{v\}$. Then*

$$\epsilon\left(dc\left(G\right), dc\left(G \setminus B\right)\right) \leq p_{dc}(v)$$

holds.

Proof. Since $d(u) = 1$, there is only one node v in $N(u)$. This node is on position $p_{dc}(v)$ in $dc(G)$ and it is the only node affected in $G \setminus B$. Thus, at most $p_{dc}(v)$ nodes are affected. □

A similar observation can be made for ϵ_N:

Lemma IV.5. *Let $G = (V, E)$ be a graph with $|V| = n$ and blue nodes $B \subset V$ with $B = \{u\}$ where $G \setminus B$ is still connected. Let further $|N(u)| = 1$, that is, $d(u) = 1$. Then*

$$\epsilon_N(dc(G), dc(G \setminus B)) \leq 2$$

holds.

Proof. Let $a_1 = dc(G)$ and $a_2 = dc(G \setminus B)$. If $d(u) = 1$, there is only one node v in $N(u)$. This node is on position $p_{dc}(v)$ in a_1 and it is the only node affected in $G \setminus B$. Thus, either it is at the same position in a_2 or on a different one which will affect the nodes on position $p_{dc}(u) - 1$ and $p_{dc}(u) + 1$ in a_1 and $p_{dc}(u) - 1$ and $p_{dc}(u) + 1$ in a_2. Thus

$$\epsilon_N(dc(G), dc(G \setminus B)) \leq 2$$

holds. □

While degree centrality is a local centrality measure, betweenness is a global measure. Since u lies only on shortest paths between u and any other node in the graph, we can make the following observation:

Lemma IV.6. *Let $G = (V, E)$ be a graph with $|V| = n$ and blue nodes $B \subset V$ with $B = \{u\}$ where $G \setminus B$ is still connected. Let further $N(u) = \{v\}$ and let*

$$t = \max\left\{n - 1, \sum_{w \neq y} P_v(w, y)\right\}.$$

Then

$$\epsilon(bc(G), bc(G \setminus B)) \leq t$$

holds.

Proof. Let $a_1 = bc(G)$ and $a_2 = bc(G \setminus B)$.

Since $d(u) = 1$, there is only one particular node $v \in N(u)$. Thus, all shortest paths containing u will include v. The highest impact of removing u will hence be on v. Moreover, $n - 1$ shortest paths that include u exist in $G \setminus B$. Thus, the first part of the maximum holds.

In general, $s = \sum_{w \neq y} P_v(w, y)$ shortest paths in G include v. Thus, removing u will also change the betweenness for s nodes and the second part of the maximum holds. □

The evaluation of ϵ_N will—in general—decrease the worst-case scenario:

Lemma IV.7. *Let $G = (V, E)$ be a graph with $|V| = n$ and blue nodes $B \subset V$ with $B = \{u\}$ where $G \setminus B$ is still connected. Let further $N(u) = \{v\}$ and let*

Let

$$z = \max\left\{2\sum_{w \neq y} P_u(w, y), 2\sum_{w \neq y} P_v(w, y)\right\}.$$

Then

$$\epsilon_N(bc(G), bc(G \setminus B)) \leq z$$

holds.

Proof. Let $a_1 = bc(G)$ and $a_2 = bc(G \setminus B)$. Since $d(u) = 1$, there is only one particular node $v \in N(u)$. Thus, all shortest paths containing u will include v. Moreover, $n - 1$ such paths exist and the highest impact of removing u will be on v. But since we are interested in the ordering of nodes, the total number of reordered entries in a_2 may be just a factor. We can estimate this factor with the total number of shortest paths containing u which is $\sum_{w \neq y} P_u(w, y)$.

In general, again, $s = \sum_{w \neq y} P_v(w, y)$ shortest paths in G include v. Thus, removing u will also change the betweenness for s nodes and the second part of the maximum holds. □

These error estimations are not sharp. In addition, if the size of B increases, it will be even more challenging to specify the error rates. But together with our experimental results, these estimations offer us a first impression of problematic graph structures having a great impact on ϵ and ϵ_N.

We could show that blue nodes in clusters have a great influence on both ϵ and ϵ_N while those nodes with a small neighborhood have a rather small influence on ϵ_N. This gives a first idea why in general scale-free networks are more robust regarding ϵ_N. The degree centrality is only influenced by local structures but in general the errors are higher while the betweenness centrality is in general more complex and the results of this paper can only give some hints, but further research needs to be done here.

V. Discussion and Outlook

This paper investigates the impact on two particular centrality measures of graphs with multiple layers compared to single-purpose graphs. We presented an experimental environment to evaluate two different centrality measures – degree and betweenness centrality – on random graphs inspired by social network analysis: small-world and scale-free networks. The result clearly shows that the graph structures and topology has a great impact on its robustness for additional data stored. In particular, we could identify nodes with a high node degree and closely connected communities or clusters as problematic for reordering the centrality measures. Thus, we could show that small-world networks are rather less robust than scale-free networks.

Although the experimental analysis of random graphs allows us to make some basic observations, we could also present some very preliminary error approximations for two cases: A node within a cluster C_k and a node v with $d(v) = 1$. These results underline the experimental results. We need to mention that a lot of research needs to be done in this field, because we only considered degree and betweenness centrality.

In particular, we can identify the following questions for further research: Is it possible to find good error approximations for larger sets of blue nodes B? How do ϵ and ϵ_N behave on any given node $v \in B \subset V$ with $d(v) = m$? What are (other) graph structures that have a great impact on the stability of networks for degree, betweenness and other centralities?

To sum up, it is valid to extend single-purpose networks with data from other sources. In particular, we considered random social networks as a basis. Thus, extending social networks with other information layers is possible, although it will change the behavior of measurements like network centrality. The effect highly depends on the given graph structure. More interdisciplinary research is needed to investigate the impact on real-world data within the context of humanities. In addition, further research needs to be done on the robustness of other centrality measures.

References

[1] D. Suárez, J. M. Díaz-Puente, and M. Bettoni, "Risks identification and management related to rural innovation projects through social networks analysis: A case study in spain," *Land*, vol. 10, no. 6, p. 613, 2021.

[2] L. M. Berhan, A. L. Adams, W. L. McKether, and R. Kumar, "Board 14: Social networks analysis of african american engineering students at a pwi and an hbcu–a comparative study," in *2019 ASEE Annual Conference & Exposition*, 2019.

[3] C. Rollinger, "Amicitia sanctissime colenda," *Freundschaft und soziale Netzwerke in der Späten Republik*, 2014.

[4] J. Dörpinghaus and A. Stefan, "Knowledge extraction and applications utilizing context data in knowledge graphs," in *2019 Federated Conference on Computer Science and Information Systems (FedCSIS)*. IEEE, 2019, pp. 265–272.

[5] G. Rossetti, S. Citraro, and L. Milli, "Conformity: A path-aware homophily measure for node-attributed networks," *IEEE Intelligent Systems*, vol. 36, no. 1, pp. 25–34, 2021.

[6] D. Fensel, U. Şimşek, K. Angele, E. Huaman, E. Kärle, O. Panasiuk, I. Toma, J. Umbrich, and A. Wahler, *Introduction: What Is a Knowledge Graph?* Cham: Springer International Publishing, 2020, pp. 1–10. [Online]. Available: https://doi.org/10.1007/978-3-030-37439-6_1

[7] L. Ehrlinger and W. Wöß, "Towards a definition of knowledge graphs." *SEMANTiCS (Posters, Demos, SuCCESS)*, vol. , no. 48, 2016.

[8] H. Paulheim, "Knowledge graph refinement: A survey of approaches and evaluation methods," *Semantic web*, vol. 8, no. 3, pp. 489–508, 2017.

[9] M. A. Rodriguez and P. Neubauer, "The graph traversal pattern," in *Graph data management: Techniques and applications*. IGI Global, 2012, pp. 29–46.

[10] ——, "Constructions from dots and lines," *Bulletin of the American Society for Information Science and Technology*, vol. 36, no. 6, pp. 35–41, 2010.

[11] R. Diestel, *Graphentheorie*. Berlin: Springer, 2012, vol. 4. Auflage, korrigierter Nachdruck 2012.

[12] J. Matoušek, J. Nešetřil, and H. Mielke, *Diskrete Mathematik*. Berlin: Springer, 2007.

[13] M. O. Jackson, *Social and Economic Networks*. Princeton: University Press, 2010.

[14] D. J. Watts, "Networks, dynamics, and the small-world phenomenon," *American Journal of sociology*, vol. 105, no. 2, pp. 493–527, 1999.

[15] L. C. Freeman, "Centrality in social networks conceptual clarification," *Social Networks*, vol. 1, no. 3, pp. 215–239, 1978.

[16] P. J. Carrington, J. Scott, and S. Wasserman, *Models and methods in social network analysis*, ser. Structural Analyses in the Social Sciences, 27. Cambridge: University Press, 2005, vol. .

[17] L. C. Freeman, "A set of measures of centrality based on betweenness," *Sociometry*, pp. 35–41, 1977.

[18] D. R. White and S. P. Borgatti, "Betweenness centrality measures for directed graphs," *Social networks*, vol. 16, no. 4, pp. 335–346, 1994.

[19] T. Schweizer, *Muster sozialer Ordnung: Netzwerkanalyse als Fundament der Sozialethnologie*. Berlin: D. Reimer, 1996.

[20] P. Bonacich, "Factoring and weighting approaches to status scores and clique identification," *Journal of mathematical sociology*, vol. 2, no. 1, pp. 113–120, 1972.

[21] S. P. Borgatti, "Centrality and network flow," *Social networks*, vol. 27, no. 1, pp. 55–71, 2005.

[22] M. Ditsworth and J. Ruths, "Community detection via katz and eigenvector centrality," *arXiv preprint arXiv:1909.03916*, 2019.

[23] B. Bollobás, C. Borgs, J. T. Chayes, and O. Riordan, "Directed scale-free graphs." in *SODA*, vol. 3, 2003, pp. 132–139.

[24] B. Bollobás and O. M. Riordan, "Mathematical results on scale-free random graphs," *Handbook of graphs and networks: from the genome to the internet*, pp. 1–34, 2003.

[25] M. Kivelä, A. Arenas, M. Barthelemy, J. P. Gleeson, Y. Moreno, and M. A. Porter, "Multilayer networks," *Journal of complex networks*, vol. 2, no. 3, pp. 203–271, 2014.

[26] M. Newman and D. Watts, "Renormalization group analysis of the small-world network model," *Physics Letters A*, vol. 263, no. 4, pp. 341–346, 1999. [Online]. Available: https://www.sciencedirect.com/science/article/pii/S0375960199007574

[27] J. Aarstad, H. Ness, and S. A. Haugland, "In what ways are small-world and scale-free networks interrelated?" in *2013 IEEE International Conference on Industrial Technology (ICIT)*. IEEE, 2013, pp. 1483–1487.

[28] K. Klemm and V. M. Eguiluz, "Growing scale-free networks with small-world behavior," *Physical Review E*, vol. 65, no. 5, p. 057102, 2002.

6th Workshop on Internet of Things—Enablers, Challenges and Applications

THE Internet of Things is a technology which is rapidly emerging the world. IoT applications include: smart city initiatives, wearable devices aimed to real-time health monitoring, smart homes and buildings, smart vehicles, environment monitoring, intelligent border protection, logistics support. The Internet of Things is a paradigm that assumes a pervasive presence in the environment of many smart things, including sensors, actuators, embedded systems and other similar devices. Widespread connectivity, getting cheaper smart devices and a great demand for data, testify to that the IoT will continue to grow by leaps and bounds. The business models of various industries are being redesigned on basis of the IoT paradigm. But the successful deployment of the IoT is conditioned by the progress in solving many problems. These issues are as the following:

- The integration of heterogeneous sensors and systems with different technologies taking account environmental constraints, and data confidentiality levels;
- Big challenges on information management for the applications of IoT in different fields (trustworthiness, provenance, privacy);
- Security challenges related to co-existence and interconnection of many IoT networks;
- Challenges related to reliability and dependability, especially when the IoT becomes the mission critical component;
- Zero-configuration or other convenient approaches to simplify the deployment and configuration of IoT and self-healing of IoT networks;
- Knowledge discovery, especially semantic and syntactical discovering of the information from data provided by IoT.

The IoT technical session is seeking original, high quality research papers related to such topics. The session will also solicit papers about current implementation efforts, research results, as well as position statements from industry and academia regarding applications of IoT. The focus areas will be, but not limited to, the challenges on networking and information management, security and ensuring privacy, logistics, situation awareness, and medical care.

TOPICS

The IoT session is seeking original, high quality research papers related to following topics:

- Future communication technologies (Future Internet; Wireless Sensor Networks; Web-services, 5G, 4G, LTE, LTE-Advanced; WLAN, WPAN; Small cell Networks...) for IoT,
- Intelligent Internet Communication,
- IoT Standards,
- Networking Technologies for IoT,
- Protocols and Algorithms for IoT,
- Self-Organization and Self-Healing of IoT Networks,
- Object Naming, Security and Privacy in the IoT Environment,
- Security Issues of IoT,
- Integration of Heterogeneous Networks, Sensors and Systems,
- Context Modeling, Reasoning and Context-aware Computing,
- Fault-Tolerant Networking for Content Dissemination,
- IoT Architecture Design, Interoperability and Technologies,
- Data or Power Management for IoT,
- Fog—Cloud Interactions and Enabling Protocols,
- Reliability and Dependability of mission critical IoT,
- Unmanned-Aerial-Vehicles (UAV) Platforms, Swarms and Networking,
- Data Analytics for IoT,
- Artificial Intelligence and IoT,
- Applications of IoT (Healthcare, Military, Logistics, Supply Chains, Agriculture, ...),
- E-commerce and IoT.

The session will also solicit papers about current implementation efforts, research results, as well as position statements from industry and academia regarding applications of IoT. Focus areas will be, but not limited to above mentioned topics.

TECHNICAL SESSION CHAIRS

- **Cao, Ning,** College of Information Engineering, Qingdao Binhai University
- **Chudzikiewicz, Jan,** Military University of Technology, Poland
- **Zieliński, Zbigniew,** Military University of Technology, Poland

Communication Papers of the of the 17th Conference on Computer Science and Intelligence Systems pp. 173–180
DOI: 10.15439/2022F234
ISSN 2300-5963 ACSIS, Vol. 32

A comprehensive framework for designing behavior of UAV swarms

Piotr Cybulski
Military University of Technology
in Warsaw
ul. Gen. Sylwestra Kaliskiego 2,
00-908 Warszawa, Poland
Email: piotr.cybulski@wat.edu.pl

Zbigniew Zieliński
Military University of Technology
in Warsaw
ul. Gen. Sylwestra Kaliskiego 2,
00-908 Warszawa, Poland
Email: zbigniew.zielinski@wat.edu.pl

***Abstract*—This paper aims to present a method of designing the behavior of robotic swarms, emphasizing swarms of unmanned aerial vehicles using bigraphs. The method's primary goal is to define a set of actions to be performed in subsequent moments by the members of a swarm that lead to the completion of the given task. In addition to formal definitions, an example use case is also included to demonstrate how utilizing our method allows overcoming typical difficulties related to swarm robotics engineering. The example covers verifying non-functional requirements and scaling a task both horizontally and vertically.**

I. Introduction

ROBOTIC swarm (SR) is a special case of multi-agent system [8] (MAS), and as such have been the subject of study for many years[10][9]. Beyond attributes typically associated with MAS, such as agent's independence, decentralized control, and the lack of access to information about the global state of a system, they can be attributed to features of real-world swarms[11][13]. These can be features of both individual members of the swarm and the swarm as a whole. The former group consists of the ability to interact with the environment or other members of the swarm, local perception capabilities, and relatively low cognitive capacity. On the other hand, the features attributed to the swarm are robustness, scalability, and flexibility. Finally, one aspect of robotic swarms that is often emphasized is that their emergent behavior is more complex than its members' behavior alone. From now on, by swarm behavior, we shall understand the behavior of its members.

Current research results on robotic swarms can be categorized by how they fit on multiple different axes[16][12]. Most common are the size of a swarm, ability to communicate (one-to-one, one-to-all, etc.), communication bandwidth, computational capabilities, or whether the swarm is homogeneous or heterogeneous. There are also classifications not by attributes of the swarm itself but whether it was designed with a top-down or bottom-up approach[17].

In the literature on robot swarms, there is a clear tendency to consider the goal posed to the swarm as a variant of tasks from a predefined set [11][14][15]. Tasks that exhibit the highest potential for practical application include moving in formation, area coverage, rendezvous, and foraging.

Main difficulties in designing swarms of robots arise from expectations that we do not have of ordinary multi-agent systems. In particular, the low capabilities of a single element of the swarm and, consequently, the problems with communication and control of the whole swarm[18]. Another issue will be to define a level of automation[4] of a swarm element. The more autonomous the swarm is expected to be, the more difficult it becomes to self-control itself in real-time, or the given task has to be less unpredictable. For highly autonomous swarms, there is also the problem of collective decision-making [19]. On the other hand, swarms that are highly dependent on an external operator may become useless in practice due to difficulties described in [18].

Existing methods for designing the behavior of a robot swarm can be divided into those that try to find similarities in the behavior of the designed swarm to the operating mechanisms of systems well understood within other areas of science and those that try to be universal. The former group consists of bio-inspired methods[25][26], physics-inspired ones [27][28][29] (with the strong emphasis on particles repulsion/attraction interactions), and those that considers members of the swarm as a dynamical system with their knowledge modeled with graph theory[30]. The latter group of methods for designing tries not to use analogies to well-studied phenomena and instead proposes its schemes, often with multiple stages[20][21][22]. We would also include in this group methods that use specially designed abstract mathematical structures. The most important of these would be amorphous[23] and aggregated[24] computing due to their resemblance to the concept of swarms.

Bigraphs[3] are formal structures that allow to model systems, in which spatial arrangement and interconnection of elements play an important role. It is also feasible to define the dynamics of a system within bigraphs framework. So far they have been found useful in designing Internet of Things [31][32] and computer networks [33]. The applicability of bigraphs in the process of designing behavior of a multi-agent system's elements requires further research. Most of existing works [34][35] focus merely on utilizing bigraphs to represent a system, without taking under consideration how its elements should operate to accomplish a given goal. These works [36]

that include also this aspect of the design process do so with an additional level of abstraction.

This work aims to present a method for designing swarm behavior using bigraphs. It is a summary of work previously presented in [2] and [1] extended with a formal definition of the schedule of actions. Section II defines all the formal structures together with how they can be used to develop a swarm behavior performing a designer-defined task. Section III presents a minimal example of a problem that can be solved using the proposed method. It covers alternative scenarios for executing the given task, verifying non-function requirements, and scaling the task both horizontally and vertically. Section IV is devoted to further direction of work related to the development of the presented method.

The design method described further on does not impose restrictions on the designed swarm members. Later in this paper, we will consider swarms whose members are small unmanned aerial vehicles (UAVs), called drones.

II. Designing UAV swarm behavior

A. Assumptions and limitations of designed swarms

The following will define, in a condensed form, a method for designing the behavior of elements of a multi-agent system [2]. It allows the development of a manner in which a designer-defined task can be completed successfully.

Developing a swarm behavior is a process of constructing a *schedule of actions* (defined formally later in this paper) for all members of the swarm. A schedule can be interpreted as a set of operations or activities to be carried out at specific moments. A schedule also indicates a role played by each member of the swarm participating in any action. The designing process begins with defining a task and an initial state of a system. By system, we will understand all elements of the real world that are relevant to the specified task. It is also necessary to define all kinds of activities that may happen within the system. An example of an activity can be a movement of drones between areas or picking up an object. Activities may involve multiple members of the swarm or its single member. Within each activity, each participant may play a different role. Both the initial state and the activities are described in with *bigraph* notation. The next step is to define all states of the system that are reachable from the initial state by performing any combination of activities from the set defined earlier. *Tracking transition systems* are used to describe both states and activities, along with roles played in each of them. The next objective is to find a sequence of activities that, when performed, allow to transform the system from being in its initial state into the desired state. To do this, a structure called *state space* has been proposed, where each state is reduced to a vertex (forgetting its bigraphical representation) of a directed multigraph, and arcs between vertices denote an activity enabling a change from one state to the other. Additionally, each arc has assigned a *mission progress function* which describes relations between swarm elements participating in the activity in a computationally inexpensive manner. Within this structure, searching for a sequence of actions that allows accomplishing the given task can be considered a problem of finding a walk (in graph theory meaning) between two vertices. A method for finding all walks of specified length has been developed to solve this problem. The last step is to transform one of the founded walks into a schedule of actions. Having such a schedule, we can verify whether executing the given task meets the non-functional requirements.

If we consider designing UAV behavior as a decision process, then designing with our method can be regarded as a level 7 automatic process according to the scale proposed in [4]. This level of automation means that the designer may leave the designing process to a specialized tool after providing initial parameters.

Components of systems for which behavior can be designed using this method can be divided into three categories: *elements of the environment*, *passive objects* and *active objects*. Environmental objects can not initiate any action, and time-lapse is irrelevant to them. An example of such elements may be areas between which drones can travel or an object that can be lifted by at most one drone. Passive objects can not initiate any action, but the passage of time has to be considered for these kinds of objects. An example of such an object can be an item multiple drones can possess during task execution. The last kind of system components we recognize are active objects which can both initialize actions and time relevant to them during a mission. Drones are an example of such objects. It is assumed that every active object in a system can be controlled. It means there are no active objects in the system that may act unexpectedly. The final limitation is that the number of objects (both active and passive) is constant during task execution.

Knowing the above, we can classify swarms for which the behavior we will try to design as “set & forget“. If we consider the execution of a task as a decision process, where the decisions regarding whether and, if so, how to perform actions not included in a schedule, then this process is level 8 or 9 on the autonomy scale mentioned earlier. Level 8 means that a swarm executes a given task and gives feedback when the operator requests it. Level 9 means that feedback is at the discretion of the swarm performing a task.

B. Bigraphs

The primary formal tool utilised in our method are bigraphs [3]. They allow for modeling ubiquitous computing with just graphical notation.

Below, we define the key concepts necessary to understand later parts of the paper. For more in dept introduction we refer to [5].

A (concrete) bigraph over the signature $(\mathcal{K}, ar : \mathcal{K} \to \mathbb{N})$ is defined as:

$$B = (\mathbb{V}_B, \mathbb{E}_B, ctrl_B, G_B^P, G_B^L) : I \to O$$

where:

- $\mathbb{V}_B$ - is a set of vertex identifiers;
- $\mathbb{E}_B$ - is a set of hyperedges identifiers;
- $ctrl_B : \mathbb{V}_B \to \mathcal{K}$ - is a function assigning controls to vertices;

- G^P_B, G^L_B - is a place graph G^P_B and a link graph G^L_B comprising the bigraph B:
  - $G^P_B = \langle \mathbb{V}_B, ctrl_B, prnt_B \rangle : m \to n$ - is the place graph of bigraph B with m sites and n roots. Both m and n are finite ordinals of the form $x\{0, 1, \ldots, x-1\}$. A function $prnt_B : m \uplus \mathbb{V}_B \to \mathbb{V}_B \uplus n$ defines a hierarchical relationship between vertices, sites and roots. It is important to emphasize that the map $prnt$ defines a set of rooted trees.
  - $G^L_B = \langle \mathbb{V}_B, \mathbb{E}_B, ctrl_B, link_B \rangle : X \to Y$ - is the link graph of bigraph B, with inner names X and outer names Y. A link map $link_B : X \uplus P_B \to \mathbb{E}_B \uplus Y$ defines connections from vertices and inner names to hyperedges and outer names of the link graph. A set $P_B = \{(v, i) \mid i \in ar(ctrl_B(v))\}$ is the set of ports of G^L_B. Its elements (v, i) shall be interpreted as ith port of vertex v.
- $I = \langle m, X \rangle$ and $O = \langle n, Y \rangle$ are the inner and outer interface of the bigraph B.

We use $\uplus$ to denote a union of sets assumed to be disjoint.

Dynamics of systems modeled with bigraphs can be expressed with reaction rules. In this paper we will use *linear parametric reaction rules* proposed in [6], extended with *tracking*. Formally this kind of a reaction rule is defined as:

$$r = (R : \langle m, \emptyset \rangle \to \langle n, X \rangle, R' : \langle m, \emptyset \rangle \to \langle n, X \rangle, \tau)$$

where:

- R - is a bigraph called *redex* of reaction rule *r*;
- R' - is a bigraph called *reactum* of reaction rule *r*;
- $\tau : \mathbb{V}_{R'} \to \mathbb{V}_R$ - is a *tracking map* indicating which vertices in redex correspond to which vertices in reactum. If this function is partial, or if it is not a surjection, then it means that as a result of action represented by this reaction rule some of the elements either have been created or disappeared.

For the purpose of this introduction we will just indicate that applying a reaction rule means finding occurrences of the redex in a target bigraph and replacing them with reactum. Details of these operations are skipped in this paper.

C. Tracking transition system

Apart from defining actions (reaction rules) that may happen in the system and specifying when preconditions for each of them are satisfied (finding redexes), we need to answer the following question regarding the dynamics of the system:

- Who participates in an action that transforms a system state in a particular way?
- Which elements of a state resulting from the transformation are "residue" of the state before the action?

To answer these questions, a structure called *tracking transition system* has been proposed in [2] and later refined in [1]. It is an extension of the basic transition systems defined in [7].

Formally, a tracking transition system is a seven tuple $TTS = (Agt, Red, Lab, Apl, Par, Res, Tra)$ where:

- Agt - is a set of bigraphs;
- Red - is a set of redexes of reaction rules;
- Lab - is a set of labels of the reaction rules. They are meant to distinguish different types of actions in the system.
- $Apl \subseteq Agt \times Lab$ - is an applicability relation. It indicates which reaction rules can be applied from which bigraph;
- $Par = \{\mathbb{V}_b \to \mathbb{V}_r \mid b \in Agt,\ r \in Red\}$ - is a set of *participation* functions. Each of them maps vertices in a redex from Red to vertices in a bigraph from Agt. Every function $par \in Par$ is injective.
- $Res = \{\mathbb{V}_{b_1} \to \mathbb{V}_{b_2} \mid b_1, b_2 \in Agt\}$ - is a set of residue functions. Each of them maps vertices in a bigraph representing a state after an action to vertices in a bigraph representing a state where the action has happened;
- $Tra \subseteq Apl \times Agt \times Par \times Res$ - a transition relation. Elements of this set will hereafter be referred to as "transitions".

A tracking transition system can be interpreted as follows. The set Agt represents the reachable states of the system after performing any sequence of actions. At this stage, the time-lapse for objects is not considered, so the actual set of possible states might be smaller. Elements of Red can be viewed as preconditions necessary to occur in the states for any action to happen, modeled as a reaction rule. The binary relation Apl allows marking which action (Lab) can occur in which state of the system (Agt). The set of functions Par makes it possible to indicate which elements (vertices) of a state play what role in an action (reaction rule) with particular redex. Let us adopt the following convention, a state from which an action may be performed will be called an *input state*, while a state being the result of acting will be called an *output state*. The set of functions Res allows mapping elements of an output state corresponding to elements of an input state. If such a function is partial, then not all output state elements have the corresponding element in the input state. Thus, these "untracked" elements are new to the system. If, on the other hand, such a function is not surjective, then some of the elements in the input state are not existing in the output state. Thus these elements have vanished from the system. The set of transitions Tra utilizes the above elements to describe feasible alterations in the system.

D. State space

Having a tracking transition system (TTS), we can indicate roles in an action played by each element of an input state. Still, we can not determine how participating in a single activity affects the possibility of interacting with other system elements in different actions. To overcome this, a structure called *state space* has been proposed. It can be constructed as a directed multigraph from a TTS, where each arc has a *mission progress function* assigned to it. By mission, we understand any course of actions made by a swarm, leading to successful task completion.

A state space of a system consisting of n_o objects and n_s states is a tuple:

$$SS = (S, E, L, I, C, T, M_f)$$

where subsequent tuple's elements are as follows:

- $S \subset \mathbb{N}$ - is a set of states of the modelled system. Each state in the state space corresponds to exactly one element of Agt in the TTS;
- $E \subseteq S \times S$ - a multiset of arcs between states;
- L - a set of labels describing possible changes in the system. Each label unambiguously indicate a single transition in the TTS. To determine the order in which actions are evaluated another set is introduced $\mathbb{H} = \{l_t \mid l \in L, t \in \mathbb{N}\}$;
- $I \subset \mathbb{N}_1^2 \times \cdots \times \mathbb{N}_{n_o}^2$ - is a set of state-at-time (SaT) configurations. With this set it is possible to define order of objects (both active and passive) as well as the moment of time in which each of them is;
- $C \subset (I \times 2^{\mathbb{H}}) \cup \{0\}$ - a set of mission courses. Consists of the current SaT configuration and subsequent actions that have led to it. Element 0 indicates an unfeasible course of a mission and will be used as to mark states of the system that are unreachable by expanding an existing course of a mission;
- $T = \{f_i : C \times \mathbb{N} \to C \mid i \in \mathbb{N}\} \cup \{f_{null}\}$ - is a set of *mission progress functions*. Each of these functions takes as an argument the current course of a mission and the number of actions currently evaluated. A set $T_{i,j} \subset T$ consist of all mission progress functions from *i*th state to the *j*th state. Function f_{null} returns 0 (unfeasible course of a mission) regardless of input;
- $M_f : E \to T$ - a bijection assigning mission progress functions to arcs.

A walk in a state space from the state recognized as initial to one of the satisfying final states is *behavior policy*. An algorithm for finding all walks of specified length, in a state space has been presented in [2]. Below are defined its main components:

- $K_s^t = \sum_{i=1} c_i \quad c_i \in C$ - a finite sequence of mission courses of a length t to a state s. A function $n_K : K_s^t \to \mathbb{N}$ returns the number of elements in the provided sequence;
- $F_{i,j}^t = \sum_{f \in T_{i,j}} f(x,t) \quad i,j \in \{0, \cdots, n_s - 1\}, x \in C$ - a finite sequence whose elements are mission progress functions from *i*th state to the *j*th state. Each of these functions takes two arguments x and t. Only a value of t is know at the moment of constructing a sequence.
- $\mathbb{M}_K^t = \begin{bmatrix} K_0^t & \cdots & K_{n_s-1}^t \end{bmatrix}$
- $\mathbb{M}_F^t = \begin{bmatrix} F_{0,0}^t & \cdots & F_{0,(n_s-1)}^t \\ \cdots & \cdots & \cdots \\ F_{(n_s-1),0}^t & \cdots & F_{(n_s-1),(n_s-1)}^t \end{bmatrix}$

Additionally, two operations are defined:

- $K_s^t \circ F_{i,j}^t = \sum_{f \in F_{i,j}^t} \sum_{i=1}^{n_K(K_s^t)} f(c_i, t)$ - a convolution of sequences;
- $\mathbb{M}_K^{t+1} = \mathbb{M}_K^t \cdot \mathbb{M}_F^t$ - a multiplication of a matrix $\mathbb{M}_K^t$ by a matrix $\mathbb{M}_F^t$. Elements of the result matrix are calculated according to the formula:

$$K_j^{t+1} = \sum_{i=0}^{n_s-1} K_i^t \circ F_{i,j}^t$$

In order to find all behavior policies of a specified length t it necessary to perform just as many multiplications $\mathbb{M}_K^t \cdot \mathbb{M}_F^t$, with each multiplication the t parameter will be incremented and the matrix $\mathbb{M}_K^t$ will be the result of the previous product.

The number of steps required to find all walks of a specified length is dependent on four parameters:

- the length of sought walks - l;
- a sum of all mission progress functions - n_f;
- the number of states in a system - n_s;
- a sum of all mission courses in a matrix $\mathbb{M}_K^0$ - n_k;

and it will be denoted as $t^{(l)}(n_s, n_f, n_k)$.

A set of functions asymptotically bounded above by a function $g(n)$ is defined as:

$$O(g(n)) = \{f(n) \mid \exists c, n_0 \forall n > n_0 \quad 0 \leq f(n) \leq c \cdot g(n)\}$$

Using the above notations, the number of steps required to find all walks of a specified length is bounded above asymptotically by $l \cdot n_s^2 + n_k \cdot \frac{(n_f)^{l+1}-1}{n_f-1}$. This in turn can be written as:

$$t^{(l)}(n_s, n_f, n_c) \in O(l \cdot n_s^2 + n_k \cdot \frac{(n_f)^{l+1} - 1}{n_f - 1})$$

E. Schedule of actions

The last component required to define behavior for swarm elements is a *schedule of actions* for every active object. An algorithm verifying the correctness of a behavior policy has been described in [1]. It returns a set of ordered elements, each comprising three items. The first is a system state at a specified moment. The state is in the form of a bigraph. The second component is a function assigning *unique identifiers* to every vertex of the bigraph. The last component is a SaT configuration of the state. Knowing that every task element (whether this being an environmental element or an object) is distinguishable with a unique identifier, we want to define how each of these elements will behave. Unique identifiers for task elements are drawn from an infinite set $\mathcal{U}$.

Formally, a schedule of actions is a triple:

- A binary relation $Assignment : \mathcal{U} \times (T \times Lab \times \mathbb{N})$ which assigns mission progress functions, a label of an activity represented by that function and a moment of time to mission elements. The time here represents a moment the activity shall began to be executed.
- A function $role : \mathcal{U} \times (T \times Lab \times \mathbb{N}) \to \mathbb{V}_r$ assigning roles to task elements participating in an activity. Roles are indicated by vertices of the redex in a reaction rule

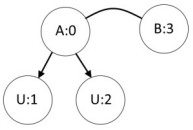

Fig. 1. Initial state of the system.

corresponding to a mission progress function provided as an argument.
- A function $duration : T \to \mathbb{N}$ which assigns how long does each of the activities take time.

Although, the main goal of the schedule of actions is to define how each element of a swarm shall behave during a mission, it is also possible to apply this structure to verify non-functional requirements.

III. Results

The structures defined in Section II can be used to design the behavior of members of a UAV swarm. A schedule of actions allows to complete a task (hence fulfill functional requirements) and makes it possible to verify if non-functional requirements are also satisfied.

This chapter aims to demonstrate a simple example of practical usage of the structures described in this paper. To do this, the following scenario will be used. Let us consider a UAV swarm consisting of two drones whose goal is to move between two areas, namely area *A* and *B*. Assume they can do this in two ways. The first one allows each of the drones to move independently; this method of movement is power-efficient (it is assumed that moving this way for an hour consumes 20Wh) and takes two units of time for a drone to complete a transition from an area A to an area B. Internally, each drone is responsible for both obstacle detection and avoiding and determining the trajectory of a movement. The second way of moving between the areas requires cooperation. It is more energy-consuming (here, assume that each drone moving this method is a 50W device), but it is twice as fast, which means it requires only one unit of time for both drones to move from an area A to an area B. Internally, we can think of this kind of movement as an activity where one of the drones follows the other, but each is responsible for different functions during the movement. By functions, we understand things like obstacle detection and avoidance and determine the trajectory of the flight. The first kind of transition will be denoted as *r1*, while the second as *r2*. The unit of time in this example is to be understood as 6 minutes. Reaction rules representing both kinds of transitions are listed in Table I. The initial state of the system is depicted in Figure 1. Vertices with control *U* represent drones, while those with control *A* and *B* represent areas.

Figure 2 presents a graphical form of a tracking transition system for the system described above. Circles denote states of the system. Every arc represents a single transition (a possible action) between states. Types of actions (either *r1* or *r2*) along with functions par and res are placed inside each arc. There

TABLE I
Reaction rules for two kinds of drones movement. Both of the τ functions are identities.

Reaction rule	Graphical notation
r_1	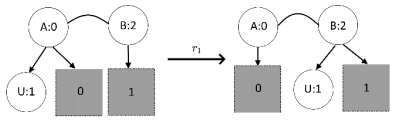
r_2	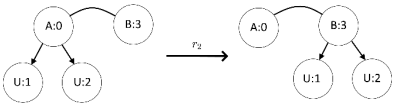

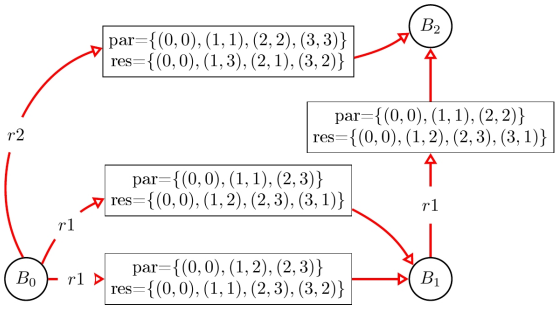

Fig. 2. A graphical form of the TTS for the example system.

are three possible states of the system. First one (B_0) is equal to the bigraph from Figure 1. B_1 represents a situation where one of the drones has already moved from *A* to *B*. There are two transitions between B_0 and B_1 because any of the drones can move between the areas. Which one actually participated in the activity is indicated by the functions par and res. The B_2 state is equal to the situation where both drones are in the *B* area. Knowing that, there is only one transition between the state B_1 to the state B_2 because regardless of which one of the drones has previously moved, only the second one can participate in *r1* activity. If we differentiate functions par and res between the same states, only by their domains and codomains, rather than actual mappings, then there can only be one transition from the state B_0 to B_2 representing an execution of *r2* activity.

Figure 3 shows a state space transformed from TTS in Figure 2. Only drones are classified as objects in the task, so mission mission courses (elements of the set C) comprise of tuples of pairs. Mission progress functions definitions are listed below. A convention was adopted that each function takes the form of $f_x(c,t)$ where c is a current mission course, and t is the length of the course (number of included activities). A mission course can either be of the form $[\langle(a,x),(b,y)\rangle, \mathbb{H}']$ or 0. In the first case a and b are objects identifiers in a SaT, while x and y are moments of time these objects are at. Knowing this, each subsequent mission progress function will transform a given course of the mission as follows:

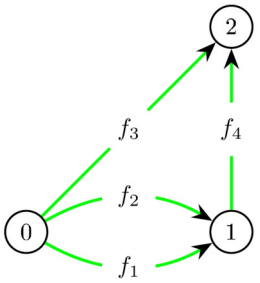

Fig. 3. A state space transformed from the TTS in Figure 2.

$$1)\ \begin{cases} \left[\langle (b,y),(a,x+2)\rangle, \mathbb{H}' \cup \{r1^1_{t+1}\}\right] & c \neq 0 \\ 0 & c = 0 \end{cases}$$

$$2)\ \begin{cases} \left[\langle (a,x),(b,y+2)\rangle, \mathbb{H}' \cup \{r1^2_{t+1}\}\right] & c \neq 0 \\ 0 & c = 0 \end{cases}$$

$$3)\ \begin{cases} \left[\langle (a,x+1),(b,y+1)\rangle, \mathbb{H}' \cup \{r2^3_{t+1}\}\right] & c \neq 0 \wedge x = y \\ 0 & c = 0 \vee x \neq y \end{cases}$$

$$4)\ \begin{cases} \left[\langle (b,y),(a,x+2)\rangle, \mathbb{H}' \cup \{r1^4_{t+1}\}\right] & c \neq 0 \\ 0 & c = 0 \end{cases}$$

A permutation of SaT components depends on the order of a bigraph's vertices that correspond to task objects, and it derives directly from function res and par. Incrementing x and y values results from the assumptions taken about the time needed for *r1* and *r2* activities to be completed. The set $\mathbb{H}'$ represents a currently constructed walk in the state space.

Having all mission progress functions defined we can proceed to constructing a behavior policy. Assuming that the task can only be started from the state denoted as *0* in Figure 2 and both drones commence the task execution at the same time (let us denote this moment as 0) the matrix $\mathbb{M}^0_K$ is of the form:

$$\mathbb{M}^0_K = \left[\left[\langle (1,0),(2,0)\rangle, \emptyset\right] \quad 0 \quad 0\right]$$

Based on the state space in Figure 3 the matrix $\mathbb{M}^t_F$ takes the form:

$$\mathbb{M}^t_F = \begin{bmatrix} f_{null} & f_1 + f_2 & f_3 \\ f_{null} & f_{null} & f_4 \\ f_{null} & f_{null} & f_{null} \end{bmatrix}$$

Multiplying the above matrices we get all possible behavior policies for drones. Successive $\mathbb{M}^t_K$ matrices are as follows:

$$\mathbb{M}^1_K = \mathbb{M}^0_K \cdot \mathbb{M}^0_F$$

$$\mathbb{M}^1_K = \begin{bmatrix} 0 \\ \left[\langle (2,0),(1,2)\rangle, \{r1^1_1\}\right] + \left[\langle (1,0),(2,2)\rangle, \{r1^2_1\}\right] \\ \left[\langle (1,1),(2,1)\rangle, \{r2^3_1\}\right] \end{bmatrix}^\intercal$$

$[\quad]^\intercal$ denotes the transpose of a matrix $[\quad]$.

$$\mathbb{M}^2_K = \mathbb{M}^1_K \cdot \mathbb{M}^1_F =$$

$$\begin{bmatrix} 0 \\ 0 \\ \left[\langle (1,2),(2,2)\rangle, \{r1^1_1, r1^4_2\}\right] + \left[\langle (2,2),(1,2)\rangle, \{r1^2_1, r1^4_2\}\right] \end{bmatrix}^\intercal$$

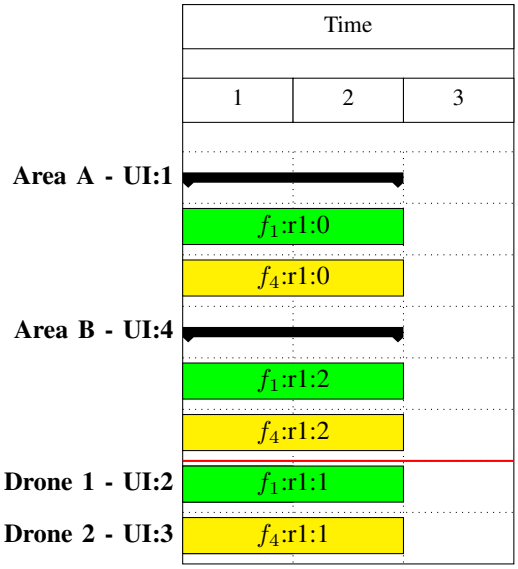

Fig. 4. A schedule of actions for all task elements based on the walk $0 \xrightarrow{f_1} 1 \xrightarrow{f_4} 2$. Areas A and B, being elements of the environment, can participate in multiple activities concurrently. Colors indicate different mission progress functions (activities). The text inside inform about a mission progress function, type of an activity it corresponds to and a role an element plays in the activity.

$\mathbb{M}^1_K$ matrix indicates there are two walks leading to the state 1 of the length 1. There there is also a single walk to the state 2 of the same length. The matrix $\mathbb{M}^2_K$ shows there are two walks to the state 2 of the length 2.

Having behavior policies, it is now possible to construct a schedule of actions for swarm elements. Using the algorithm described in [1] one can check that all found behavior policies produce a valid schedule. Figure 4 shows a schedule of actions from a walk of the form $0 \xrightarrow{f_1} 1 \xrightarrow{f_4} 2$. The formal definition of the same schedule is as follows:

- $Assignment = \left\{ \begin{array}{l} (1,(f_1,\mathrm{r1},0)),(1,(f_4,\mathrm{r1},0)), \\ (2,(f_1,\mathrm{r1},0)),(2,(f_4,\mathrm{r1},0)), \\ (3,(f_1,\mathrm{r1},0)),(4,(f_4,\mathrm{r1},0)) \end{array} \right\}$
- $role = \left\{ \begin{array}{l} ((1,(f_1,\mathrm{r1},0)),0),((1,(f_4,\mathrm{r1},0)),0), \\ ((4,(f_1,\mathrm{r1},0)),2),((4,(f_4,\mathrm{r1},0)),2), \\ ((2,(f_1,\mathrm{r1},0)),1),((3,(f_4,\mathrm{r1},0)),1) \end{array} \right\}$
- $duration = \{(f_1,2),(f_4,2)\}$

The developed framework allows scaling a task both horizontally and vertically. Scaling a task horizontally is expanding the current task by including more elements. For example, scaling the example covered in this section horizontally can increase the number of drones. To modify a task this way, the designer has to change the system's initial state. This requires a reconstruction of the tracking transition system and the state space. Hence, any modifications of this kind are very intrusive to the existing model because it requires a change in a structure that every other relies on. Vertical scaling is expanding a task by new functional requirements or additional stages. It is significantly less intrusive to an already constructed model because it does not imply changes to current structures. A new

Algorithm 1 Finding the moment of last finished action

Require: $assignment; duration$
1: $current\_max \leftarrow 0$;
2: $unchecked = assignment$;
3: **while** $unchecked \neq \emptyset$ **do**
4: $u, (fun, act, start) \leftarrow unchecked.Pick$
5: $req\_time \leftarrow duration.Find(fun)$
6: **if** $current\_max < start + req\_time$ **then**
7: $current\_max = start + req\_time$;
8: **end if**
9: **end while**
10: **return** $current\_max$;

stage may be treated as a new task starting where the previous one has ended, both in terms of bigraph representation of the initial state and the SaT configuration in the matrix $\mathbb{M}^0_K$. An example of vertical scaling of the task from this chapter can consist of requiring drones to return to the area *A*.

The last aspect of behavior designing that our framework covers is verifying non-functional requirements. While verification of functional requirements comes down to finding a certain bigraph in a TTS, verification of non-functional requirements is more complex. It is mainly because such verification depends on the insight how system changes internally while the task is executed. This implies that the verification can only be performed after a schedule of actions is available. For the task in this chapter, two non-functional requirements will be considered. The first one limits the time it can take to complete the task to 8 minutes. Whether this requirement is satisfied can be verified using the $Assignment$ relation and the $duration$ function, both components of a schedule of actions. Algorithm 1 shows how both structures can be utilized to verify the non-function requirement. It calculates the moment when each activity ends and chooses the latest one. This moment is later converted from abstract units to time in the real world. In this example, one unit of time is equal to 6 minutes. The execution of the task according to the schedule of activities in Figure 4 takes two units of time. It means that the last activity will be finished twelve minutes after the start of the task, which means that the walk $0 \xrightarrow{f_1} 1 \xrightarrow{f_4} 2$ does not produce a schedule satisfying this non-functional requirement. A fix might be to use a schedule based on another behavior policy and verify if it satisfies the requirement.

Another example of non-functional requirement regards staying within power source capacity during a mission. Let us assume that each drone is powered with a 4.5 Wh battery. We can use $role$ and a higher-order function that transforms this function to a value representing the maximum energy consumption by any task element during a mission. The mention higher-order function can be of the form:

$$f(role) = max \circ power(role)$$

where:

- $power$ is a higher-order function that assigns power consumption to each task element (represented by their unique identifiers). It is important to remember that not all elements participating in an activity use energy. For example areas between which drones are moving do not consumes energy during that process. So it is not only the label of an activity that indicates the power usage but also the role played by an element participating in it. A role is indicated by a vertex in the redex of a reaction rule representing an activity. A function calculating power usage for each task element is defined as a set of pairs (u, p), with u being a unique identifier of a task element and p being a power usage during a whole mission. This function is of the form:

$$\left\{ (u,p) \mid p = \sum_{((u,(f,a,t)),v) \in role} cons(a,v) \right\}$$

The $cons$ function calculates energy consumption in watt-hours given a type of an activity and a role in it:

$$cons(a,v) = \begin{cases} 20 \cdot 0.2 & \text{if } a = \text{r1} \wedge v = 2 \\ 50 \cdot 0.1 & \text{if } a = \text{r2} \wedge (v = 1 \vee v = 2) \\ 0 & \text{in other cases} \end{cases}$$

For example, a drone participating in *r1* activity for an hour uses 20Wh. After adjusting for a fact that a single transition between a pair of areas A and B takes 2 units of time (12 minutes = 0.2 hour), energy consumption of that single transition is equal to $20 \cdot 0.2 = 4$ Wh. A role of element participating in an activity is checked against set of vertices indicating drones. The vertex identifier of a drone in *r1* activity denoted with reaction rule from Table I is 2, hence the condition $v = 2$.
- $max : (\mathcal{U} \to \mathbb{N}) \to \mathbb{N}$ is a higher-order function that returns maximum value in codomain of the input function.

For the example covered in this section, function $power$ takes the following form:

$$power = \{(1,0), (2,4), (3,4), (4,0)\}$$

It says that task elements with unique identifiers 1 and 4 do not use any energy, while elements with identifiers 2 and 4 use 4Wh during the whole mission.

IV. Conclusions

Designing a behavior of robotic swarms is an iterative process, where subsequent iterations consider the designed behavior with a higher level of detail. This paper presents a framework that enables design of behavior for a UAV swarm members within a single iteration. It is highly automated and enables leaving the designing process to a specialized tool after providing initial task parameters and a swarm. It takes into account verification of both functional and non-functional requirements, as well as scaling an existing task vertically and horizontally.

Practical limitations of the described method come down to the computational capacity and complexity of the modeled system. The time needed for developing behavior for elements

of a system consisting of thousands of states and a few dozens of thousands of transitions is in the order of minutes. It has to be emphasized that even for such systems, dozens of gigabytes of available memory are required. The most significant limitation of the modeled tasks is the lack of active objects that can not be fully controlled, such as humans.

There are three directions for further developing the method described in this article. The first one is by developing a high-quality tool allowing for the convenient development of schedules of actions for system elements. The currently available software shall be regarded as a proof of concept. The second direction is to improve the efficiency of methods in the behavior designing process. As was already mentioned, a relatively small system can exceed the capabilities of a modern desktop computer. There are currently intense studies on algorithms for bigraphs matching problems, which may further accelerate sub-processes in the framework. The last direction to improve is to extend the method to allow active objects not fully controlled in the system or to enable a variable number of objects (both active and passive) during a mission.

REFERENCES

[1] P. Cybulski, Z. Zieliński, "Design and Verification of Multi-Agent Systems with the Use of Bigraphs", Applied Sciences, https://www.mdpi.com/2076-3417/11/18/8291, DOI:10.3390/app11188291

[2] P. Cybulski, Z. Zieliński, "UAV Swarms Behavior Modeling Using Tracking Bigraphical Reactive Systems", Sensors, https://www.mdpi.com/1424-8220/21/2/622, DOI:10.3390/s21020622

[3] R. Milner, 2009, "The Space and Motion of Communicating Agents", ISBN=978-0-521-73833-0, Cambridge University Press, DOI:10.1017/CBO9780511626661

[4] T. Sheridan, W. Verplank, "Human and Computer Control of Undersea Teleoperators", 1978.

[5] S. Benford, M. Calder, T. Rodden, M. Sevegnani, "On Lions, Impala, and Bigraphs: Modelling Interactions in Physical/Virtual Spaces", ACM Trans. Comput.-Hum. Interact., May 2016, DOI:10.1145/2882784

[6] J. Krivine, R. Milner, A. Troina, "Stochastic Bigraphs", Electronic Notes in Theoretical Computer Science, year = 2008, https://www.sciencedirect.com/science/article/pii/S1571066108004003, DOI:10.1016/j.entcs.2008.10.006

[7] O. H. Jensen, "Mobile Processes in Bigraphs", 2006, https://www.cl.cam.ac.uk/archive/rm135/Jensen-monograph.pdf.

[8] P. Stone, M. Veloso, Multiagent Systems: A Survey from a Machine Learning Perspective. Autonomous Robots 8, 345–383 (2000). DOI:10.1023/A:1008942012299

[9] H. Hamann. (2018). Swarm Robotics: A Formal Approach. DOI:10.1007/978-3-319-74528-2.

[10] Y. Mohan and S. G. Ponnambalam, "An extensive review of research in swarm robotics," 2009 World Congress on Nature & Biologically Inspired Computing (NaBIC), 2009, pp. 140-145, DOI:10.1109/NABIC.2009.5393617.

[11] Brambilla, Manuele & Ferrante, Eliseo & Birattari, Mauro & Dorigo, Marco. (2013). Swarm Robotics: A Review from the Swarm Engineering Perspective. Swarm Intelligence. 7. 1-41. DOI:10.1007/s11721-012-0075-2

[12] Navarro, Iñaki & Matía, Fernando. (2013). An Introduction to Swarm Robotics. ISRN Robotics. 2013. DOI:10.5402/2013/608164

[13] Iocchi, Luca & Nardi, Daniele & Salerno, Massimiliano & Hannebauer, Markus & Wendler, Jan & Pagello, Enrico. (2001). Reactivity and Deliberation: A Survey on Multi-Robot Systems. 2103. 9-32. DOI:10.1007/3-540-44568-4_2.

[14] Nedjah, Nadia & Silva Junior, Luneque. (2019). Review of methodologies and tasks in swarm robotics towards standardization. Swarm and Evolutionary Computation. 50. 100565. DOI:10.1016/j.swevo.2019.100565

[15] Bayindir, Levent. (2015). A Review of Swarm Robotics Tasks. Neurocomputing. 172. DOI:10.1016/j.neucom.2015.05.116

[16] Dudek, G., Jenkin, M.R., Parker, L.E., & Lin, L. (2003). A Taxonomy of Multirobot Systems.

[17] Crespi, V., Galstyan, A.G., & Lerman, K. (2008). Top-down vs bottom-up methodologies in multi-agent system design. Autonomous Robots, 24, 303-313.

[18] A. Kolling, P. Walker, N. Chakraborty, K. Sycara and M. Lewis, "Human Interaction With Robot Swarms: A Survey," in IEEE Transactions on Human-Machine Systems, vol. 46, no. 1, pp. 9-26, Feb. 2016, DOI:10.1109/THMS.2015.2480801

[19] Valentini, Gabriele. (2017). Achieving Consensus in Robot Swarms. DOI:10.1007/978-3-319-53609-5

[20] Francesca, Gianpiero & Brambilla, Manuele & Brutschy, Arne & Trianni, Vito & Birattari, Mauro. (2014). AutoMoDe: A novel approach to the automatic design of control software for robot swarms. Swarm Intell. 8. 1-24. DOI:10.1007/s11721-014-0092-4

[21] Brambilla, Manuele & Brutschy, Arne & Dorigo, Marco & Birattari, Mauro. (2014). Property-Driven Design for Robot Swarms. ACM Transactions on Autonomous and Adaptive Systems. 9. 1-28. DOI:10.1145/2700318

[22] E. Pereira, C. Potiron, C. M. Kirsch and R. Sengupta, "Modeling and controlling the structure of heterogeneous mobile robotic systems: A bigactor approach," 2013 IEEE International Systems Conference (SysCon), 2013, pp. 442-447, DOI:10.1109/SysCon.2013.6549920

[23] Bachrach, Jonathan & Mclurkin, James & Grue, Anthony. (2008). Protoswarm: A language for programming multi-robot systems using the amorphous medium abstraction. 2. 1175-1178.

[24] Pianini, D., Viroli, M., & Beal, J. (2015). Engineering multi-agent systems with aggregate computing.

[25] Byrski, Aleksander & Drezewski, Rafal & Siwik, Leszek & Kisiel-Dorohinicki, Marek. (2015). Evolutionary multi-agent systems. The Knowledge Engineering Review. 30. 171-186. DOI:10.1017/S0269888914000289

[26] Floreano, Dario & Mattiussi, Claudio. (2008). Bio-Inspired Artificial Intelligence: Theories, Methods, and Technologies. ISBN:978-0262062718

[27] Spears, William & Spears, Diana & Hamann, Jerry & Heil, Rodney. (2004). Distributed, Physics-Based Control of Swarms of Vehicles. Auton. Robots. 2. DOI:10.1023/B:AURO.0000033970.96785.f2

[28] Çelikkanat, Hande & Sahin, Erol. (2010). Steering self-organized robot flocks through externally guided individuals. Neural Computing and Applications. 19. 849-865. DOI:10.1007/s00521-010-0355-y

[29] J. Yu, S. M. LaValle and D. Liberzon, "Rendezvous Without Coordinates," in IEEE Transactions on Automatic Control, vol. 57, no. 2, pp. 421-434, Feb. 2012, DOI:10.1109/TAC.2011.2158172

[30] Bullo, F & Cortés, J & Martínez, S. (2009). Distributed Control of Robotics Networks. ISBN:9780691141954

[31] Souad, Marir and Faiza, Belala and Nabil, Hameurlain. Formal Modeling IoT Systems on the Basis of BiAgents and Maude, DOI:10.1109/ICAASE51408.2020.9380126

[32] Archibald, Blair and Shieh, Min-Zheng and Hu, Yu-Hsuan and Sevegnani, Michele and Lin, Yi-Bing, BigraphTalk: Verified Design of IoT Applications, DOI:10.1109/JIOT.2020.2964026

[33] Muffy Calder and Alexandros Koliousis and Michele Sevegnani and Joseph Sventek, Real-time verification of wireless home networks using bigraphs with sharing, DOI:10.1016/j.scico.2013.08.004

[34] Mansutti, Alessio and Miculan, Marino and Peressotti, Marco", editor="Magoutis, Kostas and Pietzuch, Peter, Multi-agent Systems Design and Prototyping with Bigraphical Reactive Systems, DOI:10.1007/978-3-662-43352-2_16

[35] DIB, Ahmed Taki Eddine and MAAMRI, Ramdane, Bigraphical Modelling and Design of Multi-Agent Systems, DOI:10.1145/3467707.3467762

[36] Pereira, Eloi and Potiron, Camille and Kirsch, Chirstoph M. and Sengupta, Raja, Modeling and controlling the structure of heterogeneous mobile robotic systems: A bigactor approach, DOI:10.1109/SysCon.2013.6549920

3rd International Forum on Cyber Security, Privacy and Trust

NOWADAYS, information security works as a backbone for protecting both user data and electronic transactions. Protecting communications and data infrastructures of an increasingly inter-connected world have become vital nowadays. Security has emerged as an important scientific discipline whose many multifaceted complexities deserve the attention and synergy of computer science, engineering, and information systems communities. Information security has some well-founded technical research directions which encompass access level (user authentication and authorization), protocol security, software security, and data cryptography. Moreover, some other emerging topics related to organizational security aspects have appeared beyond the long-standing research directions.

The International Forum of Cyber Security, Privacy, and Trust (NEMESIS'22) as a successor of International Conference on Cyber Security, Privacy, and Trust (INSERT'19) focuses on the diversity of the cyber information security developments and deployments in order to highlight the most recent challenges and report the most recent researches. The session is an umbrella for all cyber security technical aspects, user privacy techniques, and trust. In addition, it goes beyond the technicalities and covers some emerging topics like social and organizational security research directions. NEMESIS'22 serves as a forum of presentation of theoretical, applied research papers, case studies, implementation experiences as well as work-in-progress results in cyber security. NEMESIS'22 is intended to attract researchers and practitioners from academia and industry and provides an international discussion forum in order to share their experiences and their ideas concerning emerging aspects in information security met in different application domains. This opens doors for highlighting unknown research directions and tackling modern research challenges. The objectives of the NEMESIS'22 can be summarized as follows:

- To review and conclude research findings in cyber security and other security domains, focused on the protection of different kinds of assets and processes, and to identify approaches that may be useful in the application domains of information security.
- To find synergy between different approaches, allowing elaborating integrated security solutions, e.g. integrate different risk-based management systems.
- To exchange security-related knowledge and experience between experts to improve existing methods and tools and adopt them to new application areas

TOPICS

- Biometric technologies
- Cryptography and cryptanalysis
- Critical infrastructure protection
- Security of wireless sensor networks
- Hardware-oriented information security
- Organization- related information security
- Social engineering and human aspects in cyber security
- Individuals identification and privacy protection methods
- Pedagogical approaches for information security education
- Information security and business continuity management
- Tools supporting security management and development
- Decision support systems for information security
- Trust in emerging technologies and applications
- Digital right management and data protection
- Threats and countermeasures for cybercrimes
- Ethical challenges in user privacy and trust
- Cyber and physical security infrastructures
- Risk assessment and management
- Steganography and watermarking
- Digital forensics and crime science
- Security knowledge management
- Security of cyber-physical systems
- Privacy enhancing technologies
- Trust and reputation models
- Misuse and intrusion detection
- Data hide and watermarking
- Cloud and big data security
- Computer network security
- Assurance methods
- Security statistics

TECHNICAL SESSION CHAIRS

- **Awad, Ali Ismail,** Luleå University of Technology, Sweden
- **Bialas, Andrzej,** Research Network Lukasiewicz – Institute of Innovative Technologies EMAG, Poland

Communication Papers of the of the 17th Conference on Computer Science and Intelligence Systems pp. 183–189
DOI: 10.15439/2022F162
ISSN 2300-5963 ACSIS, Vol. 32

Information security management in German local government

Frank Moses, Kurt Sandkuhl
University of Rostock, Institute of Computer Science, Albert-Einstein-Str. 22, 18057 Rostock, Germany Email: {frank.moses, kurt.sandkuhl}@uni-rostock.de

Thomas Kemmerich
University of Bremen, TZI
Bibliothekstraße 1, 28359 Bremen, Germany Email: Thomas.kemmerich@uni-bremen.de

***Abstract*—The growing importance of information security in organizations is undisputed. This is particularly true of local governments, because modern administrative action is no longer conceivable today without electronic communication media and IT procedures. The complexity of information technology, the increasing degree of networking (also with citizens) and the dependence of the administration on IT-supported procedures has led to the fact that the security of information technology and associated processes must be given a higher priority and a corresponding cybersecurity strategy must be substantiated. Existing approaches either fall short or cannot be applied to the context of local government without revision and adaptation. In this article, case studies of implementations of IT security projects in local government are examined. Specific focus is on the differences between information security management system (ISMS) implementations of different hierarchical levels of governmental organizations. The results show current challenges in increasing the resilience of the local government.**

I. Introduction

INFORMATION security is a comparatively new topic in the domain of local government. The automated processing of data and information now plays a key role in the fulfilment of tasks in small and medium-sized enterprises (SMEs) and also in local governments [1, S. 429–431, 435], [2, S. 1]. All essential processes are significantly supported by information and communication technology (ICT) [3, S. 137f.]. Furthermore, legal requirements such as the General Data Protection Regulation (EU-GDPR), the Online Access Act (OZG) and the E-Government Act are driving forces of digitization in the domain. [4], [5], [6].

Increased reliance on modern ICT has significantly increased the risk of information infrastructures being adversely affected by deliberate attacks from inside and outside, negligent action, ignorance or technical failure, both qualitatively and quantitatively.[7, S. 86 u. 107], [8, S. 196]. Lack of information security can lead to disruptions in the performance of tasks, which can reduce the performance of authorities and, in extreme cases, bring their business processes to a standstill [9, S. 688]. Against this background, ensuring information security is one of the central tasks of local governments, within the framework of which an appropriate level of security in business processes and the associated (IT) infrastructures must be organized. [10, S. 650].
This need is underlined in particular by the recent successful cyber-attacks in various federal states, especially against authorities [11], [12]. Public authorities in particular are institutions of high importance for the state community. Impairments or failures may result in public service shortages, significant disruption of public security or other serious consequences [13]. In order to study the information security of local governments, a case study analysis was carried out. The aim of the work descripted here is to identify the state of information security of local governments and critical public infrastructures in order to contribute to the research field of information security in the domain of local government. Specific focus is on the differences between information security management system (ISMS) implementations of different hierarchical levels of governmental organizations.

II. Research Method

Work presented in this paper is part of a PhD project aiming at methodological and technological support for information security management that is tailored to the needs of small and medium-sized local government units. The PhD project follows the paradigm of design science research [14] and started with an analysis of (a) existing scientific work in the field of information security management (ISM) for local governments and (b) an analysis of typical problems in local government's ISM as visible in information security audit reports. The detailed results of both steps are available in [15]; the literature analysis is summarized in section III.

As the audit reports analyzed in (b) mainly reflected shortcomings of ISM implementations, we decided to also look for successful elements of ISM implementations by analyzing ISM cases. This paper focuses on these cases that – in a DSR context - contribute to the investigation of problem relevance and to requirements for the envisioned artifact. The research question for this work is: What are the differences (if any) between ISMS implementations of different kind and hierarchical levels of governmental organizations?

The introduction of information security management systems (ISM) usually represents an intervention in existing business processes and is influenced by various success fac-

tors. Case studies and retrospective analyses are research strategies [16] for qualitative data collection, which are very well suited to investigate the complex issues in the real environment [17]. Methods of qualitative data analysis help to understand process sequences and the dynamics of concrete situations under certain framework conditions and to derive results from them [18].

Thus, we analyzed various ISM cases. Although our cases show many characteristics of qualitative case studies as described by [16] (e.g., defined boundaries, defined research question, rich set of qualitative material, etc.), we prefer the term "ISM case", because most of the case material was not collected with the case study research method in mind but evaluated ex-post as case material. Here, eXperience methodology [19] supports the research work on the one hand in the uniform preparation of the ISM cases and on the other hand it can be ensured that the ISM cases are made comparable in order to derive concrete results from them.

III. Summary of Literature Analysis

In order to identify relevant literature on the status-of-research of ISM in local government sector, a structured literature search was carried out following [6]. The literature search was conducted in the databases EBSCO EconLit and WISO (Public Ser-vice, Business Administration), SSOAR (Administrative Sciences) and Scopus (various scientific disciplines) with a combination of the search terms: "cybersecurity, public sector, information security". In addition, references to relevant systematic works from the publication period 2013 to 2021 were reviewed.

The initial search resulted in more than 1,500 hits, which were in several steps reduced to 85 articles by examining the titles, keywords and abstract. It followed an assessment of their relevance using the content, quality and citation frequency. Finally, 26 papers were classified relevant and grouped into thematic areas. Table I shows these areas and the relevant papers.

TABLE I.
RELEVANT LITERATURE SORTED INTO THEMATIC AREAS

Thematic area	Literature
Validation of technical components	[20], [21]
Analysis of factors hindering the development of cybersecurity strategies in the public sector	[22]
Analysis of cyber attacks and preventive measures	[23], [24], [25], [26]
Development an establishment of ISMS	[27]
Awareness measures	[28], [29], [30], [31], [32], [33]
Lack of skilled workers in public sector and effects	[34], [35]
Physical Security and Security Assessment	[36], [37], [38], [39], [40]
Legal framework parameters in cybersecurity domain	[41], [42]
Maturity models	[43], [44]

Most papers deal with the safeguarding of the technical components or tackle the analysis of cyber-attacks and possible preventive measures. It is striking that a large number of papers put the staff in the focus and examine how their awareness for cybersecurity can be increased.

Also, a substantial number of papers address options for the protection of physical security and security assessments and discuss the lack of skilled workers in the public sector.

Furthermore, papers regarding the legal frame-work and digital sovereignty must be mentioned.

Since the introduction of EU-GDPR in 2018, information and cybersecurity have been used more and more synonymously and very often set in relation to data protection and data protection issues. In contrast, only one relevant article addresses the structure and establishment of ISM systems.

IV. ISM Cases

Although the topic of information security in local government has only recently been given more attention in Germany, corresponding concepts for the development and establishment of information security management systems already exist [45], [46]. With support of these concepts, a few local governments have already dealt with the topic of information security and set up a corresponding management system.

The municipalities examined in the focus of this research are mainly in the two federal states of Germany, namely Bavaria and Saarland. These organizations are motivated by funding programs of the respective state government to introduce and operate a corresponding security management system.

A. Case material

One of the authors supervises various institutions in setting up Information Security Management systems to increase the resiliency of the respective organization. The associated ISM cases were conducted in the years 2018 to 2022 and cover a wide range of state, city and local government and an SME as well as a critical infrastructure from four federal states.

Various municipal organizations throughout Germany were asked to participate in the ISM cases. In addition, further municipal case study participants from other federal states without a funding program and three medium-sized companies were sought as a comparison group who were willing to have the development of their information security management system scientifically accompanied. The cases consist of local governments (small to medium-sized), district council offices, city administrations, state companies, state administration and a company as well as a hospital network. For this contribution, 24 ISM cases were selected that exemplify the situation in German local government.

In all ISM cases, the documentation of ISMS, including organization structure and processes were available and analyzed. Furthermore, access to the stakeholders in the organization was possible to collect required information from other reports. This was used during ISM case analysis.

TABLE II.
ISM CASES ANALYZED IN THIS PAPER

No.	Governmental Organization	Federal State	Type of organization
1	Gemeinde ****dorf	BY	Local government
2	Gemeinde Ma******	SL	Local government
3	Gemeinde Post*****-****	BY	Local government
4	Landeshauptkasse Saarland	SL	State administration
5	Zentrales Travelmanagement Saarland	SL	State administration
6	Landratsamt Frei****	BY	District Office
7	Landratsamt Neu*****	BY	District Office
8	LEG-Service GmbH	SL	Enterprise
9	Markt ***bach	BY	Local government
10	Markt ******dorf	BY	Local government
11	Performa Nord GmbH	HB	Enterprise
12	SlyCon GmbH	SL	SME
13	Stadt Hi****	NW	Municipality
14	Stadt ***heim	BY	Municipality
15	Stadt Neuburg a.d. Donau	BY	Municipality
16	Stadt *******furt	BY	Municipality
17	Stadt S*****fen	BY	Municipality
18	Stadt St. *******	SL	Municipality
19	Stadt ****bach	SL	Municipality
20	Stadt *******hausen	BY	Municipality
21	Stadtwerke *******hausen	BY	Municipal Utilities (critical)
22	Stadt *****burg	BY	Municipality
23	VG Neumarkt i.d. Oberpfalz	BY	Local government
24	VG ****beuren	BY	Local government

B. Coding for Cross-Case Analysis

The cases listed in the previous section cover different hierarchical levels of local government and also different IT security areas. The aim of the case analysis was to identify patterns, similarities and differences in the cases, which allow conclusions to be drawn about generally valid relationships, proven process models and framework conditions relevant for success.

The case material was examined. In order to give the analysis more significance, the following criteria were coded in advance according to Mayring [48], followed by a content analysis of the case material so that corresponding core statements could be derived. The following describes the coding.

Management attention (Coding 1): Essential for the development of an information security management system is the assumption of the responsibility of the management level for the topic per se [45, S. 7], [49, S. 24–27]. Against this background, the analysis focused on the extent to which the respective management level was involved in the ISMS process.

TABLE III.
CODING SCHEME FOR THE QUALITATIVE CONTENT ANALYSIS OF THE ISM CASES

No.	Coding
1	Managementattention
2	Leadership
3	Organizational structure
4	Process organization
5	Employee awareness
6	PDCA-Cycle
7	Guidelines and other documentation tasks
8	Use of tools (ISMS-Tools, Controlling-Tools, usw.)
9	Implementation of measures (Increased IT security)
10	Risk management
11	CIP process (Assessment and measurement)

Leadership (Coding 2): The management initiative is the basic prerequisite for successfully setting up an ISMS in an organization. Nevertheless, the complex topic of ISMS requires concrete control and management tasks, which in the best case are taken over by the management itself or delegated accordingly and then performed.

Organizational structure (Coding 3): The planning and implementation of the security process includes the definition of organizational structures and the definition of roles and tasks [45, S. 28]. With this coding, all places in the ISM cases are marked, which provide information regarding the organizational structure in the context of security concept.

Process organization (Coding 4): Many tasks in organizations are organized as processes, with a specific process owner, a person in charge, and a description. The structure of a security management system includes in particular the recurring processing of maintenance, fault and change processes. The qualitative implementation of these processes form the foundation of an ISMS and are therefore marked with code 4.

Employee awareness (Coding 5): Especially the recent attacks on public infrastructures have shown that a gateway is formed by the employees of the organization itself. [7, S. 54] and these must be sensitized accordingly [50]. Against this background, it is interesting to find out which measures have been planned and implemented by the organizations with regard to employee awareness.

PDCA-Cycle (Cycle 6): A management system thrives on the recurring sequence of planning, implementation, review and initiation of corrective measures [45, S. 17]. In the analysis of the ISM cases, great emphasis was placed on coding No. 6. Essentially, it is a matter of determining whether only an ISMS is being set up in order to obtain a one-time certifi-

cate or whether the organization operates the ISMS sustainably.

Guidelines and Documentation task (Coding 7): The documentation task is indispensable [45, S. 21] and in an ISMS project ranges from the guideline for information security, through further planning and guideline documents to clear process descriptions and verification documents. It is precisely this documentation task that poses major challenges for small and medium-sized enterprises as well as for local governments. Policy documents belong to the PDCA cycle planning category, and without a good plan, the goal is often not achieved. Therefore, as part of the analysis of the ISM cases, exactly this component of an ISMS will be analyzed.

Use of tools (Coding 8): Within the framework of an ISMS project, there is a need for tool support for the ISMS as well as for other tasks within the framework of the security concept, e.g. monitoring of network activities with the help of special tools. Especially the use of tools is an important success factor in order to fulfill or monitor the multitude of different tasks. Against this background, statements regarding the use of tools are coded accordingly.

Implementation of measures (Coding 9): A holistic ISMS pursues the goal of implementing and planning both preventive measures and measures to remedy security incidents. When analyzing the ISM cases, it is to be examined which type of measures (organizational, personnel, infrastructural and technical security measures) have been planned and implemented and what contribution they make to increasing security.

Risk management (Coding 10): The operation of any process or IT infrastructure is associated with risks. The risk management process is thus one of the foundations of a security management system [51, S. 7]. Experience has shown that risk identification and treatment is particularly difficult for local governments. To identify how risk management is embedded in the security process, Coding 10 will play an important role in the analysis of the ISM cases.

Continuous improvement - CIP (Coding 11): In order to maintain information security, it must be subject to permanent improvement. Logically, this necessitates continuous measurement and, above all, evaluation. [46]. How and with which results the CIP process was implemented in the respective ISM cases is marked with the code 11 and later evaluated accordingly.

V. Case Analysis

A. Groups of Cases and their Difference

Based on the coding and analysis of the available case material, groups of governmental organizations were identified and differences in their ISM implementations recognized. These groups are summarized in the following.

Local Government cases – Adoption and Diffusion of an ISMS

The eight ISM cases from the domain of local government essentially address the challenges of setting up and establishing an information security management system in a small administrative organization (max. 25 employees). At the same time, these "small" local governments have to meet the increased demands on administrative processes due to increasing digitization. Furthermore, due to the tight tariff structure of the public service, organizations are often unable to engage employees with the appropriate qualifications, so that in addition to IT technology, both internal and cross-organizational challenges have been identified that must be solved for successful implementation. Furthermore, the documentation task is one of the biggest challenges in small local governments. In addition, there is a lack of suitable tools that support the development and establishment of the information security management system for this target group.

District Administration cases – Implementation of the Security Requirement

In the case of the two ISM cases from the domain of district administration, a different picture emerges. The necessary human and financial resources are available here. Nevertheless, additional tasks have to be performed within this domain, which are necessary as a service for the subordinate administrative levels. The ISM cases focused on the challenges that arise from the development of an information security management system in organizations. Essentially, in large administrative organizations, the management attention and the role definition and process descriptions, especially in the IT and security domain, are suboptimal. Due to hierarchical levels with in parts of a wide lead span, losses occur at the organizational interfaces (structure and process organization). Furthermore, the involvement of stakeholders and their training and sensitization as well as employees for the requirements of information security is a major challenge.

City Administration cases – Security in Organizational Processes

The eight city administrations have to cope with different challenges in terms of IT security compared to other municipal organizations. The processing of sensitive (often private) data requires a particularly secure handling of this data. Based on the introduced information security management system, the established strategy is supplemented by modern measures for data backup and process automation. Furthermore, the maturity level derived from the information security management system can be used to obtain data that can be used to support further management decisions. For example, it can be used to secure make-it or buy-it decisions that have the goal of outsourcing certain services, both for economic and security reasons. Furthermore, this strategy replaces heterogeneous risk landscape in favor of new uniform risk assessments. The use of suitable tools to support the ISMS process was essential in these ISM cases.

State Administration cases – Secure Business Processes for Financial and Travel Transactions

The ISM cases use the example of a "state accounting" and central travel management to describe the challenges there in the context of IT security. In addition to the administration of a large amount of private data within the scope of

the tasks of the travel management process, the business process " state accounting " in particular forms a core process of a state administration. In this process, all bookings of a state administration converge. Many interfaces (e.g. with banks, debtors and creditors) have to be secured both organizationally, contractually and technically. The information security management system, which has been established in the meantime, forms the foundation for further strategies to secure information security, especially in the area of payment transactions and travel management. This is based on advanced risk management, which provides a dashboard that aggregates and provides data from different sources. The C-Level-Management is now in a position to identify and treat aggregated risks that were previously not the focus of the implementation of measures as individual risks.

National Company case – IT Security at an Airport Operator

The main focus of the ISM case at an airport operator are the reactions of the ransomware attack that took place there in autumn 2020. This attack has given the impetus to implement planned measures more quickly.

At the same time, the attack and the associated ransom demand have increased the management attention accordingly. As a result, both human and financial resources were made available to build up the non-existent risk management and to promote the implementation of measures to increase IT security.

The forensic analysis revealed that a lack of employee sensitization and training and, partly, organizational failure were one of the main causes of the successful cyberattack. As a result, the following points can be mentioned in order to better defend against targeted attacks on a critical infrastructure in the future:

- Implementation of a sustainable organization-wide IT security concept,
- Streamline the threat detection process and
- Increase in the ability to deal with threats,
- Further establishment of an open cooperation of all those responsible and
- Use of suitable tools (e.g. monitoring PDCA cycle, risk and maturity model)

Clinic Network case – IT Security at a Hospital Network and Municipal Utilities

Another ISM case was carried out in a clinic network. German hospitals, as part of the public critical infrastructure, are motivated on the one hand by various successful cyberattacks against hospital infrastructures on the other hand by legal requirements to introduce an information security management system [47, S. 196]. The central topic of the ISM case in the hospital network and in the critical infrastructure of the municipal utilities examined is the use of suitable tools that accompany and optimize the introduction and implementation of a information security management system taking into account different standards (e.g. BSI Compendium 2022 and the B3S[1] of the German Hospital Association).

B. Application of Coding Scheme

Using the coding presented in section IV.b. all ISM cases were examined with respect to the maturity the individual case showed for the aspect represented by the coding. The maturity levels used were from level 1 (low maturity – only basic implementation) to level 5 (high maturity - managed and optimized status). All ISM cases focused on the introduction of an information security management system to increase the resiliency against cyber-attacks of the respective organization.

As part of the ISM cases, a prototypical process model developed by one of the authors was used [52, S. 61ff]. This process model attempts to eliminate the shortcomings that have been revealed in the analysis of the audit reports. In essence, a positive result was achieved for all facilities. Some of the above-mentioned organizations have already successfully passed an audit; others are still working towards it.

An analysis of the audit reports of the subjects from the ISM cases as well as the ISM cases themselves showed a significant improvement in the individual codes. Thus, a strong improvement in the maturity level of the information security management system and organizational resilience can be observed. The results can be found in Table IV.

TABLE IV.
DISTRIBUTION OF MATURITY LEVELS IN THE ISM CASES FOR THE DIFFERENT CODING[2]

	Distribution of encodings in %				
Coding	**1**	**2**	**3**	**4**	**5**
1	4,2	8,3	58,3	20,8	8,3
2	4,2	8,3	66,7	12,5	8,3
3	0,0	12,5	75,0	8,3	4,2
4	8,3	20,8	50,0	16,7	4,2
5	4,2	8,3	45,8	29,2	12,5
6	4,2	20,8	41,7	29,2	4,2
7	0,0	4,2	37,5	54,2	4,2
8	0,0	0,0	20,8	75,0	4,2
9	0,0	0,0	41,7	50,0	8,3
10	4,2	20,8	54,2	16,7	4,2
11	8,3	8,3	62,5	16,7	4,2

VI. SUMMARY AND DISCUSSION

24 ISM cases were carried out, which qualitatively examined projects to increase IT security, IT security concepts or individual IT security measures of different levels of German local governments from four federal states.

A prototypical procedure was used for the supported organizations, which enables the organizations to implement corresponding projects to ensure information security in a practicable way. At the same time, a basis was created for incorporating the findings made in the preliminary analysis into

[1]B3S – Branch-Specific Security Standard
[2]Values are rounded to one decimal place.

the process model. As a result, the respective organization is supported organizationally, technically as well as structurally.

In order to identify patterns in the ISM case series, a cross-case analysis in the form of a qualitative content analysis according to Mayring was carried out after the completion of the projects.

To secure the process model, this was also applied in a domain outside the local government. The results obtained confirm the findings from the primary research domain.

This article contributes to the understanding of the overall context of successful IT security projects for the implementation of IT security concepts in local government.

For the present work, the methodological limitations of case studies apply. Nevertheless, the generalizability of the results is possible, which the comparison group with 3 companies has shown. Further research will show whether qualitative and quantitative research based on this confirms the similarities and differences found.

One of the biggest limitations of our work is the focus on German local governments when it comes to the ISM cases used. The conclusions drawn from this material cannot be transferred to other countries but might help to identify the focus of attention for future analysis efforts in other federal governmental structures. However, this limitation does not apply for the analysis of the state-of-research, i.e., we see a clear need for more research on ISM in small and medium-sized governmental units.

REFERENCES

[1] A. Schönbohm, „Flexibilität und Unabhängigkeit - Rahmenbedingungen für eine gesellschaftliche Cyber-Sicherheit“, in Digitalisierung im Spannungs-feld von Politik, Wirtschaft, Wissenschaft und Recht, Bd. 1, C. Bär, T. Grä-d-ler, und R. Mayr, Hrsg. Berlin: Springer Gabler, 2018.

[2] S. Mierowski, Datenschutz nach DS-GVO und Informationssicherheit gewährleisten: eine kompakte Praxishilfe zur Maßnahmenauswahl: Prozess ZAWAS 4.0. Wiesbaden: Springer Vieweg, 2021.

[3] H. Gulden, „Digitalisierung und IT-Sicherheit“, in Digitalisierung im Spannungsfeld von Politik, Wirtschaft, Wissenschaft und Recht, Bd. 1, C. Bär, T. Grädler, und R. Mayr, Hrsg. Berlin: Springer Gabler, 2018.

[4] VERORDNUNG (EU) 2016/679 DES EUROPÄISCHEN PARLAMENTS UND DES RATES. 2016. Zugegriffen: 27. Oktober 2021. [Online]. Verfügbar unter: https://eur-lex.europa.eu/legal-content/DE/TXT/HTML/?uri=CELEX:02016R0679-20160504&from=DE

[5] OZG - Gesetz zur Verbesserung des Onlinezugangs zu Verwaltungsleistungen. Zugegriffen: 27. Oktober 2021. [Online]. Verfügbar unter: https://www.gesetze-im-internet.de/ozg/

[6] EGovG - Gesetz zur Förderung der elektronischen Verwaltung. Zugegriffen: 27. Oktober 2021. [Online]. Verfügbar unter: https://www.gesetze-im-internet.de/egovg/BJNR274910013.html

[7] D. C. Leeser, Digitalisierung in KMU kompakt: Compliance und IT-Security. Berlin [Heidelberg]: Springer Vieweg, 2020. doi: 10.1007/978-3-662-59738-5.

[8] N. Pohlmann, „Ohne IT-Sicherheit gelingt keine nachhaltige Digitalisierung“, in Digitalisierung im Spannungsfeld von Politik, Wirtschaft, Wissenschaft und Recht, Bd. 1, C. Bär, T. Grädler, und R. Mayr, Hrsg. Berlin: Springer Gabler, 2018.

[9] I. Henseler-Unger und A. Hillebrand, „Aktuelle Lage der IT-Sicherheit in KMU: Wie kann man die Umsetzungslücke schließen?“, Datenschutz Daten-sicherheit - DuD, Bd. 42, Nr. 11, S. 686–690, Nov. 2018, doi: 10.1007/s11623-018-1025-y.

[10] D. Kammerloher, „Cybersecurity: Ein sicheres Fundament für den digitalen Staat“, Datenschutz Datensicherheit - DuD, Bd. 45, Nr. 10, S. 649–653, Okt. 2021, doi: 10.1007/s11623-021-1508-0.

[11] Gernot Heller, „Immer mehr Cyberangriffe: IT-Sicherheitsbehörde BSI schlägt Alarm - Professionalität steigt: IT-Sicherheitsbehörde BSI schlägt Alarm - Professionalität steigt“, Passau. Neue Presse Vom 22102021, Okt. 2021, Zugegriffen: 28. Oktober 2021. [Online]. Verfügbar unter: https://www.wiso-net.de/document/PNP__2991743112

[12] T. Kuhn, „Warum deutsche Kommunen so anfällig für Cyberattacken sind: ‚Das kannst Du doch keinem erklären‘“, Wirtsch. Online 21102021, Okt. 2021, Zugegriffen: 28. Oktober 2021. [Online]. Verfügbar unter: https://www.wiso-net.de/document/WWON__WW27723492

[13] A. Schönbohm, Die Lage der IT-Sicherheit in Deutschland 2021. Bonn: BSI.

[14] A. R. Hevner, S. T. March, J. Park, und S. Ram, „Design Science in Information Systems Research“, MIS Q., Bd. 28, Nr. 1, S. 75–105, 2004, doi: 10.2307/25148625.

[15] F. Moses, K. Sandkuhl, und T. Kemmerich, „Empirical Study on the State of Practice of Information Securty Maturity Management in Local Government.“, in Human Centred Intelligent Systems 2022 - Proceeding of the 15th International Conference on Human Centred Intelligent Systems (KES-HCIS-22). Smart Innovation, Systems and Technologies., A. Zimmermann, Hrsg. Springer. Accepted for publication. To appear June 2022., 2022.

[16] R. K. Yin, „The Case Study Crisis: Some Answers“, Adm. Sci. Q., Bd. 26, Nr. 1, S. 58, März 1981, doi: 10.2307/2392599.

[17] K. M. Eisenhardt, „Building Theories from Case Study Research“, Acad. Manage. Rev., Bd. 14, Nr. 4, S. 532–550, Okt. 1989, doi: 10.5465/amr.1989.4308385.

[18] T. Wilde und T. Hess, „Methodenspektrum der Wirtschaftsinformatik: Über-blick und Portfoliobildung“.

[19] P. Schubert und K. Bhaskaran, „The eXperience Methodology for Writing IS Case Studies“, AMCIS 2007 Proc., S. 16, 2007.

[20] A. Weber u. a., „Sichere IT ohne Schwachstellen und Hintertüren“, TATuP - Z. Für Tech. Theor. Prax., Bd. 29, Nr. 1, S. 30–36, Apr. 2020, doi: 10.14512/tatup.29.1.30.

[21] K. Weber, M. Christen, und D. Herrmann, „Bedrohung, Verwundbarkeit, Werte und Schaden: Cyberattacken und Cybersicherheit als Thema der Technikfolgenabschätzung“, TATuP - Z. Für Tech. Theor. Prax., Bd. 29, Nr. 1, S. 11–15, Apr. 2020, doi: 10.14512/tatup.29.1.11.

[22] W. Aman und J. A. Shukaili, „A Classification of Essential Factors for the Development and Implementation of Cyber Security Strategy in Public Sec-tor Organizations“, Int. J. Adv. Comput. Sci. Appl., Bd. 12, Nr. 8, 2021, doi: 10.14569/IJACSA.2021.0120820.

[23] S. U. Ahmad, S. Kashyap, S. D. Shetty, und N. Sood, „Cybersecurity During COVID-19“, in Information and Communication Technology for Competitive Strategies (ICTCS 2020), Bd. 191, A. Joshi, M. Mahmud, R. G. Ragel, und N. V. Thakur, Hrsg. Singapore: Springer Singapore, 2022, S. 1045–1056. doi: 10.1007/978-981-16-0739-4_96.

[24] S. Alagarsamy, K. Selvaraj, V. Govindaraj, A. A. Kumar, S. HariShankar, und G. L. Narasimman, „Automated Data analytics approach for examining the background economy of Cybercrime“, in 2021 Third International Con-ference on Inventive Research in Computing Applications (ICIRCA), Coim-batore, India, Sep. 2021, S. 332–336. doi: 10.1109/ICIRCA51532.2021.9544845.

[25] J. P. Kesan und L. Zhang, „An Empirical Investigation of the Relationship between Local Government Budgets, IT Expenditures, and Cyber Losses“, IEEE Trans. Emerg. Top. Comput., Bd. 9, Nr. 2, S. 582–596, Apr. 2021, doi: 10.1109/TETC.2019.2915098.

[26] K. Bouzoubaa, Y. Taher, und B. Nsiri, „Predicting DOS-DDOS Attacks: Re-view and Evaluation Study of Feature Selection Methods based on Wrapper Process“, Int. J. Adv. Comput. Sci. Appl., Bd. 12, Nr. 5, 2021, doi: 10.14569/IJACSA.2021.0120517.

[27] N. Müller, „Es muss nicht kompliziert sein“, Tech. Sicherh., Bd. 10, Nr. 03, S. 16–18, 2020, doi: 10.37544/2191-0073-2020-03-16.

[28] S. S. Alhashim und M. M. H. Rahman, „Cybersecurity Threats in Line with Awareness in Saudi Arabia“, in 2021 International Conference on Infor-mation Technology (ICIT), Amman, Jordan, Juli 2021, S. 314–319. doi: 10.1109/ICIT52682.2021.9491711.

[29] A. Andreasson, H. Artman, J. Brynielsson, und U. Franke, „A Census of Swedish Public Sector Employee Communication on Cybersecurity during the COVID-19 Pandemic“, in 2021 International Conference on Cyber Situ-ational Awareness, Data Analytics and Assessment (CyberSA), Dublin, Ire-land, Juni 2021, S. 1–8. doi: 10.1109/CyberSA52016.2021.9478241.

[30] B. W. Wirtz und J. C. Weyerer, „Cyberterrorism and Cyber Attacks in the Public Sector: How Public Administration Copes with Digital Threats“, Int. J. Public Adm., Bd. 40, Nr. 13, S. 1085–1100, Nov. 2017, doi: 10.1080/01900692.2016.1242614.

[31] S.-K. Park, S.-H. Lee, T.-Y. Kim, H.-J. Jun, und T.-S. Kim, „A performance evaluation of information security training in public sector“, J. Comput. Vi-rol. Hacking Tech., Bd. 13, Nr. 4, S. 289–296, Nov. 2017, doi: 10.1007/s11416-017-0305-7.

[32] M. A. Alharbe, „Measuring the Influence of Methods to Raise the E-Awareness of Cybersecurity for Medina Region Employees“, in Advances on Smart and Soft Computing, Bd. 1188, F. Saeed, T. Al-Hadhrami, F. Mo-hammed, und E. Mohammed, Hrsg. Singapore: Springer Singapore, 2021, S. 403–410. doi: 10.1007/978-981-15-6048-4_35.

[33] L. Coppolino, S. D'Antonio, G. Mazzeo, L. Romano, und L. Sgaglione, „How to Protect Public Administration from Cybersecurity Threats: The COMPACT Project“, in 2018 32nd International Conference on Advanced Information Networking and Applications Workshops (WAINA), Krakow, Mai 2018, S. 573–578. doi: 10.1109/WAINA.2018.00147.

[34] J. Drmola, F. Kasl, P. Loutocký, M. Mareš, T. Pitner, und J. Vostoupal, „The Matter of Cybersecurity Expert Workforce Scarcity in the Czech Republic and Its Alleviation Through the Proposed Qualifications Framework“, in The 16th International Conference on Availability, Reliability and Security, Vi-enna Austria, Aug. 2021, S. 1–6. doi: 10.1145/3465481.3469186.

[35] M. Lehto, ECCWS 2020 19th European Conference on Cyber Warfare: Warfare and Security. 2020.

[36] M. Phelps, „The role of the private sector in counter-terrorism: a scoping re-view of the literature on emergency responses to terrorism“, Secur. J., Bd. 34, Nr. 4, S. 599–620, Dez. 2021, doi: 10.1057/s41284-020-00250-6.

[37] I. Choi, J. Lee, T. Kwon, K. Kim, Y. Choi, und J. Song, „An Easy-to-use Framework to Build and Operate AI-based Intrusion Detection for In-situ Monitoring“, in 2021 16th Asia Joint Conference on Information Security (AsiaJCIS), Seoul, Korea, Republic of, Aug. 2021, S. 1–8. doi: 10.1109/AsiaJCIS53848.2021.00011.

[38] R. Dreyling, E. Jackson, und I. Pappel, „Cyber Security Risk Analysis for a Virtual Assistant G2C Digital Service Using FAIR Model“, in 2021 Eighth International Conference on eDemocracy & eGovernment (ICEDEG), Quito, Ecuador, Juli 2021, S. 33–40. doi: 10.1109/ICEDEG52154.2021.9530938.

[39] C. Mironeanu, A. Archip, C.-M. Amarandei, und M. Craus, „Experimental Cyber Attack Detection Framework“, Electronics, Bd. 10, Nr. 14, S. 1682, Juli 2021, doi: 10.3390/electronics10141682.

[40] R. Savold, N. Dagher, P. Frazier, und D. McCallam, „Architecting Cyber Defense: A Survey of the Leading Cyber Reference Architectures and Frameworks“, in 2017 IEEE 4th International Conference on Cyber Security and Cloud Computing (CSCloud), New York, NY, USA, Juni 2017, S. 127–138. doi: 10.1109/CSCloud.2017.37.

[41] L. Maglaras, G. Drivas, N. Chouliaras, E. Boiten, C. Lambrinoudakis, und S. Ioannidis, „Cybersecurity in the Era of Digital Transformation: The case of Greece“, in 2020 International Conference on Internet of Things and Intelli-gent Applications (ITIA), Zhenjiang, China, Nov. 2020, S. 1–5. doi: 10.1109/ITIA50152.2020.9312297.

[42] A. Bendiek, M. Schallbruch, und Stiftung Wissenschaft Und Politik, „Eu-rope's third way in cyberspace: what part does the new EU Cybersecurity Act play?“, SWP Comment, 2019, doi: 10.18449/2019C52.

[43] A. A. Garba, M. M. Siraj, und S. H. Othman, „An Explanatory Review on Cybersecurity Capability Maturity Models“, Adv. Sci. Technol. Eng. Syst. J., Bd. 5, Nr. 4, S. 762–769, 2020, doi: 10.25046/aj050490.

[44] K. N. Zakaria, A. Zainal, S. H. Othman, und M. N. Kassim, „Feature Extrac-tion and Selection Method of Cyber-Attack and Threat Profiling in Cyberse-curity Audit“, in 2019 International Conference on Cybersecurity (ICoCSec), Negeri Sembilan, Malaysia, Sep. 2019, S. 1–6. doi: 10.1109/ICoCSec47621.2019.8970786.

[45] „BSI-Standard 200-1: Managementsysteme für Informationssicherheit (ISMS)“, Bundesamt für Sicherheit in der Informationstechnik. https://www.bsi.bund.de/SharedDocs/Downloads/DE/BSI/Grundschutz/BSI_Standards/standard_200_1.html?nn=128578 (zugegriffen 26. Februar 2022).

[46] DIN ISO/IEC 27001. DIN, 2018.

[47] R. Studier und epubli GmbH, Sozialgesetzbuch Fünftes Buch (SGB V) Ge-setzliche Krankenversicherung. 2021.

[48] P. Mayring, Qualitative Inhaltsanalyse: Grundlagen und Techniken, 12., Überarb. Aufl. Weinheim Basel: Beltz, 2015.

[49] U. Pfeiffer, „Eine starke Unternehmenskultur minimiert Cyberrisiken“, Digit. Welt, Bd. 6, Nr. 1, S. 24–27, 2022, doi: 10.1007/s42354-022-0429-x.

[50] T. Meuche, „Dilemmata und Wege zur Digitalisierung der öffentlichen Ver-waltung“, Gr. Interakt. Organ. Z. Für Angew. Organ. GIO, 2022, doi: 10.1007/s11612-021-00612-7.

[51] „BSI-Standard 200-3: Risikomanagement“, Bundesamt für Sicherheit in der Informationstechnik. https://www.bsi.bund.de/SharedDocs/Downloads/DE/BSI/Grundschutz/BSI_Standards/standard_200_3.html?nn=128620 (zugegriffen 26. Februar 2022).

[52] F. Moses und T. Rehbohm, „<kes> Die Zeitschrift für Informations-Sicherheit“, Nr. 1, 38. Jahrgang, 2022.

Communication Papers of the of the 17th Conference on Computer Science and Intelligence Systems pp. 191–197
DOI: 10.15439/2022F206
ISSN 2300-5963 ACSIS, Vol. 32

Performance Analysis and Application of Mobile Blockchain in Mobile Edge Computing Architecture

Thiago José, Admilson de Ribamar Lima Ribeiro and Edward David Moreno
Federal University of Sergipe (UFS)
DCOMP and PROCC at UFS
Jd. Rosa Elze, CEP 49100-000, São Cristovão, Sergipe, Brazil
Email: {thiago.melo, admilson, edward}@dcomp.ufs.br

***Abstract*—Blockchain is a system that allows the track process of the sending and receiving of some types of information over the internet. They are pieces of code generated online that carry information connected – like blocks of data that form a chain. As the technology blockchain continues to evolve, it has ever-increasing opportunities to help applications for mobile devices increasing the security aspects coming of the security characteristics of these networks. This is interesting for mobile security, as it has become increasingly important due to the growth in the use of mobile applications for financial transactions. In this paper, a blockchain benchmark study is carried out in mobile devices, illustrating its process with the help of architecture that allows the best blockchain performance on mobile devices using edge computing. With this benchmark, with regard to the performance achieved, it is possible to compare the difference between use of blockchain in a mobile edge computing architecture and without that architecture. So, we validate that adding edge computing to the mobile blockchain mining process increases its efficiency.**

I. Introduction

AS BLOCKCHAIN technology continues to evolve, it has increasing opportunities to help mobile applications with their secure network. In this sense, this is interesting for mobile security, as it has become increasingly important due to the growing use of mobile applications for financial transactions [1].

In light of this scenario, although blockchain has been widely adopted in many applications (e.g. finance, healthcare and logistics), its application in mobile services is still limited. This is due to the fact that blockchain users have to solve predefined proof-of-work puzzles to add new data (i.e. a block) to the blockchain. Solving the proof of work, however, consumes substantial resources in terms of CPU time and power, which is not suitable for mobile devices with limited resources [2].

Among the existing approaches to solve this reported performance problem, in the mobile blockchain, one that is currently used is edge computing. This is because, for a mobile user, it is unrealistic to continuously run such a computationally difficult program that it requires a large amount of energy and time. Due to the outstanding characteristics of edge computing such as low latency, mobility and wide geographic distribution; it is considered to transfer the mining tasks to Edge Servers [3].

In this sense, this paper brings results that confirm the efficiency of edge computing in improving the performance of mobile blockchain. These results come from a benchmark performed using mobile devices and edge computing technologies. With this in mind, the work is divided into 6 sections, including this introduction section. The next section is dedicated to concepts. It describes the main important concepts for a better understanding of this paper. In the third section, the works related to this area are placed, including the following topics that relate to each other: blockchain, mobile devices and edge computing. The fourth section describes the performance evaluation methodology used in the work, as well as architectures, devices and metrics. In the fifth section, the results of the performed benchmark are shown and analyzed. Some tests are done by varying metrics, devices, and edge computing technologies. Correlations of the results are also made for a better understanding of them. Finally, the sixth section is the conclusion that contains the achievements of the paper and ideas for future works.

II. Concepts

A. Information Security

According to Lyra [4], information security is characterized by the proper application of protection devices on an asset or a set of assets in order to preserve the value that it has for organizations. The application of these protections seeks to preserve confidentiality, integrity and availability, not only being restricted to systems or applications, but also information stored or transmitted in different media besides electronic or paper.

B. Blockchain

The technology known as blockchain was first revealed by Satoshi Nakamoto in his article “Bitcoin: A Peer to Peer ATM System”[1], which established the mathematical basis for the Bitcoin cryptocurrency. While this was a groundbreaking article, it was never actually submitted to a traditional peer-reviewed journal, and the true identity of the author is unknown. Blockchain technology is not only at the foundation of all cryptocurrencies, but has found wide application in the more traditional financial sector. It also opened the door to new applications such as smart contracts [5].

Federal University of Sergipe

[1]https://bitcoin.org/bitcoin.pdf

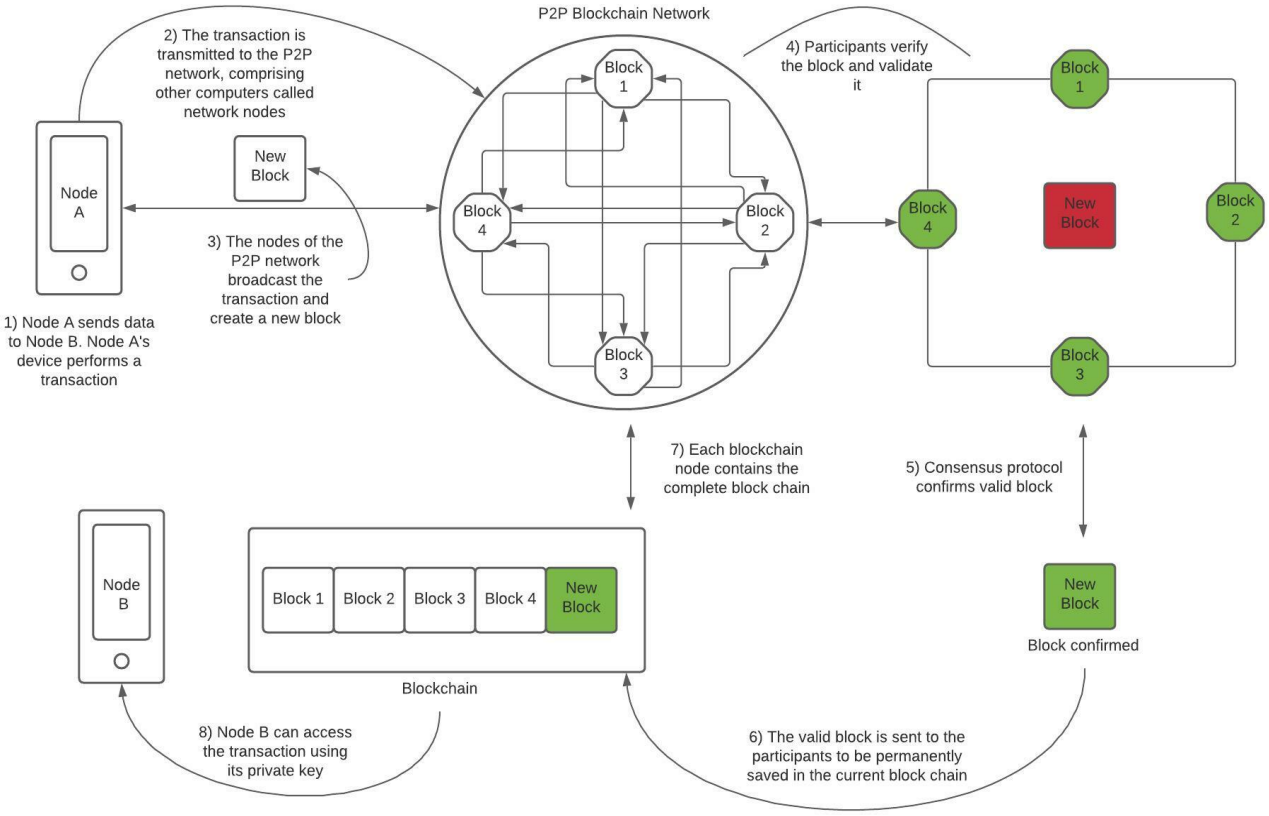

Fig. 1. Blockchain network with mobile nodes

C. Difficulty

The concept of difficulty is the measure that determines how difficult it is to mine a specific block for a given cryptocurrency. A high difficulty means that additional computing power will be needed to verify transactions entering the blockchain network. For a higher difficulty, higher is the security of the blockchain network, and more computing power will be required for breaking into the network [6].

In this sense, in this paper, the difficulty is adjusted every 2016 blocks. Blockchains adjust the difficulty automatically. For example, Bitcoin difficulty is adjusted every 2016 blocks or every 2 weeks. Ethereum's difficulty, on the other hand, is adjusted in every block, in approximately 15 seconds [7].

D. Proof of Work

The concept of "proof of work" (PoW) is defined as a consensus algorithm in which it is expensive and time consuming to produce a piece of data, but in the other hand, it is easy for others to verify that the data are correct. Bitcoin, the main cryptocurrency on the market, uses the Proof of Work Hashcash system [8].

In order for a block to be accepted by the network, miners need to complete a proof of work to verify all transactions on the block. The difficulty of this job is not always the same, it keeps adjusting so that new blocks can be generated in every 10 minutes. There is a very low probability of successful generation, so it is unpredictable which network employee will produce the next block [9].

E. Mobile Blockchain

Blockchain can be used to develop applications with mobile devices. However, to support the blockchain-based service, there is a set of miners continuously running a consensus protocol to confirm and secure data or distributed transactions in the background. Digital miners are required to solve a PoW puzzle. The mining process is conducted in a tournament structure, and miners chase each other for the solution. The figure 1 better illustrates how this process occurs on mobile devices.

F. Edge Computing

The Mobile Edge Computing (MEC) architecture was introduced to leverage the computing power available in mobile environments. On-premises data centers and servers are deployed by a service provider at the "edge" of mobile networks, such as base stations on radio access networks. MEC is the key technology to meet the stringent low latency requirements of fifth generation (5G) networks.

Mobile devices can access edge servers to enhance their computing power (e.g. processing IoT detection data). With this feature, edge computing becomes a promising solution for mobile blockchain applications whose benefits are as follows. First, by incorporating more miners, the robustness of the blockchain network is naturally improved. Second, mobile users have an incentive from the reward obtained in the consensus process.

However, edge computing services are deployed by the provider to maximize their benefits. As such, a question of price for edge services arises. Likewise, given the price adopted by the edge computing service provider, miners also need to optimize their demand for edge computing service to solve PoW and maximize their earnings [10].

III. Related Works

In [11], it is argued that it is a challenge to apply the blockchain technique to mobile applications, since mobile devices cannot afford the computing resources required by mining processes. However, edge computing architectures can help mobile blockchain applications. The figure 2 shows some possible architectures.

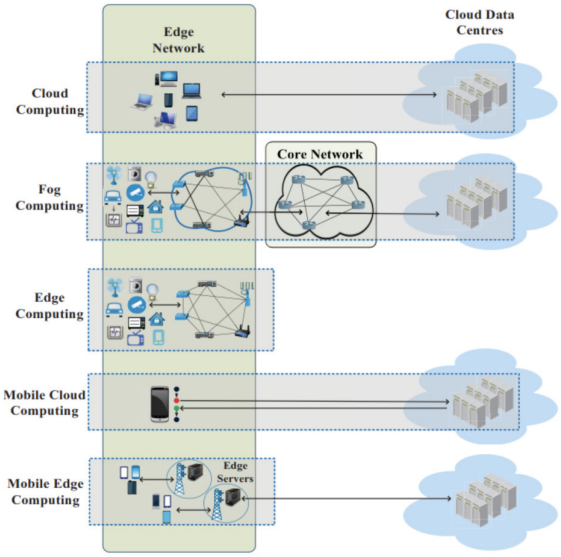

Fig. 2. Edge Computing Architectures - Source: [16]

This article proposes a mechanism based on a combinatorial double auction to offload the mining process from miners to edge servers. The mechanism is formulated as a resource allocation problem. Corresponding allocation algorithms and payment scheme are proposed to allocate resources and calculate trade prices, respectively. Furthermore, this article proves that the proposed mechanism is efficient in terms of calculation, and satisfies three properties of economic auction which are budget balance, individual rationality and veracity. Experimental results show that the proposed mechanism is capable of yielding higher total utility along with good scalability.

In [12], it is said that blockchain development in mobile apps is restricted as well. In this article, edge computing is considered as the network enabler for mobile blockchain. In particular, we study the management of edge computing resources based on optimal pricing to support mobile blockchain applications where the mining process can be offloaded to an edge computing service provider (ESP). In this way, a two-stage Stackelberg game is adopted to jointly maximize the ESP profit and the individual utilities of different miners.

In [13], blockchain is discussed as an effective security solution applied to many mobile devices. But due to storage limits and computational capabilities, it is difficult for mobile devices to run blockchain applications locally. To solve this challenge, blockchain applications are offloaded to edge servers with mobile edge computing (MEC). However, most of the existing auction mechanisms on the mobile blockchain are unable to utilize parallel execution and long-term performance has not been handled well.

Thus, this paper investigates the offloading problem of mobile blockchain computing task to improve the total utility of auction participants. An auction mechanism called POEM+ solving an NP-hard multiple-choice multidimensional knapsack problem is proposed.

In [14], it is discussed that in a mobile blockchain network, many mobile devices have insufficient computing power to perform computationally intensive tasks locally. To solve this problem, blockchain tasks can be transferred to edge servers with the help of an auction. However, most auction engines on the mobile blockchain ignore automatic parallel execution and long-term performance. This article aims to solve the problem of offloading computing on a mobile blockchain network.

This problem has been transformed into a multiple choice multidimensional knapsack problem that is NP-hard. To improve the total utility of auction participants, this paper proposes a smart contract-based dual auction mechanism called long-term auction for mobile blockchain (LAMB). Subtasks can be offloaded from a mobile device to heterogeneous edge servers. Furthermore, LAMB satisfies the economic properties of an auction engine.

The experimental results demonstrate that the utility to utilization ratio can be achieved by 130.55% higher and 138.64% higher, respectively, compared to the existing WBD auction algorithm. Furthermore, the proposed LAMB can guarantee long-term performance for offloading tasks and can achieve automatic execution in an autonomous and secure environment.

IV. Performance Evaluation Methodology

"In computing, benchmark is the act of running a computer program, a set of programs, or other operations in order to assess the relative performance of an object, typically by running a series of standard tests and trials on it. The term -benchmark - is also commonly used for the (benchmark) programs themselves developed to execute the process. Typically, benchmark is associated for evaluating the performance characteristics of a computer hardware, for example, the performance of a CPU's

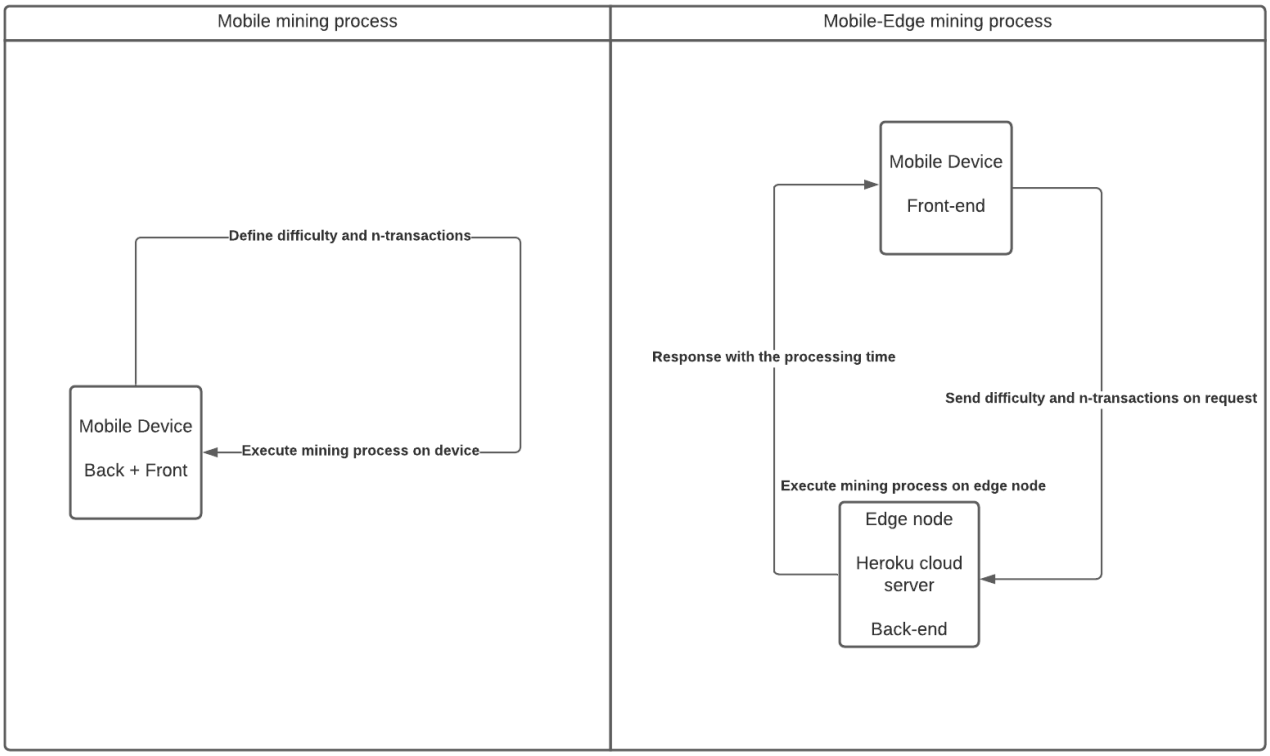

Fig. 3. Used architectures

floating point operation, but there are circumstances where the technique is also applicable to software." [15]

In this work, the circumstance is the performance evaluation of the mobile blockchain in two (2) different architectures and three (3) hardware with different specifications.

During the tests performed, 1 physical device, 1 Android device emulated through Android Studio and 1 IOS device simulated through XCode were used, both in an AVELL A62 MUV machine. In addition to these devices, the Back4App, Firebase and Heroku platforms were used, platforms as a service that provided the edge nodes in the edge computing architecture used in this work.

A. Architectures

For the present work, two architectures were considered. They are compared to see which one performs better.

On the left side of figure 3, we have the standard architecture of the mobile blockchain mining process on a mobile device. In this case,we used wallet back-end and front-end which are concentrated on the mobile device. In the application itself, the difficulty and number of transactions involved in the mining process are defined. After that, the mining process is done on the mobile device itself.

On the right side of figure 3, we have the mobile edge computing architecture. Only the front-end of the virtual wallet is kept in the application, while the back-end is on an edge node, and a server in the cloud.

B. Devices, softwares and technologies used

TABLE I
DEVICES AND SPECIFICATIONS

Device	CPU	RAM
Xiaomi Redmi 7 (Physical device)	Octa-core Max. 1.80GHx	3GB
Avell A62 MUV	Intel Core i7-9750H	64GB
Pixel 3A (Emulated)	Intel Core i7-9750H	4GB
Iphone 12 (Simulated)	Intel Core i7-9750H	4GB

*1) **Physical device - Xiaomi Redmi 7**:* the physical device used in the benchmark of this work was the Xiaomi Redmi 7. This device has a RAM of 3 GB and an Octa-core CPU with Max. 1.80GHx.

*2) **AVELL A62 MUV Machine**:* the Workstation used in this work was an Avell A62 MUV Machine. This machine was used to run the Android device program and emulator as well as the IoS device program and simulator. Both Android and IoS devices, as well as their programs, are discussed further on. This machine features an Intel® Core™ i7-9750H Coffee Lake Refresh CPU, with 12MB Cache (2.6 GHz up to 4.5 GHz with Intel® Turbo Boost) and a 64GB memory (2666MHz).

*3) **Android Studio**:* Android Studio is the development environment used to develop programs for devices using the Android operating system. In it, there is an aggregate of tools that help in this process. One of them is AVD Manager,

a program responsible for providing emulators for Android devices.

*4) **Android device Emulated in AVD Manager - Pixel 3A**:* an Android Pixel 3A device with an Intel® Core™ i7-9750H Coffee Lake Refresh CPU, 12MB Cache (2.6 GHz up to 4.5 GHz with Intel® Turbo Boost) and 4GB (2666 MHZ) of memory was emulated using the AVD Manager. allocated. The decision to use emulation was thought to be able to make use of different hardware specifications.

*5) **XCode**:* Xcode is an open source and integrated development environment from Apple Inc. for managing projects related to the macOS operating system. Xcode has tools for the user to create and improve their applications. Through XCode, it is possible to simulate some IOS devices, among them is the iPhone 12, used in this work.

*6) **Simulated IOS Device - iPhone 12 with IOS 14.4**:* using XCode, an IPhone 12 device with IOS 14.4, Intel® Core™ i7-9750H Coffee Lake Refresh CPU, 12MB Cache (2.6 GHz to 4.5 GHz with Intel® Turbo Boost) and allocated memory of 64GB (2666 MHZ) was simulated.

*7) **Heroku**:* Heroku is a PaaS (Platform as a Service) and is one of the pioneers of cloud service providers. Before it came on the scene, there was a huge challenge in building and configuring servers, not to mention the downside of shared hosting and the various complexities that come with hosting and deploying any strategies in the cloud. Heroku brought a system that made building, scaling and deploying apps so easy that it didn't take long for it to become a household name in the developer community.

*8) **Back4App**:* Back4app is a back-end platform for mobile apps. The company automates back-end development and allows companies to bring their applications to market faster and scale without infrastructure issues.

*9) **Firebase**:* by pairing the Cloud Functions service and Firebase Hosting, the users can build REST APIs as microservices. Cloud Functions for Firebase lets to developers automatically run back-end code in response to HTTPS requests. Thus, the code is stored in the Google cloud and runs in a managed environment.

C. Metrics

The metrics considered relevant to this benchmark were:

- **CPU and memory consumption of the physical device:** these measures should indicate the efficiency of the physical device used in this work in relation to its computational capacity;
- **Battery consumption:** this measurement is measured in the physical device used in this work;
- **Number of transactions:** this measure indicates the number of times that a new block of information was added to the blockchain network;
- **Difficulty:** difficulty is a measure of how difficult it is to extract a block of information or, in more technical terms, to find a hash value below a given target;
- **Time:** time is used to measure performance according to the variation of other metrics used in this work.

V. Results

In this section we present the results. We have used two scenarios. The figure 4 shows the mobile architecture without edge computing and figure 5 shows the scenario using mobile edge computing.

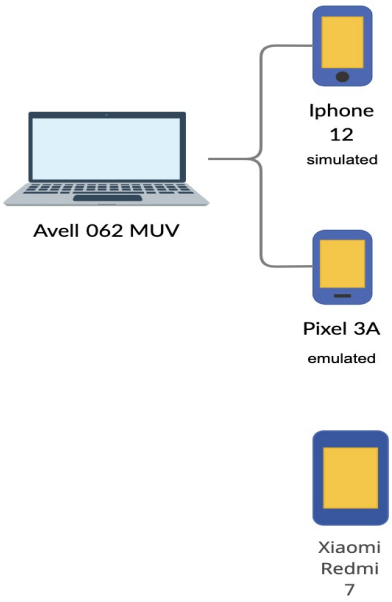

Fig. 4. Mobile architecture scenario without edge computing

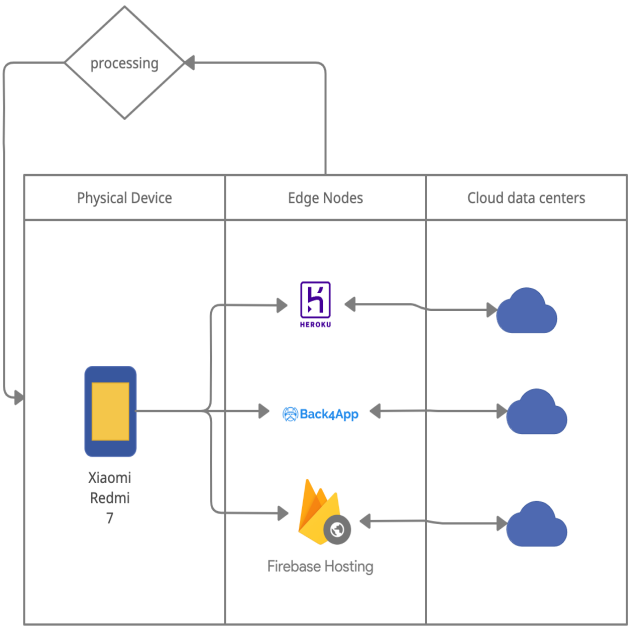

Fig. 5. Mobile edge computing architecture scenario

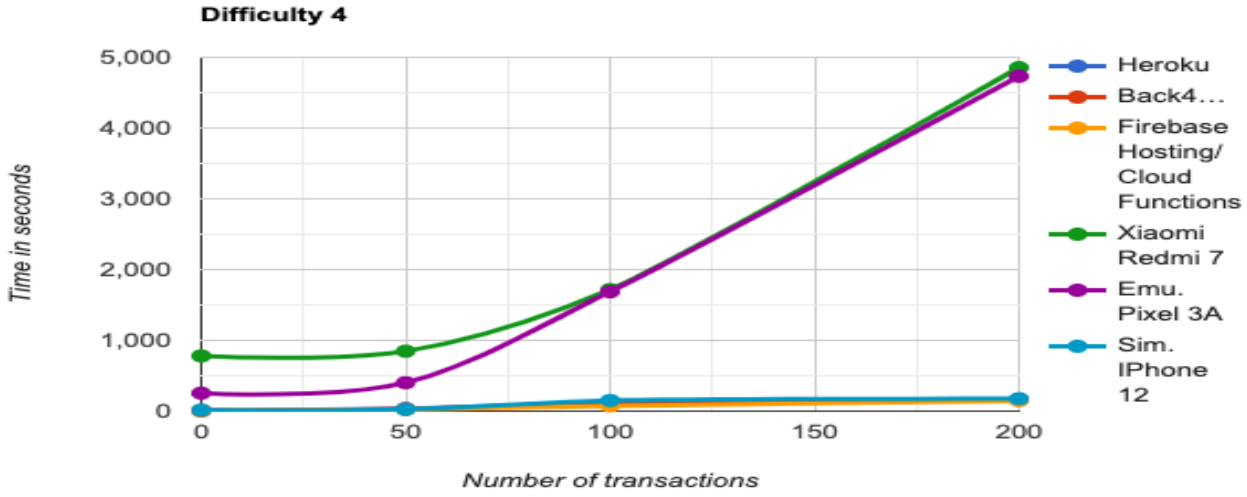

Fig. 6. Comparison between architectures - number of transactions per time in seconds with difficulty 4

A. Comparison of performance between the two architectures

1) Time and number of transactions: it is possible to compare the performance by placing the time reached by each device used without the aid of edge computing and the time achieved using Xiaomi Redmi 7 that used the mobile edge architecture for the difficulty 4, varying the number of transactions from 10 to 200. The figure 6 shows the difference that becomes evident when an edge node service is used versus not using it during blockchain network processing.

2) CPU consumption and memory consumption: it is also possible to compare the CPU and memory consumption of the physical device architecture when using these two scenarios: architecture without edge computing and when using edge computing. The figures 7 and 8 illustrate this, consecutively.

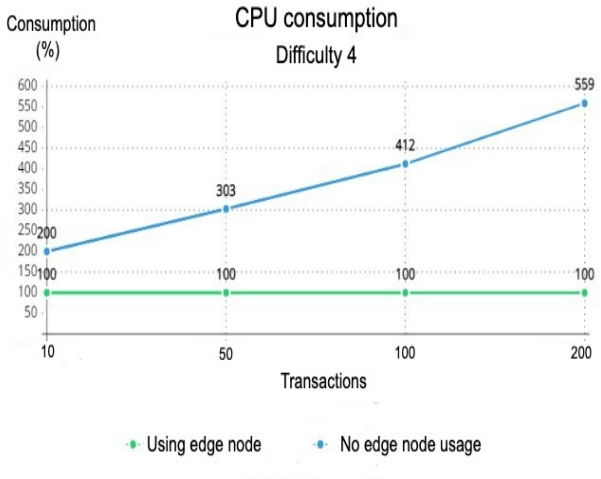

Fig. 7. Architectures comparison - CPU consumption with difficulty 4

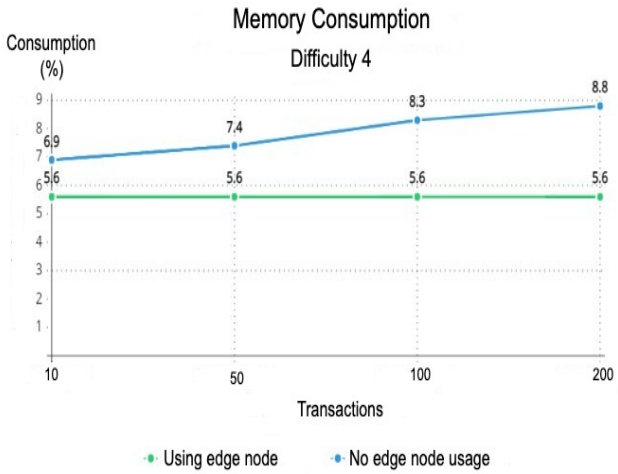

Fig. 8. Architectures comparison - Memory consumption with difficulty 4

3) Battery consumption: as far as battery consumption is concerned, this can be compared by isolating the most demanding case: difficulty 4 with 200 transactions. When using edge computing in the blockchain network mining process, the battery remains without level loss since it is not necessary to have the device always on and performing this processing on the physical device. This assignment, unlike the architecture that does not use the edge node, leaves the physical device (which becomes just a visual interface) and goes to the edge node. When there is no use of the edge node, the battery drops proportionally to the execution time, memory usage and CPU spent in the mining operation being performed on the physical device. The figure 9 demonstrates this behavior. With the passage of time, as expected, the battery level tends to decrease.

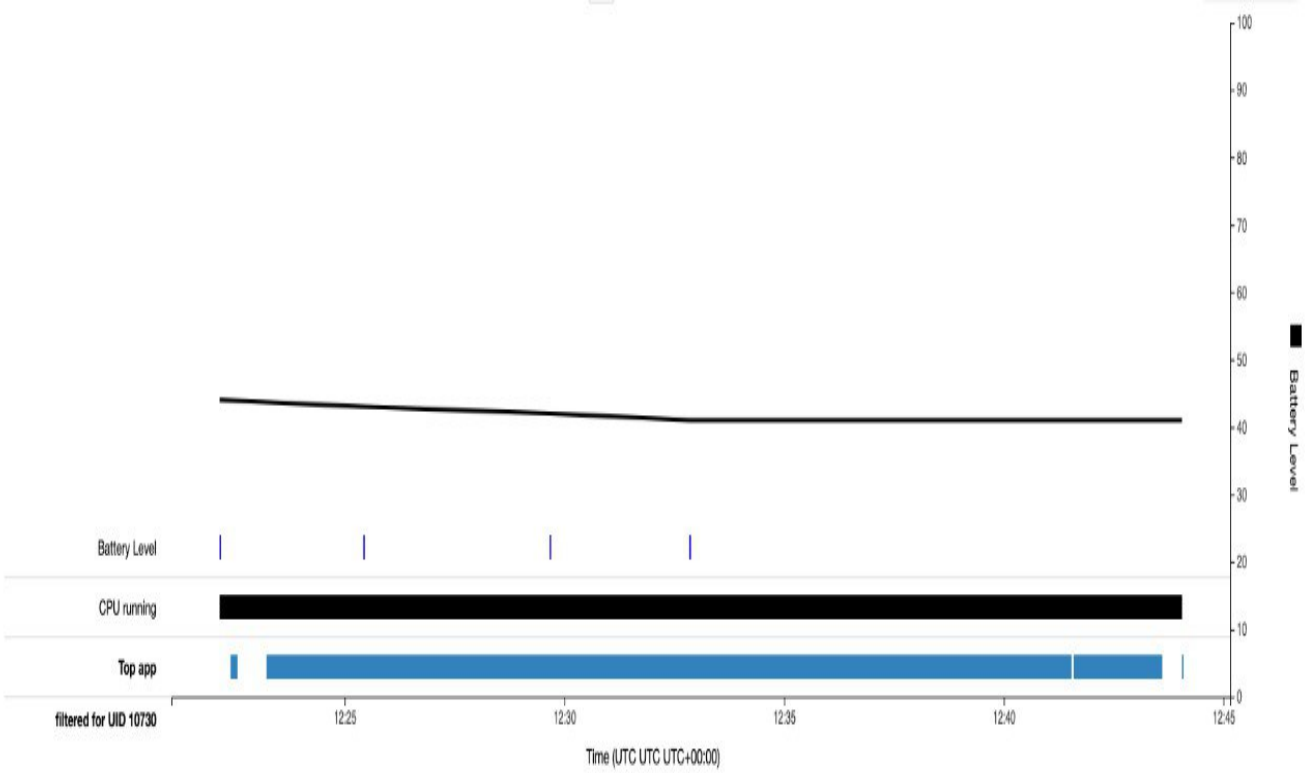

Fig. 9. Difficulty 4 - battery drain with 200 transactions without an edge node

VI. Conclusion

Finally, the conclusion drawn from this benchmark is the greater the difficulty of the blockchain network, more efficient the use of edge computing to assist in the mining process. This is more evident in our experiments since it is possible to notice the considerable difference in mining time when using the edge computing architecture compared to not using it. In this paper we showed the impact evaluating three metrics (time processing, memory and battery consumption). For future works, a prototype of the mobile blockchain application can be developed with the aim of to show how is the application of blockchain in a voting system using mobile devices.

References

[1] Aurélio, R., Oliveira, L. & Alves, M. A Tecnologia da Informação e o Uso do Mobile Banking. (In Portuguese) *Anais Do Congresso Nacional Universidade, EAD E Software Livre*. (2018)

[2] Xiong, Z., Zhang, Y., Niyato, D., Wang, P. & Han, Z. When mobile blockchain meets edge computing. *IEEE Communications Magazine*. (2018)

[3] Jiao, Y., Wang, P., Niyato, D. & Xiong, Z. Social welfare maximization auction in edge computing resource allocation for mobile blockchain. *2018 IEEE International Conference On Communications (ICC)*. pp. 1-6 (2018)

[4] Lyra, M. Governança da segurança da informação. *Brasília: Nd*. (2015)

[5] Di Pierro, M. What is the blockchain?. *Computing In Science & Engineering*. **19**, 92-95 (2017)

[6] Frankenfield, J. What Is Cryptocurrency Difficulty?. *Investopedia*. (2022,1), https://www.investopedia.com/terms/d/difficulty-cryptocurrencies.asp, [Online; accessed 15. Jan. 2022]

[7] Don Tapscott, A. Blockchain revolution. (Senai-SP Editora,2018)

[8] Loredo, J. Moedas virtuais e Bitcoin, a rede de pagamento inovadora. (Niterói,2016)

[9] Bastiani, A. O que é e como funciona o Proof of Work?. *CriptoFácil*. (2020,5), https://www.criptofacil.com/o-que-e-e-como-funciona-o-proof-of-work, [Online; accessed 15. Jan. 2022]

[10] Xiong, Z., Zhang, Y., Niyato, D., Wang, P. & Han, Z. When mobile blockchain meets edge computing. *IEEE Communications Magazine*. **56**, 33-39 (2018)

[11] Liu, X., Wu, J., Chen, L. & Xia, C. Efficient auction mechanism for edge computing resource allocation in mobile blockchain. *2019 IEEE 21st International Conference On High Performance Computing And Communications; IEEE 17th International Conference On Smart City; IEEE 5th International Conference On Data Science And Systems (HPCC/SmartCity/DSS)*. pp. 871-876 (2019)

[12] Xiong, Z., Feng, S., Niyato, D., Wang, P. & Han, Z. Optimal pricing-based edge computing resource management in mobile blockchain. *2018 IEEE International Conference On Communications (ICC)*. pp. 1-6 (2018)

[13] Li, Y., Wu, J. & Chen, L. POEM+: Pricing longer for mobile blockchain computation offloading with edge computing. *2019 IEEE 21st International Conference On High Performance Computing And Communications; IEEE 17th International Conference On Smart City; IEEE 5th International Conference On Data Science And Systems (HPCC/SmartCity/DSS)*. pp. 162-167 (2019)

[14] Liu, T., Wu, J., Chen, L., Wu, Y. & Li, Y. Smart Contract-Based Long-Term Auction for Mobile Blockchain Computation Offloading. *IEEE Access*. **8** pp. 36029-36042 (2020)

[15] Wikipédia Benchmark (computação) — Wikipédia, a enciclopédia livre. *Wikipédia*. (2022), https://pt.wikipedia.org/w/index.php?title=Benchmark_(computa\%C3\%A7\%C3\%A3o)&oldid=61821323), [Online; acessado em 17 de Janeiro de 2022]

[16] Mahmud, R., Kotagiri, R. & Buyya, R. Fog computing: A taxonomy, survey and future directions. *Internet Of Everything*. pp. 103-130 (2018)

Communication Papers of the of the 17th Conference on Computer Science and Intelligence Systems pp. 199–206
DOI: 10.15439/2022F54
ISSN 2300-5963 ACSIS, Vol. 32

On $D(n,q)$ quotients of large girth and hidden homomorphism based cryptographic protocols

Vasyl Ustymenko
Institute of Mathematics
Marie Curie-Sklodowska University
Pl. M. Curie-Skłodowskiej 5
Lublin, 20-031, Poland
Email: vasyl@hektor.umcs.lublin.pl

Michał Klisowski
Institute of Computer Science
Marie Curie-Sklodowska University
Pl. M. Curie-Skłodowskiej 5
Lublin, 20-031, Poland
Email: michal.klisowski@umcs.lublin.pl

***Abstract*—Noncommutative cryptography is based on applications of algebraic structures like noncommutative groups, semigroups, and noncommutative rings. Its intersection with Multivariate cryptography contains studies of cryptographic applications of subsemigroups and subgroups of affine Cremona semigroups defined over finite commutative rings. Efficiently computed homomorphisms between stable subsemigroups of affine Cremona semigroups can be used in tame homomorphisms protocols schemes and their inverse versions. The implementation scheme with the sequence of subgroups of affine Cremona group that defines the projective limit was already suggested. We present the implementation of another scheme that uses two projective limits which define two different infinite groups and the homomorphism between them. The security of the corresponding algorithm is based on complexity of the decomposition problem for an element of affine Cremona semigroup into a product of given generators. These algorithms may be used in postquantum technologies.**

***Index Terms*—Multivariate Cryptography, stable transformation groups and semigroups, decomposition problem of nonlinear multivariate map into given generators, tame homomorphisms, key exchange protocols, cryptosystems, algebraic graphs**

Support. This research is partially supported by British Academy Fellowship for Researchers at Risk 2022.

I. Introduction

LET k be a natural number ≥ 3. The problem of approximation of k-regular tree by the family of k-regular graphs of increasing order and increasing girth, i.e. minimal length of cycle in the graph, is very important. Solution of this broblem can be used in many applications, like computer implementations of branching process, construction of low density parity check codes, various application to Opimisation Graph Theory and Cryptography (see [30], [32] and further references). Families of k-regular graphs Γ_i of increasing order v_i of increasing girth satisfying to one of the following 3 properties are especially interesting:

1) to be a family of large girth, i.e. family such that $g_i \geq C \log_{k-1}(v_i)$ for certain constant C and each i,
2) to have a tree well defined projective limit of Γ_i when i tends to infinity,
3) to be a *family of small world graphs*, i.e. family such that diameter d_i of graphs Γ_i is at most $c \log_k(v_i)$.

The known families satisfying properties (1) and (2) were the families of q-regular graphs $D(n,q)$, $n = 1, 2, \ldots$ and q are prime powers and their connected components $CD(n,q)$.

In recent publication [33], [34], were announced that special homomorphic images quotients $A(n,q)$ of graphs $D(n,q)$ form a family satisfying (1), (2) and (3) for each value of parameter q.

Cryptographic applications of $A(n,q)$ were already known. In particular, in paper [30] postquantum secure protocols which uses standard homomorphisms between $D(n,q)$ and $D(m,q)$ $(n \geq m)$ (or $A(n,q)$ and $A(m,q)$) were used for the construction of protocols of Noncommutative Cryptography.

Current paper is dedicated to protocols of Postquantum Cryptography which use "hidden" remarkable homomorphisms between $D(n,q)$ and $A(n,q)$. In the generalisation of these protocols general finite commutative ring K can be used instead of finite field. We hope that the usage of remarkable graph homomorphism leads a strong postquantum secure protocol.

II. On ideas of Noncommutative Cryptography with platforms of transformations of Multivariate Cryptography

Post Quantum Cryptography serves for the research of asymmetrical cryptographic algorithms which can be potentially resistant against attacks with the usage of a quantum computer. The security of currently popular algorithms is based on the complexity of the following well known three hard problems: integer factorization, discrete logarithm problem, discrete logarithm for elliptic curves. Each of these problems can be solved in polynomial time by Peter Shor's algorithm for the theoretical quantum computer. In fact, some rather old cryptosystems which were suggested in the late '70s of the 20 century potentially may have some resistance to attacks on quantum computers (see for instance McEliece cryptosystem [18]).

Modern PQC is divided into several directions such as Multivariate Cryptography, Nonlinear Cryptography, Lattice-based Cryptography, Hash-based Cryptography, Code-based Cryptography, studies of isogenies for superelliptic curves, Noncommutative cryptography, and others.

The Multivariate Cryptography (see [4], [12], [6]) uses polynomial maps of affine space K^n defined over a finite commutative ring into itself as encryption tools. It exploits the complexity of finding a solution of a system of nonlinear equations from many variables. Multivariate cryptography uses as encryption tools nonlinear polynomial transformations of kind $x_1 \to f_1(x_1, x_2, \ldots, x_n), x_2, \to f_2(x_1, x_2, \ldots, x_n), \ldots, x_n \to f_n(x_1, x_2, \ldots, x_n))$, transforming affine space K^n, where $f_i : K[x_1, x_2, \ldots, x_n]$, $i = 1, 2, \ldots, n$ are multivariate polynomials usually given in a standard form, i.e. via a list of monomials in a chosen order.

Noncommutative cryptography appeared with attempts to apply the Combinatorial group theory to Information Security. If G is a noncommutative group then correspondents can use conjugations of elements involved in the protocol, some algorithms of this kind were suggested in [19], [22], [23], [7], where group G is given with the usage of generators and relations. The security of such algorithms is connected to Conjugacy Search Problem (CSP) and Power Conjugacy Search Problem (PCSP), which combine CSP and Discrete Logarithm Problem and their generalizations. Currently, Noncommutative cryptography is essentially wider than group-based cryptography. It is an active area of cryptology, where the cryptographic primitives and systems are based on algebraic structures like groups, semigroups, and noncommutative rings (see [20], [3], [5], [21], [1], [2], [11], [17], [13]). This direction of security research has very rapid development (see [16], [14] and further references in these publications).

One of the earliest applications of noncommutative algebraic structures for cryptographic purposes was the usage of braid groups to develop cryptographic protocols. Later several other noncommutative structures like Tompson groups and Grigorchuk groups have been identified as potential candidates for cryptographic post-quantum applications. The standard way of presentations of groups and semigroups is the usage of generators and relations (Combinatorial Group Theory). Semigroup based cryptography consists of general cryptographic schemes defined in terms of wide classes of semigroups and their implementations for chosen semigroup families (so-called platform semigroups).

The paper is devoted to some research on the intersection of Noncommutative and Multivariate Cryptographies. We try to use some abstract schemes in terms of Combinatorial Semigroup Theory for the implementation with platforms which are semigroups and groups of polynomial transformations of free modules K^n where K is a commutative ring.

The most popular form of Multivariate cryptosystem is the usage of a single very special map f in a public key mode. The first examples were based on families of quadratic bijective transformation fn(see [4], [12], [6]), such choice implies a rather fast encryption process. The paper is devoted to other aspects of Multivariate cryptography when some subsemigroup of affine Cremona semigroup of all polynomial transformations is used instead of a single transformation. Let us discuss a case of subsemigroup with a single generator. Everybody knows that Diffie-Hellman key exchange protocol can be formally considered in general case of any finite group or semigroup G. In the case of group G, the corresponding ElGamal cryptosystem can be introduced. Notice that the security of this algorithm depends not only on abstract group G but on the way of its generation in computer memory. For instance, if $G = Z_p^*$ is a multiplicative group of a large prime field then the discrete logarithm problem (DLP) is a difficult one and guarantees the security of the protocol. If the same abstract group is given as an additive group of Z_{p-1} protocol is insecure because DLP will be given by linear equation.

Notice that the implementation of the idea to use a multivariate generator in its standard form has to overcome essential difficulties. At first glance, the Diffie-Hellman protocol in affine Cremona semigroup looks like an unrealistic one because the composition of two maps of degree r and s taken in "general position" will be a transformation of degree rs. So in majority of cases $deg(F) = d$, $d > 1$ implies very fast growth of function $d(r) = deg(F^r)$. Of course in the case of the generator in common position, not only a degree but also a density (total number of monomial terms of the map in its standard forms) grows exponentially.

So we have to find special conditions on a subsemigroup of affine Cremona group which guarantees the polynomial complexity of procedure to compute the composition of several elements from subsemigroup. Such conditions can define a basis of Noncommutative Multivariate Cryptography. Hopefully, at least two conditions of this kind are already known [26] (see further references) and [28]. We consider them in the following section.

III. On stable subsemigroups of Affine Cremona Semigroup, Eulerian transformations and corresponding cryptographic scheme

Stability condition demands that the degree of each transformation of the subsemigroup of affine Cremona semigroup has to be bounded by independent constant d. We refer to such subsemigroup as a stable subsemigroup of degree d. Examples of known families of stable subgroups of degree $d = 3$ reader can find in [26] (see further references) or [30]. Applications of such families to Symmetric Cryptography could be found in [32]. Some examples of stable families of subgroups of degree 2 are given in [25].

The eulerian condition demands that all transformations of subsemigroup of affine Cremona subgroup are given in a standard form $(x_1, x_2, \ldots, x_n) \to (f_1(x_1, x_2, \ldots, x_n), f_2(x_1, x_2, \ldots, x_n), \ldots, f_n(x_1, x_2, \ldots, x_n))$ where each f_i has density 1. All transformations of this kind form General Eulerian Semigroup ${}^nGES(K)$ of transformations of kind $x_1 \to \mu_1 x_1^{a(1,1)} x_2^{a(1,2)} \ldots x_n^{a(1,n)}, x_2 \to \mu_2 x_1^{a(2,1)} x_2^{a(2,2)} \ldots x_n^{a(2,n)}, \ldots, x_n \to \mu_n x_1^{a(n,1)} x_2^{a(n,2)} \ldots x_n^{a(n,n)}$ where $a(i, j)$ are positive integers and $\mu_i \in K$.

First cryptosystems of Nonlinear Multivariate Cryptography in terms of ${}^nGES(K)$ are suggested in [28].

The *discrete logarithm problem* is the special simplest case of the *word decomposition problem* for semigroups. Let S' be a subsemigroup of S generated by elements $g_1, g_2, \ldots, g_t$. The *word problem* (WP) of finding the decomposition of $g \in S$ into a product of generators g_i is difficult, i.e. polynomial algorithms to solve it with Turing machine or Quantum Computer are unknown. The idea to apply this problem in Cryptography was considered in [39] where some general schemes to use WP for constructions of algorithms of Noncommutative Cryptography were suggested. Of course, the complexity of the problem depends heavily on the choice of S and the way of a presentation of the semigroup. In the cases of families of affine Cremona semigroups or $S =^n GES(K)$, the problem WP is computationally infeasible with a Turing machine and with Quantum Computer.

We are working on implementations of the following formal schemes of usage of the complexity of WP. Tame map means computable in polynomial time from parameter m.

a) TORIC TAHOMA CRYPTOSYSTEM: Let K be a commutative ring, subgroups ${}^nG$ of ${}^nGES(K)$ act naturally on $(K^*)^n$, ${}^mS(n,K)$ is a subsemigroup of ${}^mGES(K)$ such that there is a tame homomorphisn $\Delta = \Delta(m,n)$ of ${}^mS(n,K)$ onto ${}^nG$. We assume that $m = m(n)$ where $m > n$ and consider the following *toric tahoma cryptosystem*:

Alice takes $b_1, b_2, \ldots, b_s$, $s > 1$ from ${}^mS(n,K)$ and $a_1, a_2, \ldots$, as where $a_i = \Delta(b_i)^{-1}$. She takes $g \in^m EG(K)$ and $h \in^n EG(K)$ and forms pairs $(g_i, h_i) = (g^{-1}b_i g, h^{-1}a_i h)$, $i = 1, 2, \ldots, s$ and sends them to Bob.

He writes the word $w(z_1, z_2, \ldots, z_s)$ in the alphabet $z_1, z_2, \ldots, z_s$ together with the reverse word $w'(z_1, z_2, \ldots, z_s)$ formed by characters of w written in the reverse order. He computes element $b = w(g_1, g_2, \ldots, g_s)$ via specialization $z_i = g_i$ and $a = w'(h_1, h_2, \ldots, h_s)$ via specialization $z_i = h_i$. Bob keeps a for himself and sends b to Alice. She computes a^{-1} as $h^{-1}\Delta(gbg^{-1})h$.

Alice writes her message $(p_1, p_2, \ldots, p_n)$ and sends ciphertext $a^{-1}(p_1, p_2, \ldots, p_n)$ to Bob. He decrypts with his function a. Symmetrically Bob sends his ciphertext $a(p_1, p_2, \ldots, p_n)$ to Alice and she decrypts with a^{-1}.

The problems of constructions of large subgroups G of ${}^nGES(K)$, pairs (g, g^{-1}), $g \in G$, and tame Eulerian homomorphisms $\mu : G \to H$, i.e. computable in polynomial time $t(n)$ homomorphisms of subgroup G of ${}^nGES(K)$ onto $H <^m GES(K)$ are motivated by tasks of Nonlinear Cryptography.

The first platforms for this scheme and some other abstract schemes are suggested in [28].

b) AFFINE TAHOMA CRYPTOSYSTEM: If we change semigroup ${}^mGES(K)$ for affine Cremona semigroup $S(K^m)$ we obtain the following *Affine Tahoma Cryptosystem* on stable transformations.

Let K be a commutative ring, stable subgroups n^G of $S(K^n)$ act naturally on K^n and ${}^mS(n,K)$ be a subgroup of $S(K^m)$ such that there is a tame homomorphisn $\Delta = \Delta(m,n)$ of ${}^mS(n,K)$ onto ${}^nG$. We assume that $m = m(n)$ where $m > n$.

Alice takes $b_1, b_2, \ldots, b_s, s > 1$ from ${}^mS(n,K)$ and $a_1, a_2, \ldots, a_s$ where $a_i = \Delta(b_i)^{-1}$. She takes $g \in C(Q^m)$ and $h \in C(R^n)$ where R and Q are extensions of the commutative ring K and forms pairs $(g_i, h_i) = (g^{-1}b_i g, h^{-1}a_i h)$, $i = 1, 2, \ldots, s$ and sends them to Bob. We assume that $g = g'T$, $h = h'T'$ where semigroup $\langle g', {}^m S(n,K)\rangle$ generated by g' and elements of ${}^mS(n,K)$ and group $\langle h', G\rangle$ are stable semigroups of degree d and $T \in AGL_n(R)$, $T' \in AGL_m(Q)$.

As in the previous algorithm Bob writes the word $w(z_1, z_2, \ldots, z_s)$ in the alphabet $z_1, z_2, \ldots, z_s$ together with the reverse word $w'(z_1, z_2, \ldots, z_s)$ formed by characters of w written in the reverse order. He computes element $b = w(g_1, g_2, \ldots, g_s)$ via specialization $z_i = g_i$ and $a = w'(h_1, h_2, \ldots, h_s)$ via specialization $z_i = h_i$. Bob keeps a for himself and sends b to Alice. She computes a^{-1} as $h^{-1}\Delta(gbg^{-1})h$.

Alice writes her message $(p_1, p_2, \ldots, p_n)$ from R^n and sends ciphertext $a^{-1}(p_1, p_2, \ldots, p_n)$ to Bob. He decrypts with his function a. Symmetrically Bob sends his ciphertext $a(p_1, p_2, \ldots, p_n)$ to Alice and she decrypts with a^{-1} (see [27]). Let ${}^nTC(K, R, Q)$ stand for affine Tahoma cryptosystem as above.

In [25] quadratic stable subsemigroups with corresponding homomorphisms are suggested as platforms of this scheme. Some other schemes are also implemented there with these platforms. Some cubical platforms were suggested in [27].

Only one family of platforms was investigated via computer implementation. Paper [31] is devoted to implementations of Affine Tahoma scheme with platforms of cubical stable groups. They were defined via families of linguistic graphs that form projective limits and the standard homomorphisms between two members of these sequences. So we have pairs $(G_n, \Delta n)$ where $G_n < S(K^n)$, Δn is a homomorphism of G_n onto G_m, $m = m(n)$ such that projective limits $\lim(G_n)$, $n \to \infty$ and $\lim(\Delta(G_n))$, $n \to \infty$ coincide with the same infinite transformation group G.

This article is devoted to another computer experiment with the new platform which uses the same groups G_n but different tame homomorphisms η_n . In the new scheme $\lim(G_n)$, $n \to \infty$ equals to G, but $\lim(\eta_n(G_n))$, $n \to \infty$ coincides with the image of homomorphism of G with an infinite kernel.

We believe that the option to vary tame homomorphisms in the chosen sequence of semigroup makes the task of cryptanalytic much more difficult.

We use projective limits $D(K)$ and $A(K)$ of the well known graphs $D(n,K)$ (see [15], [35]) and $A(n,K)$ (see [31] and further references) defined over arbitrary finite commutative rings. Walks on the graphs $D(K)$ and $A(K)$ allow to define groups $GD(K)$ and $GA(K)$ of cubic transformations of infinite dimensional affine space over K. Group $GA(K)$ is a homomorphic image of $GD(K)$, both groups can be obtained as projective limits of sequences $GA_n(K)$ and $GD_n(K)$,$n = 1, 2, \ldots$ of finite cubical stable groups. We suggest key exchange protocols based on homomorphisms of $GD_j(K)$ onto $GA_i(K)$ for some i and j.

Computer simulations demonstrate an interesting effect of density stabilization of generated cubical maps. The time execution tables for algorithms of generation of maps and numbers of monomial terms are given. They demonstrate the feasibility of algorithms. The method of generation allows constructing for each bijective transformation of the free module over K its inverse map. Multivariate nature of collision maps allows using these algorithms for the safe exchange of multivariate transformations. Various *deformation rules* can be used for this purpose (see formal schemes of [27], [26], [25]).

IV. Some basic definitions

Let us consider basic algebraic objects of multivariate cryptography, which are important for the choice of appropriate pairs of maps f, f^{-1} in both cases of public key approach or idea of asymmetric algorithms with protected encryption rules. Let us consider the totality $SF_n(K)$ of all rules of kind: $x_1 \to f_1(x_1, x_2, \dots, x_n)$, $x2 \to f_2(x_1, x_2, \dots, x_n)$, $\dots$, $x_n \to f_n(x_1, x_2, \dots, x_n)$ acting on the affine space K^n, where f_i, $i = 1, 2, \dots, n$ are elements of $K[x_1, x_2, \dots, x_n]$ with natural operation of composition. We refer to this semigroup as semigroup of formal transformation $SF_n(K)$ of free module K^n. In fact it is a totality of all endomorphisms of ring $K[x_1, x_2, \dots, x_k]$ with the operation of their superposition. Each rule f from $SF_n(K)$ induces transformation $t(f)$ which sends tuple $(p_1, p_2, \dots, p_n)$ into $(f_1(p1, p2, \dots, p_n)$, $f_2(p_1, p_2, \dots, p_n)$, $\dots$,$f_n(p_1, p_2, \dots, p_n))$. Affine Cremona semigroup $S(K_n)$ is a totality of all transformations of kind $t(f)$. The canonical homomorphism $t \to t(f)$ maps infinite semigroup $SF_n(K)$ onto finite semigroup $S(K_n)$ in the case of finite commutative ring K.

We refer to pair (f, f') of elements $SF_n(K)$ such that ff' and $f'f$ are two copies of identical rule $x_i \to x_i$, $i = 1, 2, \dots, n$ as pair of invertible elements. If (f, f') is such a pair, then product $t(f)t(f')$ is an identity map. Let us consider the subgroup $CF_n(K)$ of all invertible elements of $SF_n(K)$ (group of formal maps). It means f is an element of $CF_n(K)$ if and only if there is f' such that ff' and $f'f$ are identity maps. It is clear that the image of a restriction of t on $CF_n(K)$ is affine Cremona group $C_n(K)$ of all transformations of K^n onto K^n for which there exists a polynomial inverse.

We say that a family of subsemigroups S_n of $SF_n(K)$ (or $S(K_n)$) is stable of degree d if maximal degree of elements from S_n is an independent constant d, $d > 1$. If K is a finite commutative ring then stable semigroup has to be a finite set.

Condition $d > 1$ is natural because of elements from the group $AGL_n(K)$ of all affine bijective transformations, i.e. elements of affine Cremona group of degree 1.

V. On linguistic graphs and related semigroups of affine transformations

Linguistic graph I of type $(1, 1, n-1)$ over commutative ring K is a bipartite graph with partition sets $P = K^n$ (set of points) anf $L = K^n$ (set of lines) such that point $\mathrm{p} = (p_1, p_2, \dots, p_n)$ is incident to line $\mathrm{l} = [l_1, l_2, \dots, l_n]$ if and only if $a_2p_2 + b_2l_2 = f_1(p_1, l_1)$, $a_3p_3 + b_3l_3 = f_2(p_1, p_2, l_1, l_2)$, $\dots$, $a_np_n + b_nl_n = f_{n-1}(p_1, p_2, \dots, p_{n-1}, l_1, l_2, \dots, l_{n-1})$ where a_i and b_i are elements of K^* and f_i are multivariate polynomials with coefficients from K. We define colours of points and lines as $\rho(\mathrm{p}) = p_1$ and $\rho(\mathrm{l}) = l_1$. In linguistic graph for each vertex there is a unique neighbour with chosen colour. Symplectic homomorphism of lingustic graph is the homomorphism induced by selecting coordinates p_i of points and l_i where i is an element of selected proper subset of $\{2, 3, \dots, n\}$. Elements of theory of linguistic graphs and their applications to graph based encryption reader can find in [29]. Some applications of linguistic graphs of type $(1, 1, n-1)$ are described in [24], [36], [38].

Let us concentrate on linguistic graphs of type $1, 1, m$. Let $N(a, v)$ be the operator of taking neighbour of the vertex v with colour $a \in K$. We refer to sequences $(f_1, f_2, \dots, f_s)$ with $f_1 \in K[x_1]$ of even length s as symbolic strings. On the totality S1,1 (K) of such sequences we consider the product $(f_1, f_2, \dots, f_s)(g_1, g_2, \dots, g_r) = (f_1, f_2, \dots, f_s, g_1(f_s(x_1)), g_2(f_s(x_1)), \dots, g_r(f_s(x_1)))$.

Proposition 1. *Elements of $S_{1,1}(K)$ with defined product form a semigroup.*

If Q is an extension of the ground commutative ring K then linguistic graph $I(Q)$ and can be defined via the same set of equations. Let us take $Q = K[x_1, x_2, \dots, x_n]$ and consider infinite linguistic graph $I' = I(K[x_1, x_2, \dots, x_n])$ with partition sets P' and L' isomorphic to variety $K[x_1, x_2, \dots, x_n]^n$. For each symbolic string $(f_1, f_2, \dots, f_s)$ from $S_{1,1}(K)$ and consider the symbolic computation $C(f_1, f_2, \dots, f_s)$ which is a walk in I' with starting point $X = (x_1, x_2, \dots, x_n)$ are generic elements of the commutative ring $K[x_1, x_2, \dots, x_n]$, other elements of the walk are $X_1 = N(f_1, X)$, $X_2 = N(f_2, X_1)$, $\dots$, $X_s = N(f_s, X_{s-1})$. Notice that operators $N(f_i, X_{i-1})$ are computed in the graph I'.

It is easy to see that $X_s = (f_s(x_1), g_2(x_1, x_2), \dots, g_n(x_1, x_2, \dots, x_n))$, where $g_i \in K[x_1, x_2, \dots, x_i]$. The rule $(x_1 \to f_s(x_1)$, $x_2 \to g_2(x_1, x_2), \dots, x_n \to g_n(x_1, x_2, \dots, x_n))$ defines the map from $S(K^n)$ into itself. We denote this map as $\Delta I(K)(f_1, f_2, \dots, f_s)$ and refer to it as a map of symbolic computation.

Proposition 2. *A map $\Delta I(K)$ from $S_{1,1}(K)$ into $s(K^n)$ sending symbolic string $(f_1, f_2, \dots, f_s)$ to $\Delta I(K)(f_1, f_2, \dots, f_s)$ is a homomorphism of $S_{1,1}(K)$ into $s(K^n)$.*

We refer to the image $PS(I(K))$ of homomorphism of proposition 2 as semigroup of symbolic point to point computations and refer to $\Delta I(K)$ as linguistic compression (lc) homomorphism. We define a semigroup $LS(I(K))$ of line-to-line computations via simple change of points for lines in I and I'.

Proposition 3. *A symplectic homomorphism δ of linguistic graphs ${}^1I(K)$ and ${}^2I(K)$ of type $(1, 1, n)$ induces canonical*

homomorphism of $PS({}^1I(K))$ onto $PS({}^2I(K))$.

Let us consider subsemigroup $\Sigma(K)$ of $S_{1,1}(K)$ generated by symbolic shifting strings of kind $(x_1+a_1, x_1+a_2, \dots, x_1+a_s)$, where a_i, $i = 1, 2, \dots, s$ are elements of K. We identify tuple $C = (x_1 + a_1, x_1 + a_2, \dots, x_1 + a_s)$ with its code $\langle a_1, a_2, \dots, a_s\rangle$.

Proposition 4. *For each linguistic graph $I(K)$ of type $(1, 1, n-1)$ the image $\Sigma(I(K))$ of $\Sigma(K)$ under the linguistic compression homomorphism onto $PS(I(K))$ is a subgroup of affine Cremona group.*

In fact for invertibility of $\delta(f_1, f_2, \dots, f_s) \in PS(I(K))$ the bijectivity of f_s is a sufficient and necessary condition. We refer to $\Sigma(I(K))$ as group of walks on points of linguistic graph $I(K)$.

Let $C = (x_1 + a_1, x_1 + a_2, \dots, x_1 + a_s)$ be a shifting symbolic string from the semigroup $\Sigma(K)$. We refer to $Rev(C) = (x_1 - a_s + a_{s-1}, x_1 - a_s + a_{s-2}, \dots, x_1 - a_s + a_1, x_1 - a_s)$ as revering string for x.

Lemma. *Let $\Delta = \Delta I(K)$ be linguistic compression map from $S_{1,1}(K)$ onto $PS(I(K))$ and $x \in \Sigma(K)$. Then inverse map for $\Delta(x)$ coincides with $\Delta(Rev(x))$.*

VI. Stable groups of cubical maps defined in terms of linguistic graphs and their homomorphisms

Let K be a commutative ring. We define $A(n, K)$ as bipartite graph with the point set $P = K^n$ and line set $L = K^n$ (two copies of a Cartesian power of K are used). We will use brackets and parenthesis to distinguish tuples from P and L. So $(p) = (p_1, p_2, \dots, p_n) \in P_n$ and $[l] = [l_1, l_2, \dots, l_n] \in L_n$. The incidence relation $I = A(n, K)$ (or corresponding bipartite graph I) is given by condition pIl if and only if the equations of the following kind hold

$$p_2-l_2 = l_1p_1, \quad p_3-l_3 = p_1l_2, \quad p_4-l_4 = l_1p_3, \quad p_5-l_3 = p_1l_4,$$
$$\dots \quad , p_n-l_n = p_1l_{n-1} \text{ for odd } n \text{ and } p_n-l_n = l_1p_{n-1} \text{ for even } n.$$

Let us consider the case of finite commutative ring K, $|K| = m$. As it instantly follows from the definition the order of our bipartite graph $A(n, K)$ is $2m^n$. The graph is m-regular. In fact the neighbour of given point p is given by above equations, where parameters $p_1, p_2, \dots, p_n$ are fixed elements of the ring and symbols $l_1, l_2, \dots, l_n$ are variables. It is easy to see that the value for l_1 could be freely chosen. This choice uniformly establishes values for $l_2, l_3, \dots, l_n$. So each point has precisely m neighbours. In a similar way, we observe the neighbourhood of the line, which also contains m neighbours. We introduce the colour $\rho(p)$ of the point p and the colour $\rho(l)$ of line l as parameter p_1 and l_1 respectively.

It means that graphs $A(n, K)$ with colouring ρ belong to the class of Γ linguistic graphs of type $(1, 1, n-1)$.

Let $GA(n, K) = \Sigma(A(n, K))$ stands for the group of walks on points of $A(n, K)$. We have a natural homomorphism $GA(n+1, K)$ onto $GA(n, K)$ induced by symplectic homomorphism Δ from $A(n+1, K)$ onto $A(n, K)$ sending point $(x_1, x_2, \dots, x_n, x_{n+1})$ to $(x_1, x_2, \dots, x_n)$ and line $[x_1, x_2, \dots, x_n, x_{n+1}]$ to $[x_1, x_2, \dots, x_n]$. It means that there is well defined projective limit $A(K)$ of graphs $A(n, K)$ and groups $GA(K)$ of groups $G(n, K)$ when n is growing to infinity. As it stated in [37] case of $K = F_q$, $q > 2$ infinite graph $A(F_q)$ is a tree. Some properties of infinite groups $GA(K)$ of transformation of infinite dimensional affine space over commutative ring K the reader can find in [31].

Other family $D(n, K)$ of linguistic graphs of type $(1, 1, n-1)$ defined over the commutative ring K were defined in [35] but its definition in the case of $K = F_q$ was known earlier. In fact graphs $D(n, q) = D(n, F_q)$ are widely known due to their applications in Extremal Graph Theory, in Theory of LDPC codes and Cryptography. Graphs $D(n, K)$ are bipartite with set of vertices $V = P \cup L, |P \cap L| = 0$. A subset of the vertices P is called the set of points and another subset L is called the set of lines. Let P and L be two copies of Cartesian power K^n, where $n \geq 2$ is an integer. Two types of brackets are used in order to distinguish points from lines. It has a set of vertices (collection of points and lines), which are n-dimensional vectors over K : $(p) = (p_1, p_2, p_3, p_4, \dots, p_i, p_{i+1}, p_{i+2}, p_{i+3}, \dots, p_n)$, $[l] = [l_1, l_2, l_3, l_4, \dots, l_i, l_{i+1}, l_{i+2}, l_{i+3}, \dots, l_n]$. The point (p) is incident with the line $[l]$, if the following relations between their coordinates hold: $l_2 - p_2 = l_1p_1$, $l_3 - p_3 = l_2p_1$, $l_4 - p_4 = l_1p_2$, $l_i - p_i = l_1p_{i-2}$, $l_{i+1} - p_{i+1} = l_{i-1}p_1$, $l_{i+2} - p_{i+2} = l_ip_1$, $l_{i+3} - p_{i+3} = l_1p_{i+1}$ where $i \geq 5$. Connected component of edge-transitive graph $D(n, q)$ is denoted by $CD(n, q)$ [15]. Notice that all connected components of the natural projective limit $D(q)$ of graphs $D(n, q)$, $n \to \infty$ are q-regular trees. Let $D(K)$ stands for the projective limit of graphs $D(n, K)$.

Let us denote as $GD(n, K)$ and $GD(K)$ the groups $\Sigma(D(n, K))$ and $\Sigma(D(K))$ of walks on points of graphs $D(n, K)$ and $D(K)$ respectively. For the description of certain symplectic quotients we will use the alternative description of graphs $D(K)$. It is based on the connections of these graphs with Kac-Moody Lie algebra with extended diagram A_1.The vertices of $D(K)$ are infinite dimensional tuples over K. We write them in the following way $(p) = (p_{0,1}, p_{1,1}, p_{1,2}, p_{2,1}, p_{2,2}, p'_{2,2}, p_{2,3}, \dots, p_{i,i}, p'_{i,i}, p_{i,i+1}, p_{i+1,i}, \dots)$, $[l] = [l_{1,0}, l_{1,1}, l_{1,2}, l_{2,1}, l_{2,2}, l'_{2,2}, l_{2,3}, \dots, l_{i,i}, l'_{i,i}, l_{i,i+1}, l_{i+1,i}, \dots]$. We assume that almost all components of points and lines are zeros. The condition of incidence of point (p) and line $[l]$ ($(p)I[l]$) can be written via the list of equations below.

$$l_{i,i} - p_{i,i} = l_{1,0}p_{i-1,i}, \quad l'_{i,i} - p'_{i,i} = l_{i,i-1}p_{0,1},$$
$$l_{i,i+1} - p_{i,i+1} = l_{i,i}p_{0,1}, \quad l_{i+1,i} - p_{i+1,i} = l_{1,0}p'_{i,i}.$$

This four relations are defined for $i \geq 1$, ($p'_{1,1} = p_{1,1}$, $l'_{1,1} = l_{1,1}$).

Similarly, we can define the projective limit $A(K)$ of graphs $A(n, K)$, $n > 1$.

We can describe the bipartite infinite graph $A(K)$ on the vertex set consisting on points and lines $(p) = (p_{0,1}, p_{1,1}, p_{1,2}, p_{2,1}, p_{2,2}, p_{2,3}, \dots, p_{i,i}, p_{i,i+1}, \dots)$.

$[l] = [l_{1,0}, l_{1,1}, l_{1,2}, l_{2,1}, l_{2,2}, l_{2,3}, \ldots, l_{i,i}, l_{i,i+1}, \ldots]$ such that point (p) is incident with the line $[l]$ ($(p)I[l]$, if the following relations between their coordinates hold: $l_{i,i} - p_{i,i} = l_{1,0}p_{i-1,i}$, $l_{i,i+1} - p_{i,i+1} = l_{i,i}p_{0,1}$.

It is clear that the set of indices $A = \{(1,0), (0,1), (1,1), (1,2), (2,2), (2,3), \ldots, (i-1,i), (i,i)\}$ is a subset in $D = \{(1,0), (0,1), (1,1), (1,2), (2,2), (2,2)', \ldots, (i-1,i), (i,i-1), (i,i), (i,i)', \ldots\}$. So graph $A(K)$ is a symplectic quotient of linguistic incidence structure $D(K)$. Let us use symbol Ψ for the corresponding symplectic homomorphism. For each positive integer $m \geq 2$ we consider subsets $M = A^m$ and $M = D^m$ containing of first $m-2$ elements of $A' = A - \{(1,0), (0,1)\}$ and $D' = D - \{(1,0), (0,1)\}$ with respect to the above orders and obtain symplectic quotients I_M of $D(K)$ and $A(K)$. One can check that corresponding quotients are isomorphic to graphs $D(m,K)$ and $A(m,K)$. The investigation of pair A^m, D^m leads to following statement [35].

Proposition 5. *For each $n \geq 4$ there are a symplectic homomorphisms of $D(2n,K)$ onto $A(m,k)$, $2 \geq m \geq n+1$ and $D(2n+1,K)$ onto $A(m,K)$, $2 \geq m \geq n+2$. Notice that $D(n,K) = A(n,K)$ for $n = 2,3$.*

Proposition 6. *Groups $GD(K)$ and $GA(K)$ are stable cubical transformations of infinite-dimensional affine space over a commutative ring K. Graph homomorphism of Proposition 5 induces group homomorphism Σ of $GD(n,K)$ onto $GA(n,K)$.*

Corollary. *$GD(n,K)$ and $GA(n,K)$ are stable cubical subgroups of Cremona group $C(K^n)$.*

A. Tahoma word cryptosystem

Alice selects commutative ring K and parameters n and m as in Proposition 5. She will prepare data for Affine Tahoma Cryptosystem presented in Section II in the simplest case of $K = Q = R$. She selects strings $C_i = \langle {}^i\alpha_1, {}^i\alpha_2, \ldots, {}^i\alpha_{t(1)} \rangle$, $i = 1,2,\ldots,r$ from $\Sigma(Q)$ and elements $B = \langle \beta_1, \beta_2, \ldots, \beta_s \rangle$ from $\Sigma(K)$ and $D = \langle \gamma_1, \gamma_2, \ldots, \gamma_k \rangle$ from $\Sigma(K)$. Alice computes $Rev(B)$ and $Rev(D)$. She takes affine transformations $T_1 \in AGL_n(K)$ and T_2 from $AGL_m(K)$.

Alice forms strings $B_i = Rev(B)C_iB$ and $D_i = Rev(D)Rev(C_i)D$, $i = 1,2,\ldots,r$ in $\Sigma(K)$ and $\Sigma(R)$. She computes images CB_i and CD_i of linguistic compression homomorphism $\Delta^{D(n,K)}$ and $\Delta^{A(m,K)}$ on elements B_i and D_i. Finally Alice computes elements $T_1^{-1}CB_iT_1 = G_i$ and $F_i = T_2^{-1}CD_iT_2$ which are elements of affine Cremona groups $C(K^n)$ and $C(R^m)$.

Alice keeps the pairs (G_i, F_i) and computes additionally for herself $H = T_1^{-1}\Delta^{D(n,K)}(Rev(B))$, $H^{-1} = \Delta^{D(n,K)}(B)T_1$ and $Z = T_2^{-1}\Delta^{DA(m,K)}(Rev(D))$, $Z^{-1} = \Delta^{A(m,K)}(D)T_2$. Alice sends pairs G_i and F_i to Bob and correspondents execute steps of the cryptosystem with this data.

The homomorphism $\delta : GD(n,Q) \to GA(m,Q)$ of the diagram is tame, i.e. its image can be computed in polynomial time in variable n. The triple $(GD(n,Q), A(m,Q), \delta)$ can be considered as a platform of Tahoma protocol introduced in [27], word tahoma stands for an abbreviation of tame homomorphism.

VII. Graphs $A(n,q)$ and $D(n,q)$, digital condenced matters physics effect

We can substitute graph $A(n,K)$ for other linguistic graph L of type $(1,1,n-1)$ defined over the commutative ring K and rewrite the content of section VI. We use graphs $A(n,K)$ and well known linguistic graph $D(n,K)$ of this type to implement all algorithm of previous section. Graphs $D(n,K)$ are bipartite with set of vertices $V = P \cup L$, $|P \cap L = 0|$. A subset of the vertices P is called the set of points and another subset L is called the set of lines. Let P and L be two copies of Cartesian power K^n, where $n \geq 2$ is an integer. Two types of brackets are used in order to distinguish points from lines. It has a set of vertices (collection of points and lines), which are n-dimensional vectors over K : $(p) = (p_1, p_2, p_3, p_4, \ldots, p_i, p_{i+1}, p_{i+2}, p_{i+3}, \ldots, p_n)$, $[l] = [l_1, l_2, l_3, l_4, \ldots, l_i, l_{i+1}, l_{i+2}, l_{i+3}, \ldots, l_n]$. The point (p) is incident with the line $[l]$, if the following relations between their coordinates hold: $l_2 - p_2 = l_1p_1$, $l_3 - p_3 = l_2p_1$, $l_4 - p_4 = l_1p_2$, $l_i - p_i = l_1p_{i-2}$, $l_{i+1} - p_{i+1} = l_{i-1}p_1$, $l_i + 2 - p_{i+2} = l_ip_1$, $l_{i+3} - p_{i+3} = l_1p_{i+1}$ where $i \geq 5$. Connected component of edge-transitive graph $D(n,q)$ is denoted by $CD(n,q)$ [15]. Notice that all connected components of the natural projective limit $D(q)$ of graphs $D(n,q)$, $n \to \infty$ infinite graph $D(q)$ are q-regular trees.

Let us denote as $G'(n,K)$ the group of elements of kind $g = \eta(C)$ of *irreducible computation* computation $C = (a_1, a_2, \ldots, a_t)$ in the case of graphs $D(n,K)$.

We present time of generation (in ms) of element g from $G(n,K)$ and $G'(n,K)$ in the cases of graphs $A(n,K)$ and $D(n,K)$ and number $M(g)$ of monomial terms for g.

We refer to parameter t as *length of word*. We can see the "condensed matters physics" digital effect. If t is "sufficiently large", then $M(g)$ is independent from t constant c. It means that the density of cubical collision map in all algorithm is simply c.

We have written a program for generating of elements and for encrypting text using the generated public key. The program is written in C++ and compiled with the gcc compiler. We used an average PC with processor Pentium 3.00 GHz, 2GB memory RAM and system Windows 7. We have implemented three cases:

1) T and T_1 are identities,
2) T and T_1 are maps of kind $x_1 \to x_1 + a_2x_2 + a_3x_3 + \ldots + a_tx_t, x_2 \to x_2, x_3 \to x_3, \ldots, x_t \to x_t, a_i \neq 0$, $i = 1,2,\ldots,t$ (linear time of computing for T and T_1), where $t = n$ and $t = m$, respectively,
3) $T = Ax+b$, $T_1 = A_1x+b_1$; matrices A, A_1 and vectors b, b_1 have mostly nonzero elements.

The tables I–II present the number of monomials depending on the number of variables (n) and the password length in the second and third case and the family of graphs $A(n,K)$,

where K is a finite field of characteristic 2. The tables III–IV present the time (in milliseconds) of the generation of public key monomials depending on the number of variables n and the length of the word in the second and third case and the family of graphs $A(n,K)$. In [8], [10], [9] the similar program for the case when K is Boolean ring was used for investigation of classical Diffie-Hellman protocol for cyclic group $\langle g\rangle$ and corresponding ElGamal cryptosystem. Currently, we expand this computer package on the case of commutative rings Z_m, where m is the power of 2.

TABLE I
NUMBER OF MONOMIAL TERMS OF THE CUBIC MAP INDUCED BY THE GRAPH $A(n,\mathbb{F}_{2^{32}})$, CASE II

	length of the word				
n	16	32	64	128	256
16	5623	5623	5623	5623	5623
32	53581	62252	62252	62252	62252
64	454375	680750	781087	781087	781087
128	3607741	6237144	9519921	10826616	10826616

TABLE II
NUMBER OF MONOMIAL TERMS OF THE CUBIC MAP INDUCED BY THE GRAPH $A(n,\mathbb{F}_{2^{32}})$, CASE III

	length of the word				
n	16	32	64	128	256
16	6544	6544	6544	6544	6544
32	50720	50720	50720	50720	50720
64	399424	399424	399424	399424	399424
128	3170432	3170432	3170432	3170432	3170432

TABLE III
PUBLIC MAP GENERATION TIME (MS), $A(n,\mathbb{F}_{2^{32}})$, CASE II

	length of the word				
n	16	32	64	128	256
16	20	60	128	260	540
32	308	788	1776	3760	7716
64	3193	8858	23231	53196	113148
128	54031	137201	368460	950849	2164037

TABLE IV
PUBLIC MAP GENERATION TIME (MS), $A(n,\mathbb{F}_{2^{32}})$, CASE III

	length of the word				
n	16	32	64	128	256
16	76	148	288	576	1148
32	1268	2420	4700	9268	18405
64	22144	40948	78551	153784	304240
128	460200	819498	1532277	2970743	5836938

CONCLUSION

We propose Post Quantum Cryptography information security solutions based on the complexity of the following problem Cremona Semigroup Word Decomposition (CSWD).

Thus we hope that introduced algorithms can be considered as serious candidates to be postquantum cryptographical tools. We believe that future studies of cryptanalytics confirm that CSWD problem remains unsolvable on ordinary Turing Machine and Quantum Computer under the condition of stability of platform S. Hope that the idea of an alternative disclosure of hidden homomorphism will attract the attention of cryptanalytics.

Complexity estimates for both correspondents demonstrate the possibility of the current usage of algorithms. Computer simulations demonstrate an interesting phase-transition effect that allows predicting the density of the collision maps of key exchange protocols and their inverse forms. This effect also demonstrates the feasibility of proposed cryptographic schemes. Direct and inverse protocols to elaborate collision multivariate transformation of free module K^n of predictable density can be used together with stream cipher working with data written in alphabet K or passwords written in this alphabet.

Correspondents can use collision maps to add them to part of a password or part of a plaintext or part of a ciphertext. There is an option to deform part of passwords, plaintext and ciphertext by outcomes of inverse protocols.

Reader can find various examples of protocol usage in [29]. Applications of graphs $A(n,K)$ to the development of stream ciphers reader can find in [40], [41].

REFERENCES

[1] M. Anshel, M. Anshel, and D. Goldfeld. An algebraic method for public-key cryptography. *Math. Res. Lett.*, 6:287–291, 1999.

[2] S. Blackburn and S. Galbraith. Cryptanalysis of two cryptosystems based on group actions. In K. Lam, C. Xing, and E. Okamoto, editors, *Advances in Cryptology – ASIACRYPT '99*, Lecture Notes in Computer Science, pages 52–61. Springer, 1999.

[3] Z. Cao. *New Directions of Modern Cryptography*. CRC Press, 2012.

[4] J. Ding, J. E. Gower, and D. S. Schmidt. *Multivariate Public Key Cryptosystems*. Advances in Information Security. Springer, 2006.

[5] B. Fine, M. Habeeb, D. Kahrobaei, and G. Rosenberger. Aspects of nonabelian group based cryptography: A survey and open problems. arXiv:1103.4093 [cs.CR], 2011. http://arxiv.org/.

[6] L. Goubin, J. Patarin, and B.-Y. Yang. Multivariate cryptography. In *Encyclopedia of Cryptography and Security*, pages 824–828. Springer US, Boston, MA, 2011.

[7] D. Kahrobaei and B. Khan. A non-commutative generalization of elgamal key exchange using polycyclic groups. In *IEEE GLOBECOM 2006 - 2006 Global Telecommunications Conference*, 12 2006.

[8] M. Klisowski. *Zwiększenie bezpieczeństwa kryptograficznych algorytmów wielu zmiennych bazujących na algebraicznej teorii grafów*. PhD thesis, Politechnika Częstochowska, 2015.

[9] M. Klisowski and V. Ustimenko. On the comparison of cryptographical properties of two different families of graphs with large cycle indicator. *Mathematics in Computer Science*, 6(2):181–198, 2012.

[10] M. Klisowski and V. Ustimenko. Graph based cubical multivariate maps and their cryptographical applications. In L. Beshaj, T. Shaska, and E. Zhupa, editors, *Advances on Superelliptic Curves and their Applications*, volume 41 of *NATO Science for Peace and Security Series - D: Information and Communication Security*, pages 305–327. IOS Press, 2015.

[11] K. H. Ko, S. J. Lee, J. H. Cheon, J. W. Han, J.-S. Kang, and C. Park. New public-key cryptosystem using braid groups. In M. Bellare, editor, *Advances in Cryptology — CRYPTO 2000*, pages 166–183, Berlin, Heidelberg, 2000. Springer Berlin Heidelberg.

[12] N. Koblitz. *Algebraic Aspects of Cryptography*. Springer-Verlag, Berlin, Heidelberg, 1998.

[13] P. H. Kropholler, S. J. Pride, W. A. M. Othman, K. B. Wong, and P. C. Wong. Properties of certain semigroups and their potential as platforms for cryptosystems. *Semigroup Forum*, 81(1):172–186, 2010.

[14] G. Kumar and H. Saini. Novel noncommutative cryptography scheme using extra special group. *Security and Communication Networks*, 2017:1–21, 01 2017.

[15] F. Lazebnik, V. A. Ustimenko, and A. J. Woldar. A new series of dense graphs of high girth. *Bull. Amer. Math. Soc.*, 32:73–79, 1995.

[16] J. A. Lopez-Ramos, J. Rosenthal, D. Schipani, and R. Schnyder. Group key management based on semigroup actions. *J. Algebra Appl.*, 16(8), 2017.

[17] G. Maze, C. Monico, and J. Rosenthal. Public key cryptography based on semigroup actions. *Adv. Math. Commun.*, 1(4):489–507, 2007.

[18] R. J. McEliece. A public-key cryptosystem based on algebraic coding theory. *DSN Progress Report*, 44:114–116, Jan 1978.

[19] D. N. Moldovyan and N. A. Moldovyan. A new hard problem over non-commutative finite groups for cryptographic protocols. In I. Kotenko and V. Skormin, editors, *Computer Network Security*, pages 183–194, Berlin, Heidelberg, 2010. Springer Berlin Heidelberg.

[20] A. Myasnikov, V. Shpilrain, and A. Ushakov. *Group-based Cryptography*. Advanced Courses in Mathematics — CRM Barcelona. Springer Basel AG, 2008.

[21] A. Myasnikov, V. Shpilrain, and A. Ushakov. *Non-commutative Cryptography and Complexity of Group-theoretic Problems*. Mathematical surveys and monographs. American Mathematical Society, 2011.

[22] E. Sakalauskas, P. Tvarijonas, and A. Raulynaitis. Key agreement protocol (kap) using conjugacy and discrete logarithm problems in group representation level. *Informatica, Lith. Acad. Sci.*, 18:115–124, 01 2007.

[23] V. Shpilrain and A. Ushakov. The conjugacy search problem in public key cryptography: Unnecessary and insufficient. *Applicable Algebra in Engineering, Communication and Computing*, 17(3):285–289, 2006.

[24] V. Ustimenko. On linguistic dynamical systems, families of graphs of large girth, and cryptography. *J. Math. Sci.*, 140(3):461–471, 2007.

[25] V. Ustimenko. On desynchronised multivariate el gamal algorithm. Cryptology ePrint Archive, Report 2017/712, 2017. https://eprint.iacr.org/2017/712.

[26] V. Ustimenko. On the families of stable multivariate transformations of large order and their cryptographical applications. *Tatra Mt. Math Publ.*, 70:107–117, 2017.

[27] V. Ustimenko. On new symbolic key exchange protocols and cryptosystems based on a hidden tame homomorphism. *Reports of the National Academy of Sciences of Ukraine*, (10):26–36, 2018.

[28] V. Ustimenko. On semigroups of multiplicative cremona transformations and new solutions of post quantum cryptography. Cryptology ePrint Archive, Report 2019/133, 2019. https://eprint.iacr.org/2019/133.

[29] V. Ustimenko and M. Klisowski. On noncommutative cryptography and homomorphism of stable cubical multivariate transformation groups of infinite dimensional affine spaces. Cryptology ePrint Archive, Report 2019/593, 2019. https://eprint.iacr.org/2019/593.

[30] V. Ustimenko and M. Klisowski. On noncommutative cryptography with cubical multivariate maps of predictable density. In K. Arai, R. Bhatia, and S. Kapoor, editors, *Intelligent Computing: Proceedings of the 2019 Computing Conference, Volume 2*, number 998 in Advances in Intelligent Systems and Computing, pages 654–674. Springer, 2019.

[31] V. Ustimenko and U. Romańczuk. On extremal graph theory, explicit algebraic constructions of extremal graphs and corresponding turing encryption machines. In *Artificial Intelligence, Evolutionary Computing and Metaheuristics*, pages 257–285. Springer, 2013.

[32] V. Ustimenko, U. Romańczuk-Polubiec, A. Wróblewska, M. K. Polak, and E. Zhupa. On the constructions of new symmetric ciphers based on nonbijective multivariate maps of prescribed degree. *Secur. Commun. Netw.*, 2019, 2019.

[33] V. Ustimenko. On new results of Extremal Graph Theory and Postquantum Cryptography. International Algebraic Conference "At the End of the Year 2021", December 27-28, 2021 Kyiv, Ukraine ABSTRACTS, p. 29.

[34] V. Ustimenko. On new results on Extremal Graph Theory, Theory of Algebraic Graphs and their applications in Cryptography and Coding Theory. Cryptology ePrint Archive, Report 2022/296, 2022. https://eprint.iacr.org/2022/296.

[35] V. A. Ustimenko. Coordinatization of regular tree and its quotients. In P. Engel and H. Syta, editors, *Voronoĭ's Impact on Modern Science*, number 2 in Proceedings of the institute of mathematics of the national academy of sciences of Ukraine. Institute of Mathematics, National Academy of Sciences of Ukraine, 1998.

[36] V. A. Ustimenko. Graphs with special arcs and cryptography. *Acta Applicandae Mathematicae*, 74, 2002.

[37] V. A. Ustimenko. Maximality of affine group, and hidden graph cryptosystems. *Alg. Dis. Mthm.*, 2005(1):133–150, 2005.

[38] V. A. Ustimenko. On graph-based cryptography and symbolic computations. *Serdica Journal of Computing*, 1(2):131–156, 2007.

[39] N. R. Wagner and M. R. Magyarik. A public key cryptosystem based on the word problem. In *Proceedings of CRYPTO 84 on Advances in Cryptology*, pages 19–36, New York, NY, USA, 1985. Springer-Verlag New York, Inc.

[40] V. Ustimenko, S. Kotorowicz, and U. Romanczuk. On the implementation of stream ciphers based on a new family of algebraic graphs. In M. Ganzha, L. A. Maciaszek, and M. Paprzycki, editors, *Federated Conference on Computer Science and Information Systems, FedCSIS 2011, Szczecin, Poland, 18-21 September 2011, Proceedings*, pages 485–490, 2011.

[41] V. Ustimenko, U. Romanczuk-Polubiec, A. Wróblewska, M. Polak, and E. Zhupa. On the implementation of new symmetric ciphers based on non-bijective multivariate maps. In M. Ganzha, L. A. Maciaszek, and M. Paprzycki, editors, *Proceedings of the 2018 Federated Conference on Computer Science and Information Systems, FedCSIS 2018, Poznań, Poland, September 9-12, 2018*, volume 15 of *Annals of Computer Science and Information Systems*, pages 397–405, 2018.

Advances in Information Systems and Technologies

AIST is a FedCSIS conference track aiming at integrating and creating synergy between disciplines of information technology, information systems, and social sciences. The track addresses the issues relevant to information technology and necessary for practical, everyday needs of business, other organizations and society at large. This track takes a socio-technical view on information systems and, at the same time, relates to ethical, social and political issues raised by information systems.

AIST provides a forum for academics and professionals to share the latest developments and advances in the knowledge and practice of these fields. It seeks new studies in many disciplines to foster a growing body of conceptual, theoretical, experimental, and applied research that could inform design, deployment and usage choices for information systems and technology within business and public organizations as well as households.

We call for papers covering a broad spectrum of topics which bring together sciences of information systems, information technologies, and social sciences, i.e., economics, management, business, finance, and education. The track bridges the diversity of approaches that contributors bring to the conference. The main topics covered are:

- Advances in information systems and technologies for business;
- Advances in information systems and technologies for governments;
- Advances in information systems and technologies for education;
- Advances in information systems and technologies for healthcare;
- Advances in information systems and technologies for smart cities; and
- Advances in information systems and technologies for sustainable development.

AIST invites papers covering the most recent innovations, current trends, professional experiences and new challenges in the several perspectives of information systems and technologies, i.e. design, implementation, stabilization, continuous improvement, and transformation. It seeks new works from researchers and practitioners in business intelligence, big data, data mining, machine learning, cloud computing, mobile applications, social networks, internet of thing, sustainable technologies and systems, blockchain, etc.

Extended versions of high-marked papers presented at technical sessions of AIST 2015-2021 have been published with Springer in volumes of Lecture Notes in Business Information Processing: LNBIP 243, LNBIP 277, LNBIP 311, LNBIP 346, LNBIP 380, LNBIP 413 and LNBIP 442.

Extended versions of selected papers presented during AIST 2022 will be published in Lecture Notes in Business Information Processing series(LNBIP, Springer).

- Data Science in Health, Ecology and Commerce (4th Workshop DSH'22)
- Information Systems Management (17th Conference ISM'22)
- Knowledge Acquisition and Management (28^{th} Conference KAM'22)

TRACK CHAIRS

- **Ziemba, Ewa,** University of Economics in Katowice, Poland
- **Chmielarz, Witold,** University of Warsaw, Poland
- **Cano, Alberto,** Virginia Commonwealth University, Richmond, United States

PROGRAM CHAIRS

- **Chmielarz, Witold,** University of Warsaw, Poland
- **Miller, Gloria,** maxmetrics, Germany
- **Wątróbski, Jarosław,** University of Szczecin, Poland
- **Ziemba, Ewa,** University of Economics in Katowice, Poland

PROGRAM COMMITTEE

- **Ben-Assuli, Ofir,** Ono Academic College, Israel
- **Białas, Andrzej,** Instytut Technik Innowacyjnych EMAG, Poland
- **Byrski, Aleksander,** AGH University Science and Technology, Poland
- **Christozov, Dimitar,** American University in Bulgaria, Bulgaria
- **Dang, Tuan,** Posts and Telecommunications Institute of Technology, Vietnam
- **Dias, Gonçalo,** University of Aveiro, Portugal
- **Drezewski, Rafal,** AGH University of Science and Technology, Poland
- **Grabara, Dariusz,** University of Economics in Katowice, Poland
- **Halawi, Leila,** Embry-Riddle Aeronautical University, USA
- **Kania, Krzysztof,** University of Economics in Katowice, Poland
- **Kapczyński, Adrian,** Silesian University of Technology, Poland
- **Kluza, Krzysztof,** AGH University of Science and Technology, Poland
- **Kovatcheva, Eugenia,** University of Library Studies and Information Technologies, Bulgaria

- **Kozak, Jan,** University of Economics in Katowice, Poland
- **Ligeza, Antoni,** AGH University of Science and Technology, Poland
- **Ludwig, Andre,** Kühne Logistics University, Germany
- **Luna, Jose Maria,** University of Cordoba, Spain
- **Michalik, Krzysztof,** University of Economics in Katowice, Poland
- **Naldi, Maurizio,** LUMSA University, Italy
- **Nguyen, Thi Anh Thu,** The University of Danang, Vietnam
- **Pham, Van Tuan,** Danang University of Science and Technology, Vietnam
- **Rechavi, Amit,** Ruppin Academic Center, Israel
- **Rizun, Nina,** Gdansk University of Technology, Poland
- **Rollo, Federica,** University of Modena and Reggio Emilia, Italy
- **Rusho, Yonit,** Shenkar College of Engineering and Design, Israel
- **Sałabun, Wojciech,** West Pomeranian University of Technology, Poland
- **Santiago, Joanna,** Universidade de Lisboa – ISEG, Portugal
- **Sikorski, Marcin,** Gdank University of Technology, Poland
- **Solanki, Vijender Kumar,** CMR Institute of Technology(Autonomous), Hyderabad, TS, India
- **Taglino, Francesco,** IASI-CNR, Italy
- **Tomczyk, Łukasz,** Pedagogical University of Cracow, Poland
- **Webber, Julian,** Osaka University, Japan
- **Ziemba, Paweł,** University of Szczecin, Poland

Communication Papers of the of the 17th Conference on Computer Science and Intelligence Systems pp. 209–216
DOI: 10.15439/2022F110
ISSN 2300-5963 ACSIS, Vol. 32

High-tech offers on ecommerce platform during war in Ukraine

Dariusz Grabara
University of Economics in Katowice
1 Maja 50 st., 40-287 Katowice, Poland
Email: dariusz.grabara@ue.katowice.pl

***Abstract*—Ecommerce plays a key role in market development. High-tech supports ecommerce, as well as being the subject of sales. However, the regional military conflict such as the war in Ukraine may change sellers' behavior. This article investigates changes on the Polish Allegro ecommerce trading platform before and during the four-week war periods in the high-tech smartphone category. During war maintaining communication in a foreign country is crucial. From this point of view, Xiaomi offers were discussed using Spearman rho coefficient. The study revealed that some high tier smartphone models like '11T Pro' are positively corelated (0.390), while most of the lower positioned devices in Redmi group are strongly and negatively correlated. This includes models like the 'Redmi Note 10' (-0.881), 'Redmi 10' (-0.829), or 'Redmi 9A' (-0.825). A possible explanation as migration shows the moderating effect of the correlation of Mi smartphones (0.422) and Redmi sub-brand (0.518) offers with the number of people crossing the border.**

I. Introduction

ECOMMERCE is perceived as a key player in the growth of the global market. Its continued growth is forcing companies to change their behavior in building new distribution channels or customer support channels. However, ecommerce does not develop independently of market disruptions. Disruptions are often related to problems of transfer, production and sale of goods and supplies. In the final stage of sales, it affects the retail customer in the form of a change in the number of goods offered on e-commerce platforms.

Disruption can be perceived from different points of view. The basic division is the scale of the event. In this sense, events can be of global or regional type. An example of one such event is the recent COVID-19 pandemic affected every aspect of ecommerce [1], [2]. The traffic bans were the fastest felt effect of COVID-19 on the retail market. However, in this context, it was ecommerce that thrived and gained momentum. Further analysis of ecommerce sales provided insight into customer behavior.

The second type of event is the regional type. From this perspective, a regional military conflict appears to be game changer for market growth. An example of regional event is Russia's invasion of Ukraine launched on February 24, 2022. It triggered a new assessment of the security situation in Europe. Concerns about the conflict spill-over to European Union countries are changing the economies. Ecommerce is also not fully immune to these changes.

Against this background, Poland was the most affected country by migration from Ukraine. In the period of more than 2 months, from February 2nd, 2022 to April 30th, 2022, the number of people crossing the border reported by Polish Border Guard (*Straż Graniczna*) was more than 3 million (3.076 million) [3]. The population of Poland is estimated at 38,057 thousand people, according to the central statistical office, Statistics Poland [4]. From this perspective, migration from Ukraine accounts for more than 8% of the native population.

People arriving from an invaded country can feel lost and abandoned. However, mobile devices and electronic services provided by the governments of Ukraine and Poland for evacuees can be quickly accessed through smartphones. In this context not having access to a smartphone for evacuee in foreign country is like losing major communication channel. It can therefore be assumed that ensuring the availability of smartphones is an equivalent of providing a basic need for those fleeing the war. Therefore, it is important to study the ecommerce market for much-needed devices, such as smartphones, in times of disrupted communications.

During a regional conflict, the transfer of goods from neighboring countries is disrupted. Embargoes are imposed and supply lines are severed. In the case of Poland, embargoes were imposed on the exchange of goods with Russia and Belarus, while disruptions affected transfers to and from Ukraine. Ecommerce platforms have also been affected by the disruptions. One form of ecommerce is selling on electronic trading platforms. The speed at which auctions/offers are issued makes them an appropriate observation point for changes in the number of issued offers. On this basis, the Allegro auction platform was chosen. Platform, originally developed in Poland, plays a key role in ecommerce in Europe and is one of ten most recognized ecommerce sites in the world [5].

Smartphones are also the most well-known high-tech devices available on the retail market. However, the trading platform offers all types of mobile devices. It is crucial then to obtain proper categories for time series analysis of offers. Product diversity is considered as a key to product and services platform competitiveness [6]. Wide availability of goods for each customer registered on the platform with conjunction of appropriately chosen categories, should provide adequate set of information.

In this perspective the article focuses on changes in the market for smartphone offerings that may be related to the large number of people migrating from a neighboring invaded country and fills a research gap on market decay caused by unexpected high-profile events.

Therefore, the aim of this study was to assess how regional military conflict affected the ecommerce auction platform in the field of high-tech.

Hypothesis H1 was issued stated that regional military conflict influenced the volume of offers through:

1. H1.1 offers change before and during war periods,
2. H1.2 existing correlation between volume of offers and number of people crossing border from country affected by military conflict.

Research methods used for hypotheses verification comprise of calculation of the Spearman rho correlations and iterative algorithm for smartphone segmentation. R-CRAN and Microsoft Excel software were used to provide results.

The remainder of this paper is organized as follows: section II reviews related literature, section III described used methods for smartphones' segmentation process, study timeframe, procedure and data analysis, section IV presents results divided by before and during war periods, and migration analysis results, section V presents discussion, section VI analyzes limitation of the study, and finally last section provides conclusions.

II. Literature Review

High-tech goods market is influenced by wide range of features. Perceived value of brand could be one of them. Smartphone studies such as Yeh et. al [7] point to brand identification as having a positive effect on brand loyalty, thus highly valued brands would attract more buyers. However, brands, especially in the high-tech field, are subjects to subsidies from the state and are aided by technology theft. China's emerging technology leaders are benefiting from this kind of extra help [8]. Thus, analyzing offers from Chinese companies, should be a better indicator in times of great uncertainty, when there is no time for potential customers to research products in the market. Relying on brand awareness and perception seems a reasonable assumption for choosing a brand. Unfortunately, capturing brand value is subject of brand perception through the prestigious perceived quality of a brand like Apple. Wang [9] observed the second-hand smartphone market and found that it was dominated by Apple, as this brand provided more recovery value. As the study stated, the market analysis is limited, thus analyzing a wider range of products should give a better representation of market models. However, Wang study is one of the few to include time series analysis in the smartphone market. The Apple brand is popular due to its quality. Chatrattikorn and Buavaraporn [10] or Hwang and Su [11] focused their findings on iPhone models, while a broader perspective would be beneficial.

Analyzing the state of the market from the perspective of unexpected events can yield new information about the behavior of buyers and sellers. The other approach is the well-known fact that military conflicts affect the development of high-tech industries. Zilberfarb [12] noticed that electronics sector grew rapidly after the war. Unfortunately, such growth could be viewed from perspective of years, while regional conflicts could quickly dissipate. Another issue of perceiving war in the long term is the shock state at its onset.

Market analysis is often provided by the perception of technology through the goods offered. This kind of study shows the state of an ecommerce platform through the number of offers. Grabara [2] indicated the state of the COVID-19 pandemic through a count of premium device offers. However, the author tried to determine changes in the long term, and samples were given in two-week periods. In the war in Ukraine humanitarian crisis each day brings catastrophic information about fatalities and huge material losses. Therefore, a higher frequency of captured changes will add value to the research. Unfortunately, this work also lacked a comparative period before the unexpected event occurred. The presented article offers a much deeper insights, also due to the higher frequency of samples taken (daily). Another novelty is the different nature of the event.

Another type of research relates to sustainable smartphone practices. Svenson [13] focused on growing potential for proper usage of high-tech, enabling customer to be more aware to environmental needs than to consumerism. Unfortunately, the qualitative type of research makes impossible comparison between different timepoints and type of phones.

Brief literature summary has been presented in table 1.

III. Methods

A. Smartphones' segmentation

In the scope of high-tech field, smartphone offers have been recognized as the best available high-tech in the retail market. However, smartphones differ in terms of their most valuable features. According to Chmielarz [14], this set includes high quality, and design. This suggests that a wide variety of smartphones from a particular brand should be available at the same time during survey. In other words, selected brand should include high-end smartphones and entry-

Table 1. Selected studies related to the high-tech field and/or market disruption events

Study	Study subject / information
Yeh C. H. at al. (2016)	Smartphone market brand loyalty prediction
International Economy (2019)	Discussed subsidies to high-tech sector in China
Wang G.-Y. (2021)	Study discussion of high-tech iPhone customers behavior
Chatrattikorn S. and Buavaraporn N. (2015)	Study discussed factors affecting purchase decision of smartphones
Su Y. and Hwang J. S. (2020)	Study focused on sustained usage time for different brands
Zilberfarb B. Z. (2018)	Discussed effect of war on high-tech industry
Grabara D. (2021)	Study discussed smartphones' market during COVID-19 pandemic
Svenson F. (2018)	Study focused on addressing sustainability issues on the market as smartphone crises

level devices. The Xiaomi smartphone brand was chosen to achieve this goal. After launching its first smartphone in 2011, Xiaomi has reached the status of the world's fourth largest manufacturer in 2019 [15]. Xiaomi was a recognized brand in Poland due to its high functionality. It was confirmed in Dąbrowski's survey on finding accuracy of geopotential models in Poland [16]. One of the key elements of Xiaomi's strategy is pricing. Established price levels could be considered as aggressive pricing strategy [17]. Xiaomi offers wide diversity of smartphones designated for different group of customers, allowing customers to choose between products with different levels of added features. In the presented study, 99 categories were found for various models listed on the Allegro platform. Second in terms of models was Samsung with 90 models. Models' selection was based on:

- availability of models through all days in survey timeframe,
- device positioning.

Positioning was determined by main brand and sub-brand. Xiaomi's main brand was Mi-based smartphones, while the Redmi brand was chosen as the sub-brand. The division exhausted the assumption of smartphone segmentation. However, additional differentiation was applied within the main brand. Xiaomi produces different varieties of products. For the actual model, there are versions with added features, which are represented by the naming convention 'Pro' or 'Ultra'. Other versions include the addition of the letter 'T' or word 'Lite'. In this scope, models with naming convention 'Pro' or 'Ultra' were considered high tier smartphones, while other smartphones were considered base tier smartphones. Within the group of high and base tier smartphones, the most frequently offered models were selected as representatives.

The Redmi sub-brand was chosen in similar fashion. However, the process was adjusted to divide devices into high tier smartphones group when they were marked with the keyword 'Note' and base tier smartphones without this designation. The 'Note' designation refers to Redmi sub-brand devices with improved hardware compared to base models. The next concern addressed in the selection of smartphones was the generation of smartphones. The highest generation of Xiaomi brand available on the platform on January 27th, 2022, was generation 11. For the study, previous generations were also of interests, as they could provide an insightful point of view on vendor behavior. Therefore, two generations preceding generation 11 were chosen for the study. A similar procedure was applied to the Redmi sub-brand. However, in the case of the Redmi sub-brand the highest generation comprised base and high tier product versions was generation 10. The selection process is shown in fig. 1.

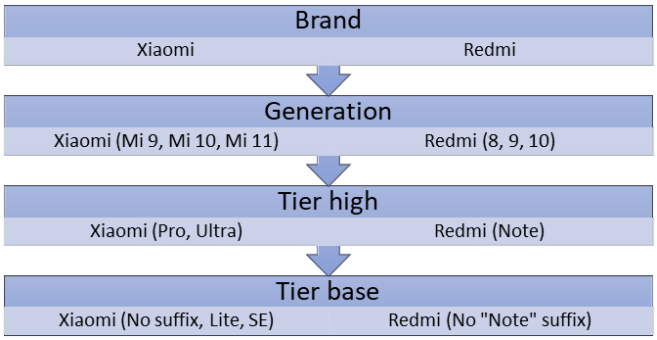

Fig. 1. Smartphones' segmentation process (Author's own work)

To find brand and sub-brand positions, Xiaomi Mi and Redmi representatives were summed and grouping variables were calculated (named 'Xiaomi group' and 'Redmi group' variables).

Additional Xiaomi smartphone launches were recorded during analyzed period. However, the impact was small, as the maximum offers were 49 for Redmi Note 11s. The dates of smartphone launches are shown in fig. 2.

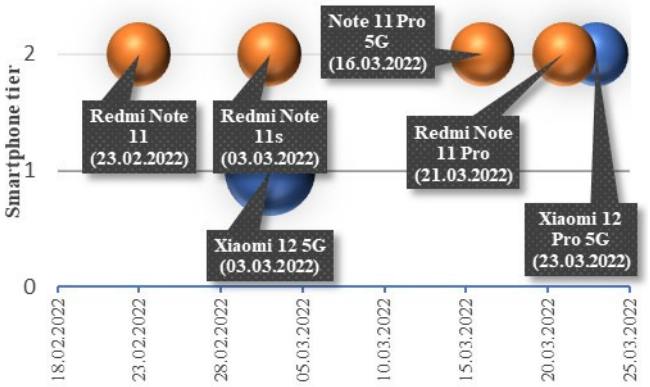

Fig. 2. Additional Xiaomi smartphone launches during study period

Table 3. Smartphones volume descriptive statistics before war (BWP)

Smartphone	Mean	±SD	Q1	Q3	IQR	Min	Max
Mi 9T	131.57	2.95	129.50	134.00	4.50	125	136
Mi 9T Pro	94.68	1.85	93.75	95.00	1.25	91	99
Mi 10T	138.54	4.23	135.00	142.00	7.00	133	146
Mi 10T Pro	85.86	4.13	83.50	89.00	5.50	79	94
Mi 11 Lite	699.82	32.99	668.50	714.25	45.75	661	762
11T Pro	136.57	21.50	118.00	154.00	36.00	102	178
Redmi 8	83.00	4.06	81.75	85.00	3.25	74	91
Redmi Note 8 Pro	262.43	9.45	255.75	266.00	10.25	251	283
Redmi 9A	623.54	27.67	601.50	647.00	45.50	573	663
Redmi Note 9 Pro	515.21	24.93	507.50	530.25	22.75	468	555
Redmi 10	330.00	43.35	301.50	373.25	71.75	253	396
Redmi Note 10	535.21	39.28	500.25	562.00	61.75	481	613
Mi (Group)	**1,287.04**	**30.66**	**1,277.75**	**1,303.25**	**25.50**	**1,219**	**1,335**
Redmi (Group)	**2,349.39**	**138.25**	**2,252.25**	**2,453.75**	**201.50**	**2,131**	**2,588**
Total	**3,636.43**	**152.67**	**3,569.25**	**3,726.25**	**157.00**	**3,364**	**3,892**

While diversity of models was a priority, Xiaomi is also recognized as the second largest smartphone vendor in Poland (25%) with preceding Samsung (31%). Globally, Xiaomi ranks third (12.7%) [18, 19].

In terms of the target group, due to the lack of Ukrainian language support on the ecommerce platform, the target group remained Polish language users.

B. Timeframe

The study was divided into two periods aligned to the same day of the week. Week alignment was applied to avoid biases from seasonal weekday changes. Each period consisted of four weeks.

The first period (also referred to as before war period - BWP) was set as four weeks before the war in Ukraine. The starting point was set for January 27th, 2022, and the ending point for February 23rd, 2022, the day before the start of the war.

The second period (also referred to as during war period - DWP) was chosen as four weeks from the start of the war. The starting point was set at February 24th, 2022, and the ending point was set at March 23rd, 2022. The fourth week of the second period represented timeframe in which the shock of the regional conflict should turn into a more stabilized state. In this perspective, the fourth week of the second period was the first in which the number of people crossing the border from Ukraine to Poland fell to the level of the first day of the war (30,081 people on March 21st, 2022, versus 31,178 on February 24th, 2022).

C. Procedure and data analysis

The data for the migration assessment were extracted from Polish Border Guard databases [20]. Offer volume data on the Allegro trading platform were recorded each. No personal information was recorded.

Analysis for each tier of smartphones was provided by comparing the time series before the war (BWP) and during the war periods (DWP). Spearman's rho correlation coefficient was calculated, and its statistical significance assessed. The coefficient is considered as one of the good assessment tools for evaluating monotonic relations [21]. In the presented study there is an expected trend in offers volume, thus Spearman coefficient is sufficient to detect vendor behavior. An additional argument in favor of using the Spearman correlation coefficient is that the coefficient is based on a ranking system thus correlation does not depend on the data distribution. The significance level was set at 5%. In addition, basic descriptive statistics was also provided.

R-CRAN version 4.0.3 and Microsoft Excel 2021 were used to analyze the data. R-CRAN software provides the necessary packages for statistical analysis and interaction with databases as well as allows design of research procedures in form of scripts.

IV. RESULTS

A. Before and during war periods analysis

Descriptive statistics are presented in tables 2 and 3.

A total number of offers with an average volume of 3,636 offers before the war period and more than 3,734 offers during the war period was observed. The number of offers from the Redmi group increased on average from more than 2,349 to 2,480 offers, while Mi group declined from 1.287 to 1.254.

The 'Mi 11 lite' smartphone model had the most offers before the war period with 762 offers, while during the war period the most offers were found for the 'Redmi Note 10' (698 offers). On average, the 'Mi 11 lite' model was also the most frequently offered before the war period with almost 700 offers per day (699.82). The situation changed during the war period, when the 'Redmi Note 10' was the most frequently offered smartphone (644.36 offers on average).

The Redmi group was represented by a higher volume of offers. Before the war period, offers from the Redmi group averaged 1.82 times more (182.54%) than Mi group of offers. This state was also observed during the war period,

Table 2. Smartphones volume descriptive statistics during war period (DWP)

Smartphone	Mean	±SD	Q1	Q3	IQR	Min	Max
Mi 9T	128.04	2.99	126.00	129.25	3.25	123	134
Mi 9T Pro	104.50	5.21	102.00	108.25	6.25	94	117
Mi 10T	138.00	5.37	134.00	141.25	7.25	131	150
Mi 10T Pro	97.75	4.19	95.00	101.25	6.25	91	107
Mi 11 Lite	611.50	37.47	568.75	642.25	73.50	560	664
11T Pro	174.68	14.02	167.25	184.25	17.00	148	201
Redmi 8	95.79	9.20	91.75	100.50	8.75	76	113
Redmi Note 8 Pro	290.46	10.04	284.00	294.75	10.75	278	312
Redmi 9A	598.00	46.48	568.00	616.50	48.50	527	683
Redmi Note 9 Pro	583.93	11.18	576.75	591.50	14.75	551	605
Redmi 10	363.54	41.20	323.50	407.25	83.75	294	434
Redmi Note 10	644.36	20.05	630.00	654.00	24.00	619	698
Mi (Group)	**1,254.46**	**46.26**	**1,213.75**	**1,288.25**	**74.50**	**1,171**	**1,324**
Redmi (Group)	**2,480.29**	**60.96**	**2,446.00**	**2,519.25**	**73.25**	**2,368**	**2,585**
Total	**3,734.75**	**103.42**	**3,649.00**	**3,795.75**	**146.75**	**3,539**	**3,905**

when the Redmi group outnumbered the Mi group even more (197.72%).

The average volume of offers before and during the war is shown in fig. 3 and 4.

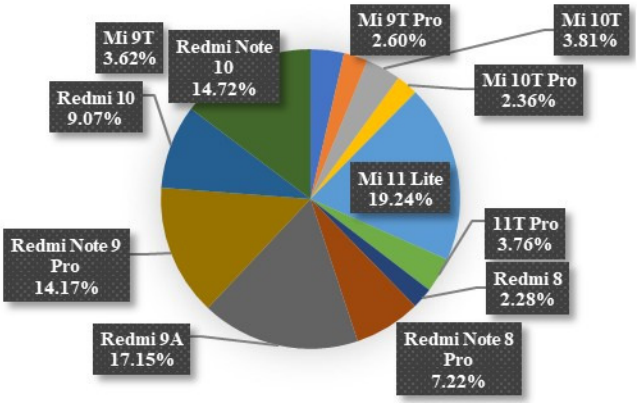

Fig. 3 Average offer numbers before the war period (Author's own work)

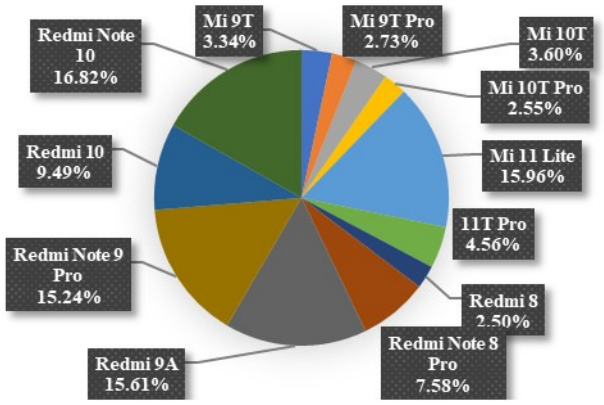

Fig. 4. Average offer numbers during the war period (Author's own work)

The group of most-offered smartphones is dominated by the Redmi sub-brand. The share above 10% of offers on average before the war period were achieved by 'Mi 11 lite' (19.24%), 'Redmi 9A' (17.15%), 'Redmi Note 10' (14.72%), and 'Redmi Note 9 Pro' (14.17%). During the war period shares above 10% were achieved by 'Redmi Note 10' (16.82%), 'Mi 11 lite' (15.96%), 'Redmi 9A' (15.61%), and 'Redmi Note 9 Pro' (15.24%).

The average percentage change in the volume of smartphones available before and during the war periods is shown in fig. 5.

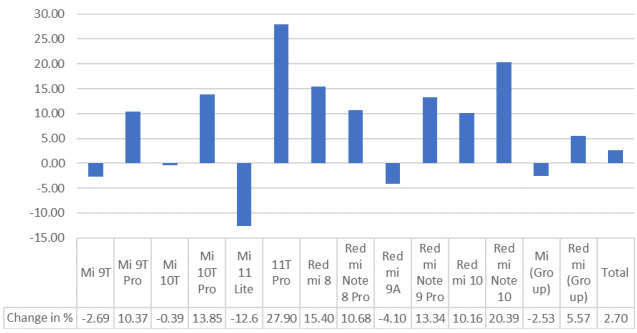

Fig. 5. Average change in percentage of smartphone offers before the war and during the war periods (Author's own work)

The total number of smartphones offers changed in favor of during the war period (2.70%). However, the changes were not the same for the Mi brand and Redmi sub-brand. The Redmi sub-brand gained 5.57%, while the Mi brand declined 2.53%. Higher positioned devices were offered in smaller volume of offers, while lower positioned devices were offered in higher volume.

Military conflicts may indicate that sellers are applying changes to their offers. To find these changes, correlations were calculated before and during the war periods. The calculated correlations are presented in table 4.

The analysis revealed that among Mi smartphones the 'Mi 9T Pro' and '11T Pro' had a statistically significant correlation. However, 'Mi 9T Pro' had a negative and moderate coefficient value (-0.468). Interestingly, there is a positive and moderate coefficient value (0.390) for the latest generation of the Mi '11T Pro' smartphone.

Table 4. Spearman *rho* coefficient of Xiaomi offered smartphones before and during war periods

Smartphone	Spearman *rho*	t	p-value
Mi 9T	-0.023	3,736.82	0.909
Mi 9T Pro	-0.468 *	5,362.60	0.012
Mi 10T	-0.237	4,520.30	0.224
Mi 10T Pro	-0.055	3,854.66	0.781
Mi 11 Lite	-0.005	3,674.05	0.978
11T Pro	0.390 *	2,228.28	0.040
Redmi 8	0.163	3,058.42	0.407
Redmi Note 8 Pro	0.662 *	1,233.38	<0.001
Redmi 9A	-0.825 *	6,666.89	<0.001
Redmi Note 9 Pro	0.564 *	1,592.77	0.002
Redmi 10	-0.829 *	6,681.83	<0.001
Redmi Note 10	-0.881 *	6,874.44	<0.001
Mi (Group)	**-0.182**	**4,318.18**	**0.355**
Redmi (Group)	**-0.568 ***	**5,728.00**	**0.002**
Total	**0.451 ***	**2,006.00**	**0.017**

*p<0.05

Among the Redmi sub-brand, there is an increased number of devices negatively correlated between studied periods. 'Redmi Note 10' (-0.881), 'Redmi 10' (-0.829), and 'Redmi 9a' (-0.825) showed strong negative correlation. 'Redmi Note 8 Pro' showed a positive moderate correlation (0.662), so did 'Redmi Note 9 Pro' (0.564).

Smartphones in the Redmi group also achieved a statistically significant correlation value (-0.568). A moderate effect would indicate that military conflict affects lower positioned devices. In contrast to the result for the Redmi group, combined offers of all smartphones showed positive correlation (0.451) and, in that perspective, more frequent than before the war issuing of offers.

B. During war period migration and smartphone offers analysis

During the first four weeks of the war, the number of people crossing the border reported by the Polish Border Guard was more than 2 million (2,198,749), and the number of evacuees was more than 1.6 million (1,675,505). This represents 5,78% and 4,40% of Poland population, respectively. The total number of offers and the number of people crossing the border are shown on fig. 5.

Data obtained from the Polish Statistical Office [20] were then further used to calculate the Spearman rho coefficient between Xiaomi smartphone offers and the number of people crossing the Polish border from Ukraine. The results are shown in table 6.

The results of the correlation of the number of people crossing the border from Ukraine to Poland may indicate that migration may be in some part related to the smartphone offering. The group of higher-positioned devices (Mi group) and the group of lower-positioned devices (Redmi group) showed a moderate correlation value.

For the Mi group, the correlation was 0.422 and for the Redmi group it was 0.518. The correlation of both groups was statistically significant. In that perspective, the combined group of offers also showed positive moderate correlation strength of 0.503. However, not all smartphone models behaved the same way. 'Redmi Note 10', the most offered smartphone during the war period (an average of 16.82% of all offers), showed a strong negative correlation of -0.772. This is the high tier model of the 10th generation of Redmi smartphones and the most advanced analyzed model of the Redmi sub-brand. Other negatively correlated smartphones are 'Mi 10T Pro' (-0.584), and 'Mi 9T Pro' (-0.482). They represent high tier models of previous generations of the Mi brand. However, they accounted for only 5% of the market's offers.

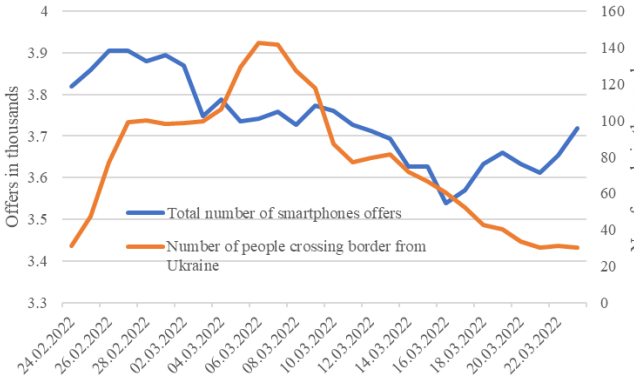

Fig. 6. Total offers of smartphones and number of people crossing the border from Ukraine (Author's own work)

Offers of several other models showed different behavior. 'Redmi 9A', 'Redmi 10' revealed positive correlation of 0.584 and 0.581. In the same way 'Mi 11 lite' and 'Mi 10T' correlated with a coefficient of 0.520, and 0.473, respectively.

V. DISCUSSION

The total number of smartphone offers increased from before to during the war period by 2,70%. A value lower than 3% may indicate, that full military conflict in a neighboring country has not changed the market for high-tech offers in

Table 5. Spearman *rho* coefficient between Xiaomi smartphones offers and number of people crossing Poland border from Ukraine during war period

Smartphone	Spearman *rho*	t	p-value
Mi 9T	0.016	3,595.49	0.936
Mi 9T Pro	-0.482 *	5,416.67	0.009
Mi 10T	0.473 *	1,924.12	0.011
Mi 10T Pro	-0.584 *	5,786.12	0.001
Mi 11 Lite	0.520 *	1,752.96	0.005
11T Pro	0.070	3,399.83	0.725
Redmi 8	0.178	3,002.84	0.364
Redmi Note 8 Pro	-0.347	4,923.70	0.070
Redmi 9A	0.584 *	1,520.42	0.001
Redmi Note 9 Pro	0.163	3,059.10	0.408
Redmi 10	0.581 *	1,530.84	0.001
Redmi Note 10	-0.772 *	6,474.86	<0.001
Mi (Group)	**0.422** *	**2,111.79**	0.025
Redmi (Group)	**0.518** *	**1,760.00**	0.005
Total	**0.503** *	**1,817.75**	0.006

*p<0.05

the short term. This assumption was also pointed out by Grabara in his work [2], where the market disruption in iPhone 11 category was related to problem of supplies. While this is true for globally supplied goods, in the context of regionalization problematic changes in selected markets, it may be of different kind.

Another interesting finding is the change observed among smartphone generations. 'Mi 9T Pro' premiered two generations earlier in 2019 and '11T Pro' in 2021, but their correlations had a different sign. While the older generation 'Mi 9T Pro' was negatively correlated, the '11T Pro' was positively correlated, meaning that customers can expect more offers of newer generation and higher-priced smartphones. According to Primanto et.al [22] price is negatively correlated with sales. Findings may indicate that cheaper products, like the previous generation 'Mi 9T Pro', will sell out at a much higher rate than '11T Pro', leaving the market with higher-priced products. Hwang and Su [11] observed that the average sustained smartphones' usage time among customers ranged from 14 to 18 months. 'Mi 9T Pro' and '11T Pro' are close enough to that distance in time, suggesting that negative correlation may be the result of switching smartphones to newer versions.

Another reason for the lower volume of the previous generation's offers are fears of inflation. According to intelligence analysts [1], the global smartphone market will be hampered. Negatively correlated results for the 'Mi 9T Pro', 'Redmi 9A', 'Redmi 10' and 'Redmi Note 10' smartphones suggest that the military conflict is affecting the smartphone market in the same way i.e., cheaper positioned smartphones will sell faster.

The volume of offers has changed with the type of smartphone. Changes in the market may be due to the number of people migrating. An unprecedented wave of migration with more than 3 million people in 2 months may shake the stabilized ecommerce market. Migration may be responsible for changing smartphone offers in the ecommerce market in Poland. Allegro trading platform saw an opportunity to attract new customers and made its services in Ukrainian [23]. However, availability of another language is not provided in the short term.

The rapidly escalating conflict and its impact on the smartphone market can be seen in terms of social media crises. Social media is considered as one of the key players in brand promotion. Study like Zahid and Dastane [24] shows that social influence would mostly affect purchase intentions. With more people crossing the border, the need for good quality smartphones in the starting point of their lifecycles would be a good investment. In that perspective, the 'Redmi Note 10' plays its role with a strong negative correlation between number of people crossing the border from Ukraine and volume of the offers.

'Redmi Note 10' was also the one that had a larger growth in perspective of the number of offers from before the war period to during the war period. On average the number of offers increased from 535 to 644. As study of Gao et al. [25] shows, the appearance of new sellers can be responsible for such event. The arrival of new potential active users of the ecommerce platform may be one of the reasons for the increase.

Brose argues in his work that high-tech plays the key role not only in future military conflicts, but also in current ones [24]. The scarcity of high-tech implementation in the armed forces make the US war simulations lost to China. What is more, all the needed technologies are in use by America's military men and women. Its importance in the retail market during the war is also evidenced by differences in the availability of smartphones through changes in the number of offers for a higher-positioned device such as the 'Mi 11 lite' (down 12.6%, from nearly 700 BWP to an average of 611 DWP offers).

In the context of discussed results, the statistically significant correlation partially supported hypothesis H1.1 stating that the volume of offers changed before and during the war

periods. Hypothesis H1.2 stating that the existing correlation between the volume of offers and the number of people crossing the border from country affected by military conflict was also true for the total number of offers and group of brands, but not for each smartphone model.

VI. Limitation of the Study

One of the key assumptions of the study was to track the offerings of the selected brand. While the Xiaomi brand provides variety of products with appropriate positioning strategy, Xiaomi is not taking over the smartphone market. The resulting changes are interesting but should be further enhanced with the analysis of different brands.

The other limitation of the study is the segmentation process. Xiaomi offers a wide variety of smartphones, thus finding representative by selecting the most offered model is one of the key assumptions of the analysis. However, providing different kind of segmentation may bring new type of findings in future studies.

VII. Conclusions and Further Research Directions

The regional conflict did not affect high-tech smartphones market in the short term. On the contrary the market grew steadily. However, the details are important. To find the changes, one need to look at smartphone features needed by customers, and these are provided by specific smartphone models. Then significant changes in number of offers of key player models may be observed.

High-tech is available through different devices, but one type is for sure known to all people – smartphones. In this context, the Xiaomi smartphone study showed that military conflicts changed availability of high-tech to retail customers. Another conclusion is that importance of availability of high-tech is not only valid for military forces but also for the customers during regional military conflicts.

VIII. References

[1] D. Wu, "Global Smartphone Market Had Worst Drop Since Virus Outbreak", *Bloomberg*. (2022) 1. https://www.bloomberg.com/news/articles/2022-04-20/global-smartphone-market-had-worst-drop-since-virus-outbreak (accessed April 30, 2022).

[2] D. Grabara, "iPhone 11 premium mobile device offers on e-commerce auction platform in the context of Marketing Mix framework and COVID-19 pandemic", in: *Procedia Comput. Sci. 192C*, 2021: pp. 1720–1729.

[3] Straż Graniczna, „Straż Graniczna na Twitterze", (2022). https://twitter.com/Straz_Graniczna/status/1520643611192619008?cxt=HHwWgMDTsdjTtJoqAAAA (accessed May 1, 2022).

[4] Statistics Poland, "Basic data", (2022). https://stat.gov.pl/en/basic-data/ (accessed April 15, 2022).

[5] Ecommerce News, "Allegro enters global top 10 biggest ecommerce websites", *Ecommerce News Eur.* (2020). https://ecommercenews.eu/allegro-enters-global-top-10-biggest-ecommerce-websites/ (accessed November 10, 2020).

[6] Y. Chen, Y. Sun, "Determinants of platform ecosystem health: An exploration based on grounded theory", *J. Bus. Econ. Manag.* 22 (2021) 1142–1159. https://doi.org/10.3846/jbem.2021.15047.

[7] C. H. Yeh, Y. S. Wang, K. Yieh, "Predicting smartphone brand loyalty: Consumer value and consumer-brand identification perspectives", *Int. J. Inf. Manage.* 36 (2016) 245–257. https://doi.org/10.1016/j.ijinfomgt.2015.11.013.

[8] International Economy, "Party Hacks and the End of the Deng Era", *Int. Econ.* 33 (2019) 4–4.

[9] G.-Y. Wang, "The Brand Effect: A Case Study in Taiwan Second-Hand Smartphone Market", *J. Soc. Econ. Stat.* 10 (2021) 30–42. https://doi.org/10.2478/jses-2021-0003.

[10] S. Chatrattikorn, N. Buavaraporn, "Investigating factors affecting purchase", *UTCC Int. J. Bus. Econ.* 7 (2015) 113–130.

[11] Y. Su, J. S. Hwang, "Integration of customer satisfaction and sustained use of a product for value assessment", *Total Qual. Manag. Bus. Excell.* 31 (2020) 1760–1773. https://doi.org/10.1080/14783363.2018.1509697.

[12] B. Z. Zilberfarb, "The short- and long-term effects of the Six Day War on the Israeli economy", *Isr. Aff.* 24 (2018) 785–798. https://doi.org/10.1080/13537121.2018.1505476.

[13] F. Svenson, "Smartphone crises and adjustments in a virtual P3 community–doing sustainability oriented smartphone consumption", *J. Mark. Manag.* 34 (2018) 664–693. https://doi.org/10.1080/0267257X.2018.1464495.

[14] W. Chmielarz, "The usage of smartphone and mobile applications from the point of view of customers in Poland", Inf. 11 (2020). https://doi.org/10.3390/INFO11040220.

[15] N. A. Brabo, A. I. Karif, S. D. Lestari, A. Sriyanto, "The Effect of Brand Page Commitment, Brand Awareness, Electronic Word Of Mouth and Brand Image on Purchase Intention of Xiaomi Smartphone on Social Media", *GATR J. Manag. Mark. Rev.* 6 (2021) 235–244. https://doi.org/10.35609/jmmr.2021.6.4(4).

[16] P. S. Dabrowski, "Accuracy of Geopotential Models Used in Smartphone Positioning in the Territory of Poland", *IOP Conf. Ser. Earth Environ. Sci*. 221 (2019). https://doi.org/10.1088/1755-1315/221/1/012080.

[17] R. Tabassum, S. Ahmed, "Xiaomi invades the smartphone market in India", *Decision.* 47 (2020) 215–228. https://doi.org/10.1007/s40622-020-00242-w.

[18] Serwis Rzeczypospolitej Polskiej, „Dane statystyczne osób ewakuowanych do Polski z terytorium Ukrainy", (2022). https://dane.gov.pl/pl/dataset/2705,dane-statystyczne-dotyczace-sytuacji-na-granicy-z-Ukraina/resource/37768/chart?page=1&q= (accessed June 01, 2022).

[19] Orange, „Najpopularniejsze marki telefonów, czyli jak wygląda rynek smartfonów na świecie i w Polsce", (2022), https://www.orange.pl/poradnik/smartfony-i-inne-urzadzenia/najpopularniejsze-marki-telefonow-czyli-jak-wyglada-rynek-smartfonow-na-swiecie-i-w-polsce/, (accessed July 07, 2022).

[20] International Data Corporation, „Smartphone Market Share, Updated: 23 June 2022", (2022), https://www.idc.com/promo/smartphone-market-share, (accessed July 08, 2022).

[21] E. van den Heuvel, Z. Zhan, "Myths About Linear and Monotonic Associations: Pearson's r, Spearman's ρ, and Kendall's τ", *Am. Stat.* 76 (2022) 44–52. https://doi.org/10.1080/00031305.2021.2004922.

[22] A. B. Primanto, M. K. ABS, A. R. Slamet, "A Study of The Best Selling Smartphone in The Two Biggest Marketplace in Indonesia*", J. Terap. Manaj. Dan Bisnis.* 4 (2018) 17–24. https://doi.org/10.26737/jtmb.v4i1.487.

[23] Allegro, „Allegro od teraz również po ukraińsku", (2022).

[24] W. Zahid, O. Dastane, "Factors affecting purchase intention of South East Asian (SEA) young adults", *Asean Mark. J.* (2016) 66–84. https://www.researchgate.net/publication/313250323_Factors_Affecting_Purchase_Intention_of_South_East_Asian_SEA_Young_Adults_towards_Global_Smartphone_Brands.

[25] B. Gao, W. K. Chan, L. Chi, X. Deng, "Size and growth dynamics of online stores: A case of China's Taobao.com", Electron. Commer. *Res. Appl.* 17 (2016) 161–172. https://doi.org/10.1016/j.elerap.2016.04.005.

[26] C. Brose, "The Kill Chain: Defending America in the Future of High-Tech Warfare", Hachette Books, 2020.

Communication Papers of the of the 17th Conference on Computer Science and Intelligence Systems pp. 217–221
DOI: 10.15439/2022F29
ISSN 2300-5963 ACSIS, Vol. 32

Digital Business Transformation Methodologies: A Quasi-systematic Review of Literature

Adriano M. S. Lima, Francisco L. de Azevedo Neto, Methanias Colaço Júnior, Rogério Patrício Chagas do Nascimento
Departamento de Computação (DCOMP)
Universidade Federal de Sergipe (UFS)
Aracaju, Brasil
ssa.adriano@gmail.com, francisco.neto@dcomp.ufs.br, methanias@ufs.br, rogerio@dcomp.ufs.br

***Abstract*— The globalized scenario of great competition in the corporate world and the use of new disruptive technologies, which are associated with a revolutionary innovation process, are leveraging current business models and awakening the latent need for companies to adapt definitively to this historic moment of transformation digital driven by the Pandemic of the new Coronavirus.**

In addition to the new commercial relationships using technology as a support base for all business processes, they are also highly dependent on the care with the privacy of the personal data used. Security incidents that occur with this data can drastically compromise the image of companies and also imply serious sanctions provided for in privacy laws such as the Brazilian LGPD - General Data Protection Law.

Thus, this work aims to map state-of-the-art articles that address Digital Business Transformation Methodologies, aiming to understand how these methodologies can be replicated in companies to accelerate the reach of this new industrial revolution. A quasi-systematic review of the literature was carried out, involving the main methodologies created from the year 2011 and 127 studies were analyzed, and which 12 were considered relevant.

The results show that the number of works related to Digital Transformation Methodologies is still very small and that it started to grow from 2017. The COVID-19 is one of the main reasons for last year's research. there is a diversity of countries studying the theme. Few articles refer to adequacy to the requirements of the privacy laws and protection of personal data existing in their countries.

***IndexTerms*—Business Transformation, Digital Transformation, Process Modeling, Process Management, Agile.**

I. Introduction

The digital transformation is reshaping competition in many well-established industries [1]. Companies are being challenged to adapt to the new wave of digital transformation that the world is experiencing or, otherwise, they will become obsolete.

But what would be the definition of digital transformation and what is its relationship with digitization. Digital transformation describes the changes imposed by information technologies as a means to automatize tasks [2]. In other hand, the digitization is the process of changing from analog to digital form.

According to the World Economic Forum, only 1% of investments in digital transformation in 2018 would have met expectations [3]. It shows the necessity for the existence of a strategy or planning for the adaptation of companies in relation to the ideas and possibilities of the current world, such as, for example, to have a digital channel in their commercial relations for the sale of products and services.

When the confrontation of the new coronavirus (COVID-19) started mainly with social isolations, these adaptations needed to be accelerated. All sectors of the economy were affected, even companies that were already starting their digital transformation processes. Face-to-face activities from that moment on needed to be virtual, papers became emails and documents that were physically stored, needed to become digital. Organizations that have failed to adapt have been left behind.

With this information in mind, this systematic mapping aims to find studies that present methodologies or models that can be adopted by companies that need to enter the world of digital transformation.

Thus, the mapping is divided as follows: Section 2 is presented the methodology used for this mapping. In section 3, the analysis of the results obtained is presented. In section 4 the completion of the mapping that is followed by the references.

II. Methodology

This article aims to map studies that present models of strategies in which companies use technology to improve their performance, expand their reach and optimize their results, this process is what we call digital transformation. For this, the article was adopted the method of systematic literature mapping (SLM) which, according to Petersen [4], consists of defining research questions, conducting the search and selection of relevant studies, extracting data and mapping the results.

This Section describes how the process of searching and selecting the studies was performed.

A. Research Questions

Reaching the objective proposed by this mapping, the following research questions were elaborated:

Q1). What is the growth of studies on digital transformation methodologies in the last 10 years?

Q2). Which countries have contributed the most to studies on digital transformation methodologies?

Q3). Were the studies driven from the context of the COVID-19 Pandemic?

Q4). What studies are oriented to data privacy laws such as GDPR or LGPD?

B. *Search and Selection Strategies*

To elaborate this mapping, the following databases were used: ACM Digital Library, IEEE Xplore, Science Direct, Scopus and Springer Link. To access the publications without restrictions, was used the CAPES journal portal (http://www.periodicos.capes.gov.br).

To perform the searches on the bases listed above, an English search term was constructed using the keywords, originating the following term: (("business transformation" OR "company transformation") AND "digital transformation") AND ("team management" OR "squad management" OR "talent management" OR "process management" OR "process modeling" OR "agile" OR "agility").

The searches were carried out in April 2021 and 127 articles were found, 4 articles found in the ACM database, 1 article from the IEEE Xplore database, 18 articles from the ScienceDirect database, 90 articles on the Scopus database and 14 articles on the SpringerLink database.

TABLE I.
RESULTS OF SEARCHES ON THE BASES

Base	Search results
ACM Digital Library	4
IEEE Xplore	1
Science Direct	18
Scopus	90
SpringerLink	14

According to TABLE 1, Scopus was the basis with the highest number of results representing 70.8% of the total and the IEEE Xplore with the lowest result with only 1 article found.

After the search, the articles were submitted to a filtering process through the selection and exclusion criteria. It is worth noting that in the first stage of the searches, studies with more than 10 years of publication have been filtered and that are not in the Portuguese or English languages.

C. *Selection Criteria*

In order to filter the most relevant articles of the mapping, inclusion and exclusion criteria were defined which are:

Only studies in the languages Portuguese and English were included; and articles proposing methodologies or frameworks aimed at digital transformation and related to business transformation.

Studies that are not directly associated with research questions; duplicate texts; and studies not made available in full for free download were excluded.

After applying the criteria, of the 127 studies found 8 were rejected because they were duplicated, 85 were rejected because they were not directly associated with research questions and 3 because they were not available free of charge. From this, 30 articles were selected to make up the studies.

TABLE 2 shows how the results were after the application of the criteria, however we can see that only the ACM Digital Library database not presented relevant studies for systematic mapping.

The remaining articles were submitted to some quality criteria, where 4 objective questions were applied where they can be answered with "yes" representing 1 point, "partially" representing, 0.5 point and "no" representing 0 point. With this, each article can reach a maximum of 4 points. Articles that have reached a cutoff score of 1.4 points are accepted by the quality criteria. Thus, the following questions were elaborated:

TABLE II.
RESULTS OF STUDIES AFTER THE APPLICATION OF INCLUSION AND EXCLUSION CRITERIA.

Base	Results before	Results after
ACM Digital Library	4	0
IEEE Xplore	1	1
Science Direct	18	5
Scopus	90	22
SpringerLink	14	2

1. Did the study prove the validity of the results obtained statistically?
2. Did the study create a new digital transformation methodology?
3. Did the study structure the methodology so that it is replicable?
4. Did the study show the result of the application of the methodology in a real environment?

Of the 30 articles that reached this phase, 12 articles reached the cutoff score and were accepted and considered relevant for the study. In Figure 1 we can graphically visualize this result.

After quality selection and evaluation, the studies were forwarded for in-depth reading and analysis and the results can be found in the data analysis and discussion section.

III. DATA ANALYSIS AND DISCUSSION

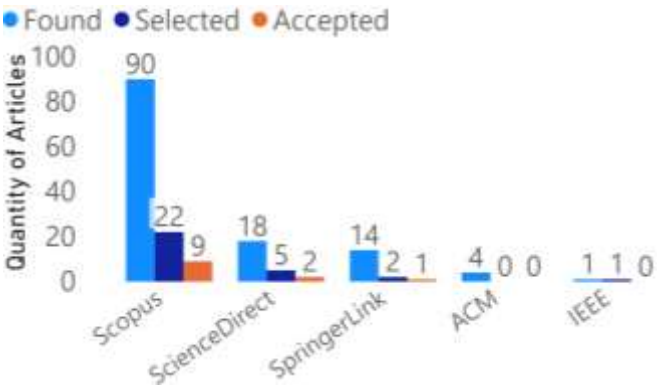

Fig 1. Quantitative of articles that were found, selected and accepted by each search base.

A. *Data Analysis and interpretation*

In this section, the results obtained from the analysis of the studies are presented, answering the research questions.

Q1). What is the growth of studies on digital transformation methodologies in the last 10 years?

The objective of this issue is to identify the annual growth of studies involving digital transformation methodologies and seek future perspectives on the subject.

Figure 2 shows the growth of studies based on the selected articles. We can observe that from 2011 to 2016 there were no publications accepted by the criteria determined. Only from 2017 relevant articles began to be published, with the exception of 2019.

It is important to remember that in 2021 with only 4 months, already has the same amount of articles from the previous year. This occurrence may signal a significant increase in the number of publications until the end of the year. One fact that may cause an increase in the last year is the great need for forced adaptation for companies of all branches due to the COVID-19 Pandemic, however, it is believed that in the coming years there will be a growing publication of studies related to the subject.

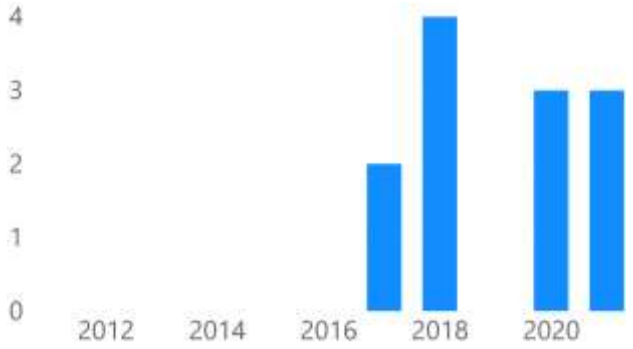

Fig 2. Quantitative studies per year in the last 10 years.

Reference of the articles recorded in question Q1.

2017: [11; 16]

2018: [6; 7; 12; 15]

2020: [5; 10; 14]

2021: [7; 8; 13]

Q2). Which countries have contributed the most to studies on digital transformation methodologies?

This issue aims to present a survey of which countries have contributed the most in the last 10 years with studies.

According to Figure 3, it can be seen that Germany and the Czech Republic are the leaders in publications, with 2 each. The other 8 countries are also tied with only 1 publication. However, despite the simple superiority of Germany and the Czech Republic, the most important information that can be absorbed is the diversity that is presented in the chart below:

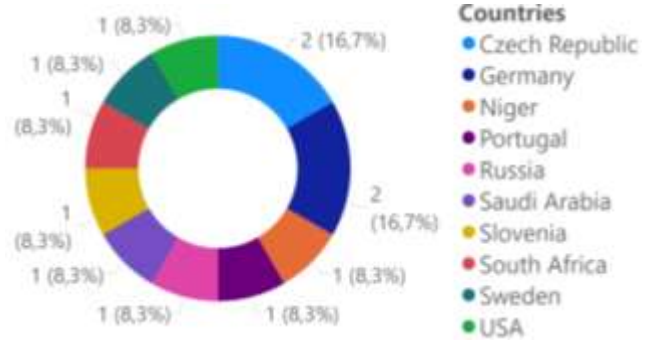

Fig 3. Quantitative studies by country of publication.

Reference of the articles recorded in question Q2.

Czech Republic: [7; 15]

Germany: [5; 6]

Niger: [13]

Portugal: [16]

Russia: [9]

Saudi Arabia: [14]

Slovenia: [10]

South Africa: [11]

Sweden: [12]

USA: [8]

Q3). Were the studies driven from the context of the COVID-19 Pandemic?

This question aims to identify the impact of COVID-19 on studies related to digital and business transformation.

Figure 4 shows in a graph the percentage of articles that refer to COVID-19. Through this indicator, the influence of this Pandemic can be observed to search for business transformation methodologies.

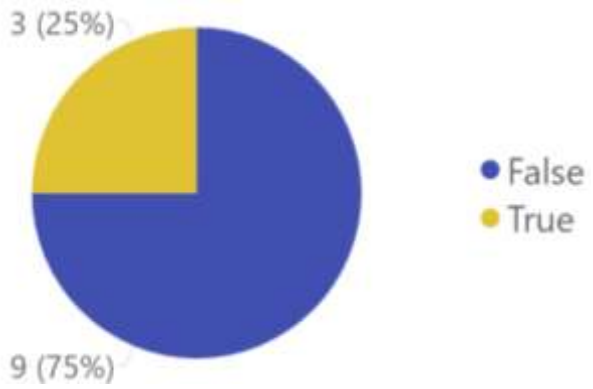

Fig 4. Quantitative of articles mentioning COVID-19.

Reference of the articles recorded in question Q3.

True: [8; 13; 14]

False: [5; 6; 7; 9; 10; 11; 12; 15; 16]

In 6 articles published between 2020 and 2021, 3 were motivated by COVID-19, which we can conclude that the pandemic is of great importance for the results obtained in recent years and may continue to be the focus of many future studies.

Q4). What studies are oriented to data privacy laws such as GDPR or LGPD?

The issue concerns the adequacy of the methodologies found to the privacy and protection laws of personal data. From these laws, both companies and government institutions will need to adapt their business processes, but the reality of the selected studies is totally opposite.

As we can see in the Figure 5, in 12 selected studies, only 3 mention data protection, all of which were published in the years 2020 and 2021, moments that the concern with the subject took higher proportions.

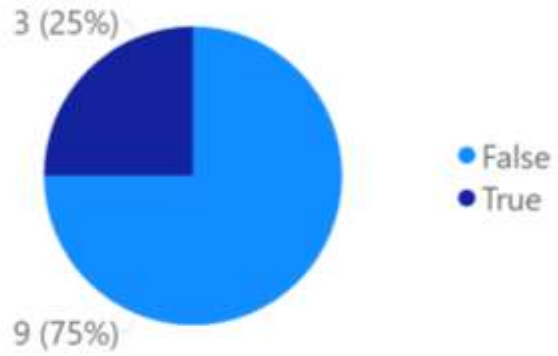

Fig 5. Quantitative of articles that took into account the LGPD or GDPR.

B. *Threats to validity*

During systematic mapping there were some factors that may have affected the results obtained. These factors are described below.

Internal factors: The date of the searches at the databases, because it was performed before the end of the first semester may have influenced the number of studies found that were published in 2021.

External Factors: This systematic mapping was still performed during the Pandemic period, however, we cannot say that in the post-pandemic period, the trends will remain the same. After the end of the pandemic, the need to be included in the digital environment may decrease, although many of the "digital" customs have come to stay.

IV. Conclusion

This study aimed to analyze how the world is reacting to adapt to the digital transformations that have been happening in the last 10 years, through a systematic mapping of the literature.

In the process, Petersen's systematic mapping method was used, which assisted in the elaboration of the process of searching, selecting and filtering articles. With the search terms defined, searches were performed in the following databases: ACM Digital Library, IEEE Xplore, Science Direct, Scopus and SpringerLink. At the end of the search, a total of 127 were found, all of which were articles in English. In the articles found, filtrations were applied through inclusion, exclusion and quality criteria, 12 articles were selected.

From the analysis and detailed reading of the selected articles, it was possible to answer the research questions. Therefore, despite presenting a possible interest on the subject only in recent years, the expectation is that the next few years it will be increasingly addressed (Q1), Germany and the Czech Republic were the 2 countries that most published studies on the subject (Q2), it could be observed a great influence of COVID-19 in the results of the studies, representing 50% of the articles of the last 2 years (2020 and 2021) of the (Q3) and 25% of the articles approach the theme LGPD (Q4). However, we can say that there are still few studies on the subject, but the trend is that, due to the pandemic, in the coming years there will be more patterns of digital transformation methodologies.

Thus, it is believed that this study can help academics and entrepreneurs who seek information and support involving new methodologies of digital transformation.

This review can be extended by changing the inclusion, exclusion and quality criteria, such as searching for articles that are not directly related to methodologies, but that deal with essential actions and projects to be carried out in companies for insertion in the context of Digital Transformation.

References

[1] M. Porter and J. Heppelmann, “How Smart, Connected Products are Transforming Competition,” Harv. Bus. Rev., no. November, pp. 65–88, 2014.

[2] LEGNER, C.; EYMANN, T.; HESS, T. Business & Information Systems Engineering. Bus Inf Syst Eng, Switzerland, v. 59, p. 301-308, ago. 2017 2363-7005, 1867-0202. DOI: https://doi.org/10.1007/s12599-017-0484-2.

[3] World Economic Forum, “The Digital Enterprise: Moving from experimentation to transformation,” 2018.

[4] PETERSEN, K., FELDT, R., MUFTABA, S. AND MATTSON, M., 2008. Systematic mapping studies in software engineering. In: Proceedings of the 12th International Conference on Evaluation and Assessment in Software Engineering, 68-77.

[5] Alt, Rainer. “Electronic Markets on Business Model Development”. Electronic Markets 30, nº 3 (setembro de 2020): 405–11. https://doi.org/10.1007/s12525-020-00438-z.

[6] Denner, Marie-Sophie, Louis Christian Püschel, e Maximilian Röglinger. “How to Exploit the Digitalization Potential of Business Processes”. Business & Information Systems Engineering 60, nº 4 (agosto de 2018): 331–49. https://doi.org/10.1007/s12599-017-0509-x.

[7] Diener, Florian, e Miroslav Špacek. “Digital Transformation in Banking: A Managerial Perspective on Barriers to Change”. Sustainability 13, nº 4 (13 de fevereiro de 2021): 2032. https://doi.org/10.3390/su13042032.

[8] Huang, Arthur, e Melissa Farboudi Jahromi. “Resilience Building in Service Firms during and Post COVID-19”. The Service Industries Journal 41, nº 1–2 (25 de janeiro de 2021): 138–67. https://doi.org/10.1080/02642069.2020.1862092.

[9] Isaev, Evgeniy, Nina Korovkina, e Maria Tabakova. “Evaluation of the readiness of a company’s IT department for digital business transformation”. Business Informatics 2018, nº 2 (30 de junho de 2018): 55–64. https://doi.org/10.17323/1998-0663.2018.2.55.64.

[10] KU Leuven, Faculty of Economics and Business, Leuven, Belgium, Ziboud Van Veldhoven, Jan Vanthienen, e KU Leuven, Faculty of Economics and Business, Leuven, Belgium. “Designing a Comprehensive Understanding of Digital Transformation and its Impact”. In Humanizing Technology for a Sustainable Society, 745–63. University of Maribor Press, 2019. https://doi.org/10.18690/978-961-286-280-0.39.

[11] Leipzig, T. von, M. Gamp, D. Manz, K. Schöttle, P. Ohlhausen, G. Oosthuizen, D. Palm, e K. von Leipzig. “Initialising Customer-Orientated Digital Transformation in Enterprises”. Procedia Manufacturing 8 (2017): 517–24. https://doi.org/10.1016/j.promfg.2017.02.066.

[12] Michalik, Alexander, Frederik Möller, Michael Henke, e Boris Otto. “Towards Utilizing Customer Data for Business Model Innovation: The Case of a German Manufacturer”. Procedia CIRP 73 (2018): 310–16. https://doi.org/10.1016/j.procir.2018.04.006.

[13] Olokundun, Maxwell, Stephen Ibidunni, Mercy Ogbari, Hezekiah Falola, e Odunayo Salau. “COVID-19 Pandemic and Antecedents for Digital Transformation in the Workplace: A Conceptual Framework”. Open Access Macedonian Journal of Medical Sciences 9, nº F (5 de janeiro de 2021): 41–46. https://doi.org/10.3889/oamjms.2021.4952.

[14] Omar, Abdulfattah, e Ahmed almaghthawi. “Towards an Integrated Model of Data Governance and Integration for the Implementation of Digital Transformation Processes in the Saudi Universities”. International Journal of Advanced Computer Science and Applications 11, nº 8 (2020). https://doi.org/10.14569/IJACSA.2020.0110873.

[15] Schwer, Karlheinz, e Christian Hitz. “Designing Organizational Structure In The Age Of Digitization”. Journal of Eastern European and

Central Asian Research 5, nº 1 (20 de abril de 2018). https://doi.org/10.15549/jeecar.v5i1.213.

[16] STIC – Universidade de Aveiro, Cristiano Pereira, Carlos Ferreira, DEGEI/IEETA – Universidade de Aveiro, Luis Amaral, e Universidade do Minho. “SHAPE A BUSINESS CASE PROCESS: AN IT GOVERNANCE AND IT VALUE MANAGEMENT PRACTICES VIEWPOINT WITH COBIT 5.0”. In Atas da 17ª Conferência da Associação Portuguesa de Sistemas de Informação, 60–75. Associação Portuguesa de Sistemas de Informação, APSI, 2017. https://doi.org/10.18803/capsi.v17.60-75.

Communication Papers of the of the 17th Conference on Computer Science and Intelligence Systems pp. 223–230
DOI: 10.15439/2022F41
ISSN 2300-5963 ACSIS, Vol. 32

Using Information and Distributed Ledger Technologies to Combat Public Procurement Corruption: A South African Perspective

Johnny Prins
University of Cape Town, Private Bag, Rondebosch, 7701, South Africa

Jean-Paul Van Belle
University of Cape Town, Private Bag, Rondebosch, 7701, South Africa.
Email: jean-paul.vanbelle@uct.ac.za

Marita Turpin
Department of Informatics, University of Pretoria, Private Bag X20, Hatfield, 0028, South Africa

***Abstract*— Corruption has had a detrimental impact on the South African economy. The use of Information Communication Technology (ICT) in combatting corruption is undervalued in e-government contexts, while insufficient empirical data exists to gauge the effectiveness of distributed digital technology in combatting malfeasance. This study explores perceptions on the use of ICT in the procurement corruption investigation sector. Legal and factual perspectives of ICTs, and specifically on Digital Ledger Technology (DLT)'s usefulness in combatting public sector procurement corruption in South Africa was found to be limited. This empirical study found that most respondents in the corruption investigation field had encounters with it in the Public Procurement field of the Supply Chain Management (SCM) function. Human interference in the ICT system appears to be the main contributing factor in corrupting the system. Monitoring of user activity logs is recommended as well as strict regulations to prevent ghost users from corrupting ICT systems.**

***Keywords*— Corruption fighting; e-government; Distributed Ledger Technology; Blockchain in Government.**

I. Introduction

DISTRIBUTED Ledger Technology (DLT) is a new and fast-evolving approach to record and share data across multiple ledgers and it allows for the sharing, recording and synchronization of transactions across a distribution of network participants [1]. In South Africa, anti-corruption agencies such as the Directorate for Priority Crime Investigations ("DPCI"), also known as the Hawks, and the Special Investigating Unit ("SIU") often finds themselves investigating alleged acts of malfeasance long after the deed has been done and proceeds thereof has been funneled elsewhere. A laborious search for documentary evidence to prove or disprove these allegations are often frustrated by the prescription law which prescribes that an investigation should generally not have happened three years after one became aware of it. Information and Communication Technology (ICT) has been misused in the form of corruption to benefit individuals and governments. This study focuses on ICTs and their potential use in fighting procurement corruption and seeks to understand whether DLT could assist in investigations of a procurement nature, and even prevent it from happening.

Corruption can be defined as a subversion of constitutional principles upon which the public procurement system is based. The government's failure to control and prevent public procurement corruption at all government procurement levels is regarded as a failure in its constitutional mandate [2].

This study evaluates whether current ICT applications are effectively used in the fight against procurement corruption and seeks to analyze how DLT can be used to impact the reduction of procurement corruption.

The research objectives of this study are:

- *The evaluation of the current effective uses of ICT in the fight against procurement corruption.*
- *Analyzing how DLT can be used to impact the reduction of procurement corruption.*

II. Literature Review

This section provides an overview of current literature on ICT's use to combat procurement corruption, its effectiveness and the legal frameworks that underpin its use. A theoretical review follows and a conceptual model that is used to guide the study is introduced.

A. ICTs employed to combat procurement corruption

Procurement corruption happens mostly during the process of procuring goods and services in that prices are often inflated or manipulated, or in awarding contracts to close relatives or friends [3]. This can happen when tenders are advertised, and tender bid committee systems are not properly constituted.

Reference [4] found it too early to assess applications powered by blockchain as tools to fight corruption but call for further experimentations, innovation, as well as rigorous research on the topic. They suggest governments should endeavor to digitize paper-based processes into blockchain applications if it is found to be of value, as well as improved transparency in conducting government to the citizen, government to business, and government to government electronic (e-government) services.

Blockchain is a digital ledger, in which data about transactions are recorded uniquely due to the distributed and decentralized nature of the blockchain [5]. Blockchain enables instant, synchronized replication, and shares the updated state of the ledger to the participants in the block-chain, the so-called "nodes", who should agree on the legitimacy of the transaction [5]. The new block in the chain

is linked to the previous which maintains the shared and agreed upon state of the blockchain [6].

Reference [7] refers to the eastern and southern African common markets' use of blockchain to implement real-time digital free trade area amongst buyers and sellers thereby increasing e-commerce transaction security with certification of origin generation and with assurance and security. The digital free trade area resulted in savings of approximately $450 million in eliminating administrative bureaucracy [7].

In their quest to answer whether emerging technologies are helping in the fight against corruption, [4] assessed the use and came up with empirical findings on the use of the following technologies and tools.

- *Digital public services* enable internal supervisors to monitor officials' activities; these can reduce corrupt behaviors rooted in the principle-agent.
- *Crowdsourcing platforms*: these allow citizens to report corruption incidences by using the internet or telephone.
- *Whistleblowing tools* are platforms that enable people to report wrongdoing by public officials, usually designed for gathering detailed reports of individual cases of grand corruption to support a criminal prosecution.
- *Transparency portals* are online platforms usually run by governments or NGOs that publish information on government operations.
- *Distributed ledger technology (DLT) and blockchain* refer to a decentralized and synchronized database maintained by a peer-to-peer network where each user holds a copy of the blockchain. All information is transmitted, verified, and saved in the distributed ledger as blocks that cannot be changed or deleted [4].

Whether the technologies in everyday use contribute to the success of ICT-enabled initiatives as an anti-corruption strategy will largely depend on implementation, education, culture, and infrastructure, among others [8]. Another factor related to its success is citizen acceptance of ICTs because environmental barriers to ICT adoption can be transnational.

B. DLT employed on the African continent

Digital Ledger Technology (DLT) is seen as a new and fast-evolving approach to record and share data across multiple data ledgers. Single layered ledgers with shared permissions that are accessed and edited by vetted participants on a network are not new but the concept of a decentralized, distributed and immutable ledger was realized for the first time through DLT [1]. DLT has great potential to provide increased public sector accountability [4]. DLT technology has found allies on the African continent in John Magufuli, the President of Tanzania, in 2015; he is a strong proponent in fighting corruption. Nigeria's customs service also uses blockchain technology to assist in the reduction of corruption and increased its revenue collection while Ghana used blockchain technology for the creation of trackable landowner records for unregistered landowners who do not have title deeds [7]. In Kenya, blockchain technology is applied in the financial services sector through micro-lending facilities that enable trust and cooperation among farmers [7]. The Ethiopian Government applied blockchain technology to track coffee exports by implementing genetic sampling of the coffee to identify its origin (the farm on which it was produced), species type, the pesticide used in its production, as well as its exposure to the different chemicals to authenticate the coffee [7].

C. E-government and corruption

E-government can be defined as the application of ICT in delivering government services to its citizens, the business community and across government [9]. Blockchain technologies brought about indirect benefits which include a reduction in bureaucracy, the reduction of paper use, reducing transacting costs, and the reduction and control of corruption which in turn changes a governance eco-system with increased trust from citizens [10]. An exposition of the key features in blockchain and their justified use in e-government is tabulated in Table 1 [10].

Table 1: Features of BCT and use in e-government [10].

Feature	**Justification**
Reduction of human errors	Advance authentication of user devices with identities before accessing the network
Increase in public trust	All network participants are authenticated, and individuals have control over their information
Great scalability	New devices and users can be added to the network automatically following the consensus mechanism because the system can easily scale up.
Improving reliability	Data can only be altered when all participants agree so because of the consensus protocol and data being stored in multiple locations.
Increasing resiliency	The system is resilient to malware, DoS, and DDoS attacks because Single point of failures is avoided
Improving auditability	All transactions remain unchanged in the network making it easy to trace back the history.
Greater verifiability	Validation of transactions by peers participating in blockchain addition
Information ownership	Individual responsibility for authorizing access to their information
Improving access to information	Multiple location storage of information which enhance speed and ease of access
Increasing data quality	Validation in advance of all transaction record in storage on the system with authentication required
Great transparency	All nodes in the network share the same copy of the blockchain is shared by all nodes in the network and transactions are consensus based
Reduction of operational costs	No third party needed in processing transactions
Improving efficiency and speed	All records are subjected to the accessibility privilege and all new transactions are distributed to all participating nodes

Project Khokha (an isiZulu word, meaning 'pay') is an experimental DLT initiative that was introduced by the South African Reserve Bank (SARB) early in 2018, to serve as a mechanism for managing wholesale payments settlement between banks [11].

Reference [12] explain the complex and confusing nature of people, business and government approaches to

Blockchain Technology (BCT) and their hesitant misconception and association with the bitcoin cryptocurrency. Blockchain technology has applications that do not only include cryptocurrencies. Reference [4] contrasts the use of emerging technologies in the fight against corruption and empirically finds that the use of digital public services can be beneficial if it is realized through appropriate infrastructure, regulations, finance, and trained staff availability. Other findings relate to Distributed Ledger Technology (DLT) and blockchain where blockchain's anticorruption impact is seen to be largely untested and that it also poses a challenge to data security and regulation that could enable the transfer of corrupt funds.

The risk of corruption in public procurement is worsened by the increased reliance on public officials in the procurement process, known as the agency problem [13]. Blockchain technology provides a unique method of joining previously unknown parties in database generation and maintenance on a complete and distributed basis [14]. A blockchain framework model can be derived from introducing IoT into traditional objects, converting it into smart objects with key applications related to logistic management functions.

D. Corruption

Corruption, is generally understood as the misuse of public office for private gain, can be a principal (citizens) agent (government officials) problem, where citizens are perceived to be the principals and government officials acting agents on citizens' behalf [4]. As such the principal-agency theory was considered to establish the framework for this study. However, this model is often used by economists in situations where the principal through his/her position induces the agent, to perform tasks that favors the principal and not necessarily those of the agent [15]. However, in an investigation scenario, enabling agents sometimes possesses more power in terms of information and discretion of a political nature on the distribution of resources, which potentially makes room for corruption.

South Africa has been besieged with corruption and malfeasance which recently gained prominence with the commissioning of a State Capture enquiry emanating from a Public Protector report by the same name. With promises of a new dawn and a general onset of corruption fatigue in society, the question on whether corruption can be stopped and if the criminal justice system is still a deterrent remains.

Limited studies have been conducted into the legal and factual perspectives of DLT's usefulness in combatting public sector procurement fraud, as well as legal barriers to its potential use in South Africa. Despite all the media attention that blockchain receives in South Africa, the technology is still in its infancy and its embryonic nature has meant that there has been limited government regulation and scant legal academic exposition on the topic [5]. Blockchain is viewed as a data structure that makes the digital ledger of transactions it hosts tamper-proof while cryptography allows access to add securely to the ledger. Due to these features blockchain can arguably make it possible to reduce or eliminate integrity violations such as fraud and corruption [16]. However, most fraud are committed where human interventions with technology occurs.

E. Conceptual Framework: TOE

This study was underpinned by the Technology-Organization-Environment (TOE) framework for organizational technology adoption [17]. In this study, TOE was used as a guide to interpret collected data for analysis purposes, not for theory development [18]. Factors that influence the use of ICT have been studied by various scholars. Extant literature on the Technology Organization and Environment theory (TOE) provides a broad applicability and possesses explanatory power across several technological, industrial, and national/ cultural contexts [19]. The technological context of the TOE framework relates to the availability of technology to an organization, with a focus on the characteristics of technologies that influence their adoption [21]. The organizational context describes the characteristics of an organization which includes the organization size, its degree of centralization, formalization, the complexity of its managerial structure and the quality of its human resources as well as the amount of slack resources available internally [21]. Factors external to the organization present constraints and opportunities to technological innovation. This external environmental context is the place in which an organization conducts its business within the context of the industry, its competitors, government regulations and relations [20].

III. RESEARCH METHODOLOGY

The study adopted a qualitative approach and sought to evaluate whether ICT is used effectively to combat public procurement corruption. The population sampling was drawn from within the procurement investigations' space. The purpose of this research is exploratory and seeks to establish whether DLT is an effective ICT to combat the scourge of corruption in South Africa.

The sample size for this study was based on practical implications namely the COVID-19 restrictions in place at the time. The total number of investigators dealing with Public Administration investigations in the Public Service Commission is fourteen (14) for both the national office, as well as the nine provincial offices. The collection of data was initiated with an anonymous linked open-ended questionnaire developed with the TOE framework as a guide. The survey instrument aimed to elicit responses on the participants' experiences in using ICT as a tool to investigate procurement corruption. It also sought to understand whether current ICTs are effective and in line with the factors regarding the availability of technology in the TOE framework. A second section of the questionnaire sought to introduce DLT as an ICT to respondents with the intention to evaluate whether they conceive it to be a potential tool for use within the ICT environment to combat

procurement corruption. The questions related to whether the innovative use of ICT to combat public procurement corruption is being considered by management.

The NVivo data analysis tool was used to analyze data as well while memoranda and summaries of all data was recorded. The questionnaire responses were subjected to thematic analysis to find patterns in the data used in conjunction with the conceptual framework. The six-step framework for thematic analysis was seen as the best tool [22]. These steps are familiarization with the data; initial code generation; initial theme generation; reviewing themes; refining, defining and naming themes; and producing the final report.

This research was approved by the University of Cape Town's Ethics in Research Committee.

IV. FINDINGS

In this section the data collected from the nine participants who responded to the semi-structured questions in the anonymous survey are presented. The findings point to a call for better ICT training for investigators, infrastructure investment by doing away with outdated mainframe technology and embracing new technology. The participants are experienced investigators based mainly in Gauteng Province with affiliation or membership to the Association of Certified Fraud Examiners (ACFE). The section is divided into three sections which include the demographics of respondents, the empirical findings on the current use of ICT and its effectiveness and DLT as an ICT option to prevent procurement corruption.

A. Demographics details

During the study period, the COVID-19 pandemic put paid to almost all person-to-person research activities. Thus, an open-ended survey was used instead of interviews. The mean years of experience among respondents were an average of fifteen years as indicated in Table 2 above, with a 75% majority being members of the Association of Certified Fraud Examiners. Respondents were unanimous in defining procurement in the supply chain management function as a source of corruption encountered, in line with extant literature [23].

Table 2: Sample Demographics

P#	Exp (yrs)	Prof?	Losing C-battle?	SCM function where C occurs	RSA lags continent?
P1	15	Yes	Yes	Tenders	Unsure
P2	15	Yes	No	Procurement	N/A
P3	16	No	Yes	Local Govt.	No
P4	15	Yes	Yes	Procurement	Yes
P5	20	No	Yes	Cover quoting	Yes
P6	28	Yes	Yes	Purchasing	N/A
P7	1	No	Yes	Procurement	Yes
P9	14	Yes	No	Procurement	50%
Legend: Exp = Experience (in years); **Prof** = Professional membership					

Seventy-five percent (75%) of respondents share the view that the battle against corruption is being lost. This is strongly evident in responses from (participant 6) who stated "***Yes. Although there are several law enforcement agencies that are actively fighting corruption, the little success of the outcomes is not effective to deter people/officials to commit corruption. So, my answer to this is yes. If officials that are in senior positions are rot, the rest (officials) will also become rotten. If law enforcement and the NPA do not do their part, then justice will not prevail***" and (participant 7) with a view that "***the battle has long been lost. Incompetent staff with a tainted employment record are appointed & the corruption continues***". These views are in contrast with (participant 9) who believes that "***South Africa is slowly getting rid of corruption. But there are some cases that are not solved as a result of lack of knowledge in ICT and DLT***". The data responses support the literature as reflected in the global corruption barometer on the perception that corruption has increased in South Africa [24].

B. Current use of ICT and its effectiveness

In this section we address the first research objective: evaluation of the current effective uses of ICT in the fight against procurement corruption. It is widely accepted that ICT integration leads to open and interactive governments that can develop more responsive policies, improved decision-making and a reduction in corruption and bribery [25]. It is against this background that the responses on the public procurement of goods and services through the National Treasury's Central Supplier Database as the best use of ICT to combat corruption can be understood as not supported because respondents placed their emphasis on current control measures. This is evident in the responses of (participant 6) whose statement that "***No, not at all. The issue has nothing to do with any database. It is all about control measures that must be adhered to, segregation of duties, accountability, integrity, and management that plays a role. The issue is that no one wants to take accountability or discipline their colleagues due to several reasons, which I am not willing to discuss***" and (participant 7) who stated "***No, there has to be a better mechanism & control, allowing a decentralized approach, not impacting service delivery. Software red flagging public servants with interests in enterprises, doing business with the state, for example***".

On analysis of the data, it is evident that the respondents such as (participant 5) believe that "***registered suppliers can also be part of corrupt activities***" while (participant 4) believes "***There are more advanced ways to combat corruption in South Africa***". While the data shows a negative view on the reliance on this database system to combat procurement corruption.

Reference [26] found that attitude was the most decisive factor in explaining the behavioral intention to adopt ICTs such as e-government services in South Africa and this is

confirmed by the data that ICT applications are not optimally used to assist in investigating procurement corruption. This was evident in responses from (participant 3) who stated that "***ICT use is primarily not utilized due to my peer's lack of knowledge of the exploitative capabilities of ICT in the investigation space***", (participant 4) "***No not really. Investigators are not necessarily tech savvy***" and (participant 9) who held that "***most of the investigators lack knowledge on how to use ICT applications***". (Participants 6 & 7) pointed to the need for training: "***The lack of knowledge and embracing new technology***" and lack of innovation "***government red tape & outdated server mainframe technology***", respectively.

The data on participants' perception on whether ICT applications are used effectively in the South African public procurement space elicited negative responses from respondents. (Participant 6 & 3) expressed as examples personal incidents related to "***SAP as an example. It has many controls in place, but in my view, if a person/official is corrupt, no ICT system will prevent it as it will take a human to control/manipulate the system, unless there are user activity logs in place. However, ghost users can be created that will make such a system useless***" and "***The current use of ICT is ineffective in assisting me in the fight against corruption because I have asked for analysis software countless times with no success***". The response from (participant 6), "***It depends what systems and policies are in place and if they employ the correct people to deal with such investigations***" is supported by literature. Reference [20] contends that the technological context of the TOE framework relates to technological availability to an organization with a focus on the characteristics of technologies that influence their adoption. Accordingly, [21] indicate that the availability of technology was a choice, but the need of technology itself was the reason to implement the software in the technological context of the TOE model.

C. Digital Ledger Technology as an ICT option

In this section we address the second research objective: Analyzing how DLT can be used to impact the reduction of procurement corruption. The research points to a need for training. As participant 13 notes: "***Training. Most of the decision makers would agree that DLT is needed but the problem is who can train our corruption busters, where can we find people that are experienced in using it, etc"*** but for less bureaucracy: (participant 4) ***"Training. Most of the decision makers would agree that DLT is needed but the problem is who can train our corruption busters, where can we find people that are experienced in using it, etc"*** and in favor of DLT adoption with better regulations (participant 4) "***Yes, but within a regulatory environment*** "

The advantages of blockchain is that it provides a platform for connecting multiple decision makers with multiple sources of information and generates a richer informational landscape for Operational Management (OM) applications which compliments other ways of collecting and sharing information such as proprietary networked systems, smart sensors, internet, mobile apps while other advantages are the low cost associated with adding new nodes, its data encryption and its record validation [27]. They also note possible disadvantages of using blockchain technology, namely that information may be used for unintended purposes, the difficulty of deleting false records and the difficult management of privacy and access rights. Reference [25] notes the possibilities that Africa can derive from an increased uptake of frontier technologies such as the Internet of Things (IoT), big data and blockchain to address agricultural, health care, educational and social protection needs.

Concerning the respondents' knowledge and understanding on the use of ICTs such as DLT to combat procurement corruption: respondents were gauged and while the concept was not well understood by some with (participant 3) noting "***I have a very vague understanding of DLT. The name perhaps suggests it is software that allows access to an accounting ledger from different access points. However, I have no idea what Blockchain or Ethereum contracts are"***, "***ICT technology that can financially profile employees and prospective suppliers. Computer technology that enables a government vetting agency to trace suspicious payments easily***" and (participant 6) who thinks that "***it is similar to the ledger that banks hold to monitor all the digital transactions we make using fiat currency***", it (DLT) received support for implementation from most respondents but only "***within a regulatory environment***" and the "***retraining of investigators***" according to (participant 4). However, (Participant 3) notes that "***User access to ICT should be restricted as much as possible in the public sector until work ethics are improved***".

The data suggests that respondents were divided on the capabilities of DLT as an implementable ICT, and suggest more awareness and training to happen before its implementation and use, as noted by (participant 6) "***Not if people are not 100% trained or aware of such a application/system but I believe that we have the ability to excel if we embrace the technology"***.

Some respondents think that DLT can make an impact in the fight against corruption in the public procurement sector but point to practical dilemmas that may ensue. (Participant 3) has doubts about DLT use and notes that if "***my understanding of the term is correct, I doubt whether it would positively impact the fight against corruption in the public sector***" because "***DLT applications in South Africa could prove to be disastrous because it would enable public procurement corruption instead of preventing it***". This view is somewhat shared by (participant 9) who states that "***it is not as effective as it could be because with few investigators who capable of using ICT technology"*** and (participant 7) who notes that it can "***Definitely assist with record keeping, especially where evidence was destroyed but may not completely eradicate***" public procurement corruption. Data suggests that some respondents prefer a

neutral wait-and-see stance like (participant 6) who cautiously noted "***Yes and no. What if the transaction is sent to a blockchain ledger in another country and they will not give their cooperation" and therefor "don't think we are ready for this***" technology.? Respondents could not be drawn on whether DLT will have an impact on corruption and were for the most part unsure of recommending the introduction of DLT in public procurement.

V. Discussion

This section discusses the above empirical findings in the light of previous literature and the South African context.

A. Current use of ICT and its effectiveness

The research shows that South Africa lags the rest of the continent when it comes to pioneering the use of effective use of ICT. This is confirmed with a clear response from (participant 9) who indicated that while "***South Africa is the most sophisticated country in Africa. Most of the cyber crimes are committed here and as a pacesetter, South Africa could have implemented DLT long time ago***".

Reference [25] notes the disruption that the innovation and technology development brought on traditional practices ensured an important interactive role between Government and its people. This can be seen in the following South African case studies of e-Government services to prevent corruption. They are:

- The South African Revenue Service (SARS) e-filing system of tax collection and tax administration,
- The smart identification card system with better security features launched by the Department of Home Affairs,
- The National Traffic Information System (NATIS): Car and License Registration functionality for the registration and renewal of motor vehicle services where users reside,
- The State Information Technology Agency (SITA) developing a Government-to-Government (G2G) and Government-to-Citizens (G2C) system. The (G2G) systems which include the Basic Accounting System (BAS), Logistic Management Information System (LOGIS), National Population Register (NPR), Social Pension Fund (SOCPEN), Police Crime Administration System (CAS) and the electronic National Transport Information System (e-Natis). G2G systems developed include Government Websites, Batho Pele Gateway, Department of Labour (DoL) U-Filing and Department of Health (DHA) "Trace and Trace, and
- The mobile telephone penetration that has reached 100% in South Africa and there has been advancement in development of mobile innovations. Mobile applications supporting e-Government services include the Find & Fix mobile application by the Johannesburg Road Agency (JRA) that enables the public to report potholes, faulty traffic signals, storm water drains, manhole covers, and other infrastructure issues related to JRA.

The increased use of ICT service delivery improves efficiency of public institutions, offers wide accessibility to all citizens, promotes transparency and accountability, and also mitigates against corruption. Prior to April 2016, all government departments maintained their own database of suppliers, individuals, and companies from whom it procured goods and services. Due to nepotism, cronyism, fraud and corruption within this public procurement system, the National Treasury called for the establishment and regulation of suppliers, individuals, and companies on its Central Supplier Database (CSD) from which all public procurement was vetted and administered. The CSD system, which came into operation in 2016, allowed for a single registration as a supplier with no physical requirements to submit proof of business registration and tax clearances. However, the change in technology relied on a centrally located mainframe system that required (mostly) slower internet network connectivity, requiring longer access to the database because of increased traffic to a limited set of data. This often resulted in manual retrieval, if data is lost.

Literature confirms that the success of ICT-enabled initiatives as an anti-corruption strategy will largely depend on implementation, education, culture, and infrastructure, among others [8]. Reference [21] includes all aspects related to technology and IT availability, as well as the human resource and IT infrastructure to this anti-corruption strategy.

B. Digital Ledger Technology as an ICT option

The most important feature of DLTs are in the control that several network participants have instead of one entity or participant [1]. This contrasts with the project of centralizing the South African National Treasury Central Supplier Database (CSD). The CSD was centralized because of the corruption that infiltrated its provincial sections. It was viewed as a single layered ledger with shared permissions that were accessed and edited by vetted participants on a network. In contrast the concept of a decentralized, distributed and immutable ledger technology was realized for the first time through DLT [1]. Some of the respondents feared the use of DLT applications in South Africa may aid public procurement corruption instead of assisting in combatting public procurement corruption while a majority was in favor thereof. This is evident in the response from (Participant 3) who noted that "***DLT applications in South Africa could prove to be disastrous because it would enable public procurement corruption instead of preventing it***". The individual influence factor of the TOE theory was also observed.

Technological factors in the TOE theory were observed where respondents pointed to **"*outdated backend main frames & server***" use in when comparing South Africa to the rest of the continent in using of DLT to combat corruption. The data indicates Environmental factor influence to DLT adoption where respondents perceived the lack of knowledge (training), bureaucratic red tape, and outdated technology as barriers to the adoption of DLT to combat public procurement corruption.

The only inference to the possible adoption of blockchain technology in South Africa is found in the experimental

Project Khokha that was initiated in the banking sector by the South African Reserve Bank (SARB) [11]. The aim of the DLT project was to reduce costs associated with reliability and inefficiencies related to availability against cyber-attacks or equipment failure. By replicating the clearing of money transfers and settlements through a permissioned blockchain network the SARB wanted to assess whether the technology improved performance, scalability, and confidential payments of real time simulated payments. Even though the project was successfully modelled its potential was acknowledged by being awarding the distributed ledger initiative by Central Banking Publications.

The barriers to blockchain adoption include the incumbent governments' reluctance to create immutable, transparent records of their activities if such technology will constrain their scope for private gain through corruption. The promised implementation of blockchain to curb procurement corruption will depend on the strength of a South African public and private institutions and their integrity.

Permissioned blockchains require safeguards to terms and policies of organizations and involves the incorporation of pre-approved nodes while permissionless blockchain (public or decentralized blockchains) can be used by anyone who can create and access the blockchain and publish the self-executing contract (smart contract). Therefore, as in the organizational context of the TOE model the adoption of DLT will be hampered. The anonymous nature of cryptocurrencies makes them vulnerable to money laundering and illicit financial regulatory activities, such as drug and human trafficking as well as terrorism which frustrates regulatory prosecutorial efforts. Legality of and uncertain regulations regarding blockchain transactions blockchains' distributive nature gives rise to conflicts of law, jurisdictional issues due to the locations of the nodes and the concurrent liabilities.

VI. CONCLUSION

This research study had as its aim the evaluation of the potential use of distributed digital ledger (DLT) as an ICT tool to detect and possibly prevent public procurement corruption. The study focused on DLT implementation and perceived barriers of its use in a public and private sector environment. Individual user factors such as employing competent people to deal with such investigations and that those investigators were not necessarily tech savvy were identified as a barrier to adoption of DLT in combatting public procurement corruption. The study also discovered that respondents were not knowledgeable on the use of Ethereum contracts in contractual arrangements in the procurement process. A lack of training was identified as a problem due the lack of experience and knowledge in using ICT to prevent and investigate corruption. While some respondents believed that South Africa is the most sophisticated country in Africa, most respondents perceive it to lag the rest of Africa in DLT adoption and as a pace setter could have implemented DLT long time ago.

Individual user factors in the TOE framework model that was used point to implicated individuals that corrupt ICT systems, even those with enforced user logs. Government policy will have to be updated to enforce the monitoring of user activity logs as a measure to combat corruption and particularly to prevent the creation of ghost users which have the potential to render any ICT system useless.

This study has some limitations. Literature on the use of DLT to combat procurement corruption are limited, particularly in the South African environment. A low response rate to the anonymous semi-structured questionnaire was experienced and the cross-sectional nature of the study did not lend itself to observing data over longer period. A longitudinal study would allow for correlational research of variables over a longer period. This would also negate the effects and limitations that COVID-19 placed on researchers to conduct conventional data collection methods in observable setups.

While this qualitative study cannot generalize its findings, it recommends that public procurement corruption can be prevented to a larger extent by an interim government policy enforcing the monitoring of user activity logs as a measure to combat corruption and to assist in preventing corruption in the interim. Furthermore, it is suggested that government initiates action on white paper discussions on the introduction of permissioned DLTs in its procurement system, including its National Treasury Central Supplier Database system.

REFERENCES

[1] H. Natarajan, S. Krause, and H. Gradstein, "Distributed Ledger Technology (DLT) and Blockchain," *FinTech Note*, 1, 2017, pp. 1–60.

[2] P. Sewpersadh and J.C. Mubangizi, "Using the law to combat public procurement corruption in South Africa: Lessons from Hong Kong," *Potchefstroom Electronic Law Journal*, 20(1), 2017, https://doi.org/10.17159/1727-3781/2017/v20i0a1359

[3] S. Kruger, "Journal of transport and supply chain management – Editorial," *Journal of Transport and Supply Chain Management*, 13, 2019, pp. 1–8, https://doi.org/10.4102/jtscm.v13i0.480

[4] I. Adam, and M. Fazekas, "Are Emerging Technologies Helping Win the Fight Against Corruption in Developing Countries?" *Pathways for Prosperity Commission Background Paper Series*, 21, April 2018, p. 34.

[5] V. Brilliantova, and T.W. Thurner, "Blockchain and the future of energy," *Technology in Society*, 57, November 2018, pp 38–45, https://doi.org/10.1016/j.techsoc.2018.11.001

[6] T. Clohessy, H. Treiblmaier, T. Acton and N. Rogers, "Antecedents of blockchain adoption: An integrative framework," *Strategic Change*, 29(5), 2020, pp.501-515, https://doi.org/10.1002/jsc.2360

[7] C. Kombe, A. Sam, M. Ally and A. Finne, "Blockchain Technology in Sub-Saharan Africa: Where does it fit in Healthcare Systems: A case of Tanzania," *Journal of Health Informatics in Developing Countries*, *13*(2), 2019.

[8] J. C. Bertot, P.T. Jaeger and J.M. Grimes, "Using ICTs to create a culture of transparency: E-government and social media as openness and anti-corruption tools for societies," *Government Information Quarterly*, 27(3), 2020, pp. 264–271. https://doi.org/10.1016/j.giq.2010.03.001

[9] J. Chipeta, "A Review of E-government Development in Africa: A case of Zambia," *Journal of E-Government Studies and Best*

Practices, January 2018, pp. 1–13, https://doi.org/10.5171/2018.973845
[10] N. Elisa, L. Yang, F. Chao and Y. Cao, "A framework of blockchain-based secure and privacy-preserving E-government system," *Wireless Networks*, 2018, pp. 1-11*,* https://doi.org/10.1007/s11276-018-1883-0
[11] South African Reserve Bank, "Project Khokha Fintech Report," *Project Khokha*, 2018, pp. 1–80.
[12] C. Aristidou and E. Marcou, "Blockchain standards and government applications," *Journal of ICT Standardization*, *7*(3), 2019, pp. 287–312, https://doi.org/10.13052/jicts2245-800X.736
[13] S. Williams-Elegbe, "Public Procurement, Corruption and Blockchain Technology in South Africa: A Preliminary Legal Inquiry," *SSRN Electronic Journal,* 2019, https://doi.org/10.2139/ssrn.3458877
[14] B. Q. Tan, F. Wang, J. Liu, K. Kang and F. Costa, "A blockchain-based framework for green logistics in supply chains," *Sustainability*, 12(11), 2020, p. 4656, https://doi.org/10.3390/su12114656
[15] T. M. Okello and A Kihara, "Effect of Procurement Lifecycle on Performance of Government Ministries in Kenya," *International Journal of Supply Chain and Logistics*, 3(2), 2019, pp.105–128.
[16] N. Kshetri, "Will blockchain emerge as a tool to break the poverty chain in the Global South?" *Third World Quarterly*, 38(8), 2017, pp. 1710–1732, https://doi.org/10.1080/01436597.2017.1298438
[17] R. DePietro, E. Wiarda and M. Fleischer, "The context for change: Organization, technology and environment", in L.G. Tornatzky and M. Fleischer, (Eds.) *The processes of technological innovation*, Lexington Books: Lexington, MA., 1990, pp. 151–175.
[18] I. Korstjens and A. Moser, "Series: Practical guidance to qualitative research. Part 4: Trustworthiness and publishing," *European Journal of General Practice*, 24(1), 2018, pp. 120–124. https://doi.org/10.1080/13814788.2017.1375092
[19] Y.K. Dwivedi, M.R. Wade and S.L. Schneberger, *Informations Systems Theory: Vol.2*. Springer, 28 November 2012, 461. https://doi.org/10.1007/978-1-4419-6108-2
[20] I. Arpaci, Y.C. Yardimci, S. Ozkan, and O. Turetken, "Organizational Adoption of Information Technologies: A Literature Review," *International Journal of EBusiness and EGovernment Studies*, 4(2), 2012, pp. 37–50.
[21] A. Ahmi, and S. Kent, "The utilisation of generalized audit software (GAS) by external auditors," *Managerial Auditing Journal*, 28(2), 2013, pp. 88–113. https://doi.org/10.1108/02686901311284522.
[22] V. Braun and V. Clarke, "Using thematic analysis in psychology," *Qualitative Research in Psychology*, 3(2), 2006, pp. 77–101, https://doi.org/10.1191/1478088706qp063oa
[23] K.O. Odeku, "Endemic corruption in supply chain and procurement in the local sphere of government in South Africa," *Journal of Distribution Science*, 16(9), 2018, pp.43–52, https://doi.org/10.15722/jds.16.9.201809.43
[24] C. Pring and J. Vrushi, "Global Corruption Barometer Africa: Citizen's Views and Experiences of Corruption," In *Afrobarometer*, 2019.
[25] United Nations, "E-Government Survey 2020. Digital Government in the Decade of action for sustainable development," In *UN E-Government Knowledgebase,* 2020, publicadministration.un.org
[26] S.F. Verkijika and L. De Wet, "E-government adoption in sub-Saharan Africa," *Electronic Commerce Research and Applications*, 30*,* February 2018, pp. 83–93, https://doi.org/10.1016/j.elerap.2018.05.012
[27] V. Babich and G. Hilary, "Blockchain and other distributed ledger technologies in operations," *Foundations and Trends in Technology, Information and Operations Management*, 12(2–3), 2019, pp. 152–172, https://doi.org/10.1561/0200000084

4th Workshop on Data Science in Health, Ecology and Commerce

DATA Science in Health, Ecology and Commerce is a forum on all forms of data analysis, data economics, information systems and data based research, focusing on the interaction of those three fields. Here, data-driven solutions can be generated by understanding complex real-world (health) related problems, critical thinking and analytics to derive knowledge from (big) data. The past years have shown a forthcoming interest on innovative data technology and analytics solutions that link and utilize large amounts of data across individual digital ecosystems. First applications scenarios in the field of health, smart cities or agriculture merge data from various IoT devices, social media or application systems and demonstrate the great potential for gaining new insights, supporting decisions or providing smarter services. Together with inexpensive sensors and computing power we are ahead of a world that bases its decisions on data. However, we are only at the beginning of this journey and we need to further explore the required methods and technologies as well as the potential application fields and the impact on society and economy. This endeavor needs the knowledge of researchers from different fields applying diverse perspectives and using different methodological directions to find a way to grasp and fully understand the power and opportunities of data science.

This is a joint track by WIG2, the Scientific Institute for health economics and health service research, the Information Systems Institute of Leipzig University and the Helmholtz Center for Environmental Research.

Topics

We embrace a rich array of issues on data science and offer a platform for research from diverse methodological directions, including quantitative empirical research as well as qualitative contributions. We welcome research from a medical, technological, economic, political and societal perspective. The topics of interest therefore include but are not limited to:

- Data analysis in health, ecology and commerce
- Data analysis in climate change adoptation
- Data analysis in commerce
- (Health) Data management
- Health economics
- 5G(/6G) in health
- Data economics
- Data integration
- Semantic data analysis
- AI based data analysis
- Data based health service research
- Smart Service Engineering
- Integrating data in integrated care
- AI in integrated care
- Spatial health economics
- Risk adjustment and Predictive modelling
- Privacy in data science

Technical Session Chairs

- **Franczyk, Bogdan,** University of Leipzig, Germany
- **Militzer-Horstmann, Carsta,** WIG2 Institute for health economics and health service research, Leipzig, Germany
- **Häckl, Dennis,** University of Leipzig, Germany and WIG2 Institute for health economics and health service research, Leipzig, Germany
- **Bumberger, Jan,** Helmholtz-Centre for Environmental Research – UFZ, Germany
- **Reinhold, Olaf,** University of Leipzig / Social CRM Research Center, Germany

Program Committee

- **Alpkoçak, Adil,** Dokuz Eylul University
- **Ansari, Alireza,** Leipzig University, Germany and IORA Regional Center for Science and Technology Transfer, Iran
- **Arruda Filho, Emílio José Montero,** Universidad Federal do Para and University of Amazon, Brazil
- **Dey, Nilanjan,** Techno India College of Technology, India
- **Fass, Eric,** WIG2 Institute for Health Economics and Health Service Research
- **Hernes, Marcin,** Wroclaw University of Economics and Business, Poland
- **Kozak, Karol,** Fraunhofer and Uniklinikum Dresden, Germany
- **Müller, Marco,** WIG2 Institute for Health Economics and Health Service Research
- **Popowski, Piotr,** Medical University of Gdańsk, Poland
- **Rot, Artur,** Wroclaw University of Economics and Business, Poland
- **Sachdeva, Shelly,** National Institute of Technology Delhi, India
- **Siennicka, Agnieszka Wroclaw Medical University,** Poland

- **Timpel, Patrick,** WIG2 Institute for Health Economics and Health Service Research, Leipzig, Germany and Technical University Dresden, Germany
- **Wasielewska-Michniewska, Katarzyna,** Systems Research Institute of the Polish Academy of Sciences, Poland

Communication Papers of the of the 17th Conference on Computer Science and Intelligence Systems pp. 233–240
DOI: 10.15439/2022F20
ISSN 2300-5963 ACSIS, Vol. 32

Financial News Effect Analysis on Stock Price Prediction Using a Stacked LSTM Model

Alexandre Heiden
Santa Catarina State University
Graduate Program in Applied Computing
Joinville, SC – Brazil
Email: alexandreheiden@hotmail.com

Rafael Stubs Parpinelli
Santa Catarina State University
Graduate Program in Applied Computing
Joinville, SC – Brazil
Email: rafael.parpinelli@udesc.br

***Abstract*—In the age of information, it is understood that social media provides valuable reference for many contexts, including the financial market. Although having high volume, publications on social media are not necessarily reliable. In this context, this research aims to examine the influence of financial news coming from a more transparent source, the newspaper The New York Times. This source provides fact-checked news, but the volume of information is lower compared to social media. The strategy proposes a difficult challenge, the application of a Machine Learning model on a limited dataset. The LSTM-based stock price prediction model proposed has two features, news sentiment and historical data of the assets. Experiments indicate that the model performs better when the news' sentiments are considered and demonstrates potential to accurately predict stock prices up to around 35 days into the future, comparing the results obtained with the real prices on the period.**

I. Introduction

THE formidable technology present in the current financial market provides a great quantity of indicators for the investors to guide their decisions in a more positive way. This information requires resources to be processed and analyzed, resources that are dominated by big fintechs and usually lacks in the hands of the small investors. An investor without tools faces uncertainty towards their investment decisions, due to the high volatility of the stock market.

This volatility is explained due to the fact that the stock price depends directly on the decisions taken by the companies [1], decisions that are unpredictable to some extent, supported by the high competitiveness of the market. The market requires adaptability from the investors to build a portfolio able to balance the risk and return factors. To achieve this, investors have a framework of mathematical models, which can help them building their portfolio.

The primordial attempt to abstract the responsibility of the analysis and decision-making of the investor was the development of the Portfolio Optimization Problem (POP). The fundamentals to the problem revolves around optimally allocating an amount of capital based on the historical stock prices time series, in order to maximize the portfolio returns. Several models have already been implemented to solve this problem [2].

While POP provides enough tools to analyze the current state of the market, the future is completely undefined. The results gathered using an ordinary POP model are not able to truly determine the next movements of the market. To accomplish this, the model needs to analyze not only the historical prices of the assets, but also more market indicators.

Recently, Machine Learning (ML) models have been studied and developed to take an even more ambitious step in the area of investment portfolio optimization: the stock price prediction. The ML models can be trained using a wide array of factors, including but not limited to financial news related to companies and socio-economic factors. These models are generally used to predict the stock price movement during a period of time, in order to aid the investor's decision-making process. The predominant techniques are based on supervised learning models, such as bagging, boosting ensemble classifiers, and Artificial Neural Networks (ANN) for making stock price predictions.

In this research, along with the classic indicator, being the historical data of the assets prices, the model developed is paired with the sentiment analysis of financial news related to the companies, collected from the newspaper The New York Times. The model is based on the Long Short-Term Memory (LSTM) artificial recurrent neural network, which is properly tuned with an AutoML strategy in order to verify the effect of news sentiment on the results and to predict raw stock prices on a pre-defined time window.

The literature showcases a few studies confirming the relevance of news sentiments in the stock price prediction process, but the majority of the results are only applied on a theoretical scope. These assertions should only be truly accepted if the model results are also replicated in a real investment scenario, to create evidence of the news sentiments' relevance and also investigate the longevity of the accuracy of the predictions generated by the model.

For this reason, the predictions generated are applied in a real investment scenario, using a risk/return strategy for the creation of portfolios based on the predicted stock price values, in order to evaluate the ability of the model in creating portfolios with high accuracy for a relatively long period of time. The experiments indicate the possibility of maintaining high accuracy up until around 35 days in the future when the model considers the investors' general sentiments acquired via financial news.

The remainder of this paper is organized as follows. Section 2 briefly discusses the relevancy of the study and further details on the stock price prediction approaches; Section 3 displays related work on the area; Section 4 elaborates the architecture and characteristics of the proposed model; Section 5 discusses about the validation and results of the model; and Section 6 points out the conclusions, limitations of this study and future work.

II. Background

A. Sentiment Analysis

At least in a financial context, it is hard to evaluate the efficiency of a sentiment analysis model individually. It is difficult to evaluate this component by itself due to the fact that it cannot be treated as a detached component, because the result of the sentiment analysis model is directly consumed by the prediction model. Furthermore, sentiment analysis models are usually generic, with no evidence displaying a better performance for a specific scenario, in this case, on financial news. The only factor that can truly influence the choice of a sentiment analysis model is the database selected, as there are faster models (for databases with large volume, such as Twitter) and more robust models (for databases with small volume, such as newspapers).

B. Valence Aware Dictionary for Sentiment Reasoning (VADER)

In order to workaround the lack of information, a sentiment analysis model that works well with a small database should be applied when working with a newspaper as source of news. The VADER sentiment analysis model accomplishes this need and is explored in this work, because the model does not require a large database to achieve high accuracy [3].

The creators of VADER have demonstrated the model's potential by comparing it with several other strategies. The results were better than all of them, both for an analysis of comments on social networks and for analysis of newspaper news. Although VADER is not specially designed to work in an investment market scope, the results showed great generalization. The application of the model on this paper will verify VADER's efficiency on a purely financial context.

C. Stock Price Prediction

Prediction methods generally fall into three categories: fundamental analysis, technical analysis or Machine Learning.

Technical analysis denotes the study of past prices, using charts as the main tool. This analysis assumes that market reactions to news are instantaneous and therefore does not take them into account in its attempts at predictions. The objective of technical analysis is to identify patterns in historical series, in order to anticipate changes in the market [4].

Fundamental analysis looks at indicators that affect supply and demand in the market. The idea is to collect and process the information before it reflects its consequences in the market. This in-between represents an opportunity to dispose of stocks that are about to go down or buy stocks that are about to go up. This type of analysis uses data about companies to predict market movements, with news as the main source.

Machine Learning denoted a transition to more technological and robust prediction models. It is very common for ML-based strategies to overlap the fundamental analysis concept, as the models generally use a number of indicators and/or an amount of market data. ML techniques are also useful to analyze how the stocks behave when subject to different market scenarios, in order for the investors to be able to make decisions with more confidence.

D. Long Short-Term Memory (LSTM)

Unlike sentiment analysis, the predictive model has an approach that stands out. Recent studies indicate that the LSTM network, an architecture specially designed to process data in the form of historical series, has better performance than the other identified models [5], but there is a lack of evidence to prove that the results are good enough to generate efficient portfolios scenarios with real data.

What makes the LSTM artificial neural network stand out from the other models is the ability of identifying long-term dependencies, as long as the training data is properly segmented into sub-sequences with a well-defined beginning and end [6]. This requirement is fulfilled when analyzing any kind of historical series, as any sequential subset of the series can be effectively listed as training data. The model's performance is directly affected by the quantity and size of these subsets: a model with a small number of subsets or with a window too short could have it's memorization capacity inhibited and, on the other hand, a model with a large number of subsets or with a window too large could suffer an execution bottleneck during model training.

III. Related Work

Stock price prediction is an inherently complex task due mainly to the volatility of the investment market [7]. Since the investment market presents the possibility of large returns in a relatively short period of time, naturally it draws a lot of interest. Researchers from all around have presented several different approaches to tackle the problem.

Rana, Uddin, and Mhoque [8] proposed three prediction models: Linear Regression (LR), Support Vector Regression (SVR), and LSTM. The authors compared the three models and highlighted the superiority of the LSTM model. For the LSTM model, different activation functions and optimizers were paired, reaching the conclusion that the combination that generated the best accuracy was the activation by Hyperbolic Tangent with the Adam optimizer.

Du and Tanaka-Ishii [9] created their own sentiment analysis model and applied on news extracted from the Wall Street Journal (WSJ) and the Reuters & Bloomberg database (R&B), weighting each news item in relation to its respective stock. The authors used a Multi Layer Perceptron (MLP) for the prediction model and the results were computed by an optimization model based on the classic Markowitz model [10]. The authors evaluated their strategy observing 18 selected stocks

from the American market. Their model obtained better results for the R&B database than other models on the literature.

The work of Xing, Hoang, and Vo [11] shows a prediction model based on an MLP network, which is applied on the currency trading scenario. The authors attempt to predict the appreciation or not of the US Dollar and the Euro. The analysis performed by the authors is extremely complete, and by comparing their results on several investment fronts, they confirm the predictive power of a model using high frequency news without any kind of technical analysis.

Maqsood *et al* [12] proposed a Convoluted Neural Network (CNN) model to work with the 4 major stocks from the US, Hong Kong, Turkey and Pakistan. The model uses historical series of stocks and a simple sentiment analysis strategy based on the proposal of the SentiWordNet lexical resource, mapping sentiments from Twitter publications in a dictionary of 4000 words. The authors concluded that not all events impact the financial market, but the sentiment analysis implemented is too simple for this statement to be generalized.

Patil, Wu, Potika, and Orang [13] combined graph theory with CNN analyzing spatiotemporal relationships between different stocks, modeling the financial market as a graph. The model used financial indicators and news as input to predict prices for 30 US stocks. The results indicate that the application of graph theory produces better results than ordinary statistical models for time series prediction.

Jin, Yang, and Liu [14] implemented an LSTM model for predicting Apple stock prices. The model applies a type of decomposition to the historical price series, in order to simplify the sequences and make them more predictable. A CNN model was developed for binary categorization (positive, negative) of posts from a forum to make the prediction model more robust, considering the content of posts. The model showed good results, but it is not possible to generalize any results due to the fact that the experiments were performed with only one stock.

An overview of the works can be seen in Table I. The focus of the research was precisely works that combine sentiment analysis with price prediction, so most of the materials present in the table explore both premises. Differences between works in terms of study scenario, algorithms used, and evaluation metrics are also highlighted in the table. There is considerable heterogeneity in the choice of sentiment analysis model, indicating that the application scenario strongly influences the choice of model. For the prediction model, CNN and LSTM stand out, having studies with relevant and recent contributions. At the end of the table, in bold, the model proposal for this work is presented.

IV. Proposed Model

The essence of the model presented in this work is highlighted in two steps: sentiment analysis and price prediction. Both stages have different requirements and will end up working together.

The first stage, sentiment analysis, has the purpose of processing the raw news of the companies studied to define the position of investors during the period studied. The values obtained are used to create the training and validation samples necessary for the model.

The second stage, stock price predictions, has the goal of developing a prediction model intelligent enough to generalize results to all studied stocks, which represent a subset of the universe of assets on a stock exchange.

A. Database Description

The experiments are carried out with the historical series of assets that make up the Top 50 of the S&P Index, with indicators for the first quarter of 2021. The stocks considered are presented in Table II.

All the data used in this research is publicly available, the historical series of assets being extracted from Yahoo Finances and the news from the New York Times newspaper's API. The period studied starts in January 1, 2016 and ends in December 31, 2020. In the 5 years considered, a maximum of 500 news per asset were extracted, with priority for the most relevant news from the section with the theme "finance". The number 500 was selected empirically, as the majority of the companies studied did not have more than 500 news on the period considered.

The separation between training and validation data is not done randomly, a strategy commonly applied in artificial neural networks. As the data is a historical series, the values are dependent on their predecessors, for example: the price of the day d depends directly on the price of the days $d-1$, $d-2$ and so on, therefore, the separation of the sets is carried out according to the closing date. The training/validation split is given at $80/20$, culminating in the years 2016-2019 being used for training and the year 2020 being used for validation.

TABLE I
Main Approaches Identified in Literature

Reference	Scenario	Sentiment Analysis	Prediction Model	Evaluation Metrics
[8]	Spain	-	LR, SVR, LSTM	RMSE
[9]	USA	Original	MLP	Return
[11]	Exchange	BERT	MLP	Accuracy
[12]	USA, Hong Kong, Turkey, Pakistan	SentiWordNet	CNN	RMSE, MAE
[13]	USA	-	Graphs + CNN	RMSE, MAPE, MAE
[14]	USA	CNN+word2vec	LSTM	MAE, RMSE, MAPE
This work	**USA**	**VADER**	**LSTM**	**RMSE, MAPE**

B. Portfolio Selection

To analyze the results on a real investment scenario, the predictions generated are subjected to a portfolio selection strategy. This strategy is unrelated to the model, and is only used as a performance measure.

With the predictions value at hand, it is possible to calculate the expected returns for every asset, as well as the measured risk. By calculating the risk and return, portfolios can be selected in three different ways: (I) maximizing returns; (II) minimizing risk, and (III) maximizing return/risk ratio.

Maximizing returns is the most aggressive strategy, as the risk values are not considering at any point of the portfolio selection. In the other hand, minimizing risk is the most conservative strategy. The strategy used in this work is to maximize the return to risk ratio, which aims to pick the assets producing high returns while offering a somewhat low risk. In order to add security to the portfolio, it is good practice to dilute the investment in a number of assets. This number represents the portfolio's cardinality (k). There is not a set in stone to find the value for k, but there is evidence that k should always be at least 3 [15], which is the value for the cardinality in this research.

C. Model Operation

In the sentiment analysis stage, the news of each asset were individually submitted to the VADER model, resulting in a sentiment value calculated for every news. This value is in the $[-1, 1]$ interval, with $s = -1$ representing the most negative sentiment possible, 1 representing the most positive sentiment possible and 0 representing a completely neutral sentiment.

As 500 news are considered for every year, some days will necessarily have more than one news for an asset. In these cases, the average of the news' sentiments is calculated for those specific days. There is also the possibility of a day having no news for an asset. In these cases, the neutral value $s = 0$ is considered.

The product of this stage is the calculation of sentiment values for each closing day for each analyzed asset. These values are fundamental for the creation of training and validation samples on the next step. The samples have the sentiment values and historical stock prices for every asset.

In the price prediction stage, the LSTM model is implemented. An ordinary LSTM model consists of three layers: a regular input layer, an LSTM layer of size n, and a dense layer with a single node, responsible for the consolidation of the LSTM layer output into a palpable prediction value. The model proposed in this work has an additional LSTM layer. Stacking LSTM layers has an interesting trade-off: it allows the model to represent more complex patterns, but increases the computational cost of every epoch. The architecture was defined empirically.

TABLE II
TICKERS CONSIDERED

AAPL	ABBV	ABT	ACN	ADBE
AMZN	AVGO	BAC	BRK-B	CMCSA
COST	CRM	CSCO	CVX	DHR
DIS	FB	GOOG	GOOGL	HD
INTC	JNJ	JPM	KO	LLY
MA	MCD	MDT	MRK	MSFT
NEE	NFLX	NKE	NVDA	ORCL
PEP	PFE	PG	PM	PYPL
T	TMO	TSLA	TXN	UNH
V	VZ	WFC	WMT	XOM

D. Parameter Tuning

One of the most important and difficult to tackle problems when working with ML algorithms is parameter tuning. An ordinary ML algorithm has a set of adjustable parameters, a fact that is also common to the model in this work. In the design of any ANN, the number of layers must be adjusted, the size of each layer, which training algorithm will be used, as well as other parameters.

The fact is that in the face of an universe of adjustable parameters, an infinite number of configurations can be established. Training a ML model until it reaches convergence is a time consuming process, so training a large number of configurations is completely unfeasible. There are strategies to reduce the amount of configurations to be trained, such as empirical experiments and sub-divisions of the search space.

There is also the possibility of applying Auto-ML, algorithms that configure the parameters of a model automatically. These algorithms abstract much of the manual decision-making during the adjustment, but it is interesting that at least some empirical testing is done beforehand to define the intervals where the algorithm should search. In this work, the *Hyperband* algorithm from the *KerasTuner* library is applied to perform the parameter adjustment.

The empiric tests performed beforehand indicates that the model's architecture should have no more than four layers, two of them being hidden layers and the remaining two being the input and output layers [16]. The hyperparameters subjected to tuning are:

- Number of nodes in the LSTM layers: minimum 16 nodes, maximum 128 nodes, with a step of 16 nodes;
- Learning rate: values of 10^{-2}, 10^{-3}, and 10^{-4};
- Window size: minimum 30 days, maximum 120 days, with a step of 30 days.

This generates a set of $8 * 8 * 3 * 4 = 768$ combinations of configurations, a number rather large of models needed to be tuned. Hyperband's ability of computing models with early stopping and remarkable speedup prove to be almost a necessity on a scenario with this many possible configurations.

V. EXPERIMENTS & RESULTS

The general idea of the experiments on this paper are summarized to four points: (I) parameter tuning of the proposed model; (II) analysis of financial news influence on the prediction model; (III) generation of stock price predictions for a set time window, and (IV) application of the generated predictions on a real investment scenario.

The model was implemented using the Python language and all experiments were carried out in a controlled environment, in equipment with the following specifications: Intel i7 Core™ i7-4770 processor operating at 3.9 GHz, with 16 Gigabytes of RAM and running a GNU/Linux operational system with kernel 4.8.10.

A. Parameter Tuning

Before submitting the model to any experiments, the calculation of the news' sentiments was performed with the VADER model, using the implementation exposed by the creators in [3]. This stage is not necessarily a part of the LSTM model itself, but is necessary to create the input data.

With the sentiments calculated and paired with the historical series of the stocks, the LSTM model has all the data necessary for it to be fitted. The execution hyperparameters are refined using the strategy defined on Section IV-D. This is performed for both the model without sentiment values as a feature and with. Hyperband was executed with a factor of $f = 2$ and a total budget of $e = 10000$ epochs for a total of 50 times and the results were collected.

1) Results for the Model without Sentiments: The five best configurations generated for the model without sentiments are presented on Table III, from best (1) to worst (5), based on their Mean Absolute Percentage Error (MAPE) values, a performance metric which measures the model accuracy as a ratio. The model was fitted for 100 epochs using these configurations 50 times each, having the value for MAPE calculated. The mean of the results for the 50 trials of each configuration is shown on Fig. 1.

TABLE III
BEST CONFIGURATIONS GENERATED BY HYPERBAND FOR THE MODEL WITHOUT SENTIMENTS

Label	Layer #1	Layer #2	Learning Rate	Window Size
1	64	48	10^{-2}	60
2	48	48	10^{-2}	60
3	32	48	10^{-2}	90
4	48	32	10^{-2}	120
5	48	48	10^{-2}	30

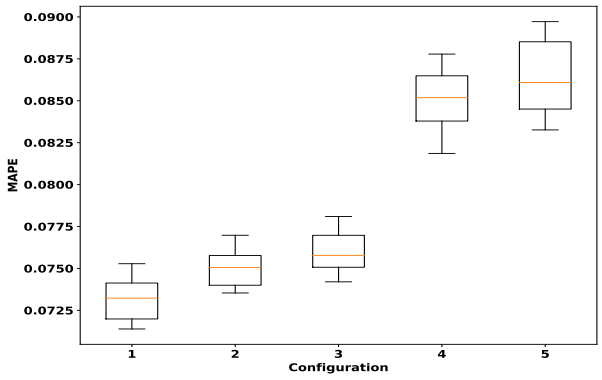

Fig. 1. MAPE for the 5 Best Configurations

TABLE IV
ONE-FACTOR ANOVA FOR CONFIGURATIONS 1 AND 2

Source	SS	df	MS	F	p-value
Treatment	0.0002	2	0.0001	83.2989	1.1102×10^{-16}
Error	0.0002	147	0		
Total	0.0004	149			

Configurations (1), (2), and (3) stand out from (4) and (5), specially configuration (1), which has the best results for MAPE. An one-factor ANOVA test is applied on the samples for configurations (1), (2), and (3) to verify if the difference between samples are statistically significant. Table IV presents the results, which suggests that at least one treatment is significantly different with a significance level of $\alpha = 0.05$. To identify the difference in between each treatment, a post-hoc test such as the Tukey HSD is indicated on this situation.

To run the Tukey test based on the $k = 3$ treatments, $df = 147$ degrees of freedom for the error and significance levels $\alpha = 0.01$ and $\alpha = 0.05$, the critical values $Q_{\alpha=0.01}^{k=3,df=147} = 4.1850$ and $Q_{\alpha=0.05}^{k=3,df=147} = 3.3487$ are obtained, respectively. To find the value for the Tukey HSD Q statistic, the Equations 1 and 2 are calculated.

$$Q_{i,j} = \frac{|\bar{x_i} - \bar{x_j}|}{s_{i,j}} \tag{1}$$

$$s_{i,j} = \frac{\sigma_\epsilon}{\sqrt{H_{i,j}}} \tag{2}$$

$H_{i,j}$ is the harmonic mean of the observations from configurations (i) and (j). σ_ϵ is the square root of the mean squared error calculated on the ANOVA test precursor of the Tukey test. The results, shown in Table V, assert the ANOVA test by confirming statistical difference for every pair of configurations. Therefore, configuration (1) is proven to be statistically better than configurations (2) and (3) and is used for the remaining experiments.

2) Results for the Model with Sentiments: Similarly, the experiment is performed for the model with sentiments. The five best configurations generated are presented on Table VI, from best (1) to worst (5). MAPE is calculated on the same way and is shown on Fig. 2.

It looks like the best configuration outperforms the remaining configurations by quite a margin, even the runner-up. Both the minimum value and the median are better for configuration (1). Selecting configurations (1) and (2), the one-factor ANOVA test is applied to verify if the difference

TABLE V
TUKEY HSD FOR CONFIGURATIONS (1) AND (2)

Pair	Tukey HSD Q	p-value	Inference
(1), (2)	11.7179	$p < 10^{-3}$	Significant
(1), (3)	17.9798	$p < 10^{-3}$	Significant
(2), (3)	6.2618	$p < 10^{-3}$	Significant

TABLE VI
BEST CONFIGURATIONS GENERATED BY HYPERBAND FOR THE MODEL WITH SENTIMENTS

Label	Layer #1	Layer #2	Learning Rate	Window Size
1	48	48	10^{-2}	60
2	48	64	10^{-2}	60
3	16	48	10^{-2}	90
4	48	16	10^{-2}	120
5	16	48	10^{-2}	30

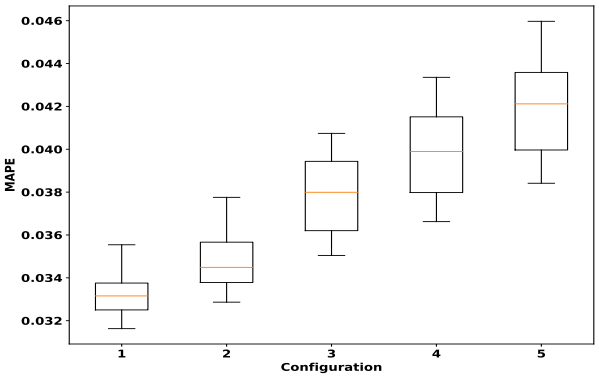

Fig. 2. MAPE for the 5 Best Configurations

between the samples are statistically significant. Table VII shows the test results, which suggests the treatments are indeed significantly different with a significance level $\alpha = 0.05$.

With the data acquired on the ANOVA test, a Tukey test was carried out to confirm the difference between the pair of configurations (1) and (2). For the test with $k = 2$ treatments, $df = 98$ degrees of freedom for the error and significance levels $\alpha = 0.01$ and $\alpha = 0.05$, the critical values $Q_{\alpha=0.01}^{k=2,df=98} = 3.7150$ and $Q_{\alpha=0.05}^{k=2,df=98} = 2.8065$ are obtained, respectively. With the values at hand, the confidence limits for the pair of configurations are set and the Tukey HSD Q are calculated, using Equations 1 and 2.

The final result is shown on Table VIII. The tests confirms the hypothesis from ANOVA, reassuring that configurations (1) and (2) are statistically different. Therefore, configuration (1) is proven to be statistically better than configuration (2) and is used for the remaining experiments.

B. Analyzing Financial News Influence

The first tests after establishing the tuning of the model aims to investigate the influence of applying news sentiments to historical series to make predictions. The model, with

TABLE VII
ONE-FACTOR ANOVA FOR CONFIGURATIONS 1 AND 2

Source	SS	df	MS	F	p-value
Treatment	0.0001	1	0.0001	34.8378	5.1488×10^{-8}
Error	0.0002	98	0		
Total	0.0002	99			

TABLE VIII
TUKEY HSD FOR CONFIGURATIONS (1) AND (2)

Pair	Tukey HSD Q	p-value	Inference
(1), (2)	8.3472	$p < 10^{-3}$	Significant

tuning referring to the best configurations without and with sentiments identified on Section V-A, was executed 50 times without the sentiment attribute and 50 times with the sentiment attribute, on the dataset containing the 5 years of series historical and news stories. Root Mean Squared Error (RMSE) was calculated at the end of each execution for every ticker, as well as the average of the normalized RMSE, represented by RMSE-N. The objective of normalizing the RMSE is to mitigate the discrepancies generated by the gross share price: a company with more expensive shares has a higher RMSE than a company with cheaper shares, even in scenarios where the proportional error is smaller. The average RMSE-N values calculated for each asset are shown in the Table IX.

The results show superiority of the model using sentiments as a feature, having a better performance for every ticker analyzed. The RMSE-N values are similar for every ticker, indicating the capabilities of generalization from the model. To confirm the results on Table IX, on Fig. 3 the boxplots referent to the RMSE-N values for the 50 tickers are presented. The mean of the RMSE-N is approximately three times higher for the model without sentiments as a feature, certifying the efficiency of the application of news' sentiments.

Furthermore, to validate the hyperparameters tuning, the average of training and validation losses curves for the 50 runs of the model with sentiments feature are displayed on Fig. 4. Results show both curves decaying to a certain point of stabil-

TABLE IX
MODELS COMPARISON (WITH AND WITHOUT SENTIMENT FEATURE)

	RMSE-N			RMSE-N	
Ticker	Without	With	Ticker	Without	With
AAPL	0.16217	0.03641	MA	0.17366	0.05188
ABBV	0.09216	0.04734	MCD	0.08461	0.04920
ABT	0.14920	0.05156	MDT	0.06753	0.05126
ACN	0.15730	0.04010	MRK	0.18300	0.06483
ADBE	0.23952	0.04764	MSFT	0.21505	0.04691
AMZN	0.17517	0.05637	NEE	0.17395	0.05358
AVGO	0.07489	0.03368	NFLX	0.20258	0.05361
BAC	0.18811	0.05210	NKE	0.08748	0.03864
BRK-B	0.19654	0.06785	NVDA	0.16485	0.04028
CMCSA	0.11541	0.04631	ORCL	0.10840	0.04493
COST	0.32205	0.04946	PEP	0.09034	0.05540
CRM	0.17471	0.04560	PFE	0.05463	0.05287
CSCO	0.13646	0.06998	PG	0.18623	0.05203
CVX	0.16035	0.05146	PM	0.33774	0.05437
DHR	0.17426	0.03413	PYPL	0.13417	0.03225
DIS	0.04160	0.03896	T	0.11346	0.05044
FB	0.10427	0.05738	TMO	0.19514	0.03491
GOOG	0.16468	0.04464	TSLA	0.09386	0.06502
GOOGL	0.17081	0.04911	TXN	0.21595	0.05035
HD	0.08458	0.04226	UNH	0.15182	0.04465
INTC	0.25737	0.06388	V	0.18331	0.06031
JNJ	0.11604	0.07057	VZ	0.12535	0.07817
JPM	0.19586	0.05880	WFC	0.13376	0.03780
KO	0.05499	0.06043	WMT	0.24476	0.05127
LLY	0.23789	0.11573	XOM	0.21062	0.04595

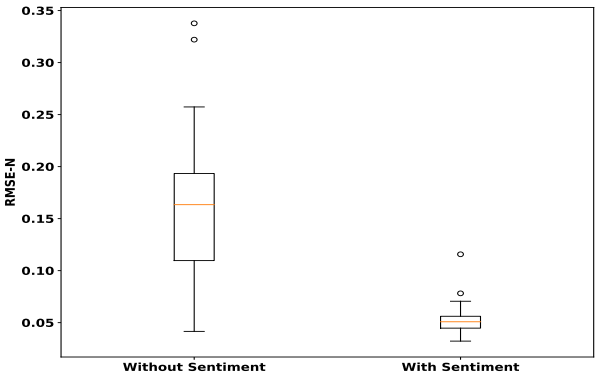

Fig. 3. RMSE-N for the 50 Stocks for the Model with and without Sentiment

ity, with a small gap between them. The first fact indicates that the model was trained enough to generalize well with the data input, and continuing the training would eventually culminate in over-fitting. The second fact is expected, since the model's loss for training should be lower than the loss for validation. The results indicate that the model is well trained.

C. Predicting Stock Prices into the Future

The main objective of the model is predicting stock prices for the 50 tickers analyzed. As explained before, the LSTM model works with a window size to represent the memorization capacity. This is crucial to understand why is it so difficult to predict prices into the future: the model has to operate with limited points of real data.

In this experiment, the model is used to predict the stock prices for the next 50 days for every ticker. The RMSE-N of the predictions generated are listed in Table X. As expected, the RMSE-N values are noticeably higher for the predictions, since the model works with data not used during the training process. Naturally, creating the predictions outside of the training scope is the biggest challenge for the model, and a decrease in accuracy is expected as the predictions distance themselves from the training scope, in other words, the further into the future, the worse the quality of predictions.

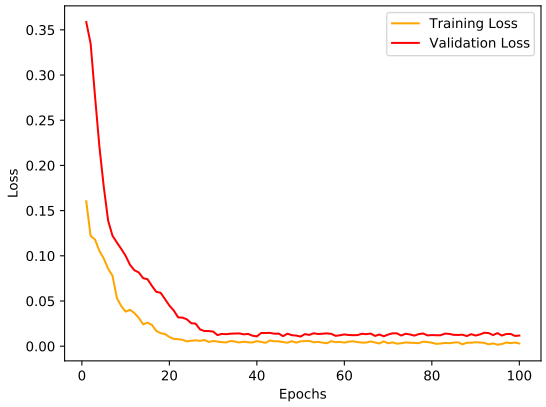

Fig. 4. Training and Validation Losses

TABLE X
NORMALIZED RMSE COMPARISON FOR TRAINING AND PREDICTIONS

	RMSE-N			RMSE-N	
Ticker	Training	Predictions	Ticker	Training	Predictions
AAPL	0.03641	0.43611	MA	0.05188	0.30879
ABBV	0.04734	0.94908	MCD	0.04920	0.52883
ABT	0.05156	0.85740	MDT	0.05126	0.48973
ACN	0.04010	0.71989	MRK	0.06483	0.70439
ADBE	0.04764	0.35472	MSFT	0.04691	0.35621
AMZN	0.05637	1.15072	NEE	0.05358	0.39933
AVGO	0.03368	1.65071	NFLX	0.05361	0.97983
BAC	0.05210	0.44360	NKE	0.03864	1.40680
BRK-B	0.06785	0.5726	NVDA	0.04028	0.95906
CMCSA	0.04631	0.55155	ORCL	0.04493	0.38606
COST	0.04946	0.31010	PEP	0.05540	0.79192
CRM	0.04560	0.39452	PFE	0.05287	0.87950
CSCO	0.06998	0.32509	PG	0.05203	0.48418
CVX	0.05146	0.24973	PM	0.05437	0.41451
DHR	0.03413	0.78150	PYPL	0.03225	1.11321
DIS	0.03896	1.07256	T	0.05044	0.64139
FB	0.05738	1.00459	TMO	0.03491	0.56151
GOOG	0.04464	0.79797	TSLA	0.06502	1.65771
GOOGL	0.04911	0.78201	TXN	0.05035	0.91743
HD	0.04226	0.59678	UNH	0.04465	0.68341
INTC	0.06388	0.55860	V	0.06031	0.25727
JNJ	0.07057	0.87682	VZ	0.07817	1.11059
JPM	0.05880	0.56786	WFC	0.03780	0.24410
KO	0.06043	1.39544	WMT	0.05127	0.25203
LLY	0.11573	0.84523	XOM	0.04595	0.38433

D. Investigating the Predictions on a Real Investment Scenario

The final experiment has the goal of moving the prediction results from a theoretical standpoint to a practical analysis. Using the predictions generated, a portfolio is setup and compared to a baseline, being the S&P 500 index. The best way to generate this portfolio would be using the RMSE of the predictions, but on a realistic scenario the RMSE is impossible to calculate, due to the real values being unknown.

The solution is to pick the portfolio based on the calculated risk of the predictions generated, as explained on Section IV-B. The portfolio selected has a cardinality value of $k = 3$, in order to create a minimum degree of diversification, consisting of the three stocks with the smallest values of CVaR, being the tickers WFC, WMT, and V. Fig. 5 display the predicted and real performance of the portfolio, assuming an equal portion of investment in each stock being $1/3$ of the total capital. Alongside, the performance on the S&P Index is also exhibited as a baseline measure.

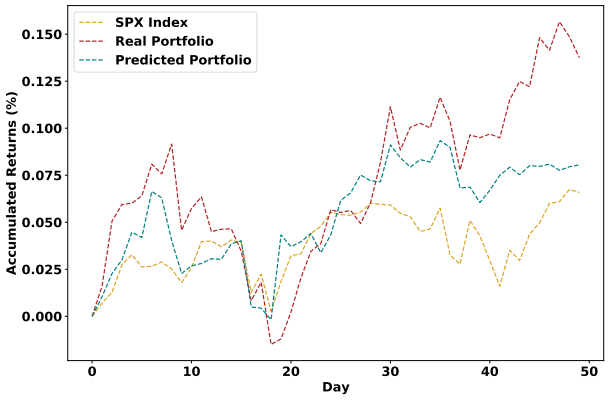

Fig. 5. Portfolio Performance & Comparison

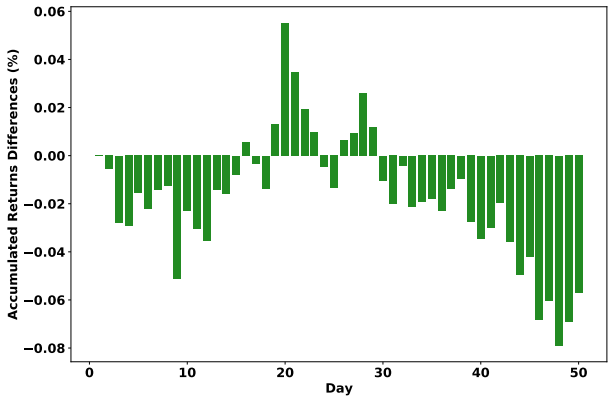

Fig. 6. Accumulated Returns Difference for Predicted and Real Portfolios

Many insights can be extracted from this experiment. The first positive fact is both the real and predicted portfolios have a better accumulated return value than the baseline compared. On the other hand, the final predicted value is a bit distant than the real value. It's noticeable that the model's predictions follow the real values really well up until the mark of 35 days, but the accuracy collapses after this point. It is understandable and expected that the accuracy would decrease as the days passes, and the breakpoint in this model seem to be around day 35. Fig. 6 displays the accumulated returns difference for predicted and real portfolios to show a less visual, more mathematical perspective for the analysis. The model objective is to keep the difference as close as possible to zero, and it is noticeable that the difference rapidly rises beyond day 35.

VI. Conclusion and Future Work

The prediction of asset prices in the financial market proves to be an ambitious and complicated task, due to the market being affected by many different factors. In this paper, one of these factors, financial news associated to the companies, was aggregated to the classic analysis of the historical series of stock prices. The model proposed presents two stages, beginning with the sentiment analysis of the news collected from the New York Times newspaper performed by VADER and ending on a stock price prediction model based on the LSTM architecture. The model also showcased the use of a robust parameter tuning strategy, being *AutoKeras' Hyperband*.

Pairing financial news sentiments with the assets historical prices gives more abstraction power to the prediction model, especially one with a dominant recurrence strategy such as LSTM. The model itself has no limitations for the application of even more features, although further investigation would be required to not only gather a new and improved dataset, but for the creation of the input samples as well.

The experiments included the tickers composing the Top 50 of the S&P 500 index, on a period of 5 years. The results indicate that the model is able to predict prices with good accuracy within a time window of around 35 days, given the scenario in which the model was applied and it's configuration. The results were validated by simulating the construction of a portfolio using the values for the three tickers with best return/risk ratio and comparing with the real values for the same portfolio. The simulation sustained the results, displaying a very similar performance for the predicted and real portfolios up until around day 35. The predicted portfolio also displayed better performance than the SPX index, which is relevant for the possibility of using the model on the real investment market.

Even after a display of good results, there is room for improvement. The five year period studied is enough for demonstration, but a realistic investigation could use a longer period to generate more data points for model training. With more training samples, the prediction could be attempted into a more distant future, while still maintaining good accuracy. Another possibility is focusing on short-time instead, a strategy used by day traders.

References

[1] E. F. Fama, "Efficient Capital Markets: II", *The journal of finance*, vol. 46, 1991, pp. 1575–1617.

[2] K. Liagkouras, K. Metaxiotis, "Efficient Portfolio Construction with the Use of Multiobjective Evolutionary Algorithms: Best Practices and Performance Metrics", *International Journal of Information Technology & Decision Making*, vol. 14, 2015, pp. 535–564, DOI: 10.1142/S0219622015300013.

[3] C. Hutto, E. Gilbert, "VADER: A Parsimonious Rule-based Model for Sentiment Analysis of Social Media Text", *International AAAI Conference on Web and Social Media*, vol. 8, 2014.

[4] R. Schumaker, H. Chen. "Textual Analysis of Stock Market Prediction Using Financial News Articles", *AMCIS Proceedings*, 2006, p. 185.

[5] M. Roondiwala, H. Patel, S. Varma, "Predicting Stock Prices Using LSTM", *International Journal of Science and Research (IJSR)*, vol. 6, 2017, pp. 1754–1756.

[6] F. A. Gers, J. Schmidhuber, F. Cummins, "Learning to Forget: Continual Prediction with LSTM", *Neural Computation*, vol. 12, 2000, pp. 2451–2471, DOI: 10.1162/089976600300015015.

[7] K. Adam, A. Marcet, J. P. Nicolini, "Stock Market Volatility and Learning", *The Journal of Finance*, vol. 71, 2016, pp 33–82, DOI: 10.1111/jofi.12364.

[8] M. Rana, M. M. Uddin, M. M. Mhoque. "Effects of Activation Functions and Optimizers on Stock Price Prediction Using LSTM Recurrent Networks", *International Conference on Computer Science and Artificial Intelligence*, vol. 3, 2019, pp. 354–358, DOI: 10.1145/3374587.3374622.

[9] X. Du, K. Tanaka-Ishii, "Stock Embeddings Acquired From News Articles and Price History, and an Application to Portfolio Optimization", *Annual Meeting of the Association for Computational Linguistics*, vol. 58, 2020, pp. 3353–3363, DOI: 10.18653/v1/2020.acl-main.307.

[10] H. Markowitz, "Portfolio Selection", *The Journal of Finance*, vol. 7, 1952, pp. 77–91.

[11] F. Xing, D. H. Hoang, D.-V. Vo, "High-frequency News Sentiment and its Application to Forex Market Prediction", *Hawaii International Conference on System Sciences*, vol. 54, 2020.

[12] H. Maqsood *et al*. "A Local and Global Event Sentiment Based Efficient Stock Exchange Forecasting Using Deep Learning", *International Journal of Information Management*, vol. 50, 2020, pp. 432–451, DOI: 10.1016/j.ijinfomgt.2019.07.011.

[13] P. Patil, C. S. M. Wu, K. Potika, M. Orang, "Stock Market Prediction Using Ensemble of Graph Theory, Machine Learning and Deep Learning Models", *International Conference on Software Engineering and Information Management*, vol. 3, 2020, pp. 85–92, DOI: 10.1145/3378936.3378972.

[14] Z. Jin, Y. Yang, Y. Liu, "Stock Closing Price Prediction Based on Sentiment Analysis and LSTM", *Neural Computing and Applications*, vol. 32, 2020, pp. 9713–9729, DOI: 10.1007/s00521-019-04504-2.

[15] R. Cheng, J. Gao. "On Cardinality Constrained Mean-CVaR Portfolio Optimization", *27th Chinese Control and Decision Conference*, 2015, p. 1074–1079, DOI: 10.1109/CCDC.2015.7162076.

[16] A. Heiden, R. Parpinelli. "Applying LSTM for Stock Price Prediction with Sentiment Analysis", *15th Brazilian Congress of Computational Intelligence*, 2021, p. 1–8, DOI: 10.21528/CBIC2021-45.

Communication Papers of the of the 17th Conference on Computer Science and Intelligence Systems pp. 241–249
DOI: 10.15439/2022F32
ISSN 2300-5963 ACSIS, Vol. 32

Visually Enhanced Python Functions for Clinical Equality of Measurement Assessment

Mauro Nascimben
Università del Piemonte Orientale,
Dept. of Health Sciences,
Novara, Italy
Enginsoft SpA, Padua, Italy
Email: m.nascimben@enginsoft.com

Lia Rimondini
Università del Piemonte Orientale,
Dept. of Health Sciences,
CAAD, Corso Trieste 15,
Novara, Italy
Email: lia.rimondini@med.uniupo.it

***Abstract*—Equivalence testing requires specific procedures usually provided by specialized statistical software. The proposed package includes customized methods to assess biomedical equivalence and focuses on translating the outcomes into visual reports. The functions are coded in an object-oriented framework, contain improved plots or novel graphs to facilitate interpretation of the results, and are accompanied by console textual outputs to support users with additional explanations. Special attention has been devoted to verifying the preliminary assumptions of the statistical tests with automatic routines. The current module covers four aspects of biomedical statistics (equivalence, Bland-Altman and ROC analyses, effect size, and confidence intervals interpretation), offering these methodologies to the biomedical community as accessible stand-alone functions. The manuscript defines software's functions and innovations with examples and theoretical explanations.**

I. Introduction

COMPARATIVE statistical tests could not address the interchangeability of measurements obtained from different laboratory devices or the similarity between two treatments. For example, the output values returned by a new and an old laboratory system require specific statistical analysis to demonstrate that the outcomes from the two machines are equivalent [1]. In comparative inference, the lack of a significant effect does not necessarily mean equality. Analyzing the equivalence means reversing the null hypothesis of standard biostatistical testing by validating the alternative hypothesis of no difference between measurements. The importance of this topic is particularly relevant for the medical sector, especially for the biopharmaceutical industry, with guidelines for therapeutic equivalence between drugs established by regulatory agencies like USA Food and Drug Administration (i.e., FDA) [2]. According to FDA, therapeutic equivalence implies that the two drugs have the same clinical effect on patients and follow the same safety profile. The FDA requires *two one-sided tests* procedure (i.e., TOST) to prove that formulations of two drugs are bioequivalent. The TOST approach determines, for a certain significance level α, if the $(1-\alpha)\times 100$ confidence interval of the average difference between drugs falls inside the regulatory boundaries $\pm\delta$. The equivalence implies that the efficacy of the new therapy is within δ units from the efficacy of a drug taken as reference, usually already on the market. FDA recommends a 90% confidence interval to determine biosimilarity, even if recently scholars suggested raising the interval range to 95% [3]. Thanks to the simplicity of TOST to prove similarity, the methodology started to be applied in other domains like medicine and chemistry [4].

The *sensitivity* (aka true positive fraction) and *specificity* (aka true negative fraction) assessment is another kind of equivalence analysis between diagnostic tests characterized by dichotic outcomes. For their estimation, a cross table is initially assembled containing the frequencies of a laboratory outcome versus the truth "disease status" in a population of subjects. Alternatively, the frequency table could be employed to contrast one lab measurement versus a gold standard. The continuous laboratory outcomes are categorized into "positives" or "negatives" based on a threshold: subjects with lab values above the threshold (or below, depending on the analysis) are labeled as positives, meaning the lab test detected the disease. Conversely, all the others are the negatives from the laboratory results. The same nomenclature is used to distinguish subjects' actual status: those carrying the illness (positives) or not (negatives). The frequency table contains the terms "false positives" (the lab procedure erroneously identified the illness in certain samples) and "false negatives" (the lab test incorrectly labeled a few samples as disease-free), also known as type I and type II errors, respectively. The sensitivity and specificity of a lab test can be deducted from the frequency cross table and describe the validity of the diagnostic examination, and they are assumed to be independent of the prior probability of having a disease [5]; however, they depend on the threshold selected to categorize the laboratory outcomes. A series of thresholds could be picked out to circumvent this limitation, thus obtaining different sensitivity and specificity pairs for each cut-off point. The *receiver operating characteristic* (i.e., ROC) curve shows over a graph the sensitivity and (1- specificity) values corresponding to each threshold. The area under the ROC curve is a metric to judge the efficacy of two laboratory tests in determining the same disease or the inter-observer variability. This latter situation is

This project has received funding from the European Union's Horizon 2020 research and innovation program under the Marie Sklodowska Curie grant agreement No 860462.

critical in medical exams involving the interpretation of the outcomes where diagnostic procedures are dependent on the investigator's skills and experience (for example, microscopic examination of cytologic samples or radiographic imaging). In addition, a certain degree of disparity between laboratory data revolves around different protocols. Consequently, the same test results might not be in perfect accordance if carried out in different hospitals or inside the same hospital by different operators.

Another pillar in the investigation of the agreement between measurements is the *Bland-Altman* analysis [6] (i.e., BA). The approach verifies if the difference between observations is contained inside acceptable agreement limits. In the original method, the two limits correspond to the $\overline{m} \pm 1.96 \times sd_m$, where $\overline{m}$ is the mean difference, and sd_m is its standard deviation. They approximate the 2.5^{th} and 97.5^{th} percentiles of the distribution of the differences, theoretically enclosing 95% of the differential values. Given the differential measurements obtained from a reference method and a new device $(New - Ref)$, approximately 95% of the time, the measurements from the new machine should be $\overline{(New - Ref)} - 1.96 \times sd$ units below the reference and $\overline{(New - Ref)} + 1.96 \times sd$ units above the reference. Before employing BA analysis, researchers should check the assumptions that the differences are normally distributed and exhibit constant variance. Moreover, studies usually include the degree of uncertainty in estimating the limits of agreement by reporting their confidence intervals. The 95% confidence interval around the agreement limits $\overline{(New - Ref)} \pm 1.96 \times sd$ can be computed as $\pm 1.96 \times SE$ where $SE = sd \times \sqrt{3/n}$ is the standard error of the limits and n the number of samples. Sampling errors might cause the agreement limits fluctuations incorporated by the confidence intervals; they restrict the initial agreement limits, but they will scale down as the sample size increases. The decision to accept the agreement intervals is taken according to clinical and biological objectives because BA analysis does not provide conclusions for statistical inference.

Confidence intervals (i.e., CI) play a fundamental role in addressing bioequivalence but can also highlight situations where a new treatment is *non-inferior* or *superior* to an existing one. The non-inferiority test requires the identification of a lower boundary $-\delta$, needed to verify if the CI obtained by the difference between treatments remains above it. A treatment is considered "as good as" the reference method if this happens. A drug's superiority to an available one is determined if the difference between treatments' CI lies above zero. In general, CIs express a certain level of probability that by randomly sampling a population an infinite number of times, one can obtain the true population parameter inside the interval. Closely connected to CI is the concept of quantifying the amount of difference between treatments to facilitate efficacy comparisons (aka effect size [7]). Standardizing the size of treatment effects produces unit-free measures that identify analogies between biomarkers and allow meta-analysis.

A. Aim of the Proposed Software Tools

Python is a general-purpose programming language widely adopted by the data science community. Its intuitive syntax and universality allow scholars to deal with various aspects of quantitative analysis. However, as for other non-commercial software, it relies on the efforts of the users to create libraries of functions able to solve specific data analysis tasks. Another popular free program for data science, for certain aspects complementary to python, is R, a statistically centered software. R might be preferred for deep statistical analysis over python, especially for creating visually interpretable statistical graphs. Alternatively, commercial software provides valuable statistical analysis tools. The present work presents a set of statistical functions in an object-oriented python library to deal with several aspects of equivalence testing. The importance is two-fold: provide specialized or improved functions usually found in other environments and share source code for future reusability by the scientific community. This latter aspect has been emphasized by the European Union's efforts for the "open science" paradigm [8].

II. Python functions

This manuscript section explains the essential functions and innovations included in the package referencing the relevant theoretical parts but accompanied by textual descriptions rather than formulas. This approach has been preferred to focus on the graphical interpretation of the outcomes. However, only a selected number of plots could be included in the current document, and only a few console outputs were discussed. The present library of visual functions has been coded in an object-oriented fashion; for didactic purposes, code snippets have been inserted throughout the document accompanied by full-length imports so users can match functions to the code organized in the Github folders. Code examples do not incorporate all function inputs, accepting the tacit defaults. Each function also provides textual outputs in the console to strengthen the analysis' conclusions. One of the key features is the preference for probability density distributions to visualize continuous data representations over a range of values rather than histograms: this avoids the process of selecting bin widths. Apart from standard python libraries, the module requires a few external dependencies: Numpy, Scipy, Pandas, Seaborn, and Matplotlib. Table I outlines the methodologies subdividing the procedures into four macro-areas as described in the "Introduction."

A. Bland-Altman Analysis

The proposed implementation controls the preliminary assumptions required to run this investigation. Indeed, calculating the limits of agreement depends on the prerequisite that the measurements' differences follow a normal homoscedastic distribution [9]. The function's code silently checks these assumptions and forces the user to meet this specification. Normalcy is assessed by the Shapiro-Wilks test, while homogeneity of variance is by Levene statistics. A practical example has been provided to illustrate the application of the

TABLE I
OVERVIEW OF THE METHODOLOGIES IMPLEMENTED IN THE PYTHON FUNCTIONS

Macro-area	Folder	Operations	Characteristics
Equivalence	EIS	TOST	Independent or paired two one-sided t-tests
	EIS	TOST	Fixed margin $\delta = f \times \sigma_{Ref}$ equivalence test
	EIS	TOST	Modified Wald with maximum likelihood estimator
	EIS	TOST	Paired inputs, sample size and statistical power dedicated functions
	EIS	TOST	Heteroscedastic inputs, sample size and statistical power dedicated functions
	EIS	Non-inferiority	Measurement vs. parameter or two-sample statistics
	EIS	Superiority	Measurement vs. parameter or two-sample statistics
	EIS	ROPE	Region of practical equivalence by equally-tailed or highest density intervals
ROC	ROC	2×2 freq. table	Confusion matrix and derivation of 34 performance indexes
	ROC	Radar plots	Circular graphs to compare cross-table's indexes (single/paired/bars) between two treatments
	ROC	ROC visual interpr.	ROC computation, Youden index, k-index, MID, non-parametric CI
	ROC	ROC Statistics	DeLong and Venkatraman independent or dependent methods
	ROC	Ranking plots	False positive rate vs. true positive rate with statistics and precision vs. recall with AUC
Effect size and CI	ES	Cohen's d	Independent or paired inputs, non-overlapping indexes
	ES	Re-testing	Repeated measurements' minimal detectable change
	ES	Responsiveness	Guyatt coeff., standardized response mean, effecct size, normalized ratio, reliable change index
	ES	Exploratory stats	Equivalence estimation based on CI analysis between biomarkers
	CI	Margin value study	Stacked CI representations to study the optimal equivalence margin
	CI	Paired Cat's Eyes	Biased or unbiased representation of two biomarkers
	CI	Car's Eye vs. p value	Single biomarker visual two-tailed analysis of CI vs. p significance
Bland-Altman	EQU	BA analysis	Revisited graphical interpretation, approximated and exact limits, min. detectable change
	EQU	Regress. diagnostics	Residuals interpretation, spread-location plot with Cook distances, influential points graphs
	EQU	Inherent imprecision	Graphical inherent imprecision with Chebyshev interval adjustment

Bland-Altman analysis. Two variables simulating the data of two different treatments were generated randomly by sampling two Gaussian distributions: the first variable represents a new treatment (`var1`), while the second is the reference method (`var2`). As summarized below, the initialization of `eq_BA` with default parameters creates an object whose methods incorporate the BA evaluation procedures:

```
from equiv_med.EQU import eq_BA
BA=eq_BA.BA_analysis(var1,var2)
BA.run_analysis()
BA.minimal_detectable_change()
```

The output of `run_analysis` is a graph exhibiting a novel interpretation of the Bland-Altman plot, as shown in Fig. 1. The typical illustration produced by statistical programs contains less information and is featured in Figure 12 of [9]. In the peculiar design supplied by the python function, each differential value is shown as a gray bar at the bottom of Fig. 1; the probability distribution overlays the graph, and the data range is the dark green horizontal dashed line. The light green dashed vertical line references the zero while the red dashed vertical line is the mean difference between measurements (aka the *bias*). Theoretically, if two measurements are equivalent, their difference should be zero. At the bottom, the standard deviation (i.e., SD) and standard error (i.e., SE) of the mean difference are visualized as horizontal bars. The SD line encloses 68% of the differences between measurements, providing the spread of the central portion of differences. The

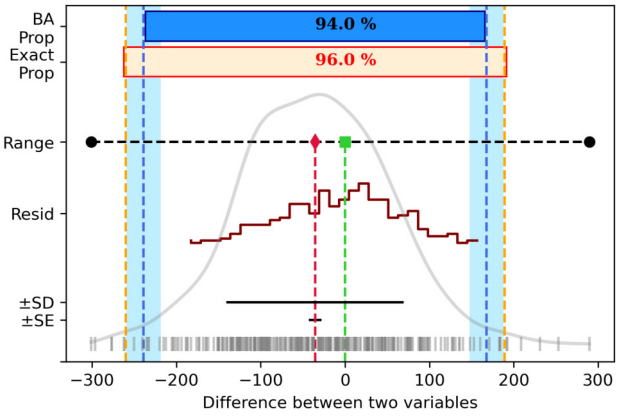

Fig. 1. Alternative design of the Bland-Altman plot as found in the `BA_analysis` class, using function `run_analysis`.

blue dashed vertical lines are the default limits of agreement at 1.96, with shaded areas representing their confidence intervals. The "BA Prop" rectangle at the top shows the effective percentage of values encompassed by the approximated limits of agreement (theoretically expected 95%, actual 94%); the rectangle length is scaled to show the proportion of actual data exceeding computed limits. Indeed, the "BA Prop" rectangle does not overcome the computed limits of 1% in length, and its horizontal boundaries are inside the blue vertical dashed lines. The orange dashed vertical lines are the exact limits

of agreement obtained by the procedure of [10]. The "Exact prop" rectangle shows the proportion of values falling inside the exact limits of agreement, with the rectangle length scaled to highlight the actual data behavior compared to the computed limits. The last information portrayed by the figure is the residuals of the linear regression between measurement values. The residuals histogram is expected to gather values around zero, and dispersion around it may emphasize the incomplete agreement between treatment measurements. The graph is accompanied by textual statistical information:

- Identification of a systematic difference between treatments (also called a fixed bias) or not by one-sample t-test
- The proportion of values in the two measurements that fall outside the approximated or exact limits of agreement

The second function in the code above allows users to detect the `minimal_detectable_change` parameter from the width of the approximated and exact limits of agreement. The minimal detectable change is the most negligible modification not attributed to an instruments measurement error. If the parameter values are less than a "minimal clinically important change" deduced from literature or clinical practice, the methods are in accordance with each other.

The sample size is a critical element in BA analysis for biomarker compliance: the class `eq_BA` offers two features to help researchers study this aspect for the exact limits of agreement (methods `exact_Bound_sample_size` and `exact_Bound_assurance`). The first function establishes the sample size by building the two-sided equal-tailed interval, given a certain CI width around the limits and significance level (i.e., $\alpha = 0.05$). Users may vary the width input parameter to adjust the required sample size. The second function supports the users in setting up the sample size, relating the theoretical to the actual probability of getting the desired CI width.

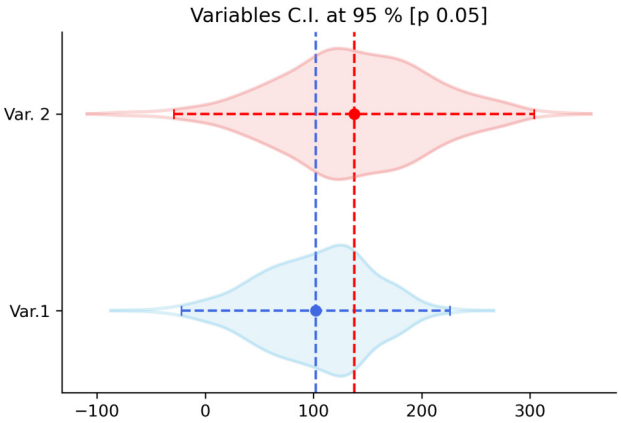

Fig. 2. Comparison between Cat's-Eye plots in `run_ce_unbiased` function.

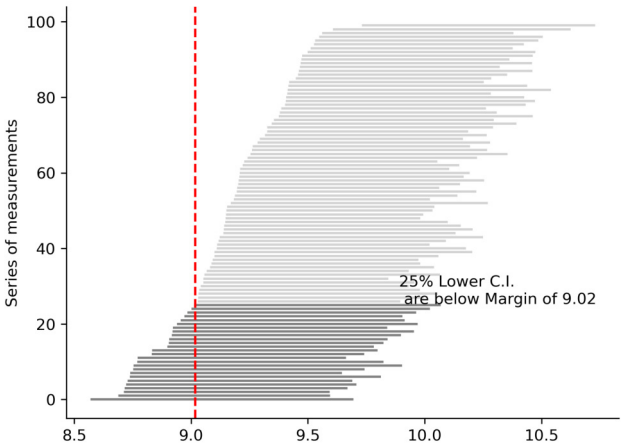

Fig. 3. Stacked CI representations of `decision_margin` function.

B. Visual Representations of Confidence Intervals

Interval estimation is directly related to p-values of null hypothesis statistical significance testing and helps interpret the precision of effect size [11]. CIs are advantageous in meta-analysis to compare data from previous studies, or in the case of longitudinal studies, they provide quickly interpretable insights. The proposed python function computes CI visual analysis creating a Cat's-Eye plot accompanied by statistical information. The function call `eq_CatEyes` is summarized below, keeping the same random variable characteristics to simulate two measurements as in the previous example:

```
from equiv_med.CI import eq_Cateyes
ce=eq_Cateyes.Cat_Eye_2var(var1,var2)
ce.run_ce_unbiased(95)
ce.single_cat_eye(var1,95)
```

The line of code with `run_ce_unbiased` verifies if the 95% CI of the first measurement is contained in the second one and vice-versa at default $\alpha = 0.05$. The console output is "At 5.0% probability: The first variable C.I. is entirely inside the C.I. of the second variable (open interval)". If the two CI match, the function inspects the interval type by checking the inclusion of the endpoints (open interval) or not (close interval). Calling `run_ce_unbiased`, users can plot the Cat's-Eyes of the two measurements, with eye shape depicting the probability density function of the data mirrored vertically (Fig. 2). The pupil of the eye, marked as a dot, is the mean, with horizontal lines providing references to evaluate the CI range and vertical dashed lines to feature the difference between averages. Alternatively, function `run_ce` shows the eyes with standard gaussian density estimation. Another function, `single_cat_eye`, allows users to investigate the plausibility of confidence intervals at different α values.

A different class, `Id_margin`, contains a method `decision_margin` that illustrates the positioning of a series of simulated CIs by bootstrap statistics built knowing the average and coefficient of variation of a biomarker (Fig. 3). The CIs are sorted and plotted together with a value acting as an equivalence margin: it might help examine the behavior of a specific regulatory boundary during equivalence testing.

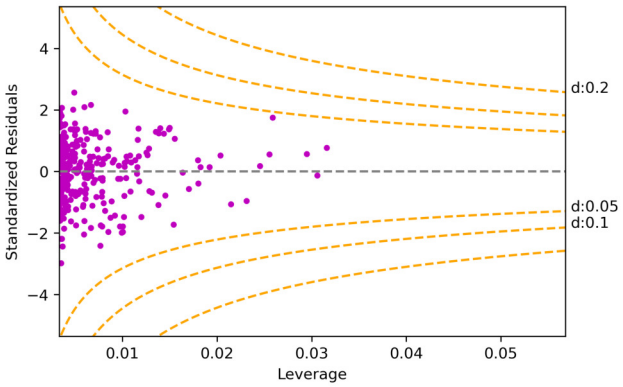

Fig. 4. Residuals vs. leverage with superimposed Cook distances of `run_diagnostic` function in `eq_Regr`.

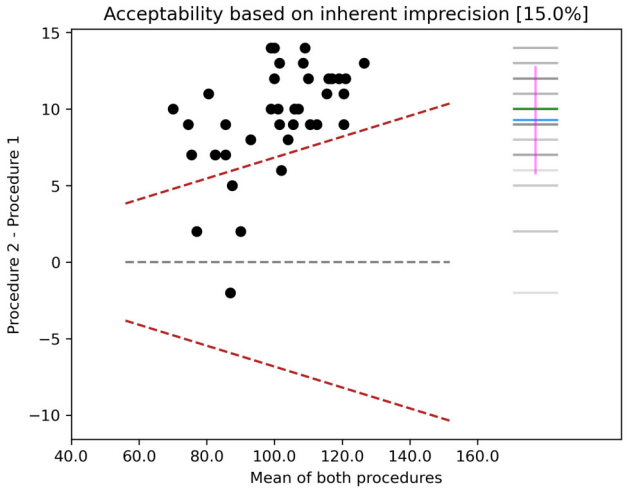

Fig. 5. Plot comparing imprecision of two measurement methods by `eq_ICI` function.

C. Regression Diagnostics

The correlation between two treatments could be examined through linear regression using `eq_Regr`. Despite not being an equivalence assessment methodology, linear regression in the presence of correlation might expose a relationship between measurements.

```
from equiv_med.EQU import eq_Regr
regr=eq_Regr.Regr_diagn(var1,var2)
regr.run_diagnostic([0.05,0.1,0.2])
```

Among the plots produced by `run_diagnostic`, there is a visual determination of Cook's distances over the residuals versus leverage graph. Users input a list of possible distances plotted as dashed orange lines: points that overcome a certain distance might be considered "highly influential" on regression outcomes. This investigation of scattered values far from zero on the y-axis and with high leverage provides an understanding of which points have a high impact on the linear model. In addition, if the graph returns stable residuals as a function of leverage, it might be perceived as an indicator of homoscedasticity. In automatic, the `run_diagnostic` method also apprises the user if the residuals are normally distributed by performing Jarque-Bera statistics: this test evaluates skewness and kurtosis to classify gaussianity or not. Another prerequisite is the independence of the errors, and the function displays the Durbin-Watson test result. Further method users can apply to study influential values is `influential_points` which shows DIFITS and DFBETAS in relation to empirical thresholds.

D. Acceptance Limits based on Inherent Imprecision

A method measuring values on a continuous scale might be characterized by a certain degree of variability in quantifying an underlying unknown true amount. The imprecision in defining the ground truth is associated with the "random error," usually measured by the coefficient of variation (i.e., CV). The CV may catch uncertainty in the repeatability or reproducibility of results. In such situations, estimating the random error (and consequently the imprecision) could be possible with the `ICI_bounds` class's method `run_ICI`:

```
from equiv_med.EQU import eq_ICI
ici=eq_ICI.ICI_bounds(var1,var2)
ici.run_ICI(2,4)
```

The python code produces the graph in Fig. 5: the number of observations by both methods has been reduced to 40 for a less crowded and more readable plot. The mean of both measurements is shown over the x-axis, while on the y-axis the difference between them. The two dashed lines in red are the acceptance limits computed as $bias \pm z \times CV_{mean}$, with $bias = 0$ and $z = 1.96$. The $CV_{mean} = \sqrt{CV^2_{procedure1} + CV^2_{procedure2}}$ requires knowledge of the CVs related to each procedure or instrument. It is a number available after carrying out laboratory experiments or from previous literature. In the example, it has been set $CV_{procedure1} = 2$ and $CV_{procedure2} = 4$. The python routine checks if the differences between measurements are normally distributed, and if not, adjusts the σ value according to the Chebyshev interval $1 - \frac{1}{z^2}$. If the Chebyshev adjustment is performed, the limits of agreement are in red otherwise, if normality is found the limits are in orange. The title also reports the number of inliers inside bounds as a percentage. On the right side of Fig. 5, users can observe the frequency distribution of the differences between measurements as grey horizontal lines. Further lines detail the median (in green), and the mean (in blue) plotted together with one standard deviation extension from the mean difference as a vertical bar (in violet). The function also produces textual outputs that explain the operations executed on the data in detail.

E. Standardized Mean Difference and Indexes of Non-overlapping

The standardized mean difference (aka Cohen's d) exposes effect size about two normally distributed measurements. Cohen d computation undertakes different formulas depending

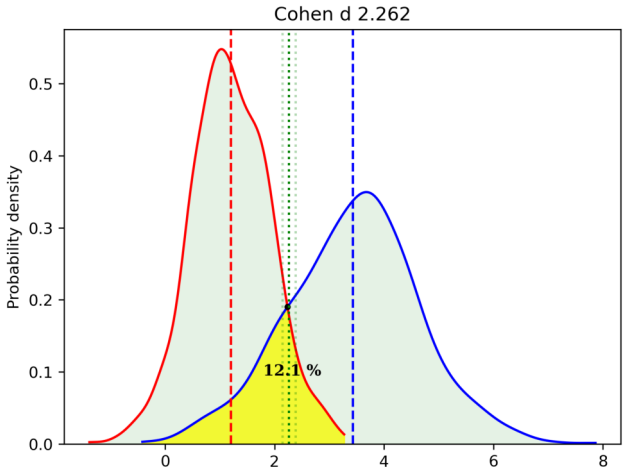

Fig. 6. Overlapping of two measurement methods by `plotting` function of `Cohen_es`. The Cohen's d CI are plotted as green dotted vertical lines.

on input values, whether they are paired or not, and whether variances are homogeneous. In two groups designs with equal variances, it is $\frac{\overline{method_1}-\overline{method_2}}{sd_{pooled}}$, and it summarizes the number of standard deviations the means of two groups differ. However, when the sample size is small, Cohen *d* is corrected to obtain an unbiased version, called Hedges *g*. During the initialization of the class `Cohen_family`, the user can decide the experimental design of the two input variables (paired or not, default is not). The function `Cohen_es` automatically checks the prerequisites and selects the proper formulation, possibly applying the small sample size correction factor using the Gamma function [12].

```
from equiv_med.ES import Cohen_family
D_meas=Cohen_family.Cohen_es(var1,var2)
D_meas.nonoverlap_measures()
D_meas.plotting()
```

The literature on Cohen's d computation in case of unequal variances reports different approaches for determining the right effect size. In the default implementation with equality of variances, computations follow [12], with results in the case of heteroskedasticity personalizable using formulas suggested by [13], [14], [15]. Among the methods of class `Cohen_family`, the `nonoverlap_measures` returns three indexes upon verifying that input data are normally distributed and with equal variability:

- Cohen's U_3, also called "percentile standing." Indeed, effect size might be interpreted as the average percentile standing of the average experimental measurement relative to the average control.
- Cohen's U_2, as U_3 is quantified using the cumulative density function, but of $d/2$ rather than d as in U_3
- Cohen's $U_1 = \frac{2\times U_2}{U_2}$ is the non-overlap percentage between the measurement areas subtended by the probability density functions.

These indexes complete the information supplied by d. With `plotting`, a visual interpretation of the data is shown as in Fig. 6. The two distributions' overlapping area is colored in yellow, with the overlap percentage added near the intersection point. Vertical dashed lines are the means of the two groups, while vertical dotted lines are the Cohen's d and its CI estimated via the "non-centrality" method.

Another class, called `Retesting`, calculates the *minimal detectable change* for repeated measurements using the same instrument on different occasions [16]. It tests the consistency of the scores by automatically switching between Pearson product-moment or Spearman correlation depending on the gaussianity of the data. This peculiar function has been inserted in the same folder as the Cohen's d, because there is a relation between d and the coefficient of correlation $r = \frac{d}{\sqrt{d^2+a}}$, with $a = 4$ if the two input measurements have same length. So theoretically, the correlation could be inferred from d, although the current implementation calculates the correlation indexes directly. The class `Responsiveness` contains other metrics to characterize devices' properties in case of repeated measurements recorded from two instruments over time.

F. Equivalence, Non-inferiority and Superiority

Analytical biosimilarity testing by TOST (`EIS` folder) executes two one-sided t-tests to verify the positioning of the mean difference between measurements in relation to the regulatory boundaries $\pm\delta$. In statistical terms the equivalence tests implemented in the python library aim to check:

$$H_0 : \overline{m_1} - \overline{m_2} \leq -\delta \quad or \quad \overline{m_1} - \overline{m_2} \geq \delta$$

$$H_1 : -\delta < \overline{m_1} - \overline{m_2} < \delta$$

In situations where measurements are independent, the function `run_Tost_indep` could be employed, while for paired biomarkers `run_Tost_dep`. When biomarkers do not have equal variances in these two functions, degrees of freedom are computed by the Satterthwaite formula, and the t-test is replaced by Welch's t-test. Assumption of normally distributed input data is checked automatically by Shapiro-Wilks statistic. The python package also contains two equivalence tests that tackle the biosimilarity problem from a slightly different point of view. In `Tost_Alt` class, the method `run_TOST_T` performs the similarity procedure of [17], fixing the margin at $\delta = f \times \sigma_2$ where f is a multiplication factor, and σ_2 is the standard deviation of the reference method. The f multiplier should be selected to accommodate statistical power based on sample size. The authors of [17] suggested $f = 1.5$. Inside the same `Tost_Alt` class, the method `run_TOST_MW` provides the methodology studied in [18] to control the type I errors. In standard TOST, the type I error rate is restrained by $\alpha = 0.05$, while the authors introduced a modified Wald test to assess the standard error by the maximum likelihood estimator. This operation should better control type I errors in repeated measurements involving samples of small size. The section dedicated to bioequivalence contains two additional procedures: paired

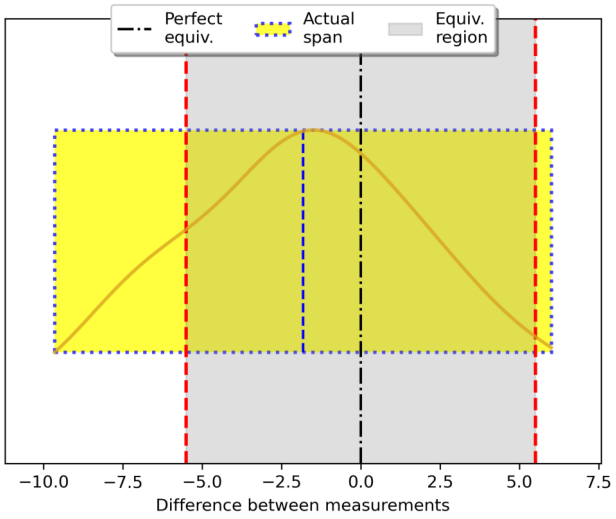

Fig. 7. Plot showing equivalence region and the actual CI extension of the difference between biomarkers, using `Tost_paired`.

measurements could be investigated with the methodology of [19] (class `Tost_paired`, Fig. 7), while in the case of heteroscedasticity, the TOST methods in `WS_eq` perform the Welch-Satterthwaite as suggested in [20]. These classes also include specialized function calls to calculate the minimal desired sample size and related statistical power. In Fig. 7, the red vertical dashed lines are the user-defined equivalence margins (set to ± 5.5). As remarked in the "Introduction," this value should be deducted from literature or clinical experience. The yellow rectangle represents the extent of the input data, and it has a length that overcomes the limits, thus not allowing to establish equivalence between the datasets. Inside the yellow rectangle, the probability distribution is shown together with a vertical dashed blue line depicting the mean difference of biomarker values.

```
from equiv_med.EIS import Standard_Tost as ST
from equiv_med.EIS import Tost_NCP,Tost_WS
from equiv_med.EIS import Tost_Alt
res1=ST.EQU(var1,var2,-5.5,5.5)
res1.run_Tost_indep()
res1.run_Tost_dep()
res2=Tost_Alt.TOST_T(var1,var2)
res2.run_TOST_T()
res2.run_TOST_MW()
res3=Tost_NCP.Tost_paired(var1,var2,5.5)
res3.run_tost()
res4=Tost_WS.WS_eq(var1,var2,5.5)
res4.run_TOST()
```

As a final remark, equivalence testing could be integrated into standard inferential statistics analysis pipelines. Indeed, equivalence assessment can clarify null-hypothesis significance tests. When $p > \alpha$, biomakers are classified as "not different" in traditional inference, but only equivalence determines their exchangeability. Conversely, it might be possible to find a significant difference ($p < \alpha$) during traditional inference and, at the same time, equivalence inside certain boundaries.

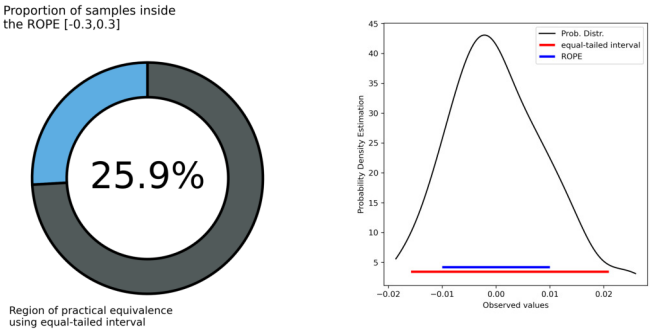

Fig. 8. Region of practical equivalence as shown by `plot_rope` of class `ROPE`. The right plot is visualized only if the sample size is larger than 50.

Non-inferiority analysis establishes that the efficacy of a new therapy is not lower than δ units than the current one:

$$H_0 : \overline{m_1} - \overline{m_2} \leq -\delta$$

$$H_1 : \overline{m_1} - \overline{m_2} > -\delta$$

Superiority evaluates if there is a difference between measurements by usually fixing $\delta = 0$:

$$H_0 : \overline{m_1} - \overline{m_2} \geq \delta$$

$$H_1 : \overline{m_1} - \overline{m_2} < \delta$$

Non-inferiority (`non_inferiority`) and superiority (`superiority`) tests were implemented following [21] as methods of the class `IoS`.

```
from equiv_med.EIS import Inf_or_Sup as IS
res5=IS.IoS(var1,var2)
res5.non_inferiority(ni_bound=0.1)
res5.superiority(sup_bound=0)
```

The region of practical equivalence (i.e., ROPE, developed inside `ROPE` class) has been introduced in [22] as a Bayesian probabilistic framework that does not rely on statistical significance. This approach considers the data sample as a probabilistic representation of the underlying real population of values. The user selects the region of practical equivalence, and it corresponds to the "null" hypothesis. The functions check the percentage of samples that fall inside the ROPE; this proportion is called the credibility interval, and it could be built using the highest density principle (`rope_hdi`) or as an equal-tailed interval (`rope_calc`). The intervals obtained from these two processes are the same when dealing with symmetric distributions, but skewed distributions might show different extensions; the python functions warn the user about this possibility. The credibility interval conceptualizes the idea that points comprehended inside it are more credible representatives of the data than external points, and it could be set to 95% or restricted to 89%. When the percentage of credibility interval within the ROPE is sufficiently low, the ROPE "null" hypothesis is rejected. Users can visualize the test result using `plot_rope`, as shown in Fig. 8.

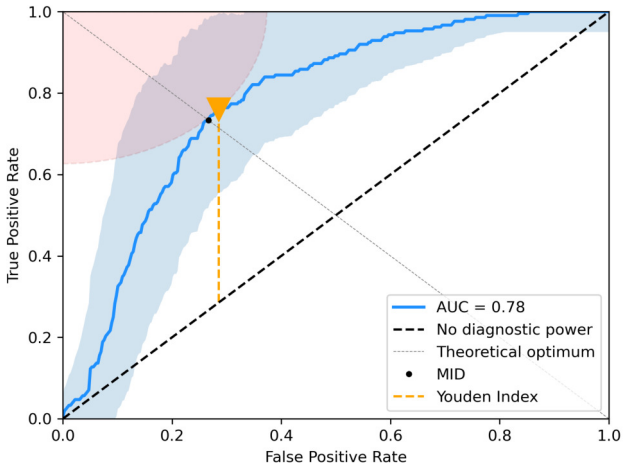

Fig. 9. ROC with CI, Youden index and K-index as shown by `plot_roc_youden`.

G. ROC Analysis

Diagnostic procedures can be evaluated in terms of ROC curves without proving any distributional assumption. Using the function `plot_roc_youden` of the class `Roc_youden`, users can visualize a ROC curve as in Fig. 9. The curve displays different threshold values determining the positivity to a medical test and the trade-off between true positive and false positive fractions. The more a ROC curve is close to the upper-left corner of the box enclosing the plot, the better the test's diagnostic power. The function automatically checks the side of the curve with the Mann-Whitney U rank test and consequently adapts computations. In the following examples, the results of a medical test are the first input variable (`test_res`) while `true_labels` represent the disease status of the subjects:

```
from equiv_med.ROC import Roc_youden as Ry
roc=Ry.Youden_Roc(test_res,true_labels)
roc.plot_roc_youden()
```

In ROC curves, it is fundamental to represent also the CIs: for their computation reckoned by non-parametric technique, `plot_roc_youden` exploits the algorithm in [23]. In addition, the plot contains the area under the curve (i.e., AUC), an accuracy metric often applied to compare different methodologies, while the Gini index is shown as textual output on the console. The orange triangle marks the Youden index, the point of maximal effectiveness of a medical test. At the Youden level, the sensitivity and specificity are balanced, thus highlighting the optimum cut-off point for the procedure. The Youden point might be close to the theoretical optimum, as happens in Fig. 9. Another index included in the graph is the K-index, represented as the pale red circle sector centered on the upper-left corner. It is the distance between the best result (the upper-left corner) and the optimum identified by the Youden index. The smaller this quarter-circle is, and better the medical test. Moreover, any ROC point that enters the K-index space is preferable to the threshold selected to determine the positives of the test. The black point "MID" is the *minimal important difference* detected by the anchor method. The MID value might also be called "minimally important change," even if it has been suggested to refer to MID only for between-subjects differences [24]. The MID value could help examine thresholds of treatments relating them to clinical improvements in health patient status.

The python package also offers four classes to statistically compare the ROC curves of two biomarkers, acquired as independent or repeated experiments. These statistics require two ROCs having the same direction:

- *DeLong* techniques in fast version [25], accomplished relating the Heaviside function to the samples mid-ranks
  - `DeLong_dependent`
  - `DeLong_independent`
- *Venkatraman* methods, performing pointwise comparison [26], [27]. This procedure requires the exchangeability assumption.
  - `Venkatraman_dependent`
  - `Venkatraman_independent`

During statistical equivalence, the ROC direction is detected by Mann-Whitney U. Intriguingly, there is a direct relation between ROC's AUC and Mann-Whitney U being $AUC = \frac{U}{n_0 \times n_1}$, with n_0 and n_1 number of negative and positive cases.

The class `Ranking_plots` allows users to visualize the precision vs. recall plot, including the calculation of area under this curve, and the true positive vs. false positive rates graph, containing the Kolmogorov-Smirnov statistic in the standard and truncated forms. Both provide an interpretation of the distance between true positive vs. false positive rate lines, but the truncated formula is less sensitive to noise.

H. The 2x2 Frequency Table and Performance Indexes

Dichotomous outcomes of diagnostic tests are generally summarized by a two-by-two frequency table, also known as two-class confusion matrix (displayed calling `frequency_plot`). Multiple performance indexes could be derived from the frequency table: these attributes are computed on a single threshold rather than several thresholds like for ROC. The python library contains the class `Frequency_table`, which calculates 34 indexes. These performance indexes support the validation of a new test against a gold standard. The `Radar` class offers comparisons of performance indexes from one or two instruments in two types of charts: a radar plot with or without overlapping input indexes or a circular paired bar graph.

```
from equiv_med.ROC import Frequency_table as ft
from equiv_med.ROC import Radars
t1=ft.Freq_table(test_res1,true_labels)
out1=t1.performance_indexes()
t2=ft.Freq_table(test_res2,true_labels)
out2=t2.performance_indexes()
rd=Radars.Radar_plots(indexes_list)
rd.radar_plots(out1,out2,overlapping=True)
```

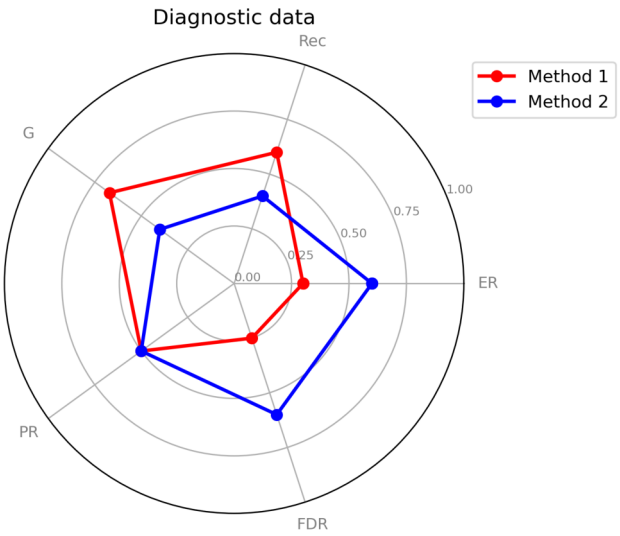

Fig. 10. Radar graphs comparing the indexes of two diagnostic tests using `radar_plots` of `Radars` class.

In Fig. 10, the radar illustrates five indexes pre-selected by the user passing the list of names during `Radar_plots` initialization. The function automatically abbreviates indexes names; in the example of Fig. 10, "Error Rate" is "ER," "Recall" as "Rec," "G" is "G measure," "Prevalence" as "PR," and "False Discovery Rate" is "FDR."

III. Conclusions

A python library for visual understanding of medical-related statistical tests targeting several aspects of bioequivalence has been presented. It offers a free alternative to commercial software. Functions are highly automated and produce enhanced graphs to facilitate the interpretation of the output parameters. Minimal working examples were included to aid in reproducing the results. Future versions will expand and improve the implemented methodologies maintaining the spotlight on producing visual insights.

Appendix

The source code of the functions described in the document (current version 0.11) has been uploaded to GitHub (https://github.com/m89p067/equiv_med) and archived on Zenodo (https://zenodo.org/record/6504217). Installation of the package directly from GitHub through pip.

References

[1] S. C. Gad, *Safety evaluation of pharmaceuticals and medical devices: international regulatory guidelines*. Springer Science & Business Media, 2010.

[2] F. Home, "Orange book: approved drug products with therapeutic equivalence evaluations," *US Food Drug Adm*, 2013.

[3] S.-C. Chow and S. J. Lee, "Current issues in analytical similarity assessment," *Statistics in Biopharmaceutical Research*, vol. 13, no. 2, pp. 203–209, 2021. doi: 10.1080/19466315.2020.1801497

[4] A. Munk, J. Gene Hwang, and L. D. Brown, "Testing average equivalencefinding a compromise between theory and practice," *Biometrical Journal: Journal of Mathematical Methods in Biosciences*, vol. 42, no. 5, pp. 531–551, 2000.

[5] J. A. Hanley and B. J. McNeil, "The meaning and use of the area under a receiver operating characteristic (roc) curve." *Radiology*, vol. 143, no. 1, pp. 29–36, 1982.

[6] J. M. Bland and D. Altman, "Statistical methods for assessing agreement between two methods of clinical measurement," *The lancet*, vol. 327, no. 8476, pp. 307–310, 1986.

[7] G. Cumming, "The new statistics: Why and how," *Psychological science*, vol. 25, no. 1, pp. 7–29, 2014.

[8] C. O'Carroll, B. Rentier *et al.*, "*Evaluation of research careers fully acknowledging open science practices-rewards, incentives and/or recognition for researchers practicing open science*," Publication Office of the Europen Union, Tech. Rep., 2017.

[9] J. M. Bland and D. G. Altman, "Applying the right statistics: analyses of measurement studies," *Ultrasound in Obstetrics and Gynecology: The Official Journal of the International Society of Ultrasound in Obstetrics and Gynecology*, vol. 22, no. 1, pp. 85–93, 2003.

[10] S.-L. Jan and G. Shieh, "The bland-altman range of agreement: Exact interval procedure and sample size determination," *Computers in Biology and Medicine*, vol. 100, pp. 247–252, 2018. doi: https://doi.org/10.1016/j.compbiomed.2018.06.020

[11] G. Cumming, *Understanding the new statistics: Effect sizes, confidence intervals, and meta-analysis*. Routledge, 2013.

[12] J.-C. Goulet-Pelletier and D. Cousineau, "A review of effect sizes and their confidence intervals, part i: The cohensd family," *The Quantitative Methods for Psychology*, vol. 14, no. 4, pp. 242–265, 2018.

[13] G. Shieh, "Confidence intervals and sample size calculations for the standardized mean difference effect size between two normal populations under heteroscedasticity," *Behavior research methods*, vol. 45, no. 4, pp. 955–967, 2013.

[14] M. Delacre, D. Lakens, C. Ley, L. Liu, and C. Leys, "Why hedges g*s based on the non-pooled standard deviation should be reported with welchs t-test," May 2021. [Online]. Available: psyarxiv.com/tu6mp

[15] D. Cousineau, "Approximating the distribution of cohens dp in within-subject designs," *Quant. Methods Psychol*, vol. 16, pp. 418–421, 2020.

[16] Y. Shou, M. Sellbom, and H.-F. Chen, "Fundamentals of measurement in clinical psychology," in *Reference Module in Neuroscience and Biobehavioral Psychology*. Elsevier, 2021. ISBN 978-0-12-809324-5

[17] Y. Tsong, X. Dong, and M. Shen, "Development of statistical methods for analytical similarity assessment," *Journal of biopharmaceutical statistics*, vol. 27, no. 2, pp. 197–205, 2017.

[18] Y.-T. Weng, Y. Tsong, M. Shen, and C. Wang, "Improved wald test for equivalence assessment of analytical biosimilarity," *International Journal of Clinical Biostatistics and Biometrics*, vol. 4, no. 1, pp. 1–10, 2018.

[19] G. Shieh, "Assessing agreement between two methods of quantitative measurements: Exact test procedure and sample size calculation," *Statistics in Biopharmaceutical Research*, vol. 12, no. 3, pp. 352–359, 2020. doi: 10.1080/19466315.2019.1677495

[20] G. Shieh, S.-L. Jan, and C.-S. Leu, "Exact properties of some heteroscedastic tost alternatives for bioequivalence," *Statistics in Biopharmaceutical Research*, pp. 1–10, 2021.

[21] S. Wellek, *Testing statistical hypotheses of equivalence*. Chapman and Hall/CRC, 2002.

[22] J. K. Kruschke and T. M. Liddell, "The bayesian new statistics: Hypothesis testing, estimation, meta-analysis, and power analysis from a bayesian perspective," *Psychonomic bulletin & review*, vol. 25, no. 1, pp. 178–206, 2018.

[23] P. Martínez-Camblor, S. Pérez-Fernández, and N. Corral, "Efficient nonparametric confidence bands for receiver operating-characteristic curves," *Statistical Methods in Medical Research*, vol. 27, no. 6, pp. 1892–1908, 2018.

[24] H. C. De Vet, R. W. Ostelo, Terwee *et al.*, "Minimally important change determined by a visual method integrating an anchor-based and a distribution-based approach," *Quality of life research*, vol. 16, no. 1, pp. 131–142, 2007.

[25] X. Sun and W. Xu, "Fast implementation of delongs algorithm for comparing the areas under correlated receiver operating characteristic curves," *IEEE Signal Processing Letters*, vol. 21, no. 11, pp. 1389–1393, 2014.

[26] E. S. Venkatraman and C. B. Begg, "A distribution-free procedure for comparing receiver operating characteristic curves from a paired experiment," *Biometrika*, vol. 83, no. 4, pp. 835–848, 1996.

[27] E. Venkatraman, "A permutation test to compare receiver operating characteristic curves," *Biometrics*, vol. 56, no. 4, pp. 1134–1138, 2000.

Communication Papers of the of the 17th Conference on Computer Science and Intelligence Systems pp. 251–258
DOI: 10.15439/2022F50
ISSN 2300-5963 ACSIS, Vol. 32

The Mood of the Silver Economy: A Data Science Analysis of the Mood States of Older Adults and the Implications on their Wellbeing

Marco A. Palomino,
Rohan Allen, Farida Aider,
Francesca A. Tirotto and Ioanna Giorgi
University of Plymouth
SECaM
Plymouth, PL4 8AA
United Kingdom
Email: {marco.palomino, rohan.allen-13,
farida.aider, francesca.tirotto,
ioanna.giorgi}@plymouth.ac.uk

Hazel Alexander
Plymouth Community Homes
Plumer House
Plymouth, PL6 5DH
United Kingdom
Email: hazel.alexander@pch.co.uk

Giovanni L. Masala
University of Kent
School of Computing
Kent, CT2 7NZ
United Kingdom
Email: g.masala@kent.ac.uk

***Abstract*—For the first time in the history of humanity, the number of people over 65 surpassed those under 5 in 2018. Undoubtedly, older people will play a significant role in the future of the economy and society in general, and technological innovation will be indispensable to support them. Thus, we were interested in learning how home automation could enable older people to live independently for longer. To better understand this, we held focus groups with UK senior citizens in 2021, and we analyzed the data derived from them from the perspective of affective computing. We have trained a machine learning classifier capable of distinguishing moods commonly associated with older adults. We have identified depression, sadness and anger as the most prominent mood states conveyed in our focus groups. Our practical insights can aid the design of strategic choices concerning the wellbeing of the ageing population.**

I. Introduction

IN THE Europe of 2060, one in three inhabitants will be over 65 [1]. A similar trend of increasing life expectancy and reversal of the population pyramid will be followed by the rest of the developed countries [2]. The forms of consumption will therefore change and older people will become the engine of the so-called *silver economy* [3].

The silver economy includes all the economic activities, products and services designed to meet the needs of older adults [4]. The concept derived from the *silver market* that emerged in Japan—the country with the highest percentage of people over 65—during the 1970s [5], and brings together sectors as diverse as health, banking, automotive, energy, housing, leisure and tourism. Scientific advances and joint efforts will be critical to address the unique health challenges of the ageing population and their communities [3]. Undoubtedly, the ageing of the population will lead to the creation of jobs and the emergence of careers related to the silver economy.

†The authors acknowledge the funding provided by the Interreg 2 Seas Mers Zeeën AGE IN project (2S05-014).

Regrettably, mental health problems in older adults are frequent. Indeed, late life depression is common, and it is typically associated with disability, reduced quality of life, mortality, and high health care costs [6]. Moreover, depressed older adults frequently have comorbid medical illnesses and cognitive impairments [6]. Life events such as moving from a private residence to a nursing home, or an assisted-living facility, can trigger symptoms such as anxiety, confusion, hopelessness, and loneliness. This is part of a nursing diagnosis now known as *relocation stress syndrome* [7].

In an attempt to prevent relocation stress, the *AGE IN* project endeavours to propose a strategy to keep the ageing population independent for longer in their own homes [8]. AGE IN has suggested a combination of house adaptations and the development of a local ecosystem for the silver economy [8]. As shown in recent studies [9], one of the keys to the silver economy will be technological innovation. Advances in home automation, artificial intelligence, the Internet of Things, eHealth and other services typical of smart cities, will prove relevant to support the ageing population.

To bring the AGE IN strategy to fruition, it is vital to understand the needs and concerns of older adults. Consequently, we organized a series of focus groups in the summer of 2021, where UK senior citizens participated in discussions about independent living, house adaptations, isolation, and their concerns about the future. Due to the sensitive nature of the focus groups, we undertook the ethical approval process required by the *University of Plymouth*, which is where the focus groups were held. Our ethical approval was recorded under the title "AGE IN Robot Home" through the *Plymouth Ethics Online System* (PEOS) [10]. Our approach was reinforced by a white paper published by the *UK Ministry of Housing, Communities and Local Government* in 2020 [11].

Transcriptions of the conversations which took place during

the focus groups that we organized allowed us to gather opinions and relevant feedback. We then processed these transcriptions with the use of text mining techniques and machine-learning algorithms to extract knowledge and insights into the feelings and emotions expressed by older adults. We expect the practical insights derived from our study to aid in the decision-making of strategic choices concerning the mental health of the ageing population—especially, as a considerable amount of fear and depression were expressed by the senior citizens who participated in our focus groups.

The remainder of this paper is organized as follows. We start by summarising the related work on emotion analysis and its links to older adults in Section II. Afterwards, we describe our dataset in Section III and its processing in Section IV. Then, we present our results in Section V, and we discuss them in Section VI. Finally, we draw our conclusions in Section VII.

II. Related Work

Plenty of multidisciplinary research has demonstrated through text analysis that word use is a reliable indicator of a person's psychological state [12]. Thus, *sentiment analysis* has been amply used to analyze people's evaluations, appraisals, and attitudes towards products, services, and topics [13], [14], [15]. However, most sentiment analysis work focuses on assigning a positive or negative rating—*polarity*—to a piece of text [16], whereas we aim to recognise a range of emotional categories, which is the goal of *affective computing* [17].

Emotions are critical for the interaction of human beings, as they enable people to express their reactions to any stimulus they experience [18]. Although the idea of employing computers to recognise emotions was first introduced by Picard in 1997 [19], it is only recently when the advances in machine learning have boosted *natural language processing* (NLP) to reach human-level performance [20].

Over the past decade, we have witnessed the publication of a great deal of literature interested in identifying emotions in text. Most of this literature has adopted supervised machine learning approaches to recognise specific sets of emotions. An example of this is Chaffar and Inkpen's research, which combined emotion-annotated news headlines, fairy tales and blogs to create a suitable training set [21]. Chaffar and Inkpen claim to have achieved a much better performance with a *support vector machine* (SVM) classifier than with any other alternative. Moreover, their SVM classifier generalises well on unseen examples [21].

We were keen on testing approaches that depart from the traditional methods followed by sentiment analysis, which used lexicons and bag-of-words models. We are aware of the improvements reported by researchers who have worked with sequences of characters, without pre-processing the text that becomes the input of a *recurrent neural network* (RNN). Colnerič and Demšar [22] implemented one of such approaches and used it to classify tweets into emotional categories. Their work is particularly relevant to ours.

Following Colnerič and Demšar [22], we have also implemented our own emotion classifier, though we did not consider the models developed by Paul Ekman [23] and Robert Plutchik [24], as Colnerič and Demšar did. Instead, we concentrated on a different model for the reasons explained below.

Ekman studied facial expressions to define six universally recognisable emotions: anger, disgust, fear, joy, sadness and surprise [23]. Even though facial recognition is an area which we wish to explore in the long term, we are currently unable to apply it. Thus, Ekman's model is not suitable for our work.

Plutchik considered eight basic, pairwise, contrasting emotions: joy vs. sadness, trust vs. disgust, fear vs. anger, and surprise vs. anticipation [24]. Even though we plan to widen the range of emotions analyzed by our classifiers as our research progresses, the lack of annotated training collections complicates any attempts to implement Plutchik's model. Ultimately, we could pursue Colnerič and Demšar's approach—that is, consider each emotion as a separate category and disregard the different levels of intensities that Plutchik defined [22]. Regrettably, such a simplification would diminish the value and full extent of Plutchik's model. Additionally, we would prefer to fine-tune our implementation for a smaller number of emotions before involving a wider range.

We favored the implementation of a third emotion model, different from Ekman's and Plutchik's, as we also wanted to identify an alternative approach that is more suitable for the study of the ageing population. This led us to consider the *Profile of Mood States* (POMS) [25], which contemplates *fatigue* and *depression*—two states of mood often associated with older adults.

In the following sections, we explain how we gathered our dataset and how we implemented our classifier.

III. Dataset

We organized meetings with 17 British senior citizens who currently live in the city of Plymouth (UK). We invited them to participate in our focus groups through our professional partnership with *Plymouth Community Homes* (`https://www.plymouthcommunityhomes.co.uk/`). We refer to these older adults hereafter as *participants*, and they were separated into three groups:

- **Group 1:** Participants whose ages were 59–80 and required daily support with mobility issues—for example, a wheelchair, a prosthetic leg or a walking aid.
- **Group 2:** Participants whose ages were 66–80 and did not require support with mobility issues.
- **Group 3:** Participants whose ages were 57–63 and did not require support with mobility issues.

For a whole morning or afternoon, the participants visited the University of Plymouth on 27–29 July 2021 and had conversations with a group of academic researchers about their views on ageing, isolation, their own future, and the relevance of using technological and automation tools to keep their independence at home. Apart from the conversations, the participants had an opportunity to attend a brief presentation delivered by *Pepper*, a semi-humanoid robot [26].

Although Pepper is not a functional robot for domestic use, it is intended to enhance people's lives and facilitate

relationships [26]. Pepper did help the researchers to establish rapport with the participants of the focus groups and start the conversation about technological and automation tools.

We recorded all the conversations held during the focus groups, abiding by the guidance provided by the *University of Plymouth Ethic's Committee* [10]. Later, we transcribed all the conversations using *Trint* [27], an audio transcription software. Once the conversations were converted into transcribed text, we proceeded to manually label by gender each line of the conversations, so that we could associate each line with a female or male participant, despite removing their names for ethical considerations. We were interested in identifying the gender of the participants, as we are aware of gender differences when diagnosing conditions such as depression. Indeed, we were hoping to contribute to the research aimed at determining whether elderly women are at greater risk for depression than elderly men [28], or vice versa.

To identify the main topics of conversation in the focus groups, we performed a lexical analysis of the transcribed text. We started by undertaking some pre-processing steps commonly associated with NLP:

- **Tokenisation:** The process of splitting a piece of text into its parts, called *tokens*, while disposing of certain characters, such as punctuation. Tokens are loosely referred to as "words" in this paper.
- **Stop-word removal:** The process of eliminating extremely common and semantically non-selective words. The stop-word list that we used was built by Salton and Buckley for the experimental *SMART* information retrieval system [29] and contains 571 words.
- **Lemmatization:** The process of reducing inflectional and derivational related forms of a word to a common base [30]. Although lemmatization is slower than stemming, we favored its use based on the recent results reported by Haynes *et al.* [31].

According to *term frequency–inverse document frequency* (TF-IDF) [30], the most characteristic nouns employed by the participants of the focus groups were *people*, *family*, *home*, *friend*, *technology*, *stairs* and *shopping*, which are reflective of their everyday concerns and interests. All the characteristic keywords discovered by TF-IDF are depicted in Fig. 1 using a word cloud.

IV. Methods

POMS is a psychological instrument for assessing an individual's mood state [32]. It is a standard validated psychological test formulated by McNair *et al.* [33]. It defines 65 adjectives that are rated by the individual on a five-point scale. Each adjective contributes to one of seven categories: anger, confusion, depression, fatigue, friendliness, tension and vigour. For example, an individual who uses adjectives such as *exhausted*, *worn out* or *weary* to describe her own mood would contribute to classify her state within the *fatigue* category.

POMS has been widely used to assess both medical patients and the normal population, with a large body of sports and

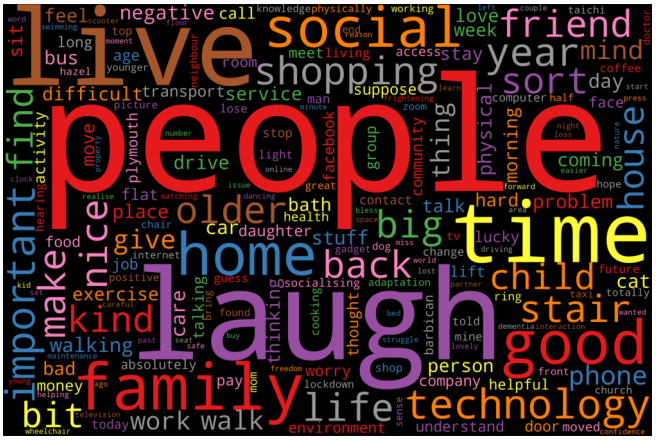

Fig. 1. Word Cloud displaying the most characteristic keywords identified by the TF-IDF weighting in the transcribed conversations of the focus groups.

exercise investigation based extensively on it [34], [35]. Also, instead of its intended use as an administered questionnaire, POMS has been adapted to work with large textual corpora, showing its potential benefits for measuring mood in NLP research [36], [37].

Research on loneliness has reported that fatigue—both mental and physical—is an ever-present challenge for older adults, largely owing to factors linked to loss—loss of loved ones, loss of purpose, or loss of health and vigour. For instance, Morita *et al.* [38] have studied the correlation between emotion and body movements. As an older adult's range of movement becomes limited by pain or fear of pain, confidence and specific age-related considerations—including a decline in muscle mass—contribute to a physical sense of fatigue. Thus, we were interested in a model that takes fatigue into account. This is precisely what POMS contributes.

Depression is another mood commonly associated with the ageing population. While depression, particularly late-onset depression, is not a sign of ageing, it is often perceived as such—the *Royal Society for Public Health* has found that one in four people between 18 and 34 think that being depressed in old age is normal [39]. Chronic pain, multiple medications [40], and loss and changes in lifestyle [41], all contribute to people not recognising or seeking help for depression, which can lead to untreated conditions and misdiagnoses [42].

Given that depression significantly reduces quality of life and cognitive abilities, and can be an antecedent and precursor of dementia [43], we were keen on using an emotion model that recognises depression. POMS contributed this to our work too. Based on POMS, adjectives such as *unworthy*, *miserable* or *gloomy* used to describe a person's feelings contribute to classify her state within the *depression* category [44].

We experimented with the following classifiers: SVM [45], Naïve Bayes [46], logistic regression [47], random forests [48]—the number of trees was selected using linear search—and long short term memory (LSTM) [49].

To train the classifiers, we used Colnerič and Demšar's training set, which is based on a dataset comprising 73 billion

tweets annotated using distant supervision [22]. Regrettably, the random forest was too slow; thus, we built forests with a maximum of 100 trees. Still, training 100 trees using bi-grams took longer than a day on *Colab* [50]. All our work was carried out using the `scikit-learn` library [51], and all the parameters were left at their default values.

Regarding neural network architectures, we decided to use an RNN, as it can naturally handle texts of variable lengths, which would be of help when working with transcribed text. We understand that there are other architectures which may suitable, but we will have to test them in the future.

Instead of pre-processing the transcriptions, we treated each line of a conversation as a sequence of characters, and pass such characters one by one into the neural network. Then, the task of the network was to combine the characters into a suitable representation and predict the moods expressed. The neural network had to learn which sequences of characters form words, since space was not treated differently from any other character. The benefit of this character-based approach is that it does not require any pre-processing. If we were working with words, we would need a tokenizer first and then we would have to decide which morphological variations of the words are similar enough to consider them equivalent for their representation, which is what stemming and lemmatization do. However, in our character setting approach, all those decisions were left to the neural network to figure out.

Our embeddings consist of sequences of characters mapped into vectors. We used only characters that occurred in the training dataset 25 times or more, which yielded a set of 410 characters, and we removed emoticons and other symbols that were not part of our transcriptions. The embeddings were then passed through the RNN layer. We experimented exclusively with the LSTM variant, as Peng has shown that LSTM produces valuable results for text classification [52].

Although POMS comprises seven mood states, we removed the *friendliness* mood from our classifier, as Norcross *et al.* have found that the adjectives corresponding to it are too weak to ensure valid classification [25]. We also complemented the model with other adjectives derived from the *BrianMac Sports Coach* website [44]. Table I shows the full list of adjectives that we employed to identify each of the mood states.

We complemented our results with `text2emotion` [53], a well-regarded Python library to determine the emotions expressed in text. Note that `text2emotion` is based on the original work by Diaz *et al.* [18].

TABLE I
PROFILE OF MOOD STATES (POMS)—CHOSEN ADJECTIVES

Mood state	Adjectives
anger	angry, peeved, grouchy, spiteful, annoyed, resentful, bitter, ready to fight, deceived, furious, bad tempered, rebellious
confusion	forgetful, unable to concentrate, muddled, confused, bewildered, uncertain about things
depression	sorry for things done, unworthy, guilty, worthless, desperate, hopeless, helpless, lonely, terrified, discouraged, miserable, gloomy, sad, unhappy
fatigue	fatigued, exhausted, bushed, sluggish, worn out, weary, listless
tension	tense, panicky, anxious, shaky, on edge, uneasy, restless, nervous
vigour	active, energetic, full of pep, lively, vigorous, cheerful, carefree, alert

V. RESULTS

The participants of Focus Group 1 were more technologically orientated than the others. Keywords such as *Internet*, *technology* and *Zoom* were among the most characteristic keywords employed in the conversations held by the participants of this focus group. Coincidentally, the first focus group was also the one with the largest number of male participants.

Studies suggest that females feel less confident in their interaction with technology, because they have learned less and practiced less, and feel more anxious about using computers when compared with their male counterparts [54]. Nevertheless, the presence of keywords such as *Facebook*, *WhatsApp*, *computer* and *mobile* with high TF-IDF weights across the three focus groups reveals that all the participants were familiar with a variety of modern applications and items.

Generally, the focus groups conversations confirm that older adults appreciate the benefits of technology. Still, negative attitudes towards technology were expressed when referring to the inconveniences associated with it. This seems to be in line with the work of Mitzner *et al.* [55].

For illustration purposes, we have listed below a few comments extracted from the conversations that took place in the focus groups and discuss the benefits and inconveniences of interacting with technology.

- **Benefit 1:** "*I mean, I wouldn't have been able to see my family without the internet!*"
- **Benefit 2:** "*And I use it digitally for communicating with my children with a portal which is a magic machine. I just make telephone calls by saying to the television, please ring Harry and Harry's on the television.*"
- **Benefit 3:** "*So technology is good. Yeah. But then you've got to know how to use it, and also be careful, being safe as well when you're using these things. That's my priority all the time.*"
- **Inconvenience 1:** "*I tell you what makes me very sad about technology is when you hear these people, these women that get sucked in by these men for all this money. [Laughs.] It's true, isn't it? That's true. Yeah.*"
- **Inconvenience 2:** "*Doctors... now... they are a nightmare! Because I'm trying to get an E-consult and if you're not on the Internet now, you can't get your prescription and you can't contact doctors. That is huge!*"
- **Inconvenience 3:** "*You want older people to embrace technology... make it easier. Make it less scary. Yeah, they*

get that. Sometimes these iPhones. I mean, I love it. I'm a geek. Yeah. As soon as there is a new technology I want it! But I've got friends that can't understand it. The technical wording is too difficult... I love it, but I don't understand a lot of it. Make it easy. We want older people or people who are scared of it to embrace the technology. Make it easy. Yeah, if that makes sense. Right?"

Using our classifier, we assigned each line in the transcriptions a probability associated with each of the POMS categories. The values displayed in Fig. 2 represent the addition of the probabilities for each category to occur in each of the lines of the transcriptions derived from Focus Group 1.

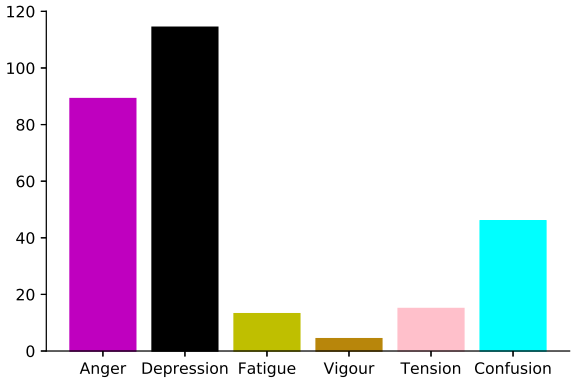

Fig. 2. Distribution of the probabilities of each of the POMS categories present in the transcriptions of Focus Group 1.

The participants in Focus Group 1 have multiple chronic health conditions and mobility impairments. In fact, some of them have already transitioned into supported-living accommodation. They have lost a degree of autonomy and are aware that their current abilities are likely to deteriorate further in the short term. Unsurprisingly, Fig. 3 shows that, according to `text2emotion`, fear is the most prominent emotion conveyed by Focus Group 1.

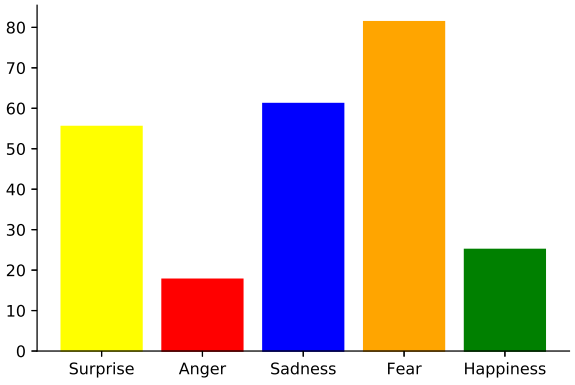

Fig. 3. Distribution of the probabilities of each of the `text2emotion` categories present in the transcriptions of Focus Group 1.

Beadle and De la Vega have pointed out that the decline of cognitive empathy frequently correlates with an increase in emotional empathy in older adults [56]. This may explain why the participants in Focus Group 2 engage in caring roles regularly, supporting others who are older or have additional concerns. While this provides them with a sense of fulfilment, it also increases their sadness both aimed at the recipients of their support and themselves. Fig. 4 corroborates that sadness is the most prominent emotion found in Focus Group 2.

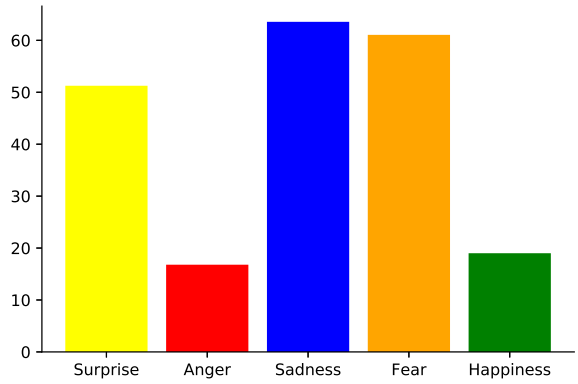

Fig. 4. Distribution of the probabilities of each of the `text2emotion` categories present in the transcriptions of Focus Group 2.

Our POMS classifier yielded very similar results across the three focus groups. Depression, anger, and confusion are the most prominent moods in all cases. The only difference is the amount associated with each mood. Fig. 5 displays the distribution for Focus Group 2.

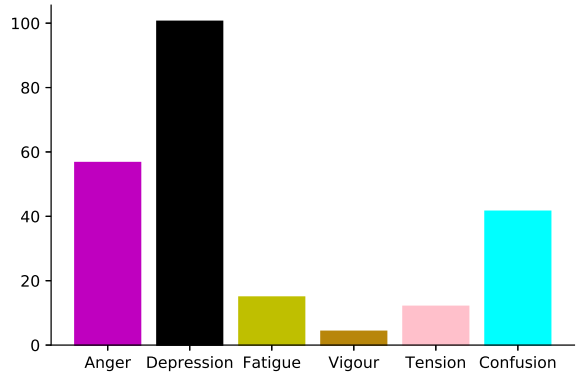

Fig. 5. Distribution of the probabilities of each of the POMS categories present in the transcriptions of Focus Group 2.

Focus Group 3 expressed a higher level of surprise than all the others, as it can be seen in Fig. 6. To explain this, it is important to examine the meaning of *surprise*. Peirce [57] and Pollard [58] define "surprise" as a reflective moment of self-realization or a new viewpoint previously unconsidered. As a younger group, with fewer health concerns, the conversations held in Focus Group 3 were mainly hypothetical or based on the participants' observations of the experiences of others.

Focus Group 3 drew on examples of older adults in their families and social circles, realizing what might be to come for

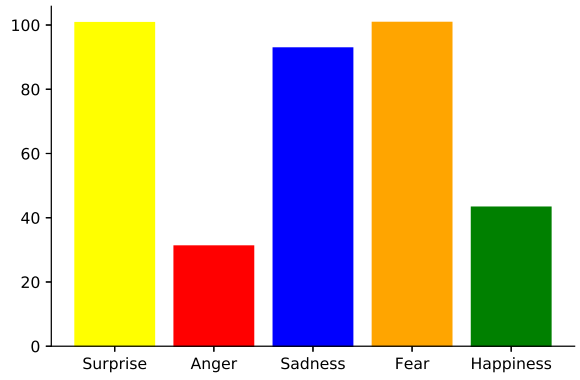

Fig. 6. Distribution of the probabilities of each of the `text2emotion` categories present in the transcriptions of Focus Group 3.

them. These participants were more likely to look for comparisons within the group to reflect on their own ageing process, as Sayag and Kavé have suggested [59]. Fig. 7 displays the POMS distribution for Focus Group 3.

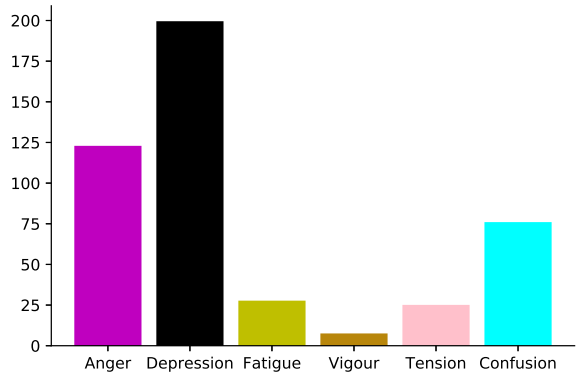

Fig. 7. Distribution of the probabilities of each of the POMS categories present in the transcriptions of Focus Group 3.

VI. Discussion

There are common themes of conversation among older adults which generate anger, depression, sadness and fear—for example, admittance into a care home [60] or susceptibility to scams [61]. However, there are also differences that can explain the variations in the mood states expressed by the participants of our focus groups. To start with, women live longer than men, on average, even when mortality is high—for instance, during severe famines and epidemics [62]. Whilst part of the gender longevity disparity can be accounted for by the nature of the work and leisure activities that a proportion of men engaged in, there is clear evidence to suggest that women live longer than men in almost all modern populations [63]. Undoubtedly, loneliness, depression, and social isolation are critical to explain why men die younger [64].

Older women have larger social networks and maintain more ties to people outside their households than older men [65]. Men who have previously relied on their partners to maintain family structures and relationships can be left without the social skills to retain and extend their connections when they lose their partners. Also, Mann [66] has explained that men's desire to demonstrate and impart their knowledge and experience can be severely impacted when they lose contacts in their late lives. As a result, men are more likely to experience depression in later life [67]. Unsurprisingly, widowed men are more prone to subsequent depression than widowed women [67]. This may be the reason why our POMS classifier detected more depression and anger from men when the analysis of Focus Group 1 was divided by gender. Fig. 8 shows the differences in moods between genders in Focus Group 1.

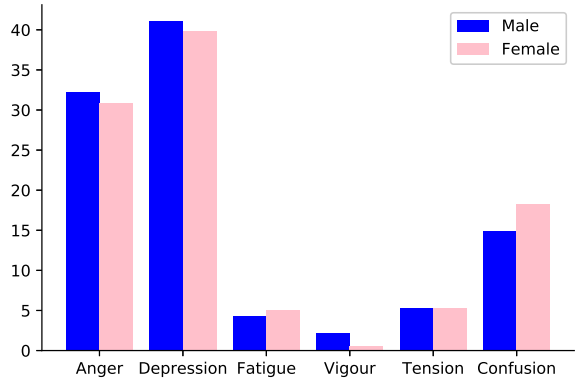

Fig. 8. Differences in moods between men and women in Focus Group 1. The histograms display the distribution of the probabilities of each of the POMS categories present in the transcriptions of Focus Group 1.

In our focus groups, men expressed more anger at falling—which is another common theme among older adults [68]—than women; whereas women identified the loss of social connections as paramount, which has also been noticed by Goll *et al.*, in a sample of older adults living independently in London, England [69].

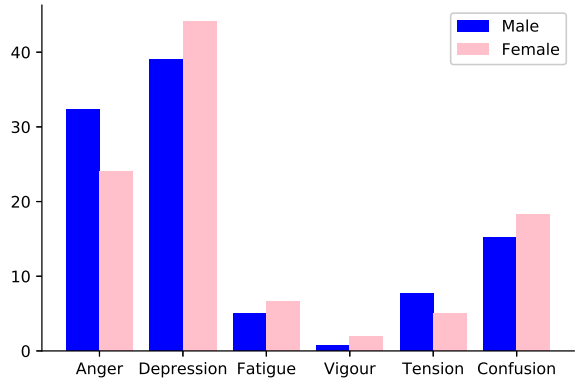

Fig. 9. Differences in moods between men and women in Focus Group 2. The histograms display the distribution of the probabilities of each of the POMS categories present in the transcriptions of Focus Group 2.

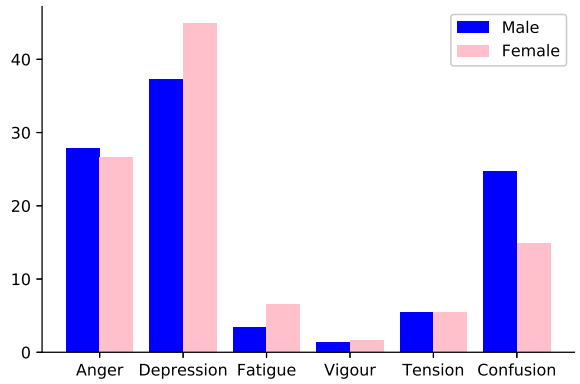

Fig. 10. Differences in moods between men and women in Focus Group 3. The histograms display the distribution of the probabilities of each of the POMS categories present in the transcriptions of Focus Group 3.

VII. Conclusions

Words matter because our attitudes towards a subject are frequently implicit in our lexical choices. Words are reflective and expressive of our attitudes and emotions, and can also explain how we think [70], [71]. The words people use to communicate not only express what they are thinking about, but also how they are feeling. Thus, an appropriate way to examine the attitudes of people towards an issue is to analyze the words they use to describe it, and the linguistic sentiment inherent in those words [72]. This is where the main contribution of the work presented here lies.

We have applied machine learning to analyze conversations recorded with older adults. Our analysis provides practical insights, and it can aid in the decision-making of strategic choices concerning the ageing population. The advantages of using POMS over other emotion classifiers have been discussed, and we expect to start the search for other models that are applicable for the study of older adults. This certainly helps in building a comprehensive view of senior citizens, which opens new possibilities to identify their problems and find ways to boost their wellbeing.

The *UK Office for National Statistics* has confirmed that we are living longer lives because of medical advances and safer workplaces, among other conditions [73]. Given this trend, it seems to be time to rethink how we support older adults, as well as the way in which society approaches the finances, housing, health, and care of the silver economy. Precisely, one of the current *Grand Challenge Missions* set out by the UK Government is to ensure that people can enjoy at least 5 extra healthy, independent years of life by 2035 [74]. Our current work and future developments attempt to harness the power of innovation to help meet the needs of an ageing society.

Acknowledgment

The authors thank Plymouth Community Homes for their help in the organisation of the focus groups and the participants for their time and insights.

References

[1] A. Ahtonen, "Healthy and active ageing: Turning the 'silver' economy into gold," *Policy Brief*, vol. 12, no. 3, p. 2012, 2012.
[2] Iberdrola, "Silver Economy," 2022, https://www.iberdrola.com/innovation/silver-economy.
[3] F. Bran, M.-L. Popescu, and P. Stanciu, "Perspectives of silver economy in the European Union," *Revista de Management Comparat International*, vol. 17, no. 2, p. 130, 2016.
[4] A. S. Zueva and T. S. Khrolenko, "Population ageing: Demographic security threat or silver industry development potential," *RUDN Journal of Public Administration*, vol. 6, no. 3, pp. 234–242, 2019.
[5] A. Klimczuk, "Comparative analysis of national and regional models of the silver economy in the European Union," *A. Klimczuk, Comparative Analysis of National and Regional Models of the Silver Economy in the European Union,"International Journal of Ageing and Later Life*, vol. 10, no. 2, pp. 31–59, 2016.
[6] J. Unützer and M. L. Bruce, "The elderly," *Mental Health Services Research*, vol. 4, no. 4, pp. 245–247, 2002.
[7] C. Walker, L. C. Curry, and M. O. Hogstel, "Relocation stress syndrome in older adults transitioning from home to a long-term care facility: Myth or reality?" *Journal of Psychosocial Nursing and Mental Health Services*, vol. 45, no. 1, pp. 38–45, 2007.
[8] Interreg 2 Seas Mers Zeeën, "AGE IN," 2022, https://www.interreg2seas.eu/en/AGEIN.
[9] A. Ollevier, G. Aguiar, M. Palomino, and I. S. Simpelaere, "How can technology support ageing in place in healthy older adults? A systematic review," *Public Health Reviews*, vol. 41, no. 1, pp. 1–12, 2020.
[10] University of Plymouth, "Plymouth Ethics Online System (PEOS)," 2022, https://www.plymouth.ac.uk/research/plymouth-ethics-online-system.
[11] Council Housing and Housing Association, "The charter for social housing residents," Ministry of Housing, Communities and Local Government, Tech. Rep., Nov. 2020, https://assets.publishing.service.gov.uk/government/uploads/system/uploads/attachment_data/file/936098/The_charter_for_social_housing_residents_-_social_housing_white_paper.pdf.
[12] C. K. Chung and J. W. Pennebaker, "Using computerized text analysis to assess threatening communications and behavior," *Threatening Communications and Behavior: Perspectives on the Pursuit of Public Figures*, pp. 3–32, 2011.
[13] B. Liu, "Sentiment analysis and opinion mining," *Synthesis Lectures on Human Language Technologies*, vol. 5, no. 1, pp. 1–167, 2012.
[14] P. Gonçalves, M. Araújo, F. Benevenuto, and M. Cha, "Comparing and combining sentiment analysis methods," in *Proceedings of the ACM Conference on Online Social Networks*, 2013, pp. 27–38.
[15] M. A. Palomino, A. P. Varma, G. K. Bedala, and A. Connelly, "Investigating the Lack of Consensus Among Sentiment Analysis Tools," in *Human Language Technology. Challenges for Computer Science and Linguistics*, Z. Vetulani, P. Paroubek, and M. Kubis, Eds. Cham: Springer International Publishing, 2020, pp. 58–72.
[16] R. A. Calvo and S. D'Mello, "Affect detection: An interdisciplinary review of models, methods, and their applications," *IEEE Transactions on Affective Computing*, vol. 1, no. 1, pp. 18–37, 2010.
[17] J. Tao and T. Tan, "Affective computing: A review," in *International Conference on Affective Computing and Intelligent Interaction*. Springer, 2005, pp. 981–995.
[18] S. S. Díaz *et al.*, "Intelligent execution of behaviors in a NAO robot exposed to audiovisual stimulus," in *IEEE Colombian Conference on Robotics and Automation (CCRA)*. IEEE, 2018, pp. 1–6.
[19] R. W. Picard, *Affective Computing*. MIT press, 2000.
[20] M. Spruit, S. Verkleij, K. de Schepper, and F. Scheepers, "Exploring language markers of mental health in psychiatric stories," *Applied Sciences*, vol. 12, no. 4, p. 2179, 2022.
[21] S. Chaffar and D. Inkpen, "Using a heterogeneous dataset for emotion analysis in text," in *Advances in Artificial Intelligence*, C. Butz and P. Lingras, Eds. Berlin, Heidelberg: Springer Berlin Heidelberg, 2011, pp. 62–67.
[22] N. Colnerič and J. Demšar, "Emotion recognition on Twitter: comparative study and training a unison model," *IEEE Transactions on Affective Computing*, vol. 11, no. 3, pp. 433–446, 2018.
[23] P. Ekman, "An argument for basic emotions," *Cognition & emotion*, vol. 6, no. 3-4, pp. 169–200, 1992.
[24] R. Plutchik, "A general psychoevolutionary theory of emotion," in *Theories of Emotion*. Elsevier, 1980, pp. 3–33.

[25] J. C. Norcross, E. Guadagnoli, and J. O. Prochaska, "Factor structure of the profile of mood states (POMS): Two partial replications," *Journal of Clinical Psychology*, vol. 40, no. 5, pp. 1270–1277, 1984.

[26] A. K. Pandey, R. Gelin, and A. Robot, "Pepper: The first machine of its kind," *IEEE Robotics & Automation Magazine*, vol. 25, no. 3, pp. 40–48, 2018.

[27] Trint Ltd., "Trint: Audio Transcription Software," 2022, https://trint.com/.

[28] J. S. Girgus, K. Yang, and C. V. Ferri, "The gender difference in depression: Are elderly women at greater risk for depression than elderly men?" *Geriatrics*, vol. 2, no. 4, 2017. [Online]. Available: https://www.mdpi.com/2308-3417/2/4/35

[29] C. Buckley, "Implementation of the SMART information retrieval system [technical report]," *Cornell University, TR85-686*, vol. 4, no. 4, p. 4, 1985.

[30] H. Schütze, C. D. Manning, and P. Raghavan, *Introduction to Information Retrieval*. Cambridge University Press Cambridge, 2008.

[31] C. Haynes *et al.*, "Automatic classification of National Health Service feedback," *Mathematics*, vol. 10, no. 6, p. 983, 2022.

[32] B. G. Berger and R. W. Motl, "Exercise and mood: A selective review and synthesis of research employing the profile of mood states," *Journal of Applied Sport Psychology*, vol. 12, no. 1, pp. 69–92, 2000.

[33] D. M. McNair, M. Lorr, and L. F. Droppleman, *Manual Profile of Mood States*. Educational & Industrial Testing Service, 1971.

[34] A. Leunes and J. Burger, "Profile of mood states research in sport and exercise psychology: Past, present, and future," *Journal of Applied Sport Psychology*, vol. 12, no. 1, pp. 5–15, 2000.

[35] S. Y. Cheung and E. T. Lam, "An innovative shortened bilingual version of the profile of mood states (POMS-SBV)," *School Psychology International*, vol. 26, no. 1, pp. 121–128, 2005.

[36] A. Pepe and J. Bollen, "Between conjecture and memento: Shaping a collective emotional perception of the future," in *AAAI Spring Symposium: Emotion, Personality, and Social Behavior*, 2008, pp. 111–116.

[37] J. Bollen, H. Mao, and A. Pepe, "Modeling public mood and emotion: Twitter sentiment and socio-economic phenomena," in *Proceedings of the AAAI Conference on Web and Social Media*, vol. 5, no. 1, 2011, pp. 450–453.

[38] J. Morita, Y. Nagai, and T. Moritsu, "Relations between body motion and emotion: Analysis based on laban movement analysis," in *Proceedings of the Annual Meeting of the Cognitive Science Society*, vol. 35, no. 35, 2013.

[39] M. Makita, A. Mas-Bleda, E. Stuart, and M. Thelwall, "Ageing, old age and older adults: A social media analysis of dominant topics and discourses," *Ageing & Society*, vol. 41, no. 2, pp. 247–272, 2021.

[40] R. M. Kok and C. F. Reynolds, "Management of depression in older adults: a review," *Jama*, vol. 317, no. 20, pp. 2114–2122, 2017.

[41] A. Fiske, J. L. Wetherell, and M. Gatz, "Depression in older adults," *Annual review of clinical psychology*, vol. 5, pp. 363–389, 2009.

[42] R. Briggs, K. Tobin, R. A. Kenny, and S. P. Kennelly, "What is the prevalence of untreated depression and death ideation in older people? Data from the Irish longitudinal study on aging," *International psychogeriatrics*, vol. 30, no. 9, pp. 1393–1401, 2018.

[43] B. E. Leonard, "Inflammation, depression and dementia: Are they connected?" *Neurochemical research*, vol. 32, no. 10, pp. 1749–1756, 2007.

[44] Mackenzie, B, "Scoring for POMS," 2022, https://www.brianmac.co.uk/pomscoring.htm.

[45] W. S. Noble, "What is a support vector machine?" *Nature biotechnology*, vol. 24, no. 12, pp. 1565–1567, 2006.

[46] D. Berrar, "Bayes' theorem and naive bayes classifier," *Encyclopedia of Bioinformatics and Computational Biology: ABC of Bioinformatics*, vol. 403, 2018.

[47] D. G. Kleinbaum, K. Dietz, M. Gail, M. Klein, and M. Klein, *Logistic Regression*. Springer, 2002.

[48] G. Biau, "Analysis of a random forests model," *The Journal of Machine Learning Research*, vol. 13, no. 1, pp. 1063–1095, 2012.

[49] J. Nowak, A. Taspinar, and R. Scherer, "LSTM recurrent neural networks for short text and sentiment classification," in *International Conference on Artificial Intelligence and Soft Computing*. Springer, 2017, pp. 553–562.

[50] G. Research, "Google Colaboratory," 2022, https://colab.research.google.com/.

[51] F. Pedregosa, G. Varoquaux, A. Gramfort, V. Michel, B. Thirion, O. Grisel, M. Blondel, P. Prettenhofer, R. Weiss, V. Dubourg, J. Vanderplas, A. Passos, D. Cournapeau, M. Brucher, M. Perrot, and E. Duchesnay, "Scikit-learn: Machine learning in Python," *Journal of Machine Learning Research*, vol. 12, pp. 2825–2830, 2011.

[52] X. Peng, "A comparative study of neural network for text classification," in *2020 IEEE Conference on Telecommunications, Optics and Computer Science (TOCS)*. IEEE, 2020, pp. 214–218.

[53] Python Software Foundation, "text2emotion 0.0.5," 2022, https://pypi.org/project/text2emotion/.

[54] J. He and L. A. Freeman, "Are men more technology-oriented than women? the role of gender on the development of general computer self-efficacy of college students," *Journal of Information Systems Education*, vol. 21, no. 2, pp. 203–212, 2010.

[55] T. L. Mitzner, J. B. Boron, C. B. Fausset, A. E. Adams, N. Charness, S. J. Czaja, K. Dijkstra, A. D. Fisk, W. A. Rogers, and J. Sharit, "Older adults talk technology: Technology usage and attitudes," *Computers in human behavior*, vol. 26, no. 6, pp. 1710–1721, 2010.

[56] J. N. Beadle and C. E. De la Vega, "Impact of aging on empathy: Review of psychological and neural mechanisms," *Frontiers in psychiatry*, vol. 10, p. 331, 2019.

[57] J. Buchler, *Philosophical writings of Peirce*. Dover, 1955.

[58] V. Pollard, "Ethics and reflective practice: Continuing the conversation," *Reflective Practice*, vol. 9, no. 4, pp. 399–407, 2008.

[59] M. Sayag and G. Kavé, "The effects of social comparisons on subjective age and self-rated health," *Ageing & Society*, pp. 1–14, 2021.

[60] S. Quine and S. Morrell, "Fear of loss of independence and nursing home admission in older Australians," *Health & Social Care in the Community*, vol. 15, no. 3, pp. 212–220, 2007.

[61] B. D. James, P. A. Boyle, and D. A. Bennett, "Correlates of susceptibility to scams in older adults without dementia," *Journal of elder abuse & neglect*, vol. 26, no. 2, pp. 107–122, 2014.

[62] V. Zarulli, J. A. B. Jones, A. Oksuzyan, R. Lindahl-Jacobsen, K. Christensen, and J. W. Vaupel, "Women live longer than men even during severe famines and epidemics," *Proceedings of the National Academy of Sciences*, vol. 115, no. 4, pp. E832–E840, 2018.

[63] J. Lemaire, "Why do females live longer than males?" *North American Actuarial Journal*, vol. 6, no. 4, pp. 21–37, 2002.

[64] A. Steptoe, A. Shankar, P. Demakakos, and J. Wardle, "Social isolation, loneliness, and all-cause mortality in older men and women," *Proceedings of the National Academy of Sciences*, vol. 110, no. 15, pp. 5797–5801, 2013.

[65] B. Cornwell, "Independence through social networks: Bridging potential among older women and men," *Journals of Gerontology Series B: Psychological Sciences and Social Sciences*, vol. 66, no. 6, pp. 782–794, 2011.

[66] R. Mann, "Out of the shadows?: Grandfatherhood, age and masculinities," *Journal of Aging Studies*, vol. 21, no. 4, pp. 281–291, 2007.

[67] F. Förster, A. Pabst, J. Stein, S. Röhr, M. Löbner, K. Heser, L. Miebach, A. Stark, A. Hajek, B. Wiese *et al.*, "Are older men more vulnerable to depression than women after losing their spouse? evidence from three german old-age cohorts (agedifferent.de platform)," *Journal of Affective Disorders*, vol. 256, pp. 650–657, 2019.

[68] R. W. Kressig, S. L. Wolf, R. W. Sattin, M. O'Grady, A. Greenspan, A. Curns, and M. Kutner, "Associations of demographic, functional, and behavioral characteristics with activity-related fear of falling among older adults transitioning to frailty," *Journal of the American Geriatrics Society*, vol. 49, no. 11, pp. 1456–1462, 2001.

[69] J. C. Goll, G. Charlesworth, K. Scior, and J. Stott, "Barriers to social participation among lonely older adults: The influence of social fears and identity," *PloS one*, vol. 10, no. 2, 2015.

[70] T. Holtgraves, "Social psychology and language: Words, utterances, and conversations," *Handbook of Social Psychology*, 2010.

[71] Y. R. Tausczik and J. W. Pennebaker, "The psychological meaning of words: LIWC and computerized text analysis methods," *Journal of language and social psychology*, vol. 29, no. 1, pp. 24–54, 2010.

[72] S. Eggly, M. A. Manning, R. B. Slatcher, R. A. Berg, D. L. Wessel, C. J. Newth, T. P. Shanley, R. Harrison, H. Dalton, J. M. Dean *et al.*, "Language analysis as a window to bereaved parents' emotions during a parent—physician bereavement meeting," *Journal of Language and Social Psychology*, vol. 34, no. 2, pp. 181–199, 2015.

[73] A. Storey, N. Coombs, and S. Leib, "Living longer: Caring in later working life," UK Office for National Statistics, Tech. Rep., Mar. 2019.

[74] Department for Business, Energy & Industrial Strategy, "The grand challenge missions," Industrial Strategy, Tech. Rep., Jan. 2021.

17th Conference on Information Systems Management

THIS event constitutes a forum for the exchange of ideas for practitioners and theorists working in the broad area of information systems management in organizations. The conference invites papers coming from three complimentary directions: management of information systems in an organization, uses of information systems to empower managers, and information ssytems for sutainable development. The conference is interested in all aspects of planning, organizing, resourcing, coordinating, controlling and leading the management function to ensure a smooth operation of information systems in organizations. Moreover, the papers that discuss the uses of information systems and information technology to automate or otherwise facilitate the management function are specifically welcome. Papers about the influence of information systems on sustainability are also expected.

TOPICS

- Management of Information Systems in an Organization:
  - Modern IT project management methods
  - User-oriented project management methods
  - Business Process Management in project management
  - Managing global systems
  - Influence of Enterprise Architecture on management
  - Effectiveness of information systems
  - Efficiency of information systems
  - Security of information systems
  - Privacy consideration of information systems
  - Mobile digital platforms for information systems management
  - Cloud computing for information systems management
- Uses of Information Systems to Empower Managers
  - Achieving alignment of business and information technology
  - Assessing business value of information systems
  - Risk factors in information systems projects
  - IT governance
  - Sourcing, selecting and delivering information systems
  - Planning and organizing information systems
  - Staffing information systems
  - Coordinating information systems
  - Controlling and monitoring information systems
  - Formation of business policies for information systems
  - Portfolio management,
  - CIO and information systems management roles
- Information Systems for Sustainability
  - Sustainable business models, financial sustainability, sustainable marketing
  - Qualitative and quantitative approaches to digital sustainability
  - Decision support methods for sustainable management

TECHNICAL SESSION CHAIRS

- **Arogyaswami, Bernard,** Le Moyne University, USA
- **Chmielarz, Witold,** University of Warsaw, Poland
- **Jankowski, Jarosław,** West Pomeranian University of Technology in Szczecin, Poland
- **Kisielnicki, Jerzy,** University of Warsaw, Poland
- **Ziemba, Ewa,** University of Economics in Katowice, Poland

PROGRAM COMMITTEE

- **Bicevska, Zane,** University of Latvia, Latvia
- **Bicevskis, Janis,** University of Latvia, Latvia
- **Carchiolo, Vincenza,** Universita di Catania, Italy
- **Czarnacka-Chrobot, Beata,** Warsaw School of Economics, Poland
- **De Juana-Espinosa, Susana,** Universidad de Alicante, Spain
- **Duan, Yanqing,** University of Bedfordshire, UK
- **Eisenbardt, Monika,** Univeristy of Economics Katowice, Poland
- **Gabryelczyk, Renata,** University of Warsaw, Poland
- **Geri, Nitza,** The Open University of Israel, Israel
- **Leyh, Christian,** Technische Universität Dresden, Germany
- **Malgeri, Michele,** Universita' degli Studi di Catania, Italy
- **Muszyńska, Karolina,** University of Szczecin, Poland
- **Nikiforova, Anastasija,** University of Tartu, Estonia
- **Rizun, Nina,** Gdansk University of Technology, Poland
- **Rozevskis, Uldis,** University of Latvia, Latvia
- **Sobczak, Andrzej,** Warsaw School of Economics, Poland
- **Swacha, Jakub,** University of Szczecin, Poland
- **Symeonidis, Symeon,** Democritus Univesity of Thrace, Greece

Communication Papers of the of the 17th Conference on Computer Science and Intelligence Systems pp. 261–267
DOI: 10.15439/2022F104
ISSN 2300-5963 ACSIS, Vol. 32

Required Quality of Service attributes in the context of various types of Web Services

Maksymilian Iwanow, Helena Dudycz, Krzysztof Michalak
Wroclaw University of Economics and Business, ul. Komandorska 118/120, Wroclaw, Poland
Email: {maksymilian.iwanow, helena.dudycz, krzysztof.michalak}@ue.wroc.pl

***Abstract*—Nowadays, many business units are based on network solutions on the Internet. Various industry branches are entering the Web and offering their services. Customers differ a lot in terms of what services quality requirements they want to be ensured. Functional conditions are defined at the level of business process implementation, but quality issues are also very important there. This study concerns the analysis of non-functional requirements for different groups of users of Web Services. The main objective is to identify differences in user expectations in the context of distinct services offering various functionalities on the Internet. The research was carried out via a systematic literature review within the Web of Science database using keyword chains. As a result of this work, 21 publications describing case studies of the implementation of Web Services and their qualitative attributes were identified. In the context of 20 different types of Web Services, a total of 23 quality attributes were listed.**

I. Introduction

A Web Service is a self-describing, self-contained module providing a certain kind of functionality on the Internet [1]. The module is independent of the user's hardware or software configuration, and the implementation ensures operation on a black box basis – the service reacts to user input and returns a certain result [2]. A very important factor in the analysis of the service operation is the Quality of Service – QoS [3], which can be defined as a set of certain non-functional attributes that should be maintained at a fixed level in order to make the functionality of the service as friendly as possible to the end user.

The subject of QoS criteria is a very broad area, which is described in more detail in [4]. This paper presents a list of identified authors who proposed various sets of quality attributes relevant to application contexts in which they studied the use of Web Services. Most often, the groups of quality attributes consisted of five metrics. In general, the most popular criterion was the time metric (usually formulated as response time), followed by availability, reliability, price and throughput [5-7]. The analysis of the publications showed that the vast majority of the works are related to Web Service selection, composition, optimization and prediction in the field of QoS.

No doubt, in today's world, almost all areas of life are affected by Internetization [8]. Private and public institutions provide more and more services and web applications with more and more functionalities. Many of them operate on the user's private and secret information, hence they should be secure and guarantee protection against attacks from potential hackers. Others, on the other hand, due to their specificity, should work quickly and guarantee an instant response to human actions. Some should be available basically non-stop and have a sufficiently developed Continuous Integration/Continuous Delivery (CI/CD) process so that when a new version is deployed on the servers, continuous operation is guaranteed for the user [9].

The areas in which the services operate are different, the users are different, and the functionalities are different – hence it can be assumed that customer groups have quite different expectations regarding each service. The aim of this paper is to analyze the types of Web Services studied by researchers and draw conclusions, using case study examples, as to what quality characteristics are taken into account in the context of which service. Unraveling the problem of which quality parameters are most important for various services can be a key aspect of a multi-criteria optimization of complex services.

The paper has the following structure: in the next section, we describe the context and the methodology of the study; then the research results are presented and discussed; finally, directions for further research and future works are described.

II. Research Context and Methodology

Every Web Service should meet several requirements. The basic ones are, of course, functional. Each Web Service operates in a certain context, usually the scope of an organization, a company or an operational unit. On the other

This work was supported by the Ministry of Science and Higher Education in Poland

hand, non-functional quality requirements also have to be satisfied. After all, no one is able to use even the best-adapted functionality if it is unavailable to customers or if the system response time is too long.

The importance of non-functional features of Web Services can be identified on the basis of the following questions: Are all users willing to allow a one-second delay at the expense of greater transaction security in the context of a banking service? And in the field of a purchasing service, will such an exchange not be acceptable? Do customers measure the login sub-system and the medical appointments ordering sub-system within the same medical application with exactly the same quality metrics? Do users have different quality requirements for order approval in a food-ordering application and order approval in a clothing store system? With the help of a reasonable systematization, we may not be able to answer those doubts with specific, numerical outcomes, but we will surely obtain an overview of the situation and a clue to correctly identify the problem.

Based on these considerations, the following research questions emerged:

RQ1. Which QoS metrics are the most important in the context of which types of services?

RQ2. What are the differences in quality requirements in the context of the same functionality but different Web Services?

RQ3. What are the differences in quality requirements in the context of different functionalities within a single Web Service?

A systematic literature review was conducted to identify answers to these research questions. The study was carried out according to the procedure described below.

The Web of Science platform was chosen as the source of articles due to the strictest policy in the peer-to-peer review process and because this database seeks to publish high-standard papers. The queries used to find the articles are defined in Table 1. We limited ourselves to English language articles and abstracts-based searches as the most important parts of the articles in terms of presenting their vision.

The first search focused on the quality requirements in the enterprise context of Web Services. We wanted to understand how researchers define fixed initial QoS metrics in the aspect of different systems. The second search stemmed strictly from the first one – we found that the best way to determine quality requirements is to focus on case studies.

The articles were analyzed in three iterations. The first consisted of reading the abstracts and determining which articles would in any way help answer the research questions posed. The second iteration allowed for digging more deeply into the selected writings and confirming or rejecting the selection. The final iteration involved an in-depth analysis of the full text of selected articles. In total, over the two searches, 21 publications were identified that contributed a lot to the topic of the relationship between services and the required quality in the context of their types (Table A in the Appendix).

TABLE I.
SAMPLE QUERIES TO THE SEARCH ENGINE (WEB OF SCIENCE) CONTAINING PUBLICATIONS

Search Engine	Phrase	Keywords	Date	Quantity
Web of Science	AB=("web servic*" AND (enterpr* OR compan* OR busin* OR corporat* OR "econom* unit*") AND qos AND (requiremen* OR prerequisi* OR constrain*))	Web Service, Enterprise, Company, Business, Corporate, Economic Unit, QoS, requirements, constraints, prerequisites	02.08.2021	193
Web of Science	AB=("case stud*" and "web servic*" and (quality or qos))	Case Study, Web Service, Quality, QoS	22.08.2021	206

III. RESULTS

The results of the study are two matrixes. The first one (Table A in the APPENDIX) contains a systematic summary of the identified and analyzed publications. The second (Table 2), on the other hand, presents the analysis and relationships between the types of Web Services and the quality metrics. In total, there are 23 quality attributes considered by researchers in the context of 20 different types of Web Services. Many of the quality metrics need to be standardized because, for example, not every "time" is a "response time", and, for instance, performance or scalability are such broad concepts that they probably consist of several smaller sub-attributes.

The marking key to Table 2 is organized as follows:

- Columns:
  (1) Time (Response Time, Speed); (2) Reliability (Precision); (3) Availability; (4) Cost (Price); (5) Recall (Frequency of Invocations, Answers); (6) Performance; (7) Accuracy; (8) Reputation (Brand, Trust); (9) Security; (10) Accessibility; (11) Integrity; (12) Robustness; (13) Benefit; (14) Capacity; (15) Exception Handling; (16) Regulatory; (17) Interoperability; (18) Privacy; (19) Responsiveness; (20) Scalability; (21) Network-Related QoS Requirement; (22) Successability; (23) Throughput; (No. 2) Number of various metrics within a given service type; (No. 3) Number of times a service type is mentioned in the articles.
- Rows:
  (A) Hotel Service; (B) Medical Service; (C) Purchasing Service; (D) Telecom Service; (E) Travel Agency Service; (F) Insurance Company Service; (G) Language

Translation Service; (H) Social Security Sector Service; (I) Engineering Service; (J) Public Employment Service; (K) Activity (Sport) Service; (L) Film Service; (M) Geospatial Application; (N) Loan Service; (O) Ordering Food Service; (P) Weather Service; (R) Advertisement Service; (S) Bioinformatic Service; (T) Government Service; (U) Industrial Automation Platform; (No. 1) Number of occurrences of a metric among services.

In the next section, conclusions resulting from the conducted research are discussed.

IV. Discussion of the Results

Referring to Table 2., there is no doubt that by far the most important factor for virtually all Web Services is the Response Time – it is omitted by the researchers only in 3 types of services – Advertisement, Bioinformatic and Geospatial applications. The second most popular metric is Reliability, indicated by researchers in 14 different types of services, and in the third place, with 13 references – is Availability. Then there is Price (Cost), which is cited in 8 different types of Web Services. As many as 11 of the 23 metrics appear only once. These are Benefit, Capacity, Exception Handling, Regulatory, Interoperability, Privacy, Responsiveness, Scalability, Network-Related QoS Requirement, Successability, and Throughput.

The services in the context of which the largest number of various features is extracted are Hotel and Medical services (15 and 11 metrics respectively). Each of these service types is mentioned twice in the considered group of articles. This may imply, for example, a not completely considered set of features towards the end customer – we should remember that optimization in terms of multiple criteria is very costly.

Using the Hamming Distance (the number of places where the rows in Table 2. differ), we identified service types that have the most similar quality requirements. Among the services that are mentioned by the researchers a minimum of two times, the most similar quality criteria are used for the Purchasing Service and the Travel Agency Service – the Hamming Distance equals 4. In the second place, with a distance equal to 5, there are two pairs: Language Translation Service together with Purchasing Service and Language Translation Service together with Travel Agency Service.

Answering the first research question (**RQ1**), we can clearly state that the most important quality attributes for almost all types of Web Services are: Response Time, Reliability and Availability. A specific breakdown: of which metrics are most important in the context of which services is presented in the Table 2.

When analyzing the articles, one can come across similar

TABLE II.
AN ANALYSIS OF THE MAPPING OF WEB SERVICES TYPES TO RESEARCHER-SELECTED NON-FUNCTIONAL FEATURES

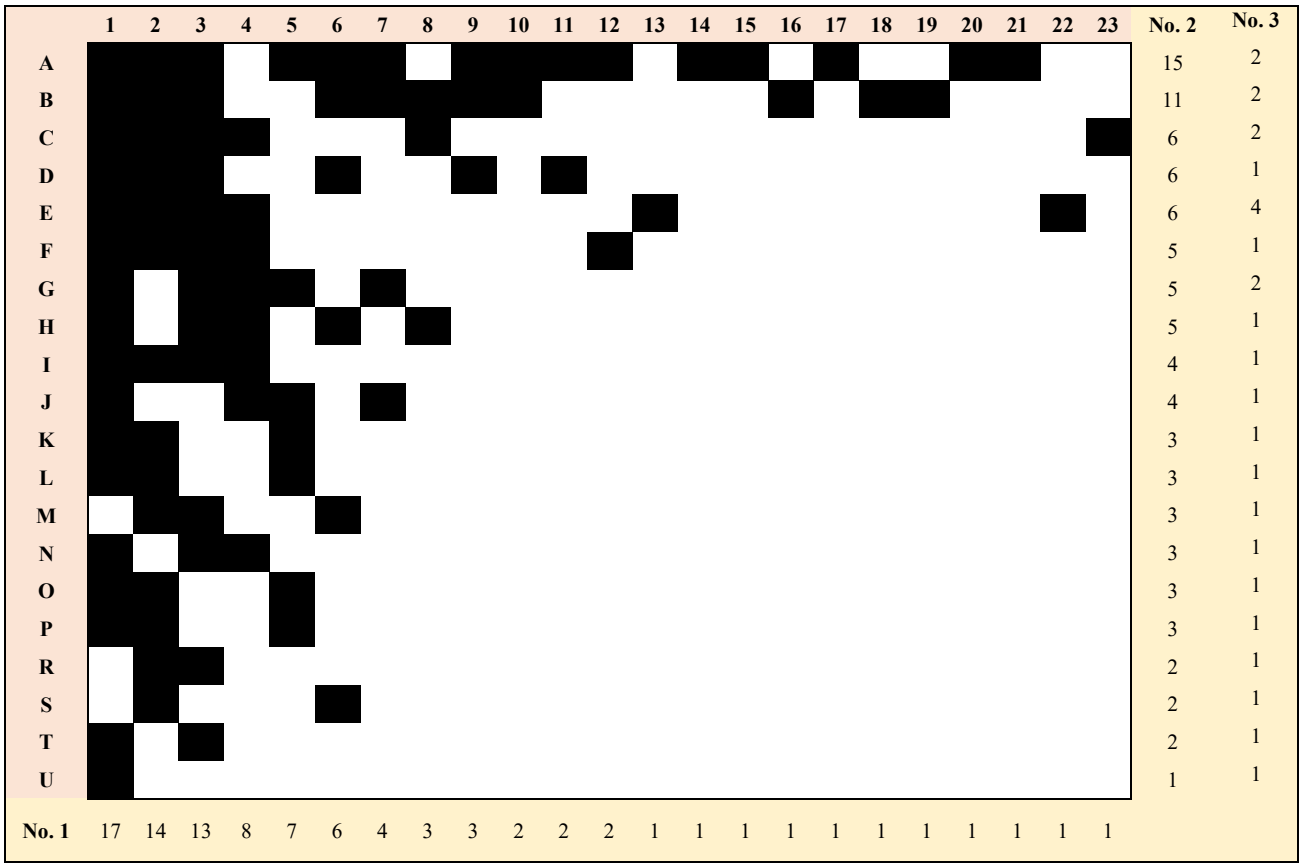

functionalities in different Web Services. As the first example, we can take the comparison of three ordering functionalities: food, computer and creating an order without an itemized product (respectively in [10], [11], [12]) within Ordering Food and Purchasing Services. Unambiguously, the greatest emphasis, unsurprisingly, is on Response Time, which is found in each of the three services. In the second place, ex aequo, we have Availability (computer and no product specified order) and Reliability (food and no product specified order). Next, Recall, Cost, Reputation, and Throughput are listed.

The next comparison regards functionalities related to traveling in the broadest sense (e.g. renting a car, booking a hotel or flight). Again, the most important factor (4/4 of the analyzed articles) turns out to be Response Time, which is hardly a surprise. In as many as three articles ([11], [13], [14]) Cost plays an important role. In the case of the Hotel Service [10] the authors still mention Recall and Reliability. In the case of three Travel Agency Services (mentioned earlier) we still have Availability, Benefit and Successability.

We can also find similar functionalities in the Travel Agency Service [15], i.e. check user action, and in the Medical Service [16], i.e. login (with email) action. In the first case, Reliability and Time are the most important issues, and in the second – Security.

The last comparison regards search functionalities in the context of the Activity Service [10], the Travel Agency Service [11], the Public Employment Service [17] and the Advertisement Service [18]. For the first three publications, in the context of functionality: the Search for an activity, the Search for an available flight, and the Search for job vacancies in a specified country, Response Time is mentioned, and Recall and Cost are also important (in 2 of the 3 articles). Availability, Reliability (also mentioned in the context of the fourth functionality – the Search for a car from the fourth article) and Accuracy also appear.

Summarizing the second research question (**RQ2**), we made the following conclusions:

- In the context of ordering functionalities (food, hardware and no product specified), Response Time is the most important, in the second place in the context of hardware is Availability and in the context of food is Reliability; ordering of a non-specified product combines all features.
- Leaving aside Response Time, for similar related functionalities in the Hotel Service, Recall and Reliability are more important, while in the Travel Agency Services we have Cost, Availability, Benefit and Successability.
- The functionality of logging in and checking the user in the Travel Agency Service focuses primarily on Reliability and Time, while a similar functionality in the Medical Service focuses on Security.
- The search functionality in the Activity Service, Travel Agency Service and Public Employment Service focuses primarily on Response Time, Recall and Cost. The Advertisement Service focuses on Availability and Reliability.

To analyze many different functionalities among the services of the same type, we can focus on the Medical Services. This type of service provides a large variety of functionalities like, for example, presenting relevant medical information in the context of a region [19]. In this case, we listed numerous requirements, such as Reliability, Security, Privacy, Accessibility, Responsiveness, Speed, Availability, Trust, Relevancy, Performance and Regulatory. Hence, unfortunately, we are not able to prioritize them all. However, when we look at the functionalities in [16] – we see that for any action where the patient's (and unit individual) data is processed, Security is by far the most important issue.

To explain **RQ3,** we can focus on different functionalities of Medical Services. Undoubtedly, in all actions where the user data is processed, Security is by far the most important quality requirement, while as far as other functionalities (which are mainly about presenting facts) are concerned, the importance is equally distributed among the most basic metrics like Response Time, Reliability, Availability and so on.

V. Conclusion

This paper presents findings related to the selection of quality metrics in the context of different types of Web Services. The research was conducted based on case study examples found via a systematic literature review. An attempt was made to systematize the non-functional requirements in the context of the same and different types of services and functionalities.

Twenty-one publications were identified that describe the practical implementation of Web Services and the quality attributes important to these services. The publications present 20 different types of services and a total of 23 distinct quality metrics. The most important quality attributes for almost all types of Web Services were found to be the following: Response Time, Reliability, and Availability. When the functionalities involve sensitive data processing, security remains a very important issue.

Further research in this direction should also address the popular services that are missing from our set of case studies, such as online wallet services or social media. Gray literature should also be analyzed (studies carried out by companies providing Web Services). It would also be advisable to conduct interviews and surveys with users (Web Services customers) to determine what quality features are the most important to them in this context. Another direction of research could be focused on different multi-criteria optimization approaches with respect to the quality requirements identified as important for different types of services.

APPENDIX

Table A. Selected publications analyzed by service type, specified functionalities and quality requirements

Year	Authors	Analyzed Systems	Analyzed Functionalities	Non-functional Requirements
2006	H. Wang, D.G. Yang; Y.H. Zhao; Y. Gao [18]	Advertisement Service	• Search for a car	Reputation (i.e. Availability + Reliability)
2006	F. De Paoli, G. Lulli, A. Maurino [17]	Public Employment Service	• Search for job vacancies in a specified country • Glue together and rank retrieved job vacancies • Translate job offers in different languages • Notify end-users of results via different communication channels	Time, Cost, Accuracy, Answers
2008	J.K. Lee, S.H. Kuk, H.S. Kim, S.W. Park [20]	Engineering Service	---	Cost, Reliability, Availability, Time
2008	C. Riedl, T. Bohmann, M. Rosemann, H. Krcmar [21]	Government Service (Business Name Renewal Service)	• Renew business name registrations • Pay a fee for using a service	Response Time, Availability
2008	W.L. Lin, C.C. Lo, K.M. Chao, M. Younas [22]	Hotel Service	• Book a hotel • Book a flight (integration with other WS) • Rent a car (integration with other WS)	Performance, Reliability, Scalability, Capacity, Robustness, Exception Handling, Accuracy, Integrity, Accessibility, Availability, Interoperability, Security, Network-Related QoS Requirement
2008	V. Patankar, R. Hewett [23]	Insurance Company Service	• View the patient's past medical records	Price, Availability, Response Time, Robustness, Reliability
2008	M. Fantinato, M.B.F. De Toledo, I.M.D. Gimenes, [24]	Telecom Service	• Outsource a charging service from one company to the CRM of Telecom company	Availability, Response Time, Security, Integrity, Reliability, Performance
2009	T. Cucinotta, A. Mancina, G.F. Anastasi, G. Lipari, L. Mangeruca, R. Checcozzo, F. Rusina [25]	Industrial Automation Platform	• Stream multimedia (view from 2 IP cameras): what is going on inside the plant • Start/Stop translation	Response Time
2009	T. Neubauer, C. Stummer [26]	Social Security Sector Service	• Consolidate the existing system architecture based on a given set of business processes	Availability, Performance (Time), Reputation, Cost (Revenue, Initial/Running Costs)
2010	M.A. Serhani, A. Jaffar, P. Campbell, Y. Atif [27]	Language Translation Service	• Translate from static, dynamic, active content (with different sizes) • Control version • Track changes	Availability, Quality of Translation (i.e. Time + Accuracy of Translation), Frequency of Service Invocation
2011	K. Xu, Q. Yu, Q. Liu, J. Zhang, A. Bouguettaya [28]	Bioinformatic Service	• Analyze the colorectal cancer studies	Reliability, Performance
2012	V. Vescoukis, N. Doulamis, S.Haragiorgou [29]	Geospatial Application (Integrated Information System for Forest Fire Management)	• Support the monitoring and decisions in the event of a real forest fire incident • Plan early and develop the scenario	Real Time (i.e. Performance + Availability + Reliability)
2013	R.Z. Xu, B.T. Ji, B. Zhang, P.Y. Nie [13]	Travel Agency Service	• Ensure flight services • Ensure hotel services • Ensure other, independent tourism	Benefit, Cost, Time

			services	
2013	D. Bruneo, S. Distefano, F. Longo, M. Scarpa [15]	Travel Agency Service	• Check user • Check credit card • Book a flight • Pay • Cancel reservation	Reliability, Time
2013	M.M. Chen, T.H. Tan, J. Sun, Y. Liu, J. Pang, X.H. Li [11]	Travel Agency Service, Purchasing Service, Loan Service	• Buy a computer, pay with a credit card • Apply for a loan • Search for an available flight, hotel, transport, local agents' services with given user requirements	Response Time, Availability, Cost
2014	D.H. Lin, T. Ishida, Y. Murakami, M. Tanaka [30]	Language Translation Service	• Translate including human and machine activities	Adequacy (Accuracy), Time, Cost
2015	M. Fahad, N. Moalla, Y. Ourzout [12]	Purchasing Service	• Create order	Availability, Response Time, Reputation, Throughput, Reliability
2015	A. Akhunzada, A. Gani, S. Hussain, A.A. Khan, Ashrafullah [14]	Travel Agency Service	• Reserve a ticket • Reserve accommodation • Reserve a car • Reserve all tickets, accommodation, car • Reserve 2 from 3 services	Price, Successability (Probability of Success), Time
2016	G.Buyukozkan, O. Feyzioglu, F. Gocer [19]	Medical Service	• Provide sufficient medical information within a region	Reliability, Security, Privacy, Accessibility, Responsiveness, Speed (Response Time), Availability, Trust (Reputation), Relevancy (Accuracy), Performance, Regulatory *[Metrics that were not related to strict functionalities of Web Services components themselves, like friendly user Interface were not included]*
2016	I. El Kassmi, Z. Jarir, A. Obaid [16]	Medical Service	• Ensure health authentication action • Ensure login action • Ensure login with email action • Ensure patient permission action • Ensure data permission action • Ensure page permission action • Ensure module permission action	Security
2020	M. Driss, A. Aljehani, W. Boulila, H.W. Ghandorh, M. Al-Sarem, [10]	Weather Service, Activity (Sport) Service, Hotel Service, Film Service, Ordering Food Service	• Search for an activity • Forecast weather • Rent a car • Book a hotel • Watch a film • Order food	Response Time, Recall (Frequency of Invocations), Precision (Reliability)

ACKNOWLEDGMENT

The project is financed by the Ministry of Science and Higher Education in Poland under the programme "Regional Initiative of Excellence" 2019 - 2022 project number 015/RID/2018/19 total funding amount 10 721 040,00 PLN.

REFERENCES

[1] M. Papazoglou, "*Web Services: Principles and Technology*". Pearson Prentice Hall, 2007.

[2] D. Fensel and Ch. Bussler, "The Web service modeling framework WSMF", *Electronic Commerce Research and Applications*, vol. 1, no. 2, pp. 113-137, 2002. DOI: 10.1016/S1567-4223(02)00015-7

[3] Y. Hao, Y. Zhang and J. Cao, "A novel QoS model and computation framework in web service selection", *World Wide Web*, vol. 15, no. 5, pp. 663-684, 2012. DOI: 10.1007/s11280-012-0157-5

[4] M. Iwanow, H. Dudycz and K. Michalak, "Quality of Service Attributes for Evaluation of Web Services. A systematic Literature Review", in *14th International Conference on Computational Collective Intelligence*, submitted for publication.

[5] H. Chen, T. Yu, and K.J. Lin, "QCWS: An implementation of QoS-capable multimedia web services", in *5th IEEE International Symposium on Multimedia Software Engineering*, 2003. DOI: 10.1109/MMSE.2003.1254420

[6] D. Dumitriu, A.A. Purcarea and E. Fleaca, "Information Technology Management And Quality Of Services Oriented Architecture", *Management of Technological Changes*, vol. 2, pp. 753-756, 2009.

[7] M. Younas, I. Awan and D. Duce, "An efficient composition of web services with active net-work support", *Expert Systems with Applications*, vol. 31, no. 4, pp. 859-869, 2006. DOI: 10.1016/j.eswa.2006.01.008

[8] S. Ran, "A model for web services discovery with QoS", *ACM SIGecom Exchanges*, 2003. DOI: 10.1145/844357.844360

[9] B.N. Barreto, A. Rezende de Sa and A.R.L. Ribeiro, "A Fog Computing Architecture for Security and Quality of Service", Position Papers of the 2019 Federated Conference on Computer Science and Information Systems, vol. 19, pp. 69–73, 2019. DOI: 10.15439/2019F348

[10] M. Driss, A. Aljehani, W. Boulila, H.W. Ghandorh, and M. Al-Sarem, "Servicing Your Requirements: An FCA and RCA-Driven Approach for Semantic Web Services Composition", *IEEE Access*, vol. 8, pp. 59326-59339, 2020. DOI: 10.1109/ACCESS.2020.2982592

[11] M.M. Chen, T.H. Tan, J. Sun, Y. Liu, J. Pang and X.H. Li, "Verification of Functional and Non-functional Requirements of Web Service Composition. Formal Methods and Software Engineering", *Lecture Notes in Computer Science*, no. 8144, 2013. DOI: 10.1007/978-3-642-41202-8_21

[12] M. Fahad, N. Moalla and Y. Ourzout, "Dynamic Execution of a Business Process via Web Service Selection and Orchestration", *Procedia Computer Science*, vol. 51, pp. 1655–1664, 2015. DOI: 10.1016/j.procs.2015.05.299

[13] R.Z. Xu, B.T. Ji, B. Zhang and P.Y. Nie, "Research on dynamic business composition based on web service proxies", *Simulation Modelling Practice and Theory*, 2013. DOI: 10.1016/j.simpat.2013.05.008

[14] A. Akhunzada, A. Gani, S. Hussain, A.A. Khan and Ashrafullah, "A Formal Framework for Web Service Broker to Compose QoS Measures", in *SAI Intelligent Systems Conference*, pp. 532-536, 2015. DOI: 10.1109/IntelliSys.2015.7361191

[15] D. Bruneo, S. Distefano, F. Longo and M. Scarpa, "Stochastic Evaluation of QoS in Service-Based Systems", *IEEE Transactions on Parallel and Distributed Systems*, vol. 24, no. 10, pp. 2090-2099, 2013. DOI: 10.1109/TPDS.2012.313

[16] I. El Kassmi, Z. Jarir and A. Obaid, "Non-Functional Requirements Interdependencies in Web Service Composition", in *Third International Conference on Systems of Collaboration (SysCo)*, pp. 1-6, 2016. DOI: 10.1109/SYSCO.2016.7831332

[17] F. De Paoli, G. Lulli and A. Maurino, "Design of quality-based composite web services", *Service-Oriented Computing, Lecture Notes in Computer Science*, vol. 4294, 2006. DOI: 10.1007/11948148_13

[18] H. Wang, D.G. Yang, Y.H. Zhao and Y. Gao, "Multiagent system for reputation-based Web services selection", in *Sixth International Conference on Quality Software (QSIC'06)*, pp. 429-434, 2006. DOI: 10.1109/QSIC.2006.43

[19] G. Buyukozkan, O. Feyzioglu and F. Gocer, "Evaluation of Hospital Web Services Using Intuitionistic Fuzzy AHP and Intuitionistic Fuzzy VIKOR", in *IEEE International Conference on Industrial Engineering and Engineering Management (IEEM)*, pp. 607-611, 2016. DOI: 10.1109/IEEM.2016.7797947

[20] J.L. Lee, S.H. Kuk, H.S. Kim and S.W. Park, "Extended BPEL System for e-Engineering Framework Considering the Characteristics of Mechanical Engineering Services", in *IEEE International Conference on Services Computing*, pp. 481-484, 2008. DOI: 10.1109/SCC.2008.151

[21] C. Riedl, T. Bohmann, M. Rosemann and H. Krcmar, "Quality management in service ecosystems", *Information Systems and e-Business Management*, vol. 7, no. 2, pp. 199-221, 2008. DOI:10.1007/s10257-008-0080-6

[22] W.L. Lin, C.C. Lo, K.M. Chao and M. Younas, "Consumer-centric QoS-aware selection of web services", *Journal of Computer and System Sciences*, vol. 74, no. 2, pp. 211-231, 2008. DOI: 10.1016/j.jcss.2007.04.009

[23] V. Patankar and R. Hewett, "Automated Negotiations in Web Service Procurement", in *Third International Conference on Internet and Web Applications and Services*, pp. 620-625, 2008. DOI: 10.1109/ICIW.2008.102

[24] M. Fantinato, M.B.F. De Toledo and I.M.D. Gimenes, "WS-contract establishment with QoS: An approach based on feature modeling", *International Journal of Cooperative Information Systems*, vol. 17, no. 3, pp. 373-407, 2008. DOI: 10.1142/S0218843008001889

[25] T. Cucinotta, A. Mancina, G.F. Anastasi, G. Lipari, L. Mangeruca, R. Checcozzo and F. Rusina, "A Real-Time Service-Oriented Architecture for Industrial Automation", *IEEE Transactions on Industrial Informatics*, vol. 5, no. 3, pp. 267-277, 2009. DOI:10.1109/TII.2009.2027013

[26] T. Neubauer and C. Stummer, "Interactive selection of Web services under multiple objectives", *Information Technology and Management*, vol. 11, no. 1, pp. 25-4, 2009. DOI:10.1007/s10799-009-0058-1

[27] M.A. Serhani, A. Jaffar, P. Campbell and Y. Atif, "Enterprise web services-enabled translation framework", *Information Systems & e-Business Management*, vol. 9, no. 4, pp. 497-517, 2010. DOI: 10.1007/s10257-010-0162-0

[28] K. Xu, Q. Yu, Q. Liu, J. Zhang and A. Bouguettaya, "Web Service management system for bioinformatics research: a case study", *Service Oriented Computing and Applications*, vol. 5, no. 1, pp. 1-15, 2011. DOI: 10.1007/s11761-011-0076-9

[29] V. Vescoukis, N. Doulamis and S. Karagiorgou, "A service oriented architecture for decision support systems in environmental crisis management", *Future Generation Computer Systems*, vol. 28, no. 3, pp. 593-604, 2012. DOI: 10.1016/j.future.2011.03.010

[30] D.H. Lin, T. Ishida, Y. Murakami and M. Tanaka, "QoS Analysis for Service Composition by Human and Web Services", *IEICE Transactions on Information and Systems*, vol. E97.D, no. 4, pp. 762-769, 2014. DOI:10.1587/transinf.E97.D.762

Communication Papers of the of the 17th Conference on Computer Science and Intelligence Systems pp. 269–274
DOI: 10.15439/2022F147
ISSN 2300-5963 ACSIS, Vol. 32

Web Intrusion Detection Using Character Level Machine Learning Approaches with Upsampled Data

1st Talya Tümer Sivri
Defense and Information Systems
BITES
Ankara, TURKEY
talya.tumer@bites.com.tr

2nd Nergis Pervan Akman
Defense and Information Systems
BITES
Ankara, TURKEY
nergis.pervan@bites.com.tr

3rd Ali Berkol
Defense and Information Systems
BITES
Ankara, TURKEY
ali.berkol@bites.com.tr

4th Can PEKER
Training Tech. and Digital Platforms
BITES
Ankara, TURKEY
can.peker@bites.com.tr

***Abstract*—Today, people fulfill their needs in many areas such as shopping, health, and finance online. Besides many well-meaning people who use websites for their own needs, there are also people who send attack requests to get these people's personal data, get website owners' information, and damage the application. The attack types such as SQL injection and XSS can seriously harm web applications and users. Detecting these cyber-attacks manually is very time-consuming and difficult to adapt to new attack types. Our proposed study performs attack detection using different machine learning and deep learning approaches with a larger dataset obtained by combining CSIC 2012 and ECML/PKDD datasets. In this study, we evaluated our classification results which experimented with different algorithms based on computation time and accuracy. In addition to applying different algorithms, experiments on various learning models were applied with our data upsample method for balancing the dataset labels. As a result of the binary classification, LSTM achieves the best result in terms of accuracy, and a positive effect of the upsampled data on accuracy has been observed. LightGBM was the algorithm with the highest performance in terms of computation time.**

***Index Terms*—Web Application Firewall, Intrusion Detection, Data Upsampling, CNN, LSTM, XGBoost, LightGBM, Random Forest, Deep Learning**

I. Introduction

With the increase of devices and applications such as the Internet of Things (IoT), efforts to ensure the security of these applications are also increasing. Ensuring the security of web applications is a critical step for the continuity of the application. The Verizon 2020 Data Breach Investigations Report [5] found that web application attacks doubled in 2019, to nearly 43% of all attacks analyzed in the report. It is still an actively used approach to detect and prevent Hyper Text Transfer Protocol (HTTP) requests from coming into the application with rule-based software. However, in rule-based software, attack detection depends on the rule. It is not adapted for incoming attacks outside the rules. Apart from detecting attacks with the signature-based software, there are studies in the literature that classify using traditional machine learning [1], [2] and deep learning algorithms [4], [18], [23].

Along with detecting incoming attacks with high accuracy, rapid detection is also important for quick intervention [3]. For this reason, machine learning algorithms used in this study, which take less training time and detection time and need less data, have great importance in attack detection.

Hoang et al. [8] have included Naive Bayes, Support Vector Machine (SVM), Decision Tree, and Random Forest (RF) for binary classification. The best performance is obtained with RF, and the worst is Naive Bayes. The highest performance with 99.68% accuracy is obtained with RF.

The use of Natural Language Processing (NLP) techniques is common due to the frequent use of meaningful or meaningless characters in extracting the attributes of requests coming to the application. Since character-level Convolutional Neural Network (CNN) is constructed using vectors of a limited character string, it is very advantageous in terms of computational costs [4]. They build traditional CNN with two convolutional layers and also build CNN architecture which is merged final layers in parallel. They proposed a faster and less computational approach owing to character representation.

As a different feature extraction approach, the vectors of words are extracted and classified by deep learning. Zhang [3] et al. split HTTP requests according to certain characters and extract words and generate word vectors using Word2Vec, which is a word embedding algorithm. Then they calculated the Term Frequency — Inverse Document Frequency (TF-

IDF) value from the word vectors for dimension reduction. One of the two algorithms used in this study, Light Gradient Boosting Machine (LightGBM), has lower accuracy than another algorithm, Category Boosting (CatBoost), using three available datasets, namely, HTTP DATASET CSIC 2010, UNSW-NB15, and malicious Uniform Resource Locators (URL). Different word embedding algorithms such as Global Vectors (Glove) for Word Representation and Fasttext are compared with accuracy, true-positive rate, and false-positive rate performance metrics.

With the increase in the use of machine learning algorithms, the need for data increases, and the importance of approaches such as systems that need less data, data augmentation studies, and automatic data generation are increasing at the same level. Therefore, machine learning-based studies are now moving towards high-quality data augmentation [20]–[22] of data or producing an effective model with fewer data.

Both speed and accuracy are of great importance in intrusion detection. In this study, we aimed to demonstrate this evaluation by conducting experiments on different algorithms. In addition, one of the biggest aims of this study is to increase the data by diversifying the different headers in the data. In this way, we have generalized the headers that appear only in attacks or only in normal requests.

The main contributions of this study are as follows: i) In a binary classification of HTTP requests, both time and accuracy performances of traditional machine learning algorithms and deep learning algorithms are compared. ii) The effect of increasing the dataset size using upsampling approaches on the obtained model accuracies is observed.

II. Related Work

Intrusion detection is vital for vulnerable machines and applications by enabling the detection and subsequent prevention of malicious software or activity. Before the anomaly detection step algorithmically, feature selection and extraction [10]–[14] of HTTP requests is an important step that affects performance. In addition to these traditional feature analysis studies, there are also information extraction studies using NLP techniques. Liu et al. [15] developed a system that works together with the optimized SVM algorithm and feature analysis work. HTTP requests were analyzed and selected using expert knowledge. SVM is used as a classification algorithm, and a grid search algorithm is used for parameter optimization. The results of this study, using the CSIC 2010 dataset, can detect attacks with high accuracy performance.

Providing intrusion detection, which is the first step, can be achieved automatically with machine learning methods. While Pham et al. [6] used the most important traditional machine learning methods such as decision tree, logistic regression, and random forest to detect an anomaly, the best result is achieved with logistic regression. The CSIC 2010 dataset, which is used in the evaluation of many studies and consists of requests coming to an e-commerce site, is used. In general, in this study, different studies are included in the step of feature extraction of the text.

In addition to such automatic anomaly detection studies, signature-based studies still produce effective results. Adem et al. [7] present a hybrid study using both signature-based and anomaly detection approaches. With a rule-based study based on character, word, and request length, a faster detection is made on CSIC 2010, ECML-PKDD 2007, and WUGD 2015 datasets with 95% accuracy.

Duy et al. [9], as a different approach, also consider user behavior in anomaly detection. In this study, the attributes of user behaviors on HTTP requests are determined. For feature extraction, TF-IDF and common feature approaches are used together with the random forest algorithm, and TF-IDF achieves a better result with a 4% difference.

Current malware acts as a benign request to evade attack detection. In this study [16], the difference between benign and malicious software is revealed by using a language-based approach to detect malicious requests. An importance score calculation is made between the characters of good and bad-tempered requests, and word order is created according to the order of importance. Then, a vector representation was created with doc2vec, which is a document-based approach to creating a feature vector.

Jemal et al. [18] made CNN, one of the best working deep learning algorithms, a three-step evaluation for each classification step, such as variations of the input vector and hyperparameter tuning. As the first evaluation step, the representation of the HTTP request as presentation and splitting is being worked on. As a second evaluation, different CNN hyperparameter combinations are compared, and as a final evaluation, the selection of the best deep learning toolbox. At the end of the study, the effect of the input vector and hyperparameter tuning on the CNN model is analyzed.

The biggest reason why detecting cyber attacks is problematic is that attacks are constantly being updated and become more complex. In order to cope with this problem, it is necessary to develop systems that are more flexible and adaptable to new types of attacks. Zhao et al. [17] have attempted to overcome this challenge with the semi-supervised Discriminant Autoencoder (AUE) classification method. The purpose of the algorithm is to ensure that unidentified samples get a place based on their nearest neighbors. In this way, it is to produce a generalized model by understanding the nature of the previously undefined attack.

Eduardo et al. [19] have also done a study as a solution to intrusion detection models that become obsolete and outdated over time. They provide anomaly detection with semi-supervised learning in order to update the existing model without human intervention. The experiments carried out within the scope of the study were carried out by considering the real network traffic of one year, and it is observed that the accuracy of the new data continues to be preserved. In the case of no model update, approximately 10% of the data is rejected, while in the case of a model update, this value becomes approximately 3%.

Bhati et al. [26] proposed an Intrusion Detection System (IDS) on an ensemble method using Extreme Gradient

Boosting (XGBoost), which provides the balance of bias-variance. The KDD-Cup99 dataset was used in the proposed model training and the obtained accuracy of the method is 99.95

Liu et al. [27] used the LightGBM ensemble technique to create a Network Intrusion Detection System (NIDS). By creating synthetic samples with the Adaptive Synthetic (ADASYN) oversampling method, the authors addressed the problem of class imbalance. In the suggested study, categorization is accomplished utilizing the datasets CICIDS2017, NSL-KDD and UNSW-NB15. According to their findings, LightGBM and ADASYN perform better than other traditional ML algorithms.

III. Method

Detecting malicious requests with high accuracy and high speed is a vital process in order to prevent systems from important damage. In our work, we aimed to find the best fit for this purpose. The techniques we applied in the experiments are divided into two parts. The first technique focuses on the classification of malicious and normal HTTP requests trained and tested by different models such as CNN, LSTM, XGBoost, LightGBM, and Random Forest. This study also focuses on fast detection of attacks as well as good accuracy results. The second technique focuses on new data upsampling algorithm for increasing the variety of normal requests since it aims to decrease disadvantages, for instance, lack of diversity and imbalance between classes.

A. Data

In this study, two different publicly available datasets have been taking considered. The first one is the CSIC dataset published and produced by the Spanish Research National Council (CSIC) [24], and it contains over 74000 requests with three different labels, which are normal, anomalous, Structured Query Language (SQL) injection, Cross-site scripting (XSS), Server-Side Includes Injection (SSI), buffer overflow, Carriage Return Line Feed injection (CRLFi), XML Path Language (XPATH) injection, Lightweight Directory Access Protocol injection (LDAPi), and format string. Dataset has been generated artificially via semi-automatic tools. Second dataset is the Discovery Challange Data [25] which was provided LIRMM (Laboratoire dInformatique, de Robotique et de Microelectronique de Montpellier, FRANCE) and the LGI2P (Ecole des Mines dAlcs, FRANCE) to use in ECML/PKDD Discovery Challenge. The dataset was named in this work as ECML. It was based on a dataset of real-world web traffic in conjunction with Bee Ware. It has eight labels which are normal, SQL injection, path traversal, command execution, LDAPi, XPATH injection, SSI injection and cross-site scripting. There are over 50000 requests in the dataset.

1) Data Preprocessing: Some important data preprocessing steps were applied to datasets in order to standardize the data since two different datasets were used to perform binary classification. Firstly, common header names were chosen,

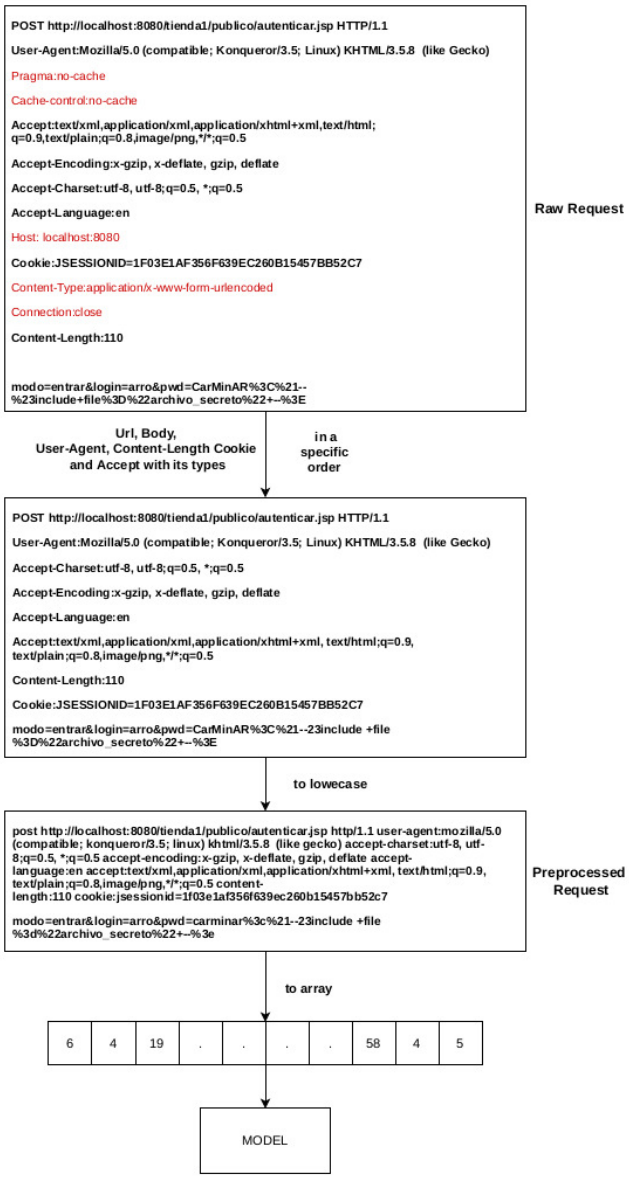

Fig. 1: An example of data preprocessing.

considering which header includes the attack in a specific order. More precisely, "User-Agent", "Accept", "Accept-Charset", "Accept-Encoding", "Accept-Language", "Content-Length", "Content-Encoding", and "Cookie" were used with the request type, URL, and the body part of the HTTP request. If there is no header in the original request, the header name will be added only the header name. Second, labels were changed to binary labels, i.e., normal requests labeled as "0" and different types of anomalous and malicious attack types labeled as "1". Finally, all characters turned into lowercase. See Fig. 1.

2) Data Upsampling: Data upsampling techniques can be used where a dataset has unbalanced data. In the appended dataset, we have 62.54% attack requests and 37.46% normal

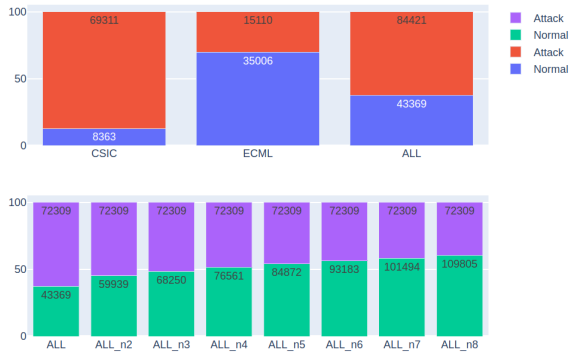

Fig. 2: Data distributions. In the red/blue part original dataset class distributions can be observed. In the purple/green part upsampled data class distributions can be observed. n_i where $i = 2, ..., 8$ means that CSIC's normal requests upsampled i times.

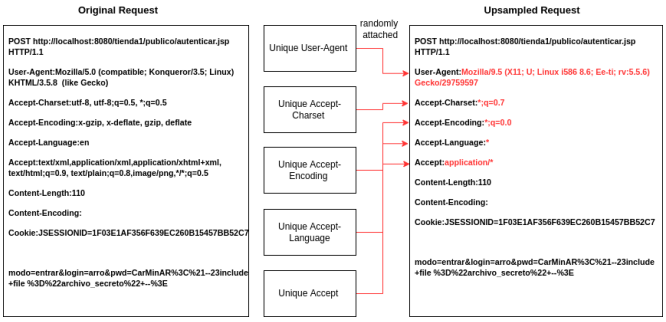

Fig. 3: An example of our upsampling method. While upsampling algorithm works, header values are randomly replaced from a unique list obtained from ECML for each header name. For example, "Accept-Language" header value was changed from "en" to "*".

requests, which refers to unbalanced data (see Fig. 2). We developed a new data upsampling technique for normal HTTP requests in order to provide a balanced dataset. Firstly, we found the number of unique header values for each header name considering labels (see Table I). As it can be seen in Table I, ECML has an excessive amount of unique values in both attack and normal requests. On the contrary, CSIC has a narrow range of unique values.

TABLE I: The numbers of unique header values

Header Name	Dataset Name	Attack	Normal
ACCEPT	ECML	4440	9044
	CSIC	6	2
ACCEPT Charset	ECML	5559	11738
	CSIC	2	1
ACCEPT Encoding	ECML	3257	6154
	CSIC	3	1
ACCEPT Language	ECML	6543	14210
	CSIC	3	1
User Agent	ECML	15075	35006
	CSIC	8664	1

Due to the few numbers of normal requests of CSIC and lacking unique values, we decided to upsample normal requests of this dataset using ECML's normal requests header values. The algorithm works in a way that randomly replaces the header values for each normal HTTP request of CSIC. See an example of replacing headers in Fig. 3. To examine if our upsampling technique works well and due to the number of samples we need, we applied this process for many times, i.e., 2 to 8 times. According to each dataset, normal and attack request percentages and the number of each label and total data of each upsampled dataset and the original datasets can be seen in Fig. 2. Moreover, each request converted character level arrays, i.e., each character has an integer value.

B. Models

Ensemble and deep learning methods are highly used in classification problems. In this paper, we would like to compare these methods' outcomes. Ensembles like RF, XGBoost, and LightGBM use a technique that combines different base models to produce one ideal predictive model. On the other hand, deep learning methods like CNN and LSTM provide automatic feature extraction techniques through filters/kernels and patterns across time, respectively, with learning parameters via forward and backward propagations. In our work, we applied input as character level which means that each character is translated into its corresponding integer. We divided the dataset into train, validation and test subsets with percentages of 60, 20, 20, respectively.

RF, XGBoost, and LightGBM classification models were fitted using default hyperparameters where estimators were evaluated using K-Fold cross-validation, where K is 5. Moreover, CNN and LSTM models are applied. Using hyperparameter tuning, decided hyperparameters are as follows. For the CNN model, the learning rate is 0.0001, the optimizer is Stochastic Gradient Descent (SGD), and filter and kernel sizes are 64 and 7, respectively. For the LSTM model, the learning rate is 0.001, and the optimizer is Adam. In Fig.4, each models layers can be seen. Additionally, both models are trained with batch sizes 32, and 5 epochs with an input size of 750.

IV. Results

Our work has two different outcomes. The first one is model-based and the second one is data-based outcomes. In model-based evaluation results, the binary LSTM classification model gave the best results in terms of accuracy, f1 score, precision, recall, and false-negative rate. Moreover, although LSTM is better than CNN except for the false-positive rate, CNN gave the best result on the evaluation of the false-positive rate. On the other hand, the RF classification model gave the worst results in terms of all numeric results, see Table II. Moreover, it can be easily seen that ensemble methods like XGBoost and LightGBM are as good as learning methods like CNN. However, RF was not able to perform like other methods even though it is a kind of ensemble algorithm. In

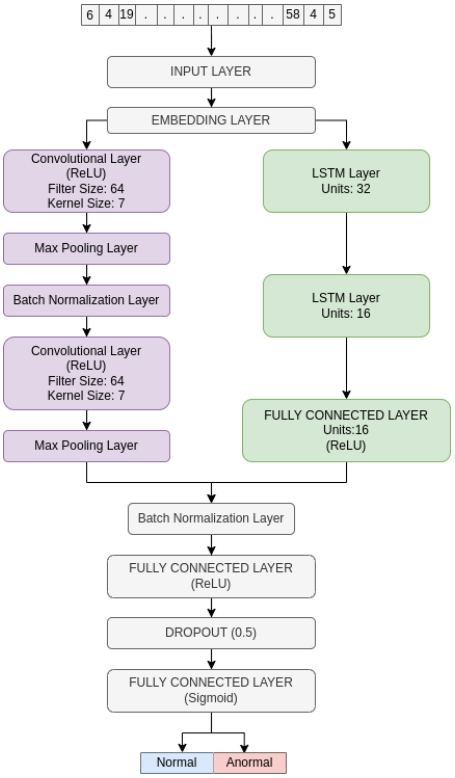

Fig. 4: Illustrations of CNN and LSTM classifier models. CNN and LSTM models have different layers. Separated by purple part shows CNN layers and separated by yellow part shows LSTM layers.

Table II, numeric results which is written in blue refers to the best results according to comparison type. Solely, the red refers to the worst results according to comparison type.

Secondly, we compared results between models and upsampled data (see Table II). In general, the LSTM model concluded that the best results are in accuracy, f1 score, precision, recall and false negative rate. However, some results of applications on false-positive rates CNN gave the best results. As expected from the model-based approach, the RF model gave the worst results for all numeric outputs. When we examine the training time outputs, we can easily observe that there is a vital difference between LSTM and LightGBM models (see Table II).

V. Conclusion

In this work, we tried to illustrate the effectiveness of different models which are CNN, LSTM, XGBoost, LightGBM and RF and to illustrate our new method for data upsampling and prove its efficiency. According to the results, LSTM is the best algorithm for character-level binary classification problems with HTTP requests. Additionally, ensemble methods such as XGBoost and LightGBM work as efficiently as CNN and LSTM. However, there is a serious trade-off between training time and the best model since LSTM average training time is approximately 85 times higher than LightGBM average training time. Furthermore, we explained our new data upsampling method for balancing datasets that have an unbalanced amount of classes. According to numerical results, our algorithm worked fine and proved its efficiency. In most cases, it improves the accuracy, f1 score, precision, recall, false-negative rate, and false-positive rate results.

VI. Future Work

Classification of HTTP requests as attack or not is essential for cyber security applications since hackers are waiting to steal any confidential information to use them to their advantage. Balancing the attack types in the dataset will increase the capability of detecting attacks for models. As a future work, we are planning to work on synthetic data generation and develop different upsampling methods for balancing attack types in the dataset.

References

[1] Isiker, B., and Sogukpinar, I. (2021). Machine learning based web application firewall. 2021 2nd International Informatics and Software Engineering Conference (IISEC). https://doi.org/10.1109/iisec54230.2021.9672335

[2] Pham, T. S., Hoang, T. H., and Van Canh, V. (2016). Machine learning techniques for web intrusion detection — a comparison. 2016 Eighth International Conference on Knowledge and Systems Engineering (KSE). https://doi.org/10.1109/kse.2016.7758069

[3] Li, J., Zhang, H., and Wei, Z. (2020). The weighted word2vec paragraph vectors for anomaly detection over HTTP traffic. IEEE Access, 8, 141787–141798. https://doi.org/10.1109/access.2020.3013849

[4] Ito, M., and Iyatomi, H. (2018). Web application firewall using character-level convolutional neural network. 2018 IEEE 14th International Colloquium on Signal Processing amp; Its Applications (CSPA). https://doi.org/10.1109/cspa.2018.8368694

[5] Bassett, G., Hylender, C. D., Langlois, P., Pinto, A., Widup, S. (2020). Verizon data breach investigations report. doi:10.13140/RG.2.2.21300.48008

[6] T. S. Pham, T. H. Hoang and V. Van Canh, "Machine learning techniques for web intrusion detection — A comparison," 2016 Eighth International Conference on Knowledge and Systems Engineering (KSE), 2016, pp. 291-297, doi: 10.1109/KSE.2016.7758069.

[7] Tekerek, A., Gemci, C., and Bay, Ö. F. (2016). Web tabanlı saldırı önleme sistemi tasarımı ve gerçekleştirilmesi: yeni bir hibrit model. Gazi Üniversitesi Mühendislik-Mimarlık Fakültesi Dergisi, 31(3). https://doi.org/10.17341/gummfd.63355

[8] Hoang, X. D. (2020). Detecting common web attacks based on machine learning using web log. Advances in Engineering Research and Application, 311–318. https://doi.org/10.1007/978-3-030-64719-3_35

[9] Duy, P. H., Thuy, N. T. T., and Diep, N. N. (2020). Anomaly detection system of web access using user behavior features. Southeast Asian J. Sciences, 7(2).

[10] Li, M., Wang, H., Yang, L., Liang, Y., Shang, Z., and Wan, H. (2020). Fast hybrid dimensionality reduction method for classification based on feature selection and grouped feature extraction. Expert Systems with Applications, 150, 113277. https://doi.org/10.1016/j.eswa.2020.113277

[11] Torrano-Gimenez, C., Nguyen, H. T., Alvarez, G., Petrovic, S., and Franke, K. (2011). Applying feature selection to payload-based web application firewalls. 2011 Third International Workshop on Security and Communication Networks (IWSCN). https://doi.org/10.1109/iwscn.2011.6827720

[12] Nguyen, H. T., Torrano-Gimenez, C., Alvarez, G., Petrović, S., and Franke, K. (2011). Application of the generic feature selection measure in detection of web attacks. Computational Intelligence in Security for Information Systems, 25–32. https://doi.org/10.1007/978-3-642-21323-6_4

[13] Li, H., Guo, W., Wu, G., and Li, Y. (2018). A RF-PSO based hybrid feature selection model in Intrusion detection system. 2018 IEEE Third International Conference on Data Science in Cyberspace (DSC). https://doi.org/10.1109/dsc.2018.00128

TABLE II: Model result with all datasets

Model Name	Data Name	Accuracy	F1 Score	Precision	Recall	FPRate	FNRate	Training Time(sec)
CNN	ALL	0.9549	0.9553	0.9595	0.9549	0.0014	0.0713	666.55
	ALL_n2	0.9666	0.9666	0.9684	0.9666	0.0040	0.0575	752.43
	ALL_n3	0.9678	0.9678	0.9695	0.9678	0.0028	0.0596	676.87
	ALL_n4	0.9710	0.9710	0.9722	0.9710	0.0031	0.0565	722.64
	ALL_n5	0.9692	0.9691	0.9703	0.9692	0.0044	0.0616	813.08
	ALL_n6	0.9756	0.9755	0.9761	0.9756	0.0058	0.0484	681.81
	ALL_n7	0.9777	0.9776	0.9781	0.9777	0.0053	0.0463	706.86
	ALL_n8	0.9780	0.9779	0.9784	0.9780	0.0039	0.0494	834.70
LSTM	ALL	0.9815	0.9816	0.9820	0.9815	0.0086	0.0243	3544.32
	ALL_n2	0.9867	0.9867	0.9869	0.9867	0.0035	0.0214	3987.73
	ALL_n3	0.9880	0.9881	0.9882	0.9880	0.0034	0.0199	4217.64
	ALL_n4	0.9886	0.9886	0.9887	0.9886	0.0043	0.0189	4489.10
	ALL_n5	0.9880	0.9880	0.9881	0.9880	0.0058	0.0192	4519.91
	ALL_n6	0.9860	0.9860	0.9860	0.9860	0.0140	0.0140	4750.85
	ALL_n7	0.9918	0.9917	0.9918	0.9918	0.0020	0.0171	5150.77
	ALL_n8	0.9927	0.9927	0.9927	0.9927	0.0030	0.0138	5617.30
XGBoost	ALL	0.9529	0.9532	0.9556	0.9529	0.0207	0.0627	47.16
	ALL_n2	0.9576	0.9577	0.9593	0.9576	0.0161	0.0639	56.82
	ALL_n3	0.9601	0.9601	0.9613	0.9601	0.0156	0.0628	62.98
	ALL_n4	0.9630	0.9629	0.9639	0.9630	0.0143	0.0613	67.61
	ALL_n5	0.9632	0.9631	0.9641	0.9632	0.0121	0.0657	55.49
	ALL_n6	0.9667	0.9666	0.9675	0.9667	0.0100	0.0633	63.81
	ALL_n7	0.9695	0.9694	0.9700	0.9695	0.0095	0.0600	82.74
	ALL_n8	0.9703	0.9702	0.9708	0.9703	0.0090	0.0612	106.40
LightGBM	ALL	0.9383	0.9389	0.9434	0.9383	0.0227	0.0847	51.51
	ALL_n2	0.9463	0.9464	0.9493	0.9463	0.0170	0.0839	40.59
	ALL_n3	0.9483	0.9483	0.9508	0.9483	0.0158	0.0855	53.76
	ALL_n4	0.9527	0.9526	0.9544	0.9527	0.0159	0.0808	55.59
	ALL_n5	0.9524	0.9522	0.9541	0.9524	0.0143	0.0868	58.44
	ALL_n6	0.9563	0.9561	0.9576	0.9563	0.0130	0.0833	54.13
	ALL_n7	0.9597	0.9595	0.9608	0.9597	0.0109	0.0815	57.15
	ALL_n8	0.9602	0.9599	0.9611	0.9602	0.0110	0.0836	57.23
RF	ALL	0.8986	0.8999	0.9099	0.8986	0.0437	0.1355	115.76
	ALL_n2	0.9149	0.9151	0.9220	0.9149	0.0271	0.1328	124.59
	ALL_n3	0.9179	0.9177	0.9238	0.9179	0.0252	0.1358	121.28
	ALL_n4	0.9243	0.9240	0.9285	0.9243	0.0241	0.1308	126.20
	ALL_n5	0.9265	0.9260	0.9306	0.9265	0.0201	0.1362	132.78
	ALL_n6	0.9304	0.9298	0.9338	0.9304	0.0184	0.1357	137.53
	ALL_n7	0.9350	0.9343	0.9376	0.9350	0.0177	0.1315	145.36
	ALL_n8	0.9372	0.9365	0.9393	0.9372	0.0181	0.1306	124.78

[14] J. Gupta and J. Singh, "Detecting anomaly based network intrusion using feature extraction and classification techniques," Int. J. Adv. Res. Comput. Sci., vol. 8, no. 5, pp. 1453–1456, 2017

[15] Liu, C., Yang, J., and Wu, J. (2020). Web intrusion detection system combined with feature analysis and SVM Optimization. EURASIP Journal on Wireless Communications and Networking, 2020(1). https://doi.org/10.1186/s13638-019-1591-1

[16] Mimura, M. (2020). Adjusting lexical features of actual proxy logs for intrusion detection. Journal of Information Security and Applications, 50, 102408. https://doi.org/10.1016/j.jisa.2019.102408

[17] Zhao, F., Zhang, H., Peng, J., Zhuang, X., and Na, S.-G. (2020). A semi-self-taught network intrusion detection system. Neural Computing and Applications, 32(23), 17169–17179. https://doi.org/10.1007/s00521-020-04914-7

[18] Jemal, I., Haddar, M. A., Cheikhrouhou, O., and Mahfoudhi, A. (2021). Performance evaluation of Convolutional Neural Network for web security. Computer Communications, 175, 58–67. https://doi.org/10.1016/j.comcom.2021.04.029

[19] Viegas, E. K., Santin, A. O., Cogo, V. V., and Abreu, V. (2020). A reliable semi-supervised Intrusion Detection Model: One year of network traffic anomalies. ICC 2020 - 2020 IEEE International Conference on Communications (ICC). https://doi.org/10.1109/icc40277.2020.9148916

[20] H. Zhang, X. Yu, P. Ren, C. Luo and G. Min, "Deep adversarial learning in intrusion detection: A data augmentation enhanced framework", arXiv:1901.07949, 2019

[21] Yuan, D., Ota, K., Dong, M., Zhu, X., Wu, T., Zhang, L., and Ma, J. (2020). Intrusion detection for smart home security based on data augmentation with Edge Computing. ICC 2020 - 2020 IEEE International Conference on Communications (ICC). https://doi.org/10.1109/icc40277.2020.9148632

[22] Wang, Y., lv, S., Liu, J., Chang, X., and Wang, J. (2020). On the combination of data augmentation method and gated convolution model for building effective and robust intrusion detection. Cybersecurity, 3(1). https://doi.org/10.1186/s42400-020-00063-5

[23] Farea, A. A., Wang, C., Farea, E., and Ba Alawi, A. (2021). Cross-site scripting (XSS) and SQL injection attacks multi-classification using bidirectional LSTM recurrent neural network. 2021 IEEE International Conference on Progress in Informatics and Computing (PIC). https://doi.org/10.1109/pic53636.2021.9687064

[24] Torpeda. (n.d.). Retrieved May 6, 2022, from https://www.tic.itefi.csic.es/torpeda/datasets.html

[25] Analyzing web traffic ECML/PKDD 2007 discovery challenge September 17-21, 2007, Warsaw, Poland. Attack Challenge - ECML/PKDD Workshop. (n.d.). Retrieved May 6, 2022, from https://www.lirmm.fr/pkdd2007-challenge/

[26] Bhati BS., Chugh G., Al-Turjman F., and Bhati NS. An improved ensemble based intrusion detection technique using XGBoost.Trans EmergTelecommun Technol. 2020.https://doi.org/10.1002/ett.4076

[27] Liu J., Gao Y., and Hu F. A fast network intrusion detection system using adaptive synthetic oversampling and LightGBM. Comput. Security 2021;106. doi:10.1016/j.cose.2021.102289

28th Conference on Knowledge Acquisition and Management

KNOWLEDGE management is a large multidisciplinary field having its roots in Management and Artificial Intelligence. Activity of an extended organization should be supported by an organized and optimized flow of knowledge to effectively help all participants in their work.

We have the pleasure to invite you to contribute to and to participate in the conference “Knowledge Acquisition and Management". The predecessor of the KAM conference has been organized for the first time in 1992, as a venue for scientists and practitioners to address different aspects of usage of advanced information technologies in management, with focus on intelligent techniques and knowledge management. In 2003 the conference changed somewhat its focus and was organized for the first under its current name. Furthermore, the KAM conference became an international event, with participants from around the world. In 2012 we’ve joined to Federated Conference on Computer Science and Systems becoming one of the oldest event.

The aim of this event is to create possibility of presenting and discussing approaches, techniques and tools in the knowledge acquisition and other knowledge management areas with focus on contribution of artificial intelligence for improvement of human-machine intelligence and face the challenges of this century. We expect that the conference&workshop will enable exchange of information and experiences, and delve into current trends of methodological, technological and implementation aspects of knowledge management processes.

TOPICS

- Knowledge discovery from databases and data warehouses
- Methods and tools for knowledge acquisition
- New emerging technologies for management
- Organizing the knowledge centers and knowledge distribution
- Knowledge creation and validation
- Knowledge dynamics and machine learning
- Distance learning and knowledge sharing
- Knowledge representation models
- Management of enterprise knowledge versus personal knowledge
- Knowledge managers and workers
- Knowledge coaching and diffusion
- Knowledge engineering and software engineering
- Managerial knowledge evolution with focus on managing of best practice and cooperative activities
- Knowledge grid and social networks
- Knowledge management for design, innovation and eco-innovation process
- Business Intelligence environment for supporting knowledge management
- Knowledge management in virtual advisors and training
- Management of the innovation and eco-innovation process
- Human-machine interfaces and knowledge visualization

TECHNICAL SESSION CHAIRS

- **Hauke, Krzysztof,** Wroclaw University of Economics, Poland
- **Nycz, Malgorzata,** Wroclaw University of Economics, Poland
- **Owoc, Mieczyslaw,** Wroclaw University of Economics, Poland
- **Pondel, Maciej,** Wroclaw University of Economics, Poland

PROGRAM COMMITTEE

- **Andres, Frederic,** National Institute of Informatics, Tokyo, Japan
- **Berka, Petr,** Prague University of Economics and Business, Czech Republic
- **Bodyanskiy, Yevgeniy,** Kharkiv National University of Radio Electronics, NURE, Ukraine
- **Chomiak-Orsa, Iwona,** Wroclaw University of Economics and Business, Poland
- **Christozov, Dimitar,** The American University in Bulgaria
- **Chudán, David,** University of Economics, Prague, Czech Republic
- **Hernes, Marcin,** Wrocław University of Economics and Business, Poland
- **Jan, Vanthienen,** Katholieke Universiteit Leuven, Belgium
- **Kliegr, Tomáš,** Prague University of Economics and Business, Czech Republic
- **Kluza, Krzysztof,** AGH University of Science and Technology, Poland
- **Ligęza, Antoni,** AGH University of Science and Technology, Poland
- **Mercier-Laurent, Eunika,** Jean Moulin Lyon 3 University, France
- **Perechuda, Kazimierz,** Wroclaw University of Economics and Business, Poland

Communication Papers of the of the 17th Conference on Computer Science and Intelligence Systems pp. 277–285
DOI: 10.15439/2022F35
ISSN 2300-5963 ACSIS, Vol. 32

Elaboration of Financial Fraud Ontology

1st Adamu Hussaini
Université de Reims Champagne Ardenne, France.
(CReSTIC EA 3804, 51097 Reims, France.)
adamu.hussaini@etudiant.univ-reims.fr

2nd Zahia Guessoum
Université de Reims Champagne Ardenne, France
(CReSTIC EA 3804, 51097 Reims, France.)
zahia.guessoum@univ-reims.fr
0000-0003-2303-7263

3rd Eunika Mercier-Laurent
Université de Reims Champagne Ardenne, France
(CReSTIC EA 3804, 51097 Reims, France.)
eunika.mercier-laurent@univ-reims.fr
0000-0003-2303-7263

***Abstract*—Financial Frauds have dynamically changed, the fraudsters are becoming more sophisticated. There has been an estimated global loss of 5.127 trillion dollars each year due to various forms of financial frauds. Industries like banking, insurance, e-commerce and telecommunication are the main targets for financial frauds. Several techniques have been proposed and applied to understand and detect financial frauds. In this paper we propose an ontology to describe financial frauds and related knowledge. The aim of this ontology is to provide a semantic framework for the detection of financial frauds. Theoretical ontology has been elaborated exploring various sources of information.**

After describing the research objectives, related works and research methodology, this paper presents details of theoretical ontology. It is followed by its validation using real datasets. Discussion of the obtained results gives some perspectives for the future work.

***Index Terms*—Fraud, Detection, Ontology, Concepts, Class, Entities, Validation, Dataset.**

I. Introduction

FINANCIAL frauds exist in different aspects of our life. Detection and prevention of those frauds represent an important question relevant to many academic disciplines. Fraud is an economically significant issue, that leads to depressions, bankruptcies and unfortunately suicide.

Ontology is used to study concepts, it has been applied to solve various problems in several domains such as medicine, computing, and economics. The objective of this research work is to understand the existing frauds and to propose a system able to detect them in order to prevent damages. This challenge is ambitious because the addressed problem is complex and dynamic - the fraudsters learn from failures and invent new ways of fraud. We can find in the literature various approaches to face this threat.

The paper is organized as follows. Section one is the introduction of financial frauds and the use of ontologies to detect financial frauds. In Section 2, we discuss the research challenge. Research methodology is described in Section 3, and related works in Section 4. While elaboration of the ontology, which includes theoretical development, validation, and discussion, is presented in Section 5. Finally, conclusion and some future works are proposed in Section 6.

II. Research Challenge

Financial institutions are facing several challenges in preventing and detection of frauds. Many firms proposed to use artificial intelligence and other advanced detection approaches.

In this paper the main challenges are to develop and validate a theoretical ontology for financial frauds that will understand and identify patterns for fraud detection and prevention. While undergoing the research, we must identify and provide a comprehensive solution to the problem of domain modeling, knowledge extraction, as well as creation of concepts.

III. Methodology

The research methodology focuses on heavyweight research methods that provide comprehensive detail of the research work process. Several development stages proposed in this research work are heavily influenced by one another. These stages suggest a routinely certain activities, which include:

- The understanding of the various types of frauds and related fraudsters' methods: The research work relies on publicly available information, consulting experts with the aim of understanding different types of financial frauds, while at the same time learning and deducing various fraud patterns used by the fraudsters. This methodology facilitates the organization of the frauds into different classes.
- Hypothesis, the research pointed out a possible expectation or prediction expected from the ontology, which include understanding of financial frauds' behaviors. The hypothesis of the research noted a possible change of behavior from the fraudsters. Hence, modification and change in the ontology will be needed from time to time.
- Study the state of the art: The section studies the domain of financial frauds, as well as other related entities of financial frauds that have a direct impact with the aims and objectives of the research. Understanding the existing

works makes it possible to achieve the goal of this research.

- Search for existing ontologies for possible reusing: Existing ontologies help to reposition the research as well as getting the right document we need for the creation of concepts, entities and other semantic content of our ontology. Some elements of the knowledge extracted are to be used as concepts that can be mapped to an ontology, some of the extracted knowledge are more complicated to be transformed into a concept.
- Adaptation and elaboration of theoretical ontology considering the types of frauds: This stage provides us with a theoretical implementation of the concepts and sub concepts of the ontology, the section iterates the overview of the ontology. Adaptation of this approach is the key point to the successful development of the ontology.
- Validation using datasets: The validation is proposed to help users to develop a confidence in the semantic content of the ontology. We use the dataset-based validation process due to the available resources and quality of the validation technique. We use various kinds of datasets for different types of frauds to validate the content of this ontology.
- Discussion of results and improvement: This stage of the research work will consider the aim and objective of the research work, compared with the validation result. The discussion of the result highlights if the goal of the research has been achieved. This section will give us a prediction of possible future improvement and modification of the ontology.

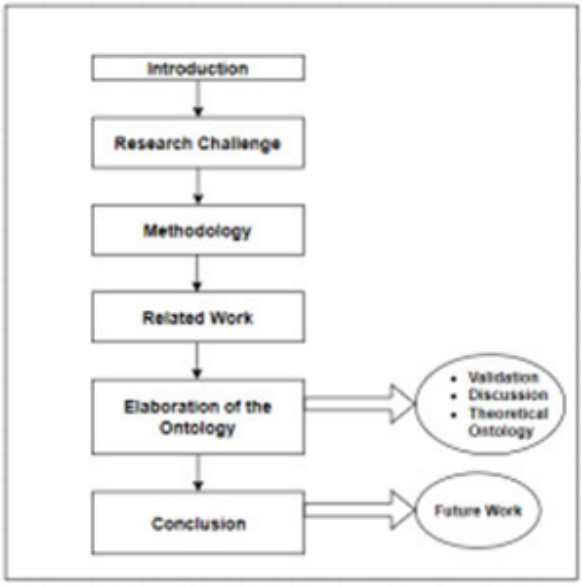

Fig. 1. The structure of the paper.

IV. Related Work

There are a considerable number of ontologies for finance, and fraud detection and prevention that have been proposed and developed.

Alexopoulos et al. [1] this propose provide an ontological basis which serves as a base on which the classification of ontology layers can be created. Generic, domain and case specific layers proposed. These three independent but interconnected layers, each one defining its own set of ontologies. We use the approach proposed in this ontology to implement to design our ontology. For example Generic layer of financial fraud, domain layer of banking fraud and the case specific layer of email fraud.

Tang et al. [2] propose an ontology to detect e-mail frauds. The ontology aims to tackle financial frauds, using formal ontological repositories as well as multilingual terminological resources. This ontology makes it possible to detect a fraud indicator within email content no matter how the fraudster tries to manipulate the content. The knowledge extraction process used to extract fraud indicators within emails is updated regularly. Hence, automatic rules are inserted in the knowledge extraction process. The approach provides a methodology of knowledge extraction, the extracted knowledge is used to built lexicons for semantic annotations. While this is important, the words processing without going into conceptual modelling and systematic linguistic engineering and without going deeper into semantic models of frauds, can be problematic In the cause of ontology validation.

Ontology-Based Framework Applied to Money Laundering [3] By Carnaz et al. This work provides a unified approach to represent and reason with investigation into money laundering. The approach is based on the knowledge of three money laundering steps. Placing, circulation, and integration. The ontology supports knowledge representation related to money laundering composed by several components. However, the paper does not present any framework of using real-world scenarios.The framework composed other components, preprocessing, data handling, knowledge and visualization. It has not been implemented yet. Hence, there is not test result with real-world scenarios.

Ahmed et al. [**?**] developed an ontology for electronic payment fraud prevention. The aim is detecting and preventing suspicious transactions on various electronic payment systems. The approach allows users to share an adaptive preventive rules of fraud on an ontology based on multiple and various payment systems. The paper discusses problems, issues in fraud detection and proposed prevention of financial fraud using ontology technology, among the concepts represented are legislation, legal rules from multiple countries, support reasoning about compliance with these legal rules and it represents interpretation of legislation and legal rules useful to the user.

In their article Kingston et al.m [**?**] propose a legal financial fraud ontology-based approach. The first phase of the proposed approaches aims building financial fraud concepts and the second phase aims building an ontology for laws against frauds. The ontology models the relationships where a two-way exchange is promised but only one of the two sub-transactions takes place while the second is to identify the

relations between fraud laws, facts and inferences about facts present, facts presumed or facts missing.

[**?**] introduced an ontology for detecting suspicious fraud activities by monitoring individual transactions. The authors combined expert system and ontology with three components: Ontology construction, ontology reasoning as well as query on inferred ontology. The presented approach uses anti-money laundering guidelines provided by the State Bank of Pakistan. The transactions are decomposed into groups of transactions, graphical representation of while few sample transactions updated after the application of the following steps. Rules were built on top of the OWL ontology to deduce new knowledge (suspicious transactions) from the existing knowledge. The approach used protégé built in reasoner to deduce new knowledge about the nature of a financial transaction. One of the important tasks missing in this approach is the system capability to suggest transactions that need to be further analysed. So that its strength to identify suspicious transactions can be validated.

The related works provide several unique ways of treating financial fraud problem with ontology. e.g., deducing knowledge from the user behavior for analysing words in email and basic structure of ontology. Some of the methods used in these approaches have been reused in our ontology. We reused the ontological basis approach proposed by alexopoulos et al. [1] to design the structure of our ontology. The domain of money laundering in the second layer of our ontology was reused from the framework of detecting money laundering [3] by Carnaz et al. this ontology give us an important background knowledge of money laundering life cycle. The class of email fraud in the third layer of our ontology, was reused from the approach proposed to detect e-mail frauds by Tang et al. [2]. While these ontologies have exhibited great performance of knowledge discovery in the domain of fraud detection.They are mostly single layer ontologies with focus on domain or case-specific frauds. The aim of our work is to converge these knowledge and approaches, to provide an ontology that covers the whole area of financial frauds, treating the problem of financial fraud in a wider and deep approach. The ontology will have multiple layers from generic to domain and case-specific. It will serve as a knowledge repository for the various kinds of financial frauds,

V. A new Financial Fraud Ontology

This section discusses the elaboration and overview of our proposed ontology. In this section we elaborated the knowledge in-closed in the multiple layers of the ontology, such as banking frauds, insurance frauds, identity theft and so on. The collective concepts, properties and relations matched together to give a comprehensive theoretical ontology. The properties of the concepts are keys to understanding the fraud patterns exhibited in a particular fraud domain.

A. Banking Fraud

In conceptualized context, bank fraud is using deception to steal money or assets from a bank or financial institution

Fig. 2. The ontological structure of financial frauds.

including credit unions and other financial institutions that are legally insured. This includes Federal Reserve banks, Deposit Insurance Corporation, Mortgage lending agencies, and other institutions that accept deposits of money or other financial assets. While in legal context, bank fraud is the use of potentially illegal means to obtain money, assets, or other properties owned or held by a financial institution, or to obtain money from depositors by fraudulently posing as a bank. In all instances, bank fraud is a criminal offense.

In this research we created the concept of banking fraud with other several sub concepts together with their properties, including accounting fraud, bill discounting fraud, credit card fraud, debit card fraud, ATM machine fraud, money laundering transfer, loan fraud, and wire transfer fraud.

Fig. 3. The banking fraud concept.

1) Accounting Fraud: Accounting fraud is described as a deliberate manipulation and alteration of financial records or statements. [4] In this context, bank documents are being

manipulated, the account statement of a client is deviated to represent a false financial position of the client. This could be done to an individual or company account. Accounting fraud aims to convince shareholders and investors by displaying false financial statements of the company. Attempting unlawful tax evasions by misstating assets and liabilities and revenues and expenses.

In this research we classify accounting fraud into several classes, which include embezzlement, kickback, misstating income, expenses and so on. Accounting fraud affects various sections of financial fraud, including tax fraud, money laundering, and so on. Hence, we embedded properties of accounting fraud with relation annotation. The latter describes that an entity has another relation with another entity outside its root concept.

2) ATM Machine Fraud: The automatic teller machine fraud (ATM) is becoming a target for attacks globally because fraudsters and other criminals are trying to find the machine vulnerabilities. Several entities, tools, and dimensions used for ATM frauds. Some of these are, card jamming, shoulder surfing and stolen cards which constitutes 65.2 percent of ATM frauds in countries like Nigeria. [5] The ontology proposed a joint relation between ATM fraud and other forms of financial fraud. Including identity theft, wire transfer fraud, debit card fraud and ATM card fraud. In so many cases ATM fraud occurred due to the machine design structure. For example, the machine user interface serves as the communication medium between the user and the machine. It provides the resources for the user to input his card details, some of the ATM machines as we investigated, provide a window for shoulder surfing, and card jamming, and hidden cameras. We uncovered many reported cases of ATM fraud using some of the above-mentioned cases. Shoulder surfing fraud, refers to observing someone entering the PIN at an ATM machine, it is most effective in crowded places; fraudsters stand too close to the victims, so they can see card details like pin, card number, expiry date, and cvv number. Another case of ATM fraud is using hidden cameras to capture users' pin codes. In this case the fraudsters put a concealed camera to capture the details of the user while using the ATM machine.

3) Credit Card Fraud: Credit cards are one of the most famous targets of frauds but not the only one [6]. Credit card fraud is a healthy and growing means of stealing billions of dollars from credit card companies, merchants, and consumers. Due to the rise and rapid growth of e-commerce, use of credit cards for online purchases have dramatically increased and it caused an explosion in credit card fraud. Credit cards become the most popular mode of payment for both online as well as regular purchase [7].

In this research we investigate card fraud and the patterns used by the criminals to defraud the victims. Credit card fraud provides detailed ontological understanding of credit card fraud. From entities, terminologies, relations, instances as well as data types and classes, including card-not-present fraud, counterfeit, and skimming fraud, lost or stolen card fraud, and card-never arrived-fraud. The above-mentioned cases are the most occurring credit card fraud. For example, card-not-present fraud contributes to overall credit card fraud, accounting for 75 percent. Hence, we provide several properties and relations between the card not present entity with other credit card and non-credit card fraud. The relation we proposed to make it possible to generate reasoning for other credit card fraud detection.

Fig. 4. The credit card fraud class.

4) Money Laundering: Money laundering is described as a technique for hiding proceeds of crime including transporting cash out of the country, purchasing businesses through which funds can be channeled, buying easily transportable valuables, transfer pricing, and using underground banks. [8] Money laundering is an organized crime with sophisticated multinational financial operations that transform proceeds of drug trafficking and other crimes into clean money. [9] This ontology represents the components used in money laundering such as people, organization, portfolios, messages, communication medium, and documents. We categorized people as sub concepts. These are individuals who participate in the money laundering cycle. It consists of several entities. Portfolio: The portfolio represents financial assets and products, it has many subclasses such as investment, transport, and other businesses. This class is associated with "organization", people, companies, and banks". For instance, people own accounts linked to a bank that will be used to purchase or invest in a particular business. Organization: This class describes organizations that are engaged in criminal acts of money laundering, mostly they are well-structured organizations, with many entities such as banking, securities trading, and so on. Messages: Represents all messages exchanged in the domain between people and organization. This is considered as the breaking ground or first stage of money laundering. All the activities in the domain are performed via messages, such as bank messages, trade messages. This class is associated with entities, people, orga-

nization, portfolio, and communication medium. Communication medium: This class of communication medium consists of standard and encrypted communication with subclasses such as anonymous proxy server, electronic payment server, and mail server. This entity is in relations with class of message, people, and organization. Document: The class contains all documents that can be provided by the person for identification purposes. It has many subclasses such as national card ID and passport. This entity is only associated with the entity people.

B. Identity Theft

Identity theft is considered as a mind game that favors hackers for the purpose of tricking users. There are various classes of identity theft, including email fraud. Most fraud detection researchers focused on non-semantics features of identity theft. In this type of fraud, the fraudsters try to steal none identity convincing the victims they are communicating with the intended person. In this area we classified several classes of identity theft from email to phishing and other scams.

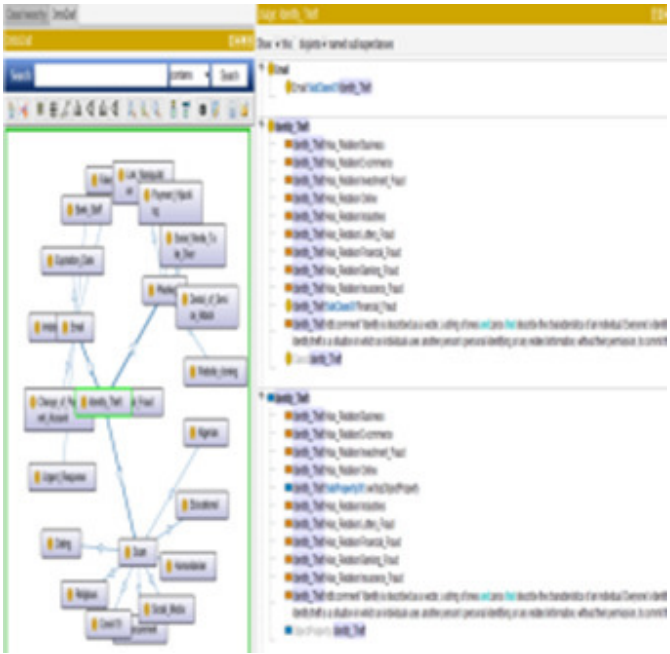

Fig. 5. The concept of identity theft.

1) Email Fraud: The use of email as a means of official and non-official communication is increasing worldwide. The number of emails sent and received globally has increased each year since 2017. While roughly 306.4 billion emails were estimated to have been sent and received each day in 2020, this figure is expected to increase to over 376.4 billion daily mails by 2025. [2] Claim that email fraud is more structured and more successful that in each 10 fraudulent emails sent, seven are delivered in the inbox, and estimated three are responded. More precisely, the incremental trust and usage of the service provide an opportunity to fraudsters to exploit the vulnerabilities. These vulnerabilities can be from both ends: sender, receiver as well as the email service providers. In our implementation we classified email fraud into various subclasses.

Fig. 6. The sub concepts of email fraud.

2) Phishing fraud: Refers to the spam that are sent by fraudsters in order to deceive their victims and obtain their personal information. Fraudsters can impersonate a service provider or institute that victims collaborate with. The fraudsters can make use of convincing techniques to obtain the victim's personal information including credit card details. The spam may also include links to fraudulent websites which again can deceive victims into revealing their personal information. In this class of ontology, we have several entities.

Fig. 7. The sub concepts of phishing fraud.

C. Lottery Fraud

The current trend of lottery fraud cannot be ignored, especially amongst elderly people. In this research, there are several behavior classifications of lottery fraud victims. On the other hand, the ontology provides a comprehensive semantic property to the kind of lotteries where fraud is more likely. For example, social media lottery fraud is more concurrent in developing countries than developed countries. This could be due to the fact that in developed countries people tend to have more available information in these kinds of fraud. While the fraudsters target elderly people, there is a concern the new trend of lottery fraud is shifting toward younger and desperate individuals.

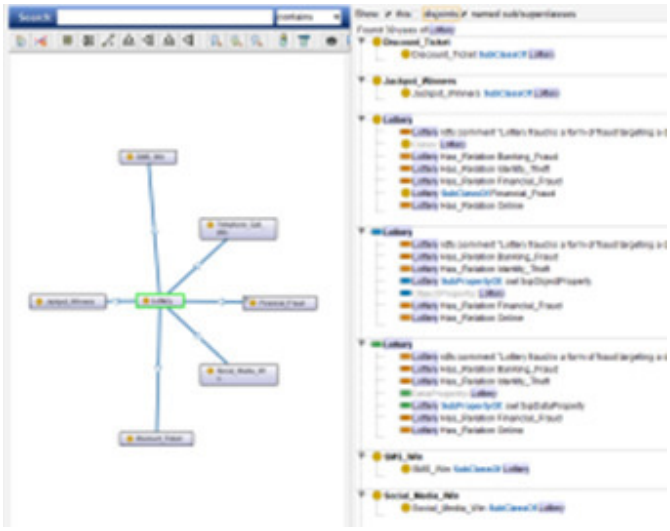

Fig. 8. The concept lottery fraud.

D. Insurance Fraud

Insurance fraud in its many forms is seen as a deliberate deception perpetrated against or by an insurance company or agent for the purpose of financial gain. Fraud may be committed at different points in the transaction by applicants, policyholders, third-party claimants, or professionals who provide services to claimants. We classified insurance fraud into internal and external, the sub concepts of this fraud are classified into health, vehicle, life insurance. We also presented common patterns of insurance frauds including padding, inflating claims, misrepresenting facts, and fake license agents.

E. Investment Fraud

The comprehensive classification of investment fraud is provided in this ontology. There are various existing investment frauds, some are old enough while some are new due to technological advancement. In investment fraud, existing investors are paid with funds collected from new investors. For example, Ponzi schemes whereby organizers often promise

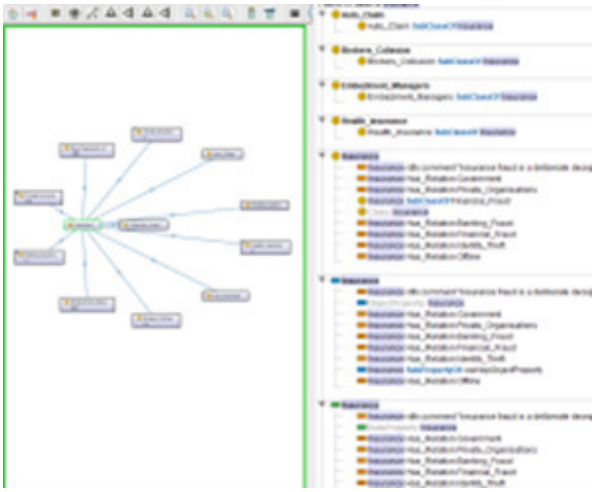

Fig. 9. The concept of insurance fraud.

investors a huge return on investment with little or no risk. We proposed several sub concepts of investment fraud, some are targeting big investment, while others target small and medium investors. These are Ponzi scheme, pyramid scheme, pump and dump, offshore, gold as well as boiler room and advance fee.

Fig. 10. The concept of investment fraud.

F. Tax Fraud

This section includes the process of classifying, constructing the various ways of tax evasion and as a means of tax fraud. The aim is to understand the tax collection structure and the main challenges they faced. Hence, we classified tax fraud into several sub concepts, from tax evasion, fake income, report, corporate tax fraud. We conclude that while avoiding tax burden is legal, there are several ways that individual, and organizations avoid tax illegally. These provide us with other entities, properties, and individual tax noncompliance activities.

G. Transaction Fraud

The transaction fraud was extracted from one of the datasets we obtained for the purpose of validating the ontology. Initially this concept of fraud was not in the ontology. We proposed

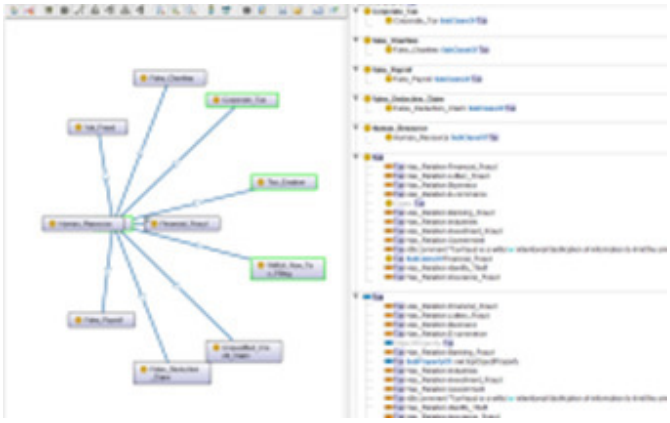

Fig. 11. The concept of tax fraud.

transaction fraud to separate it from the payment fraud, which already exists in the ontology. The concept of transaction includes various sub concepts. From fake alerts, to fake items, items not delivered, service not rendered, etc. The properties of this concept are inline and related with various concepts and sub concepts of frauds in the ontology. Hence, it is one of the most relatively related concepts in this research.

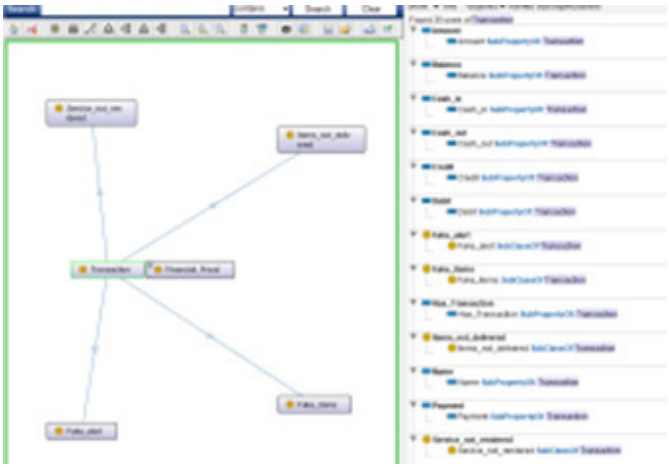

Fig. 12. The concept of transaction fraud.

H. Forex Fraud

Foreign exchange is a decentralized market for the trading of currencies, unfortunately the market has been penetrated by fraudsters, in which various frauds are proposed to the customer. In this research we focused on this fraud and declassified them into a semantic context. This concept has very few relations with other concepts in the ontology, all of its sub concepts have no relations with any concept or sub concept in the ontology. Nevertheless, the object properties have some common relation with investment fraud.

I. Cyber Violence Fraud

The act of Bullying was specifically known for teenage ages especially in schools. Cyber violence is often just other

Fig. 13. The concept of forex fraud.

sides of the same coin. The act aims at causing emotional and physical violence for the purpose of monetary exploitation from the victims. While conducting the research, we contacted some experts in cyber violence and bullying for understanding the various forms of cyberbullying. This act of fraud is on the rise especially in developed countries. We classified this concept into various sub concepts which clearly diversified the concept into a significant act of violence and fraud. While investigating this concept we understood how gender plays an important role in this fraud, for example a sexism sub concept is mainly targeted at females. While social exclusion is targeted at the male. There are not many relations between this concept and other concepts in the ontology, but identity theft and dating scam have a direct relation with this concept in the ontology.

Fig. 14. The concept of cyber violence fraud.

VI. Validation of Ontology

This ontology was designed and built based on multiple layers. Hence, the validation should be based on layer by layer or component to components. The aim of this section is to determine a concise and acceptance of the ontology to the experts and users. We identified a set of ontology quality criteria and ontology aspects that must be achieved, including accuracy, adaptability, clarity, completeness, computational efficiency, and consistency. There are several methods of ontology validation using tools and other techniques. While tools

are good with ontology consistency validation, we consider several techniques that are more consistent with knowledge and content validation. The dataset validation was performed in two ways.

A. Dataset Based Validation

This type of validation is done by using fraud-related datasets to validate the ontology, in this section we elaborate some of the dataset. The challenge with this type of validation is finding the correct data that is in line with the concepts of the ontology. Hence, we explore several options and various data sources. Financial fraud data: The dataset obtained from Kaggle, has various features simulated for mobile money transactions. The technique of concept extraction from the dataset was done by means of distributing every feature into a particular class as ontology. From the features we extracted sub concepts, entities, properties, as well as individuals.

- Matching the semantic content of the ontology concept with the dataset features. This process explored the similarity function to find the matching words that appear in both files. While using a dictionary function to identify words with several meanings to avoid missing matching. This process of validation is considered the most acceptable type of ontology content validation.
- Concept extraction validation. In this process, we studied the features of the dataset in order to extract a possible ontology concept from the dataset, then we checked the ontology if the concept is existing. Else it will be added into the ontology. Using this type of validation, we were able to add several concepts into the ontology, which include transaction fraud, forex fraud, and crypto currency fraud concepts.
- Insurance fraud data: The dataset contains insurance claim data for fraud detection, in the ontology we built several concepts including insurance fraud. Some examples of features in this dataset are employee data which include the data of the employee or agent working in the insurance company. This data is used to validate the claim of internal insurance fraud in our ontology. While the feature of vendor data is for the external agent who assists the insurance company in investigating the claims. As suggested in our ontology vendors are sometimes involved in external insurance fraud. This feature was used to validate the broker's collision class in the ontology.
- Bank Fraud Data: The banks are often exposed to fraud transactions in various forms, we use the dataset to validate the concept of banking fraud in the ontology. From the various features in the dataset, we construct the concept of banking fraud and it exactly tallies with the concept of and entities of banking fraud that exist in the ontology.
- Fraudulent Email Data: This dataset contains criminally deceptive information, usually with the intent of convincing the recipient to give the sender a large amount of money. This dataset is a huge collection of fraudulent letters sent to various recipients. The features include sender, receiver, message id, date, subject, etc. We explore this dataset and extract the concept of email fraud, in our ontology email fraud is a sub concept of identity theft. We also used this dataset to validate Nigerian scam, which is a class of fraud under sub concept termed scam.
- Cryptocurrency Fraud Data: This dataset contains rows of known fraud and valid transactions made over ethereum, a type of cryptocurrency. The various features in the dataset makes it possible to have enough entities to create the cryptocurrency concept in our ontology. Hence, we proposed a class of cryptocurrency fraud concept in the ontology. The properties of individuals as well as entities of this class were not in the ontology before we started the validation process.
- Financial fraud data: The dataset obtained from Kaggle, has various features simulated for mobile money transactions based on a sample of real. We explore these features. Concept extraction from the dataset was done by means of distributing every feature into a particular class as ontology. From the features we have those in sub concepts, entities, properties, as well as individuals. From the features we extracted, the transaction fraud concept is extracted from the dataset.
- Insurance fraud data: The dataset contains insurance claim data for fraud detection. In our ontology we built several concepts including insurance fraud. From the features, employee data include the data of the employee or agent working in the insurance company. This data is used to validate the claim of internal insurance fraud in our ontology. The feature of vendor data is for the external agent who assists the insurance company in investigating the claims. As suggested in our ontology vendors are sometimes involved in external insurance fraud. This feature was used to validate the broker's collision class in the ontology. The claims data in the dataset is for the claim-level transaction details submitted by the customer to the insurance company for reimbursement. The feature was used to validate the auto claim fraud class in the ontology.

VII. Discussion

The research proposed heavyweight ontology for financial fraud due to the multi-layer structure of the ontology. The elaboration of the ontology was done with a full compliance of the state-of-the-art methodology and advice received from the domain experts in addition to adopting various ontology development articles from several ontology developers' community. The proposed ontology consists of a number of concepts, sub concept, properties, and other semantic annotations.

The proposed domain areas constitute eleven concepts and several sub concepts. In this research work, we are constructively convinced; these areas are of great importance in the financial sector. Hence, understanding the fraud concepts will reduce a significant number of losses in the sector.

A. Semantic contents and related information

- Documentation: It provides a consistent and centrally non-technical description of the semantic content of the concept of the ontology such as concepts, classes, individual resources and properties. The documentation does not consider the proprietary format in which the information is stored in the ontology platform.
- Navigation: Is used to provide links between the information sources established, which can be employed for navigation between resources. Consider for instance when a user tries to navigate from the class of banking fraud object properties to the class of identity theft fraud data properties and vice versa.
- Retrieval: As the annotations are represented in a formal machine-interpretable ontology language, they can be exploited by appropriate browsing and querying tools.
- Definition We added definitions of entities in the individual section of the ontology. The definition will provide users with the most accurate definitions of the entity, including a semantic knowledge of the concept. For example, in Figure 1. We can see the definition of Government as described in the individual section of the ontology.
- Restrictions In OWL there are two kinds of restrictions, existential restrictions, that describe classes of individuals which participate in at least one relationship along a specified property to individuals that are members of a specified class. For example, the concept of banking fraud has a relationship called 'has a part of' with members of the Identity theft fraud concept. While universal restrictions describe classes of individuals that only have relationships along with a property that are members of a specified class.
- Visualization For a user to be able to view the ontology, there is a need for an ontology development, or ontology view platform. We recommend using Protégé ontology platform or Vowl ontology viewer to navigate to windows, then view options, there are several view options from OBO, Owl viz, Onto graph and many more.
- Ontology Instances The instances in ontology are lists of individuals that are asserted to be instances of classes. The classes are selected and assigned to each instance. For example, financial fraud is a concept and 'business' is an instance of that concept. It could be argued that business is a concept representing the different instances of financial fraud and its isotopes, etc. This is a well known and open question in ontology building. However, deciding whether something is a concept of an instance is difficult, and often depends on the application and domain.

VIII. Conclusion and future work

The paper proposed an ontological approach to various concepts of financial fraud, which could serve as first of its kind. The elaboration of the ontology provides a comprehensive and explicit terminology of financial fraud activities, we explored creating an ontological catalogue that defines the various types of fraud committed. This was largely helped by the dataset validation technique adopted. The technique allows the flexibly created fraud ontology to be modified and additional definitions made.

The validation approach used in this research work opens doors to the ontology developer's community to implement such an approach for better accuracy of ontology developed. The availability of datasets makes it possible to achieve this type of validation. But in the case of fraud and other cyber security-related ontologies, there could be a difficulty in obtaining the correct data and information needed, due to the sensitivity of the research.

We found a number of the dataset's attributes in our ontology. Using a dataset classified as transaction fraud, we perform concepts and properties extraction in the dataset, and we find a match with the number of properties in our ontology. But not enough as the unmatched attributes are more than the matched. Hence, we create the concept of transaction fraud in the dataset.

Few improvements could be included in the future work. The paper lacks semantic detection reasoning, this shall be implemented in the future work. The detection reasoning will allow for real time detection of various kinds of financial fraud. Obviously, comparison of this method with other machine learning approaches will as well be implemented. The future work identified in this section (semantic detection reasoning) will make the work an asset to financial institutions globally.

References

[1] Panos Alexopoulos, Kostas Kafentzis, Xanthi Benetou, Tassos Tagaris, and Panos Georgolios. Towards a generic fraud ontology in e-government. In *ICE-B*, pages 269–276, 2007.

[2] Koen Kerremans, Yan Tang, Rita Temmerman, and Gang Zhao. Towards ontology-based e-mail fraud detection. In *2005 portuguese conference on artificial intelligence*, pages 106–111. IEEE, 2005.

[3] Gonçalo Carnaz, Vitor Nogueira, and Mário Antunes. Ontology-based framework applied to money laundering investigations. In *Proceedings of the Seventh Conference on Informatics at the University of Evora*, pages 1–17. University of Evora Evora, 2017.

[4] Steven L Skalak, Thomas W Golden, Mona M Clayton, and Jessica S Pill. *A guide to forensic accounting investigation*. John Wiley & Sons, 2011.

[5] Johnson Olabode Adeoti. Automated teller machine (atm) frauds in nigeria: The way out. *Journal of Social Sciences*, 27(1):53–58, 2011.

[6] Linda Delamaire, Hussein Abdou, and John Pointon. Credit card fraud and detection techniques: a review. *Banks and Bank systems*, 4(2):57–68, 2009.

[7] S Benson Edwin Raj and A Annie Portia. Analysis on credit card fraud detection methods. In *2011 International Conference on Computer, Communication and Electrical Technology (ICCCET)*, pages 152–156. IEEE, 2011.

[8] Michael Levi. Money laundering and its regulation. *The Annals of the American Academy of Political and Social Science*, 582(1):181–194, 2002.

[9] Michael Levi and Peter Reuter. Money laundering. *Crime and justice*, 34(1):289–375, 2006.

Communication Papers of the of the 17th Conference on Computer Science and Intelligence Systems pp. 287–291
DOI: 10.15439/2022F152
ISSN 2300-5963 ACSIS, Vol. 32

SAP Fiori as a Cause of Innovation and Sociotechnical System

Maciej Suder
High Banking School in Wroclaw ul. Fabryczna 29/31, 53-609 Wroclaw, Poland
Email: maciej.suder@wsb.wroclaw.pl

Tadeusz Gospodarek
High Banking School in Wroclaw ul. Fabryczna 29/31, 53-609 Wroclaw, Poland
Email: tadeusz.gospodarek@wsb.wroclaw.pl

***Abstract*—Implementation of an ERP system in manufacturing organization is closely related with customization of the standard prototype of the system offered by a software house. In case of manufacturing health-care products some additional aspects to standard information circuits must be added. These mean QC, ISO, FDA requested data should be processes parallel to bookkeeping ones. In this paper the use of SAP Fiori in the QC process in inbound logistic is presented. Adding SAP Fiori to the existing SAP solution allows to create sociotechnical informal group of the users having new key competences. It allows to achieve some benefits measured with CBA method for the organization. It was concluded that integrated IT systems of ERP class may develop sociotechnical systems in organizations used them leading to re-engeneering processes and transition changes. A case study of changes inside a map of process of the manufacturing health-care products plant is presented and discussed.**

I. Introduction

THE world is changing, and all manufacturing organizations want to be competitive and strictly focused on customer demands and requirements (Kotler, 2007). The customer wants to receive a product of better quality, faster and cheaper. One of possible supports for managing organization fulfilling such demands is implementing the integrated IT system of the ERP class. It will help managers to take rational decisions based on optimization costs and a profit, based on constant monitoring of a feed-back between the initial values of a set of key performance indicators and the received response from the surroundings being recognized as the value created (Gospodarek, 2012).

There are some well-known ERP solutions for industrial enterprises, like IFS, QAD, SAPS4/HANA, Oracle E-Business Suite, (Kimberling, 2020). Each of them has some pros and cons. There are some comparisons and rankings on the Internet regarding functionality and operationality, e.g., "Top 10 ERP"[1], The Top 14 Manufacturing ERP Systems in 2022[2], Manufacturing ERP Software[3], Best ERP Software for Manufacturing Businesses[4], and more. All of ERP systems must be customized and specifically implemented in concrete organization, regarding to its map of processes and the value chain. In all cases it is necessary to define what does it mean the ERP system, because the gap between imagination how it should work from the user and the supplier point of view may be the problem in proceeding with the project realized the way using dedicated methodic approach.

A lot of specific solutions of implementations of the ERP systems are available over the Internet. In this paper some advantages of using the SAP Fiori tool[5] in the manufacturing organization of healthcare scope is presented. SAP Fiori is a design system that enables one to create business apps with a consumer-grade user experience, turning casual users into SAP experts with simple tools that run on any device (e.g., tablets and smartphones). Implementation of the SAP Fiori may be recognized as the reengineering process of the ERP use. The users are deeply involved in process of modifications its functionality and the distribution of knowledge in the organization. It resembles the SECI model of knowledge socialization (Takeuchi and Nonaka, 1995) and forming a sociotechnical system STS (Mumford, 2006) realizing the scrum idea (Takeuchi and Nonaka, 1986) during design the modification (Ghosh & Sahney, 2010). This sociotechnical informal structure inside the organization creates innovative solutions of managing the related map of processes and becomes the valuable VRIN[6] class human resources with specific key competences[7] (Barney, 1995; Gospodarek, 2012).

The aim of this research is to prove that economic aspects of introduction SAP Fiori are effective in increasing functionality of the exploited integrated IT system. It is especially suitable for agile incremental, spiral variant of expanding usability of the existing SAP system. This approach involves the users into deep interactions with technology what allows to form non formal STS increasing productivity of the whole department.

II. The ERP system

The base model of ERP function in organizations is presented on the Figure 1. The system is understanding as the tool of measurement the performance of the organization regarding influence of the surroundings on the economic score. Feedback is the base for time-depending comparisons

[1] https://www.top10erp.org/
[2] https://tipalti.com/manufacturing-erp-software/
[3] https://softwareconnect.com/manufacturing/
[4] https://www.softwaresuggest.com/erp-software/manufacturing-industry
[5] https://www.sap.com/products/fiori.html
[6] VRIN – Valuable, Rare, In-imitable, Non-substitutable (The term derived from the resource based theory).
[7] https://embapro.com/frontpage/vrioanalysis/6661-discrimination-job

of a state of the organization. The ERP system collects source data derived from different units of the organization and processes them resulting useful information supporting a decision-making process. In the most advanced form a set of key performance indicators (Parmenter, 2019) are calculated and compared along time.

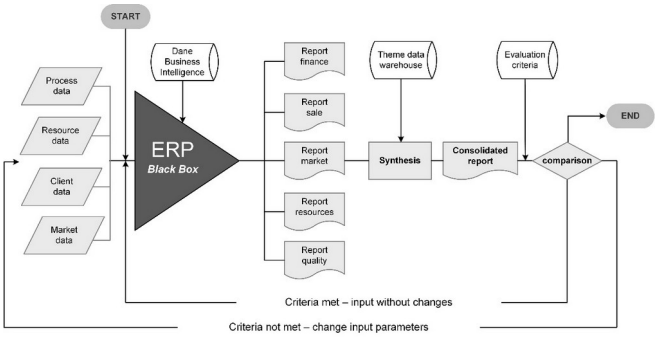

Figure 1. The ERP class integrated IT system as a tool of feed-back measurement [Source: Gospodarek T., 2015]

Practical realization of any ERP support in the manufacturing organization requires description of its value chain (Porter, 1965; Gospodarek, 2015). It needs to represent a map of organizational processes divided on single business unit or divisional parts in an architecture of processing of the ERP system. Usually, modules of the ERP system are closely related to the organizational structure of business logic.

It means that each module supports a group of specific business processes logically joined together like finance, procurement, or manufacturing – and provides employees in the related department with the information transactions and insight they need do their jobs. Every module included in the ERP system are the source of input data and the receiver of the elaborated information. Therefore, the ERP system may be treated as a single source of truth, accurate, shared data across the whole organization.

SAP A.G. is one of the world's leading producers of software for the management of business processes, developing solutions that facilitate effective data processing and information flow across organizations. In the health care business, some different from standard bookkeeping documents are used. It requires precise data collection. One of them is ISO norm fulfillment what requires for all components of a final product the source of origin and some related data. It must be determined for all processes and stages. The number of a charge of the product must be related to the place in stock. Finally, selling documents must contain the number of a product serie and date of its usefulness. It strongly complicates standard information circuit of the exploiting ERP adding some extra collections of data to the map of processes as: ISO information circuit, period of usefulness, inbound and outbound logistic information, QC control information and some more related to the CRM subsystem in the organization.

When inner auditors in subject organization analyzed how many operations had to quality technician did to release some raw materials, the organization management had decided to Implement SAP Fiori UX system for optimizing the map of processes and information circuit. SAP Fiori is a design system which enables to create business apps with a consumer-grade user experience. Common users of the SAP ERP may become experts thank to simple screens that run on any device. They better understand the processes and information exchange because some hidden knowledge is delivered from the mentioned modification of the SAP ERP system. Using the SAP Fiori design guidelines and available tools included, one can easily build and customize the existing apps adding new functionality at minimum knowledge about architecture and structure of the used integrated IT systems. This is the starting point for arising the sociotechnical subsystem and transformation of the involved in handling the process persons from costs makers for the organization to its resources offering some new key competences. It is the hidden value which appears after implementation new concept of processing data describing the process.

SAP Fiori enables multiple device applications that allow users to start a process on their desktops/laptops and continue it on a smartphone or on a tablet. It seems to be the optimum solution for multidivisional manufacturers of corporational structure at reasonable costs. For that reason, it is interesting to estimate some profit of the Fiori implementation using the cost-benefit analysis (CBA) (Sartori at all, 2015).

III. KEY STUDY OF THE ANALYZED PROCESS

In this research, the processes of quality control and inbound logistic of a raw material supply were chosen. Both are performing in the production department of the analyzed plant. Map of the standard version of the process is presented on the Figure 2A.

The plant operates 41 raw material items which are checked daily in 2 shifts. The material is delivered to stock and an appropriate document is generated for accounting records. Semantic model representing some FDA's requirement for a material released is based on the Supplier's Certificate of Analysis and in site visual control.

Before any material reaches the production department, it must undergo laboratory control. This requires certain activities not necessarily registered in the ERP system but using the related thematically IT subsystem. There are some possibilities to optimize the process structure and its map.

IV. DESCRIPTION OF THE PROCESS (STANDARD SAP ERP WORKFLOW)

Process name – Release Raw Material
Category – Main Process
Type related – Inbound delivery
Purposes – releasing raw material for production
The owner - Production manager
Participants – Warehouse operator (WH), Extended warehouse manager (EWM), Quality

technicians (QT), Production manager (PM).

IT supporting modules - SAP Quality Module, SAP Extended Warehouse Management.

Steps (actions):

1. Warehouse receives raw materials from a supplier.
2. WH moves the material to the quality stock.
3. QT receives a certificate of analysis from the supplier which is checked with parameters requested.
4. QT prints the list of materials available at batch quantities in the stock fulfilling quality requirements.
5. QT sends information containing material list to WH by e-mail and demands to prepare samples for control purposes.
6. WH prints additional label for the subjective material including some processes data, as: batch number, quantity, code for ISO purposes, etc.
7. WH collects necessary materials and moves them to a quality bin.
8. WH uses EWM SAP module and moves material from the Quality Stock to the quality bin.
9. WH informs QT that samples are ready to check.
10. QT goes to the quality bin, doing visual control of the selected material and decides which material could be release for production line.
11. QT send mail to WH and requests to move back all material from the quality bin to the quality stock.
12. WH moves back material from the quality bin to the quality stock (and issues suitable document).
13. QT uses SAP Quality Module and puts some records resulting and releases the controlled material for further processing.
14. Released raw material is moved to the production department.

One can note that the set of processed data is different from the standard ERP information circuit. Warehouse operator and Quality Technicians make nine steps, some possible to reduce:

Warehouse: Printing additional label, preparing and placing the sample elsewhere, moving material inside the system, returning back material to its physical location, returning back material into the system (5 activities).

Quality controller: Downloading the list, sending mail to WH, writing which material could be release, sending mail to WH (4 activities)

V. Modifications Inside the Workflow Derived From Fiori Implementation

New look of the workflow is presented on the Figure 3. The set of actions:

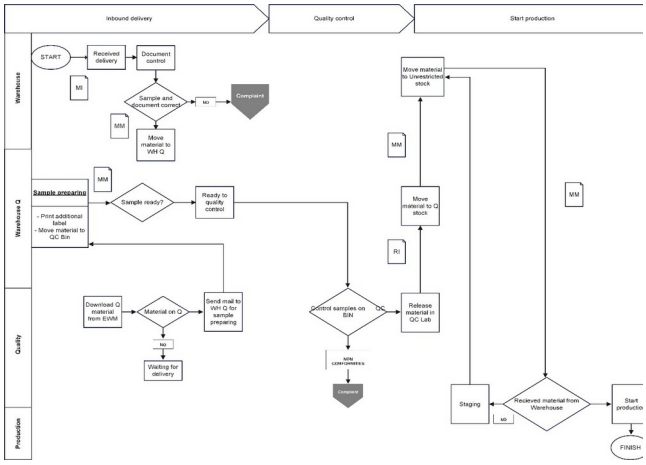

Figure 2 UML diagram of the subjected process. A – standard SAP ERP mode

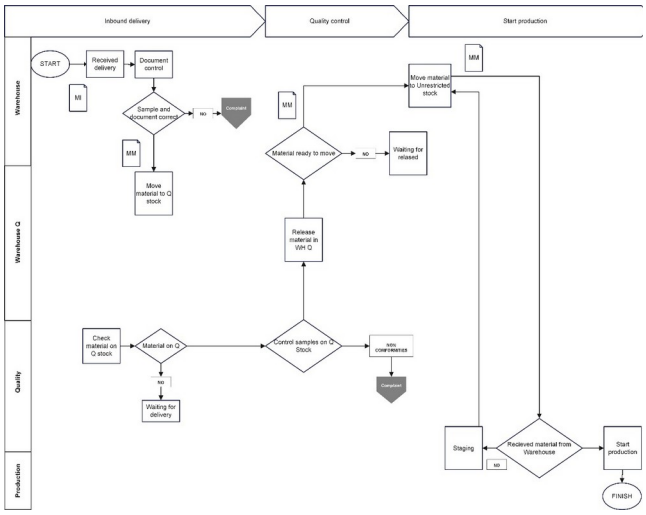

Figure 3 UML diagram of the subjected process modified SAP Fiori mode.

Steps

1. Warehouse receives raw material from the supplier
2. WH moves the material to the Quality Stock
3. QT receives certificate of quality from the supplier
4. QT goes to the quality stock, controls the subject material, records the results and makes a decision
5. The released raw material may be move to production

As it is easy to see, only 4 steps are taken in case of the SAP Fiori use. It means 2 for WH and 2 for QT. It means reduction of additional steps for the Quality Department to 66.7%, and for the Warehouse 71.5% respectively. This way WH and QT

VI. Cost Benefit-Analysis of Innovation

The cost-benefit analysis is the comparison the projected or estimated costs and benefits or possible ones, associated with a project decision (in our case – implementing SAP Fiori technology). (Layard and Glaister, 1994). It allows to

Table 1 Direct benefits obtained

Item	I shift	II shift
Saved time of release material [hour]	4	4
Number of technicians involved [EA*]	1	1
Man-hour cost [USD]	10	10
Daily savings [USD]	40	40
Total direct benefit [USD/year]	28800	

* EA – Employed active

Table 2 Indirect benefits obtained

Item	SAP	FIORI
Nonconformities identification and traceability [unit/year]	5	0
Onboarding new employees for process handling [hour]	24	16
Operations inside the process map [pcs]	14	5
Time of release material for production [hours]	20	10

determine whether the decision makes sense from an economic perspective. The main concept of the CBA approach is a monetization of the score and find a simple measure of the economic effects (Sartori at all, 2015). From the methodical point of view, the first step in CBA is to determine all components in relation to the analyzed business project. It is closely related to the Total costs of ownership approach (Cossio, 2018) applied to implementation of the SAP Fiori and its maintenance from start of the project.

Costs

1. Direct costs -related to implementing the Fiori system (such as licenses, equipment, labor, services, time wastes, learning costs, etc).
   - 6 iPads 4200 USD
   - Training new users by the Internal Subject Matter Expert 40 hours 350 USD
   - Validation of the system and documentation by a regulatory affairs associate and an Internal Subject Matter Expert: 20 hours, 1400 USD

   Total direct cost: 5950 USD
2. Indirect costs: Other expenses not directly related to the product, such as rent, utilities, or transportation costs.
   - iPads insurance 600 USD
   - iPads accessories 50 USD
   - Shipping 25 USD
   - iPads configuration 50 USD

   Total indirect cost 725 USD
3. Intangible costs: Any other costs possible to quantify e.g., brand damage if the market doesn't respond positively to the product, decreasing of production capacity if project fails. The subject organization didn't observe any intangible cost and decided to implement FIORI in the next business unit in another country.
4. Opportunity costs: The loss of opportunities caused by the decision taken. One could choose to manufacture a product more profitable. Increasing costs of licenses (Apple, Fiori).
5. Costs of potential risk (estimated): Any business project is exposed to a variety of risks. It should be considered the following:
   - Behavioral question against use FIORI,
   - Potential equipment damage,
   - Stress at work job head count,
   - Possible errors in handling the system.

Benefits[8]

1. Direct Benefits: The measurable benefits in monetary value that one can get from the project. In this case, the revenue and cash flow increasing.
2. Indirect Benefits: Benefits that you can perceive but not necessarily measure such as increased brand awareness, some risk reductions, making the STS structure inside the organization, time saving, errors reduction

It may be concluded that implementation the FIORI together with forming the STS structure grouping around the workflow presented on the Figure 2 brings measurable positive effects in the subject plant.

VII. CONCLUSION

A lot of manufacturing plants are involved in raw material control process. Additional requests for data handling out of the scope of standard ERP system cause necessity to look for new IT solutions. The most important aspect in such problem is reorganization of the map of process according to technological functionality of the offered software. Sometimes such update of the map of processes creates enhancement of economic effectiveness of the subjective organization. The best situation is observed when a group of employed for handling the modified process will take part in knowledge socialization and become a sociotechnical system. Such informal substructure may introduce a lot of benefits for the organization.

ERP systems and their modifications expanding functionality outside the set of key performance indicators mainly focused on the balanced scorecard monitoring may be good base of founding sociotechnical systems inside the organization. We've found that SAP Fiori modification is one of ef-

[8] All benefits described below were determined by an audit after a year of functioning the system.

fective examples of such mechanism. The process of moving raw materials from a stock to the production department of medical care goods was reengineered and its workflow was redesigned using the Fiori software. It was estimated direct yearly benefits round 28 800 USD (see table 1) and some indirect benefits (see table 2), which influence the profit of the organization. Reduction of quantity steps in the map of process are direct related to form the sociotechnical system operating between Warehouse operators and Quality technicians. This STS eliminate errors in handling samples for QC and reduces knowledge socialization from 24 to 16 hours for new employees.

Less number of operations for quality control and warehousing reduce no conformities of the material with requests and improve delivery raw materials faster for production. Quality control doesn't influence material flow and less backorders from customers have been observed since a year of Fiori implementation. Fiori reduced daily paper works. It was observed no nonconformities during internal audits of identification and traceability of the raw materials.

Scientific problem derived from this research seems to be very prospective. The relationship between the IT integrated systems and stimulation of forming the STS systems will be investigated in the nearest future.

References

[1] Barney, Jay. B, 1995, *Looking Inside for Competitive Advantage*, Academy of Management Executive, Vol. 9, Issue 4, pp. 49-61

[2] Cossio, Miguel, 2018, *Use Total Cost of Ownership to Optimize Costs and Increase Savings*, Gartner Research, Document No. https://www.gartner.com/en/documents/3847267

[3] Ghosh, Koustab, Sahney Sengeeta, 2010, *Organizational Sociotechnical Diagnosis of Managerial Retention: SAP – LAP Framework*, Global Journal of Flexible Systems Management, Vol.11, Nos.1 & 2, pp 75-88.

[4] Gospodarek Tadeusz, 2012, Aspekty złożoności i filozofii nauki w zarządzaniu,

[5] Gospodarek, Tadeusz, 2015, Systemy ERP. Modelowanie, projektowanie, wdrażanie, Helios, Gliwice.

[6] Kimberling, Eric, 2020, *Top 10 Manufacturing ERP Systems*, https://www.thirdstage-consulting.com/top-10-manufacturing-erp-systems/

[7] Kotler, Philip T., Armstrong, Gary, (2007), *Principles of Marketing*, Pearson, London.

[8] Layard, Richard and Glaister, Stephen, (1994) *Cost-benefit analysis*. Cambridge University Press, Cambridge, UK, http://eprints.lse.ac.uk/39614/1/Introduction_%28LSERO%29.pdf

[9] Mumford, Enid, 2006, *Researching people problems: some advice to a student*, Information Systems Journal, vol. 16 (4) pp. 383–389, doi: 10.1111/j.1365-2575.2006.00223.

[10] Parmenter, David, 2019, Key Performance Indicators: Developing, Implementing, and Using Winning KPIs, 4th Ed., John Wiley & Sons Inc, Hoboken, NJ.

[11] Porter, Michael E., 1985, Competitive Advantage: Creating and Sustaining Superior Performance, Simon and Schuster, N.Y.

[12] Nonaka, Ikujiro, Takeuchi, Hirotake, 1995, The Knowledge-Creating Company: How Japanese Companies Create the Dynamics of Innovation. Oxford University Press.

[13] Sartori Davide, Catalano Gelsomina, Genco Mario, Pancotti Chiara, Sirtori Emanuela, Vignetti Silvia, Bo Chiara del, 2015, *Guide to Cost-Benefit Analysis of Investment Projects. Economic appraisal tool for Cohesion Policy 2014-2020*, European Commission, Brussels, https://ec.europa.eu/regional_policy/sources/docgener/studies/pdf/cba_guide.pdf

[14] Takeuchi, Hirotake, Nonaka, Ikujiro, 1986, *The New New Product Development Game*, Harvard Business Review, January-February 1986, https://hbr.org/1986/01/the-new-new-product-development-game

Communication Papers of the of the 17th Conference on Computer Science and Intelligence Systems pp. 293–299
DOI: 10.15439/2022F13
ISSN 2300-5963 ACSIS, Vol. 32

Top-down and bottom-up collaboration as a factor of the technological development of smart city. The example of Taipei

Dorota Walentek
Czestochowa University of Technology,
ul. J.H. Dąbrowskiego 69,
42-201 Częstochowa, Poland
Email: dorota.walentek@pcz.pl

Dorota Jelonek
Czestochowa University of Technology,
ul. J.H. Dąbrowskiego 69,
42-201 Częstochowa, Poland
Email: dorota.jelonek@pcz.pl

Abstract— **The aim of the article was to identify the benefits and risks resulting from combining top-down and bottom-up initiatives in the context of the technological development of smart cities. In order to achieve the goal, an interview has been conducted with the Deputy Secretary General of GO Smart. It has been shown that the cooperation of top-down and bottom-up initiatives has a positive impact on the city's technological development. The most important benefits of this type of cooperation include increasing innovation and the level of creativity of technological solutions introduced in a smart city, opening the city to new opportunities, as well as increasing the activity of the private sector and the involvement of residents in the city's development. The main risks are related to determining the scope of responsibility for individual initiators when implementing a project as well as the duration of processing applications.**

I. Introduction

ACCORDING to the data provided by The World Bank, in 2020 the number of people living in cities exceeded 56% of the entire global population [1]. By 2050, the percentage of people living in urban areas will increase to 66% [2]. The process of urbanization, taking place all over the world, constitutes a major challenge for city authorities. Proper living conditions must be created in a limited urban area for a constantly increasing population. The increasing standard of living is accompanied by a constant strive to increase the quality of life of citizens.

Both of the above mentioned trends contributed to the creation of the idea of a smart city. The main feature of this concept is taking advantage of modern technologies both to improve the efficiency of an urban infrastructure and to communicate with residents. The question arises: who and how can present new technological ideas to the decision making entities and who handles their implementation. In the context of smart cities, it is possible to distinguish two main types of technological initiatives: top-down and bottom-up ones [3]. Both concepts are very important for the sustainable development of urban areas.

The aim of this article was to identify the benefits and risks resulting from combining top-down and bottom-up initiatives in the context of the smart city technological development. The city of Taipei, considered to be one of the most modern cities in the world, has been chosen for the study. Taking advantage of an interview with the Deputy Secretary of the Global Organisation of Smart Cities, Anita Chen, the Smart Taipei Collaborative Ecosystem model used in Taipei, which combines top-down and bottom-up initiatives, has been analyzed.

Individual elements and infrastructure systems of Taipei have already been described in the scientific literature. Researchers focused, for example, on public security [4], transport [5], education [6], or the role of the Taipei Smart City Project Management Office in the process of the city's technological development [7], and the top-down communication in Taipei [8] has also been analyzed.

A combination of top-down and bottom-up initiatives has also been described on numerous occasions. However, these publications concerned either models of using top-down and bottom-up in the development of other cities [9, 10, 11], or the general characteristics of the concepts mentioned above [12, 13]. This article will constitute an expansion of the knowledge concerning combining top-down and bottom-up initiatives by presenting a specific model of the Smart Taipei Collaborative Ecosystem. The information about the described model has been obtained during an interview with the Deputy Secretary General of the GO SMART organization that has been established in Taipei but has a global reach.

II. The concept of a smart city

The idea of a smart city appeared at the end of the 20th century as a result of research on the process of urbanization and the development of ICT tools. According to one of the early definitions, a city referred to as smart is an efficient and environmentally safe space of the future, in which all processes and systems are controlled electronically [14]. This space aims for an optimal interaction of individual urban infrastructure systems, such as: administration, transport, construction, waste management, education, health care, public safety, and recreational spaces [15]. Modern ICT technology constitutes the element that allows a symbiosis of the above-mentioned systems.

Smart cities are characterized by a smart management

style. Filling the public space with smart sensors, measuring devices, as well as programs and apps for collecting and processing data has an impact on the rapid flow of information among city stakeholders [16], which in turn makes it easier for urban authorities to make decisions and create plans related to further improving smart cities. In this case it is important to pay attention to all sectors of the infrastructure when allocating urban resources as well as finalizing official matters in an efficient manner.

Increasing the city's efficiency has an impact on the improvement of the well-being of citizens [15]. According to the assumptions, residents of smart cities should feel safe, and they can take advantage of convenient electronic educational platforms. Additionally, they conveniently finalize official matters thanks to using smart electronic systems. Web and smartphone apps allow them to quickly acquire information. Thanks to using modern ICT solutions, residents can also participate in citizens' initiatives, thus supporting the authorities in the process of planning the city development [11].

Sustainable energy resources play a highly significant role in smart cities [16]. It is crucial for all kinds of economic activities that contribute to urban development [17]. It is also necessary for the proper functioning of all sectors of urban infrastructure, including: heating of the buildings, the functioning of city cameras, controlling sensors, using the IoT and electric cars, or the operation of computers and telephones. In smart cities, renewable energy sources, such as photovoltaic farms, hydroelectric power plants, and wind farms, are considered to be optimal sources of energy.

Since the formation of the smart city concept, four main research areas can be distinguished, presented in Table I [18]. As shown, publications handling the subject of smart cities concern both the definition of the concept, the characteristics of specific urban centers, individual elements of smart cities infrastructure, as well as specific methods used in the process of creating and implementing smart IT solutions in terms of the city's activity.

Due to the development of subsequent technological innovations and system methods, these issues appeared in research works at different periods of time. During the initial stage of developing the smart cities concept, researchers focused primarily on implementing ICT solutions in the processes occurring in the city [19]. The aim of implementing new technologies was to increase the efficiency of the city while taking care of the ecology. Singapore was an example of a smart city during the initial stage of the concept's development [20]. Along with a significant increase in data transmission resulting from implementing new technologies in the second decade of the 21st century, the process of city's the datafcation [21] and cybersecurity began to be analyzed [22, 23]. During the same period of time, using the IoT in smart cities was also studied [24, 25]. The currently created publications concerning smart cities are mainly devoted to specific initiatives and projects increasing a city's efficiency. These projects concern, for example, analyzing large data sets [19].

III. TOP-DOWN AND BOTTOM-UP INITIATIVES

Top-down and bottom-up concepts are used to describe phenomena and behaviours in various aspects of life. In philosophical terms, they define contradictory theories regarding the rights and properties of nature [26]. In psychology, they are used to describe, among others, autobiographical memory [27]. In biology, they can describe a process of tissue formation starting from the top or bottom [28]. These concepts are also very common in management. The top-down initiative combined with bottom-up comes from 90's Knowledge Management. Here, top-down means initiating a given process by entities with a higher position in the structure of a given organization, while bottom-up means the opposite [29].

In the context of smart cities, top-down initiatives stand for actions of administrative authorities undertaken in the process of city management [30]. They usually concern long-term planning and are characterized by a comprehensive and predictable character [31]. Their aim is often to maintain stability in the city or to carry out inspections in individual sectors. The implementation of top-down a concept is ordered and hierarchical [11].

TABLE I.
MAIN RESEARCH AREAS OF THE SMART CITIES IDEA

Research area	Main topics within the research area
Concept description	Smart cities definitions, scientific discourse concerning the concept, theories of spatial development, etc.
Characteristics of specific smart cities	Smart cities rankings, new urban planning, urban problems and propositions for their solutions, promotion of tourism, the role of the public sector and city residents in relation to the goals and benefits of individual cities and countries, etc.
Elements of smart cities	Various types of sensors used in the urban infrastructure, IoT, big data, smart solutions in terms of specific sectors: education, environmental protection, tourism, transport, public safety, food supply, waste management, water management, energy, etc.
Methods of creating and developing of smart cities	Smart applications, smart government, top-down and bottom-up initiatives, ICT companies, participation of universities, etc.

Bottom-up initiatives are related to the ideas of citizens and businesses. Such initiatives are often carried out on a much smaller scale than top-down initiatives. They have a test and experimental character [11]. According to [32], these initiatives are mainly submitted by representatives of the business sphere. However, other sources point to an increasing number of apps and platforms enabling bottom-up initiatives also for citizens. Examples of these solutions include the Taipei Smart City Project Management Office [33] platform, The Open Data Organization, The Community-based Information Service Organization [34], or tens of tools addressed to bottom-up initiatives in Amsterdam [35].

Currently, local governments more and more often point to the advantages of combining top-down and bottom-up initiatives, such as increasing a city's level of technological innovativity by taking advantage of the creativity of businesses and units while maintaining standards and rules set from above. Top-down and bottom-up cooperation is possible through, for example, creating specialized development programs and dedicated online platforms, thanks to which business representatives and residents participate in the city's technological development. Examples include the Taipei Global Organization of Smart Cities [36], the China's Community Duty Planners [11], or the Smart Taipei Collaborative Ecosystem [37] model.

However, in scientific literature it is often emphasized that the relations between top-down and bottom-up initiatives are often contradictory [11], and thus combining these initiatives can be a major challenge for smart cities [30]. The main conflicts occur in terms of [11] the scope of a given initiative (comprehensiveness vs. fragmentarization), duration (long-term initiative vs. short-term testing) and the degree of standardization (complete standardization vs. creative approach).

Municipal authorities often have different goals than bottom stakeholders who have to comply with the laws from above. Bottom-up initiatives may stand in opposition to spatial development plans or other regulations imposed by municipal authorities. An example of this type of conflict of interest is the one between the politicians establishing the maritime protection zone in the UK and the fishermen [30].

Experts on the subject also draw attention to the growing dominance of IT corporations in terms of planning and designing buildings in a city. This includes the cities of Songdo in Korea, PlanIT Valley in Portugal, and Masdar in the United Arab Emirates. A similar process can be noticed in China [11]. The growing impact of corporations on the development processes of smart cities may result in an increasingly small percentage of residents' participation in the shaping of the city.

IV. Research Methodology

The aim of the presented study was to identify the benefits and risks resulting from combining the top-down and bottom-up initiatives in the context of the technological development of the city of Taipei. This aim corresponds to the fourth item in Table 1: Methods of creating and developing of smart cities. Two research hypotheses have been presented:

H1: Creating of intuitive communication channels between bottom initiators and authorities increases the involvement of residents in the technological development of a smart city.

H2: Combining of the top-down and bottom-up initiatives has a positive impact on the technological development a smart city.

Choosing Taipei as the studied city was not random. In 2021 Taipei was ranked 4th in the prestigious Smart City Index created by IMD and Singapore University of Technology and Design [38] compared to 8th place in 2020. The city also organized the Smart City Summit & Expo 2021 and 2022 [39].

To achieve the intended goal, a qualitative method has been used – a structured interview. It was conducted on 29.03.2022 with Anita Chen, Secretary General of the Global Organisation of Smart Cities (abbreviated: GO SMART), who is also the Project Manager of the Taipei Smart City Project Management Office. Anita Chen has been professionally handling the creation and implementation of Taipei government programs for over 9 years. At the same time, she possesses experience in international initiatives (4 years in terms of the smart city and 4 years in cooperation between Taiwan and India). During the interview, the focus was put on analyzing the Smart Taipei Collaborative Ecosystem model used in Taipei which combines both types of the mentioned initiatives.

The interview took the form of a video conference conducted via the ZOOM platform. The final date and time of the interview (taking into account the 6-hour time difference between Poland and Taipei) were determined on 28.03.2022 during a conversation on LinkedIn chat. At the beginning of the video conference, Anita Chen expressed her consent for recording the interview and to disclosing her name in this publication.

During the interview, the following questions were asked:

1. What are the basic elements of the Smart Taipei Collaborative Ecosystem?
2. How can bottom initiators communicate with the city authorities? How do you assess the impact of these communication channels on the city and its residents?
3. Does creating intuitive communication channels between bottom the initiators and the authorities increase the involvement of residents in the technological development of smart cities?
4. What advantages and disadvantages of top-down and bottom-up strategies do you notice?

5. What is the average time of processing a project?
6. Is, in your opinion, the Smart Taipei Collaborative Ecosystem an effective solution from the perspective of the city and residents? Do any of its elements need to be improved?

An additional method used for the purposes of this publication consisted in examining of the existing documents. 2 types of formal documents have been analyzed: a document made available by the Department of Information Technology of the City of Taipei, the Smart Taipei prospectus *Government as a Platform. City as a Living Lab* [Department…], as well as documents published by GO SMART: *GO SMART. Global Organization of Smart Cities since 2019*, *GO SMART. Annual Report 2020* and *GO SMART Opportunity Report* [GO SMART].

V. The results

On the basis of the answers given by Anita Chen and examining of the above mentioned existing documents, all the questions mentioned above have been answered. First of all, the question has been asked concerning the essence of the model of creating and the implementation of new technological solutions, referred to as the Smart Taipei Collaborative Ecosystem. The process of the city's technological development is supervised by the Taipei Smart City Project Management Office (TPMO), an entity established by the Taipei City Government in 2016. Its aim is promoting top-down and bottom-up projects in terms of creating new technologies, increasing the comfort and convenience of residents in every area of urban infrastructure. According to the director of TPMO, Dr. L. Chen-Yu, the effect of the actions undertaken by his subordinate unit should consist in transforming the city of Taipei into a living lab [40]. The remaining units responsible for the technological development of Taipei are: Department of Information Technology (DoIT), Taipei City Police Department (TCPD), Department of Urban Development (DoUD), Department of Transportation (DoT), Department of Education (DoE), Department of Health (DoH), Department of Environmental Protection (DoEP), and the Department of Industry and Business (DoIB). The main connections between the individual stages of this model are shown in Fig. 1

According to Fig. 1 the Smart Taipei Collaborative Ecosystem consists of four stages. The first of them is the Strategic Map, meaning a strategic planning of technological innovations in a smart city. It is a process initiated both by the city's administrative authorities as well as by various types of research, visions, and solutions used outside Taiwan.

The second stage consists in creating a structure of new ideas. At this stage, the difference between top-down and bottom-up initiatives becomes clear. On the government side, it proposes specific pilot programs. The private sector becomes familiar with existing programs. An important role is played by the TPMO platform, which is used to inform the private sector about the government's proposals, and the government about the proposals of the private sector.

The following stage is the Proof of Concept, the core of which are: identifying a problem/area to be improved in the city, submitting proposals for a technological solution to a problem, evaluating the submitted projects, planning the implementation as well as conducting the necessary tests. Here, combining the private and public sectors takes place. The private sector needs the support from the authorities (budget, legal regulations). While top-down initiatives must be implemented and tested with the participation of business representatives and residents. On the government side, the units involved at this stage are: TPMO, DoIT, and the department corresponding to the area of a given technological solution. The main bottom stakeholders consist in representatives of academic centers, the business sphere, and research institutes. During the testing stage, both groups of stakeholders contact each other on an ongoing basis in order to eliminate possible problems.

Submitting initiatives takes place via the TPMO platform. During the calendar year, two calls for proposals are announced. Bottom initiators can also take advantage of the help of the Taipei Global Organization of Smart Cities (www.citiesgosmart.org), an institution mediating between representatives of the business sphere and the government in term of the city's technological development. The GO Smart organization is a facilitator, facilitating contacts with the government primarily for start-ups, which due to the lack of experience and reputation on the market find it more difficult to effectively negotiate with government representatives. The establishment of TPMO and GO Smart is considered to be highly beneficial in the process of Taipei's technological development. An element that encourages proposing new initiatives is the Smart Taipei Innovation Award, which aims to select and reward high-quality technological projects.

The final stage of the model consists in promoting the accepted technological solution. It means not only introducing innovation into the city's life, but also promoting it among residents and advertising it in external environments, such as, for example, international organizations or introducing ICT solutions into force. An example of this type of organization is the previously described GO Smart.

During the interview, a question was also asked about the participation of residents in the city's technological development. According to the received answer, the main form of the residents' participation in the development of Smart Taipei is the opportunity to vote for proposals for technological solutions submitted in various types

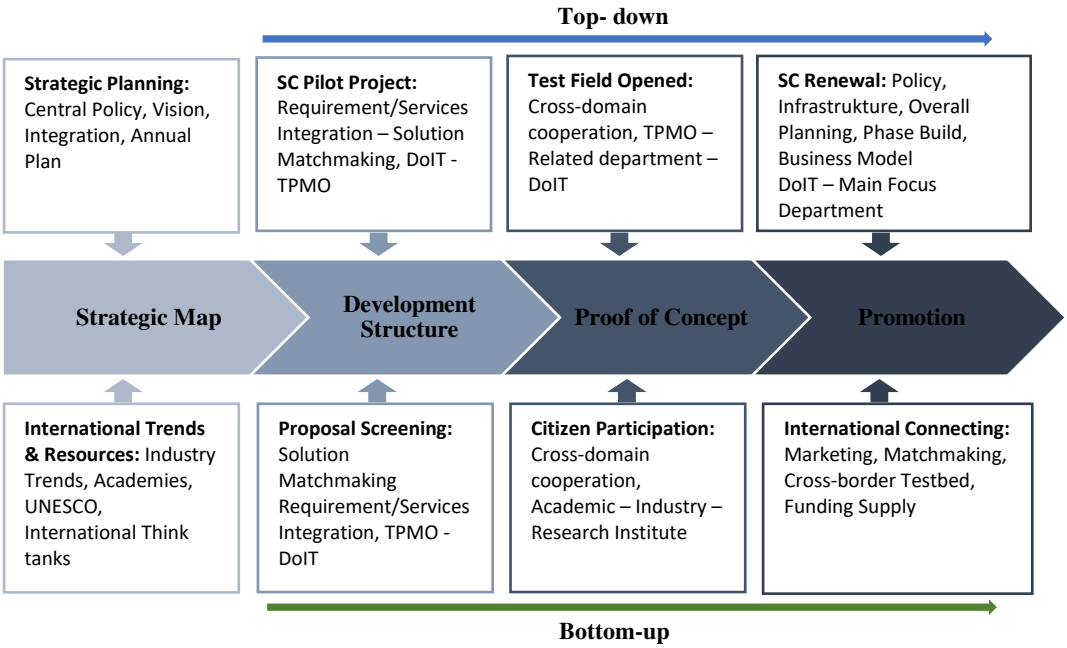

Fig 1. Smart Taipei Collaborative Ecosystem

of competitions. Voting takes place via the TPMO www.smartcity.taipei online platform, which is very convenient for the residents and increases their involvement in the development of Smart Taipei. Voting is usually carried out during the Proof of Concept stage presented in Fig. 1 of the Smart Taipei Collaborative Ecosystem model. The results are not binding: the city's authorities decide on the future of the project on the basis of their own analyses. However, the government takes into account the opinion of the residents, and they are aware of it. This answer has been considered as a confirmation of the H1 hypothesis: *Creating intuitive communication channels between bottom-up initiators and authorities increases the involvement of residents in the technological development of a smart city*.

Residents can also participate in events devoted to new technologies or build pro-innovative communities, and even participate in submitting and implementing projects devoted to the city's technological development. Surveys carried out among the residents concerning their life needs are also important from the point of view of the city authorities.

According to the Secretary General of GO Smart, both forms of projects: top-down and bottom-up, result in a number of benefits for the city. However, they are also related to challenges for initiators. The most important benefits and challenges identified during the interview have been presented collectively in Table II. Top-down initiatives usually have a larger reach than the bottom-up projects. This results mainly from easier access to funding sources and the possibility of cooperation between different departments in a short period of time. Direct access to the decision making person/people (city president or mayor) has an impact on the shortening of a project's processing. Residents can feel proud to live in a city whose authorities are open to technological development. However, at the same time, residents often consider contents provided by government units via apps or websites as less attractive. Top-down projects are usually not as creative and do not involve the business sector as much as bottom-up initiatives.

In turn, bottom-up projects have a smaller reach than top-down, which is consistent with the views presented by Zhou and Hollands [11, 32]. However, they contribute to a faster development of companies and non-governmental organizations as well as to an increase in the involvement of the residents in the city's matters. These initiatives are also regarded to be more creative than top-down initiatives. Thanks to this they often inspire subsequent people, companies, and even entire cities to introduce technological improvements. For city authorities, bottom-up initiatives are more risky, because if they fail, the people in charge will be blamed by citizens for the incorrect allocation of the taxpayers' money. For this reason, top-down initiators must devote more energy and time to conducting negotiations with representatives of the authorities.

According to Anita Chen, the Smart Taipei Collaborative Ecosystem is very beneficial for both the city and its residents. Combining these two forms of initiatives has a positive impact on the city's development, as it allows collecting creative ideas from the private sector while maintaining the order and structure established by the authorities. The city becomes more open to new possibilities. Whereas, by participating in the process of evaluating projects, the residents feel co-responsible for the technological development of Taipei and become more

TABLE II.
ADVANTAGES AND RISKS OF TOP-DOWN AND BOTTOM-UP INITIATIVES

	Top-down initiatives	Bottom-up initiatives
Advantages	▪ Often with greater reach than bottom-up; ▪ direct access to a decision making person; ▪ shorter processing path; ▪ easier access to the budget; ▪ the possibility of cooperation between several departments; ▪ the satisfaction of residents with the fact that "their" city cares for development.	▪ Development of the private sector; ▪ increasing the involvement of residents in the city's development; ▪ adding more creative content/solutions; ▪ they are an inspiration for other people/companies/cities.
Risks	▪ Content provided by government projects/apps is often unattractive to citizens; ▪ usually less creative than bottom-up; ▪ less engaging for the business sector and individual residents than bottom-up.	▪ riskier than top-down; ▪ the government fears the loss of its good image in the eyes of residents in the event of the project's failure; ▪ require longer negotiations with the authorities; ▪ require more energy from the initiator; ▪ most often with a smaller reach.

involved in the city's technological development. At the same time, the interviewed person agreed with R.G. Hollands [32] who states that bottom-up initiatives are mainly submitted by business representatives. However, at the same time, the interviewed person emphasized that the sole possibility of voting on projects submitted by other entities also significantly increases the involvement of residents in the city's development. Thus, hypothesis no. 2 has been confirmed: *The combination of top-down and bottom-up initiatives has a positive impact on the technological development of a smart city.*

During the interview, Jones' views have been confirmed [30], as according to them combining top-down and bottom-up strategies is related to risks. Anita Chen points to the often problematic issue of determining the scope of responsibility of individual entities, including the need to bear fees charged during the implementation of a project, or the responsibility to correctly prepare project documentation. An element that requires improvement is the duration of processing applications. The average time for implementing a project in 2021 was 11.3 months, with individual initiatives being processed from 1 month to as many as 44 months. It would also be desirable to increase the number of projects implemented through the Smart Taipei Collaborative Ecosystem. In 2021, the number of projects implemented via www.smartcity.taipei was 46.

VI. CONCLUSIONS

The city of Taipei has an area of 271.8 km^2. As many as 2.7 million residents live in an area almost half the size of Warsaw. Therefore, the need to create an orderly urban infrastructure, in which every resident would feel comfortable, is very justified.

On the basis of the conducted interview, it was found that public-private partnership (PPP) constitutes a very large potential for implementing technological projects in smart cities. The main benefits of combining both initiatives are faster implementation of creative technological solutions in the city, control of financing sources for a given project and increasing the involvement of residents in the construction of a functional smart city. In order to avoid excessive or too strict regulations related to public-private cooperation, it is worth taking care of intuitive communication channels between top-down and bottom-up stakeholders, such as the TPMO platform: www.smartcity.taipei. They have an impact on a faster and better flow of messages as well as increasing the involvement of residents and business representatives in the city's development.

At the same time, it is worth taking care of preparing a proper model defining the framework of interaction between top-down and bottom-up projects. An example of this type of model is the Smart Taipei Collaborative Ecosystem. Thanks to establishing clear rules for cooperation between the public and private sectors the chances of implementing creative and inspiring technological solutions in the urban area will increase, just as transforming the smart city into a living lab. Both the smart city as well as the residents will benefit from this type of regulations.

The combination of top-down and bottom-up initiatives in Taipei can also be a benchmark for smart cities in other regions of the world. In some cities, there are currently attempts to combine government initiatives with citizens' initiatives, but the transparency of the TMPO model would certainly add value to numerous urban centers, incl. in Poland.

In the future, it would be worth verifying the level of satisfaction of business representatives and individual residents concerning the possibility of participating in the smart city's technological development. Such a study would show, for example, the extent to which bottom stakeholders are satisfied with using dedicated online platforms and cooperating with institutions supporting contacts with the public sphere.

REFERENCES

[1] The World Bank, *Urban population (% of total population)*, https://data.worldbank.org/indicator/SP.URB.TOTL.IN.ZS (accessed on 28. March 2022).

[2] C.S. Lai, Y. Jia, Z. Donk, D. Wang, Y. Tao, Q. H. Lai, R. Wong, A. Zobaa, R. Wu and L. L. Lai, "A Review of Technical Standards for Smart Cities", *Clean Technologies*, vol. 2, 2020, pp. 290–310, doi:10.3390/cleantechnol2030019.

[3] K. Lenkenhoff, U. Wilkens, M. Zheng, T. Süße, B. Kuhlenk ötter, X. Ming, "Key challenges of digital business ecosystem development and how to cope with them", *10th CIRP Conference on Industrial Product-Service Systems*, IPS2, Linköping, Sweden, May 2018, pp. 29-31, https://doi.org/10.1016/j.procir.2018.04.082.

[4] C. Y. Chang, L. C. Chien, Y. H. Chang, E. C. Kuo and Y. S. Hwang, "A Smart Public Security Strategy: The New Taipei City Technology Defense Plan", *23rd KES International Conference on Knowledge-Based and Intelligent Information and Engineering Systems (KES)*, Budapest, Hungary, vol. 159, Sep. 04-06, 2019, pp. 1715-1719, doi: 10.1016/j.procs.2019.09.342.

[5] Y. S. Chen, C. K. Lin, S. F. Chen and S. H. Chen, "Two Advanced Models of the Function of MRT Public Transportation in Taipei", *Electronics*, vol. 10(9), 1048, 2021, doi: 10.3390/electronics10091048.

[6] C. F. Chen, "Design and Development of Cloud Learning Tool for English Sentence Patterns", *International Journal of English Linguistics*, vol. 9, issue 6, 2019, pp. 93-105, doi: 10.5539/ijel.v9n6p93.

[7] I. C. Chang, S. Jou, M. Chung, "Provincialising smart urbanism in Taipei: The smart city as a strategy for urban regime transition", *Urban Studies*, vol. 58(3), 2021, pp. 559-580, doi: 10.1177/0042098020947908.

[8] C. Nicolas, J. Kim and S. Chi, "Natural language processing-based characterization of top-down communication in smart cities for enhancing citizen alignment", *Sustainable Cities and Society*, vol. 66, 102674, 2021, doi: 10.1016/j.scs.2020.102674.

[9] K. Eckerberg, T. Bjarstig and A. Zachrisson, "Incentives for Collaborative Governance: Top-Down and Bottom-Up Initiatives in the Swedish Mountain Region", *Mountain Research and Development*, vol. 35, issue 3, 2015, pp. 289-298, doi: 10.1659/MRD-JOURNAL-D-14-00068.1.

[10] G. O. Huby, A. Cook and R. Kirchhoff, "Can we mandate partnership working? Top down meets bottom up in structural reforms in Scotland and Norway", *Journal of Integrated Care*, vol. 26, issue 2, 2018, pp. 109-119, doi: 10.1108/JICA-11-2017-0041.

[11] S. Zhou, H. Fu, S. Tao, Y. Han and M. Mao, "Bridging the top-down and bottom-up approaches to smart urbanization? A reflection on Beijing's Shuangjing International Sustainable Development Community Pilot", International Journal of Urban Sciences, 2021, doi: 10.1080/12265934.2021.2014939.

[12] H. Kaplan, M. Gurven, "Top-down and bottom-up research in biodemography", *Demographic Research*, vol. 19, 2008, pp. 1587-1602, doi: 10.4054/DemRes.2008.19.44.

[13] I. van Meerkerk, "Top-down versus bottom-up pathways to collaboration between governments and citizens: reflecting on different participation traps", in *Collaboration in public service delivery: promise and pitfalls*, A. Kekez, M. Howlett, M. Ramesh, Ed. 2019, pp. 149-167, doi: 10.4337/9781788978583.

[14] R. E. Hall, B. Bowerman, J. Braverman, J. Taylor, H. Todosow and U. von Wimmersperg, *The vision of a smart city*, Brookhaven National Lab., Upton, NY, 2000.

[15] J. Bélissent, "Getting Clever About Smart Cities: New Opportunities Require New Business Models", Cambridge: Forrester, 2010, pp. 244-277.

[16] M. Zuccalà, E. Verga, "Enabling energy smart cities through urban sharing ecosystems", *Energy Procedia*, vol. 111, 2017 pp. 826-835, doi: 10.1016/j.egypro.2017.03.245

[17] S. Hajduk, D. Jelonek, "A Decision-Making Approach Based on TOPSIS Method for Ranking Smart Cities in the Context of Urban Energy", *Energies*, vol. 14.9, 2691, doi: https://doi.org/10.3390/en14092691.

[18] J. Yang, Y. Kwon and D. Kim, "Regional Smart City Development Focus: The South Korean National Strategic Smart City Problem", *IEEE-Inst Electrical Electronics Engineers Inc445 Hose Lane, Piscataway, NJ 08855-4141*, vol. 9, pp. 7193-7210, doi: 10.1109/ACCESS.2020.3047139.

[19] H. Allahar, "What are the Challenges of Building a Smart City?", *Technology Innovation Management Review*, vol. 10, issue 9, 2020, pp. 38-48, doi: 10.22215/timreview/1388.

[20] A. Mahizhnan, "Smart cities: the Singapore case", *Cities*, vol. 16(1), 1999, pp. 13-18, doi: 10.1016/S0264-2751(98)00050-X.

[21] D. Walentek, "Datafication Process in the Concept of Smart Cities", *Energies*, vol. 14, issue 16, doi: 10.3390/en14164861.

[22] G. Verhulsdonck, J. Weible, S. Helser, N. Hajduk, "Smart Cities, Playable Cities, and Cybersecurity: A Systematic Review", *International Journal of Human-Computer Interaction*, 10.1080/10447318.2021.2012381.

[23] A. Alibasic, R. Junaibi, Z. Aung, W. Woon, M. Omar, "Cybersecurity for Smart Cities: A Brief Review", *Data Analytics for Renewable Energy Integration*, vol. 10097, 2017, pp. 22-30, doi: 10.1007/978-3-319-50947-1_3.

[24] A. Gyrard and M. Serrano, "A Unified Semantic Engine for Internet of Things and Smart Cities: From Sensor Data to End-Users Applications", *IEEE International Conference on Data Science and Data Intensive Systems*, Dec. 11-13, 2015, Sydney, Australia, pp. 718-725, doi: 10.1109/DSDIS.2015.59.

[25] V. K. Akram, M. Challenger, "Connectivity Maintenance in IoT-based Mobile networks: Approaches and Challenges", *Position and Communication Paper of the 16th Conference on Computer Science and Intelligence System*, vol. 26, pp. 145-149, doi: 10.15439/2021F102.

[26] L. Patton, "Kantian Essentialism in the Metaphysical Foundations", *The Monist*, vol. 100, 2017, pp. 342-356, doi: 10.1093/monist/onx014.

[27] A. Damianou, C. Ek, L. Boorman, N. Lawrence and T. Prescott, "A top-down approach for a synthetic autobiographical memory system", *Lecture Notes in Artificial Intelligence*, vol. 9222, pp. 280-292, doi: 10.1007/978-3-319-22979-9_28.

[28] C. Connon, "Approaches to corneal tissue engineering: top-down or bottom-up?", *Procedia Engineering*, vol. 110, 2015, pp. 15-20, doi: 10.1016/j.proeng.2015.07.004.

[29] Oxford Learner's Dictionaries, https://www.oxfordlearnersdictionaries.com/definition/american_english/top-down (accessed on 1. April 2022).

[30] P. Jones, "Marine protected areas in the UK: challenges in combining top-down and bottom-up approaches to governance", *Environmental Conservation*, vol. 39(3), 2012, pp. 248-258, doi: 10.1017/S0376892912000136.

[31] F. Cugurullo, "Exposing smart cities and eco-cities: Frankenstein urbanism and the sustainability challenges of the experimental city", *Environment and Planning A: Economy and Space*, vol. 50(1), 2018, pp. 73–92, doi: 10.1177/0308518X17738535.

[32] R. G. Hollands, "Critical interventions into the corporate smart city", *Cambridge Journal of Regions, Economy and Society*, vol. 8(1), 2015, pp. 61-77, doi: 10.1093/cjres/rsu011.

[33] Smart Taipei, https://smartcity.taipei/ (accessed on 1. April 2022).

[34] P. Thakuriah, L. Dirks and Y. M. Keita, "Digital infomediaries and civic hacking in emerging urban data initiatives", in: *Seeing cities through Big data,* P. Thakuriah, N. Tilahun, & M. Zellner (Eds.), Cham: Springer, 2017, pp. 189–207.

[35] S. Niederer and R. Priester, "Smart citizens: Exploring the tools of the urban bottom-up movement", *Computer Supported Cooperative Work (CSCW)*, vol. 25(2–3), 2016, pp. 137–152, doi: 10.1007/s10606-016-9249-6.

[36] Global Organisation of Smart Cities, https://www.citiesgosmart.org/publications (accessed on 25. March 2022).

[37] Departament of Information Technology Taipei City, https://smartcity.taipei/download/26/0 (accessed on 25. March 2022).

[38] Smart City Index 2022, https://www.imd.org/smart-city-observatory/home/ (accessed on 29. March 2022).

[39] Smart City Summit & Expo, https://en.smartcity.org.tw/index.php/en-us/ (accessed on 29. March 2022).

[40] L. Chen-Yu, *City Lights: Dr Chen-Yu Lee, Director, Taipei Smart City Project Management Office*, available: https://www.smartcitiesworld.net/city-lights/city-lights/city-lights-dr-chen-yu-lee-director-taipei-smart-city-project-management-office-4982 (accessed on 6. April 2022).

[41] Taipei City Government, Department of Information Technology, *Smart Taipei. Government as a Platform. City as a Living Lab*, available: https://smartcity.taipei/downloaddetail/2 (accessed on 6. April 2022).

Software, System and Service Engineering

THE S3E track emphasizes the issues relevant to developing and maintaining software systems that behave reliably, efficiently and effectively. This track investigates both established traditional approaches and modern emerging approaches to large software production and evolution.

For decades, it is still an open question in software industry, how to provide fast and effective software process and software services, and how to come to the software systems, embedded systems, autonomous systems, or cyber-physical systems that will address the open issue of supporting information management process in many, particularly complex organization systems. Even more, it is a hot issue how to provide a synergy between systems in common and software services as mandatory component of each modern organization, particularly in terms of IoT, Big Data, and Industry 4.0 paradigms.

In recent years, we are the witnesses of great movements in the area of software, system and service engineering (S3E). Such movements are both of technological and methodological nature. By this, today we have a huge selection of various technologies, tools, and methods in S3E as a discipline that helps in a support of the whole information life cycle in organization systems. Despite that, one of the hot issues in practice is still how to effectively develop and maintain complex systems from various aspects, particularly when software components are crucial for addressing declared system goals, and their successful operation. It seems that nowadays we have great theoretical potentials for application of new and more effective approaches in S3E. However, it is more likely that real deployment of such approaches in industry practice is far behind their theoretical potentials.

The main goal of Track 5 is to address open questions and real potentials for various applications of modern approaches and technologies in S3E so as to develop and implement effective software services in a support of information management and system engineering. We intend to address interdisciplinary character of a set of theories, methodologies, processes, architectures, and technologies in disciplines such as: Software Engineering Methods, Techniques, and Technologies, Cyber-Physical Systems, Lean and Agile Software Development, Design of Multimedia and Interaction Systems, Model Driven Approaches in System Development, Development of Effective Software Services and Intelligent Systems, as well as applications in various problem domains. We invite researchers from all over the world who will present their contributions, interdisciplinary approaches or case studies related to modern approaches in S3E. We express an interest in gathering scientists and practitioners interested in applying these disciplines in industry sector, as well as public and government sectors, such as healthcare, education, or security services. Experts from all sectors are welcomed.

TOPICS

Submissions to S3E are expected from, but not limited to the following topics:

- Advanced methodology approaches in S3E – new research and development issues
- Advanced S3E Process Models
- Applications of S3E in various problem domains – problems and lessons learned
- Applications of S3E in Lean Production and Lean Software Development
- Total Quality Management and Standardization for S3E
- Artificial Intelligence and Machine Learning methods in advancing S3E approaches
- S3E for Information and Business Intelligence Systems
- S3E for Embedded, Agent, Intelligent, Autonomous, and Cyber-Physical Systems
- S3E for Design of Multimedia and Interaction Systems
- S3E with User Experience and Interaction Design Methods
- S3E with Big Data and Data Science methods
- S3E with Blockchain and IoT Systems
- S3E for Cloud and Service-Oriented Systems
- S3E for Smart Data, Smart Products, and Smart Services World
- S3E in Digital Transformation
- Cyber-Physical Systems (9^{th} Workshop IWCPS-9)
- Model Driven Approaches in System Development (7th Workshop MDASD'22)
- Software Engineering (42^{th} IEEE Workshop SEW-42)

TRACK CHAIRS

- **Luković, Ivan,** Unniversity of Belgrade, Serbia
- **Kardas, ,** Geylani, Ege University International Computer Institute, Turkey

PROGRAM CHAIRS

- **Bowen, Jonathan,** Museophile Ltd., United Kingdom
- **Hinchey, Mike**(Lead Chair), Lero-the Irish Software Engineering Research Centre, Ireland
- **Szmuc, Tomasz,** AGH University of Science and Technology, Poland
- **Zalewski, Janusz,** Florida Gulf Coast University, United States
- **Seyed Hossein Haeri, ,** IOG and University of Bergen, Norway

PROGRAM COMMITTEE

- **Ahmad, Muhammad Ovais,** Karlstad University, Sweden
- **Challenger, Moharram,** University of Antwerp, Belgium
- **Dejanović, Igor,** Faculty of Technical Sciences, University of Novi Sad, Serbia
- **Derezinska, Anna,** Institute of Computer Science, Warsaw University of Technology, Poland
- **Dutta, Arpita,** National University of Singapore
- **Erata, Ferhat,** Yale University, USA
- **Escalona, M.J.,** University of Seville, Spain
- **Essebaa, Imane,** Faculté des Sciences et Techniques Mohammedia, Morocco
- **García-Mireles, Gabriel,** Universidad de Sonora, Mexico
- **Göknil, Arda,** SINTEF Digital, Norway
- **Hanslo, Ridewaan,** University of Pretoria, South Africa
- **Jarzebowicz, Aleksander,** Gdansk University of Technology, Poland
- **Kaloyanova, Kalinka,** University of Sofia, Bulgaria
- **Katic, Marija,** University of London, United Kingdom
- **Khlif, Wiem,** FSEGS, Tunisia
- **Kolukısa Tarhan, Ayça,** Hacettepe University, Turkey
- **Krdzavac, Nenad,** University of Belgrade, Serbia
- **Marcinkowski, Bartosz,** University of Gdansk, Poland
- **Milašinović, Boris,** Faculty of Electrical Engineering, University of Zagreb, Croatia
- **Milosavljevic, Gordana,** Faculty of Technical Sciences, University of Novi Sad, Serbia
- **Misra, Sanjay,** Ostfold University, Norway
- **Morales Trujillo, Miguel Ehécatl,** University of Canterbury, New Zealand
- **Ozkan, Necmettin,** Kuveyt Turk Participation Bank
- **Ozkaya, Mert,** Istanbul Kemerburgaz University, Turkey
- **Ristic, Sonja,** Faculty of Technical Sciences, University of Novi Sad, Serbia
- **Rossi, Bruno,** Masaryk University, Czech Republic
- **Sanden, Bo,** Colorado Technical University, USA
- **Sierra, Jose Luis,** Universidad Complutense de Madrid, Spain
- **Torrecilla-Salinas, Carlos,** IWT2
- **Varanda Pereira, Maria João,** Instituto Politécnico de Bragança, Portugal
- **Vescoukis, Vassilios,** National Technical University of Athens, Greece

Advances in Software, System and Service Engineering

THE S3E track emphasizes the issues relevant to developing and maintaining software systems that behave reliably, efficiently and effectively. This track investigates both established traditional approaches and modern emerging approaches to large software production and evolution.

For decades, it is still an open question in software industry, how to provide fast and effective software process and software services, and how to come to the software systems, embedded systems, autonomous systems, or cyber-physical systems that will address the open issue of supporting information management process in many, particularly complex organization systems. Even more, it is a hot issue how to provide a synergy between systems in common and software services as mandatory component of each modern organization, particularly in terms of IoT, Big Data, and Industry 4.0 paradigms.

In recent years, we are the witnesses of great movements in the area of software, system and service engineering (S3E). Such movements are both of technological and methodological nature. By this, today we have a huge selection of various technologies, tools, and methods in S3E as a discipline that helps in a support of the whole information life cycle in organization systems. Despite that, one of the hot issues in practice is still how to effectively develop and maintain complex systems from various aspects, particularly when software components are crucial for addressing declared system goals, and their successful operation. It seems that nowadays we have great theoretical potentials for application of new and more effective approaches in S3E. However, it is more likely that real deployment of such approaches in industry practice is far behind their theoretical potentials.

The main goal of Track 5 is to address open questions and real potentials for various applications of modern approaches and technologies in S3E so as to develop and implement effective software services in a support of information management and system engineering. We intend to address interdisciplinary character of a set of theories, methodologies, processes, architectures, and technologies in disciplines such as: Software Engineering Methods, Techniques, and Technologies, Cyber-Physical Systems, Lean and Agile Software Development, Design of Multimedia and Interaction Systems, Model Driven Approaches in System Development, Development of Effective Software Services and Intelligent Systems, as well as applications in various problem domains. We invite researchers from all over the world who will present their contributions, interdisciplinary approaches or case studies related to modern approaches in S3E. We express an interest in gathering scientists and practitioners interested in applying these disciplines in industry sector, as well as public and government sectors, such as healthcare, education, or security services. Experts from all sectors are welcomed.

TOPICS

Submissions to S3E are expected from, but not limited to the following topics:

- Advanced methodology approaches in S3E – new research and development issues
- Advanced S3E Process Models
- Applications of S3E in various problem domains – problems and lessons learned
- Applications of S3E in Lean Production and Lean Software Development
- Total Quality Management and Standardization for S3E
- Artificial Intelligence and Machine Learning methods in advancing S3E approaches
- S3E for Information and Business Intelligence Systems
- S3E for Embedded, Agent, Intelligent, Autonomous, and Cyber-Physical Systems
- S3E for Design of Multimedia and Interaction Systems
- S3E with User Experience and Interaction Design Methods
- S3E with Big Data and Data Science methods
- S3E with Blockchain and IoT Systems
- S3E for Cloud and Service-Oriented Systems
- S3E for Smart Data, Smart Products, and Smart Services World
- S3E in Digital Transformation
- Cyber-Physical Systems (9^{th} Workshop IWCPS-9)
- Model Driven Approaches in System Development (7th Workshop MDASD'22)
- Software Engineering (42^{th} IEEE Workshop SEW-42)

TRACK CHAIRS

- **Luković, Ivan,** Unniversity of Belgrade, Serbia
- **Kardas, ,** Geylani, Ege University International Computer Institute, Turkey

PROGRAM CHAIRS

- **Bowen, Jonathan,** Museophile Ltd., United Kingdom
- **Hinchey, Mike**(Lead Chair), Lero-the Irish Software Engineering Research Centre, Ireland
- **Szmuc, Tomasz,** AGH University of Science and Technology, Poland

- **Zalewski, Janusz,** Florida Gulf Coast University, United States
- **Seyed Hossein Haeri, ,** IOG and University of Bergen, Norway

PROGRAM COMMITTEE

- **Ahmad, Muhammad Ovais,** Karlstad University, Sweden
- **Challenger, Moharram,** University of Antwerp, Belgium
- **Dejanović, Igor,** Faculty of Technical Sciences, University of Novi Sad, Serbia
- **Derezinska, Anna,** Institute of Computer Science, Warsaw University of Technology, Poland
- **Dutta, Arpita,** National University of Singapore
- **Erata, Ferhat,** Yale University, USA
- **Escalona, M.J.,** University of Seville, Spain
- **Essebaa, Imane,** Faculté des Sciences et Techniques Mohammedia, Morocco
- **García-Mireles, Gabriel,** Universidad de Sonora, Mexico
- **Göknil, Arda,** SINTEF Digital, Norway
- **Hanslo, Ridewaan,** University of Pretoria, South Africa
- **Jarzebowicz, Aleksander,** Gdansk University of Technology, Poland
- **Kaloyanova, Kalinka,** University of Sofia, Bulgaria
- **Katic, Marija,** University of London, United Kingdom
- **Khlif, Wiem,** FSEGS, Tunisia
- **Kolukısa Tarhan, Ayça,** Hacettepe University, Turkey
- **Krdzavac, Nenad,** University of Belgrade, Serbia
- **Marcinkowski, Bartosz,** University of Gdansk, Poland
- **Milašinović, Boris,** Faculty of Electrical Engineering, University of Zagreb, Croatia
- **Milosavljevic, Gordana,** Faculty of Technical Sciences, University of Novi Sad, Serbia
- **Misra, Sanjay,** Ostfold University, Norway
- **Morales Trujillo, Miguel Ehécatl,** University of Canterbury, New Zealand
- **Ozkan, Necmettin,** Kuveyt Turk Participation Bank
- **Ozkaya, Mert,** Istanbul Kemerburgaz University, Turkey
- **Ristic, Sonja,** Faculty of Technical Sciences, University of Novi Sad, Serbia
- **Rossi, Bruno,** Masaryk University, Czech Republic
- **Sanden, Bo,** Colorado Technical University, USA
- **Sierra, Jose Luis,** Universidad Complutense de Madrid, Spain
- **Torrecilla-Salinas, Carlos,** IWT2
- **Varanda Pereira, Maria João,** Instituto Politécnico de Bragança, Portugal
- **Vescoukis, Vassilios,** National Technical University of Athens, Greece

Communication Papers of the of the 17th Conference on Computer Science and Intelligence Systems pp. 305–312
DOI: 10.15439/2022F7
ISSN 2300-5963 ACSIS, Vol. 32

Component Interface Standardization in Robotic Systems

1st Anton Hristozov
Polytechnic Institute
Purdue University
West Lafayette, Indiana, USA
ahristoz@purdue.edu

2nd Dr. Eric Matson
Polytechnic Institute
Purdue University
West Lafayette, Indiana, USA
ematson@purdue.edu

3rd Dr. Eric Dietz
Polytechnic Institute
Purdue University
West Lafayette, Indiana, USA
jedietz@purdue.edu

4th Dr. Marcus Rogers
Polytechnic Institute
Purdue University
West Lafayette, Indiana, USA
rogersmk@purdue.edu

***Abstract*—Components are heavily used in software systems, including robotic systems. The growth in sophistication and diversity of new capabilities for robotic systems presents new challenges to their architectures. Their complexity is growing exponentially with the advent of AI, smart sensors, and the complex tasks they have to accomplish. Such complexity requires a more flexible approach to creating, using, and interoperability of software components. The issue is exacerbated because robotic systems increasingly rely on third-party components for specific functions. In order to achieve this kind of interoperability, including dynamic component replacement, we need a way to standardize their interfaces. We desperately need a formal approach for specifying what an interface of a robotic software component should contain. This study analyzes the issue and presents a universal and generic approach to standardizing component interfaces for robotic systems. Our approach is inspired and influenced by well-established robotic architectures such as ROS, PX4, and Ardupilot. The study also applies to other software systems with similar characteristics to robotic systems. We consider using JSON or Domain-Specific Languages (DSL) development with tools such as Antlr or Xtext and automatic code and configuration files generation for frameworks such as ROS and PX4. A case study with ROS2 has been done as a proof of concept for the proposed methodology.**

***Index Terms*—CPS, robots, software architecture, interface, ROS, autopilot**

I. Introduction

COMPONENT interfaces have functional and non-functional parts [1]. Functional characteristics are the ones that usually receive the most attention and are considered most important. These characteristics cannot be completely independent of the overall architecture [2], and in this work, we concentrate on systems that use popular architectural paradigms such as ROS [3]. Having interfaces in explicit form is very important for analyzing and achieving component replacement and maintenance during run-time for maintenance or other objectives such as adaptation. They are important during development, too, when software components are given to third parties or bought from other organizations. Many systems do not have their interfaces presented in an explicit form in one central place. Their interfaces are dispersed in text configuration files and source code and are implicit rather than explicit, making their understanding and analysis more difficult. This is the case for systems we studied, such as ROS, PX4, and Ardupilot, as typical representative systems from the robotic field.

A. The need for standardization of robotic interfaces

Robotic systems have had typically different forms of custom implementations until recently. This has been steadily changing in the last decade, and robotic architectures are becoming more consistent and based on existing frameworks. Even when they are based on architectures such as Autosar [4] though they still do not offer a consistent model for providing interfaces for components that can become interoperable within the architecture or even between different architectures. This creates a need for a universal and consistent proposal for interface specification that can be complete and expressive and bring us closer to better interoperability among vendors of software components. This can also help us reach the possibility of better component reuse and system evolution.

In this paper, a general representation of component interfaces is proposed. The main contribution is defining a universal interface specification for software components applicable to components used in robotic systems. Another contribution is using a DSL to represent such interfaces and compare them and generate code and configuration files for different architectures. The applicability of the idea is demonstrated through a case study in ROS.

The following two sections talk about possible structural representations of interfaces through JSON and a DSL. The component interface standardization section proposes a universal interface representation and its constituent parts. The dynamic component management section defines the conditions for component interfaces to be compatible. An example is shown based on an extension of the Thrift IDL grammar. Furthermore, a case study with ROS illustrates the approach for a modern robotics framework.

B. Publish-subscribe robotic systems

Today, many robotic systems use an asynchronous architecture for message delivery based on the publish-subscribe paradigm. An example is PX4 [5] and ROS [6]. These systems are easier to use and provide many benefits for quickly adding new interfaces and components through a loosely coupled architecture. We believe that the interface standardization we

are presenting in this work will be used in a system that uses either a publish-subscribe broker or a similar message delivery mechanism. This decision is also based on the fact that publish-subscribe is common in other autopilot software systems, for example, Ardupilot. The central capability in this paradigm is that we can have software components publish topics or subscribe to topics making an arbitrary graph of connections between the components in the architecture. In this respect, we have a many-to-many relationship between components which can also be supported dynamically by components subscribing to messages at different times or advertising messages that they will publish later. This enables the possibility of adding new components at run-time and removing obsolete components, given that we follow specific rules.

C. ROS interfaces

We will focus our ROS investigations on ROS2, which is the latest version of the framework. ROS2 has been improved compared to ROS1 and is holding new promise for the future of robotics [3]. The improvements in how the system is configured and its real-time characteristics will allow new classes of applications to be possible. In addition to messages and services, ROS2 includes the concept of actions that are particularly applicable to robots in addition to messages and services. Therefore the three most essential features that ROS supports are messages, services, and actions. They are strongly related to how an interface can be described and used in our interface formulation in the next section. These interfaces can be used to achieve dynamic component exchange during run-time as part of the pursuit of fault-tolerant systems and systems that can adapt to changing conditions [7].

II. Component Interface Standardization

It is necessary to create a framework of components that can be interchangeable and compatible in a particular architecture or even between architectures. We aim to derive a comprehensive interface standardization that describes the component's interfaces. This standardization does not deal with the timing and memory characteristics of the component, which is essential but will not be addressed in this work.

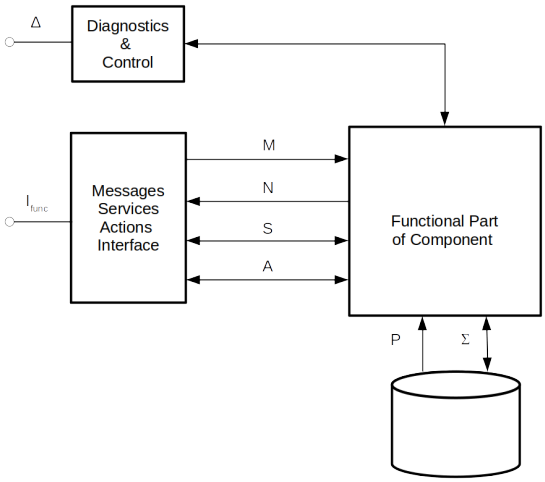

Fig. 1. Interface Standardization Diagram

Figure 1 depicts how a typical component's interface in a robotic system should look. The diagnostics portion is shown as a separate box as it can be a separate thread of execution and possess an interface Δ dedicated to diagnostics. The configuration parameters P and the component's state Σ use nonvolatile storage. The incoming messages M and outgoing N and service S and actions A are how the component communicates with other components in the system.

An interface I is a heterogeneous set formed by the union of several sets. The set I describes all common characteristics for robotic systems and even other software systems' components. Our generalization of an interface for any component is defined by equation 1.

$$I = M \cup N \cup S \cup A \cup P \cup \Sigma \cup \Delta \tag{1}$$

, where I is the interface of a component,
M is the set of subscribed messages
N is the set of published messages
S is the set of services
A is the set of actions
P is the set of configuration parameters
Σ is the set of state variables
Δ is the set of diagnostics services

A. Messages

The publish-subscribe paradigm allows many components to subscribe to any published messages. We consider two main types of messages in our analysis in a publish-subscribe model [8] or in a general case of a system using messaging. In our equation, the first set denoted as M is the set of messages the component subscribes to. The other set of messages is the messages N that the component publishes for other components to receive. We assume that the relationship is many to many with regards to both sets, and any component can subscribe to any messages and publish any messages that any other component can receive [5]. The dispatching of messages is typically handled by a message broker component that

performs the necessary bookkeeping and queuing to ensure delivery.

B. Services

Services are based on client-server interactions of one component making a service call and another component servicing this call. The client component blocks until the service finishes executing. Then the result is returned. Services can be characterized by parameters sent and results returned to the caller. The timing of services will not be part of the interface specification in this work. We concentrate on the parameters and results and assume that the service always completes with a result returned to the caller in a finite time.

C. Actions

Actions are particularly useful for some robotic operations and are supported in ROS2 [9]. This includes operations that are started, monitored, and getting a notification when the goal is reached. This allows the requester of the action to do something else while the action continues while receiving notifications asynchronously from the executor of the action. They are using messages and services to accomplish the action and thus provide a more complicated interaction and are suitable for tasks that need to continually send feedback to the client of the action. They have a goal defined as a service, feedback messages periodically sent from the action server to the client, and a result defined as another service. This ROS2 model is general enough for defining actions that can be used in many practical scenarios.

D. Configuration Parameters

The set of configuration parameters is used to configure a component at startup during the initialization process. They provide initial values for variables and constants used in the component during its lifetime. Typically these values come from a configuration file or are embedded in the source code. The parameters determine the initial state of the component and its operation. That is why they need to be part of the full interface description. A universal approach to configuration parameters is to keep them out of the source code in the form of a configuration file, preferably in a structured fashion. A possible structured format can be XML, JSON, or even some custom configuration language format.

E. State

Almost every component has some state that continually changes as the component operates as part of the system. Describing the component's state allows us to build tools that can save and recover it when needed. This is especially important when new components replace old ones while the system works. The state needs to be captured in a language-neutral form since different components may have different implementations using different technologies and languages. State variables with complex data types can be saved and retrieved using serialization and deserialization techniques. This makes it possible to restore precisely the state of every variable in a component, independently of how complex its type is. The description of a component's state at a particular point makes it transparent and can lead to new possibilities where a new component can pick up work that an old component has started without interrupting the flow of operations in a complex system. This can be a considerable advantage in architectures where the system cannot be halted and needs to be incrementally upgraded.

F. Diagnostics and Control

For a component to be useful in software architecture, it is good to have a self-diagnostics section with a well-defined interface. It makes sense to have the diagnostics work in an independent thread of execution so that it does not interfere with the main execution thread of the component. This way, other components can send queries and commands to a running component without affecting its main thread of execution. Having a separate thread for diagnostics makes it practical to have diagnostics services that can block in the requesting client and wait for a response from the diagnostics thread. This part of the interface can also be used to control a component's state, for example, running, ready, and others. Having this ability can allow the user to stop a component, save its state, load another component in its place and switch them. This adds additional non-functional abilities that can lead to many exciting scenarios.

The diagnostics and control interface should allow for control of the internal state machine of a component. If a component is in the middle of an operation that cannot be interrupted, a request to this interface can request a pause of the activities when the current operation is done. This way, we can have the notion of work transactions that cannot be interrupted and can have the opportunity to stop the component, save its state and then can unload it and load a replacement component using the saved state to continue. The approach of controlling the state machine of a component provides flexibility since we want to allow for operations to reach a steady state and results to be published before we perform any dynamic reconfiguration action in the system [10] [11].

G. Contracts in Component Interfaces

The software contract paradigm has been popular for a long time. In most cases, though, the focus has been to look at contracts in the scope of classes and functions [12]. This is appropriate for object-oriented systems and relations inside a component but is not universal for components that use different languages and are integrated based on their interfaces. There is a way to relate the software contract approach with component interfaces [13]. Our approach to embedding assumptions and guarantees into the interface makes the notion of contracts possible for software components independently of their implementation.

$$C = (A, G) \tag{2}$$

The general representation of contracts can be given with equation 2 where A represents the assumptions and G the guarantees [14]. We can apply this definition to our notion of contracts and their relation to the general interface representation we propose. The sets of services S and actions A have assumptions and guarantees since they send requests and expect responses. The messages M we subscribe to can be assumptions, and the messages N we publish are the guarantees that we promise to fulfill. The diagnostics interface also has assumptions in the interface Δ with the services it handles, and the guarantees are the responses to the user of this interface. Similarly, the configuration parameters P are only assumptions, and the state Σ has both assumptions and guarantees since we are saving and restoring it from external storage to the component. This mapping of contract obligations into the interfaces allows us to use the design by contract paradigm at the software component level.

III. Dynamic Component Management

Creating dynamically reconfigurable systems is challenging mainly because the interfaces of components are not explicitly defined. Most systems have a static architecture that does not allow for dynamic reconfiguration [15] without modifications. Systems based on publish-subscribe architectures can be extended, although many challenges need to be overcome. One of the really compelling challenges is to transfer the application state into the new instances of components from existing components [16]. This necessitates a well-defined interface that includes the description of the state. Dealing with state storage and retrieval assumes a mechanism that performs serialization and deserialization of state variables so that they are stored in nonvolatile memory.

Another challenge in dynamic reconfiguration is the impact of component replacement on the entire architecture. This effect can differ based on the component and its place in the architecture. One way to model this dependency is to create a graph where the nodes are the components, and the edges are the connections between them [17] [11]. Maintaining such a dynamic graph shows the components that can be affected by changes in a particular component. In the case of publish-subscribe, components are only coupled through messages, and this makes it easier to perform dynamic changes. This architecture of loosely coupled parts makes it easy to add and remove components at run-time. Messages are buffered by the message broker and are delivered to the component only when it is ready to retrieve them. We can also control the internal state of any component by using the diagnostics and control interface.

Another issue we have to consider for the management of components is the security of dynamically loaded components since they need to be trusted before being used [4]. The interface alone cannot solve the security, and other techniques need to be utilized. Adding some form of authentication may be needed to make sure the component can be trusted before it is loaded and run in the system. A dedicated component manager module is proposed in several works [18]. Some works propose a dedicated language for specifying component capabilities [19].

A. Interfaces and Their Role in Component Management

It is important to analyze when a new component can be a candidate for the replacement of an existing running component. Having an explicit and comprehensive interface is very important to accomplish this. We use set theory to formalize the interface definition and its constituent parts. If a component is a superset of another component, it can potentially replace it as shown in equation 3 where I_2 is the new component, and I_1 is the old component. Equation 3 is a necessary but not sufficient condition for a successful replacement.

$$\begin{aligned} I_1 &\subset I_2 \\ &or \\ M_1 &\subset M_2 \\ N_1 &\subset N_2 \\ S_1 &\subset S_2 \\ A_1 &\subset A_2 \\ P_1 &\subset P_2 \\ \Sigma_1 &\subset \Sigma_2 \\ \Delta_1 &\subset \Delta_2 \end{aligned} \tag{3}$$

A more precise definition of when a component is a successful candidate to replace another component is shown by equation 4. We show that all sets can be subsets of the new component sets, but only if the extra elements in the new sets are not used. Equation 4 can be further restricted to the equivalency case shown by equation 5 where the two components are equivalent. Equation 6 shows the conditions for equation 5 to hold true. We can consider that 6 provides a necessary and sufficient condition to achieve component compatibility. This means that all of the equivalence relationships in equation 6 should be true so that we can satisfy equation 5. The equivalence of each set in equation 5 means that they have identical number and type of elements.

$$\begin{aligned} M_1 \subset M_2, \text{ given } M_2 - M_1 \text{ is not used} \\ N_1 \subset N_2, \text{ given } N_2 - N_1 \text{ is not used} \\ S_1 \subset S_2, \text{ given } S_2 - S_1 \text{ is not used} \\ A_1 \subset A_2, \text{ given } A_2 - A_1 \text{ is not used} \\ P_1 \subset P_2, \text{ given } P_2 - P_1 \text{ is not used} \\ \Sigma_1 \subset \Sigma_2, \text{ given } \Sigma_2 - \Sigma_1 \text{ is not used} \\ \Delta_1 \subset \Delta_2, \text{ given } \Delta_2 - \Delta_1 \text{ is not used} \end{aligned} \tag{4}$$

$$I_1 \equiv I_2 \tag{5}$$

$$
\begin{aligned}
M_1 &\equiv M_2 \\
N_1 &\equiv N_2 \\
S_1 &\equiv S_2 \\
A_1 &\equiv A_2 \\
P_1 &\equiv P_2 \\
\Sigma_1 &\equiv \Sigma_2 \\
\Delta_1 &\equiv \Delta_2
\end{aligned} \tag{6}
$$

IV. Interface Representation using Json

One of the goals of capturing an interface formally is to be able to process it programmatically and make decisions at run time. Another goal is to have the interface in one place, for example, in a textual interface file. This is a significant step compared to having interfaces defined in source code and in multiple text files with different formats. There are many choices in selecting an approach for interface notation. One of them is to use formats like JSON, which is easy to parse and flexible enough for this task. A more ambitious possibility is to design a unique language to represent interfaces and have a parser that can analyze it automatically. For this study, we will use both approaches but will start with the JSON approach as our goal is to illustrate the content, not so much the format of the interface representation.

A JSON representation in a dedicated file can include all parts of an interface I in one place and keep the information in a structured form. JSON allows for the definition of complex types based on the common types, and this can be used when defining interfaces for real systems. One can use key-value pairs that define each data element's name and data type. Parsing such an interface file in JSON format becomes practical, and comparing components for their equivalence with regard to their interfaces becomes possible. One potential drawback is that the representation in this format can be rather verbose and tedious to create, but for the parsing, it really does not make a difference.

V. Domain Specific Languages for Interface Representation

Using a domain-specific language to represent an interface specification has many benefits. The main benefit is that the interface can be created using a textual language that has well-defined grammar. This textual representation has some benefits over a graphical language such as UML as it improves the formalization of the interface creation and forces users to comply with grammar rules and the associated tools that enforce them. A second benefit is that the parser can generate code and configuration files automatically while parsing the interface file. This can help automate the process of the software component creation, provide a more unified and automated approach, and reduce the margin of error, especially when different vendors do component development. Designing our DSL can be tailored to the needs of the systems. Having a language grammar imposes stricter interface specifications which makes any automation easier. The requirements we have defined for such a DSL are the following:

- to be able to represent all aspects of the component interface fully as shown in figure 1
- to be easy to read by humans
- to be in a structured format so that it can be parsed easily by automatic tools
- to be expandable in order to support future needs

A. Development Approach

Domain-specific languages are becoming easier to create by using special tools that can create parsers. One such tool is Antlr [20] although one can use any other tool that they are familiar with. The generation of parsers that are created from an Antlr grammar file is possible in several languages such as Java and C++. The grammar files used by Antlr have a traditional BNF notation. The result is a working C++ or Java parser that can be used to parse a file that complies with the grammar. Adding new features to the language happens by modifying the grammar and regeneration of C++/Java files. Many existing grammars can be downloaded and adapted as per the user's needs. Alternatively, Xtext can be used as a newer tool for creating DSLs [21]. It provides a better set of tools for the task.

B. Code Generation

Components in different frameworks are defined differently for reasons such as what architecture and programming languages are used. Having an interface file in the form of a DSL makes it easier to add code and configuration files automatically. For example, in the case of ROS, all services are created as .srv files in a folder with the name srv. Similarly, actions are in a folder with a file for each action with an .action extension. Messages are in a msg folder with a file for each message with .msg extension. All these files can be easily generated from a single interface file.

The concept of code generation can be extended to more than one platform. For example, PX4 also has msg files but does not support srv and actions, and the declarations for message topics follow a standard pattern that exists in the C++ code. This boilerplate code can be easily generated from the interface representation in a DSL. The parsing and validation of the syntax of the interface is an independent step that a target-specific code generation can follow that users can add for their specific platforms. This approach looks practical for systems with well-defined architectural patterns such as ROS, PX4, and Ardupilot.

C. Example DSL Grammar

Developing a proprietary DSL may be a time-consuming task. A practical approach is to start with an existing Antlr grammar and enhance it if needed. There are different possibilities to use. One option is to use the Apache Thrift grammar as a well-established interface definition language(IDL) [22]. Thrift already has the options to create structures and services sufficient for what is needed when creating an interface. An

equivalent interface to our earlier example is shown using the enhanced syntax based on Apache Thrift grammar, giving us a new DSL grammar in Listing 1. Using Thrift-like language

Listing 1 DSL Example Component Interface File

```
message message1 {
   string str,
   i16 i
}
message message2 {
   string str,
   float f
}
service service1 {
   string str,
   i32 i,
   string result
}
service service2 {
   i32 i,
   float f
}
action action1 {
   i32 par1,
   string s,
   string r
}
action action2 {
   double par1,
   float par2,
   string f,
   i16 result
}
configuration params{
   string param1,
   i32 param2,
   float param3,
   double param4
}
state state_variables {
   float position,
   float velocity,
   float acceleration,
   string mode
}
service diagnostics{
   string result,
   i32 r,
   string cmd
}
```

is even more intuitive, more compact, and provides the benefit of starting with a grammar that is available as an open-source file. The example above shows that Thrift may be sufficient in most cases, although its grammar can be easily extended, and a new C++ or Java parser can be developed if needed by using Antlr. The best part of having a parser is that we can add code generation based on our interface file and thus improve and standardize the development process.

The original grammar had to be enhanced with the following sections to allow us to support: actions, messages, configuration, and state portions of the interface specification, as shown in Listing 2. This allows us to parse an interface file with all the earlier sections. The file parsing confirms that the interface conforms to the rules of the defined language. In addition, we can easily generate configuration files specific to a particular platform, for example, ROS.

Listing 2 Grammar Additions to Thrift

```
definition
: const_rule | typedef_ | enum_rule |
senum | struct_ | union_ |
exception_cpp | service | action |
configuration | message | state;

message
: 'message' IDENTIFIER
'{' field* '}' type_annotations?;

action
: 'action' IDENTIFIER
'{' field* '}' type_annotations?;

configuration
: 'configuration' IDENTIFIER
'{' field* '}' type_annotations?;

state
: 'state' IDENTIFIER
'{' field* '}' type_annotations?;
```

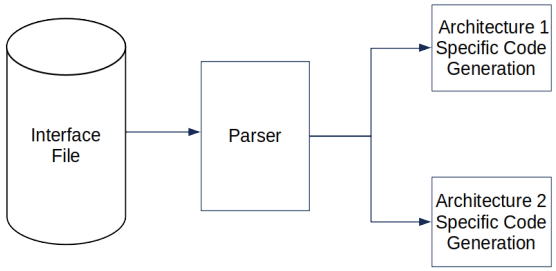

Fig. 2. Code Generation from Interface File

The code generation is shown in figure 2. The parser uses a listener or visitor pattern, allowing it to intercept each token

and make decisions based on what is necessary for the parsing logic. Since parsing is based on the grammar shown above, this is independent of the software architecture. On the other hand, the code generation portion depends on whether we need to create configuration files for ROS or for PX4, for example. The code generation architecture blocks can be added in the future depending on what new architectures need to be supported.

The most significant advantage of the formal interface design is that the interface allows for documentation of the component and for its comparison with other components with possible reuse and integration within an existing system. In addition to configuration files, we can generate code that reflects the interface design. Some systems have their interfaces in code instead of external configuration files, for example, PX4. Code generation is also applicable for the diagnostics section, where we can have a template code for diagnostics services. Even with boilerplate code generation, we will always need some manual code development.

D. Case Study with ROS

Our case study focused on how a ROS component can be represented consistently through an interface file. The prototype we developed aimed to parse the interface file and determine if it complies with the grammar of the IDL used, in this case, the Thrift-like derivative DSL we propose. Secondary, the parsing process generated configuration files for a ROS process automatically. These included message files, service files, and action files. We did not generate any source code since this is not part of the interface. The study showed that a parser could be used successfully for custom interface definition languages, and the sections of our interface standardization worked well in this experiment.

The advantages of representing the interfaces in the proposed way are that instead of using multiple files for different aspects of the interface and having some of them in the source code, we have moved the specification to a single textual file that can be parsed automatically by tools. This allows us to easily compare components from different vendors and to reason if they are compatible. Such analysis otherwise is pretty difficult and cannot be done automatically. The problem is exacerbated when components from different architectures are to be compared, where architectural specifics make the task even more difficult. The same methodology can be applied to different architectures, provided they have the same functional elements such as messages, services, and actions. The cost in time for parsing a component interface before it is loaded is not an issue. In fact, ROS does that in a more complicated manner because it has to parse multiple files and connect the data with the source code.

A promising future direction is to develop an architecture-specific tool that allows for a defined interface that can generate all the boilerplate code specific to that architecture. We described a possible implementation for ROS, but similarly, the code generation can be tailored to other systems that use different ways to represent their interfaces. This can help design components that need to be ported from one system to another. Reusing third-party components will only continue to increase, and ways to minimize efforts and introduce a common language can only help design new and expanding existing architectures.

VI. Conclusion

Interfaces represent components and their capabilities. Universally presenting them can make reuse possible and dynamic component reconfiguration at run-time and design-time. A viable first step in this direction is to formalize the representation of interfaces to make this representation easier to parse programmatically and to use as a basis for run-time architectural decisions. The presented standardization can be used in different architectures as it is pretty general and covers many component characteristics. It directly applies to systems that use ROS/ROS2 or even autopilots such as PX4 and Ardupilot. Our generic approach to defining interfaces for robotic systems can be used universally and help achieve better and more resilient architectures with new capabilities for reconfiguration and maintenance.

References

[1] O. Scheickl, M. Rudorfer, and C. Ainhauser, "How timing interfaces in autosar can improve distributed development of real-time software," *INFORMATIK 2008. Beherrschbare Systeme-dank Informatik. Band 2*, 2008.

[2] B. Y. Alkazemi, "A precise characterization of software component interfaces." *J. Softw.*, vol. 6, no. 3, pp. 349–365, 2011.

[3] I. Malavolta, G. Lewis, B. Schmerl, P. Lago, and D. Garlan, "How do you architect your robots? state of the practice and guidelines for ros-based systems," in *2020 IEEE/ACM 42nd International Conference on Software Engineering: Software Engineering in Practice (ICSE-SEIP)*, 2020, pp. 31–40.

[4] J. Axelsson and A. Kobetski, "On the conceptual design of a dynamic component model for reconfigurable autosar systems," *SIGBED Rev.*, vol. 10, no. 4, p. 45–48, dec 2013. [Online]. Available: https://doi.org/10.1145/2583687.2583698

[5] L. Meier, D. Honegger, and M. Pollefeys, "Px4: A node-based multithreaded open source robotics framework for deeply embedded platforms," in *2015 IEEE International Conference on Robotics and Automation (ICRA)*, 2015, pp. 6235–6240.

[6] M. Lauer, M. Amy, J.-C. Fabre, M. Roy, W. Excoffon, and M. Stoicescu, "Engineering adaptive fault-tolerance mechanisms for resilient computing on ros," in *2016 IEEE 17th International Symposium on High Assurance Systems Engineering (HASE)*, 2016, pp. 94–101.

[7] M. Lauer, M. Amy, J. Fabre, M. Roy, W. Excoffon, and M. Stoicescu, "Resilient computing on ros using adaptive fault tolerance," *Journal of Software: Evolution and Process*, vol. 30, 2018.

[8] P. T. Eugster, P. Felber, R. Guerraoui, and A.-M. Kermarrec, "The many faces of publish/subscribe," *ACM Comput. Surv.*, vol. 35, pp. 114–131, 2003.

[9] E. Erős, M. Dahl, K. Bengtsson, A. Hanna, and P. Falkman, "A ros2 based communication architecture for control in collaborative and intelligent automation systems," *Procedia Manufacturing*, vol. 38, pp. 349–357, 2019, 29th International Conference on Flexible Automation and Intelligent Manufacturing (FAIM 2019), June 24-28, 2019, Limerick, Ireland, Beyond Industry 4.0: Industrial Advances, Engineering Education and Intelligent Manufacturing. [Online]. Available: https://www.sciencedirect.com/science/article/pii/S2351978920300469

[10] N. T. Huynh, "An analysis view of component-based software architecture reconfiguration," 03 2019, pp. 1–6.

[11] A. Butting, R. Heim, O. Kautz, J. O. Ringert, B. Rumpe, and A. Wortmann, "A classification of dynamic reconfiguration in component and connector architecture description," in *MODELS*, 2017.

[12] G. T. Leavens and Y. Cheon, "Design by contract with jml," 2006.

[13] A. Beugnard, J.-M. Jezequel, N. Plouzeau, and D. Watkins, "Making components contract aware," *Computer*, vol. 32, no. 7, pp. 38–45, 1999.

[14] A. Sangiovanni-Vincentelli, W. Damm, and R. Passerone, "Taming dr. frankenstein: Contract-based design for cyber-physical systems," *European journal of control*, vol. 18, no. 3, pp. 217–238, 2012.

[15] D. de Leng and F. Heintz, "Dyknow: A dynamically reconfigurable stream reasoning framework as an extension to the robot operating system," in *2016 IEEE International Conference on Simulation, Modeling, and Programming for Autonomous Robots (SIMPAR)*, 2016, pp. 55–60.

[16] C. Cu, R. Culver, and Y. Zheng, "Dynamic architecture-implementation mapping for architecture-based runtime software adaptation." in *SEKE*, 2020, pp. 135–140.

[17] A. Saadi, M. C. Oussalah, Y. Hammal, and A. Henni, "An approach for the dynamic reconfiguration of software architecture," in *2018 International Conference on Applied Smart Systems (ICASS)*, 2018, pp. 1–6.

[18] S. Alhazbi and A. B. Jantan, "Safe runtime reconfiguration in component-based software systems," in *Software Engineering Research and Practice*, 2008.

[19] T. V. Batista, A. Joolia, and G. Coulson, "Managing dynamic reconfiguration in component-based systems," in *EWSA*, 2005.

[20] T. J. Parr and R. W. Quong, "Antlr: A predicated-ll(k) parser generator," *Softw. Pract. Exper.*, vol. 25, no. 7, p. 789–810, jul 1995. [Online]. Available: https://doi.org/10.1002/spe.4380250705

[21] M. Eysholdt and H. Behrens, "Xtext: Implement your language faster than the quick and dirty way," in *Proceedings of the ACM International Conference Companion on Object Oriented Programming Systems Languages and Applications Companion*, ser. OOPSLA '10. New York, NY, USA: Association for Computing Machinery, 2010, p. 307–309. [Online]. Available: https://doi.org/10.1145/1869542.1869625

[22] K. Grochowski, M. Breiter, and R. Nowak, "Serialization in object-oriented programming languages," in *Introduction to Data Science and Machine Learning*, K. Sud, P. Erdogmus, and S. Kadry, Eds. Rijeka: IntechOpen, 2020, ch. 12. [Online]. Available: https://doi.org/10.5772/intechopen.86917

Communication Papers of the of the 17th Conference on Computer Science and Intelligence Systems pp. 313–318
DOI: 10.15439/2022F171
ISSN 2300-5963 ACSIS, Vol. 32

A Data Analysis Study of Code Smells within Java Repositories

Noah Lambaria
Baylor University
One Bear Place #97141, Waco, USA
Email: Noah_Lambaria1@baylor.edu

Tomas Cerny
Baylor University
One Bear Place #97141, Waco, USA
Email: tomas_cerny@baylor.edu

***Abstract*—Although code smells are not categorized as a bug, the results can be long-lasting and decrease both maintainability and scalability of software projects. This paper presents findings from both former and current industry individuals, aiming to gauge their familiarity with such violations. Based on the feedback from these individuals, a collection of smells were extracted from a sample size of 100 Java repositories in order to validate some of the smells that are typically encountered. After analyzing these repositories, the smells typically encountered are *Long Statement*, *Magic Number*, and *Unutilized Abstraction*. The results of this study are applicable for developers and researchers who require insight on the frequencies of code smells within a typical repository.**

I. Introduction

THE term "code smell" dates back to the 1990s, where Kent Beck first defined the term. Martin Fowler was another individual responsible for popularizing the term within his book *Refactoring*, which addressed code smells with the application of Java examples [1]. Although many authors and researchers have defined an abundant amount of code smells, what is deemed to be a code smell or not is subjective and abstract. This is due to the vast variations of smells that exist, and what is considered to be a harmful and non-harmful smell. An example of a code smell that this study and future work aims to address is the *God Class*, as well as several other smells. Alves et al. mention that *God Classes* can be up to 13 times more likely to contain faults embedded within the smell itself [2]. For this reason, it is imperative to dive deeper within large classes and methods and examine their occurrences since these smells are detrimental. Our goal is to compare the frequencies of such smells compared to others with our selected tool, which will be elaborated on in further sections.

Evident in the works of Fontana et al., anti-patterns and code smells have the potential to impact Technical Debt (TD) and Architectural Degradation (AD) [3]. Their research suggested that some code anomalies were more inclined to be better indicators of TD than others. Because of instances such as these, code smells can be detrimental to software systems over the course of time. To resolve these conflicts, there are abundance of different static analyzers within the software community that assist code smell identification.

For these reasons, it is important to further examine the repercussions that code smells have, and what types of smells are common in code bases. Within these next couple of sections, we will be covering how we collected our data along with the results found based on the repositories examined. Before discussing our results, however, we want to highlight other works that have impacted our approach to our case study and rationale.

Through undertaking this study, there were many challenges we encountered. Firstly, we were unsure what static analyzers were available for Java that best fit our needs. Although there are many add-ons and plugins that assist developers in refactoring their code in common IDEs (Integrated development environment)s, we wanted to utilize a tool that was unrestricted to a specific extension. As further discussed in later sections, the accuracy of each tool can differ, which was why our goal was to find a tool that could provide extensive feedback on different smells. Thus, ensuring that false positives of particular smells proved to be concerning and a challenge. Our research challenge was to observe the frequency of the Long Method and God classes, comparing this data to related works that have highlighted the severity of smells such as these. Furthermore, we sought to determine how often they appear in repositories compared to other smells.

This paper is organized by discussing some similar studies and works that have been conducted in more recent years. We will then cover the prevalent smells we recorded out of the repositories examined, highlighting the frequency of each smells. These findings are beneficial to developers who are interested in our selected tool and the common implementation, design, and architectural smells that exist in popular Java libraries on GitHub. We also discuss potential validity concerns, and how we minimized and reduced potential risks while collecting and analyzing the data. Further studies need to be conducted to gain knowledge on various tools, which we will examine in our future work.

II. Related work

Many papers have aimed to better detect code smells within software. Within the work of Paiva et al. [4], researchers conducted comparison studies on various code smell tools.

This research was funded by National Science Foundation grant number 1854049 and a grant from Red Hat Research https://research.redhat.com

Their research suggests that each tool had a different amount of accuracy when identifying code smells such as *God Classes* or *God Methods*. The challenges of creating such tools with minimal inaccuracy is difficult, as some code smells could be erroneous or not be flagged properly.

Our selected code smell detection tool was *DesigniteJava* [1] [5]. Developed by Sharma et al., this particular tool is newer and provides a detailed assessment report about architectural, design, and implementation smells. Some of the naming conventions for each smell slightly differ, such as the terms *God Class* and *Insufficient modularization*, which are interchangeable for describing a class that can be further broken up to reduce complexity. These slightly differ from a *God Component*, which is an architectural smell that denotes an excessively large component (e.g., a package) that can be reduced or further broken up.

Further details associated with the definitions of each term (e.g. Unutilized abstraction, Deficient Encapsulation) can be found the works of Sharma et al. [6]. Although *Designite* supports the examination of C# code, we were most interested in Java projects only. The tool also offers more features and flexibility than other code smell detection tools such as *JDeodorant*.

JDeodorant, an Eclipse plug-in developed by Tsantalis et al. at Concordia University and the University of Macedonia [7], currently supports detection of 5 types of code smells at the time of this writing. Because of its dedication specifically to Java, it was a tool that was considered to be used for our selected repositories. However, the amount of time required to operate the tool on hundreds of repositories would be dramatically different due to DesigniteJava's flexibility and lack of limitations. This enables researchers the capability of creating scripts or programs to enhance the overall automation of collecting code smell results without the restriction and usage of Eclipse.

Another tool that has been used for code analsyis is *iPlasma*, which Marinescu et al. described [8]. This tool provides analysis of various metrics and can detect violations such as duplicate code. It is available in object-oriented languages such as C++ and Java.

Prior to this study, we asked ourselves what the pitfalls related to the current static analyzers and tools out there to detect various metrics were. Samarthyam, Suryanarayana, and Sharma mentioned some of the downsides to tools such as Sonargraph [9]. A non-exhaustive list of some of these worries were the following: lack of extensive support of architectural smells, lack of contextual information related to each smell, and limited availability of popular IDE (Integrated Development Environment) support for refactoring architectural smells [10]. While inspecting code smells, it is also important to filter out harmful and less severe smells. Highlighted in the upcoming sections, some of the uncertainties of these static analyzers are the filtering methods used along with the potential for false positive smells. In the works of Fontana et al. [11], they devised strong and weak filters which can be used to alleviate possible false positive instances. Furthermore, the strong filters proved to increase overall precision on detecting such smells.

[1]https://github.com/tushartushar/DesigniteJava

TABLE I
BRIEF OVERVIEW OF SOME OF THE SURVEY QUESTIONS ASKED

Question 2	On a scale from 1-5, how familiar are you with the term "code smells"?
Question 3	On a scale from 1 to 10, how often do you encounter violations within your software?
Question 6	Are you familiar with static code analyzers?
Question 7	If you answered "Yes" to the previous question, what types (or name) of tool(s) did/do you use to monitor violations (code smells) within your codebase/project?
Question 8	At your company, did you measure / use any kind of calculation to assess technical debt? (e.g., monthly reports on developer/cloud-usage cost/performance stats, etc.)
Question 9	At your company, did you use any visualization tool to assess technical debt? If so, how did you visualize it?
Question 10	Besides static code analyzers, how much time would you say you spent manually observing and inspecting code for violations per week?
Question 13	How much time did you typically spend refactoring code at your company, per week?

Similar case studies have been done in the past, such as in the writings of Sharma, Fragkoulis, and Spinellis, where they examined C# repositories in order to inform the reader about characteristics of code smells in C# code bases [6]. Their results showed that both the *Unutilized Abstraction* and *Magic Number* were the most frequently occurring smells in C# code [6]. Rather than selecting their repositories manually, they utilized *RepoReaper* [12] to gather their repositories. The overall findings are similar to our results, which will be further discussed in later sections.

III. PRACTITIONER SURVEY

Before data collection, we sought to identify the typical amount of time developers spend refactoring code and inspecting it for violations. A survey was created in order to gain insight from individual's experiences with code violations. This allowed us to attain an understanding on the currently adopted tools and how familiar the respondents were of code smells. A total of 14 questions were asked with initial questions pertaining to a generalization of technical debt and evaluating economical cost associated with it. Due to relevancy of the paper, those questions were omitted from the first table. The feedback was collected through google forms and served primarily as a basis for determining what tools were used to monitor code violations. A total of 14 individuals were surveyed and their feedback will be discussed in further sections.

Many surveys have been conducted in the past to accumulate feedback from software developers. An example of such is in the work of Yamashita and Moonen, where 85 software developers were surveyed to gain insight on their thoughts of code smells [13]. The results from this study showed that

32% of respondents had no prior knowledge of code smells. Furthermore, the most mentioned smells that were familiar to the developers were smells such as the *Large Class* and *Long Method*.

Another survey that has been conducted is evident in the works of Golubev et al. [14], where over 1100 individuals were surveyed in order to determine how often they spent refactoring code. Furthermore, they assessed how developers refactored their code. Their findings suggested that two-thirds of developers spent longer than an hour refactoring code for every instance spent working. They also found that 40.6% of developers refactored code almost every day [14].

Based on the tiny sample we collected from our survey, almost all respondents that are currently in the industry said that they spent less than 5 hours a week refactoring code. On the contrary, 70% of the respondents for the Graduate survey stated that they spent 5 hours of more a week refactoring code while they were in industry. Although further studies would need to be conducted, a possibility for this differentiation is that the Graduate students who opted to participate in the survey are newer developers or have not spent a lot of time in industry. Furthermore, these individuals could be a younger demographic that has not had an immense exposure as a software developer compared to their peers. As a result, it could take more time for those individuals to refactor code due to the lack of experience. Based on this minuscule sample-size however, much more research would need to be conducted for further evaluation and verification of the possibilities mentioned.

From the individuals surveyed, some tools utilized for code quality were SonarQube, JavaParser, and Jacoco. Others mentioned linters such as ESLint and golint to help improve the quality of production-based code while working with continuous integration pipelines. When asked whether or not there was any visualization tool used for assessing technical debt, all respondents from both surveys stated that they were unfamiliar such tools or did not employ any. For this reason, we sought tools that can be beneficial to developers, which are discussed in prior sections.

Code smells can take a lot of time to evaluate and identify. Because of the immense amount of allocated resources spent, researchers have attempted to alleviate the time spent refactoring by developing tools that can minimize the amount of time in identifying the smells to fix. This can impact the cost of the company as funds would be used for refactoring and fixing rather than innovation and enhancements, impacting profits over a long period of time.

IV. Proposed Method

A. Methodology

For this study, we gathered 100 repositories that were as close as possible to being fully written in Java due to the uncertainty of how DesigniteJava would perform. Another requirement we decided upon was that each repository contains at least 3000 lines of code for it to be considered. As mentioned in further sections, this was due to alleviating potential inconsistencies and ensuring that one particular smell would not be disproportionate to other smells. This particular minimum value was selected due to testing the tool with smaller repositories and discovering this value to be suitable and adequate for our sample size.

Most repositories examined were libraries and frameworks that were highly active and recommended when searching for repositories on GitHub. These repositories were chosen at random to prevent any biases. Each repository would also be thoroughly checked to ensure that no other languages would be scanned in by our chosen tool.

B. Data Extraction

Once validated and identified, the repositories are downloaded and unzipped. DesigniteJava is then utilized to generate an XML file, which can be read in by *QScored* [15]. Provided by Sharma et al., QScored agent is readily available for analyzing information from DesigniteJava and uploading it to QScored for a visual representation along with computing a raw score for the particular repository [15]. Our primary focus was extracting the data returned by the DesigniteJava output and parsing it to collect the summation of total smells within that particular repository as well as examining the number of instances of *God Classes or God Components* and *Long Methods* detected. For this reason, QScored was only used for initial testing to visualize some of the earlier repositories. It was also used for pinpointing files within each repository that had high levels of lines of code, which is beneficial for our future work. We tested out the feature and modified the sample python source code provided with a granted API key to see how simplistic it is to convert the XML file to a visual depiction on QScored.

To organize the data, a shell script was created for running each repository selected against DesigniteJava. This script also generated new sub-directories to store each file obtained by the tool for every repository examined. For each repository, the results were redirected from standard output and appended to one large result file. The name of the repository would also be appended subsequently after redirection occurred so that the data would have proper association for future parsing. After running the detection tool on all of the repositories, the result file would be parsed and sorted into manageable data using other programs. A majority of the original output data would be discarded and only the total lines of code, top two code smells recorded, and number of instances of particular smells for each repository would remain for the final data set. The smells that remained in our final data set were the following: *Long Method*, *Magic Number*, *Long Statement*, *God Components*, and *Unutilized Abstraction*. As further discussed in our results section, these were ultimately chosen as the remaining smells due to their popularity and sole focus of our research.

The data collected would then be easily transferable and converted to a readable format, such as an excel sheet or CSV file. The results of the study are an open data source and

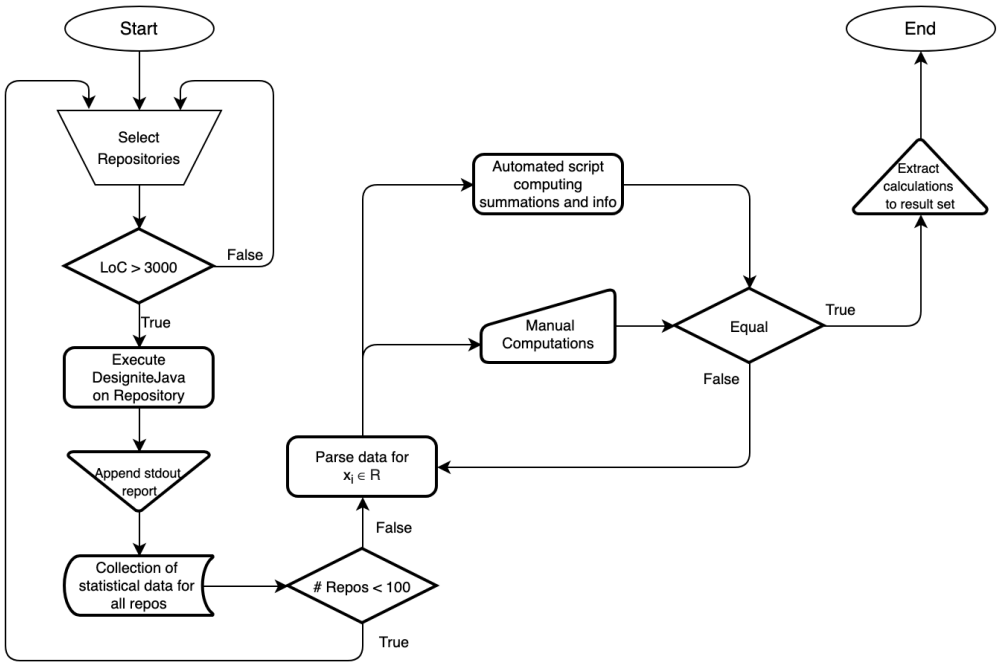

Fig. 1. Flowchart of our process

accessible through GitHub[2]. Our process for collecting the data is depicted in Figure 1, which entails each step conducted to obtain the final data set.

V. Case Study

A. Results

Prior studies have mentioned the prevalence of specific smells within software projects, however, our findings suggest that some smells such as the *Long Method* and *God Components* are fairly uncommon. Based on our results, the *Long Method* was documented for 0.144% of all methods scanned. The *Long Method* also only accounted for 0.255% of all smells collected, which is reasonably minuscule. This number was heavily impacted due to other code smells that seemed to be highly widespread. On the other hand, both the *Long Method* and *God Components* contain significantly more lines of code compared to others such as the *Magic Number*. Although they are not as prevalent, both smells still make up a significant portion of total lines of all smells. The *Magic Number* smell was one of the more common smells detected within the repositories, however, in most instances it can be omitted in real-world practices as a potential smell. It made up 48.357% of all code smells detected, making it substantial compared to other smells. The second most common smell was a *Long Statement*, which comprised of 21.425% of all smells. Both the *Magic Number* and *Long Statement* together appeared as the most common and second common code smell for 70.0% of all repositories.

[2]https://bit.ly/39L0iIH

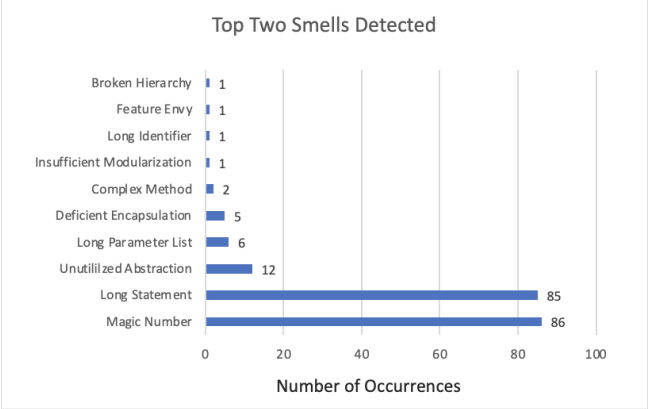

Fig. 2. Frequency of top two smells detected

TABLE II
Overall Averages of each Repository selected

Attribute	Average (AVG)
Number of Smells Detected	3924.04
Lines of Code (LoC)	59509.73
Number of Methods	6926

Some code smells are insignificant compared to others. To clarify, a few smells such as a *Magic Number* could be seen as appropriate or easily modifiable in specific instances compared to other smells that can have long-lasting effects and degrade the overall quality of the software. Because of instances where there could be valid solutions that require code segments to be

designed a particular way as well as many other factors, smells like these can be discarded under most circumstances. Other code smell that were flagged many times were *Unutilized Abstraction* and *Broken Hierarchy*. For *Unutilized Abstraction*, 6.654% of total code smells were devised of this violation. This particular smell was third most prevalent and relative to the top two smells, the overall percentage is substantially small. Out of the total lines of code analyzed, only 6.594% of all repositories contained violations. This ratio was calculated by computing the total number of smells in all 100 repositories, and divided by the total lines of code in each program. This is only an estimate, as some of the code smells could take several lines of code. The outcome was an expected result, as these libraries are likely maintained by experienced developers who practice good coding habits. Likewise, the developers are likely to follow these standards to ensure high scalability and to maintain their libraries efficiently.

From this study, we can confirm that similarly to C# code analyzed in Sharma et. al [6], that *Magic Number* and *Unutilized Abstraction* are both prevalent smells that are also common in Java repositories. Furthermore, we can conclude that the commonality between both *Long Statement* and *Magic Number* frequencies are significantly higher than other smells, which is depicted in Figure 2.

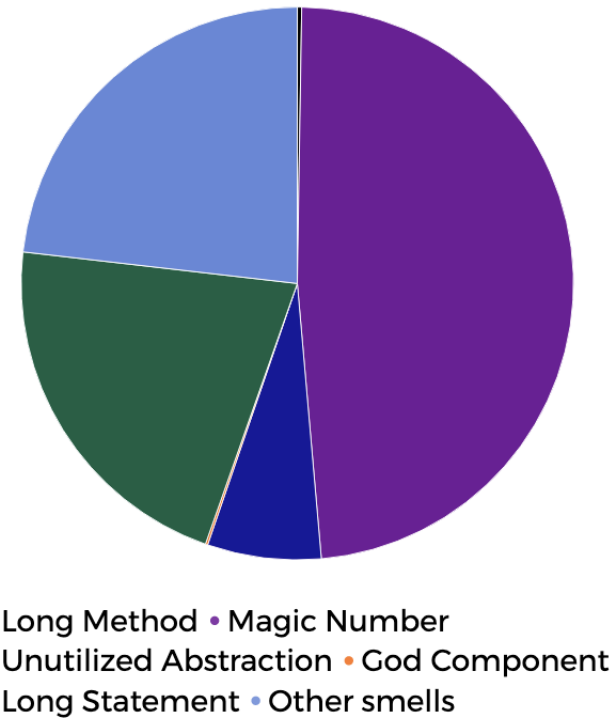

Fig. 3. Pie Chart displaying distribution percentages of particular smells out of all 100 repositories examined

B. Threats to Validity

1) Internal Validity: Bias in regards to data extraction could be a potential issue. Only Java projects were selected due to the limitations of DesigniteJava. Because of the restriction, different types of smells could potentially be more or less common in other languages. Although the data was validated through several automated checks, some of the smells were manually checked and computed. Specifically, all smells in our final data set were manually calculated.

To prevent any errors, these manual operations were compared with programs to validate that the summations equalled the summations calculated initially by hand and vice versa. In order to alleviate any potential conflicts, popular repositories from experienced developers that contained several thousands of lines of code were primarily selected to be analyzed. Because of the restrictions on the number of lines required, this removes the possibility of special cases where there could be an outlier of a particular code smell.

2) External Validity: A minor subset of individuals who were surveyed haven't been within the industry in the past couple years. To reduce these biases, the survey data was separated by those who are currently employed as a software developer, and those who recently departed from the industry, such as for Graduate School. Within the software field, new tools and technologies are rapidly evolving, which allow developers to spend significantly less time refactoring their code. As a result, these former developers could have potentially utilized outdated tools even if they have only been out of the industry for a few years, which could heavily impact the amount of time it takes to refactor code.

In regards to the repositories collected, the data extracted was reliant on the accuracy of the tool. Because of the tool being recently developed and not as widely used overall, DesigniteJava could pick up false positives of a particular smell. Conducting the study again with different static analyzers or other tools that detect code smells and comparing the results to the current data set would lessen the probability of inaccurate data. Furthermore, due to these popular repositories constantly changing with updates, the number of code smells for each repository could differ at the time of this writing.

VI. Future Work

As previously discussed, it would be beneficial to utilize these exact same repositories but with many tools to compare the rate of success and accuracy of each tool. A larger data set expanding the use of other languages would be advantageous to ensure that the most frequent smells identified within this study is widespread in other languages besides Java. Although Java and C# projects are compatible with our selected tool, further identification of analyzers that support other object-oriented languages such as Python or C++ need to be tested. This will allow for identifying potential relationships between different design, architectural, and implementation smells in contrary projects.

Because of the programs created and utilized as a result of this experiment, a data set with thousands of repositories can be applied under the same circumstances as the small selection of this case study at significant rate. The only limitation is the manual selection of each repository, since criteria must be met for every selected repository to ensure valid data collection.

For our future work, we plan to devise or identify software that will assist in fetching repositories, while adhering to our criteria. Some static analyzers only support specific languages and are potentially vulnerable to issues if conflicting files are also embedded in the same repository.

Our future work entails examining the code that was associated with the *Long Method* and *God Components* for the repositories selected, and running code smell detectors and analyzers on these sections of code. The results could potentially detect other embedded code smells within these particular smells, as well as a correlation between the creation of these oversized classes or methods. Furthermore, many tools would be utilized, ensuring that a wide range of smells are fetched from each repository.

VII. Conclusions

Based on the repositories examined, the *Long Method*, *God Components* and other architectural and design smells are typically not as detected in well-developed Java repositories compared to other code smells. The most common smells recorded were the *Long Statement* and *Magic Number*, accounting for 69.782% of all smells recorded within the chosen repositories. The *Long Method* was recorded for 0.144% of all methods in the repositories selected. It also only accounted for 0.255% of all total smells analyzed. Although insignificant smells such as the *Magic Number* disproportionately impacted other smells' percentage weight, if this smell was omitted, the *Long Method* would only slightly increase to 0.494% of all detected smells. Future studies will be conducted to gather a larger sample size and analyze the *God Components* and *Long Method* segments of code within each repository fetched. DesigniteJava is an extremely beneficial tool, which both researchers and those in industry can utilize to further evaluate production code and long-term maintainability.

Acknowledgments

This research was funded by National Science Foundation grant number 1854049 and a grant from Red Hat Research https://research.redhat.com

References

[1] M. Fowler, K. Beck, J. Brant, W. Opdyke, and D. Roberts, *Refactoring: Improving the Design of Existing Code*. USA: Addison-Wesley Longman Publishing Co., Inc., 1999.

[2] N. S. Alves, T. S. Mendes, M. G. de Mendonça, R. O. Spínola, F. Shull, and C. Seaman, "Identification and management of technical debt: A systematic mapping study," *Information and Software Technology*, vol. 70, pp. 100–121, 2016. [Online]. Available: https://www.sciencedirect.com/science/article/pii/S0950584915001743

[3] F. A. Fontana, V. Ferme, and M. Zanoni, "Towards assessing software architecture quality by exploiting code smell relations," in *2015 IEEE/ACM 2nd International Workshop on Software Architecture and Metrics*, 2015, pp. 1–7.

[4] T. Paiva, A. Damasceno, E. Figueiredo, and C. Sant'Anna, "On the evaluation of code smells and detection tools," *Journal of Software Engineering Research and Development*, vol. 5, p. 7, 12 2017.

[5] T. Sharma, "Designitejava," Dec. 2018, https://github.com/tushartushar/DesigniteJava. [Online]. Available: https://doi.org/10.5281/zenodo.2566861

[6] T. Sharma, M. Fragkoulis, and D. Spinellis, "House of cards: Code smells in open-source c# repositories," in *Proceedings of the 11th ACM/IEEE International Symposium on Empirical Software Engineering and Measurement*, ser. ESEM '17. IEEE Press, 2017, p. 424–429. [Online]. Available: https://doi-org.ezproxy.baylor.edu/10.1109/ESEM.2017.57

[7] M. Fokaefs, N. Tsantalis, E. Stroulia, and A. Chatzigeorgiou, "Jdeodorant: identification and application of extract class refactorings," in *2011 33rd International Conference on Software Engineering (ICSE)*, 2011, pp. 1037–1039.

[8] C. Marinescu, R. Marinescu, P. Mihancea, D. Ratiu, and R. Wettel, "iplasma: An integrated platform for quality assessment of object-oriented design." 01 2005, pp. 77–80.

[9] "Sonargraph-quality: A tool for assessing and monitoring technical quality." [Online]. Available: https://www.hello2morrow.com/products/sonargraph/quality

[10] G. Samarthyam, G. Suryanarayana, and T. Sharma, "Refactoring for software architecture smells," in *Proceedings of the 1st International Workshop on Software Refactoring*, ser. IWoR 2016. New York, NY, USA: Association for Computing Machinery, 2016, p. 1–4. [Online]. Available: https://doi-org.ezproxy.baylor.edu/10.1145/2975945.2975946

[11] F. A. Fontana, V. Ferme, and M. Zanoni, "Filtering code smells detection results," in *Proceedings of the 37th International Conference on Software Engineering - Volume 2*, ser. ICSE '15. IEEE Press, 2015, p. 803–804.

[12] N. Munaiah, S. Kroh, C. Cabrey, and M. Nagappan, "Curating github for engineered software projects," *PeerJ Preprints 4:e2617v1*, 2016.

[13] A. Yamashita and L. Moonen, "Do developers care about code smells? an exploratory survey," in *2013 20th Working Conference on Reverse Engineering (WCRE)*, 2013, pp. 242–251.

[14] Y. Golubev, Z. Kurbatova, E. A. AlOmar, T. Bryksin, and M. W. Mkaouer, "One thousand and one stories: A large-scale survey of software refactoring," in *Proceedings of the 29th ACM Joint Meeting on European Software Engineering Conference and Symposium on the Foundations of Software Engineering*, ser. ESEC/FSE 2021. New York, NY, USA: Association for Computing Machinery, 2021, p. 1303–1313. [Online]. Available: https://doi-org.ezproxy.baylor.edu/10.1145/3468264.3473924

[15] V. Thakur, M. Kessentini, and T. Sharma, "Qscored: An open platform for code quality ranking and visualization," in *2020 IEEE International Conference on Software Maintenance and Evolution (ICSME)*, 2020, pp. 818–821.

Joint 42nd IEEE Software Engineering Workshop and 9th International Workshop on Cyber-Physical Systems

THE IEEE Software Engineering Workshop (SEW) is the oldest Software Engineering event in the world, dating back to 1969. The workshop was originally run as the NASA Software Engineering Workshop and focused on software engineering issues relevant to NASA and the space industry. After the 25th edition, it became the NASA/IEEE Software Engineering Workshop and expanded its remit to address many more areas of software engineering with emphasis on practical issues, industrial experience and case studies in addition to traditional technical papers. Since its 31st edition, it has been sponsored by IEEE and has continued to broaden its areas of interest.

One such extremely hot new area are Cyber-physical Systems (CPS), which encompass the investigation of approaches related to the development and use of modern software systems interfacing with real world and controlling their surroundings. CPS are physical and engineering systems closely integrated with their typically networked environment. Modern airplanes, automobiles, or medical devices are practically networks of computers. Sensors, robots, and intelligent devices are abundant. Human life depends on them. CPS systems transform how people interact with the physical world just like the Internet transformed how people interact with one another.

The joint workshop aims to bring together all those researchers with an interest in software engineering, both with CPS and broader focus. Traditionally, these workshops attract industrial and government practitioners and academics pursuing the advancement of software engineering principles, techniques and practices. This joint edition will also provide a forum for reporting on past experiences, for describing new and emerging results and approaches, and for exchanging ideas on best practice and future directions.

Topics

The workshop aims to bring together all those with an interest in software engineering. Traditionally, the workshop attracts industrial and government practitioners and academics pursuing the advancement of software engineering principles, techniques and practice. The workshop provides a forum for reporting on past experiences, for describing new and emerging results and approaches, and for exchanging ideas on best practice and future directions.

Topics of interest include, but are not limited to:

- Experiments and experience reports
- Software quality assurance and metrics
- Formal methods and formal approaches to software development
- Software engineering processes and process improvement
- Agile and lean methods
- Requirements engineering
- Software architectures
- Design methodologies
- Validation and verification
- Software maintenance, reuse, and legacy systems
- Agent-based software systems
- Self-managing systems
- New approaches to software engineering (e.g., search based software engineering)
- Software engineering issues in cyber-physical systems
- Real-time software engineering
- Safety assurance & certification
- Software security
- Embedded control systems and networks
- Software aspects of the Internet of Things
- Software engineering education, laboratories and pedagogy
- Software engineering for social media

Technical Session Chairs

- **Bowen, Jonathan,** Museophile Ltd., United Kingdom
- **Hinchey, Mike**(Lead Chair), Lero-the Irish Software Engineering Research Centre, Ireland
- **Szmuc, Tomasz,** AGH University of Science and Technology, Poland
- **Zalewski, Janusz,** Florida Gulf Coast University, United States

Program Committee

- **Ait Ameur, Yamine,** Toulouse Institute for Research in Computer Science, France
- **Banach, Richard,** University of Manchester, United Kingdom
- **Challenger, Moharram,** University of Antwerp, Belgium
- **Cicirelli, Franco,** DIMES Università della Calabria, Italy
- **Gomes, Luis,** Universidade NOVA de Lisboa, Portugal
- **Gracanin, Denis,** Virginia Tech, USA

- **Havelund, Klaus,** Jet Propulsion Laboratory, USA
- **Hsiao, Michael,** Virginia Tech, USA
- **Karaduman, Burak,** University of Antwerp, Belgium
- **Katwijk, Jan van,** TU Delft, Netherlands
- **Pullum, Laura,** Oak Ridge National Laboratory, USA
- **Sekerinski, Emil,** McMaster University, Canada
- **Sojka, Michal,** Czech Technical University in Prague, Czech Republic
- **Trybus, Leszek,** Rzeszow University of Technology, Poland
- **Vardanega, Tullio,** University of Padua, Italy
- **Velev, Miroslav,** Aries Design Automation, USA

Communication Papers of the of the 17th Conference on Computer Science and Intelligence Systems pp. 321–328
DOI: 10.15439/2022F208
ISSN 2300-5963 ACSIS, Vol. 32

Towards developing a cyber-physical warehouse system for automated order-picking for online shopping

Melike Oruc
Department of Computer Science
Dokuz Eylul University
melikeoruc97@gmail.com

Onur Berker Alhas
Department of Computer Science
Dokuz Eylul University
alhasonur@gmail.com

Goksun Beren Usta
Department of Computer Science
Dokuz Eylul University
goksunberen@gmail.com

Hussein Marah
University of Antwerp &
Flanders Make Strategic Research Center
hussein.marah@uantwerpen.be

Baris Tekin Tezel
Department of Computer Science
Dokuz Eylul University
baris.tezel@deu.edu.tr

Moharram Challenger
University of Antwerp &
Flanders Make Strategic Research Center
moharram.challenger@uantwerpen.be

***Abstract*—In recent years, Cyber-Physical Systems (CPS) have been studied in various application areas. Since there are many robots that need to implement both physical and cyber sides, interact with each other and the environment, and the system has to cope with many faced difficulties, a warehouse system for automated order-picking for online shopping seems to be very suitable for being modeled and implemented as CPS. In this study, the planning and control of mobile robots in a store warehouse is defined from the perspectives of obstacle avoidance, collision detection, and solving the shortest path problem. Accordingly, a simulation environment is designed and a layered CPS development model is proposed. In the simulation environment, both object avoidance and collision detection algorithms are introduced and implemented, different shortest path-finding algorithms are adapted and implemented and their performances are evaluated.**

***Index Terms*—Online shopping, Mobile robot, Simulation, Webots, Cyber-Physical systems**

I. Introduction

Cyber-Physical Systems (CPS) are complex systems that incorporate cyber and physical components that communicate and interact with each other [5, 3]. They collect environmental data through sensors and affect the environment via actuators. CPS has pervasive applications in various fields such as health, transportation, manufacturing, etc., making our lives easier by automating many aspects.

In today's world, online shopping is spreading everywhere in society. [17]. Especially during the COVID-19 pandemic, the increasing rate of online shopping [22] started to create an extra workload for warehouses' employees. In order to reduce this workload, it's necessary to automate the processes in warehouses by using robots and smart systems. Robots in warehouses are responsible for picking and delivering packages from/to the right destination. The robots must take the shortest possible path to collect/deliver the products to avoid time loss and save energy[26]. Therefore, path-finding algorithms such as Greedy [12] and A* [13] were used to find the shortest path. Since CPS interact with the environment, another problem that may be encountered is the possibility of robots hitting any obstacle that may come their way in the warehouse. During the movement, it is necessary to prevent the robots from colliding not only with an obstacle, but also with each other. For this, a master robot transmits the information it receives from the environment to other robots, enabling them to recognize the environment dynamically and direct their movements.

The presented study identifies the planning and control of mobile robots in a shop warehouse by deploying several shortest path algorithms and comparing the performance and efficiency of these algorithms regarding the number of destinations or nodes in the simulation environment. Also, the implementation focused on the autonomy of robots (i.e., obstacle decisions) and free mobility (i.e., navigation and collision avoidance). Therefore, we try to examine and provide answers to the following research questions:

- What does the simulation environment, specifically Webots, can provide for implementing CPS?
- What are the suitable shortest path algorithms for navigation and controlling robots?
- How can the simulation environment be converted to real CPS implementation and improve the design and implementation phases?

This paper is organised as follows: Section 2 gives the related works in this field. Section 3 describes the components and technologies we used in this study. Layered CPS development model is introduced in Section 4. Section 5 is about our preliminary findings by early experimental simulation studies. Section 6 gives information about future work and concludes the paper.

II. Related Work

In the era of massive online shopping, warehouse management has become an essential and crucial factor for ensuring

safe and timed delivery. The operations in a warehouse are usually intensive and require significant effort, organization, management, accuracy, and speed to deliver packages in a reasonable time frame. Also, a warehouse requires a large space to allow vehicles to maneuver around the racks [4]. In a warehouse, autonomous robots can play a vital role in picking and delivering goods while ensuring time constraints and safety requirements (collision-free, obstacle detection, and energy efficiency). Thus, moving to partially-to-fully automated operations has been considered a priority for warehouses and big retailers in the last few years. However, implementing such intelligent systems requires using appropriate technologies. Several studies, approaches, and implementations for building autonomous robots have been introduced. Also, simulations for building such systems have been considered too. Simulation studies can be helpful to get deep insights and estimations of the requirements and performance before building and implementing the system.

In the literature, there are many implementations for robots in warehouses. For example, in the paper presented by [10], they implemented an autonomous robot equipped with RFID. The RFID reader is integrated with the PIC microcontroller as the main component. Also, a servo-motor that has an infrared sensor is used to follow the line. This project is aimed to build an autonomous robot with an RFID application. The implementation of the system used the Assembly languages. As a result of the implementation, the robots read the tag on the items to identify them, pick up those items, and then navigate to the desired location to store the item.

For most warehouses, there are many orders to be fulfilled in a given time constraint. As a result, task assignment for robots in such systems becomes one of the most crucial corners stone of the system. Thus, efficient algorithms for path-finding can boost the system's performance and achieve good results. The algorithm presented in [6] gives us a feasible adaptive task assignment algorithm for a real-time system to solve task assignment problems. With the given algorithms, such systems can be robust enough to meet the needs of huge order loads dynamically while being flexible at the same time.

The authors of the study [18] focused on investigating the robotic mobile fulfillment system (RMFS) in warehouses where there is high-density storage due to the limited space and high costs. The main focus was to assign tasks between workstations and the storage area, and this process is composed of three phases: task assignment, path planning, and traffic control. A simulation environment was implemented to evaluate the system requirements, and the results showed that 10% of storage space could be saved using the energy level. The study presented in [7] focused on the order processing problem in order to determine the time of picking and delivering the packages by the mobile robot. The topic of improving the throughput performance of Automated guided vehicles (AGV) was studied in the [24], and to achieve this, they introduced a mathematical model. The model was designed with genetic algorithm, and the main aim of this model is to achieve the shortest order completion.

Simulation of real warehouse or manufacturing environment systems has also been taken into account in the literature. For example, A simulation framework designed with ROS Gazebo simulator to simulate transport systems based on automated guided vehicles (AGVs) has been built in [19]. This framework is used for simulations by deploying algorithms and different policies in the control system. The adaptation to the Just-in-Time (JIT) concept was discussed in the [16]. In addition, a simulation model in a job shop environment was developed to improve transportation efficiency, and a dispatching algorithm was deployed in vehicles that move through stations. The paper [11], presents a strategic simulation model for comparing common fixed layouts that deploy the shortest path approach where collision avoidance is the central focus. In terms of transport capacity, the results of simulation experiments showed that dynamic free-ranging has high potential. Anyhow, the use of simulation environments have helped developers to build more dynamic and error-prone cyber-physical system (CPS) due to the favor of the valuable insights that have gained from simulation experiments.

Some of the open source simulators that have been seen in the previous works are like (Gazebo, Webots, Simbad, USARSim, RoboDK, MRDS and MisionLab) [23]. In this paper, the simulation environment has been designed and developed with Webots. In addition, an layered CPS development model is proposed to create a warehouse storage system automated order-picking for online shopping in the simulation environment. With the simulation environment and proposed architecture, both object avoidance and collision detection algorithms are introduced and implemented, as well as different shortest path-finding algorithms are applied and evaluated performances according to solving the traveling salesman problem for picking items within the optimum time.

III. Background

This section indicates the background information which relates to the components in the scope of this study. The section clarifies which algorithms such as Dijkstra, A-star, Travelling Salesman Problem and which tools such as Webots, e-Puck are used in the study.

A. Warehouse System and Order-picking for Online Shopping

Especially in the pandemic period, technical solutions to improve the manual order picking process have gained more and more importance. One of them is to do the order picking process with robots. While the ultimate goal is real robotics, it is often very beneficial to run simulations before researching with real robots. This is because simulations are easier to set up, cheaper, and more convenient to use than real robotics.

Webots: Webots is an open source robot simulator produced by Cyberbotics[20]. It is written by the developers of the open source program called Khepera Simulator, which is based on Khepera Simulator. Any type of mobile robot can be simulated using Webots. So it is really useful for the development of advanced robotics projects. The Webots library includes distance sensors, light sensors, cameras, accelerometers, touch/pressure

sensors, and GPS, and the user can process data from these sensors.

e-Puck: The e-puck robot was designed by Francesco Mondada and Michael Bonani at the Swiss Federal Institute of Technology in 2006. It is an educational robot that has helped generations of students learn about embedded systems and robotics. It has a small differential wheel, 7.4 cm in diameter, 4.5 cm in length, and weighs 150 g. It has 8 infrared sensors that measure near the light at a range of 4 cm and the proximity of obstacles. It also contains a 3-axis accelerometer, three microphones, a speaker, a 640x480-pixel color camera, and a Bluetooth interface for communicating with a host computer. The current version of the e-puck model includes distance sensors, light sensors and many more features such as a camera [21].

B. Shortest Path Algorithm

Throughout history, it has always been a question asked how people can travel from one city to another in the shortest time. This is a very simple question in everyday life that almost everyone can easily understand and find a solution to. But when the input data is large, solving the problem may not be so easy. Machines can calculate this process more accurately and faster for us. As a result, the shortest path problem is considered a basic topic in the field of computer science. The shortest path problem is defined as the shortest distance movement from a given starting point to a given target point in a given environment with obstacles at different locations.

Travelling Salesman Problem (TSP): The Traveling Salesman, which is one of the well-known NP-hard optimization problems, was formally stated by Irish mathematician William Rowan Hamilton and British mathematician Thomas Kirkman in the nineteenth century. TSP is a problem in which the distance between "n" cities is known, it is aimed to find the optimal route in which the total distance traveled during the tour is the shortest, based on the principle of returning to the starting point, provided that each city is visited only once [14]. In short, the goal in TSP is to find the shortest path through each city in a given set of cities.

Greedy Algorithm: When computer scientist and mathematician Edsger Dijkstra tried to calculate the minimum spanning tree, he came up with the greedy approach. The greedy approach means selecting the option or solution that appears to be the greatest at the time. [12]. It merely means selecting the option or solution that appears to be the greatest at the time. To reach the optimum solution, the main purpose of this is to find the best among the locally optimal solutions for each sub-task. Thus, the optimal solutions found for each sub-task will provide the optimal solution for the main task.

A-star Search Algorithm: The A* algorithm is a heuristic search algorithm for finding the shortest path between two targets. It is considered an expansion of the Dijkstra method, however, it uses a heuristic to determine the best solution to save runtime. The algorithm was first published in 1968 by Peter Hart, Nils Nilsson, and Bertram Raphael. [13].

C. Cyber-Physical Systems (CPS):

Cyber-Physical Systems encompass any structures that facilitate communication and cooperation between the physical and cyber worlds. The fundamental goal of CPS is to meet the flexible and dynamic needs of production while also increasing industrial efficiency and productivity. "Cyber-physical systems" are defined as "the integration of physical processes and computation." This gives the production process a whole new level of control, monitoring, and efficiency [25].

IV. Layered CPS development model for a warehouse system

Cyber-physical systems (CPS) are enabling technologies that connect the virtual and physical worlds to create a genuinely networked world in which intelligent objects communicate and interact. They are also self-contained onboard systems having sensors to sense their surroundings and actuators to control physical processes. Because they can receive and process data, they can control certain tasks themselves, so CPS can enable communication between humans, robots or even products. In the traditional warehouse system, many processes such as product picking and delivery are done by people. However, under the pandemic conditions that affected the whole world, this has been even more costly in terms of both resources and time. That's why there is an understanding of making smarter with robots in the emergence of this project. This understanding also lies in the use of the CPS.

This section describes in sequence the steps of developing a cyber-physical warehouse system for automated order picking for online shopping. This study aims to collect the products ordered by robots through online shopping in a warehouse environment and to minimize the time and cost. For this, some shortest path algorithms were produced and Java was used as the programming language. Although this study is intended to be implemented in the physical environment in the future, it was carried out with the help of a simulator as it would be much easier and more convenient to implement in the simulation environment at the first stage. The architecture of the proposed approach is shown in Figure 1.

A. Creation of The Simulation Environment on Webots and Inclusion of e-Puck Robots

In this study, the Webots simulator is used to model the robots and the environment. The Webots allows the creation of obstacles of different shapes and sizes. It also consists of a collection of robots, sensors, actuators, and objects. The environment in Webots is called the "world" and robot or object are created inside this "world". For this study, a 3x3 world was created, then The e-puck was added to this "world".

The e-puck robot is equipped with a wide variety of sensors and actuators such as a camera, infrared sensors, GPS, and LED sensors. It also has two wheels, each controlled by a separate servo motor, enabling it to move. Each motor is equipped with an encoder that counts the pulses sent to it. Encoders are used to obtain the true motor rotation by counting the number of ticks in a wheel. It has the ability to travel

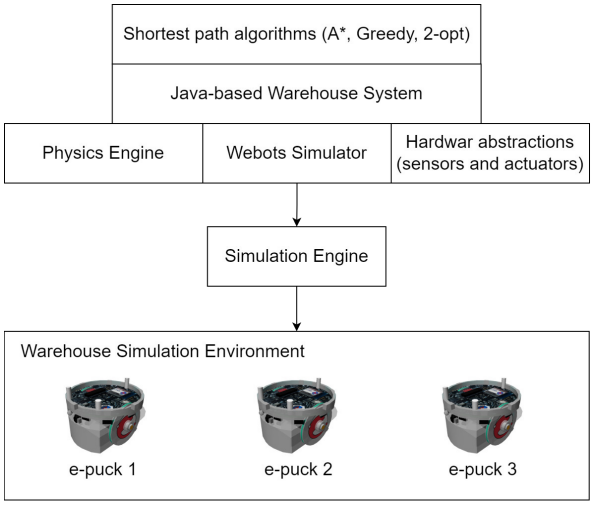

Fig. 1. The overview of the warehouse simulation architecture

forward, backward, and right or left. The wheels' maximum speed is 1000 steps per second, or one wheel revolution every second [2].

Robots drive forward and backward if the values give for the wheels are positive and negative respectively. The left wheel speed must be lower than the right wheel speed for the e-puck robot to turn left, and the right wheel speed must be lower than the left wheel speed for the robot to turn right. Functions of a derived class called $RotationalMotor$ from Webots' *Robot* node are used to move the e-puck robot as mentioned above.

B. Implementing Obstacle Avoidance for e-puck

Obstacle avoidance can never be ignored when aiming to develop a cyber-physical warehouse system for automated order picking for online shopping. Because there are many obstacles such as shelves, baskets, and objects that the robot can hit in the warehouse environment. To create the obstacle avoidance algorithm, we need to read the values of the 8 infrared sensors of the e-puck robot and activate its two wheels. The implementations for the movements of the wheels were explain in the previous section. In this section, implementations for obstacle avoidance are described.

The e-Puck has 8 IR sensors that measure the proximity of obstacles or the intensity of infrared light at a distance of 4 cm from the environment. These are named from ps0 to ps7. Figure 2 shows how the IR sensors are positioned on the e-puck. It receives as input the IR sensor values. The algorithm is created according to these input values. To get these input values, import directives must be added for the $DistanceSensor$ to use the corresponding API to the Controller.

When the 2 IR sensors ("ps1", "ps0") located on the right front of the e-puck detect the obstacle, it turns their direction to the left and continues towards the target when the obstacle is out of the distance range. Likewise, when the 2 IR sensors

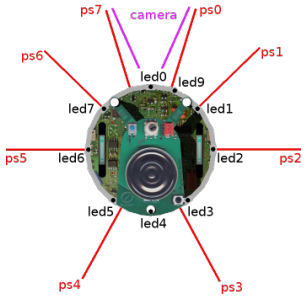

Fig. 2. Sensors, LEDs and Camera of e-puck[1]

("ps7", "ps6") on the left front detect an obstacle, it turns right and continues toward the target when the obstacle is out of the distance range.

In this case, when the e-puck robot detects an obstacle, it first stops, turns in the opposite direction, and takes action. When it is more than 4 cm away from the obstacle it detects, it adjusts its angle and continues to go towards the target again. Although this does not seem like a waste of time for a single e-puck robot and a single obstacle, it can cause a lot of wasted time when considering multiple obstacles and robots in the warehouse environment. For this reason, an obstacle avoidance algorithm was designed gradually.

Algorithm 1 An algorithm of wheel speeds for obstacle avoidance

```
1:  base ← 3
2:  count ← 0
3:  total ← 0
4:  for iteration = 0, 1, 2, 3 do
5:      if distance_sensors[iteration].getValue() ≤ 1000
    then
6:          total ← total + iteration
7:          count ← count + 1
8:      end if
9:  end for
10: if count > 0 then
11:     leftSpeed ← base + (total/count − 2) ∗ 3
12:     rightSpeed ← base − (total/count − 2) ∗ 3
13:     setVelocity(leftSpeed)
14:     setVelocity(rightSpeed)
15: else
16:     setVelocity(base)
17:     setVelocity(base)
18: end if
```

The "base" variable is used to store the base speed of the robot. The "total" variable is used to save the sum of the weights of the distance sensors that detect an object. The "count" variable saves the number of distance sensors that caught an object. The distance sensors of the e-puck robot can take values between 0 and 1000[2]. If the threshold sensor value

[1]e-puck: https://cyberbotics.com/doc/guide/epuck

[2]https://cyberbotics.com/doc/reference/distancesensor

rises above 1000, an obstacle has been detected. Conversely, if the sensor's value is 0, there is no obstacle detected.

The weights of the distance sensors which are assigned to the indexes of a loop, when the total is divided by count give a value between 0 and 4. The left-most object that the robot can detect will give 0 and the right-most object that the robot can detect will give 4. Now if we subtract 2 from the leftmost will give -2 and the rightmost will give 2 giving us the possibility of detecting which side the object is on concerning the robot.

Then we multiply this value by another weight. This weight was found by trial and error with different values for this the robots turning speed and reaction time will change. To get the separate speeds for left speed and right speed the values we get are subtracted from the base speed. The resulting values are sent to the $SetVelocity$ function of Webots' $Motor$ library. $SetVelocity$ is used to control the speed of the robot. Thus, it provides a more effective working opportunity for obstacle avoidance of the robot without slowing down. The related demonstrating video can be found on https://youtu.be/siQvDc7AbG4

C. Implementing Collision Avoidance for e-Puck

Collision avoidance is a critical feature that provides accurate, fast, and dependable warnings before a collision occurs. In particular, collision avoidance in the warehouse environment for order-picking for online shopping robots is an area of work that should be considered. Because if more than one robot does not communicate with each other, possible conflicts may occur, resulting in loss of time and work. As a result, a collision avoidance algorithm has been devised in this study, allowing e-puck robots to reach their destinations without colliding with each other or obstacles.

Improvements have been expressed in this section. The improvement was initiated by adding two more e-pucks to the "world" and controllers for them. The collision avoidance algorithm introduced in the previous section was applied to these two e-puck controllers.

Each e-puck used has a priority over the other. This situation is used in this study with Webots' "$Supervisor$" library. The supervisor has omnipotent powers, including the ability to change the environment and deliver messages to robots. In Webots, it's linked to a controller program. The Supervisor controller, unlike a conventional robot controller, will have access to advantaged operations. Any robot can be turned into a supervisor when the "supervisor" field is set to TRUE in Webots. In this way, it can provide access to other e-puck robots. Considering this situation, the algorithm has been developed.

To explain the algorithm; in the beginning, three e-puck robots are moving toward their destination. The situation of collision avoidance occurs when the Euclidean distance between the e-puck robots is less than 5 cm. Any e-puck robot, when there is a possibility of collision with another e-puck robot, allows the passage of whichever has priority by messaging between them. When the distance between them eliminates the possibility of collision, the other e-puck robot continues to go to its target. The algorithm continues until all the e-puck robots reach their targets.

Algorithm 2 An algorithm of collision avoidance

```
1: function START
2:     if CheckDistance then
3:         MOVE(0, 0)
4:     end if
5: end function

6: function MOVE(leftSpeed, rightSpeed)
7:     setVelocity(leftSpeed)
8:     setVelocity(rightSpeed)
9: end function

10: function BOOLEAN CHECKDISTANCE
11:     if Distance(getPosition(Robot_2), getPosition(Robot_1)) <
    5 then
    return TRUE
12:     else
    return FALSE
13:     end if
14: end function
```

Within the scope of this study, 3 e-puck robots were used as mentioned in this section. However, in Webots, many robots can be added to the "world", and controllers for these robots can be added. Collision avoidance status can be implemented for many robots by providing priority conditions in the controller of each. The related demonstrating video can be found on https://youtu.be/h03AbXaXYV4

D. Path Planning with Shortest Path Algorithm for Travelling Salesman Problem

Finding the shortest path in the presence of obstacles, referred to as the shortest path problem, is one of the fundamental problems in path planning. As this problem occurs in many industrial applications, it also plays an important role in the warehouse ordering robot. Because in this way, order picking for online shopping at a warehouse can effectively reduce the cost and time. Therefore, improving the route planning algorithm of the online ordering robot has a significant impact on improving transportation efficiency.

The robot receives the coordinates of all ordered products, then automatically starts moving from the starting position to the first calculated product position to complete the loading task. After all the products it needs to collect are finished, it returns to its starting position and completes its process. Therefore, this scenario can be considered a "Traveling Salesman Problem". The Traveling Salesman Problem defines a salesman who must travel between a certain number of cities. The order of the cities to be visited does not matter, as long as it is visited in one go and ends in the starting city. Each of the links between cities has one or more weights that can represent distance, time or price cost. The real problem is to

find the shortest path that starts at one point, travels through all needed destinations, and ends at the point where it started again. In the study, we test the robot's path planning through 2 algorithms for Travelling Salesman Problem. These are Greedy Algorithm and A* Algorithm. The related demonstrating videos can be found on https://youtu.be/hgCQA_o4QGs and https://youtu.be/w-z1-IhCY68, respectively.

1) Input Data Set: Within the scope of this study, the coordinates of the products that need to be collected in the warehouse environment for order picking for the online shopping robot are read from the file. The coordinates in this file are randomly generated in Python. It takes the starting position of the robot from Webots. This is also the final position.

2) Greedy Approach Algorithm for Order Picking Robot: The greedy algorithm is a strategy that contends that the best choice should be chosen under present conditions, without regard for the long-term consequences of solving a problem. The algorithm's main goal is to find the shortest path possible. Starting with the initial node, only the one with the smallest distance among the available nodes is chosen. After each selection, the selected node is marked not to be re-selected. As a result, the previously visited node is no longer visited. When there are no more nodes to visit, that is, all nodes have been visited, it returns to the starting point. This is the greedy method's idea for the Travelling Salesman Problem (TSP) solution.

The way the algorithm works for this study is as follows: The coordinates of the products that the order-picking for online shopping robot needs to collect are read from the file through the controls. Since there is a TSP problem, the start point and end point of the robot must be the same. This start and end position is automatically obtained from Webots. That is, the start point and end point of the robot can be changed dynamically. Since Greedy is an algorithm, it always chooses the closest one among the nodes it can go to. The distance was calculated with "Euclidean Distance". The weight of each node visited is changed to an "infinite" value since it will not be visited again. When all the coordinates to be visited are finished, that is, when all the ordered products are collected, the order-picking for the online shopping robot returns to its starting position and the algorithm ends.

3) A Algorithm for Order Picking Robot:* The A* algorithm is a search algorithm that searches for the shortest path between the starting and ending states. In the Greedy method, we only consider our estimated distance to the target and move in the direction where it is the least. The A* algorithm, unlike the Greedy method, takes into account heuristic cost and actual distance. This is accomplished by retaining a tree of paths that originate from the initial node and extending those paths one edge at a time until the termination requirement is fulfilled. The A* algorithm must decide which of its paths to extend at each iteration of its main loop. It does so based on the path's cost as well as an estimate of the cost of widening the way to the goal.

"Manhattan Distance" and "Euclidean Distance" can be used when calculating the cost of the road. In this study, both methods were tried on the algorithm and the results were examined. However, in [1], it has been seen that "Manhattan Distance" is recommended in case of high-dimensional data, and "Euclidean Distance" is recommended in case of lower data, as in our study. Therefore, "Euclidean Distance" was used while calculating the cost of the road [1, 9].

$f(n) = g(n) + h(n)$
$f(n)$ = total estimated cost of the path through node n
$g(n)$ = cost so far to reach node n
$h(n)$ = estimated cost from n to goal. This is the heuristic part of the cost function, so it is like a guess.

But the A* algorithm does not have a suitable scenario for the Travelling Salesman Problem (TSP) solution. In this study, the A* algorithm was adapted to TSP. For this, the robot went from the starting position to a point and then the A* algorithm was run. Thus, the scenario was made suitable for TSP. He made several attempts to decide where he should go first from his starting position. By making the robot go to the nearest node from the starting point, the A* algorithm was run. Then, on the contrary, this process made the robot go to the farthest node from the starting point, and the A* algorithm was run.

When we compared the results, it was observed that going to the farthest node from the starting point of the robot and then running the A* algorithm gave better results. For this reason, the warehouse ordering robot has been adapted to pick up the product at the furthest node from the starting position, then visit the nodes that need to be intuitively visited using the A* algorithm, collect all the ordered products, and finally return to the starting position.

V. Preliminary findings by early experimental simulation studies

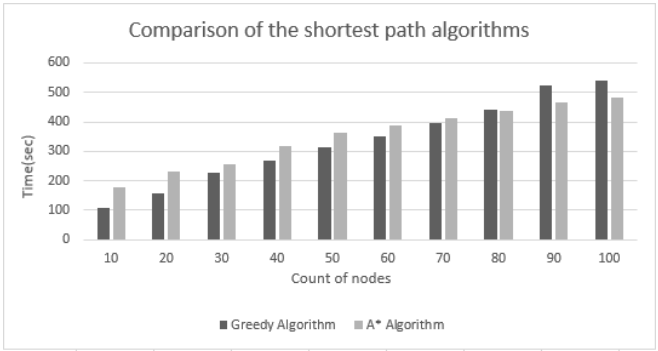

Fig. 3. Evulation of the algorithms with respect to time criteria

In this study, A* and Greedy Algorithm will be applied in the path planning of a cyber-physical warehouse system for automatic order selection for online shopping. We made some changes to adapt these algorithms to our scenario for the warehouse system. The results we obtained from the study of

these two algorithms and the comparison of these results are shown in Figure 3.

The bar chart provides information about the running times of the simulations based on the number of nodes. The number of nodes here represents the number of items to be retrieved in sequence. The number of nodes was randomly generated from 10 to 100, and the values in the graph were created by running the simulation 20 times for both algorithms and taking the average. The main reason for testing the number of nodes between 10 and 100 here is to compare the two shortest path algorithms based on the complexity of the scenario. In both shortest path algorithms, the result has been reached, but it is aimed to decide which is better in which situations. In this section, it is explained which algorithm should be used in which situations for the scenario according to the simulation completion times of the two shortest path algorithms.

Overall, the Greedy Algorithm's time to complete the simulation initially performed better than the A* Algorithm. However, at the end of the period, the A* algorithm worked faster. The most significant finding is as the number of nodes increases, the running time of the A* algorithm started to give faster results compared to the Greedy algorithm. When the number of nodes is 10, the greedy algorithm completed the path in around 100 seconds, while the star algorithm's running time was just under 200 seconds. It can be clearly seen from the bar chart that the running times of algorithms began to approach each other with the increase in the number of nodes. When the count of nodes reaches 80, the running time of the A* algorithm was slightly above 400, giving a faster result than the Greedy algorithm.

According to the result of the early experimental simulation studies, when the robot receives the order, if the number of products to be collected by the robot is less than 80, it is more efficient to use the Greedy algorithm because it works faster. When the number of products is more than 80, the A* algorithm can be used since A* performs more successfully. However, these findings have not been confirmed by any statistical test. Therefore, in order to make these results more reliable, the number of trials should be increased and the results should be tested statistically. Although the findings obtained in this state are guiding, it will not be appropriate to make a definitive judgment.

VI. Discussion

The robot travels through the points most shortly, following a certain route. One of the first problems encountered while trying to solve this step was the selection of the method used to solve the shortest path problem. It was noticed that when using the Greedy algorithm to find the shortest path, it often misses the shortest distance on the overall route, as expected since the algorithm always chooses to travel the local minimum distance. So, trying the A* algorithm and the Greedy algorithm was decided to evaluate them. Another problem encountered at this stage was that the A* algorithm was not a completely suitable method to solve the Travelling Salesman Problem, so the algorithm was modified to made it suitable for the TSP problem. After the robot went to the node with the shortest distance from the starting point, the A* algorithm was ran. With this method, it was realized that the algorithm did not show the efficiency we expected.

When we ran the A* algorithm after going to the farthest node from the starting point of the robot, more successful results were got. When the results gathered from the Greedy and A* algorithms were compared, it was observed that as the number of nodes increases, the Greedy algorithm works faster up to about 80 nodes, while adding more nodes gives slower results. This may be because Greedy runs slower since its time complexity is n^2 as it travels through all the nodes. The data structures used while implementing algorithms can also be a factor that needs to be evaluated for speed. To find a better route in the A* algorithm, prioritizing some nodes using the cost function may have provided a faster solution to finding the optimal route.

VII. Conclusion and Future Work

In this paper, we have designed and developed a simulation implementation to simulate the real behaviors of Cyber Physical System (CPS) embodied as mobile robots that operate in a warehouse or a shop. In the simulation implementation, shortest path algorithms have been designed, deployed and tested. According to the results of the early experimental simulation studies, if the number of products to be collected by the robot is less than 80, it seems more efficient to use the Greedy algorithm. However, it has been observed that A* performs more successfully when the number of products is more than 80. Besides implementing and testing shortest path-finding algorithms, object avoidance and collision detection algorithms are introduced and implemented for appropriate to the scenario and the simulation environment.

We plan to integrate the current simulation environment with an agent-based paradigm to provide a simulation implementation with smart and autonomous behaviors. Agents can provide the simulation with advanced capabilities as well as make the system actors independent, interactive and proactive. Agents can behave competitively or cooperatively in the simulation environment to form Multi-Agent Systems (MASs). The MASs may have different perspectives like a plan, interaction, organization, role, environment etc. Thanks to these different perspectives, MASs can consider the structure, behavior, interaction and environment of complex systems such as CPSs. Therefore, both agents and MASs can be an ideal alternative in the modeling and development of CPSs [8]. This as future work will be discussed and explored with a clear and obvious case study that can show reliable results.

In addition, concerning providing digital twins with agent-based simulation, we intend to extend the current simulation and integrate it with the proposed agent-based Digital Twin architecture [15]. The plan is to have a digital twin framework where services such as simulation can be run by exploiting the real-time and historical data collected from the physical components to perform several tasks (prediction, maintenance, and improvement).

REFERENCES

[1] Charu C Aggarwal, Alexander Hinneburg, and Daniel A Keim. "On the surprising behavior of distance metrics in high dimensional space". In: *International conference on database theory*. Springer. 2001, pp. 420–434.

[2] Marwah Almasri, Khaled Elleithy, and Abrar Alajlan. "Sensor fusion based model for collision free mobile robot navigation". In: *Sensors* 16.1 (2015), p. 24.

[3] Tansu Zafer Asici et al. "Applying model driven engineering techniques to the development of contiki-based iot systems". In: *2019 IEEE/ACM 1st International Workshop on Software Engineering Research & Practices for the Internet of Things (SERP4IoT)*. IEEE. 2019, pp. 25–32.

[4] Kaveh Azadeh, René De Koster, and Debjit Roy. "Robotized and automated warehouse systems: Review and recent developments". In: *Transportation Science* 53.4 (2019), pp. 917–945.

[5] Ankica Barišic et al. "Systematic Literature Review on Multi-Paradigm Modelling for Cyber-Physical Systems". In: *Technical Report, Zenodo (Archive)* DOI: 10.5281/zenodo.2528953 (2019).

[6] Ali Bolu and Ömer Korçak. "Adaptive Task Planning for Multi-Robot Smart Warehouse". In: *IEEE Access* 9 (2021), pp. 27346–27358.

[7] Nils Boysen, Dirk Briskorn, and Simon Emde. "Parts-to-picker based order processing in a rack-moving mobile robots environment". In: *European Journal of Operational Research* 262.2 (2017), pp. 550–562.

[8] Moharram Challenger et al. "Agent-based cyber-physical system development with sea_ml++". In: *Multi-Paradigm Modelling Approaches for Cyber-Physical Systems*. Elsevier, 2021, pp. 195–219.

[9] Ge Chen, Tao Wu, and Zheng Zhou. "Research on ship meteorological route based on A-star algorithm". In: *Mathematical Problems in Engineering* 2021 (2021).

[10] Loh Poh Chuan et al. "An RFID warehouse robot". In: *2007 International Conference on Intelligent and Advanced Systems*. IEEE. 2007, pp. 451–456. DOI: 10.1109/ICIAS.2007.4658428.

[11] Mark B. Duinkerken, Jaap A. Ottjes, and Gabriel Lodewijks. "Comparison of Routing Strategies for AGV Systems using Simulation". In: *Proceedings of the 2006 Winter Simulation Conference*. 2006, pp. 1523–1530. DOI: 10.1109/WSC.2006.322922.

[12] A Fitriansyah et al. "Dijkstra's algorithm to find shortest path of tourist destination in Bali". In: *Journal of Physics: Conference Series*. Vol. 1338. 1. IOP Publishing. 2019, p. 012044.

[13] Peter E Hart, Nils J Nilsson, and Bertram Raphael. "A formal basis for the heuristic determination of minimum cost paths". In: *IEEE transactions on Systems Science and Cybernetics* 4.2 (1968), pp. 100–107.

[14] Holger H. Hoos and Thomas Stützle. "1 - INTRODUCTION". In: *Stochastic Local Search*. Ed. by Holger H. Hoos and Thomas Stützle. The Morgan Kaufmann Series in Artificial Intelligence. San Francisco: Morgan Kaufmann, 2005, pp. 13–59. ISBN: 978-1-55860-872-6. DOI: https://doi.org/10.1016/B978-155860872-6/50018-4.

[15] Marah Hussein and Moharram Challenger. "Intelligent Agents and Multi Agent Systems for Modeling Smart Digital Twins". In: *Engineering Multi-Agent Systems*. 2022 (in press).

[16] Saadettin Erhan Kesen and Ömer Faruk Baykoç. "Simulation of automated guided vehicle (AGV) systems based on just-in-time (JIT) philosophy in a job-shop environment". In: *Simulation Modelling Practice and Theory* 15.3 (2007), pp. 272–284.

[17] Julia Koch, Britta Frommeyer, and Gerhard Schewe. "Online shopping motives during the COVID-19 pandemic—lessons from the crisis". In: *Sustainability* 12.24 (2020), p. 10247.

[18] Xiaowen Li et al. "A simulation study on the robotic mobile fulfillment system in high-density storage warehouses". In: *Simulation Modelling Practice and Theory* 112 (2021), p. 102366. ISSN: 1569-190X. DOI: https://doi.org/10.1016/j.simpat.2021.102366.

[19] Joaquín López, Eduardo Zalama, and Jaime Gómez-García-Bermejo. "A simulation and control framework for AGV based transport systems". In: *Simulation Modelling Practice and Theory* 116 (2022), p. 102430.

[20] Olivier Michel. "Cyberbotics Ltd. Webots™: professional mobile robot simulation". In: *International Journal of Advanced Robotic Systems* 1.1 (2004), p. 5.

[21] Francesco Mondada et al. "The e-puck, a robot designed for education in engineering". In: *Proceedings of the 9th conference on autonomous robot systems and competitions*. Vol. 1. CONF. IPCB: Instituto Politécnico de Castelo Branco. 2009, pp. 59–65.

[22] Hoang Viet Nguyen et al. "Online book shopping in Vietnam: The impact of the COVID-19 pandemic situation". In: *Publishing Research Quarterly* 36.3 (2020), pp. 437–445.

[23] Aaron Staranowicz and Gian Luca Mariottini. "A survey and comparison of commercial and open-source robotic simulator software". In: *Proceedings of the 4th International Conference on PErvasive Technologies Related to Assistive Environments*. 2011, pp. 1–8.

[24] Hongtao Tang et al. "Research on equipment configuration optimization of AGV unmanned warehouse". In: *IEEE Access* 9 (2021), pp. 47946–47959.

[25] Michael Vierhauser et al. "Towards a model-integrated runtime monitoring infrastructure for cyber-physical systems". In: *International Conference on Software Engineering: New Ideas and Emerging Results (ICSE-NIER)*. IEEE. 2021, pp. 96–100. DOI: 10.1109/ICSE-NIER52604.2021.00028.

[26] Han-ye Zhang, Wei-ming Lin, and Ai-xia Chen. "Path planning for the mobile robot: A review". In: *Symmetry* 10.10 (2018), p. 450.

7th Workshop on Model Driven Approaches in System Development

FOR many years, various approaches in system design and implementation differentiate between the specification of the system and its implementation on a particular platform. People in software industry have been using models for a precise description of systems at the appropriate abstraction level without unnecessary details. Model-Driven (MD) approaches to the system development increase the importance and power of models by shifting the focus from programming to modeling activities. Models may be used as primary artifacts in constructing software, which means that software components are generated from models. Software development tools need to automate as many as possible tasks of model construction and transformation requiring the smallest amount of human interaction.

A goal of the proposed workshop is to bring together people working on MD approaches, techniques and tools, as well as Domain Specific Modeling (DSM) and Domain Specific Languages (DSL) and applying them in the requirements engineering, information system and application development, databases, and related areas, so that they can exchange their experience, create new ideas, evaluate and improve MD approaches and spread its use. The intention is to target an interdisciplinary nature of MD approaches in software engineering, as well as research topics expressed by but not limited to acronyms such as Model Driven Software Engineering (MDSE), Model Driven Development (MDD), Domain Specific Modeling (DSM), and OMG's Model Driven Architecture (MDA).

1st Workshop on MDASD was organized in the scope of ADBIS 2010 Conference, held in Novi Sad, Serbia. From 2012, MDASD becomes a regular bi-annual FedCSIS event.

TOPICS

- MD Approaches in System Design and Implementation – Problems and Issues
- MD Approaches in Software Process Models, Software Quality and Standards
- MD Approaches in Databases, Information Systems, Embedded and Real-Time Systems
- Metamodeling, Modeling and Specification Languages, Model Transformation Languages
- Model-to-Model, Model-to-Text, and Model-to-Code Transformations in Software Process
- Transformation Techniques and Tools
- Domain Specific Languages (DSL) and Domain Specific Modeling (DSM) in System Specification and Development
- Design of Metamodeling and Modeling Languages and Tools
- MD Approaches in Requirements Engineering, Document Engineering and Business Process Modeling
- MD Approaches in System Reengineering and Reverse Engineering
- MD Approaches in HCI and UX Design, GIS Development, and Cyber-Physical Systems
- Low-Code and No-Code software development – research, experiences and challenges
- Model Based Software Verification
- Artificial Intelligence (AI) for MD and MD for AI-based system development
- Theoretical and Mathematical Foundations of MD Approaches
- Multi-View, Multi-Paradigm and Blended Modeling
- Organizational and Human Factors, Skills, and Qualifications for MD Approaches
- Teaching MD Approaches in Academic and Industrial Environments
- MD Applications, Industry Experience, Case Studies, relationship with IoT and Industry 4.0

There is a possibility of selecting extended versions of the best papers presented during the conference for further procedure in the journals: ComSIS, ISI IF(2020) = 1.167, and COLA, ISI IF(2020) = 1.271.

TECHNICAL SESSION CHAIRS

- **Luković, Ivan,** University of Novi Sad, Serbia

STEERING COMMITTEE

- **Gray, Jeff,** University of Alabama, United States
- **Mernik, Marjan,** University of Maribor, Slovenia
- **Ristić, Sonja,** University of Novi Sad, Faculty of Technical Sciences, Serbia
- **Tolvanen, Juha-Pekka,** MetaCase, Finland

PROGRAM COMMITTEE

- **Amaral, Vasco,** NOVA University Lisbon, Portugal
- **Brdjanin, Drazen,** University of Banja Luka, Faculty of Electrical Engineering, Bosnia and Herzegovina
- **Bryant, Barrett,** University of North Texas, USA
- **Budimac, Zoran,** Faculty of Sciences, University of Novi Sad, Serbia
- **Chen, Haiming,** Chinese Academy of Sciences, China
- **Erradi, Mohammed,** ENSIAS Rabat, Morocco

- **Fertalj, Krešimir,** Faculty of EE and Computing, University of Zagreb, Croatia
- **Haerting, Ralf,** Hochschule Aalen, Germany
- **Ivanovic, Mirjana,** Faculty of Sciences, University of Novi Sad, Serbia
- **Janousek, Jan,** Czech Technical University Prague, Czech Republic
- **Karagiannis, Dimitris,** University of Vienna, Austria
- **Kardaş, Geylani,** Ege University, Turkey
- **Kordić, Slavica,** Faculty of Technical Sciences, University of Novi Sad, Sebia
- **Kosar, Tomaz,** University of Maribor, Slovenia
- **Krdzavac, Nenad,** University of Belgrade, Serbia
- **Liu, Shih-Hsi,** California State University, Fresno, USA
- **Macos, Dragan,** Beuth Hochschule für Technik, Germany
- **Melo-de-Sousa, Simão,** Universidade da Beira Interior, Portugal
- **Milosavljevic, Gordana,** Faculty of Technical Sciences, University of Novi Sad, Serbia
- **Özkaya, Mert,** Istanbul Kemerburgaz University, Turkey
- **Porubän, Jaroslav,** Technical University of Košice, Slovakia
- **Rangel Henriques, Pedro,** University of Minho, Portugal
- **Selic, Bran,** Malina Software Corp., Canada
- **Sierra, Jose Luis,** Universidad Complutense de Madrid, Spain
- **Slivnik, Bostjan,** University of Ljubljana, Slovenia
- **Tavakoli Kolagari, Ramin,** Nuremberg Institute of Technology, Germany
- **Varanda Pereira, Maria João,** Instituto Politécnico de Bragança, Portugal
- **Vescoukis, Vassilios,** National Technical University of Athens, Greece
- **Wimmer, Manuel,** JKU Linz, Austria

Communication Papers of the of the 17th Conference on Computer Science and Intelligence Systems pp. 331–338
DOI: 10.15439/2022F270
ISSN 2300-5963 ACSIS, Vol. 32

ModelWeb: A Toolset for the Model-based Testing of Web Applications

Mert Ozkaya
Department Computer Engineering
Yeditepe University
Istanbul, Turkey
mozkaya@cse.yeditepe.edu.tr

Mehmet Alp Kose
Institute of Graduate Studies
Altinbas University
Istanbul, Turkey
alp.kose@ogr.altinbas.edu.tr

Arda Burak Mamur
Empa Technology
Istanbul, Turkey
arda.mamur@empa.com

Turker Koc
Kurulum Cognitive Services
Istanbul, Turkey
turker@kurul.com.tr

***Abstract*—Model-based testing promotes the specifications of abstract system behaviours and their transformations into test scenarios to enhance the quality of software testing. In this paper, we propose a modeling toolset called *ModelWeb* for the model-based testing of web applications. *ModelWeb* provides a modeling editor that offers a flowchart-based notation set for the modeling of users' functional behaviours on the web applications. *ModelWeb*'s flowchart notation set consists of a pre-defined list of user actions (e.g., click, type, login, register, select etc.) and system actions (display and return). *ModelWeb* can further transform the flowchart-based model for a web functionality (e.g., adding products to cart in an online store) into the test scenarios that are documented in accordance with the behaviour-driven development (BDD) approach for understandability and the acceptance by the web test automation tools. So finally, *ModelWeb* can automatically test the web applications against the transformed BDD scenarios using the Selenium web test automation tool and report the test results to the user. To evaluate *ModelWeb*, we asked four practitioners from diverse industries to test three different web-applications with and without *ModelWeb*. We observed that *ModelWeb* enables considerable gains on the time performance (27-41%) and the number BDD scenarios obtained (51-113%).**

***Index Terms*—model-based testing, domain-specific modeling, behaviour-driven development, Selenium, Metaedit+**

I. Introduction

MODELS are considered as the abstract representations of real systems for their better understanding and reasoning [1]–[3]. As Rumbaugh stated in [4], models can be used for various important purposes including the precise understanding and communications of the domain knowledge, making early design decisions, separating design from requirements, generating useful business products, exploring alternative solutions, and managing complexity. Today, many attempts have been made for applying modeling on the software and systems testing so as to reduce the time for generating test scenarios and increase the effectiveness of the test scenarios [5]–[7].

Model-based testing could be used in the web applications development, which has been getting more complex ever-increasingly as the web applications may require complex GUIs and further need to satisfy various quality requirements (e.g., performance). Therefore, modeling and analysing web applications and automating the implementation and test case generation from models are highly popular issues nowadays. Many modeling approaches have been proposed for the web applications development, e.g., [8]–[12], which enable to specify high-level models for the web applications with some precise textual/graphical notation sets and are supported with tools for the model transformation (e.g., the automated implementation of web applications and early model analysis and simulation). Also, many model-based testing approaches have been proposed on web applications, e.g., [13]–[19], which are discussed in Section II. Using those approaches, abstract models can be specified using various types of notation sets for different concerns about systems including functional and non-functional concerns and transformed into test scenarios.

In this paper, we propose a modeling toolset for the web applications called *ModelWeb*. *ModelWeb* is supported with a flow-chart based notation set that consists of a pre-defined list of actions (e.g., click, select, open, login, type, share, register, drag & drop, and comment) through which the functional user behaviours on the web applications can be specified. Any flowchart models can be automatically transformed into the test scenarios with path coverage matching the cyclomatic complexity of the flow-chart models. To make the generated test scenarios understandable and at the same time executable, *ModelWeb* formats the transformed scenarios in accordance with the behaviour-driven development (BDD) approach [20]. *ModelWeb* further automatically executes the BDD scenarios on a given web application using the Selenium web test automation tool[1] and reports the test results to the user.

ModelWeb's novelty is to do with its flowchart-based, simple notation set consisting of a reusable set of actions for the modeling of users' functional behaviours on web applications and support for the fully automated testing process including the automated generation of scenarios and their execution on the web applications. As shown in Table I, the current approaches offer a textual notation set supported with some formalisms and therefore require a learning curve, some use statechart notation set that is not always easy to manage for specifying the user behaviours for stakeholders due to many states and transitions to be drawn, and some offer domain-specific notation sets for the quality testing (e.g., load, vulnerability, and security). We strongly believe that

[1]Selenium web-site: https://www.selenium.dev/

TABLE I: The model-based testing approaches for web applications

Work	Notation Set	Notation Set Type	Formalism	Focus	Scenario Gen.	Test Exec.
[13]	State-chart	Graphical	No	Functionality	Automated	Automated
[14]	Domain-specific	Textual	Alloy	Security testing	No	Automated
[15]	State-chart	Textual	No	Stateful GUI testing	Automated	Automated
[16]	No	Graphical	No	Ajax web apps.	Automated	Manual
[21]	State-chart	Graphical	No	GUI testing	No	Automated
[18]	Domain-specific	Graphical	No	Load testing	No	Automated
[19]	Domain-specific	Hybrid	Regular Expression	Vulnerability testing	Automated	Automated
[22]	Domain-specific	Textual	Labelled transition system	Functionality	Automated	Automated

ModelWeb may easily be used by stakeholders with any levels of technical knowledge involved in the testing process thanks to its simple notation set with no (or very little) learning curve. Thanks to its tool support, web applications may therefore be tested for the functional user behaviours in a highly productive manner (i.e., more cases to be tested in a shorter time period).

II. Related Work

The literature includes some works on the model-based testing of web applications, which are analysed in Table I for a number of requirements (i.e., notation set, formalism, focus, scenario generation, and test execution). Concerning the notation set, state-chart based notation set is quite dominant, which prompts the users to specify different states that the web pages can be in at a time and the events that cause transitions among them. Using the state-chart notation set could essentially be useful for proving the correctness of behaviour models as many model checkers have been existing for formally verifying the state-chart models (e.g., SPIN [23] and UPPAAL [24]). However, in our work, we do not focus on the formal verification and our main intent here is to generate BDD test scenarios from user functional behaviour models. Concerning the notation set type, while some approaches offer textual, some offer visual notation sets - Lebeau etal.'s approach [19] is the only exception here which offers a hybrid notation set. Concerning the formalism support, some approaches provide notation sets that are based on formal languages so as to enable formal verification or precise modeling. However, formally-based approaches lead to notation sets with steep learning curve [25]. Concerning the focus, different approaches focus on different aspects for testing, e.g., quality testing, Ajax web applications, GUI testing, and functionality testing. Lastly, each approach is supported with a tool that either generates the test scenarios from models automatically or executes the scenarios on the web application automatically. Note that some tools perform both tasks automatically. So, we observe that *ModelWeb* is the only tool that offers a graphical, flowchart-based notation set for the modelling of functional user behaviours and supports the fully automated way of producing test scenarios from flowchart models and executing the scenarios on the web application.

III. ModelWeb Toolset

As shown in Fig. 1, *ModelWeb*'s tool architecture consists of two main tools that are each composed of some sub-tools[2]. Users firstly use the model extractor to extract the web application HTML source file structures consisting of the HTML IDs of the web components. Then, users use the modeling editor to specify the flowchart models of their web applications and map their model elements with the actual web components using the extracted HTML IDs. The BDD generator is used next to transform the flow-chart models into test scenarios in BDD. Lastly, using the scenario tester, users execute the transformed test scenarios on the web application.

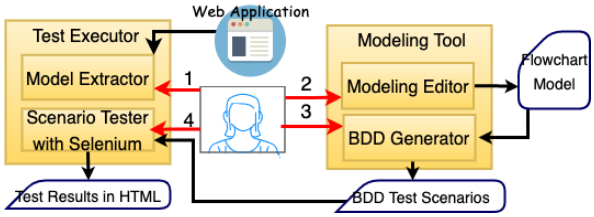

Fig. 1: *ModelWeb*'s tool architecture

IV. ModelWeb's Modeling Editor

ModelWeb's modeling editor is depicted in Fig. 2 and has been developed using the Metaedit+ meta-modeling tool [26]. Firstly, a modeling project is created via the dialog box appearing for specifying the project name and the web application URL. Then, a new editor opens for the project, through which the functionalities to be modeled for the web application can be specified in a tabular notation. Herein, for each functionality, users may record the name of the functionality and create a flowchart model for that functionality which opens up another (sub-)editor for drawing the flowchart model.

With *ModelWeb*'s editor, a flowchart model is specified using the pre-defined user and system actions. User actions represent the different types of actions that users perform while navigating through the web pages. System actions represent the system responses operated by the web application upon any user actions. As depicted in Fig. 2, any action on a flowchart model may be right-clicked and a window appears for specifying the relevant data and the HTML identifiers of the web components associated with that action. As discussed later in Section 7, each action needs to be mapped with the web application components so as to enable the automated testing of web applications for the model specifications.

[2] ModelWeb's web-site:https://sites.google.com/view/modelweblanguage

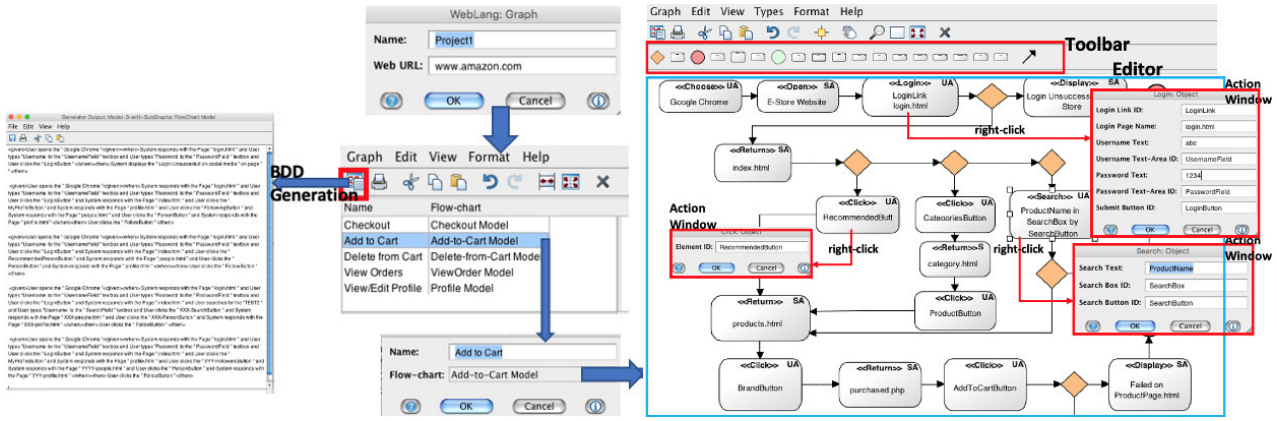

Fig. 2: *ModelWeb*'s modeling editor

To determine the user and system actions given as follows, we analysed several web applications in such industries as e-commerce, banking, and social-media, and came up with a set of actions. Then, we conducted interviews with practitioners working for an e-commerce software development company to get their feedback about the action set. We interviewed with one web developer, one support engineer, one analyst, and one manager. Each interview took 1-2 hours and aid in understanding from the practitioners' point of view to what extent the current list of actions are adequate and how the action list could be extended further.

User Actions

Choose. The choose action is intended for choosing a web browser through which the web pages of the web application under test can be requested by the user.

Open. The *open* action is intended for specifying the user action of opening a web page. To specify the open action, the name of the web page to be opened needs to be specified.

Click. The click action is for specifying the user action of clicking any web components, which can be either a button, link, text-area, drag-drop area, list (e.g., radiobutton and dropdown lists), or a list item. A click action is specified with the HTML ID of the web component to be clicked.

Type. The *type* action is for specifying the user action of typing a text on any text-area in a web page. To specify the type action, the text to be typed and the HTML ID of the text-area in which the text is to be typed need to be specified.

Login. Any *login* action for logging into a web application is specified with the login link ID, login page name, and username & password details. The login link ID is the HTML ID of the login page link. The login page name is the name of the page directed upon clicking the login link. The username and password are each specified with the IDs of the respective text-areas and the data to be provided.

Search. Any *search* action for searching information on a web page is specified with the search box ID, text, and search button ID. The search box ID is the HTML ID of the web component clicked for entering the search key. The search text is what the user enters as the search key. The search button ID is the HTML ID of the web component clicked for searching.

Select. The *select* action is intended for specifying the user action of selecting an item from a list on a web page. To specify the select action, the HTML ID of the list and the HTML ID of the list item to be selected need to be specified.

Register. The *register* action is for specifying the user action of performing a registration by filling a form. To specify the register action, a set of web components (e.g., text-area, button, dropdown list) constituting the registration form needs to be specified. For each component, the HTML ID of the component and the data that is supplied by the user for that component need to be specified by the user.

Comment. The *comment* action is for leaving a comment on a post. The comment action is specified with the comment link ID, comment text and, comment submit button ID. The comment link ID is the HTML ID of the link clicked to type comment. The comment text is the text typed by the user whenever the user clicks on the comment link ID. The comment submit button ID is the HTML ID of the button that the user clicks to submit comment.

Share. The *share* action is for sharing a post. The share action is specified with the share link ID, share text and, share submit button ID. The share link ID is the HTML ID of the link that the user clicks to share the post in question. The share text is the text that the user types on a window that appears whenever the user clicks on the share link ID. The share submit button ID is the HTML ID of the button that the user clicks to share the post with the text message.

Drag&Drop. The *drag&drop* action is intended for specifying the user action of dragging and dropping any item into a particular area of the same web page. To specify the drag&drop action, the HTML ID of the element that is dragged and dropped needs to be specified.

System Actions

Return. The *return* action is intended for specifying the system action of returning a web page upon any user action. To specify the return action, the name of the web page to be returned needs to be specified.

Display. The *display* action is intended for specifying the

system action of displaying a message on a web page upon any user action. To specify the display action, the message text and the name of the web page on which the message will be displayed need to be specified.

Note that a user action may transition to a diamond notation (as depicted in Fig. 4), whose aim is to connect the action with multiple user actions one of which can be chosen to be transitioned into. The outgoing action to be operated is decided depending on the user who performs one of the outgoing actions at that time.

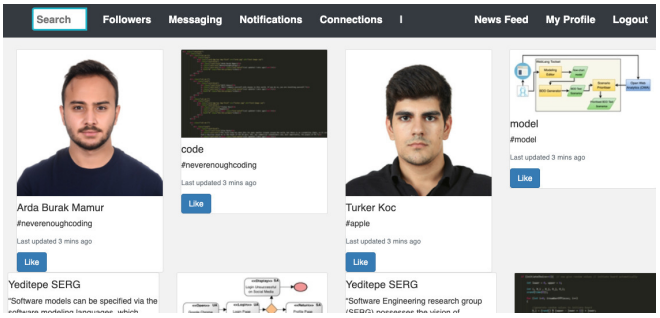

Fig. 3: A snapshot from the social networking web application's homepage

A. Case-study - Social Networking Web Application

We illustrate *ModelWeb*'s flowchart modeling notation set via a social networking web application, which allows users to connect with each other, post photos/videos/musics/documents of their interest for their connections, like each others' posts, send messages to any users, and follow/unfollow each other to get informed about each others' posts. We developed a prototype web application for social networking using PhP, whose main page is depicted in Fig. 3. Our prototype web application basically allows the users for registering themselves, logging in/out, following/unfollowing other users, clicking to like any post shared by the users, and sending messages.

Fig. 4 depicts the flowchart model of the *follow* functionality specified with *ModelWeb*, through which one may follow any users so as to be informed about their news/updates. As specified, the user starts by choosing the *Google Chrome* web-browser and opening the webpage. Then, the user attempts to login, where the necessary data are provided via the login action specification (i.e., username and password details, login link ID, and login page name). If login is unsuccessful, a message is displayed on the login page. Otherwise, the system returns the profile page. The user may now perform the *follow* functionality in three alternative ways. The user may search the name of the person whom he/she wishes to follow. The user may click to view the followers appearing on the user home page. Alternatively, the user select one of his/her connections to check the followers/following list of his/her connection. Each of those alternative ways leads to the system response that is to display the list of users where any user may be selected to follow. The system is then supposed to return the profile page of the chosen user where the follow button can be clicked to follow the user. If the follow operation is successful, the system returns the profile page of the followed user, otherwise an error message is displayed.

The full specification for the social networking web application can be found in the project web-site[2].

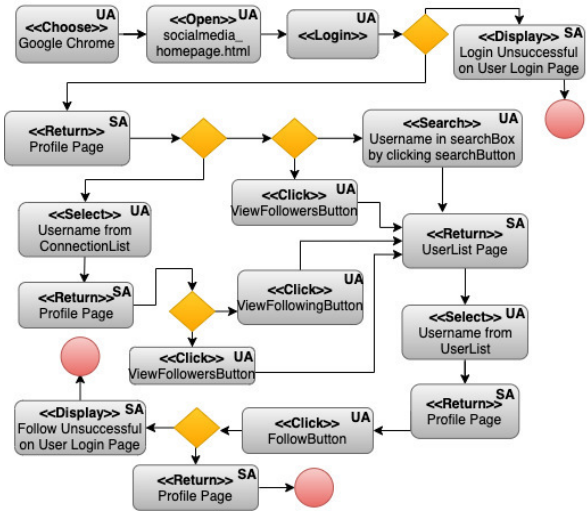

Fig. 4: The flowchart model for the "follow" functionality

V. ModelWeb's BDD Generator

To process the test scenarios generated from the flowchart models, we consider the transformation of the flowchart models in the behaviour-driven development (BDD) approach. BDD is supported by various test automation tools for executing the test scenarios on the web application under test (e.g., Selenium). Also, BDD does not require any learning curve thanks to its English-based notation set and also promotes the precise communication among non-technical stakeholders.

BDD has been proposed by Dan North in 2003 for tackling with the issues raised from the test-driven development (TDD) [27], which is mainly to do with writing test cases, testing the software systems against those test cases, and making the necessary refactoring. BDD's main focus is on the high-level system behaviour specifications rather than writing test cases that may require technical knowledge. As defined by the Gherkin language[3] that has been proposed for specifying BDD-based test scenarios and accepted by the BDD-based web test automation tools, the test scenarios that describe the expected system behaviours can be specified in terms of the *given*, *when*, and *then* clauses. *Given* here represents for a behaviour specification the pre-condition that needs to be satisfied before the behaviour is performed; *when* represents the behaviour specification itself; and, *then* represents the post-condition to be ensured after the behaviour specified.

We developed a transformation tool using Metaedit+'s MERL code-generator definition technology, which can be used via the modeling editor as depicted in Fig. 2. An icon

[3]Gherkin Language: https://cucumber.io/docs/gherkin/reference/

appears on the top-left of the editor, which is clicked to transform for any web application development project the flowchart models specified for different web functionalities of the web application. A set of BDD test scenarios are transformed from each flowchart model. The BDD generator outputs for any given web application project the generated BDD scenarios for the modeled web functionalities in XML.

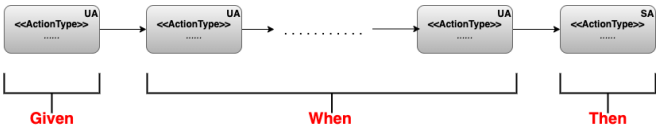

Fig. 5: Transforming a flowchart model into BDD

A. Transforming Flowchart Models in BDD

In a flowchart model, multiple paths may be existing depending on the diamond notations specified in the model. Each path is considered to be transformed into a distinct BDD test scenario. The number of paths for a flowchart model matches with the cyclomatic complexity of the model.

Given any flowchart model, the first action is supposed to be *choose* for choosing any web browser and that is considered as the pre-condition for each path of the flowchart model. As shown in Fig. 5, the first action of each path is considered as the pre-condition of the test scenario and thus transformed into a *given* clause. For each path of the flowchart model, all the actions that come after the first action in that path – except the last action – are considered as the main behaviour of the corresponding flowchart path which are expected to be operated in order given the pre-condition specified as the *given* clause is operated successfully. So, those actions are transformed as the the *when* clause, which includes the logical *AND* combinations of the actions in the same order that the actions are specified in the flowchart path. The last action on the path is considered as the post-condition of the test scenario that is ensured after the *when* behaviour is operated and thus transformed as the *then* clause. The last action on any path is expected to be a system action, which asserts that upon the user performing a behaviour for a web functionality, the system is to provide the expected response as a post-condition.

Fig. 6 illustrates how the model transformation works. The flowchart model in Fig. 6 describes the user behaviour for the ”add to cart” functionality of an e-store web application. Apparently, the flowchart model includes four different paths, which are indicated in Fig. 6. Each path here is transformed into a separate BDD scenario, where the first action is transformed as the *given* clause, the middle actions as the *when*, and the last action transformed as the *then* clause of the BDD scenario. Note that each model translation starts with the functionality description (i.e., ”add to cart”) and that is followed by the BDD scenario descriptions which are translated from each unique path of the model and started with the scenario identification number (e.g., ”Scenario 1”).

As depicted in Fig. 6, some user actions specified in a flowchart model are refined into a sequence of actions. A *search* action is transformed as clicking the search area, typing a search text, and then clicking the search button. A *select* action is transformed as clicking a list to be oopened and then clicking the item on the opened list. A *type* action is transformed as clicking the text area and typing the text on the clicked area subsequently. A *share* action is transformed as clicking the share box, typing the sharing message on the text area, and clicking the share submit button subsequently. Likewise, a *comment* action is transformed as clicking the comment box, typing the comment message on the text area, and clicking the comment submit button subsequently. A *register* action is transformed as the sequence of actions that correspond to the components composing the register form. A *login* action is transformed as clicking the login link, clicking the username text-area, typing the username, clicking the password text-area, typing the password, and clicking the submit button subsequently. By doing so, we intend to enable any flow-chart models to be transformed in a standard manner in terms of user-clicks and therefore any third-party tools (e.g., scenario prioritisation tools) may easily understand and process the transformed BDD scenarios.

VI. Test Executor

As depicted in Fig. 1, *ModelWeb*'s test executor consists of the model extractor and scenario tester tools, which are accessible via the GUI given in Fig. 7. The model extractor button in Fig. 7 is clicked for mapping the action elements in the flow-chart models with the HTML components on the web application (e.g., buttons, links, text-areas, lists, etc.). Note that to be able to test the web applications against the BDD scenarios generated from the flow-chart models, the flowchart models need to be traceable with regard to the web application implementation (i.e., the HTML sources). For instance, a click action specified needs to refer to the identifier of a clickable element on the relevant web page. So, given for any web application source HTML files, the model extractor produces and visualises the HTML element structures of each web page in a tree form. Users go through the generated tree model of web pages, learn the identifiers of the HTML elements in the web pages, and thus click any action elements on the flow-chart model as depicted in Fig. 2 so as to specify the HTML identifiers of the actions via the window opening. Then, the user may click the ”execute” button on the test executor GUI to run the scenario tester tool and perform the following activities automatically: *(i)* produce from the BDD scenarios (received as a text file from the modeling editor) a test script for the Selenium web test automation tool, *(ii)* run Selenium and execute the generated test script on the web application, and *(iii)* display the test results in HTML form as depicted in Fig. 7. In the test results screen, the test duration,the test platform, the BDD scenario tested with Selenium and the part of the BDD scenario under test (i.e., given, when, and then) that fail (red cross) or pass (green tick) are displayed. Note that the test executor in Fig. 7 also enables the scenarios to be prioritised, which is not inside the scope of this paper however.

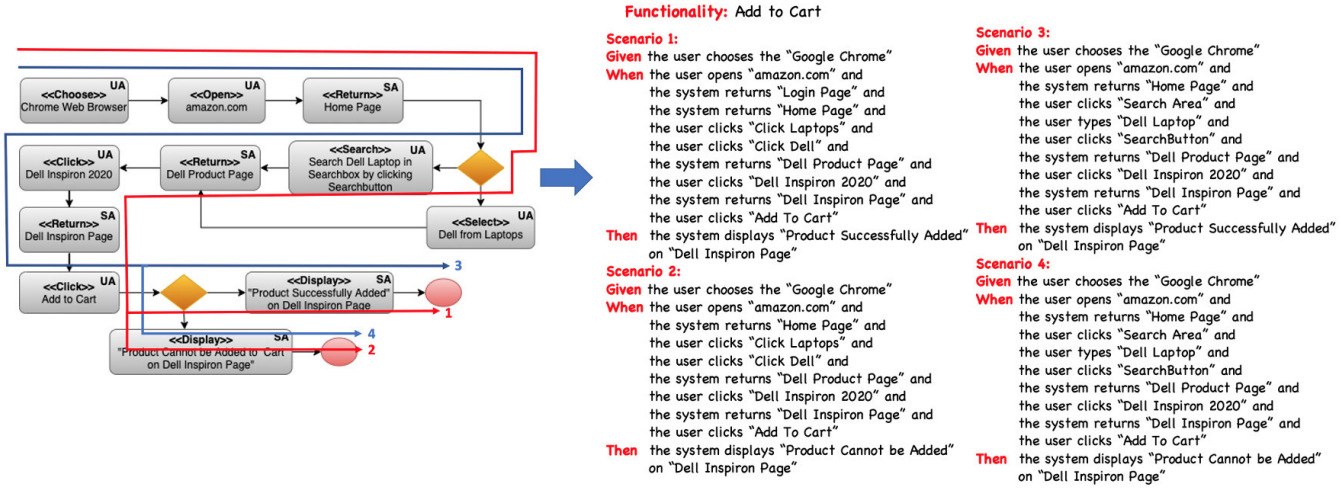

Fig. 6: Illustrating the model transformation from *ModelWeb*'s flowchart to BDD

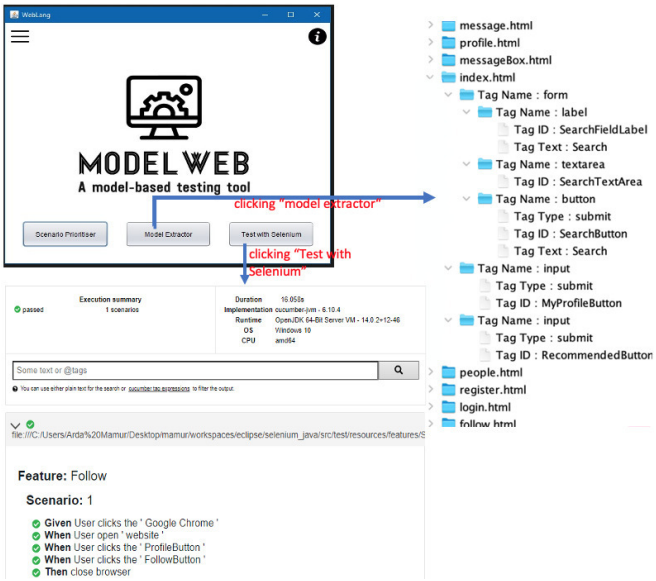

Fig. 7: The test execution GUI tool

VII. Evaluation

We discuss here *ModelWeb*'s performance evaluation, which has been conducted together with a group of practitioners for understanding to what extent *ModelWeb* provides the time performance gain when testing web applications. Note that we further conducted a usability evaluation through a series of interviews with 9 practitioners. However, due to the space restrictions, we could only discuss the performance evaluation here, and the document including the usability evaluation results discussion is accessible via the project web-site[2].

We considered the social networking, course management, and sports-store case-studies for our performance evaluation. The social networking application has been partly illustrated in Section IV-A, which provides such functionalities as following people, sending messages, and leaving likes on the posts shared by others. The course management application is used by the students to enroll for any course, retrieve materials, and upload any files. The sport-store application enables the users to do online shopping for the sports store, performing such tasks as adding any product to a cart, purchasing the products in the cart, and viewing orders. For each case-study, we developed a prototype web application in PhP. So, the practitioners who participate in the evaluation could use the web application implementations.

To choose the participants, we applied non-random sampling and selected four practitioners who work for the companies that our research group collaborates with. To reduce biases, we ensured that each participant works in a different industry, which are e-commerce, logistics, IOT, and defense, and represents a different user behaviour on web applications. Each participant completed a software engineering course in their undergraduate studies and thus has the basic modeling knowledge. Each participant has no experience on web programming and web test automation tools such as Selenium.

In the initial phase of our evaluation, we asked each participant to test the web applications without *ModelWeb*. So, each participant documented the scenarios for the functionalities of the three case-studies in BDD manually. We recorded the time here in extracting the possible scenarios given any functionality, their documentation in the BDD format, and transforming the BDD scenarios into a feature file that can be accepted by the Selenium web test automation tool. Then, each participant has been asked to use Selenium and test the corresponding web applications for the BDD scenarios specified as a feature file. In this aspect, the participants have used the Eclipse development environment that supports Selenium and perform the following activities for each web functionality: *(i)* writing the Java code for the step-definition (i.e., mapping scenarios in the feature file to the test code to be executed) and *(ii)* writing the Java code for the runner files that execute the step-definition code. The time spent on the above-listed two activities for each web functionality of each

TABLE II: The increase ratios for the time performance and the number of BDD scenarios with the use of *ModelWeb*

Case Study	Functionality	The increase ratio for the time performance (%)				The increase ratio for the number of BDD scenarios (%)			
		User (e-commerce)	User (logistics)	User (defense)	User (IoT)	User (e-commerce)	User (logistics)	User (defense)	User (IoT)
Course Management App.	Enroll for a course	25%	66%	28%	55%	200%	25%	100%	100%
	Upload submission	44%	58%	39%	30%	100%	33%	133%	100%
Sports-store App.	View orders	42%	30%	13%	45%	40%	33%	200%	25%
	Purchase a product	41%	53%	65%	63%	83%	25%	20%	0%
	Add product to cart	27%	26%	40%	30%	100%	125%	200%	133%
Social Networking App.	Follow	10%	17%	53%	23%	200%	133%	50%	300%
	Like	22%	46%	12%	47%	75%	25%	150%	33%
	Send Message	6%	28%	36%	27%	175%	29%	50%	29%
Average		**27%**	**41%**	**36%**	**40%**	**88%**	**51%**	**113%**	**90%**

web application have also been taken into consideration.

In the second phase of our evaluation, we asked the same participants to use *ModelWeb* this time. Note here that getting each participant involved in both the first and second phases may cause biases due to "carry-over effect" and thus we decided not to count the time that the participants spend on learning and understanding the functionality for the case when ModelWeb is not used and the time spent on understanding the functionality and learning the modeling notation set when ModelWeb is used. With *ModelWeb*, each participant initially used the modeling editor and the BDD generator to *(i)* specify the flowchart models for the functionalities of each web application considered and *(ii)* transform the flowchart models into BDD scenarios automatically. After obtaining the BDD scenarios, each participant used *ModelWeb*'s GUI-based executor tool so as to automatically execute the scenarios on the web applications automatically. Our test executor firstly takes the transformed BDD scenarios from the user via the GUI tool. Then the test executor produces a test script for the Selenium web test automation tool, and runs Selenium to execute the test script on the web application automatically. The test results are then displayed in HTML form.

Having collected the data from two phases of our evaluation, we calculated the increase ratios given in Table II for the time performance and the number of BDD scenarios obtained when the *ModelWeb* toolset has been used for the three case-studies. The time performance percentage indicates how much the time spent for testing is reduced when *ModelWeb* has been used, while the percentage for the BDD scenarios indicates how many more BDD scenarios are obtained when *ModelWeb* has been used. So, *ModelWeb* along with its test executor aids in improving the time performance of web applications testing considerably. Indeed, the users involved in the evaluation gained 27-41% time performance by using *ModelWeb*. Also, the users were able to maximise the number of BDD scenarios tested with the use of *ModelWeb*. Indeed, the users gained 51-113% increase on the number BDD scenarios obtained. Therefore, while the time spent have been reduced considerably, the number of the BDD scenarios tested got increased very highly thanks to *ModelWeb*. It should also be noted that using *ModelWeb* does not require learning and using any programming technologies. It is essentially enough to be capable of specifying flowchart models and the rest of the processes (test scenario generation and test execution via Selenium) are all performed by the toolset automatically in the background. On the other hand, in the case when *ModelWeb* is not used, practitioners have to use software development environments such as Eclipse and learn any required web test automation technologies such as Selenium.

VIII. Acknowledgement

This work was supported by a project of the Scientific and Technological Research Council of Turkey (TUBITAK) under grant 120E394.

IX. Conclusion

In this paper, a model-based testing toolset called *ModelWeb* for testing web applications has been proposed. *ModelWeb* is supported with a modeling editor that has been developed using the Metaedit+ meta-modeling tool. The editor enables to use a modeling notation set for specifying a flowchart model for any functionalities of web applications. A flowchart model is specified with a a pre-defined set of actions (i.e., click, type, open, choose, search, select, share, comment, register, login, and drag&drop). The modeling editor is also supplemented with a transformation tool, which can transform a flowchart model of any web functionality into the test scenarios according to the behaviour-driven development (BDD) approach. Users can further use *ModelWeb*'s test executor to execute the BDD test scenarios on the web application automatically. The test executor generates a test script for the Selenium web test automation tool and runs the test script over the Selenium platform. The test results are displayed in HTML format. Therefore, using *ModelWeb*, users may specify their functional behaviours for any web functionality with a simple, flow-chart notation set, and execute their web applications for each scenario derived from their flow-chart models automatically without having to use programming and testing technologies.

We focussed on the time performance gain that can be achieved with *ModelWeb*. That is, we developed prototype web applications for three case studies, (i.e., course management, sports-store, and social networking) and determined four practitioners from different industries to participate in the evaluation. So, we illustrated how *ModelWeb* reduces the

time spent for testing while maximising the number of BDD scenarios generated.

We further extended *ModelWeb* with a scenario prioritiser, which determines the users' usage behaviours on the web applications by analysing the sequence of user actions tracked and stored via the web analytics tools (e.g., OWA[4]), and prioritises the transformed test scenarios accordingly. Due to the space restriction, we could not discuss *ModelWeb*'s prioritisation tool here. However, a document is available in the project web-site[2] for *ModelWeb*'s prioritisation tool support.

As a future work, we will improve the modeling notation set with *(i)* user-defined action types for better expressiveness and *(ii)* the inclusion of a model within another model for managing complexity. We will also consider using some complex web applications with complex user behaviours and apply *ModelWeb* on a real environment and test real web applications using *ModelWeb* so as to validate the preliminary evaluation results.

REFERENCES

[1] E. Seidewitz, "What models mean," *IEEE Softw.*, vol. 20, no. 5, pp. 26–32, 2003. [Online]. Available: https://doi.org/10.1109/MS.2003.1231147

[2] B. Selic, "The pragmatics of model-driven development," *IEEE Softw.*, vol. 20, no. 5, pp. 19–25, 2003. [Online]. Available: https://doi.org/10.1109/MS.2003.1231146

[3] T. Kühne, "Matters of (meta-)modeling," *Software and Systems Modeling*, vol. 5, no. 4, pp. 369–385, 2006. [Online]. Available: https://doi.org/10.1007/s10270-006-0017-9

[4] J. E. Rumbaugh, I. Jacobson, and G. Booch, *The unified modeling language reference manual*. Addison-Wesley-Longman, 1999.

[5] I. Schieferdecker, "Model-based testing," pp. 14–18, 2012. [Online]. Available: https://doi.org/10.1109/MS.2012.13

[6] A. Pretschner, W. Prenninger, S. Wagner, C. Kühnel, M. Baumgartner, B. Sostawa, R. Zölch, and T. Stauner, "One evaluation of model-based testing and its automation," *CoRR*, vol. abs/1701.06815, 2017. [Online]. Available: http://arxiv.org/abs/1701.06815

[7] M. Utting, B. Legeard, F. Bouquet, E. Fourneret, F. Peureux, and A. Vernotte, "Recent advances in model-based testing," *Adv. Comput.*, vol. 101, pp. 53–120, 2016. [Online]. Available: https://doi.org/10.1016/bs.adcom.2015.11.004

[8] A. Kraus, A. Knapp, and N. Koch, "Model-driven generation of web applications in UWE," in *Proceedings of the 3rd International Workshop on Model-Driven Web Engineering MDWE 2007, Como, Italy, July 17, 2007*, ser. CEUR Workshop Proceedings, N. Koch, A. Vallecillo, and G. Houben, Eds., vol. 261. CEUR-WS.org, 2007. [Online]. Available: http://ceur-ws.org/Vol-261/paper03.pdf

[9] J. Gómez, C. Cachero, and O. Pastor, "Conceptual modeling of device-independent web applications," *IEEE Multim.*, vol. 8, no. 2, pp. 26–39, 2001. [Online]. Available: https://doi.org/10.1109/93.917969

[10] D. M. Groenewegen, Z. Hemel, L. C. L. Kats, and E. Visser, "Webdsl: a domain-specific language for dynamic web applications," in *Companion to the 23rd Annual ACM SIGPLAN Conference on Object-Oriented Programming, Systems, Languages, and Applications, OOPSLA 2008, October 19-13, 2007, Nashville, TN, USA*, G. E. Harris, Ed. ACM, 2008, pp. 779–780. [Online]. Available: https://doi.org/10.1145/1449814.1449858

[11] R. D. Virgilio, "AML: a modeling language for designing adaptive web applications," *Pers. Ubiquitous Comput.*, vol. 16, no. 5, pp. 527–541, 2012. [Online]. Available: https://doi.org/10.1007/s00779-011-0418-9

[12] G. Paolone, M. Marinelli, R. Paesani, and P. D. Felice, "Automatic code generation of MVC web applications," *Comput.*, vol. 9, no. 3, p. 56, 2020. [Online]. Available: https://doi.org/10.3390/computers9030056

[13] F. Bolis, A. Gargantini, M. Guarnieri, E. Magri, and L. Musto, "Model-driven testing for web applications using abstract state machines," in *Current Trends in Web Engineering - ICWE 2012 International Workshops: MDWE, ComposableWeb, WeRE, QWE, and Doctoral Consortium, Berlin, Germany, July 23-27, 2012, Revised Selected Papers*, ser. Lecture Notes in Computer Science, M. Grossniklaus and M. Wimmer, Eds., vol. 7703. Springer, 2012, pp. 71–78. [Online]. Available: https://doi.org/10.1007/978-3-642-35623-0_7

[14] M. Peroli, F. D. Meo, L. Viganò, and D. Guardini, "Mobster: A model-based security testing framework for web applications," *Softw. Test. Verification Reliab.*, vol. 28, no. 8, 2018. [Online]. Available: https://doi.org/10.1002/stvr.1685

[15] A. Törsel, "Automated test case generation for web applications from a domain specific model," in *Workshop Proceedings of the 35th Annual IEEE International Computer Software and Applications Conference, COMPSAC Workshops 2011, Munich, Germany, 18-22 July 2011*. IEEE Computer Society, 2011, pp. 137–142. [Online]. Available: https://doi.org/10.1109/COMPSACW.2011.32

[16] A. Marchetto, P. Tonella, and F. Ricca, "State-based testing of ajax web applications," in *First International Conference on Software Testing, Verification, and Validation, ICST 2008, Lillehammer, Norway, April 9-11, 2008*. IEEE Computer Society, 2008, pp. 121–130. [Online]. Available: https://doi.org/10.1109/ICST.2008.22

[17] P. W. M. Koopman, P. Achten, and R. Plasmeijer, "Model-based testing of thin-client web applications and navigation input," in *Practical Aspects of Declarative Languages, 10th International Symposium, PADL 2008, San Francisco, CA, USA, January 7-8, 2008*, ser. Lecture Notes in Computer Science, P. Hudak and D. S. Warren, Eds., vol. 4902. Springer, 2008, pp. 299–315. [Online]. Available: https://doi.org/10.1007/978-3-540-77442-6_20

[18] X. Wang, B. Zhou, and W. Li, "Model based load testing of web applications," in *IEEE International Symposium on Parallel and Distributed Processing with Applications, ISPA 2010, Taipei, Taiwan, 6-9 September 2010*. IEEE Computer Society, 2010, pp. 483–490. [Online]. Available: https://doi.org/10.1109/ISPA.2010.24

[19] F. Lebeau, B. Legeard, F. Peureux, and A. Vernotte, "Model-based vulnerability testing for web applications," in *Sixth IEEE International Conference on Software Testing, Verification and Validation, ICST 2013 Workshops Proceedings, Luxembourg, Luxembourg, March 18-22, 2013*. IEEE Computer Society, 2013, pp. 445–452. [Online]. Available: https://doi.org/10.1109/ICSTW.2013.58

[20] M. Wynne, A. Hellesoy, and S. Tooke, *The Cucumber Book: Behaviour-Driven Development for Testers and Developers*. Pragmatic Bookshelf, 2017.

[21] H. Reza, K. Ogaard, and A. Malge, "A model based testing technique to test web applications using statecharts," in *Fifth International Conference on Information Technology: New Generations (ITNG 2008), 7-8 April 2008, Las Vegas, Nevada, USA*, S. Latifi, Ed. IEEE Computer Society, 2008, pp. 183–188. [Online]. Available: https://doi.org/10.1109/ITNG.2008.145

[22] J. P. Ernits, R. Roo, J. Jacky, and M. Veanes, "Model-based testing of web applications using nmodel," in *Testing of Software and Communication Systems, 21st IFIP WG 6.1 International Conference, TESTCOM 2009 and 9th International Workshop, FATES 2009, Eindhoven, The Netherlands, November 2-4, 2009. Proceedings*, ser. Lecture Notes in Computer Science, M. Núñez, P. Baker, and M. G. Merayo, Eds., vol. 5826. Springer, 2009, pp. 211–216. [Online]. Available: https://doi.org/10.1007/978-3-642-05031-2_14

[23] G. J. Holzmann, "The spin model checker," vol. 23, no. 5, pp. 279–295, May 1997.

[24] K. G. Larsen, P. Pettersson, and W. Yi, "UPPAAL in a nutshell," *STTT*, vol. 1, no. 1–2, pp. 134–152, 1997.

[25] I. Malavolta, P. Lago, H. Muccini, P. Pelliccione, and A. Tang, "What industry needs from architectural languages: A survey," *IEEE Trans. Software Eng.*, vol. 39, no. 6, pp. 869–891, 2013. [Online]. Available: https://doi.org/10.1109/TSE.2012.74

[26] S. Kelly, K. Lyytinen, and M. Rossi, "Metaedit+ A fully configurable multi-user and multi-tool CASE and CAME environment," in *Seminal Contributions to Information Systems Engineering, 25 Years of CAiSE*, J. A. B. Jr., J. Krogstie, O. Pastor, B. Pernici, C. Rolland, and A. Sølvberg, Eds. Springer, 2013, pp. 109–129. [Online]. Available: http://dx.doi.org/10.1007/978-3-642-36926-1_9

[27] K. Beck, *Test Driven Development: By Example*. Addison-Wesley Professional, 2002.

[4]OWA Web-site: http://www.openwebanalytics.com/

Communication Papers of the of the 17th Conference on Computer Science and Intelligence Systems pp. 339–348
DOI: 10.15439/2022F93
ISSN 2300-5963 ACSIS, Vol. 32

From MSL to Dezyne: an Industrial Application Of QVTo

Leo van Schooten, Marco Alonso, Ronald Wiericx
Philips in Best, The Netherlands
Email: leo.van.schooten@philips.com

Mathijs Schuts
Philips in Best, The Netherlands
& Radboud University
in Nijmegen, The Netherlands

***Abstract*—At Philips Image Guided Therapy (IGT), we have developed a Domain Specific Language (DSL) that describes the behaviour of one of the subsystems of our interventional X-ray system. With the current implementation of our DSL we are able to generate C++ code that is integrated in our product software. As a next evolutionary step for our DSL, we would like to benefit from the features the Dezyne toolset offers, like C++ code generation and model checking. If all model checks pass, we know that the generated C++ code is free of certain issues. We present a model to model transformation developed in QVTo, that transforms our own DSL called the Movement Specification Language (MSL) to another DSL called Dezyne. To avoid confidentiality issues, we use a Lego robot example to explain the MSL.**

I. Introduction

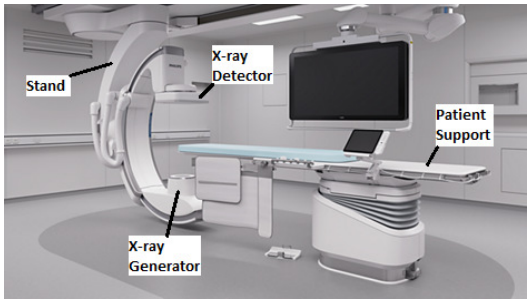

Fig. 1. Interventional X-ray system

AT Philips IGT, we develop and produce the interventional X-ray systems as shown in Figure 1. These systems are used for the diagnosis and treatment of mainly cardio and vascular diseases. One of the sub-systems is responsible for positioning the X-ray beam with respect to the patients body. A stand hanging on the ceiling holds an X-ray generator and an X-ray detector. To position the X-ray beam, the user of the system can initiate motorized movements of the stand using joysticks. Depending on the system state, these joystick requests are altered by a software component called the supervisory controller. Approximately six years ago we developed a Domain Specific Language (DSL) called: 'Movement Specification Language' (MSL). Language instances of the MSL called models describe the behaviour of the supervisory controller. To integrate a MSL model in our software, the instance is provided as input for a code generator that generates C++ code. The generated code can then be integrated in our software such that it behaves as described in the language instance.

Schuts et. al. [13] describe the evolution of the grammar of the MSL. In this paper, we describe the next evolutionary step we took to improve the MSL. We would like to replace the model to text C++ code generator by a model to model transformation. The target is a model in the Dezyne language [1]. Dezyne is a modelling language created by a Dutch company called Verum. Dezyne language instances can be checked for certain properties with the use of a model checker [2]. If all properties checks pass, C++ code can be generated with guaranteed equivalent behaviour as the checked model [2]. To be able to detect violations of certain properties in a MSL model and have C++ code that does not contain these violations we want to use the model checker and code generator provided by Dezyne.

The work described in this paper is executed by the first author of this paper during his internship at Philips. New in this paper, as compared to his master thesis [12], is that in this paper, we present and explain the QVTo instance needed for the model to model transformation.

The paper is organized as follows. We start with Section II about related work followed by Section III where we briefly describe the architecture of all the related languages and how they interact with each other. In Section IV, we introduce the case and grammar. The case will be a running example throughout this paper. Next in Section V we explain Dezyne and how the MSL example instance of Section IV maps to a Dezyne instance. Section VI describes how we have automated the transformation from MSL to Dezyne. Then we present the results in Section VII. We conclude our paper in Section VIII.

II. Related Work

The DSL that is developed at Philips IGT and described in this paper is informally described in [13] and formally described in [12]. Furthermore the Dezyne toolset is the successor of another toolset developed by Verum called ASD [3]. At Philips ASD has been successfully applied and evaluated as a valuable tool for software development. ASD, like Dezyne, is a lightweight formal software development tool. The toolset

[1]https://verum.com/discover-dezyne/

can be utilized to define and generate C++ code from finite state-machine models. Furthermore, the toolset is capable of detecting defects in the finite state-machines by means of model checking. Case studies of applying ASD at Philips IGT can be found in [5] and [11]. In both cases, the software contained less defects than when developing the software using conventional techniques of software development. Furthermore, both cases conclude that the overall development process was more efficient as time was spared because less tests had to be developed as some defects could be detected using the model checker of ASD.

The Dezyne toolset consists of a modelling language, a code generator and capabilities for model checking. In [2] the Dezyne language features are described and the transformation from the Dezyne modelling language to another modelling language called mCRL2 [6] is described. The mCRL2 models outputted by the transformation are used by the mCRL2 toolset [4] for model checking the behaviour of the Dezyne models.

Model to model transformations have been successfully applied in several occasions in the industry. For example, in [8] the authors describe a model to model transformation that was implemented at Cern[2] using the Asf+Sdf toolset [17]. The authors define a model to model transformation from a state machine DSL developed at Cern to the mCRL2 modelling language. This allowed the DSL instances from Cern to be model checked using the mCRL2 toolset and thus finding defects earlier in the development process. Furthermore, at Philips IGT a model to model transformation has successfully been applied in order to refactor state machine models from the Rhapsody [7] language to Dezyne [14]. This model to model transformation has been positively evaluated by comparing two approaches, manual transforming the models in the Rhapsody language to Dezyne and automatically transforming the Rhapsody models to Dezyne. The authors take into account the time it takes to fully implement and test a model to model transformation and the time it takes to do the transformation manually. The conclusion of the paper is that automating the transformation is a less time consuming process than doing the transformation manually.

As model transformations and, both toolsets from Verum: ASD and Dezyne have successfully been applied and positively evaluated at Philips we would like to continue on this path and therefore develop a model to model transformation that generates Dezyne language instances.

Finally, the QVTo language is an extension to the QVT language, the QVT language is described in [9] with the addition of operational mappings which is called QVTo. The extension QVTo adds new common imperative language constructs to the QVT language such as loops and conditions. Furthermore, the authors describe scenarios on which QVT can be utilized and which not. The authors discuss that the language can be seen as a general purpose model transformation language and suitable for a variety of model transformation problems. In addition they describe that the QVT language is less suitable for data transformation problems. Finally, in [16] a foundation is laid to describe QVTo transformations in a mathematical format for documentation purposes. As there are cases where the QVTo language has been evaluated for different purposes we present a practical application of QVTo in this paper.

[2]https://home.cern/

III. Model to Model Transformation Architecture

In order to be able to benefit from the advantages of Dezyne, we use Query/View/Transformation operational (QVTo) [9], defined by the Object Management Group (OMG) [10], as a language for describing a model to model transformation.

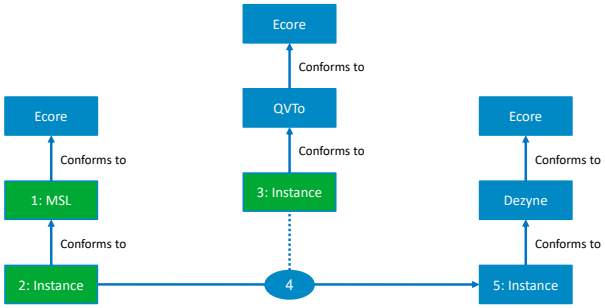

Fig. 2. Model to model transformation overview

Figure 2 provides an overview of the different languages we created and used. We make use of the Eclipse Modeling Framework (EMF) [1]. On the meta-meta-level we have Ecore, part of EMF, which is essentially a language to describe languages. The languages we use are described in Ecore. In Figure 2, all green boxes are language concepts that we developed and all blue boxes existed or are generated.

Our work consists of the following steps:

Step 1 In this step, we created a grammar for the MSL. The specifics of this language are described in [13].

Step 2 Software engineers create and alter an MSL instance to describe the behaviour of the supervisory controller.

Step 3 In this paper, we focus on the QVTo language instance we created.

Step 4 This step automatically generates Dezyne models. For the generation, a MSL instance and a QVTo instance are taken as input.

Step 5 We now have a generated Dezyne instances. Properties of the instances are tested using a model checker. If all checks pass, we generate C++ code with Dezyne and are done. If, however, there are failing properties, we have to go back to **Step 2** and change the language instance after which **Steps 4 & 5** have to be executed again.

IV. Movement Specification Language

First in order to understand the paper we will introduce the Movement Specification Language (MSL) as far as needed.

Because of confidentiality, we describe the MSL using a Lego rover example. The described example is inspired by an earlier paper we wrote about the evolution of the MSL's grammar [13].

We start this section with an introduction of the Lego Mars rover. Next we explain what Mars looks like. Then we describe how the Lego Mars rover is controlled. Last we provide an MSL example instance.

A. Rover

The Lego Mars rover has to accomplish missions on Mars Its mission is to search for water.

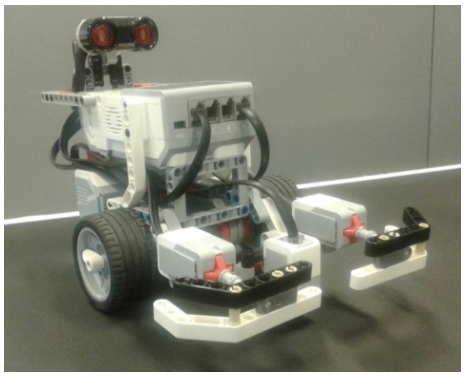

Fig. 3. Lego Mars rover

The Lego Mars rover is depicted in Figure 3. The rover has two big wheels at the front that are powered by two individual motors and the rover has a wheel at the back. Two bumpers at the front can detect if the rover has collided with an object. Between the bumpers there is a colour sensor that is used to look at the surface of Mars. At the back and on top of the rover an ultrasonic sensor looks forward.

The Lego Mars rover is remotely controlled. With joysticks the following movements can be requested: moving forward, moving backward, turn left and turn right. For all movements, the analog deflection of the joystick indicates the desired movement speed.

B. Playing Field

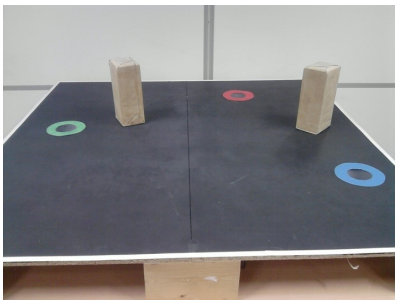

Fig. 4. Mars

For Mars we use Figure 4. Mars has the following characteristics:

- Mars has a square and flat surface.
- The surface of Mars is black and the edge has a white line.
- On the surface there are coloured lakes.
- There can be rocks on Mars.

The colour sensor is used to detect the edges of Mars. It is used to prevent driving the rover over the edge. The colour sensors can also be used to detect the colour of the lakes. Rocks can be seen at a distance using the ultrasonic sensor. Collisions with rocks are detected by the bumpers.

C. Controller

The controller of the Lego Mars rover is responsible for altering movement request that come from the remote control. The controller could alter a request based on the following examples:

1) *State:* The rover can be in a certain state for example, when the bumpers are active or when a sensor is defect the rover can reduce the speed of movement or even stop.
2) *Position:* The rover can deduce its position on the playing field. Depending on the on the position the rover can either reduce or increase its speed. For example, it can detect when it is near a lake or on the surface of Mars.
3) *Sensor value:* Sensor values of the rover can provide input that indicate that the rover should stop or reduce its speed. For example, when the collision sensor detects the rover is nearing a collision the rover should reduce its speed.

Note that: if none of the inputs trigger a reason to alter the movement request then the movement request will be executed unchanged.

D. Movement Specification Language

The DSL we describe in this section is used to describe the behaviour of our controller. We created a DSL we call MSL using the Xtext [1] Eclipse plug-in. First a few requirements are specified for the controller followed by an example of an MSL instance that implements these requirements. After that we argue that some of these requirements might lead to conflicting behaviour and how this is reflected in the MSL instance.

First consider the following requirements for our MSL instance:

1) Given the Lego Mars rover is driving on the surface of Mars then the rover should move with at most *max* speed.
2) Given the Lego Mars rover is driving near a coloured lake then the rover should move with at most a *reduced* speed.
3) Given the bumpers detect a collision then the rover should disable the ultra sonic sensor.
4) Given the bumpers detect a collision then the rover should stop immediately.

```
1 const DrivingMovements = Forward +
      Backward + TurnLeft + TurnRight
2 const ForwardMovements = Forward +
      TurnLeft + TurnRight
3
4 WHILE Inside LAKE_AREA DO MaximumSpeed
      safe APPLIES TO ForwardMovements
5 WHILE Inside MARS_AREA DO MaximumSpeed
      max APPLIES TO DrivingMovements
6 WHILE inState BUMPERS_ACTIVE In
      ULTRA_SONIC_SENSOR is disabled
      APPLIES TO allMovements
7 In ULTRA_SONIC_SENSOR, BUMPERS_SENSOR
      is enabled APPLIES TO allMovements
8 WHILE inState BUMPERS_ACTIVE DO
      QuickStop APPLIES TO allMovements
9 WHILE inState ULTRASONIC_ACTIVE DO
      NormalStop APPLIES TO allMovements
```

Listing 1. New proposal

5) Given the ultra sonic sensors detect a rock then the rover should gradually reduce speed and eventually stop.

Requirements 1 and 2 are requirements for the movement speed of the Lego Mars rover. On the flat surface of Lego Mars the rover is allowed to move with maximum speed as its collision prevention sensors are capable of preventing potential harm. However, the rover should move with at most a reduced safe speed whenever it is near a coloured lake as it is incapable of detecting when it could potentially ride into the water and thus get stuck in the water. Furthermore, requirement 3 ensures that the rover only relies on the bumper sensors when it is in a collision that the ultrasonic sensor is not able to detect. For example, when the obstacle's height is below the vision of the ultrasonic sensor. Then, the bumpers detect a collision and the ultrasonic sensor does not. Finally, requirements 4-5 are requirements that prevent the rover from colliding into obstacles. For requirement 4, the rover should stop immediately as it is already colliding with an obstacle when the bumpers detect a collision. However, when the ultrasonic sensor detects a collision, the rover has still some room to move forward. Hence, it may stop in a more gradual manner.

In Listing 1 an example MSL instance of the Lego rover is shown. It is used as a running example throughout the paper. The example instance in Listing 1 describes requirements 1-5. All the words in bold and blue are keywords i.e. part of the MSL's grammar. As explained in Section IV-C, a movement request can be altered by the controller. Lines 4-9 provide six examples of how the movement requests are altered.

First we will discuss some language concepts that help understand how the requirements are implemented. Consider line 4, the line contains a *condition*, *action* and a *set of movements*. The *condition* is denoted after the **WHILE** keyword, the *action* is denoted after the **DO** keyword and the applicable *set of movements* is denoted after the **APPLIES TO** keywords. Conditions can be considered as logical propositions and thus can be evaluated to *true* or *false*. The *actions* in the MSL instance are references to handwritten C++ classes that implement a function that takes as input a movement request and outputs an altered movement request. A typical line in the MSL instance can be interpreted as: when the *condition* is *true*, execute the *action* for movement requests related to movements in the *set of movements*. Furthermore, there are also *actions* related to enabling or disabling certain sensor inputs. Examples of such *actions* are shown on lines 6-7. These lines describe when the rover should consider or ignore the input values from certain sensors.

Recall Mars as shown in Figure 4. Line 4 describes that when a movement is requested and the rover is inside one of the lake areas of Mars the rover will move with at most a reduced *'safe'* speed. This line is applicable to all the movement requests related to driving forward i.e. moving forward, turn left and turn right. This *set of movements* is also defined in the language instance itself as shown on line 2. The line defines a *set of movements* called `ForwardMovements` to be the union of three movements being: `Forward`, `TurnLeft` and `TurnRight`. In addition, line 5 describes similar behaviour to line 4 the difference is that the rover moves at maximum speed instead of a reduced speed. These two lines essentially cover requirements 1 and 2. Next, lines 6-9 implement the behaviour required for requirements 3-5. Line 6 specifies that when the bumper sensor is active, the input from the ultrasonic sensor is disabled for all of the available movements. Furthermore, in other cases the ultrasonic sensor should be enabled and this is specified by line 7. These two lines implement the behaviour of requirement 3. In addition line 8 covers requirement 4. Line 8 states that when the bumper sensor is reporting a collision the movement should stop immediately which is represented by *action* `QuickStop`. Finally, line 9 covers requirement 5 which can be interpreted in a similar fashion as line 8, the difference being that the *condition* depends on the ultrasonic sensor input and the *action* representing a gradual stop.

E. Verification properties MSL

With the example in Listing 1 we will outline some properties that we would like to have in our MSL instance.

Recall that in a MSL instance the maximum speed of a movement can be set depending on the system state. An undesirable scenario is an instance that can set conflicting speeds for one specific movement. For example, in the MSL a developer can specify two lines where one line specifies that a movement should move with safe reduced speed while another specifies that a movement should move with maximum speed. If the *conditions* of those two lines exclude one another there is no problem i.e. the conditions can never both evaluate to *true*. However, if the two *conditions* do not exclude each other there might be cases where the speed is first set to the maximum value and then to a reduced value or vice versa. We would like to prevent such specifications as this might lead to undesirable behaviour i.e. the rover damaging itself. Hence, a

MSL instance should be free of ambiguous specifications for speed values. From now on we will refer to the property as *no conflicting speeds*.

The next property we would like our MSL model to have is that the specification is unable to simultaneously enable and disable the same sensor input. Such a specification might also lead to undesirable behaviour as it will or will not ignore certain sensor input while it is required to do so. This might occur when a developer specifies two lines where one line enables the input of a sensor and the other disables the input of a sensor and similar to property *no conflicting speeds* both conditions do not exclude each other. In addition to the *no conflicting speeds* property we would also like a MSL instance to be free of ambiguous specification where a sensor input can simultaneously be turned on and off. From now on we will refer to this property as *no ambiguous sensor status*.

V. Dezyne

In order to understand the translation we will as far as required describe the Dezyne modelling language, its features and give a small example. After that we will provide an outline to the implemented model to model transformation from the MSL to Dezyne. Dezyne language instances are called models and from now on we will refer to Dezyne languages instances as Dezyne models.

A. Dezyne toolset

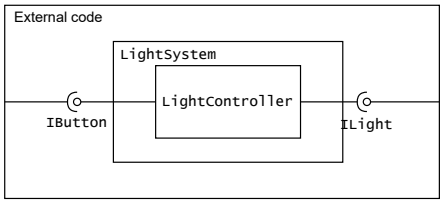

Fig. 5. System model of light system example

We start with an introduction to the Dezyne modelling language and the features of the Dezyne toolset. The Dezyne modelling language is a DSL with the purpose of designing state machine models. Dezyne models define three main concepts: interfaces, components and systems. We will explain the different types of Dezyne models by means of an example. Consider a simple light switch system where a light can be turned on and turned off by a button press. In addition the light has a requirement that whenever the light is turned on it is not allowed to turn the light on again and whenever the light is turned off it is not allowed to turn the light off again. The structure of the light switch system is depicted in Figure 5. The outside rectangle represents the external code while the inside rectangles represent a Dezyne system and component model `LightSystem` and `LightController` respectively. An arc at the end of a connection means that the Dezyne interface is required by the rectangle that it is connected to and a circle at the end of a connection means that the Dezyne interface is provided by the rectangle that it is connected to. We will now continue to zoom into these Dezyne concepts.

```
1  interface IButton {
2   in void buttonPress();
3   behaviour {
4     on buttonPress: { }
5   }
6  }
```

Listing 2. Example Dezyne interface model `IButton`

```
1  interface ILight {
2    in void turnOn();
3    in void turnOff();
4    enum State {On, Off};
5
6    behaviour {
7      State state = State.Off;
8      [state.On] on turnOff:{state = State.Off;}
9      [state.Off] on turnOff: illegal;
10     [state.On] on turnOn: illegal;
11     [state.Off] on turnOn:{state = State.On;}
12   }
13 }
```

Listing 3. Example Dezyne interface model `ILight`

1) Dezyne interface models: First, interfaces in Dezyne models describe a specification of deterministic stateful behaviour. The description of behaviour in the interface models is implemented by Dezyne component models or external C++ code. The interface models can define input events. Input events can be used as input for the implementation of a Dezyne interface. Interfaces can also define output events which occur as a consequence of certain behaviour and can be input for other implementations of the same interface. However, output events are not utilized by our Dezyne translation. Hence, we will further omit them. Furthermore, interface models can also define when certain behaviour is *illegal* meaning that the implementation is not allowed to trigger certain input events in certain states. For example, consider the interface model defined in Listing 2 for the light switch system. The model defines on line 2 one input event that corresponds to the button being pressed. The second interface model called `ILight` defined in Listing 3 defines two input events and a state type to keep track of the system's state i.e. whether the light is turned on or turned off. Furthermore, the interface specifies for each state what is allowed and what is not allowed. For example, on line 8 the interface specifies that whenever the interface is in the `On` state a `turnOff` event is allowed, while on line 9 the interface specifies that the `turnOff` event is not allowed by specifying it with the `illegal` keyword.

```
1  component LightController {
2    provides IButton provided;
3    requires ILight required;
4    behaviour {
5      ILight.State state = ILight.State.Off;
6      on provided.buttonPress(): {
7        if (state == ILight.State.Off) {
8          required.turnOn();
9          state = ILight.State.On;
10       } else if (state == ILight.State.On) {
11         required.turnOff();
12         state = ILight.State.Off;
13       }
14     }
15   }
16 }
```

Listing 4. Example Dezyne Component model `LightController`

2) Dezyne component models: The second type of models in Dezyne are component models. These component models implement the actual behaviour described by the interface models. Component models can either require or provide an interface model. The models need to adhere to the state

behaviour that is described by their provided and required interfaces. When a component requires an interface it means that the component can trigger the inputs of the interface. Furthermore, when a component provides the interface it means that the component provides the implementation of the interface i.e. the component defines what the behaviour is if certain inputs are triggered. The component model defined in Listing 4 implements the behaviour for the required interface i.e. interface `ILight`. On lines 6-14 the component model defines the behaviour of the input event `buttonPress`. The implementation triggers the input events on the required `ILight` interface according to the specification of the interface. The component ensures the behaviour of the interface by keeping track of the state and using the if else statement on lines 7 and 10 to evaluate the system state and call the correct input event on the provided interface.

```
1  component LightSystem {
2    provides IButton provided_port;
3    requires ILight required_port;
4
5    system {
6      LightController controller;
7      provided_port <=> controller.provided;
8      controller.required <=> required_port;
9    }
10 }
```

Listing 5. Example Dezyne system model `LightSystem`

3) Dezyne system models: The third type of Dezyne models are the system models. These models describe the composition of the components and interface models i.e. the models describe the structure depicted in Figure 5. Meaning that these models specify what interface is connected to what component and what interfaces are provided and required to the software that is integrating the Dezyne models. External C++ code is supposed to provide the implementation of turning the light on and off and trigger the input event on the `IButton` interface when the button is pressed. Furthermore, the Dezyne models implement the control behaviour of the light switch system. The Dezyne model that represents this structure is depicted in Listing 5. Observe that the `LightSystem` is also a component model that provides and requires interfaces. The required interfaces of the `LightSystem` will be provided by the external code. On line 6 the model states that the system consists of one component model being the `LightController`. On line 7 the model connects the implementation of the provided interface to that of the `LightController` and on line 8 the model connects the required interface of the `LightController` to the external code.

The semantics of the Dezyne models from Listings 2-5 implement the run to completion semantics [15]. The run to completion semantics imply that when a Dezyne component calls an input event on an interface the component gets blocked and awaits the result of the event that was called. These semantics are demonstrated in Figure 6. Observe that on the component the `buttonPress` event is called, as a consequence of the input event, component `LightController` calls the `turnOn` event on the required interface. Now observe that both the component and the initial caller on the component are blocked until the required interface returns.

The next feature Dezyne offers is formal verification of the behaviour that is expressed by a Dezyne model with the help of the mCRL2 model checker [2]. The general formal verification properties that Dezyne can verify are:

- Deadlock and livelock i.e. can the specification in a Dezyne model get stuck and thus no longer progress.
- Compliance i.e. does the component implement equivalent state behaviour as the provided interface description i.e. does the component not trigger illegal behaviour.
- Deterministic i.e. does a component or interface specification implement deterministic behaviour.

Finally, Dezyne models can be used as input for a C++ code generator that outputs code that is equivalent in behavior to the mCRL2 model. Whenever the model checker does not find any violations in a Dezyne model, C++ code can be generated and integrated in a system. In the case of the light switch system, the model checker found no violations which, implies that the implementation in component `LightController` is not able to trigger a `turnOn` event when the light is turned on or `turnOff` event when the light is turend off.

B. Translation outline

In this section we will describe the outline of the Dezyne models outputted by the model to model transformation. In Figure 7 an outline of all the Dezyne models generated for movement `TurnLeft` is shown. The rectangles describe component models and the connectors between the rectangles describe the interface models. An arc at the end of a connection means that the component requires the mentioned interface and a circle at the end of a connection means that the component provides the mentioned interface.

The main idea of the translation is that each distinct *action-movement* pair has its own component. Figure 7 shows the decomposition for the `TurnLeft` movement. Observe that the `TurnLeft` movement shows two components that have behaviour for an *action* i.e. component `TurnLeftUltraSonicSenor` and component `TurnLeftMaximumSpeed`. Component `TurnLeftUltraSonicSenor` implements the behaviour

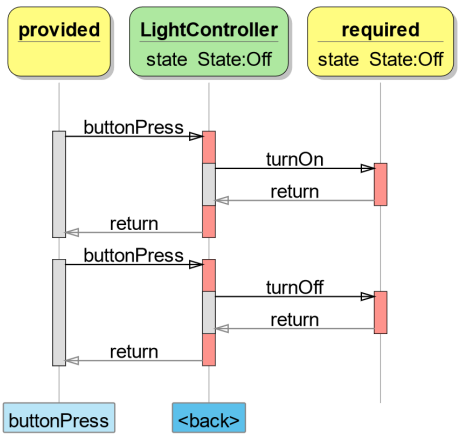

Fig. 6. Semantics Example model

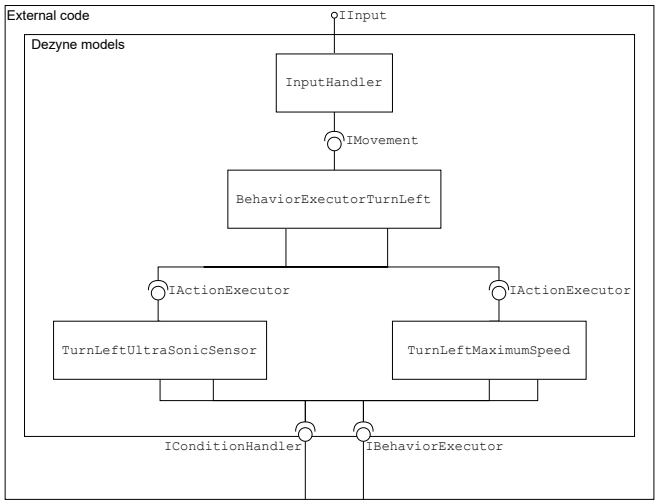

Fig. 7. Translation outline

for enabling and disabling the ultrasonic sensor and component `TurnLeftMaximumSpeed` implements the behaviour for setting the maximum speed of the movement. Recall, from the running example in Listing 1 that for movement `TurnLeft`, a `QuickStop` *action* and a `NormalStop` *action* are also defined. Our translation would also generate component models for these two actions. However, we have omitted these from Figure 7. Furthermore, the other components `BehaviorExecutorTurnLeft` and `InputHandler`, process the input coming from manually written components in the system. Movement requests are provided as input through the `IInput` interface. Depending on the request the `InputHandler` will forward the movement request to a component that maintains the behaviour for a specific movement. For example, in the case of a movement request for the `TurnLeft` movement `InputHandler` will forward the request to component `BehaviourExecutorTurnLeft` which will then forward the input to the relevant *action* components i.e. `TurnLeftUltraSonicSenor` and `TurnLeftMaximumSpeed`.

VI. QVTo

In this section, we will describe how we utilized QVTo to implement our model to model transformation. First we will provide a Dezyne model that shows how we want a generated model to look like using the model to model transformation. Second we will describe the QVTo language constructs and see how the translation is implemented.

A. Dezyne target model

```
1  component TurnLeftUltraSonicSensor {
2      requires IConditionHandler iConditionHandler;
3      requires IBehaviourExecutor iBehaviourExecutor;
4      provides IActionExecutor iActionExecutor;
5      behaviour {
6          enum State {enabled, notSet, disabled};
7          State state = State.notSet;
8          on iActionExecutor.executeBehaviours(mc): {
9              state = State.notSet;
10             bool bumpersActive = iConditionHandler.BumpersActive();
11             if (bumpersActive) {
12                 iBehaviourExecutor.Disabled(mc, UltraSonicSensor);
13                 if (!(state == State.disabled  state == State.notSet)) illegal;
14                 state = State.disabled;
15             }
16             if (true) {
17                 iBehaviourExecutor.Enabled(mc, UltraSonicSensor);
18                 if (!(state == State.enabled  state == State.notSet)) illegal;
19                 state = State.enabled;
20             }
21         }
22     }
23 }
```

Listing 6. Component specification `TurnLefUltraSonicSensort`

The Dezyne component models that are generated all have a similar structure. Listing 6 shows an example of a Dezyne model generated by our model to model transformation. The model implements the behaviour of turning the ultrasonic sensor on and off for movement `TurnLeft` as described in our running example in Listing 1. Observe that the model requires two interfaces being `IConditionHandler` and `IBehaviourExecutor`, and it provides the `IActionExecutor` interface. The required interfaces are used to evaluate *conditions* and to execute *actions*. The provided interface is there to provide the input to the Dezyne model. In the case of the model in Listing 6 the input consists of movement requests for movement `TurnLeft`. Furthermore, observe that line 11 implements the *condition* on line 6 of Listing 1. In addition line 16 implements the absent condition on line 6 of Listing 1. Hence, it is simply translated as *true*. Finally in order to verify that the *no ambiguous sensor status* property holds, the Dezyne model keeps track of the state of the sensor and triggers an *illegal* event when conflicting values for the sensor state are set. This is implemented using the if-statements on lines 13 and 18.

B. QVTo language

We will introduce QVTo as far as needed to understand this paper. The first main concept QVTo defines are the source and the target language i.e. the language that is used as input and the language that the QVTo transformation should output.

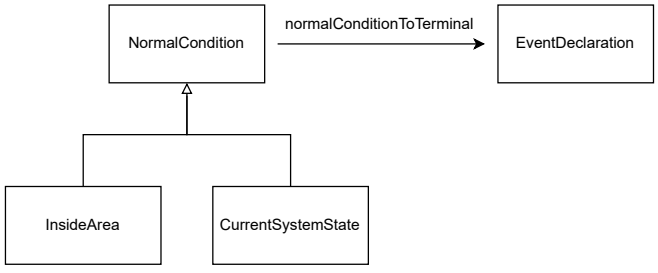

Fig. 8. Description of mappings

The second QVTo concept that we will discuss are mappings. Mappings transform a language element from the source language to a language element in the target language. Mappings are one of the main driving concepts in the QVTo language. For example, consider the *conditions* of the MSL. As mentioned earlier our MSL language conforms to the Ecore language on the meta model level. The *conditions*

```
1  mapping msl::NormalCondition::normalConditionToTerminal(...),
2  disjuncts
3  msl::InsideArea::InsideAreaToTerminal,
4  msl::CurrentSystemState::systemStateToTerminal: dzn::EventDeclaration {
5
6  }
7
8  mapping msl::InsideArea::InsideAreaToTerminal(...) : dzn::EventDeclaration {
9      name := "inside" + self.object3D.name;
10     dir := dzn::EventDirection::IN;
11     typeName := new BoolType();
12 }
13
14 mapping msl::CurrentSystemState::systemStateToTerminal(...) : dzn::
       EventDeclaration {
15     name := "inState" + self.currentState.name;
16     dir := dzn::EventDirection::IN;
17     typeName := new BoolType();
18 }
```

Listing 7. Disjunct mapping normalConditionToTerminal

```
1  query isMovementInSet(movementName : String, set : OrderedSet(csl::AMovement))
       : Boolean {
2      return set->selectOne(s | s.name = movementName) != null;
3  }
```

Listing 8. Query for movement set

are described using an Ecore class called 'NormalCondition'. This class has two subtypes called 'InsideArea' and 'CurrentSystemState'. This class decomposition is shown in Figure 8, the composition can be interpreted similar to super types and subtypes in object-oriented programming languages. QVTo mappings allow us to convert object instances of the NormalCondition type to object instances of the target Dezyne language.

Listing 7 shows an example of a mapping in QVTo. This mapping defines how objects of the 'NormalCondition' type should be transformed to 'EventDeclaration' type of Dezyne i.e. it defines events for the evaluation of system states on the `ICondtionHandler` interface. On line 1 a mapping for the 'NormalCondition' type is defined. Note that the mapping first states the input type i.e. 'NormalCondition'. Then observe on lines 2-4 that the mapping defines mappings for its subtypes 'InsideArea' and 'CurrentSystemState'. Finally, on line 4 the mapping also defines the output type of the mapping which is a type of the target language. In this case, the output type is an 'EventDeclaration'. The mappings for the subtypes are defined on lines 8-18. Typically a mapping states what values class member variables of the target class should have. For example on lines 9-11 it is shown that the EventDeclaration that is the result of the mapping 'InsideAreaToTerminal' states what name the event should have, what the direction of the event is i.e. ingoing or outgoing and finally what the type of the event is i.e. boolean.

The next language concept in QVTo are queries. Queries are typically used to retrieve information from elements in the source language. Furthermore, queries can also be utilized to return static elements of the target language. An example of a query is shown in Listing 8, the query determines if a certain movement is in a certain *set of movements*. Observe that the query is implemented similar to lambda expressions in modern object-oriented programming languages.

Furthermore, QVTo defines the notion of intermediate classes. Elements from the source language can be mapped

```
1  intermediate class BehaviourStatement {
2      name:String;
3      condition:intermediateCondition;
4      action:msl::GeneralDoAction;
5      setOfMovements:MovementSet;
6  };
```

Listing 9. Intermediate class

```
1  mapping msl::GeneralExecutionStatement::ExecutionStatementToBehaviourStatement
       (...) : BehaviourStatement {
2    name := self.name;
3    if(self.conditions != null) {
4      condition := new intermediateBoolExprCondition(self.conditions);
5    } else {
6      condition := new intermediateNoCondition();
7    };
8    action := self.actionGen;
9    setOfMovements := self.setOfMovements.xmap SetOfMovementsToSet(...);
10 };
```

Listing 10. Intermediate class mapping

to intermediate classes before they are mapped to elements of the target language. This can be beneficial as not always elements from the source language can be one to one mapped to elements in the target language. Listing 9 shows an example of a intermediate class, it describes an abstraction of a behaviour in the MSL language. Recall from the instance in Listing 1 that a line in the MSL can describe a behaviour that consists of a *condition*, *action* and an applicable *set of movements*. This intermediate class is meant to be used to extract this relevant information from a MSL model. Observe that the class also makes use of intermediate classes such 'intermediateCondition' and 'MovementSet'.

An example of how intermediate classes can be used in a QVTo mapping is shown in listing 10. The Listing defines a mapping where the language element 'GeneralExecutionStatement' gets mapped to the intermediate class 'BehaviourStatement'. The 'GeneralExecutionStatement' is the class defined in the source language that describes typical MSL statements such as the ones in the example in Listing 1. This mapping is convenient as it determines the correct condition for a behaviour statement, the correct *set of movements* and the corresponding *action*. Observe that on line 9 in Listing 10 another mapping is called to extract the correct set of movements from a 'GeneralExecutionStatement'.

Finally, in order to generate the component model of Listing 6 the mapping from the 'GeneralExecutionStatement' to the intermediate class 'BehaviourStatement' is used and then another mapping called 'BehaviourStatementToComponents' is used to generate the Dezyne component. The implementation of this mapping is shown in Listing 11. Observe that in this mapping we generate a new component for each movement action pair for a 'GeneralExecutionStatement'. The loop on line 3 in Listing 11 iterates over the applicable *set of movements* for a 'BehaviourStatement'. Then on line 5 the earlier created Dezyne component is retrieved from a mapping called 'StatementToComponent'. This mechanism is called 'resolve' in QVTo and it allows a user to retrieve results from earlier mappings in the transformation. The resolve feature is very convenient in this case as we only want to create one component for each specific *movement*, *action* pair.

```
1  mapping BehaviourStatement::BehaviourStatementToComponents(...) {
2      var actionName := self.action.name;
3      self.setOfMovements.movements->forEach(move) {
4          var componentName := move.name + actionName;
5          var component := componentName.resolveoneIn(String::
               StatementToComponent);
6          if (component == null) {
7              component := componentName.xmap StatementToComponent(...);
8          };
9
10         var ifExpr := self.condtion.xmap inermediateConditionToIfExpression
               (...)
11         var behaviourExecutorPort := component.ports->(p | p.name = "
               iBehaviourExecutor").oclAsType(dzn::PortDeclaration);
12         var actionEvent := self.action.resolveoneIn(msl::GeneralDoAction::
               generalExecutionStatementToActionEvent);
13         var then := new CompoundBehaviourStatement();
14         then.stats += new ActionOrFunctionStatement(...);
15         then.stats += GenerateCheck(...);
16         var ifStatement := new IfStatement();
17         ifStatement.expr := ifExpr;
18         ifStatement.then := then;
19
20         component.behaviour.stats->first().oclAsType(dzn::OnEventStatement).
               stat.oclAsType(dzn::CompoundBehaviourStatement).stats +=
               ifStatement;
21     }
22 }
```

Listing 11. BehaviourStatement to component

```
1  transformation Msl2DZN(in source:genmsl, out target:dzn);
2
3  main() {
4    source.rootObjects()[genmsl::GENMSLModel].xmap MSL2DZN();
5  }
6
7  mapping genmsl::GENMSLModel::MSL2DZN() : List(dzn::ModelDeclarationList) {
8    result += self.xmap actionsToEvents();
9    result += self.xmap conditionsToConditionInterface();
10   result += self.xmap movementsToInterfaceAndComponents();
11   result += self.xmap behavioursToDezyne();
12 }
```

Listing 12. BehaviourStatement to component

Furthermore, observe that the if-statement on line 6 ensures that a new Dezyne component is created if it has not been mapped before. Next lines 13-20 implement the generation of the if-statement that corresponds to evaluating the condition and executing the action. First on line 13 it maps the condition to a Dezyne if expression. Then on lines 11-12 the QVTo mapping retrieves the *action* elements in the target language in order to build the body of the if-statement. Finally on lines 13-20 the if-statement along with its body is created and added to the component. In addition on line 15 a query is called that depending on whether the component checks the *no ambiguous speed* or *no ambiguous sensor* status property, generates the if statement that contributes to the verification i.e. the if-statements on lines 13 and 18. This mapping essentially generates the Dezyne component that is shown in Listing 6.

To fit all the mappings together the final mapping that QVTo requires is to define a transformation. Listing 12 shows the definition of a transformation and the main function associated with it. Line 1 states the definition of the transformation, specifying the source and the target language. Then on line 3 the main entrypoint for the transformation is defined where we specify that the objects in the source language are to be transformed by the mapping called 'MSL2DZN'. This main mapping is defined on line 7 which specifies that it returns a list of 'ModelDeclarationList' in the target language i.e. a list of component and interface models.

VII. Results

The developed model to model transformation extended the capabilities of the MSL with model checking capabilities and the capability to use the Dezyne C++ code generator that allows us to dismiss our C++ code generator for the MSL. We will discuss the results of applying the transformation in the running example and in a MSL model of the interventional X-ray system. First we will describe the violations of the model checking properties *no conflicting speeds* and *no ambiguous sensor status* in our running example. Then we describe the transformation outcome and model checking properties violations found on a MSL model integrated in the software of the interventional X-ray system.

A. Model checking violations in running example

In our running example in Listing 1 we deliberately put violations of the *no conflicting speeds* and *no ambiguous sensor status* properties. Both the *conditions* on lines 4 and 5 can evaluate to *true* this results in an ambiguous specification for the speed value. For example, when the Mars rover is on the border of the lake and the Mars area then both the conditions `Inside LAKE_AREA` and `Inside MARS_AREA` might both evaluate to *true*. This ambiguous specification is applicable to all of the movements in the intersection of both the specified *set of movements* in both lines i.e. {Forward, TurnLeft, TurnRight}.

Furthermore, there is also a violation of the *no ambiguous sensor status* property. We have specified that both sensor input should be enabled by default (line 7) while also the ultra sonic sensor input should be ignored when the bumper sensor is active (line 6). Hence, whenever the condition `inState BUMPERS_ACTIVE` evaluates to *true*, the Mars Rover's specification is ambiguous on whether or not it should consider or ignore the sensor input from the ultra sonic sensor. The violation of the ambiguous sensor status is applicable for all of the movements the system can perform as both of the applicable *set of movements* on lines 6 and 7 are all movements.

B. Model checking violations Philips IGT system

For the software of the interventional X-ray system a MSL model has been developed that describes the behaviour that is specified by the requirements. We have applied the transformation described in this paper to generate Dezyne models that were capable of verifying the properties *no conflicting speeds* and *no ambiguous sensor status*. The transformation generated approximately 1200 Dezyne models. The amount can be explained by the fact the transformation generates a new component model for each specific movement action pair in the MSL model. In the MSL model that is integrated in the X-ray system there are 55 movements and 20 *actions*. Hence, the maximum amount of models that our transformation could generate is 55*20=1100. Then for each specific movement there is also a Dezyne model generated with the addition of the interface and composition models. These models were mostly small in size and the model checker of Dezyne was

capable of verifying most of them. The model checker of Dezyne has found 4 violations of the *no conflicting speeds* property and 17 violations of the *no ambiguous sensor status* property. Not all of the violations were issues in the software because the order in the MSL instance happened to be such that the code generator of the MSL generated C++ code that did not implement behaviour that could cause an issue. In addition some of the found ambiguous specifications between two lines in the MSL were not ambiguous because although both conditions could be *true* at the same time in theory, in practice it concerned system states that could never be *true* at the same time. Unfortunately, there were 27 generated Dezyne models that had a very vast state-space, we did not explore the state-space of all of the models but one of the models had a state-space of approximately 160 million states. The Dezyne model checker was not able to verify these models in a acceptable time period, some models could take hours or longer to verify. Finally, the C++ code generated by Dezyne was integrated in the software of the interventional X-ray system. With the Dezyne code the regression test cases passed that every code change in the X-ray system's software need to pass. Hence, we have good confidence that the behaviour described by the MSL instance is preserved in the generated Dezyne models.

VIII. Concluding Remarks

To conclude we have implemented a model to model transformation from a DSL developed at Philips IGT called the MSL to another DSL developed by Verum called Dezyne. This transformation is the next step in the evolution of the MSL. The transformation to Dezyne can be utilized as an intermediate step between developing a MSL model and generating C++ code that can be integrated in our software. The additional benefit of the generated Dezyne models is that their behaviour can be model checked and thus, we can ensure that our MSL instance does not contain certain potential issues. In the MSL a developer can make certain specifications ambiguous by specifying multiple speed values that are both set in a specific system state. Furthermore, a developer can specify that certain sensor inputs should be ignored or considered. Specifying the consideration of a sensor input could also lead to ambiguous specifications as a developer could specify to both ignore and consider a certain sensor input in a specific system state. In order to prevent such ambiguous specifications the transformation generates Dezyne models that could detect these ambiguous specifications using model checking. In total the transformation generated approximately 1200 Dezyne models which, contained 21 ambiguous specifications. These models were generated from a MSL model integrated in the software of the interventional X-ray system.

There are some improvements that can be made using this approach. As mentioned in the previous section, the Dezyne models do not contain any domain specific knowledge, leading to flagging potential issues which in practice could never occur. Furthermore, there are some Dezyne models outputted by our transformation that have a state-space that is to vast for the model checker to output a result in a acceptable time period. Therefore, as future work we would like to solve the state-space explosion problem in addition we would like our Dezyne models to be more aware of domain specific concepts such as system states that exclude each other. Finally, another improvement we could make is seeing if there are more *actions* in the MSL that are tightly coupled to each other and could for example also lead to ambiguous specifications.

References

[1] L. Bettini, *Implementing Domain-Specific Languages with Xtext and Xtend*. Packt Publishing Ltd, 2013.

[2] R. V. Beusekom, J. F. Groote, P. Hoogendijk, R. Howe, W. Wesselink, R. Wieringa, and T. A. C. Willemse, "Formalising the dezyne modelling language in mcrl2," *Lecture Notes in Computer Science Critical Systems: Formal Methods and Automated Verification*, p. 217–233, 2017.

[3] G. H. Broadfoot and P. J. Hopcroft, "Analytical software design," *Verum Consultants BV*, 2003.

[4] S. Cranen, J. F. Groote, J. J. A. Keiren, F. P. M. Stappers, E. P. D. Vink, W. Wesselink, and T. A. C. Willemse, "An overview of the mcrl2 toolset and its recent advances," *Tools and Algorithms for the Construction and Analysis of Systems Lecture Notes in Computer Science*, p. 199–213, 2013.

[5] J. F. Groote, A. Osaiweran, and J. Wesselius, "Analyzing the effects of formal methods on the development of industrial control software," in *Proceedings of the 27th IEEE International Conference on Software Maintenance (ICSM 2011, Williamsburg VA, USA, September 25-30, 2011)*. United States: Institute of Electrical and Electronics Engineers, 2011, pp. 467–472.

[6] J. F. Groote and M. R. Mousavi, *Modeling and analysis of communicating systems*. The MIT Press, 2014.

[7] D. Harel and H. Kugler, "The rhapsody semantics of statecharts (or, on the executable core of the uml)," in *Integration of Software Specification Techniques for Applications in Engineering*. Springer, 2004, pp. 325–354.

[8] Y. L. Hwong, J. J. Keiren, V. J. Kusters, S. Leemans, and T. A. Willemse, "Formalising and analysing the control software of the compact muon solenoid experiment at the large hadron collider," *Science of Computer Programming*, vol. 78, no. 12, pp. 2435–2452, 2013, special Section on International Software Product Line Conference 2010 and Fundamentals of Software Engineering (selected papers of FSEN 2011).

[9] I. Kurtev, "State of the art of qvt: A model transformation language standard," in *Applications of Graph Transformations with Industrial Relevance*, A. Schürr, M. Nagl, and A. Zündorf, Eds. Berlin, Heidelberg: Springer Berlin Heidelberg, 2008, pp. 377–393.

[10] OMG, "meta object facility (mof) 2.0 query/view/transformation specification_2008," Apr 2008.

[11] A. Osaiweran, M. Schuts, J. Hooman, J. F. Groote, and B. V. Rijnsoever, "Evaluating the effect of a lightweight formal technique in industry," *International Journal on Software Tools for Technology Transfer*, vol. 18, no. 1, p. 93–108, 2015.

[12] L. v. Schooten, "Extending a domain specific language using model transformations," Master's thesis, 2021.

[13] M. Schuts, M. Alonso, and J. Hooman, *Industrial Experiences with the Evolution of a DSL*. New York, NY, USA: Association for Computing Machinery, 2021, p. 21–30.

[14] M. Schuts, J. Hooman, and P. Tielemans, "Industrial experience with the migration of legacy models using a dsl," in *Proceedings of the Real World Domain Specific Languages Workshop 2018*, 02 2018, pp. 1–10.

[15] A. S. Tanenbaum and H. Bos, *Modern operating systems*. Prentice Hall, 2015.

[16] U. Tikhonova and T. Willemse, "Designing and describing qvto model transformations," in *2015 10th International Joint Conference on Software Technologies (ICSOFT)*, vol. 1, 2015, pp. 1–6.

[17] M. van den Brand, A. van Deursen, J. Heering, H. de Jong, M. de Jonge, T. Kuipers, P. Klint, L. Moonen, P. Olivier, J. Scheerder, J. Vinju, E. Visser, and J. Visser, "The asf+sdf meta-environment: A component-based language development environment," *Electronic Notes in Theoretical Computer Science*, vol. 44, no. 2, pp. 3–8, 2001, lDTA'01, First Workshop on Language Descriptions, Tools and Applications (a Satellite Event of ETAPS 2001).

Author Index